東京帝國大學

地震研究所彙報

第八號

昭和五年

BULLETIN

OF THE

EARTHQUAKE RESEARCH INSTITUTE

TOKYO IMPERIAL UNIVERSITY

Vol. VIII.

1930.

目　次

第八號

第一冊（昭和五年三月）

			頁
1.	地震波によつて土地の固有振動が誘起される可能度に就いて（英文）	妹澤克惟	1
2.	地殼の群塊運動の可能度に就いて（英文）	妹澤克惟 西村源六郎	13
3.	カリフォルニアに於ける地殼の變形（英文）	宮部直巳	45
4.	破壞的地震に就て（英文）	寺田寅彦	61
5.	海水面に及ぼす海流の影響竝びに波浪の影響に就て（英文）	山口生知	75
6.	大阪近傍水準測量の結果に就て（邦文）	梅本豐吉	85

第二冊（昭和五年六月）

7.	溫度分布が半無限彈性體の變形に及ぼす影響（英文）	西村源六郎	91
8.	十八米突の鐵管による地表傾斜變化の觀測（豫報）（英文）	高橋龍太郎	143
9.	昭和二年丹後地震に關聯せる丹後地方の地殼の變形に關する研究（第一報）（英文）	坪井忠二	153
10.	地表の傾斜の變化に就て（第二報）關原における地震後の觀測（佛文）	石本巳四雄	222

11. 昭和四年六月北海道駒ヶ嶽の噴火(英文)…… 津屋弘逵・坪井誠太郎・岸上冬彦・高橋龍太郎・坪井忠二・中田金市・宮部直巳 237

第三冊（昭和五年九月）

12. 彈性波の反響性及び分散性分散に就て(英文) 妹澤克惟・西村源六郎 321

13. 昭和二年丹後地震に關聯せる丹後地方の地殼の變形に關する研究(第二報)(英文)…… 坪井忠二 338

14. 筑波山に於ける傾斜變化觀測報告(邦文)…… 井上宇胤・杉山友紀 346

15. 大地震と太陽黑點との關係に就て(邦文)…… 高山威雄・鈴木武夫 364

16. 伊豆東海岸に於ける水準測量成果報告(邦文)…… 375

第四冊（昭和五年十二月）

17. 地殼の變形に因る熱の發生(英文)…… 寺田寅彦 377

18. 地殼の水平變動に就いて(英文)…… 坪井忠二 384

19. 地震と潮汐との關係(英文)…… 山口生知 393

20. 伊豆、伊東地方の地質構造に就いて(英文)… 津屋弘逵 409

21. 伊東地震と地表傾斜變化の觀測(邦文)…… 石本巳四雄・高橋龍太郎 427

Contents.

Vol. VIII.

Part 1.—March, 1930.

Page

1. K. Sezawa, Possibility of the Free-oscillations of the Surface-layer excited by the Seismic-waves. (in English) 1
2. K. Sezawa and G. Nishimura, On the Possibility of the Block Movements of the Earth Crust. (in English) 13
3. N. Miyabe, Deformation of Earthcrust in California. (in English) 45
4. T. Terada, On the Nature of Destructive Earthquakes. (in English) 61
5. S. Yamaguti, On the Effect of Ocean Current, "Kurosiwo", upon Sea Level. Effect of Waves. (in English) 75
6. T. Umemoto, Results of the Repeated Levellings in the Vicinity of Oosaka. (in Japanese) 85

Part 2.—June, 1930.

7. G. Nishimura, The Effect of Temperature Distribution on the Deformation of a Semi-infinite Elastic Body. (in English) 91
8. R. Takahasi, Preliminary Report on the Observation of the Tilting of the Earth's Crust with a Pair of Water Pipes. (in English) 143

9. C. Tsuboi, Investigation on the Deformation of the Earth's Crust in the Tango District connected with the Tango Earthquake of 1927. (Part 1.) (in English) 153

10. M. Ishimoto, Observations sur les variations de l'inclinaison de la surface terrestre (deuxième rapport). Résultats obtenus dans la région épicentrale du tremblement de terre de Sekihara. (en Français) 222

11. H. Tsuya, S. Tsuboi, F. Kishinouye, R. Takahasi, C. Tsuboi, K. Nakata and N. Miyabe, The Eruption of Komagatake, Hokkaidô, in 1929. (in English) 237

Part 3.—September, 1930.

12. K. Sezawa and G. Nishimura, Dispersion of a Shock in Echoing- and Dispersive-Elastic Bodies. (in English) 321

13. C. Tsuboi, Investigation on the Deformation of the Earth's Crust in the Tango District connected with the Tango Earthquake of 1927. (Part 2.) (in English) 338

14. W. Inouye and T. Sugiyama, On Earth-tiltings observed at Mt. Tukuba. (in Japanese) 346

15. T. Takayama and T. Suzuki, On the Relation between the Sunspot Number and the Destructive Earthquakes in Japan. (in Japanese) 364

16. Precise Levellings in the Province of Idu. (in Japanese) 375

Part 4.—December, 1930.

17. T. Terada, On the Heat generated by the Deformation of the Earth Crust. (in English) 377

18. C. Tsuboi, A Note on the Analytical Treatments of the Horizontal Deformation of the Earth's Crust. (in English) 384

19. S. Yamaguti, Relation between Tidal Phases and the Earthquakes. (in English) 393

20. H. Tsuya, On the Geological S ructure of Itô District, Idu. (in English) 409

21. M. Ishimoto et R. Takahasi, Séismes d'Itô et l'observation sur les variationsde l'inclinaison de la surface terrestre. (en japonais) 427

正　誤　表

Errata.

號 Volume	册 Part	頁 Page	行 Line	誤 *for*	正 *read*
II		31	17	$\frac{d^2H}{dy^2}+$	$\frac{d^2H}{dy^2}-$
IV		120		$\begin{cases} t=0 \\ t=0 \end{cases}$	$\begin{cases} t=0 \\ t=t \end{cases}$
VII	1	49	12, 14	$\cos(m-2p)f\,df$	$\mathrm{ch}(m-2p)f\,df$
"	1	53	4, 6		
"	3	573	18	n^2f	n^2A
"	"	579	16	$Adx=\frac{v}{\gamma P}dP + \frac{P^2-\pi^2}{P}\frac{r^4}{16\pi\eta l}dt$	$Adx=\frac{v}{\gamma P}dP + \frac{P^2-\pi^2}{P}\frac{\pi r^4}{16\eta l}dt$
"	"	"	17	$\frac{r^1}{16\pi\eta l}=B$	$\frac{\pi r^4}{16\eta l}=B$
"	"	"	24	$\frac{8\pi\eta l}{r^4}A^2\frac{dx}{dt},$	$\frac{8\eta l}{\pi r^4}A^2\frac{dx}{dt},$
"	"	580	1	$2\varepsilon=8\pi\eta lA^2/r^4$	$2\varepsilon=8\eta lA^2/\pi r^4$
"	"	"	2	$\lambda=\frac{4\pi\eta lA^2}{Mr^4}$	$\lambda=\frac{4\eta lA^2}{\pi Mr^4}$
"	"	"	3	$S=\frac{\lambda}{n^2}=\frac{\lambda T_0^2}{4\pi}$	$S=\frac{\lambda}{n}=\frac{\lambda T_0}{2\pi}$
"	"	"	4	$\lambda=1{\cdot}37\times10^2$	$\lambda=1{\cdot}05\times10^2$
"	"	"	5—6	M, A は前述の如き値として $r'/l=1{\cdot}925\times10^{-5}$ となり、$l=1$ cm. とすると $2r=0{\cdot}13$ cm. となる	MA は前述の如き値、$l=1$ cm. とすると $2r=0{\cdot}33$ mm. となる。實際に於ては l は 1 cm. 以上あり、又ゴムパッキング自身内の減衰作用も加るから穴は此程細くする必要はない。
VIII	1	14	19	is not	is
"	1	88	第二圖	大津市 130·0	大津市 1300
"	2	304	23	rack	rock
"	"	306	31	amplitudes	amplitude
"	"	307	1	result	results
"	2	312	3	hill	hill
"	3	323	17	Dispertion	Dispersion

號 Volume	册 Part	頁 Page	行 Line	誤 *for*	正 *read*
VIII	4	388	第四表 第三行	NE 0·15	1·15
"	"	"	"	WN 0·01	1·01
"	"	"	"	ΔWN 0·82	0·92
VIII	3	372—373	(附記)	高山 鈴木論文「附記」	(附記)

Cycle として得られた各の値を n とし、それの平均を ν とする、$n-\nu$ 即ち偏差が全く偶然的に起つて居るならば $\overline{|(n-\nu)/\nu|^2}=1/\nu$ なる關係式が成立すると考へられるから $\overline{|(n-\nu)/\nu|^2}$ (obs.) と $1/\nu$ (cal.) とが大體一致する場合は、ν と云ふ値は物理的意味あるものとし然らざる場合は意味を持たぬものと見做し得ると思ふ。この計算の結果は Table VI の通りである。$1/\nu$ を計算する時は ν を初めに單位としてとつた年數にて除して單なる數として計算した。

Table VI.

Cycle (max.—max.)	$\overline{\|(n-\nu)/\nu\|^2}$ (obs.)	$1/\nu$ (cal.)	Cycle (min. min.)	$\overline{\|(n-\nu)/\nu\|^2}$ (obs.)	$1/\nu$ (cal.)
81 years	0·35	0·25	81 years	0·15	0·25
97	0·3	0·24	97	0·11	0·24
103	0·23	0·24	97	0·10	0·26
154	0·22	0·26	149	0·28	0·27
184	0·17	0·25	202	0·14	0·23
200	0·15	0·25	190	0·12	0·26
240	0·07	0·25	240	0·008	0·25
34	0·13	0·29	33	0·29	0·30

Table VI より $\overline{|(n-\nu)/\nu|^2}$ と $1/\nu$ とが最もよく一致するのは 150 年と云ふ Cycle の場合である。從つて 150 年と云ふ週期は實際に存在するのではないかと思はれる。

東京帝國大學
地震研究所彙報
第八號

1. Possibility of the Free-oscillations of the Surface-layer excited by the Seismic-waves.

By Katsutada SEZAWA,

Earthquake Research Institute.

(Read Nov. 19, 1929.—Received Dec. 20, 1929.)

A few months ago Professor Imamura[1] showed that in some of the recent seismic records at Kii District there is a superposition of small vibrations of a very quick type on the main oscillations of the earthquake movement, and from this fact and other geological data he concluded that these small vibrations are chiefly the effect of self-oscillations of the surface layer as excited by the seismic waves from a very deep origin. Such an explanation will, of course, meet with the objections from the theoretical investigators in various ways. The instrumental defects may in some cases be mentioned as the cause of the oscillations and I think that the effects of the other behaviours of waves such as the dispersion and the scattering of the seismic rays will be equally important on the explanation of the present problem. These facts, however, have no much bearings on the possibility of the excitation of the free oscillations of the surface layer. Thus it is most urgent to know in the first place to what extent the free viblations of the layer can be excited in the idealised case, leaving out the question to the causes of the small oscillations of the ground.

In the present paper I have attempted to examine a simplest case in which a dilatational pulse of a purely plane type propagated vertically upwards in an elastic solid medium is partly transmitted through the

1) A. IMAMURA, "On the Earth-vibrations Induced in some Localities at the Arrival of Seismic Waves," *Bull. Earthq. Res. Inst.*, 7 (1929), 489-494.

bottom boundary of the superficial layer and partly reflected at this bottom as well as the surface bodunaries of the same layer.

1. Let the axis of x be drawn vertically upwards from the lower boundary of the layer, and let u be the displacement of the bottom medium and ρ, λ, μ the density and Lamé's elastic constants of this medium. The similar displacement, the density and the elastic constants of the surface layer of the thickness H are to be expressed by u', ρ', λ', μ'.

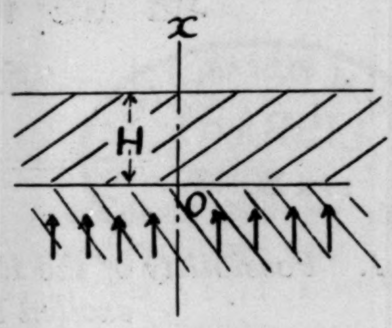

Fig. 1.

The equations of motion of the both medium can be written by

$$\rho\frac{\partial^2 u}{\partial t^2} = (\lambda+2\mu)\frac{\partial^2 u}{\partial x^2}, \quad\cdots\cdots(1)$$

$$\rho'\frac{\partial^2 u'}{\partial t^2} = (\lambda'+2\mu')\frac{\partial^2 u'}{\partial x^2}. \quad\cdots\cdots(2)$$

The solutions of these equations can be easily denoted in the forms:

$$u = e^{ih(V_1 t-x)} + Ae^{ih(V_1 t+x)}, \quad\cdots\cdots(3)$$

$$\Delta = -ih\{e^{ih(V_1 t-x)} - Ae^{ih(V_1 t+x)}\}, \quad\cdots\cdots(4)$$

$$u' = Be^{ih'(V_2 t-x)} + Ce^{ih'(V_2 t+x)}, \quad\cdots\cdots(5)$$

$$\Delta' = -ih'\{Be^{ih'(V_2 t-x)} - Ce^{ih'(V_2 t+x)}\}, \quad\cdots\cdots(6)$$

where A, B, C are arbitrary constants to be determined from the boundary conditions and

$$V_1 = \sqrt{\frac{\lambda+2\mu}{\rho}}, \qquad V_2 = \sqrt{\frac{\lambda'+2\mu'}{\rho'}}, \quad\cdots\cdots(7)$$

$$h = p/V_1, \qquad h' = p/V_2, \quad\cdots\cdots(8)$$

$$-\frac{1}{h^2}\frac{\partial \Delta}{\partial x} = u, \qquad -\frac{1}{h'^2}\frac{\partial \Delta'}{\partial x} = u'. \quad\cdots\cdots(9)$$

At the lower boundary, $x = 0$, we have

$$\left.\begin{aligned} u &= u', \\ \lambda\Delta + 2\mu\frac{\partial u}{\partial x} &= \lambda'\Delta' + 2\mu'\frac{\partial u'}{\partial x}, \end{aligned}\right\} \quad\cdots\cdots(10)$$

and at the upper boundary, $x = H$, we must have

$$\lambda' \Delta' + 2\mu' \frac{\partial u'}{\partial x} = 0. \quad \text{.........(11)}$$

From (10) and (11), we get

$$\left.\begin{aligned} A &= \frac{(1-\alpha)+(1+\alpha)\,e^{-2i\beta hH}}{(1+\alpha)+(1-\alpha)\,e^{-2i\beta hH}}, \\ B &= \frac{2}{(1+\alpha)+(1-\alpha)\,e^{-2i\beta hH}}, \\ C &= \frac{2\,e^{-2i\beta hH}}{(1+\alpha)+(1-\alpha)\,e^{-2i\beta hH}}, \end{aligned}\right\} \quad \text{.........(12)}$$

where

$$\alpha = \sqrt{\frac{\rho'(\lambda'+2\mu')}{\rho(\lambda+2\mu)}}; \quad \beta = \frac{h'}{h} = \sqrt{\frac{\rho'(\lambda+2\mu)}{\rho(\lambda'+2\mu')}}. \quad \text{.........(13)}$$

The displacement u in (3) is composed of two parts, one of them being of the type of the primary waves and the other that of reflected waves. It is therefore convenient to denote u in the form:

$$u = u_1 + u_2, \quad \text{.........(14)}$$

where

$$u_1 = e^{ih(V_1 t - x)}, \quad \text{.........(15)}$$

$$u_2 = A e^{ih(V_1 t + x)}. \quad \text{.........(16)}$$

To generalise the expressions of displacements, we introduce Fourier's double integral such that

$$f(x) = \frac{1}{2\pi}\int_{-\infty}^{\infty} dh \int_{-\infty}^{\infty} f(\sigma)\, e^{ih(x-\sigma)} d\sigma. \quad \text{.........(17)}$$

By applying this theorem, we obtain

$$u_1 = \frac{1}{2\pi}\int_{-\infty}^{\infty} dh \int_{-\infty}^{\infty} f(\sigma)\, e^{ih(V_1 t - x + \sigma)} d\sigma, \quad \text{.........(18)}$$

$$u_2 = \frac{1}{2\pi}\int_{-\infty}^{\infty} \frac{(1-\alpha)+(1+\alpha)\,e^{-2i\beta hH}}{(1+\alpha)+(1-\alpha)\,e^{-2i\beta hH}}\, dh \int_{-\infty}^{\infty} f(\sigma)\, e^{ih(V_1 t + x + \sigma)} d\sigma, \quad \text{.........(19)}$$

$$u' = \frac{1}{2\pi}\int_{-\infty}^{\infty} \frac{2\,dh}{(1+\alpha)+(1-\alpha)\,e^{-2i\beta hH}} \int_{-\infty}^{\infty} f(\sigma)\, e^{i\beta h\left(V_2 t - x + \frac{\sigma}{\beta}\right)} d\sigma$$

$$+ \frac{1}{2\pi}\int_{-\infty}^{\infty} \frac{2\,e^{-2i\beta hH} dh}{(1+\alpha)+(1-\alpha)\,e^{-2i\beta hH}} \int_{-\infty}^{\infty} f(\sigma)\, e^{i\beta h\left(V_2 t + x + \frac{\sigma}{\beta}\right)} d\sigma. \quad \text{......(20)}$$

These are the solutions of displacements at all time and positions for given primary waves of the type

$$t=0\,;\quad u=f(x). \qquad \cdots\cdots(21)$$

Now we know the expressions:

$$\left.\begin{aligned}\frac{1}{(1+\alpha)+(1-\alpha)\,e^{-2i\beta hH}}&=\frac{1}{1+\alpha}\sum_{m=0}^{\infty}(-1)^m\left(\frac{1-\alpha}{1+\alpha}\right)^m e^{-2im\beta hH},\ [\alpha<1]\\ \frac{1}{(1+\alpha)+(1-\alpha)\,e^{-2i\beta hH}}&=\frac{1}{\alpha+1}\sum_{m=0}^{\infty}\left(\frac{\alpha-1}{\alpha+1}\right)^m e^{-2im\beta hH},\qquad [\alpha>1]\end{aligned}\right\}\ (22)$$

so that (19) and (20) reduce to

$$u_2=\frac{1}{2\pi}\sum_{m=0}^{\infty}(-1)^m\left(\frac{1-\alpha}{1+\alpha}\right)^{m+1}\int_{-\infty}^{\infty}e^{-2im\beta hH}\,dh\int_{-\infty}^{\infty}f(\sigma)\,e^{ih(V_1t+x+\sigma)}\,d\sigma$$

$$+\frac{1}{2\pi}\sum_{m=0}^{\infty}(-1)^m\left(\frac{1-\alpha}{1+\alpha}\right)^{m}\int_{-\infty}^{\infty}e^{-2i\overline{m+1}\beta hH}\,dh\int_{-\infty}^{\infty}f(\sigma)\,e^{ih(V_1t+x+\sigma)}\,d\sigma,$$

$$[\alpha<1]\qquad\cdots\cdots(19')$$

$$u'=\frac{1}{\pi}\sum_{m=0}^{\infty}(-1)^m\frac{(1-\alpha)^m}{(1+\alpha)^{m+1}}\int_{-\infty}^{\infty}e^{-2im\beta hH}\,dh\int_{-\infty}^{\infty}f(\sigma)\,e^{i\beta h\left(V_2t-x+\frac{\sigma}{\beta}\right)}\,d\sigma$$

$$+\frac{1}{\pi}\sum_{m=0}^{\infty}(-1)^m\frac{(1-\alpha)^m}{(1+\alpha)^{m+1}}\int_{-\infty}^{\infty}e^{-2i\overline{m+1}\beta hH}\,dh\int_{-\infty}^{\infty}f(\sigma)\,e^{i\beta h\left(V_2t+x+\frac{\sigma}{\beta}\right)}\,d\sigma,$$

$$[\alpha<1]\qquad\cdots\cdots(20')$$

and to similar expressions of some modified forms, when $\alpha>1$.

2. We may now take a simplest case such that

$$t=0,\quad f(x)=e^{-\frac{x^2}{c^2}},\qquad\cdots\cdots(23)$$

then we find in virtue of (18), (19′), (20′),

$$u_1=e^{-\frac{(V_1t-x)^2}{c^2}},$$

$$u_2=\sum_{m=0}^{\infty}(-1)^m\left(\frac{1-\alpha}{1+\alpha}\right)^{m+1}e^{-\frac{(V_1t+x-2m\beta H)^2}{c^2}}$$

$$+\sum_{m=0}^{\infty}(-)^m\left(\frac{1-\alpha}{1+\alpha}\right)^{m}e^{-\frac{(V_1t+x-2\overline{m+1}\beta H)^2}{c^2}},$$

$$u' = 2\sum_{m=0}^{\infty}(-1)^m \frac{(1-\alpha)^m}{(1+\alpha)^{m+1}} e^{-\frac{\beta^2(V_2t-x-2mH)^2}{c^2}}$$

$$+2\sum_{m=0}^{\infty}(-1)^m \frac{(1-\alpha)^m}{(1+\alpha)^{m+1}} e^{-\frac{\beta^2(V_2t+x-2\overline{m+1}H)^2}{c^2}},$$

$$[\alpha<1] \quad \cdots\cdots\cdots(24)$$

and similarly

$$u_1 = e^{-\frac{(V_1t-x)^2}{c^2}},$$

$$u_2 = -\sum_{m=0}^{\infty}\left(\frac{\alpha-1}{\alpha+1}\right)^{m+1} e^{-\frac{(V_1t+x-2m\beta H)^2}{c^2}}$$

$$+\sum_{m=0}^{\infty}\left(\frac{\alpha-1}{\alpha+1}\right)^{m} e^{-\frac{(V_1t+x-2\overline{m+1}\beta H)^2}{c^2}},$$

$$u' = 2\sum_{m=0}^{\infty}\frac{(\alpha-1)^m}{(\alpha+1)^{m+1}} e^{-\frac{\beta^2(V_2t-x-2mH)^2}{c_2}}$$

$$+2\sum_{m=0}^{\infty}\frac{(\alpha-1)^m}{(\alpha+1)^{m+1}} e^{-\frac{\beta^2(V_2t+x-2\overline{m+1}H)^2}{c^2}}.$$

$$[\alpha>1] \quad \cdots\cdots\cdots(25)$$

The fact that the series forms of the expressions of the displacements have entered the present analysis is very reasonable. Each term of the series gives us every component of the succession of the disturbances produced by the multiple reflection and the transmission of the waves at the stratified layer, so that the series forms of the expressions have by no means been taken for the easiness of the procedure of the calculation as ordinarilly believed in other cases.

Let us here consider the viblations of the surface of the body due to the whole disturbance besides those of the most shallow portion of the bottom medium due to the receding waves vertically downwards. Putting $x=0$ in the expressions of u_2 in (24) and (25), and $x=H$ in those of u', we get

$$
\left.\begin{aligned}
u_2 &= \frac{1-\alpha}{1+\alpha}\, e^{-\frac{V_1^2 t^2}{c^2}} - 4\sum_{m=1}^{\infty}(-1)^m \frac{\alpha}{1-\alpha^2}\left(\frac{1-\alpha}{1+\alpha}\right)^m e^{-\frac{(V_1 t-2m\beta H)^2}{c^2}},\\
u' &= 4\sum_{m=0}^{\infty}(-1)^m \frac{(1-\alpha)^m}{(1+\alpha)^{m+1}}\, e^{-\frac{\beta^2(V_2 t-\overline{2m+1}H)^2}{c^2}},
\end{aligned}\right\}
$$

$[\alpha<1]$ ………(26)

$$
\left.\begin{aligned}
u_2 &= -\frac{\alpha-1}{\alpha+1}\, e^{-\frac{V_1^2 t^2}{c^2}} + 4\sum_{m=1}^{\infty} \frac{\alpha}{\alpha^2-1}\left(\frac{\alpha-1}{\alpha+1}\right)^m e^{-\frac{(V_1 t-2m\beta H)^2}{c^2}};\\
u' &= 4\sum_{m=0}^{\infty} \frac{(\alpha-1)^m}{(\alpha+1)^{m+1}}\, e^{-\frac{\beta^2(V_2 t-\overline{2m+1}H)^2}{c^2}},
\end{aligned}\right\}
$$

$[\alpha>1]$ ………(27)

where α and β are given by (13). Some special cases are plotted in the following drawings. In Figs. 2, 3, 4 the cases of $c=H$, $c=5H$, $5c=H$, besides the conditions $\alpha=\frac{1}{2}$, $\beta=1$ in common, are plotted respectively.

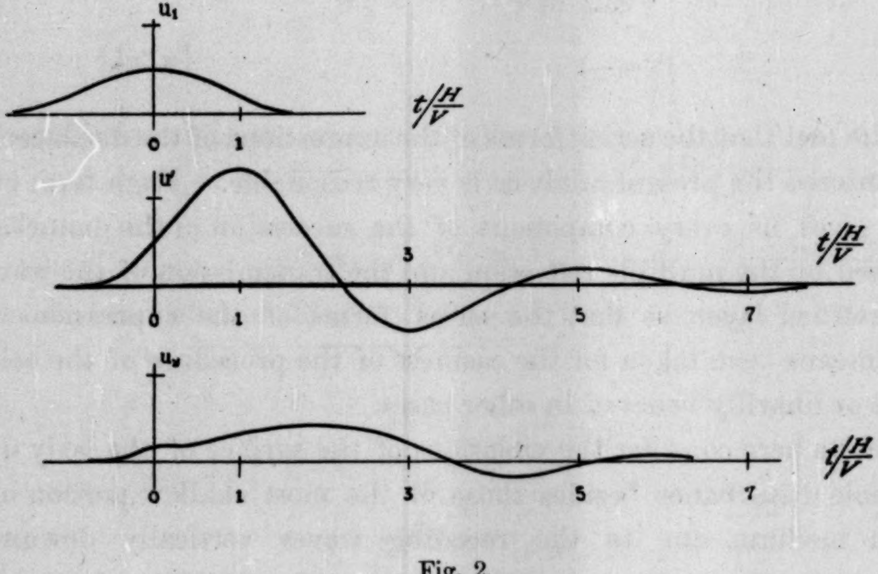

Fig. 2.

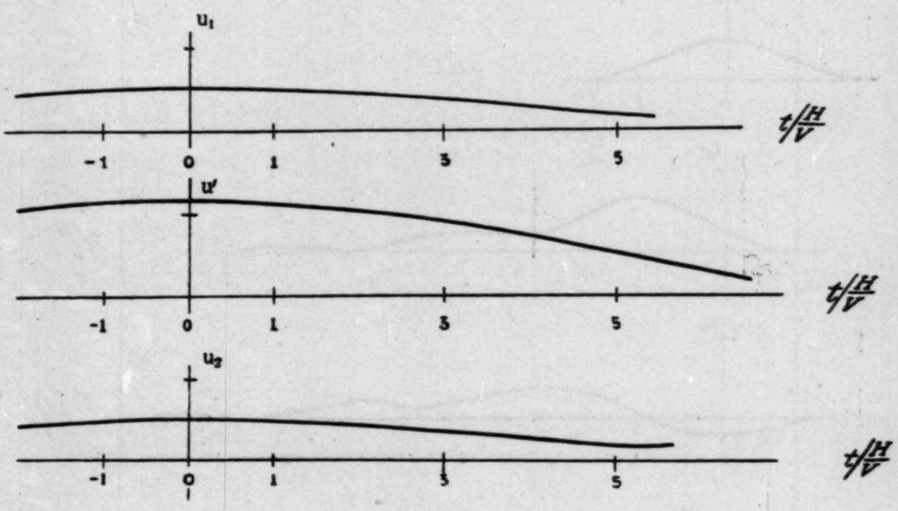

Fig. 3

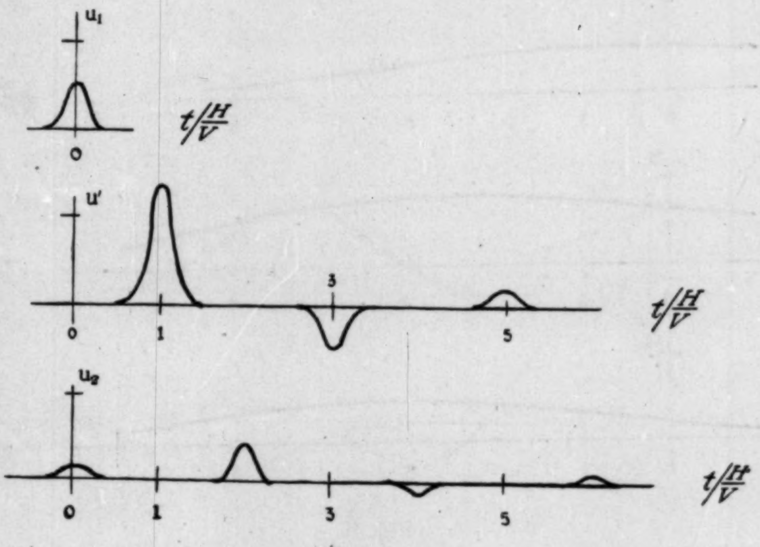

Fig. 4.

Figs. 5, 6, 7 give the similar cases under the conditions $\alpha=2$, $\beta=1$, while Fig. 8 gives us the case $\alpha=1$, $\beta=1$, i.e. the case of the semi-infinite isotropic body.

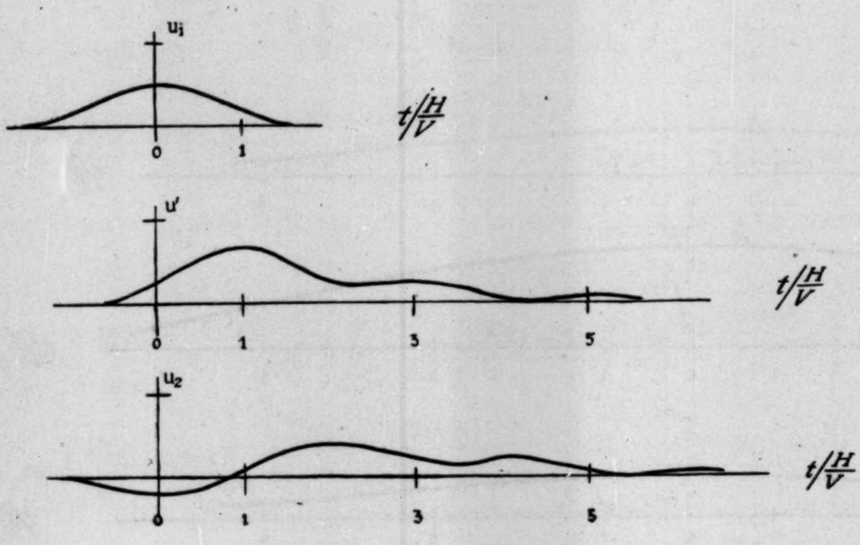

Fig. 5.

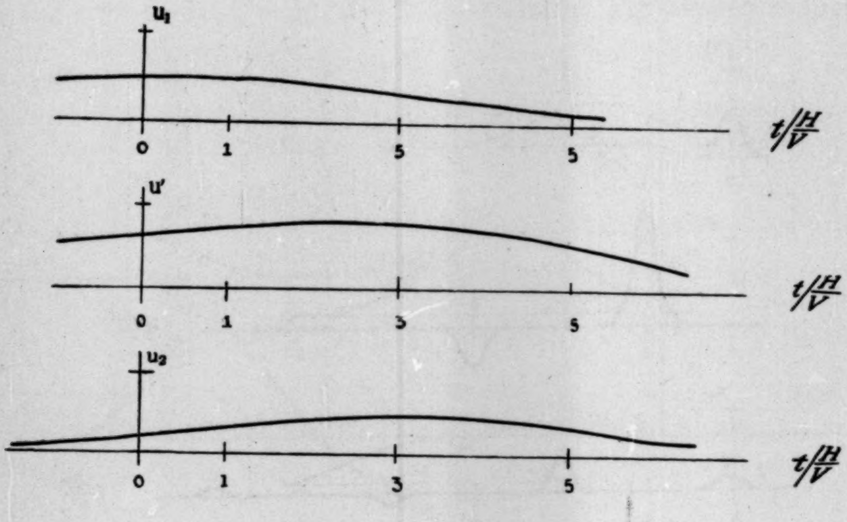

Fig. 6.

3. We may complete the present investigation by a brief notice on the results of the mathematical calculation.

It has been shewn in the preceding diagrams that, when the length of the disturbed portion of the primary shocks is small compared with

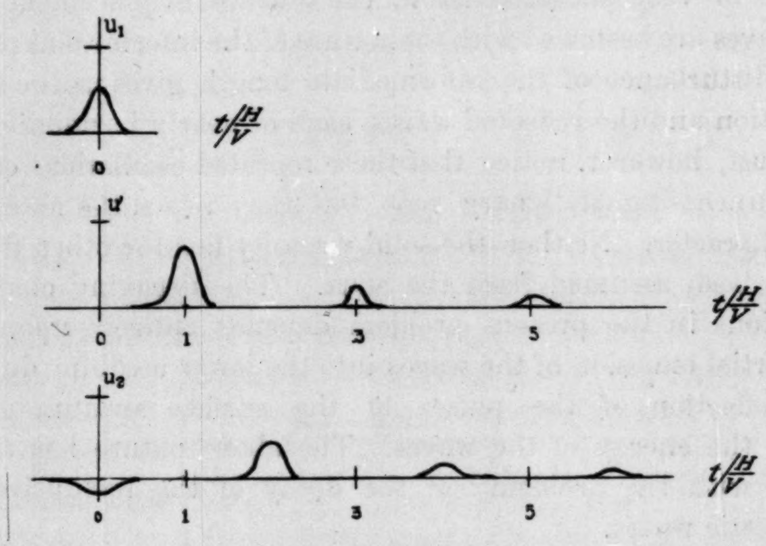

Fig. 7.

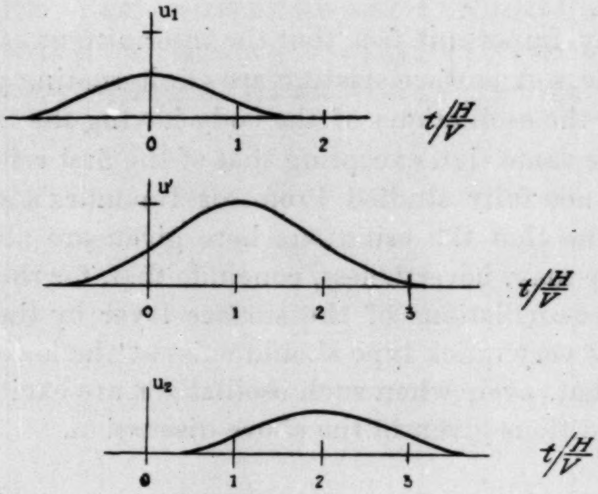

Fig. 8.

the depth of the surface stratum, the surface displacement and downward-receding waves are of periodic pulsatory types, and when the extent of the primary disturbance is large compared with the depth of the layer, no periodic pulsation can be obtained both in the surface movements

and in the reflected waves. Thus, in the extreme case of the primary disturbance of very short duration, the surface displacement and the reflected waves are bestowed with the nature of the intermittent pulsation, while the disturbance of the intermediate length gives us the resulting surface motion and the reflected waves, each of nearly harmonic type.

We must, however, notice that these repeated oscillations can never be of the unceasing stationary type, but they reveal the nature of the decaying character. Neither the solid viscosity nor the other dispersive nature has been assumed from the start. The decaying character of the oscillations in the present problem depends entirely upon the fact that the partial emission of the waves into the lower medium during the multiple reflection of the pulses at the surface stratum gradually diminishes the energy of the waves. The above nature has the direct connection with the problem[2] of the decay of the restitutive origins emitting elastic waves.

When the surface layer is more rigid than the bottom medium, the oscillatory character and the decaying nature of the waves due to the intermediate primary pulsation shew a somewhat different tendency. In this case the harmonic character is not distinct as will be seen in Fig. 5.

It is equally important fact that the intermittent oscillations of the body having the soft surface stratum are of alternatingly different signs of phases, while the oscillations of the body having the rigid layer are of the phases of the same sign excepting that of the first reflected waves.

As I have not fully studied Professor Imamura's seismic records, I cannot examine that the criterions here given are all fulfilled in the actual case. We may, nevertheless, conclude that, for the purpose of the excitation of free-oscillations of the surface layer by the seismic waves, sharp tremors of very quick type should exist at the lower medium from the start and that, even when such oscillations are excited, they should obey all the conditions given in the above discussion.

My many thanks are due to Dr. G. Nishimura who has assisted me in preparing this paper.

2) K. SEZAWA, "Scattering of Elastic Waves and Some Allied Problems," *Bull. Earthq. Res. Inst.*, 3 (1927), 35–39 (§§ 6, 7, 8).

1. 地震波によつて土地の固有振動が誘起される可能度に就いて

地震研究所 妹澤克惟

數ケ月前に今村博士は紀伊地方の或地震では土地の固有振動が誘起され得る事を地震記象の說明によつて提唱された。斯る事柄は土地の固有振動を考へなくても地震波の分散や散逸を以てすれば亦容易に說明する事が出來る。しかしこゝでは土地の固有振動を考へる事が最も適當であると假定して如何なる振動現象が可能的であるかを硏究して見たのである。

問題を簡單にする爲に一つの表面層が下の彈性體の上に置かれ，深層地震の如く平らな前進面を有する任意の第一次波が與へられる場合，地表上の點が如何なる振動をするか又反射波が如何に變形されるかもしらべた。

計算の重要な結果を摘錄すれば，

1. 衝擊波の攪動部分の長さが表面層の厚さに比較して短い時には表面上の變位と地中の反射波とは週期性を保持する事になる。しかし攪動部分の長さが表面層の厚さに比較して大きい時は斯る週期性は決して存在せぬ。
2. 又、衝擊波の攪亂部分の長さが極めて短い時は表面の振動や反射波の誘起は間歇的となる。
3. 週期的の振動が誘起されてもその次々の振動は必ず減衰的傾向を持たねばならぬ。
4. 表面層が下の媒體よりも剛い時は衝擊波が多少短くても週期性はあまり明瞭ではない。
5. 間歇的振動が誘起される樣な場合表面層が下の媒體よりも軟い時には地表面に於ける次々の振動及び地中の次々の波動形は其位相が互に逆となる。しかし表面層の剛い時は各振動は同位相となる。

2. *On the Possibility of the Block Movements of the Earth Crust.*[1]

By **Katsutada SEZAWA** and **Genrokuro NISHIMURA**,

Earthquake Research Institute.

(Read Nov. 19 and Dec. 17, 1929.—Received Dec. 20, 1929.)

1. Several years ago one[2] of the present authors studied the problem of some earthquake motions, in which the energy of the seismic waves is radiated in succession from multiple sources consisting of a series of land blocks. Taking the size of each block to be of a few kilometers in the linear scale and assuming that the volume of the earth crust as large as the faulted region at the occurrence of an earthquake is filled with the above blocks, the energy of the surface waves in a visco-elastic solid generated from these block origins was approximately equal to that estimated from the seismic records at various stations. The actual example was taken to the Great Kwanto Earthquake of 1923 and in that case, besides the total energy, even the order of the number of the oscillations was very like to that, in which the successive blocks radiate in series the respective energy of waves. Of course, the radiated energy was assumed to be equal to the strain energy of the earth crust accumulated in the earth blocks to the critical limit of the break-down of the material of the crust.

Since the time of the above investigation, many geophysicists have studied the problem of the block movement: S. Ono,[3] M. Ishimoto,[4] N. Nasu,[5] Ch. Tsuboi,[6] A. Imamura,[7] K. Muto—K. Atumi[8] are most notable among them. The works of the geological side have been excluded from the present consideration owing to our incomplete

---

1) The principal calculation involved in this paper has been carried out by G. NISHIMURA. (Added K. SEZAWA).

2) K. SEZAWA, *Colloq. Meeting of the Fac. Eng., Tokyo Imp. Univ.* (Sep. 1924).

3) S. ONO, *General Meeting of Math.-Phys. Soc., Japan,* (April 1925).

4) M. ISHIMOTO, *Bull. Earthq. Res. Inst.,* **4** (1928), 203; **6** (1929), 127.

5) N. NASU, *Bull. Earthq. Res. Inst.,* **6** (1929), 245; **7** (1929), 133.

6) Ch. TSUBOI, *Bull. Earthq. Res. Inst.,* **6** (1929), 71; **7** (1929), 103.

7) A. IMAMURA, *Proc. Imp. Acad.,* **5** (1929), 330.

8) K. MUTO-K. ATUMI, *Bull. Earthq. Res; Inst.,* **7** (1929), 503.

knowledge on such a line.[9]

These investigators seem to have explained the structures of the earth crust and the phenomenon of the earthquake principally by means of the hypothesis of the land blocks; and their excessive belief on this hypothesis appears now to be beyond the necessity of explaining the natural phenomenon to such an extent that they frequently violate both the actual facts and the well known principles of theoretical mechanics at the interpretation of the observed results.

By the encouragement of Professor Terada, one of the present authors has exerted his orthodox efforts to obtain the solutions of the stability problem[10] of determining the rough dimensions of the land blocks; but he could not get a full result with which he would satisfy. This fact meant that the nature of the configulation of the blocks at the land crust is not so distinct as to be analysed in any theoretical manner, rather than that his method of attack was incomplete. Thus his interest and persistence on this problem have been lost in the course of time.

The present authors do not think that the idea itself of the block movement is not to be excluded. Such an idea would rather become a good guidance to the discovery of the unknown nature of the geophysical evidence. Very recent investigation of some authors, however, on the earth crust in the manner of block movement gives the conclusion that the land blocks are heaped like a mosaic work and each block can be assumed to be very rigid, without any sensible action of the contact forces among respective blocks. The present authors cannot imagine that such blocks as larger than a few kilometers scale should behave like a toy mosaic in the actual gravitating and in the ordinary elastic medium. Even though the medium may be plastic, such a special nature can never be expected. These can be easily seen from very simple theories of the statics of the deformable body and of the dimensional analysis. Again, the confirmation of the actual results of the observation of the Land Survey Department made on the disturbed districts gives us the fact that any portion of the land surface has scarcely moved in the manner of rigid blocks like a mosaic which may be assumed to be too rigid for its size and weight.

9) Late Prof. N. YAMASAKI is said to have read a paper on block movements almost at the same time as that of one of the present authors. Dr. F. TADA, who is an excellent successor of Professor YAMASAKI, has published a few papers on the similar line of the research.

10) K. SEZAWA, *Colloquium at the Seism. Inst., Tokyo Imp. Univ.* (Feb. 18, 1925.)

According to the theoretical discussion of the present authors, the block movements cannot occur in the form of the assemblage of rigid blocks having no sensible connecting forces. The discontinuity of the displacement, of course, may be permitted to localise at some particular portions of the ground surface owing to the heterogeneity of the elasticity and the pre-exitence of the faulted boundaries. The general deformation, nevertheless, of the earth crust should be curved along its surface. The particular portions may give rise to the movement discontinuous in the field of the crust in combination with the general continuous movement. But such ideal displacements as an uniform overthrust or a tilting of the rigid block can never take place. It may be added that, in consequence of the combined movements of the continuous and discontinuous characters even in the most probable cases, the determination of the actual blocks and the discovery of the actual faults from the observed data would be much complicated.

Apart from the theoretical consideration, it may easily be seen that the original curvature of a tilted block among other blocks cannot be maintained owing to the geometrical configulation of the medium and the condition of the surface which is free from the stresses.

It may be asserted by some authors that in the case of the pure plastic earth crust the bodily movement of a block will be very large and the deformation relating to the curvature of the surface cannot be possible. The recent study on the plastic deformation chiefly involving the effect of the time tells us that the deformation of a plastic body is very similar to the case of the elastic body under the condition that the deformation of a body at any time is made with the state of the body at that instance as the ordinary conditions of stresses. From this fact we find that the displacement peculiar to the deformable body will become more conspicuous than the bodily displacement.

In the following calculations the pure elastic body has been assumed to exist from the start and the behaviour of the block under certain unbalanced forces has been examined. In the first section the case of the action of the uniform vertical force has been studied, and in the second place the case of the action of the varying vertical force has been discussed; while in the remaining sections the problem of the action of the horizontal forces at the vertical walls of the block is involved.

2. We shall take a two-dimensional problem in which the axis of x is directed downwards and the axis of y resides on the free surface of a body. Let us introduce Airy's function χ which satisfies

$$\nabla^4\chi = 0, \quad \cdots\cdots(1)$$

where ∇^4 stands for

$$\frac{\partial^4}{\partial x^4} + 2\frac{\partial^4}{\partial x^2 \partial y^2} + \frac{\partial^4}{\partial y^4}. \quad \cdots\cdots(2)$$

Again, take a complementary function ψ[11] which fulfils the conditions:

$$\frac{\partial^2\psi}{\partial x \partial y} = \nabla^2\chi, \quad \cdots\cdots(3)$$

$$\nabla^2\psi = 0. \quad \cdots\cdots(4)$$

Then the stresses and the displacements in a gravitating body are expressed in the forms:

$$X_x = \frac{\partial^2\chi}{\partial y^2} - \rho g x, \quad \cdots\cdots(5)^{12)}$$

$$Y_y = \frac{\partial^2\chi}{\partial x^2}, \quad \cdots\cdots(6)$$

$$X_y = -\frac{\partial^2\chi}{\partial x \partial y}, \quad \cdots\cdots(7)$$

$$2\mu u = -\frac{\partial\chi}{\partial x} + \frac{\lambda+2\mu}{2(\lambda+\mu)}\frac{\partial\psi}{\partial y} + \frac{\mu\rho g}{\lambda+2\mu}(a^2-x^2), \quad \cdots\cdots(8)$$

$$2\mu v = -\frac{\partial\chi}{\partial y} + \frac{\lambda+2\mu}{2(\lambda+\mu)}\frac{\partial\psi}{\partial x}. \quad \cdots\cdots(9)$$

When the boundary conditions of stresses and displacements are specified, the problem can be uniquely determined.

3. Let us first suppose that a gravitating rectangular block of the elastic material is wedged between other blocks and that the bottom of this block is pressed or tracted by some unbalanced forces besides the isostatic force. Then, at the contacting surfaces of the vertical walls of the block the frictional resistance of the contacting solid body will neccessarily be induced

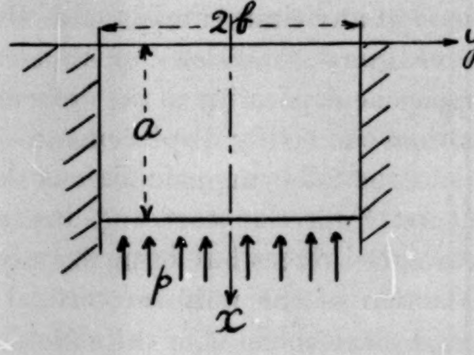

Fig. 1.

11) R. C. J. HOWLAND, *Proc. Roy. Soc., London,* 125 (1929), and other books on the theory of elasticity.

12) N. YAMAGUTI, *Jour. of Civil Eng. Soc., Tokyo,* 15 (1929), 291–304; Love, *Mathematical Theory of Elasticity, 4th ed.* (1927), 212.

owing to the lateral pressure of the gravitating mass of the block. This lateral pressure must be expected in the plastico-elastic medium, excepting the special case such as a sharp cliff.

Now we write the general solutions of the equations (1), (2), (3), (4) in the following forms:

$$\chi = \sum_m \left\{B_m y \operatorname{sh} my + C_m \operatorname{ch} my\right\} \cos mx + \sum_{m'} \left\{A'_{m'} x \operatorname{ch} m'x + B'_{m'} x \operatorname{sh} m'x + C'_{m'} \operatorname{ch} m'x + D'_{m'} \operatorname{sh} m'x\right\} \cos m'y, \qquad \text{.........(10)}$$

$$\psi = \sum_m \frac{2}{m} B_m \operatorname{sh} my \cos mx + \sum_{m'} \frac{2}{m'} \left\{A'_{m'} \operatorname{ch} m'x + B'_{m'} \operatorname{sh} m'x\right\} \sin m'y. \qquad \text{.........(11)}$$

Then the components of displacement and the stresses can be written by means of (5), (6), (7), (8), (9) in the forms:

$$2\mu u = \sum_m \left\{B_m \left(my \operatorname{sh} my + \frac{\lambda+2\mu}{\lambda+\mu} \operatorname{ch} my\right) + C_m m \operatorname{ch} my\right\} \sin mx - \sum_{m'} \left\{A'_{m'} \left(m'x \operatorname{sh} m'x - \frac{\mu}{\lambda+\mu} \operatorname{ch} m'x\right) + B'_{m'} \left(m'x \operatorname{ch} m'x - \frac{\mu}{\lambda+\mu} \operatorname{sh} m'x\right) + C'_{m'} m' \operatorname{sh} m'x + D'_{m'} m' \operatorname{ch} m'x\right\} \cos m'y + \frac{\mu\rho g}{\lambda+2\mu}(a^2-x^2), \qquad \text{.........(12)}$$

$$2\mu v = \sum_m \left\{B_m \left(\frac{\mu}{\lambda+\mu} \operatorname{sh} my - my \operatorname{ch} my\right) - C_m \operatorname{sh} my\right\} \cos mx + \sum_{m'} \left\{A'_{m'} \left(m'x \operatorname{ch} m'x + \frac{\lambda+2\mu}{\lambda+\mu} \operatorname{sh} m'x\right) + B'_{m'} \left(m'x \operatorname{sh} m'x + \frac{\lambda+2\mu}{\lambda+\mu} \operatorname{ch} m'x\right) + C'_{m'} m' \operatorname{ch} m'x + D'_{m'} \operatorname{sh} m'x\right\} \sin m'y, \qquad \text{.........(13)}$$

$$X_x = \sum_m m\left\{B_m(my \operatorname{sh} my + 2 \operatorname{ch} my) + C_m m \operatorname{ch} my\right\} \cos mx$$
$$- \sum_{m'} m'^2 \left\{A'_{m'} x \operatorname{ch} m'x + B'_{m'} x \operatorname{sh} m'x\right.$$
$$\left. + C'_{m'} \operatorname{ch} m'x + D'_{m'} \operatorname{sh} m'x\right\} \cos m'y - \rho g x, \qquad \cdots\cdots\cdots(14)$$

$$Y_y = - \sum_m m^2 \left\{B_m y \operatorname{sh} my + C_m \operatorname{ch} my\right\} \cos mx$$
$$+ \sum_{m'} m' \left\{A'_{m'} (m'x \operatorname{ch} m'x + 2 \operatorname{sh} m'x) + B'_{m'} (m'x \operatorname{sh} m'x + 2 \operatorname{ch} m'x)\right.$$
$$\left. + C'_{m'} m' \operatorname{ch} m'x + D'_{m'} m' \operatorname{sh} m'x\right\} \cos m'y, \qquad \cdots\cdots\cdots(15)$$

$$X_y = \sum_m m\left\{B_m (my \operatorname{ch} my + \operatorname{sh} my) + C_m m \operatorname{sh} my\right\} \sin mx$$
$$+ \sum_{m'} m' \left\{A'_{m'}(m'x \operatorname{sh} m'x + \operatorname{ch} m'x) + B'_{m'}(m'x \operatorname{ch} m'x + \operatorname{sh} m'x)\right.$$
$$\left. + C'_{m'} m' \operatorname{sh} m'x + D'_{m'} m' \operatorname{ch} m'x\right\} \sin m'y. \qquad \cdots\cdots\cdots(16)$$

Now we have the boundary conditions such that

$$y = \pm b, \begin{cases} u = \dfrac{\rho g}{2(\lambda+2\mu)}(a^2 - x^2), & \cdots\cdots\cdots(17) \\ v = 0, & \cdots\cdots\cdots(18) \\ X_y = \pm f \dfrac{\lambda}{\lambda+2\mu} \rho g x. & \cdots\cdots\cdots(19) \end{cases}$$

$$x = 0, \quad X_x = X_y = 0, \qquad \cdots\cdots\cdots(20), (21)$$

$$x = a, \quad X_x = -f \frac{\lambda}{\lambda+2\mu} \frac{\rho g a^2}{2b} \quad [= -\Delta p]$$

except the isostatic pressure, $\cdots\cdots\cdots$(22)

in which Δp is the isostatically unbalanced pressure and the neighbouring blocks are supposed to be very rigid, except the deformation due to its own gravitating force. The case of the ordinary deformable neighbouring blocks can easily be calculated in the manner of the addition of the correctional

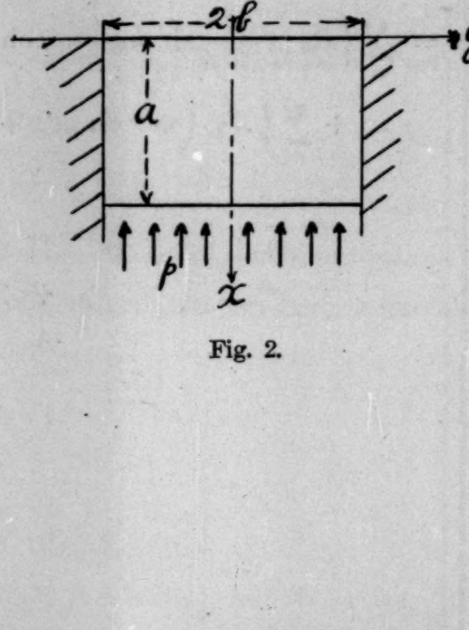

Fig. 2.

terms. In the equations (19) and (22), f is the coefficient of the friction due to the contact of the solid bodies corresponding the prescribed state. When f is smaller than a critical value, say ½, the relative movement at the contact surface cannot take place.

From (17), we find

$$m' = \frac{(2n'+1)\pi}{2b}, \quad [n' = 0, 1, 2, \cdots] \cdots\cdots\cdots(23)$$

$$B_m\left(mb \text{ sh } mb + \frac{\lambda+2\mu}{\lambda+\mu} \text{ ch } mb\right) + C_m m \text{ ch } mb = 0. \cdots\cdots\cdots(24)$$

From (18), we get

$$\sum_m \left\{B_m\left(\frac{\mu}{\lambda+\mu} \text{ sh } mb - mb \text{ ch } mb\right) - C_m m \text{ sh } mb\right\} \cos mx$$
$$+ \sum_{n'} (-1)^{n'} \left\{A'_{m'}\left(m'x \text{ ch } m'x + \frac{\lambda+2\mu}{\lambda+\mu} \text{ sh } m'x\right)\right.$$
$$+ B'_{m'}\left(m'x \text{ sh } m'x + \frac{\lambda+2\mu}{\lambda+\mu} \text{ ch } m'x\right)$$
$$\left. + C'_{m'} m' \text{ ch } m'x + D'_{m'} m' \text{ sh } m'x\right\} = 0. \cdots\cdots\cdots(25)$$

From (19),

$$\sum_m m\left\{B_m (mb \text{ ch } mb + \text{sh } mb) + C_m m \text{ sh } mb\right\} \sin mx$$
$$+ \sum_{n'} (-1)^{n'} m' \left\{A'_{m'} (m'x \text{ sh } m'x + \text{ch } m'x)\right.$$
$$+ B'_{m'} (m'x \text{ ch } m'x + \text{sh } m'x) + C'_{m'} \text{ sh } m'x$$
$$\left. + D'_{m'} m' \text{ ch } m'x\right\} = f \frac{\lambda}{\lambda+2\mu} \rho g x. \cdots\cdots\cdots(26)$$

From (20),

$$\sum_m m\left\{B_m (my \text{ sh } my + 2 \text{ ch } my) + C_m m \text{ ch } my\right\}$$
$$- \sum_{m'} m'^2 C'_{m'} \cos m'y = 0. \cdots\cdots\cdots(27)$$

From (21),

$$A'_{m'} + m' D'_{m'} = 0. \cdots\cdots\cdots\cdots\cdots\cdots\cdots\cdots\cdots\cdots(28)$$

From (22),

$$m = \frac{(2n+1)\pi}{2a}, \quad [n = 0, 1, 2, \cdots] \cdots\cdots\cdots\cdots\cdots\cdots(29)$$

and

$$\sum_{m'} m'^2 \Big\{ A'_{m'}\, a \operatorname{ch} m'a + B'_{m'}\, a \operatorname{sh} m'a + C'_{m'} \operatorname{ch} m'a + D'_{m'} \operatorname{sh} m'a \Big\} \cos m'y = f \frac{\lambda}{\lambda+2\mu} \frac{\rho g a^2}{2b}. \quad \cdots\cdots\cdots(30)$$

By applying the method of Fourier's analysis on (25), (26), (27), (30) and making use of (23), (24), (28), (29) we obtain the relations:

$$\frac{\operatorname{sh} mb \operatorname{ch} mb - mb}{\operatorname{ch} mb} B_m + (-1)^{n'} \frac{2}{a} \times \Big\{ B'_{m'} \frac{(-1)^n m'}{m^2+m'^2} \Big(ma \operatorname{sh} m'a + \frac{m(m^2-m'^2)}{m'(m^2+m'^2)} \operatorname{ch} m'a \Big) + C'_{m'} \frac{(-1)^n mm'}{m^2+m'^2} \operatorname{ch} m'a - D'_{m'} \frac{m'^2}{m^2+m'^2} \Big((-1)^n ma \operatorname{ch} m'a - (-1)^n \frac{2mm'}{m^2+m'^2} \operatorname{sh} m'a - \frac{m^2-m'^2}{m^2+m'^2} \Big) \Big\} = 0, \quad \cdots\cdots\cdots(31)$$

$$\frac{m^2 b}{\operatorname{ch} mb} B_m + (-1)^{n'} \frac{2m'}{a} \times \Big\{ B'_{m'} \frac{(-1)^n m'}{m^2+m'^2} \Big(m'a \operatorname{sh} m'a + \frac{2m^2}{m^2+m'^2} \operatorname{ch} m'a \Big) + C'_{m'} \frac{(-1)^n m'^2}{m^2+m'^2} \operatorname{ch} m'a - D'_{m'} \frac{m'^2}{m^2+m'^2} \Big((-1)^n m'a \operatorname{ch} m'a - (-1)^n \frac{m^2-m'^2}{m^2+m'^2} \operatorname{sh} m'a - \frac{2mm'}{m^2+m'^2} \Big) \Big\} = f\rho g \frac{2}{a} \frac{(-1)^n}{m^2}, \quad \cdots\cdots\cdots(32)$$

$$(-1)^{n'} \frac{2m}{b} \frac{m^2-m'^2}{(m^2+m'^2)^2} \operatorname{ch} mb\, B_m + m' C'_{m'} = 0, \quad \cdots\cdots\cdots(33)$$

$$a \operatorname{sh} m'a\, B'_{m'} + \operatorname{ch} m'a\, C'_{m'} + (\operatorname{sh} m'a - m'a \operatorname{ch} m'a) D'_{m'} = f \frac{\rho g a^2}{b^2} \frac{(-1)^{n'}}{m'^3}; \quad \cdots\cdots\cdots(34)$$

where $m = \frac{(2n+1)\pi}{2a}$ and $m' = \frac{(2n'+1)\pi}{2b}$.

From (31), (32), (33), (34), we can construct the following determinants:

$$\vartheta = \begin{vmatrix} \dfrac{\operatorname{sh} mb \operatorname{ch} mb - mb}{\operatorname{ch} mb}, & (-1)^{n+n'} \dfrac{2}{a} \dfrac{m(m^2-m'^2)}{(m^2+m'^2)^2} \operatorname{ch} m'a, & 0, & (-1)^{n'} \dfrac{2}{a} \dfrac{m'(m^2-m'^2)}{a(m^2+m'^2)^2} \left(m' - (-1)^n m \operatorname{sh} m'a \right) \\ \dfrac{mb}{\operatorname{ch} mb}, & (-1)^{n+n'} \dfrac{4}{a} \dfrac{mm'^2}{(m^2+m'^2)^2} \operatorname{ch} m'a, & 0, & (-1)^{n'} \dfrac{4}{a} \dfrac{m'^3}{(m^2+m'^2)^2} \left(m' - (-1)^n m \operatorname{sh} m'a \right) \\ (-1)^{n'} \dfrac{2m}{b} \dfrac{m^2-m'^2}{(m^2+m'^2)^2} \operatorname{ch} mb, & 0, & m', & 0 \\ 0, & a \operatorname{sh} m'a, & \operatorname{ch} m'a, & \operatorname{sh} m'a - m'a \operatorname{ch} m'a \end{vmatrix}, \quad \cdots\cdots\cdots(35)$$

and

$$\vartheta' = \begin{vmatrix} \dfrac{\operatorname{sh} mb \operatorname{ch} mb - mb}{\operatorname{ch} mb}, & (-1)^{n+n'} \dfrac{2}{a} \dfrac{m'}{m^2+m'^2} \left(ma \operatorname{sh} m'a + \dfrac{m(m^2-m'^2)}{m'(m^2+m'^2)} \operatorname{ch} m'a \right) & (-1)^{n+n'} \dfrac{2}{a} \dfrac{mm'}{m^2+m'^2} \operatorname{ch} m'a, & 0 \\ \dfrac{m^2 b}{\operatorname{ch} mb}, & (-1)^{n+n'} \dfrac{2}{a} \dfrac{m'^2}{m^2+m'^2} \left(m'a \operatorname{sh} m'a + \dfrac{2m^2}{m^2+m'^2} \operatorname{ch} m'a \right), & (-1)^{n+n'} \dfrac{2}{a} \dfrac{m'^3}{m^2+m'^2} \operatorname{ch} m'a, & \dfrac{2}{a} \dfrac{(-1)^n}{m^2} \\ (-1)^{n'} \dfrac{2m}{b} \dfrac{m^2-m'^2}{(m^2+m'^2)^2} \operatorname{ch} mb, & 0, & m', & 0 \\ 0, & a \operatorname{sh} m'a, & \operatorname{ch} m'a, & \dfrac{a^2}{b^2} \dfrac{(-1)^{n'}}{m'^3} \end{vmatrix}. \quad \cdots\cdots\cdots(36)$$

Then the vertical displacement on the surface $x = 0$, can be easily expressed, when $\lambda = \infty$, in the form:

$$u = -\frac{f\rho g}{2\mu} \sum_m \sum_{m'} \frac{m'}{m} \frac{\vartheta'}{\vartheta} \cos m'y. \quad \cdots\cdots\cdots\cdots\cdots\cdots\cdots(37)$$

The computed result of this equation is illustrated in Fig. 3. The displacement thus obtained is the vertical movement of the surface due to the unbalanced bottom pressure Δp, where

$$\Delta p = f\,\frac{\rho g a^2}{2b} \qquad \text{(38)}$$

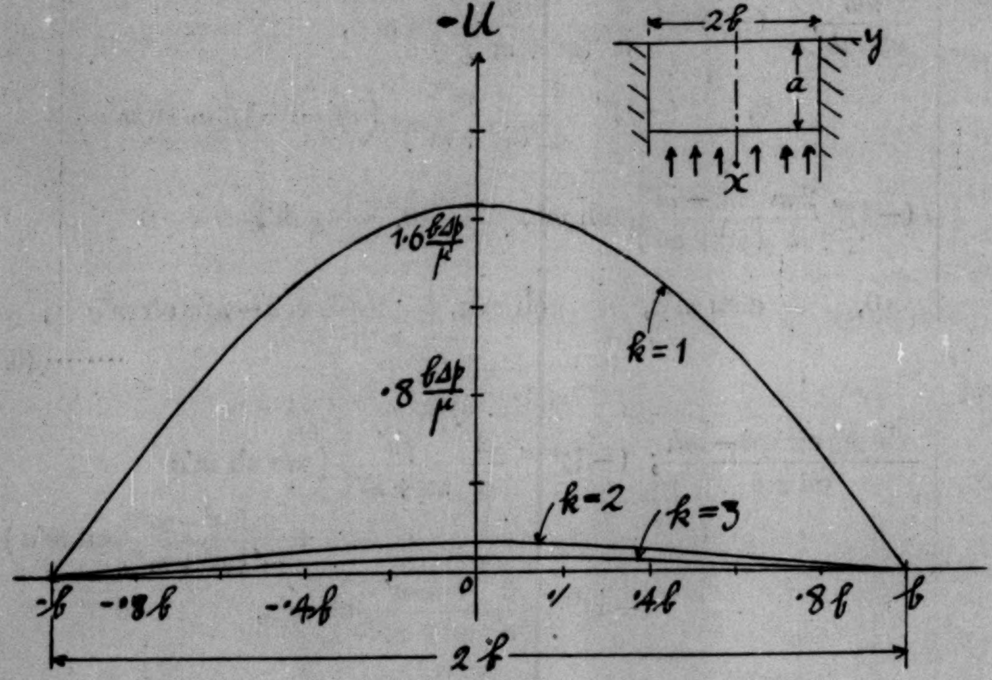

Fig. 3.

Some examples which are most probable in the actual case are tabulated below:

$k\ \left(=\frac{a}{b}\right)$	$2b$	Δp	f	max. $u_{x=0}$
½	10km.	15atm.	·0992	750cm.
1	»	»	·0247	42cm.
2	»	»	·0062	3·5cm.
3	»	»	·0027	1·75cm.

As the limit of f which gives the relative displacement at the contact surfaces $y = \pm b$ should take such a great value as $\frac{1}{4} \sim \frac{1}{2}$ in the ordinary rocks, the above results tell us the fact that even in the case

of very thin blocks the relative displacement at the surface of contact can hardly take place. The pressure change of 15 atmosphere is not small. Even in the case of the high mountain, the pressure change at the base of the isostatic support cannot be so large, because the unbalanced pressure at the surface in the neighbourhood of the mountain is diffused in the interior of the earth crust in a vast horizontal area of the crust. Some question on the nature of the solid friction at the surface of contact may be raised. Though the coefficient of rolling friction of a solid body is very small, we cannot imagine that the friction of the present case has the nature of such a rolling quality. We think that the friction at the cracks of the earth crust will be not only of the sliding type but also of normally pressing type, so that the nature of the friction will be of an eddying quality (so to call), in which the coefficient of friction is perhaps greater than that of the ordinary solid friction. Thus the sliding fault which we observe at the ground may reside in the very vicinity of the surface. This can be clearly known from the fact that the solid friction at the shallow depth, where the hydrostatic pressure of the ground is very small, cannot give its full effect on the resistance of the sliding.

It is also seen from the diagram that the surface displacement cannot take place in a straight line form. The distribution of the displacements is curved along its surface in general. Even though the sliding takes place locally at very shallow portion of the ground, the general displacement is not of a mosaic type, but of the flexure type. It may also be added that, in the present case of the pressure distribution, even the local sliding cannot be expected. Because the region of the action of the unbalanced force is very far from the surface of the body.

4. Let us next consider a similar block which is subjected to the bottom pressure varying along the edge of this bottom.

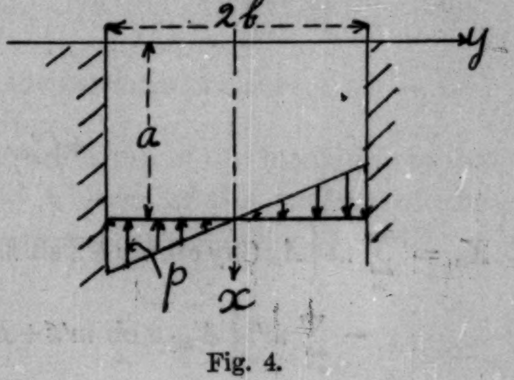

Fig. 4.

The general solutions of the equations (1), (2), (3), (4) are given in the following forms:

$$\chi = \sum_m \left\{ A_m y \operatorname{ch} my + D_m \operatorname{sh} my \right\} \cos mx$$
$$+ \sum_{m'} \left\{ A'_{m'} x \operatorname{ch} m'x + B'_{m'} x \operatorname{sh} m'x + C'_{m'} \operatorname{ch} m'x + D'_{m'} \operatorname{sh} m'x \right\} \sin m'y, \quad \text{.........(39)}$$

$$\psi = \sum_m \frac{2}{m} A_m \operatorname{ch} my \sin mx - \sum_{m'} \frac{2}{m'} \left\{ A'_{m'} m' \operatorname{ch} x + B'_{m'} \operatorname{sh} m'x \right\} \cos m'y. \quad \text{.........(40)}$$

The components of displacement and the stresses can be written in the forms:

$$2\mu u = \sum_m \left\{ A_m \left(my \operatorname{ch} my + \frac{\lambda+2\mu}{\lambda+\mu} \operatorname{ch} my \right) + D_m m \operatorname{sh} my \right\} \sin mx$$
$$+ \sum_{m'} \left\{ A'_{m'} \left(-m'x \operatorname{sh} m'x + \frac{\mu}{\lambda+\mu} \operatorname{ch} m'x \right) + B'_{m'} \left(-m'x \operatorname{ch} m'x + \frac{\mu}{\lambda+\mu} \operatorname{sh} m'x \right) - C'_{m'} m' \operatorname{sh} m'x - D'_{m'} m' \operatorname{ch} m'x \right\} \sin m'y + \frac{\mu \rho g}{\lambda+2\mu} (a^2 - x^2), \quad \text{.........(41)}$$

$$2\mu v = \sum_m \left\{ A_m \left(-my \operatorname{sh} my + \frac{\mu}{\lambda+\mu} \operatorname{ch} my \right) - D_m m \operatorname{ch} my \right\} \cos mx$$
$$- \sum_{m'} \left\{ A'_{m'} \left(m'x \operatorname{ch} m'x + \frac{\lambda+2\mu}{\lambda+\mu} \operatorname{sh} m'x \right) + B'_{m'} \left(m'x \operatorname{sh} m'x + \frac{\lambda+2\mu}{\lambda+\mu} \operatorname{ch} m'x \right) + C'_{m'} m' \operatorname{ch} m'x + D'_{m'} m' \operatorname{sh} m'x \right\} \cos m'y, \quad \text{.........(42)}$$

$$X_x = \sum_m m \left\{ A_m (my \operatorname{ch} my + 2 \operatorname{sh} my) + D_m m \operatorname{sh} my \right\} \cos mx$$
$$- \sum_{m'} m'^2 \left\{ A'_{m'} x \operatorname{ch} m'x + B'_{m'} x \operatorname{sh} m'x + C'_{m'} \operatorname{ch} m'x + D'_{m'} \operatorname{sh} m'x \right\} \sin m'y - \rho g x, \quad \text{.........(43)}$$

$$Y_y = -\sum_m m^2\left\{A_m\, y \operatorname{ch} my + D_m \operatorname{sh} my\right\} \cos mx$$

$$+\sum_{m'} m'\left\{A'_{m'}(m'x \operatorname{ch} m'x + 2 \operatorname{sh} m'x) + B'_{m'}(m'x \operatorname{sh} m'x + 2 \operatorname{ch} m'x)\right.$$

$$\left. + C'_{m'}\, m' \operatorname{ch} m'x + D'_{m'}\, m' \operatorname{sh} m'x\right\} \sin m'y, \qquad \cdots\cdots\cdots(44)$$

$$X_y = -\sum_m m\left\{A_m\,(my \operatorname{sh} my + \operatorname{ch} my) + D_m\, m \operatorname{ch} my\right\} \sin mx$$

$$+\sum_{m'} m'\left\{A'_{m'}(m'x \operatorname{sh} m'x + \operatorname{ch} m'x) + B'_{m'}(m'x \operatorname{ch} m'x + \operatorname{sh} m'x)\right.$$

$$\left. + C'_{m'}\, m' \operatorname{sh} m'x + D'_{m'}\, m' \operatorname{ch} m'x\right\} \cos m'y. \qquad \cdots\cdots\cdots(45)$$

Now we have boundary conditions:

$$y = \pm b, \quad \begin{cases} u = \dfrac{\rho g}{2(\lambda+2\mu)}(a^2 - x^2), & \cdots\cdots\cdots(46) \\ v = 0, & \cdots\cdots\cdots(47) \\ X_y = f\dfrac{\lambda}{\lambda+2\mu}\rho g x, & \cdots\cdots\cdots(48) \end{cases}$$

$$x = 0, \quad \begin{cases} v = 0, & \cdots\cdots\cdots(49) \\ X_y = 0, & \cdots\cdots\cdots(50) \end{cases}$$

$$x = a, \quad X_x = -\Delta p = -f\frac{\lambda}{\lambda+2\mu}\,\frac{3\rho g a^2}{2b^2}\,y$$

except the isostatic pressure. $\cdots\cdots\cdots(51)$

In the equation (51), the moment equilibrium of the block due to the bottom varying pressure and the solid friction of the surface of the contact caused by the hydrostatic pressure are considered.

From (46),

$$m' = \frac{n'\pi}{b}, \qquad [n' = 1, 2, 3, \cdots] \cdots\cdots\cdots(52)$$

$$A_m\left(my \operatorname{ch} my + \frac{\lambda+2\mu}{\lambda+\mu} \operatorname{sh} my\right) + D_m\, m \operatorname{sh} my = 0. \qquad \cdots\cdots\cdots(53)$$

From (47),

$$\sum_m \left\{A_m\left(-mb \operatorname{sh} mb+\frac{\mu}{\lambda+\mu} \operatorname{ch} mb\right)-D_m m \operatorname{ch} mb\right\}\cos mx$$
$$-\sum_{m'}(-1)^{n'}\left\{A'_{m'}\left(m'x \operatorname{ch} m'x+\frac{\lambda+2\mu}{\lambda+\mu} \operatorname{sh} m'x\right)\right.$$
$$+B'_{m'}\left(m'x \operatorname{sh} m'x+\frac{\lambda+2\mu}{\lambda+\mu} \operatorname{ch} m'x\right)$$
$$\left.+C'_{m'} m' \operatorname{ch} m'x+D'_{m'} m' \operatorname{sh} m'x\right\}=0. \quad \cdots\cdots(54)$$

From (48),

$$-\sum_m m\left\{A_m(mb \operatorname{sh} mb+\operatorname{ch} mb)+D_m m \operatorname{ch} mb\right\} \sin mx$$
$$+\sum_{m'}(-1)^{n'} m'\left\{A'_{m'}(m'x \operatorname{sh} m'x+\operatorname{ch} m'x)\right.$$
$$+B'_{m'}(m'x \operatorname{ch} m'x+\operatorname{sh} m'x)+C'_{m'} m' \operatorname{sh} m'x$$
$$\left.+D'_{m'} \operatorname{ch} m'x\right\}=f\frac{\lambda}{\lambda+2\mu}\rho g x. \quad \cdots\cdots\cdots\cdots(55)$$

From (49) and (50),

$$\sum_m m\left\{A_m(my \operatorname{ch} my+2 \operatorname{sh} my)+D_m m \operatorname{sh} my\right\}$$
$$-\sum_{m'} m'^2 C'_{m'} \sin m'y=0, \quad \cdots\cdots\cdots(56)$$
$$A'_{m'}+m' D'_{m'}=0. \quad \cdots\cdots\cdots\cdots\cdots\cdots\cdots\cdots\cdots\cdots\cdots(57)$$

From (51),

$$m=\frac{(2n+1)\pi}{2a}, \qquad [n=0,1,2,\cdots] \quad \cdots\cdots\cdots(58)$$

$$-\sum_{m'} m'^2\left\{A'_{m'} a \operatorname{ch} m'a+B'_{m'} a \operatorname{sh} m'a+C'_{m'} \operatorname{ch} m'a\right.$$
$$\left.+D'_{m'} \operatorname{sh} m'a\right\} \sin m'y=f\frac{\lambda}{\lambda+2\mu}\frac{3\rho g a^2}{2b^2} y. \quad \cdots\cdots\cdots(59)$$

By applying the Fourier's analysis on (54), (54), (56), (59), making use of (52), (53), (57), (58) in the same manner as in the preceding section and simplifying the result, we get

$$(-1)^n\frac{m}{m^2+m'^2}\left\{m'a \operatorname{sh} m'a+\frac{(m^2-m'^2)}{(m^2+m'^2)} \operatorname{ch} m'a\right\} B'_{m'}$$
$$+\left\{(-1)^n\frac{mm'}{m^2+m'^2} \operatorname{ch} m'a-\frac{abm'(m^2+m'^2)^2(mb+\operatorname{sh} mb \operatorname{ch} mb)}{8m^3 \operatorname{sh}^2 mb}\right\} C'_{m'}$$
$$+\frac{m'^2}{m^2+m'^2}\left\{(-1)^n\frac{2mm'}{m^2+m'^2} \operatorname{sh} m'a-(-1)^n ma \operatorname{ch} m'a+\frac{m^2-m'^2}{m^2+m'^2}\right\} D'_{m'}=0,$$
$$\cdots\cdots\cdots\cdots\cdots\cdots\cdots\cdots(60)$$

$$(-1)^n \frac{m'}{m^2+m'^2}\left\{m'a \text{ sh } m'a+\frac{2m^2}{m^2+m'^2} \text{ ch } m'a\right\} B'_{m'}$$

$$+\left\{(-1)^n \frac{m'^2}{m^2+m'^2} \text{ ch } m'a+\frac{ab^2(m^2+m'^2)^2}{8m \text{ sh}^2 mb}\right\} C'_{m'}$$

$$+\frac{m^2}{m^2+m'^2}\left\{\frac{2mm'}{m^2+m'^2}-(-1)^n m'a \text{ ch } m'a\right.$$

$$\left.-(-1)^n \frac{m^2-m'^2}{m^2+m'^2} \text{ sh } m'a\right\} D'_{m'}=(-1)^{n+n'}\frac{f\rho g}{m^2m'},$$

$$\cdots\cdots\cdots(61)$$

$$a \text{ sh } m'a\, B'_{m'}+\text{ch } m'a\, C'_{m'}+(\text{sh } m'a-m'a \text{ ch } m'a)\, D'_{m'}$$

$$=(-1)^{n'}\frac{3f\rho g a^2}{b^2m'^3}. \quad \cdots\cdots\cdots(62)$$

From (60), (61), (62), we can construct two determinants:

$$\vartheta=\begin{vmatrix} (-1)^n \dfrac{m(m^2-m'^2)}{(m^2+m'^2)^2} \text{ ch } m'a, & -\dfrac{abm'(m^2+m'^2)^2(mb+\text{sh } mb \text{ ch } mb)}{8m^3 \text{ sh}^2 mb}, & \\ & \dfrac{m'^2}{(m^2+m'^2)^2}\left\{(-1)^{n'} mm' \text{ sh } m'a+m^2-m'^2\right\} & \\ (-1)^n \dfrac{2m^2m'}{(m^2+m'^2)^2} \text{ ch } m'a, & \dfrac{ab^2(m^2+m'^2)^2}{8m \text{ sh}^2 mb}, & 0 \\ a \text{ sh } m'a, & \text{ch } m'a, & \text{sh } m'a-m'a \text{ ch } m'a \end{vmatrix},$$

$$\cdots\cdots\cdots\cdots\cdots\cdots\cdots\cdots\cdots(63)$$

and

$$\vartheta'=\begin{vmatrix} (-1)^n \dfrac{m'}{m^2+m'^2}\left\{m'a \text{ sh } m'a+\dfrac{m^2-m'^2}{m^2+m'^2} \text{ ch } m'a\right\}, & & \\ \left\{(-1)^n \dfrac{mm'}{m^2+m'^2} \text{ ch } m'a-\dfrac{abm'(m^2+m'^2)^2}{8m^3}\dfrac{(mb+\text{sh } mb \text{ ch } mb)}{\text{sh}^2 mb}\right\}, & & 0 \\ (-1)^n \dfrac{m'}{m^2+m'^2}\left\{m'a \text{ sh } m'a+\dfrac{2m^2}{m^2+m'^2} \text{ ch } m'a\right\}, & & \\ \left\{(-1)^n \dfrac{m'^2}{m^2+m'^2} \text{ ch } m'a+\dfrac{ab^2(m^2+m'^2)^2}{8m \text{ sh}^2 mb}\right\}, & & (-1)^{n+n'}\dfrac{1}{m^2m'} \\ a \text{ sh } m'a, & \text{ch } m'a, & (-1)^{n'}\dfrac{3a^2}{b^2m'^2} \end{vmatrix}.$$

$$\cdots\cdots\cdots\cdots\cdots\cdots\cdots\cdots\cdots(64)$$

The vertical displacement on the surface $x=0$, is expressed, when $\lambda=\infty$, in the form:

$$u=-\frac{f\rho g}{2\mu}\sum_{m}\sum_{m'} m'\frac{\vartheta'}{\vartheta}\sin m'y. \quad \cdots\cdots(65)$$

The computed result of this solution is shown in Fig. 5, in which the unbalanced pressure Δp is of the form:

$$\Delta p=-f\frac{3\rho g a^2}{2b^2}y. \quad \cdots\cdots(66)$$

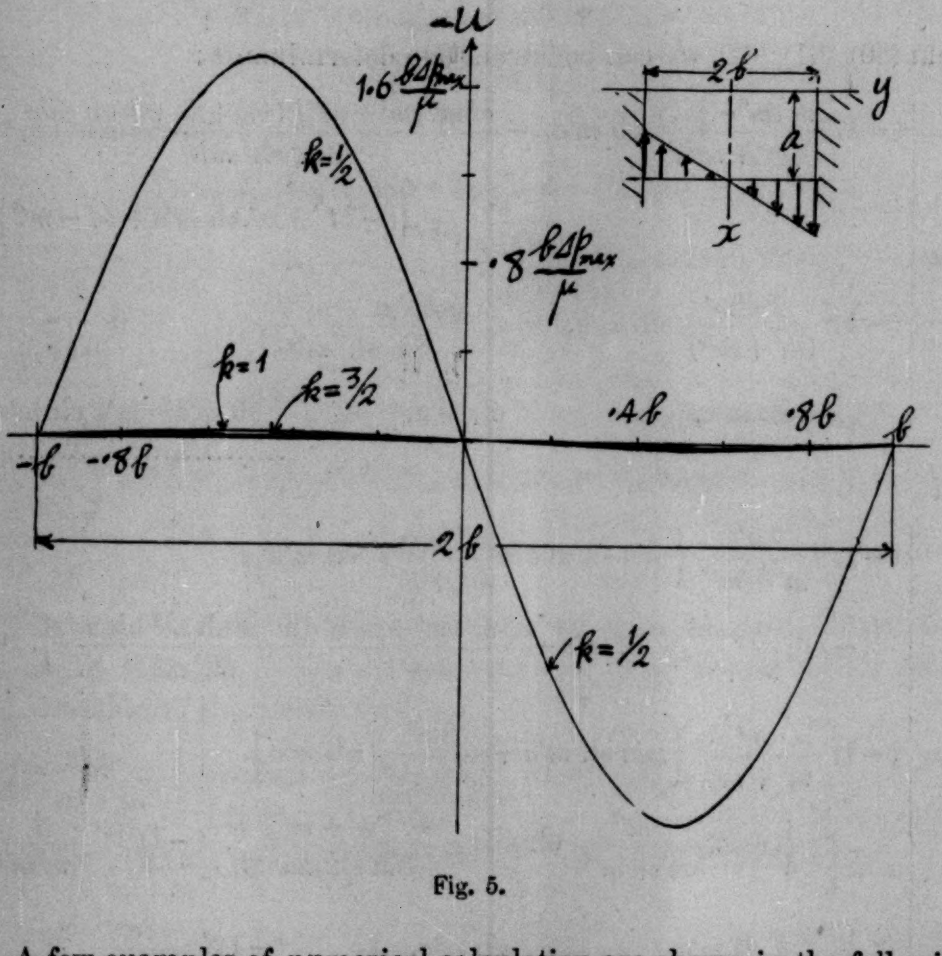

Fig. 5.

A few examples of numerical calculation are shown in the following table:

$k\left(=\frac{a}{b}\right)$	$2b$	$\Delta p_{max.}$	f	max. $u_{x=0}$
½	10^km.^	15^atm.^	·0327	43·25^cm^
¾	"	"	·0147	·35^cm^
1	"	"	·0082	·06^cm^
2	"	"	·0020	·005^cm^

It will be worth noticing that, as the induced coefficient of friction at the contact surface is very small, the slipping of the block in an ordinary state is almost impossible. The distribution of the displacements at the surface is of a flexural type. The curve of the flexure is much different from that of the preceding case. The maximum amplitude of the displacement diminishes more quickly than that of the preceding case as the ratio of the depth to the breadth of the block is increased. This is of a similar nature as that[13] in a semi-infinite body subject to internal nuclei of strain of a multiplet type.

5. In this section, we shall suppose that the block is subjected to an uniform compression or tension acting horizontally. Let $\frac{ca}{2}$ denotes the intensity of the horizontal force, then the boundary conditions can be written in the forms:

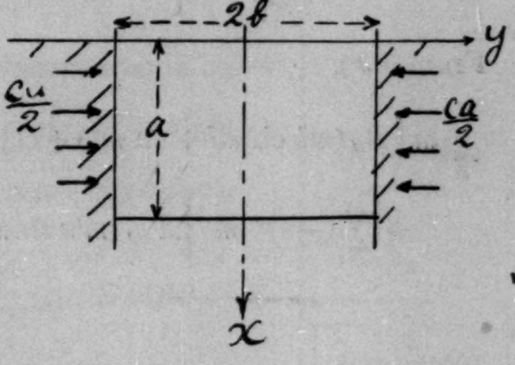

Fig. 6.

$$y=\pm b,\quad \begin{cases} u=0, & \cdots\cdots(67) \\ Y_y=\dfrac{Ca}{2}, & \cdots\cdots(68) \\ X_y=f\dfrac{\lambda}{\lambda+2\mu}\rho g x, & \cdots\cdots(69) \end{cases}$$

$$x=0,\qquad X_x=X_y=0, \quad \cdots\cdots(70),(71)$$

$$x=a,\qquad X_x=0. \quad \cdots\cdots(72)$$

13) K. Sezawa, "The Tilting of the Surface of a Semi-infinite Solid due to Internal Nuclei of Strain", *Bull. Earthq. Res. Inst.*, 7 (1929), 1-14.

The Airy's function χ, complementary function ψ, the components of displacement (u, v) and the stresses X_x, Y_y, X_y are quite of the same forms as those in (10), (11), (12), (13), (14), (15), (16).

From the nature of the problem, we can write

$$X_y \doteqdot 0, \quad \cdots\cdots(69')$$

instead of (69) in the present case.

Then we have the following system of the relations.

From (67),

$$m' = \frac{(2n'+1)\pi}{2b}, \qquad [n' = 0, 1, 2, \cdots] \quad \cdots\cdots(73)$$

$$B_m \left(mb \,\mathrm{sh}\, mb + \frac{\lambda+2\mu}{\lambda+\mu} \,\mathrm{ch}\, mb \right) + C_m \, m \,\mathrm{ch}\, mb = 0. \quad \cdots\cdots(74)$$

From (68),

$$-\sum_m m^2 \left\{ B_m \, b \,\mathrm{sh}\, mb + C_m \,\mathrm{ch}\, mb \right\} \cos mx = \frac{Ca}{2}, \quad \cdots\cdots(75)$$

From (69'),

$$\sum_m m \left\{ B_m (mb \,\mathrm{ch}\, mb + \mathrm{sh}\, mb) + C_m \, m \,\mathrm{sh}\, mb \right\} \sin mx$$

$$+ \sum_{n'} (-1)^{n'} m' \Big\{ A'_{m'} (m'x \,\mathrm{sh}\, m'x + \mathrm{ch}\, m'x) + B'_{m'} (m'x \,\mathrm{ch}\, m'x + \mathrm{sh}\, m'x)$$

$$+ C'_{m'} m' \,\mathrm{sh}\, m'x + D'_{m'} m' \,\mathrm{ch}\, m'x \Big\} = 0,$$

$$\cdots\cdots(76)$$

From (70), (71),

$$\sum_m m \left\{ B_m (my \,\mathrm{sh}\, my + 2 \,\mathrm{ch}\, my) + C_m \, m \,\mathrm{ch}\, my \right\}$$

$$- \sum_{m'} m'^2 C'_{m'} \cos m'y = 0, \quad \cdots\cdots(77)$$

and

$$A'_{m'} + m' D'_{m'} = 0. \quad \cdots\cdots(78)$$

From (72),

$$m = \frac{(2n+1)\pi}{2a}, \qquad [n = 0, 1, 2, \cdots] \quad \cdots\cdots(79)$$

and

$$A'_{m'} a \,\mathrm{ch}\, m'a + B'_{m'} a \,\mathrm{sh}\, m'a + C'_{m'} \,\mathrm{ch}\, m'a + D'_{m'} \,\mathrm{sh}\, m'a = 0. \quad \cdots\cdots(80)$$

Proceeding in the same manner as in the preceding case, we get

$$B_m = (-1)^n \frac{c}{m^2 \operatorname{ch} mb}, \quad \cdots\cdots(81)$$

$$\frac{m^2 b}{\operatorname{ch} mb} B_m + (-1)^{n'} \frac{2m'}{a} \Big\{ B'_{m'} \frac{(-1)^n m'^2}{m^2+m'^2} \Big(a \operatorname{sh} m'a + \frac{2m^2}{m'(m^2+m'^2)} \operatorname{ch} m'a \Big)$$
$$+ C'_{m'} (-1)^n \frac{m'^2}{m^2+m'^2} \operatorname{ch} m'a + D'_{m'} \frac{m'^2}{m^2+m'^2} \Big(\frac{2mm'}{m^2+m'^2}$$
$$- (-1)^n \frac{m^2-m'^2}{m^2+m'^2} \operatorname{sh} m'a - (-1)^n m'a \operatorname{ch} m'a \Big) \Big\} = 0, \quad \cdots\cdots(82)$$

$$(-1)^{n'} \frac{2m}{b} \frac{m^2-m'^2}{(m^2+m'^2)^2} \operatorname{ch} mb \, B_m + m' C'_{m'} = 0, \quad \cdots\cdots(83)$$

$$a \operatorname{sh} m'a \, B'_{m'} + \operatorname{ch} m'a \, C'_{m'} + (\operatorname{sh} m'a - m'a \operatorname{ch} m'a) D'_{m'} = 0. \quad \cdots\cdots(84)$$

From these, we may construct the determinants below:

$$\vartheta = \begin{vmatrix} (-1)^n m \operatorname{ch} m'a, & m'(m' - (-1)^n m \operatorname{sh} m'a) \\ a \operatorname{sh} m'a, & \operatorname{sh} m'a - m'a \operatorname{ch} m'a \end{vmatrix}, \quad \cdots\cdots(83)$$

$$\vartheta' = \begin{vmatrix} \dfrac{b}{\operatorname{ch} mb}, & (-1)^{n+n'} \dfrac{4m'^2}{a(m^2+m'^2)^2} \operatorname{ch} m'a, & 0 \\ (-1)^n \dfrac{2m}{b} \dfrac{m^2-m'^2}{(m^2+m'^2)^2} \operatorname{ch} mb, & 0, & m' \\ 0, & a \operatorname{sh} m'a, & \operatorname{ch} m'a \end{vmatrix}. \quad \cdots\cdots(84)$$

Then the vertical displacement on $x = 0$ is expressed, when $\lambda = \infty$, in the form:

$$u = \frac{ca}{8\mu} \sum_{n'} \sum_{n} \frac{(-1)^{n+n'}}{\operatorname{ch} mb} \times \frac{(m^2+m'^2)^2}{mm'^2} \frac{\vartheta'}{\vartheta} \cos m'y. \quad \cdots\cdots(85)$$

The compiled result of this equation is shewn in Fig. 7.

Though the magnitude of f which should be induced at the surface of contact has not been calculated for the sake of simplicity, we can easily anticipate that f takes very small value in the present case. The sliding of the surface of the contact at the superficial portion of the

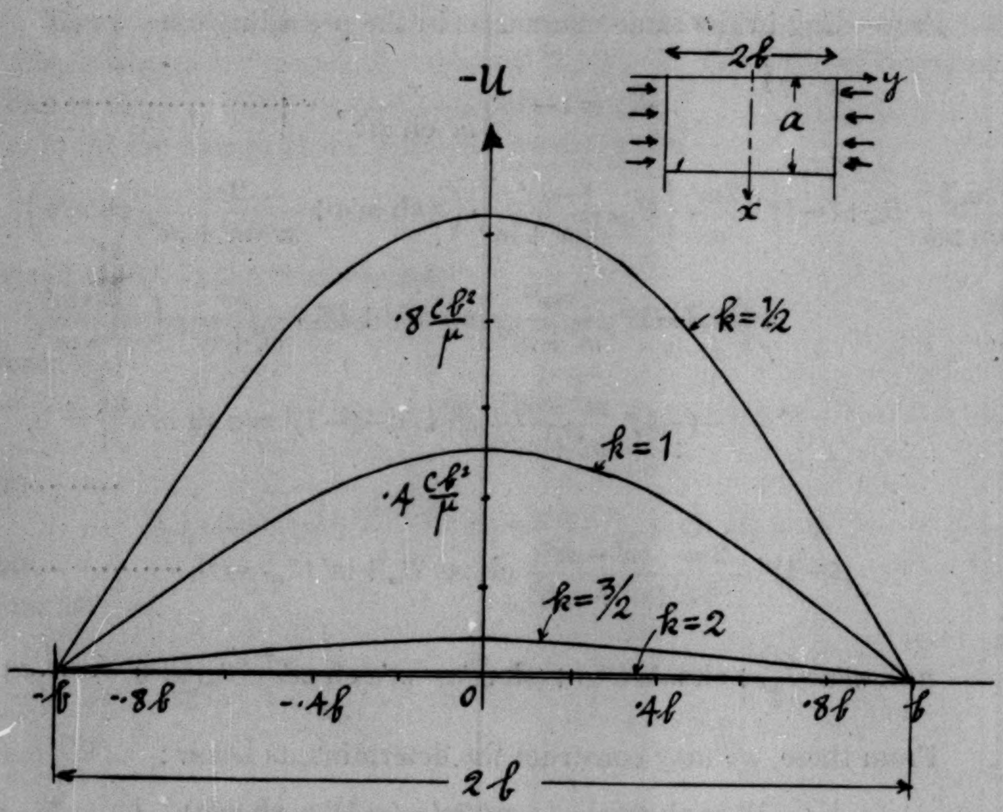

Fig. 7.

ground is very possible, because the location of the disturbing force extends to the vicinity of the surface where the limiting value of the sliding resistance is small on account of the low hydrostatic pressure. In the preceding cases the sliding resistance near the surface is, too, small, but the disturbing forces do not act directly on that surface region.

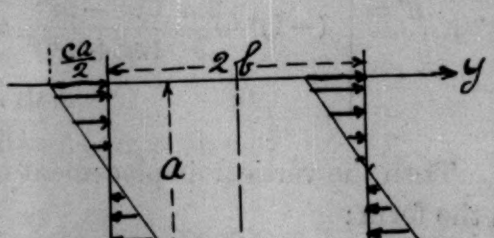

Fig. 8.

6. When the block is subjected to a varying horizontal force, the types of the Airy's function and of the complementary function are the same as those in (39) and (40). The equations of the displacement and of the stresses have similar forms, excepting some particular terms. The correct forms of them will be expressed by

$$2\mu u = \sum_{m} \left\{ A_m \left(my \operatorname{ch} my + \frac{\lambda+2\mu}{\lambda+\mu} \operatorname{sh} my \right) + D_m m \operatorname{sh} my \right\} \sin mx$$
$$+ \sum_{m'} \left\{ A'_{m'} \left(-m'x \operatorname{sh} m'x + \frac{\mu}{\lambda+\mu} \operatorname{ch} m'x \right) \right.$$
$$+ B'_{m'} \left(-m'x \operatorname{ch} m'x + \frac{\mu}{\lambda+\mu} \operatorname{sh} m'x \right)$$
$$\left. - C'_{m'} m' \operatorname{sh} m'x - D'_{m'} m' \operatorname{ch} m'x \right\} \sin m'y, \quad \cdots\cdots(86)$$

$$X_x = \sum_{m} m \left\{ A_m (my \operatorname{ch} my + 2 \operatorname{sh} my) + D_m m \operatorname{sh} my \right\} \cos mx$$
$$- \sum_{m'} m'^2 \left\{ A'_{m'} x \operatorname{ch} m'x + B'_{m'} x \operatorname{sh} m'x \right.$$
$$\left. + C'_{m'} \operatorname{ch} m'x + D'_{m'} \operatorname{sh} m'x \right\} \sin m'y,$$
$$\cdots\cdots\cdots(87)$$

$$Y = - \sum_{m} m^2 \left\{ A_m y \operatorname{ch} my + D_m \operatorname{sh} my \right\} \cos mx$$
$$+ \sum_{m'} m' \left\{ A'_{m'} (m'x \operatorname{ch} m'x + 2 \operatorname{sh} m'x) + B'_{m'} (m'x \operatorname{sh} m'x + 2 \operatorname{ch} m'x) \right.$$
$$\left. + C'_{m'} m' \operatorname{ch} m'x + D'_{m'} m' \operatorname{sh} m'x \right\} \sin m'y,$$
$$\cdots\cdots\cdots(88)$$

$$X_y = - \sum_{m} m \left\{ A_m (my \operatorname{sh} my + \operatorname{ch} my) + D_m m \operatorname{ch} my \right\} \sin mx$$
$$+ \sum_{m'} m' \left\{ A'_{m'} (m'x \operatorname{sh} m'x + \operatorname{ch} m'x) + B'_{m'} (m'x \operatorname{ch} m'x + \operatorname{sh} m'x) \right.$$
$$\left. + C'_{m'} m' \operatorname{sh} m'x + D'_{m'} m' \operatorname{ch} m'x \right\} \cos m'y.$$
$$\cdots\cdots\cdots(89)$$

Now we have the boundary conditions :

$$y = \pm b, \qquad u = 0, \cdots\cdots\cdots\cdots\cdots\cdots\cdots\cdots(90)$$

$$\left. \begin{aligned} y = +b, \qquad X_y = c\left(x - \frac{a}{2}\right), \\ y = -b, \qquad Y_y = -c\left(x - \frac{a}{2}\right), \end{aligned} \right\} \cdots\cdots\cdots\cdots(91)$$

$$y = \pm b, \qquad X_y = f\frac{\lambda}{\lambda+2\mu}\rho g x, \quad \cdots\cdots(92)$$

$$x = 0, \qquad X_x = X_y = 0, \quad \cdots\cdots(93), (94)$$

$$x = a, \qquad X_x = 0. \quad \cdots\cdots(95)$$

Substituting from (86), (87), (88), (89), in (90)—(95), we find

$$m' = \frac{n'\pi}{b}, \qquad [n' = 1, 2, 3\cdots] \quad \cdots\cdots(96)$$

$$A_m\left(mb \operatorname{ch} mb + \frac{\lambda+2\mu}{\lambda+\mu}\operatorname{sh} mb\right) + D_m m \operatorname{sh} mb = 0, \quad \cdots\cdots(97)$$

$$-\sum_m m^2\left\{A_m b \operatorname{ch} mb + D_m \operatorname{sh} mb\right\}\cos mx = c\left(x - \frac{a}{2}\right), \quad \cdots\cdots(98)$$

$$-\sum_m m\left\{A_m(mb \operatorname{sh} ma + \operatorname{ch} mb) + D_m m \operatorname{ch} mb\right\}\sin mx$$
$$+\sum_{n'}(-1)^{n'} m'\left\{A'_{m'}(m'x \operatorname{sh} m'x + \operatorname{ch} m'x) + B'_{m'}(m'x \operatorname{ch} m'x + \operatorname{sh} m'x)\right.$$
$$\left. + C'_{m'} m' \operatorname{sh} m'x + D'_{m'} m' \operatorname{ch} m'x\right\} = 0, \quad \cdots\cdots(99)$$

$$\sum_m m\left\{A_m(my \operatorname{ch} my + 2 \operatorname{sh} my) + D_m m \operatorname{sh} my\right\}$$
$$-\sum_{m'} m'^2 C'_{m'} \sin m'y = 0, \quad \cdots\cdots(100)$$

$$A'_{m'} + m' D'_{m'} = 0, \quad \cdots\cdots(101)$$

$$m = \frac{(2n+1)\pi}{2a}, \quad [n = 0, 1, 2, \cdots] \quad \cdots\cdots(102)$$

$$A'_{m'} a \operatorname{ch} m'a + B'_{m'} a \operatorname{sh} m'a + C'_{m'} \operatorname{ch} m'a + D'_{m'} \operatorname{sh} m'a = 0. \quad \cdots\cdots(103)$$

Applying the method of Fourier's analysis on (98), (99), (100) and making use of (96), (97), (101), (102), (103), we get the relations:

$$A_m\left(mb \operatorname{ch} mb + \frac{\lambda+2\mu}{\lambda+\mu}\operatorname{sh} mb\right) + D_m m \operatorname{sh} mb = 0, \quad \cdots\cdots(104)$$

$$m^2\left\{A_m\, b \operatorname{ch} mb + D_m \operatorname{sh} mb\right\} + \frac{2c}{a}\left(\frac{(-1)^n a}{2m} - \frac{1}{m^2}\right) = 0, \quad \cdots\cdots\cdots(105)$$

$$-m\left\{A_m\,(mb \operatorname{sh} mb + \operatorname{ch} mb) + D_m\, m \operatorname{ch} mb\right\}$$

$$+(-1)^{n'}\frac{2m'}{a}\Bigg[A'_{m'}\frac{m'}{m^2+m'^2}\Bigg((-1)^n\, m'a \operatorname{ch} m'a$$

$$+(-1)^n\frac{2m^2}{m^2+m'^2}\operatorname{sh} m'a + \frac{m(m^2-m'^2)}{m'(m^2+m'^2)}\Bigg)$$

$$+B'_{m'}\frac{(-1)^n\, m'}{m^2+m'^2}\left(m'a \operatorname{sh} m'a + \frac{2m^2}{m^2+m'^2}\operatorname{ch} m'a\right)$$

$$+C'_{m'}\frac{(-1)^n\, m'^2}{m^2+m'^2}\operatorname{ch} m'a + D'_{m'}\frac{m'^2}{m^2+m'^2}\left((-1)^n \operatorname{sh} m'a + \frac{m}{m'}\right)\Bigg] = 0,$$

$$\cdots\cdots\cdots(106)$$

$$\frac{2m}{b}\Bigg[A_m\frac{(-1)^{n'}\, mm'}{m^2+m'^2}\left(b \operatorname{ch} mb + \frac{2m'^2}{m(m^2+m'^2)}\operatorname{sh} mb\right)$$

$$+(-1)^{n'} D_m \frac{mm'}{m^2+m'^2}\operatorname{sh} mb\Bigg] - m'^2\, C'_{m'} = 0, \quad \cdots\cdots\cdots(107)$$

$$A'_{m'} + m'\, D'_{m'} = 0, \quad \cdots\cdots\cdots\cdots\cdots\cdots\cdots\cdots\cdots(108)$$

$$A'_{m'}\, a \operatorname{ch} m'a + B'_{m'}\, a \operatorname{sh} m'a + C'_{m'} \operatorname{ch} m'a + D'_{m'} \operatorname{sh} m'a = 0. \quad \cdots\cdots(109)$$

From these, we find the surface displacement, when $\lambda = \infty$, in the following form:

$$u = -\frac{c}{2\mu}\sum_m \sum_{m'} (-1)^{n'}\left(\frac{a(-1)^n}{2} - \frac{1}{m}\right)\frac{m^2+m'^2}{m'^3\, m^3 \operatorname{sh}^2 mb} \times \frac{\vartheta'}{\vartheta}\sin m'y,$$

$$\cdots\cdots\cdots(110)$$

where

$$\vartheta=\begin{vmatrix} (-1)^n m'a \operatorname{ch} m'a+(-1)^n \dfrac{2m^2}{m^2+m'^2} \operatorname{sh} m'a+\dfrac{m(m^2-m'^2)}{m'(m^2+m'^2)}, & & \\ (-1)^n\left(m'a \operatorname{sh} m'a+\dfrac{2m^2}{m^2+m'^2} \operatorname{ch} m'a\right), & & m'\left((-1)^n \operatorname{sh} m'a+\dfrac{m}{m'}\right) \\ 1, & 0, & m' \\ a \operatorname{ch} m'a, & a \operatorname{sh} m'a, & \operatorname{sh} m'a \end{vmatrix}, \qquad \text{(111)}$$

$$\vartheta'=\begin{vmatrix} (mb \operatorname{ch} mb+\operatorname{sh} mb), & m \operatorname{sh} mb, & 0, & 0 \\ -m(mb \operatorname{sh} mb+\operatorname{ch} mb), & -m^2 \operatorname{ch} mb, & (-1)^{n+n'} \dfrac{2m'^2}{a(m^2+m'^2)}\left(m'a \operatorname{sh} m'a+\dfrac{2m^2}{m^2+m'^2} \operatorname{ch} m'a\right), & (-1)^{n+n'} \dfrac{2m'^3}{a(m^2+m'^2)} \operatorname{ch} m'a \\ (-1)^{n'} \dfrac{2mm'(m^2-m'^2)}{b(m^2+m'^2)^2} \operatorname{sh} mb, & 0, & 0, & -m'^2 \\ 0, & 0, & a \operatorname{sh} m'a, & \operatorname{ch} m'a \end{vmatrix}. \qquad \text{(112)}$$

The compiled result of (108) is shown in Fig. 9.

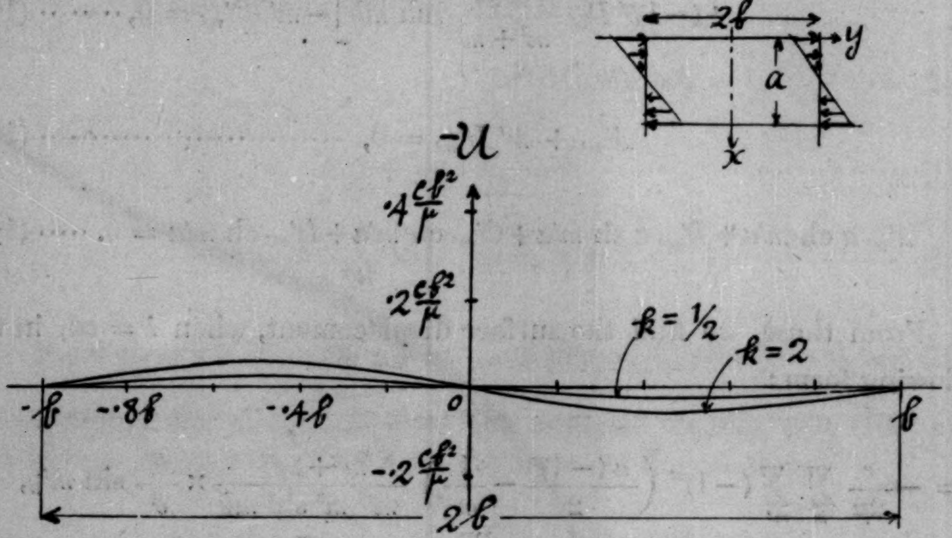

Fig. 9.

7. Now, we may combine two results in Sections 5 and 6. We can then obtain the problem of uniformly increasing compression or tension acting at the vertical wall of the block. The solutions thus obtained should satisfy the boundary conditions of the forms:

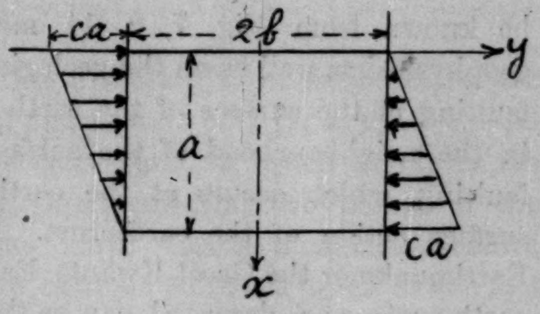

Fig. 10.

$$y = \pm b, \quad u = 0, \quad \cdots\cdots (113)$$

$$\left.\begin{array}{ll} y = +b, & Y_y = cx, \\ y = -b, & Y_y = c(a-x), \end{array}\right\} \cdots\cdots (114)$$

$$y = \pm b, \quad X_y \doteqdot f \frac{\lambda}{\lambda + 2\mu} \rho g x, \cdots\cdots (115)$$

$$x = 0, \quad X_x = X_y = 0, \cdots\cdots (116), (117)$$

$$x = a, \quad X_x = 0. \cdots\cdots (118)$$

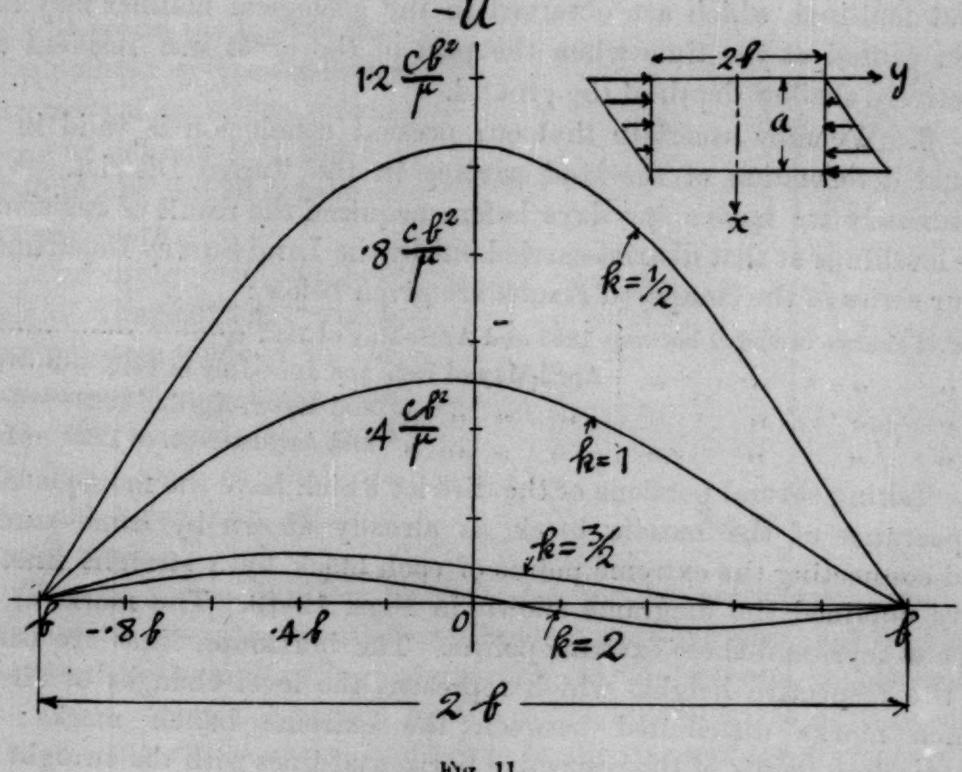

Fig. 11.

The result is plotted in Fig. 11. The general tendency which can be known from Fig. 7, 9, 11 may have some importance on the geophysical as well as on the geological problems. As already cited, the faulting of the surface of the earth crust seems to be accumulated only in the neighbourhood of the surface. The phenomena of the quick faulting, which occurs at the earthquake movement, are nearly the surface action of the earthcrust.* Even the cases of the Great Nôbi Earthquake or the Great Kwantô Earthquake, where large areas of the earth surface are damaged, can be thought to be the effect of the acting forces accumulated in the vicinity of the surface of a relatively vast extent. We have no intention to think that the forces cannot act in the deep portion of the earth. The forces cannot give their influence on the sliding of the crust at such a depth. The ordinary depth of the focus of the seismic origin may be rather shallow in the actual sense. Even though the co-existence of the deepness of the focus of the earthquake and the shallowness of the fault is permissible to a certain extent, the occurrence of the deep seated earthquake is yet wonderful. The mechanism of such a fact will be determined in the course of the development of the seismological science. Again, the evidence of great faultings which are observed in the geological manner may have been caused at the time when the part of the crust was resident at a relatively shallow depth of the ground.

8. We may ascertain that our present conclusion is valid in the actual deformation of the land surface in the Tango District. Very fortunately we have a few days before acquired the result of revision of the levellings at that district carried out by the Land Survey Department. Four series of the compared results are given below:

Level change occurred between 1888 and April-May of 1927 .... 0–I
" " " " April-May of 1927 and June-July of 1927 .... I–II
" " " " " " " " and March-April of 1928 ...... I–III
" " " " " " " " and August-Sept. of 1929 ... I–IV

Taking several portions of the district which have the most plausible appearance of the mosaic block as already shown by some student and connecting the extreme points of each block by a straight line, we have obtained the diagrams shown in Figs. 12–19. The marks of the type ● represent these extreme points. The horizontal lines are drawn at the respective heights which represent the level changes of all the bench marks distributed between the extreme bench marks: the intersection points of the respective horizontal lines with the straight line

connecting the extreme bench marks are shown successively by ▮, ○, △, □, ×. In these ▮ corresponds to the bench mark which is nearest to the left extreme mark.

If the blocks move vertically like a mosaic work as shown by the student already cited, the horizontal distribution of ▮, ○, △, □, × should be equal in proportion to that of the corresponding bench marks in the actual map projected on a straight line connecting two points of the extreme bench marks in the same map. Even a fractional shift, however, of these points between the extreme points is to tell us the fact that the displacement of the land surface is curved. We will easily see that this condition is not quite satified almost in all cases.

Moreover, the incoincidence of each series of the marks such as ▮, ○, △, □, × with respect to the vertical line in Fig. 12–19 shows that the successive level changes are not only of a mosaic type, but also of much irregular procedure. Again, we will see in the figures that some points reside outside the extreme points. These facts oblige us to know that the so-called blocks cannot behave as a mosaic work.

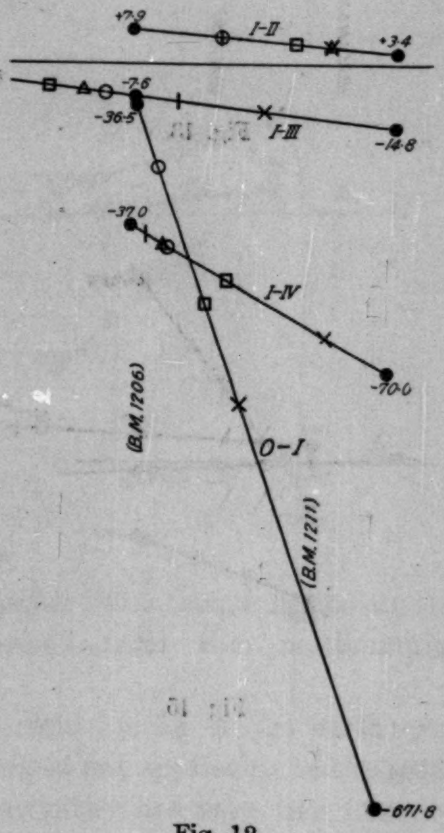

Fig. 12.

The other levelling portions of Tango-district which have not been touched in the present analysis from the start are curved in more complex forms so that we have not given any addition to such cases.

Except a few faulting lines caused by the earthquake, even the diagramatic steps of semi-discontinuous portions are not so large compared with and rather comparable to the general displacement. The faults which are caused by the earthquake seem, as already cited, to be of a superficial nature and not to be the traces of the surfaces of the

contact of the blocks in the form of a mosaic work. We have the idea that the deformations of the crust, besides the faulting, are all of the superficial nature; the mathematical mechanics of this will appear more fully in our future paper.

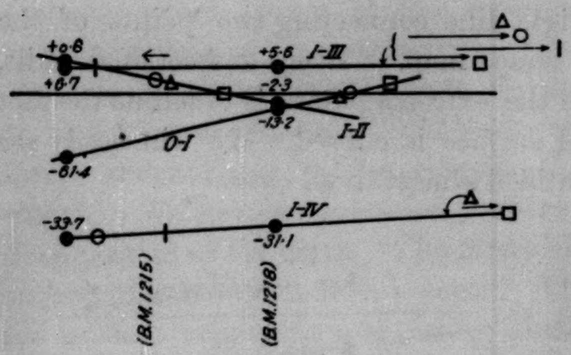

Fig. 13.

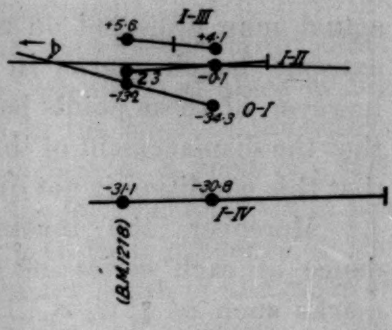

Fig. 14.

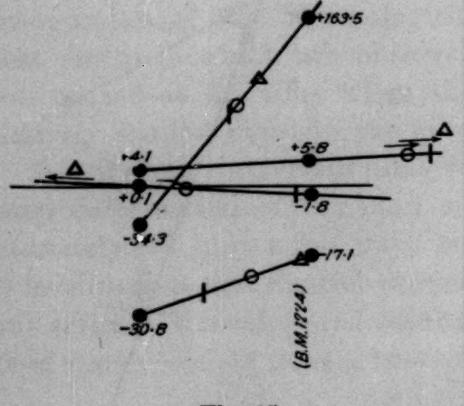

Fig. 15.

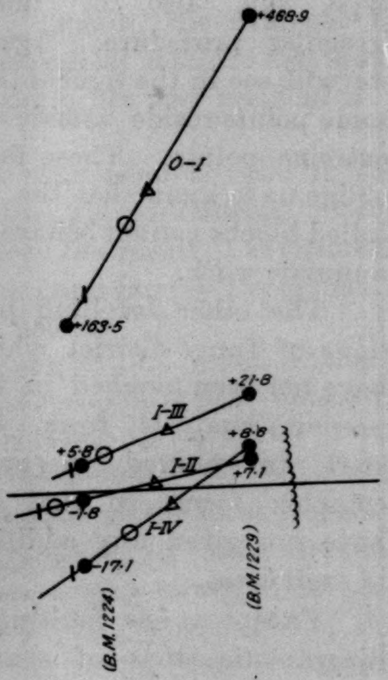

Fig. 16.

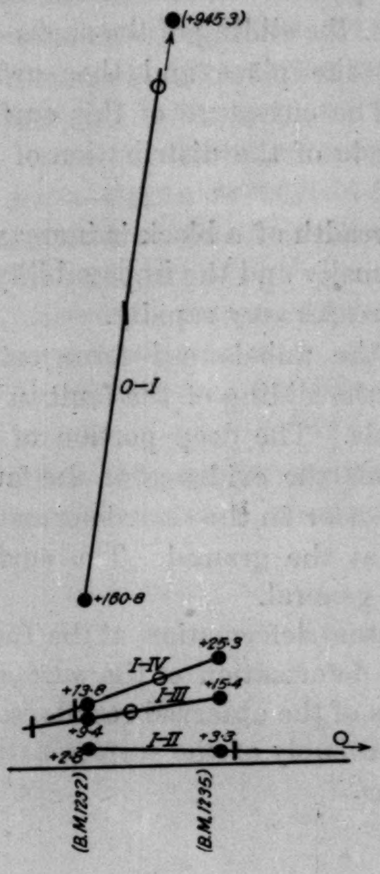

Fig. 17.

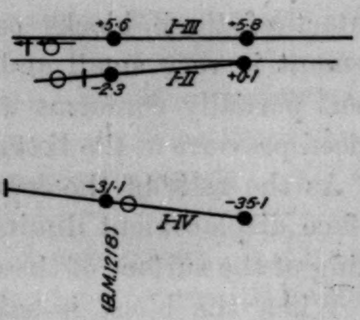

Fig. 18.

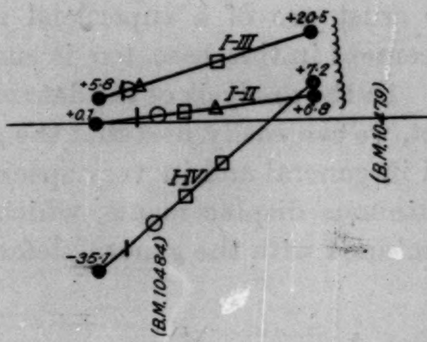

Fig. 19.

Résumé.

9. We may now complete this paper with some notice on the general results which have been obtained from this mathematical analysis.

1. The bodily movements of very rigid blocks of the earth crust are impossible. The idea of a mosaic work is not applicable to the actual earth crust where the elasticities or plasticities are very like to or less than that of the actual rocks and the solid friction at the surface of the separation of blocks (if pre-existing) is very large in gravitating masses.

2. The deformation of the surface of the earth crust must be curved in general. In particular cases of the boundary conditons or of the heterogeneous distribution of the rocks of various rigidities, the surface displacement may have certain discontinuous characters combined with the general curved flexural forms.

3. At the action of any extraordinary pressure unbalanced isostatically at the bottom of the so-called blocks, the sliding of the surface of the contact of these blocks can hardly take place and the surface displacement is very small and curved. The curvature of this surface movement partially conforms with the mode of the distribution of the unbalanced pressure at the bottom.

4. As the ratio of the depth to the breadth of a block is increased, the surface displacement diminishes anormally and the impossibility of the sliding of the surface of the contact increases very rapidly.

5. When the block is subjected to the unbalanced force acting horizontally at the surface of the contact, the sliding of the fault in the very vicinity of the surface becomes possible. The deep portion of the ground is not yet capable of sliding. Thus the evidence of the faults which are observed at the earthquake motion or in the slow deformation of the crust are of a superficial nature at the ground. The surface displacement in this case, too, is curved in general.

6. In the analysis of the data of the actual deformation, at the Tango District, we can easily find that the general deformation of the surface is curved in general and in very special cases of the observed results, some discontinuous displacements, which are probably of the surface nature, are combined with the general deformations.

---

2. 地殼の群塊運動の可能度に就いて

地震研究所 {妹澤克惟 / 西村源六郎}

地殼の變形が寄木細工の樣であり、各の地塊は殆んど完全な剛體として動く樣なものであるかどうかは多くの人々の興味を惹く所であらう。著者の一人は大正十三年頃別の意味に於ける地塊を力學的に考へた事もあるが、其後多くの人々が地塊といふ事をしきりに提案し、遂には本邦の如き地體の唯一の構造とまでも想像されて居るかの樣に見えたので、著者等は其重大さを感じ、こゝに改めて斯る事實が許せる事かどうかを吟味する事にした。

研究の方法は二次元の問題を導入してエヤリー函數を應用し、普通の彈性率を有する固體が重力に支配されて固體の表面に固體面摩擦のある事を注目して計算を施した。

研究の主要な結果を列擧すれば,

1. 普通地塊と考へて居る樣な固體では寄木細工の樣な運動は不可能である。即ち斯る大きなものでは彈性は通常のものであるのに重力の爲固體面の摩擦力が非常な影響を與へる爲めである。

2. たとひ地塊の様なものを假定しても地表面の變形は一般に曲面狀である事がわかる。極めて特別な場合、即ち剛性率の甚しく異なろ岩石塊が混入する時は其近所だけに稍不連續に見える歪みがあり、又地表等の境界條件が著しく特定の時は、表面の附近に限り上述の曲面狀變形に混合して不連續變形の存在する事がある。

3. 地塊の下部に不平衡壓力が働く時は地塊面の斷層の辷り等は殆ど不可能の事柄となる。又表面の一般變形は不平衡壓力の分布と一致せる傾向を持つには持つが其變位は極めて小さい。

4. 地塊の深さが其幅に比較して大きくなるに從ひ表面の變位は急激に少くなる。又斷層の辷りは一層困難となる。

5. 地塊が水平の不平衡力を受ける時は斷層の辷りは比較的容易になる。しかしこの辷りは表面に極く近い部分のみであり、少し深くなればやはり辷り得なくなる。即ち一般に斷層は極めて表面的のものである事が判明する。地表面の變形はこの場合でも勿論曲面狀のものを主として含む。

6. 實際の測量の結果に就て著者等が行つた分析に照しても極めて特別な場合を除いては、一般に上述の形成にあり、殊に表面の變形が著しく曲面狀をなす事が認められる。

3. *Deformation of Earthcrust in California.*

By Naomi MIYABE,

Earthquake Research Institute.

(Read Nov. 18, 1929.—Received Dec. 20, 1929.)

Introduction.

The triangulation survey was revised in the time interval of 1922–1928 in the western part of California over 1000 kilometres along the Pacific coast from Ross Mountain in the north to Cuyamaca in the south. These regions are traversed by San Andreas fault and were much disturbed at the time of the California earthquake of 1906. The result of the recent survey was compared with the result of the former ones which had been carried out before the earthquake of 1906, and thence the horizontal displacements of the triangulation points were computed.[1] For these computations, the line connecting Mt. Lola and Round Top was taken as the base, which was compared afterwards with eastern triangulation points and found to be unchanged relative to them in the direction and the length of it, during the time interval of the two successive surveys, so that the reported displacements of triangulation points in these regions may be regarded as the actual displacements which have occurred relative to the continent of America.

We calculated, from these data, divergence, rotation, shear and principal axes of strain ellipse for every triangle, the vertices of which are the triangulation points, by the same method as we have already applied for the earth movement in the Kwansai districts[2] to elucidate the mode of deformation of the earth crust in these regions.

It may be remarked that these displacements of triangulation points are affected by two different sources of disturbances, i.e., the destructive effect of the earthquake and the slow cumulative deformation of the crust. These components of displacements due to different causes are, of course, not easily separable in practice and, in the present computations, we treated the both components inclusive.

---

1) W. BOWIE, *Special Publication of the Coast & Geodetic Survey U.S.A.*, No. 151 (1928).
2) T. TERADA and N. MIYABE, *Bull. Earthq. Res. Inst.*, 7 (1929), 223.

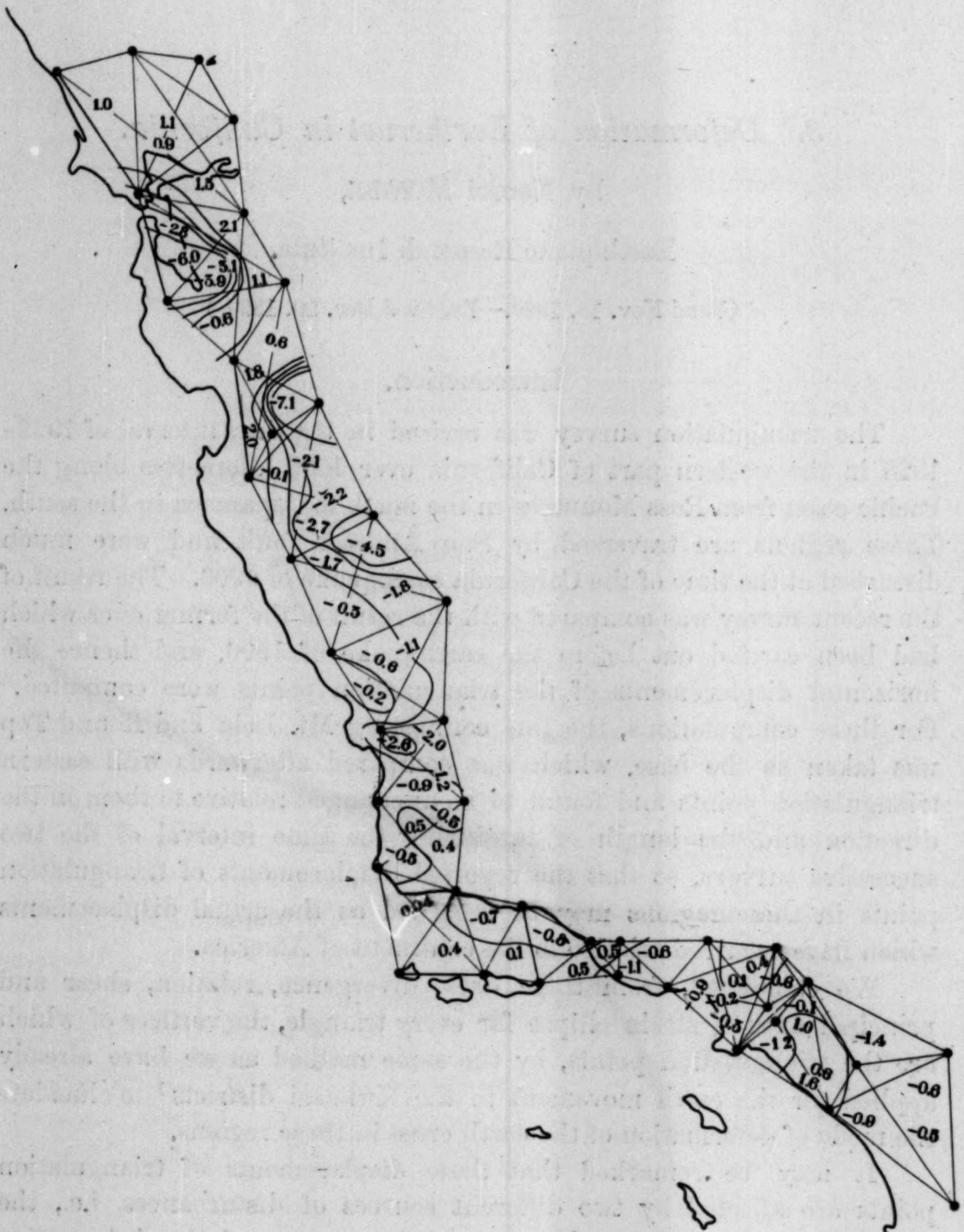

Fig. 1. Distribution of Divergence.

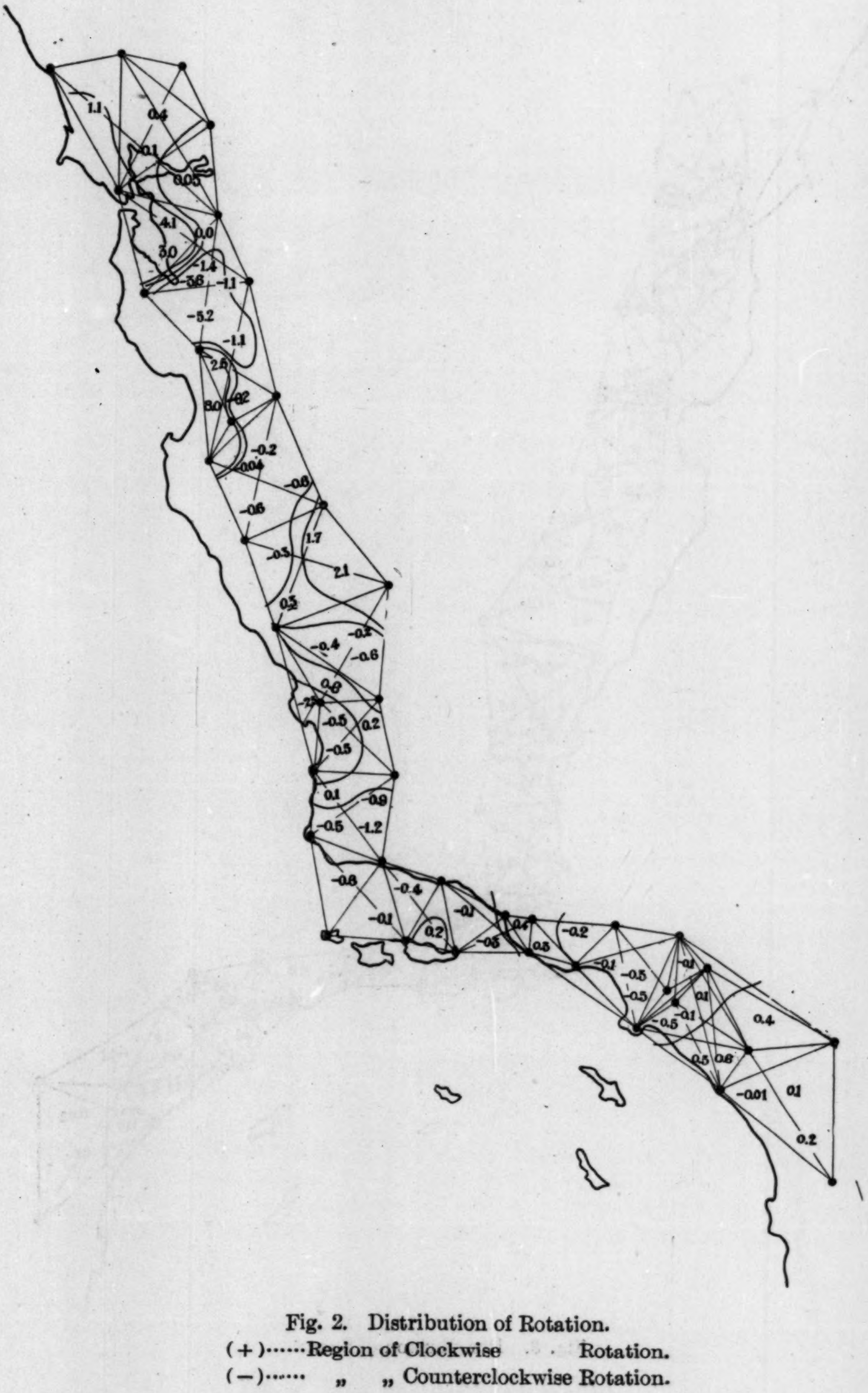

Fig. 2. Distribution of Rotation.
(+)……Region of Clockwise Rotation.
(−)…… „ „ Counterclockwise Rotation.

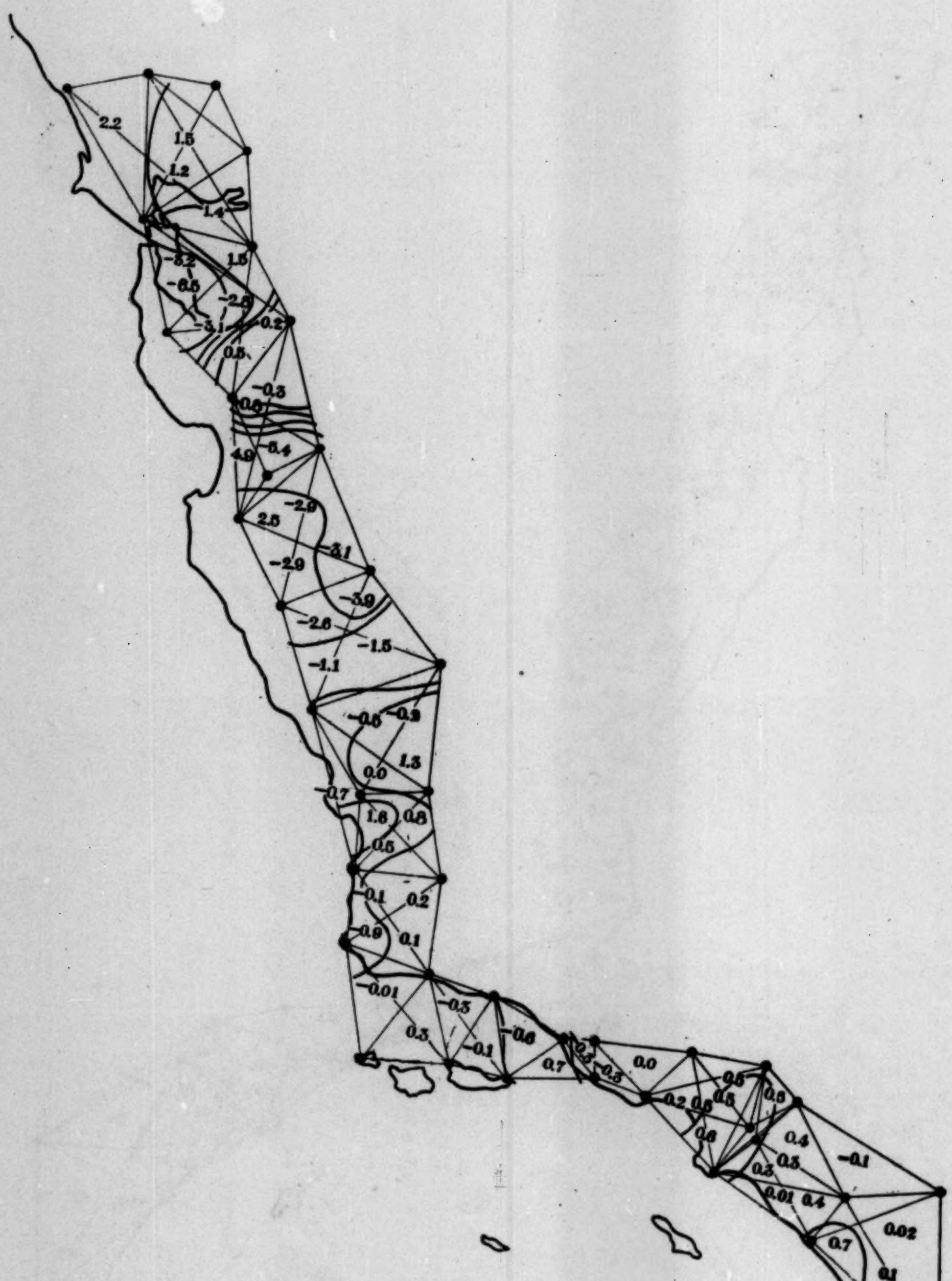

Fig. 3. Distribution of Shear.

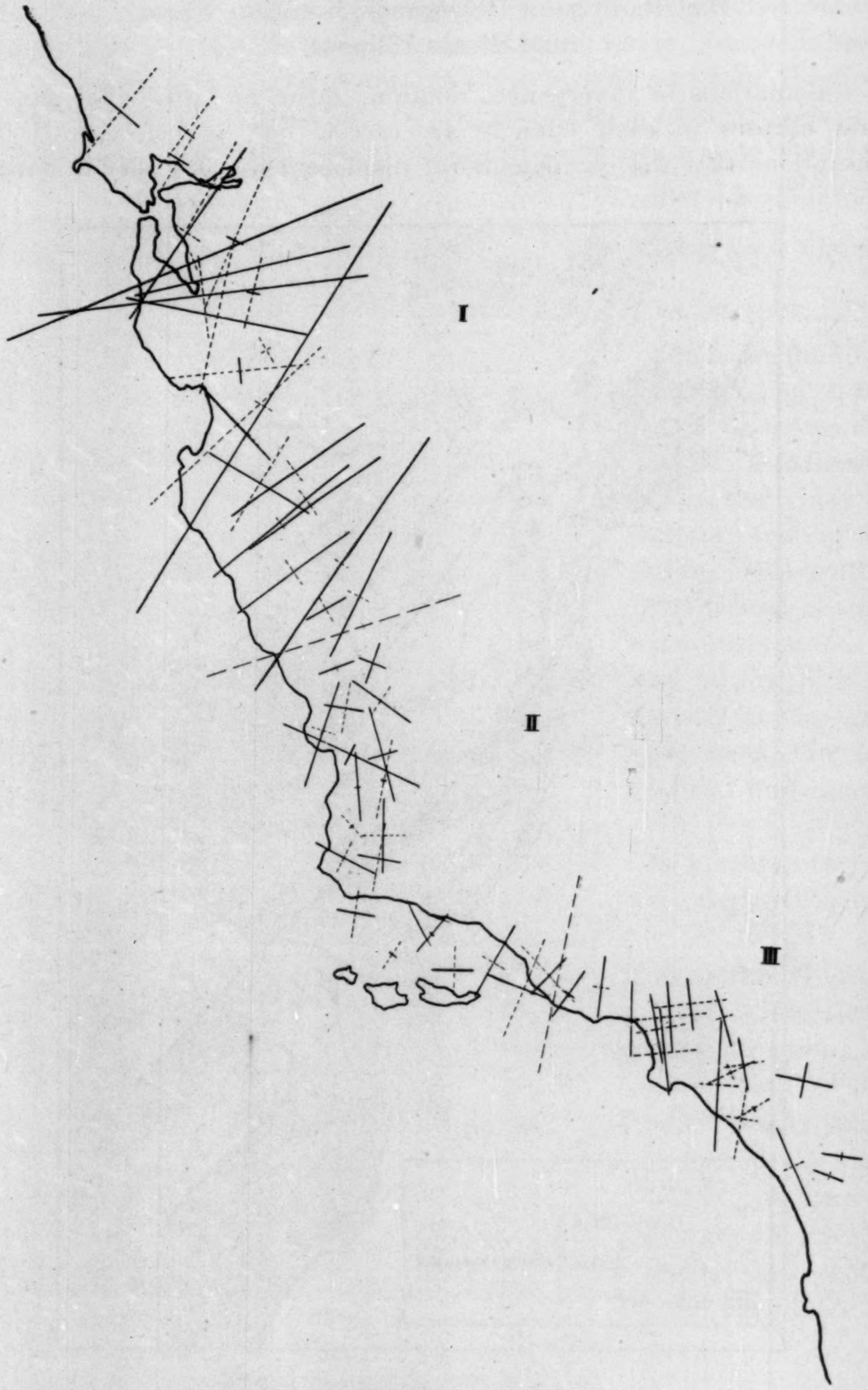

Fig. 4. Distribution of Strain Ellipses.

Full line ······Axes of Contraction.
Broken „ ······ „ „ Elongation.

Distributions of Divergence, Rotation, Shear and Strain Ellipses.

Calculations of divergence, rotation, shear and principal axes of strain ellipses in each triangle are carried out, as before, with the assumptions that the components of displacements u, v vary uniformly

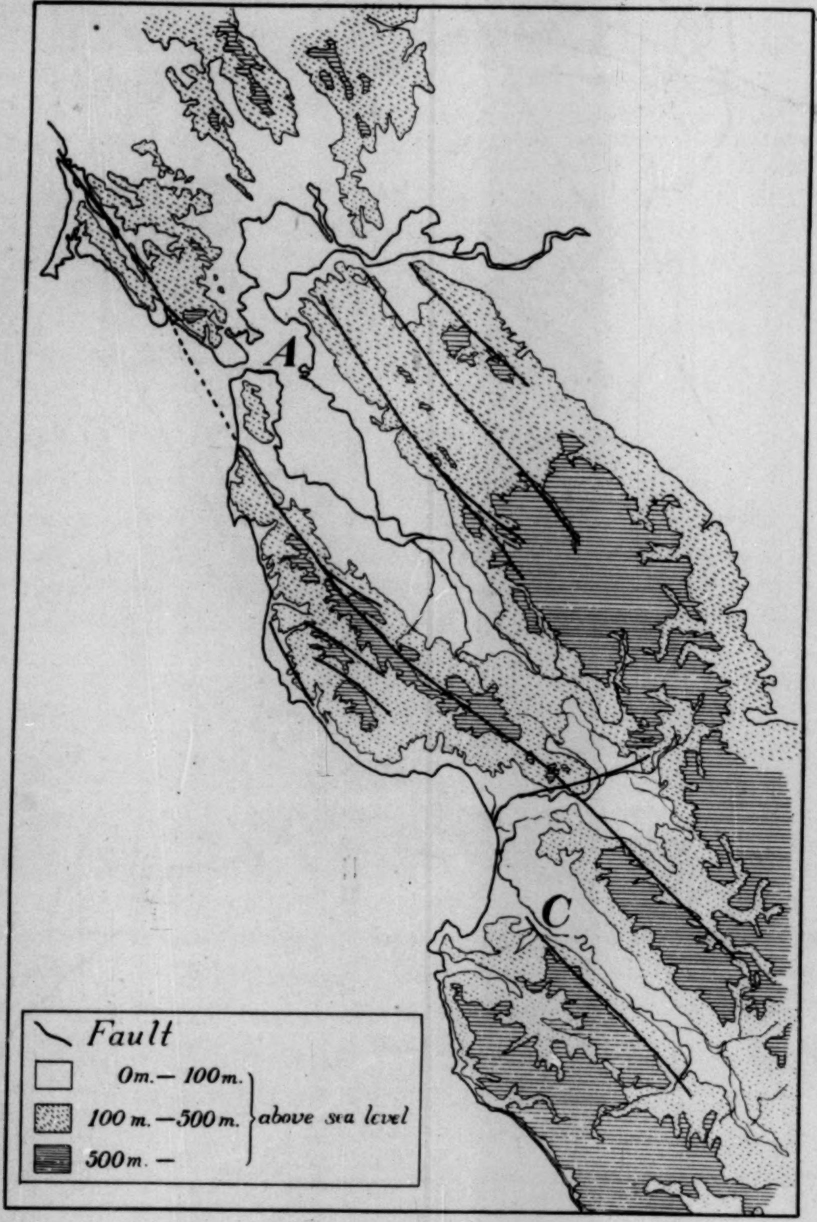

Fig. 5. Geographical Features in the Neighbourhood of San Francisco.

within a triangle and they are linear functions of the coordinates x and y. The origin of the coordinate axes was taken at Lospe, the x-axis being taken in EW-direction positive towards the east, and y-axis in NS-direction positive towards the north. Thus divergence Δ, rotation ζ, shear S, principal axes of strain ellipses γ_1 γ_2 and inclinations θ_1 of γ_1 to the x-axis are calculated in terms of $\frac{\partial u}{\partial x}$, $\frac{\partial u}{\partial y}$, $\frac{\partial v}{\partial x}$ and $\frac{\partial v}{\partial y}$, and the geographical distributions of them are shown in Figs. 1–4. Examining these figures, the followings may be noticed:

i) In the Fig. 1, showing the geographical distribution of divergence, two regions of negative divergence are remarkable which are found to correspond to the San Francisco Bay (A in Fig. 5) and the valley of the Vajaro River (C in Fig. 5) respectively. In the map showing the distribution of faults in these regions,[3] a fault is marked to the north boundary of the Vajaro valley. Between these two basins, there may be seen, on the geographical map, relatively elevated districts dividing the two basins. To the south of these regions, as a whole, the negative values of divergence are gradually decreased, that is, they tend to change into positive divergences, though accompanied with some fluctuations.

ii) As for the distribution of rotation, as shown in Fig. 2, it is somewhat interesting to see that the regions of counterclockwise and clockwise rotations are arranged alternately along the coast. In his study of the geographical features of Japan, Professor Fujiwhara[4] pointed out the existence of the same phenomena.

iii) The amount of shear is generally larger in the northern region where San Andreas fault passes, while in the southern region situated far from that fault, the amount of shear is smaller.

iv) For the investigation of the distribution of the strain ellipses, shown in Fig. 4, the whole area may conveniently be divided into three regions, I, II and III, according to the amounts and directions of principal axes of strain ellipses. In the region I, one or both of the principal axes are much larger than those in the other two regions. Examining more closely, there are some sub-regions in which the axes of elongation are larger, and other sub-regions in which the axes of contraction are larger, and these two sorts of sub-regions are alternately situated. In this region, the greater majority of longer axes, both elongation and contraction, are directed convergently, i.e., they seem to

3) Report of California Earthquake of April 18, 1906.
4) S. Fujiwhara, *Japanese Journ. Geophys.*, 3 (1925), No. 2.

converge to some limited portions to the west of the San Andreas fault. In the region II, the magnitudes of principal axes of strain ellipses are generally less than those in the region I, and yet their directional character is the same. In the region III, however, the magnitudes of the principal axes are generally smaller and the axes of elongation are directed generally in EW, while, those of contraction in NS.

Divergence and Topography.

In the study of the distribution of divergence, the distribution along the coast line is more significant than that in the direction perpendicular to it, for the triangulation points of which the horizontal displacements were calculated are poorly distributed in the latter direction. Hence, in the present case, the values of divergence for different triangles are projected on a straight line approximately parallel to the coast, which is shown in Fig. 6a.[5] In that figure, the amounts of divergence are taken as ordinates and the distance of the approximate centre of every triangle from the origin (here, the central part of Golden Gate was taken as the origin) is taken as abscissa. The mark ∘ gives the value of divergence for the individual triangle, while × means an averaged value of them for every 100 km.

The mean heights of profile[6] sections taken perpendicular to the above line were taken for every 25 km. distance from the origin and plotted on the same straight line as that for divergence, which is shown in Fig. 6b. The average height for every 100 km. is also marked by the symbol ×.

Examining these two curves, it may be noticed that, in both the cases, the curves are generally higher in the south. In the curve of divergence, however, this general tendency of the curve is interrupted by a discontinuous increase of convergence at the point corresponding to the valley of the Vajaro River. Thus, the variation of divergence may more likely be represented by the two straight lines AB and CD as shown in the figure. The southern boundary of the regions AB is roughly coincident with the conspicuous fault line.

The discordance between the above two curves may be understood, under the light of our previous results, to signify that the region corresponding to AB might be raised more or less to follow the variation of divergence. Such a rise of the crust may be expected from the

5) In the figure, abreviation G.G. means the origin, Golden Gate.
6) Profiles are due to the map issued by the "TIMES".

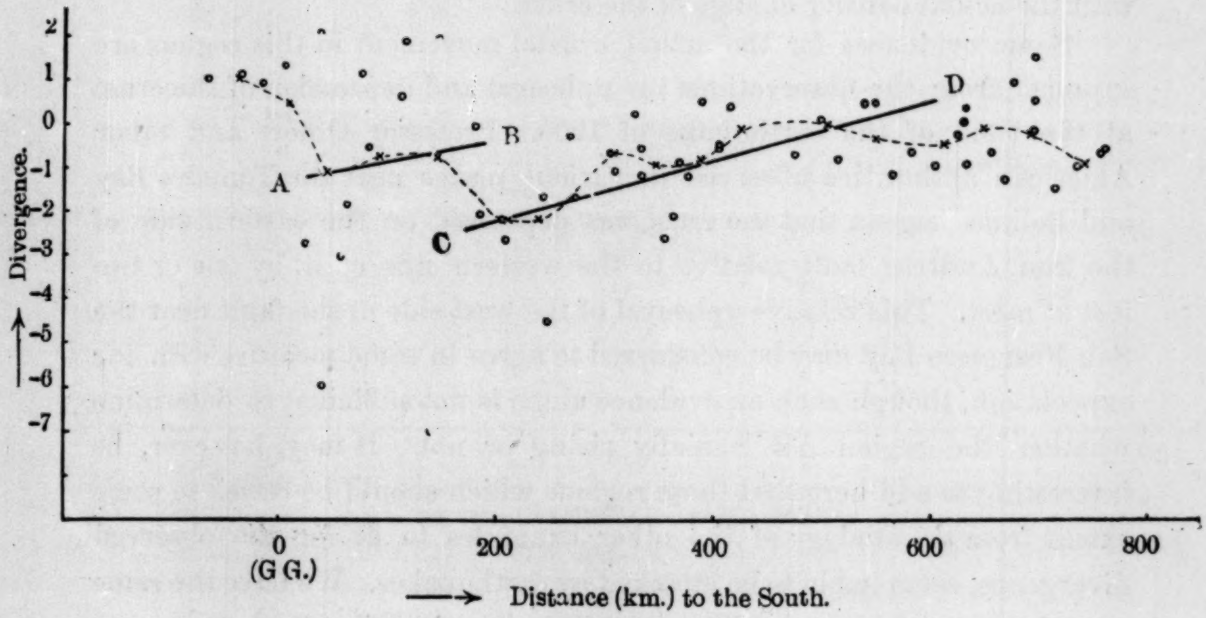
Divergence.
2
1
0
-1
-2
-3
-4
-5
-6
-7
A
B
C
D
0
(G G.)
200
400
600
800
Distance (km.) to the South.

Fig. 6a.

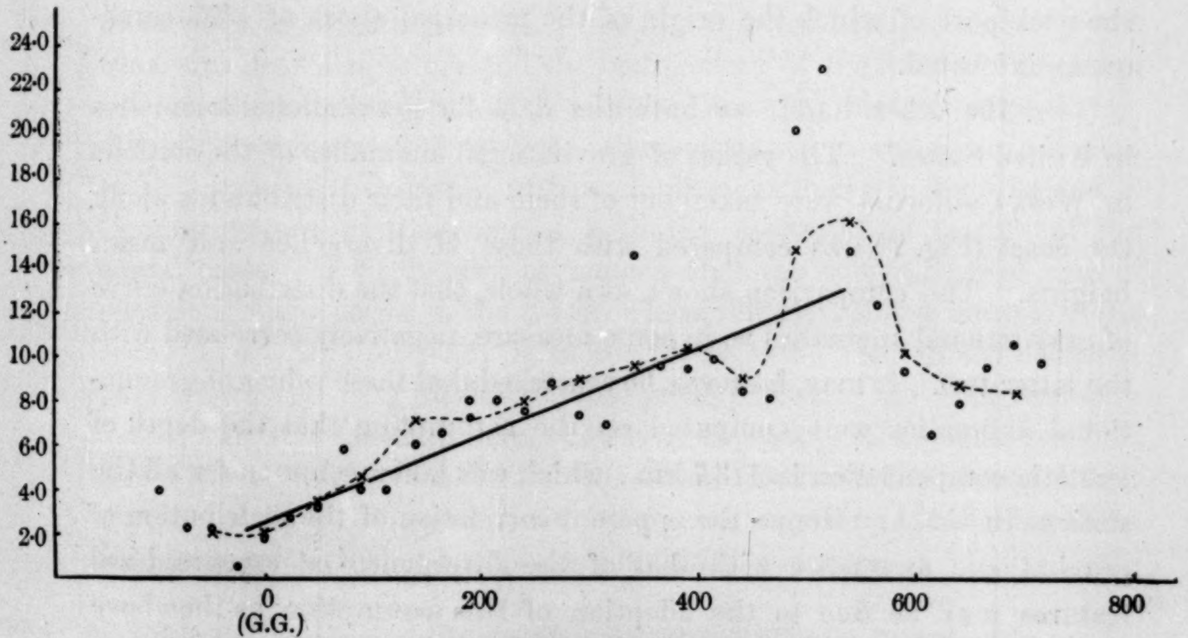
24·0
22·0
20·0
18·0
16·0
14·0
12·0
10·0
8·0
6·0
4·0
2·0
0
(G.G.)
200
400
600
800
Distance (km.) to the South.

Fig. 6b.

requirement of the theory of isostasy,[7] if the divergence may be associated with the actual density change of the crust.

Some evidences for the actual crustal movement in this region are supplied from the observations on upheaval and depression of the crust at the time of the earthquake of 1906. Professor Omori and other American authorities observed in various places near the Tomales Bay and Bolinas Lagoon that the crust was depressed on the eastern side of the San Andreas fault relative to the western side of it, by one or two feet at most. This relative upheaval of the west side of the fault near the San Francisco Bay may be considered to agree in some measure with our expectation, though such an evidence alone is not sufficient to determine whether the region AB is really rising or not. It may, however, be interesting to add here that those regions which should be raised to some extent from the analogy of the other examples to fit for the observed divergence, seem liable to be attacked by earthquakes. We have the same experience in the case of Tango earthquake of 1927. In that case, to make the distribution of divergence coincident with the topographical features, Tango-Peninsula should have been raised a little more,[8] in the neck part of which the origin of the principal shock of 1927 earthquake is located.

On the other hand, we have the data for gravitational anomalies in United States.[9] The values of gravitational anomalies of the stations in West California were taken out of them and their distributions along the coast (Fig. 7) was compared with those of divergence and mean heights. The comparison shows, as a whole, that the distribution curve of gravitational anomalies is, in some measure, negatively correlated with the latter two. It may, however, be remarked that these values of gravitational anomalies were computed on the assumption that the depth of isostatic compensation is 113.7 km., which was taken common for all the stations in U.S.A. Hence, the apparent correlation of the distribution of gravitational anomalies with that of the divergence or topographical features may be due to the adoption of this assumption, as the above depth may be unsuitable for the limited localities under consideration.

---

7) T. TERADA and N. MIYABE, *Proc. Imp. Acad.*, (1928), 218.
8) T. TERADA and N. MIYABE, *loc. cit.* 2)
9) W. BOWIE, *Special Publication of Coast & Geodetic Survey, U.S.A.*, No. 99 (1924).

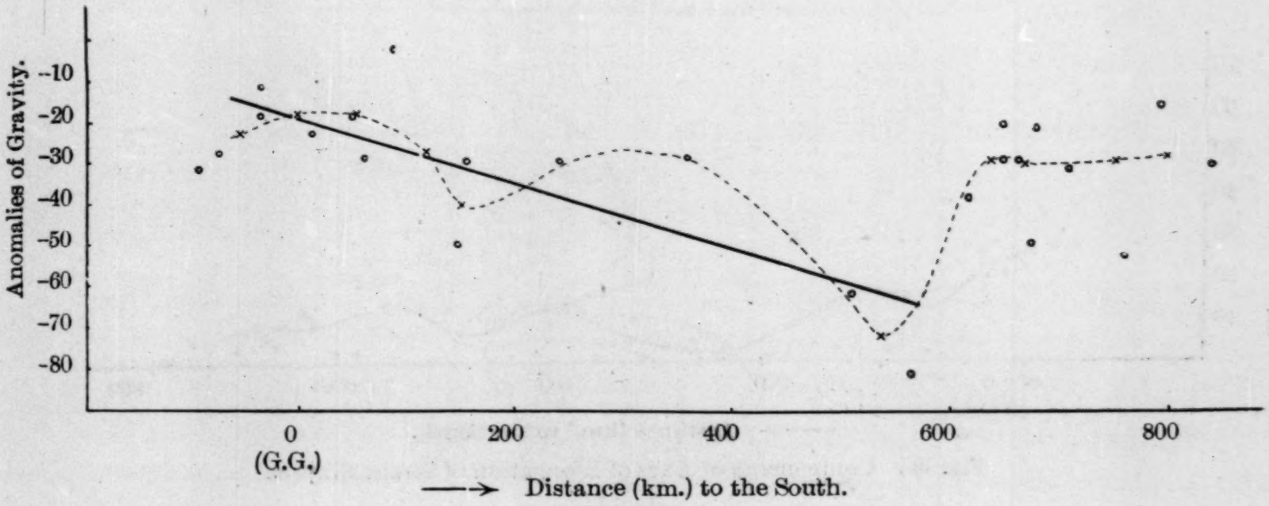

Fig. 7.

Principal Axes of Strain Ellipses and Feature of Coast Line.

We have already noticed that strain ellipses with longer axes of elongation and those with longer axes of contraction are distributed alternately in adjoining regions. A line approximately parallel to the coast was drawn as before and the components of the axes of elongation and contraction perpendicular to this line were plotted respectively, along the approximate coast line. Fluctuations in these two curves seem to be correlated negatively with each other, as shown in Figs. 8a and b. Comparing one of these curves with the geographical feature of the actual coast (Fig. 5), it may be noticed that the components of axes of contraction are larger in the region where the coast line is convex to the ocean side. This tendency is more clearly to be seen in the northern part where the magnitudes of the principal axes are comparatively larger. In the southern part, however, especially along the coast of Santa Barbara and San Pedro, the above mentioned tendency is not quite apparent. At present, we cannot say anything about what these facts may mean, without some more material evidences.

Formal Analogy with the Cases of Some Elastic Deformations.

The principal axes of the strain ellipses above obtained are joined by a system of continuous curves in such a way that the axes of contraction and those of elongation are connected respectively into lines of contraction

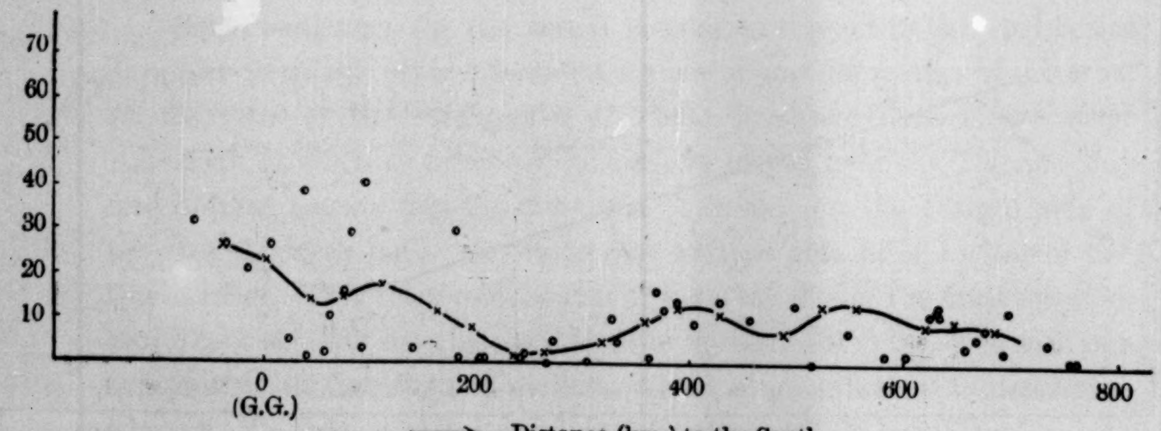

Fig. 8a. Components of Axes of Elongation of Strain Ellipses.

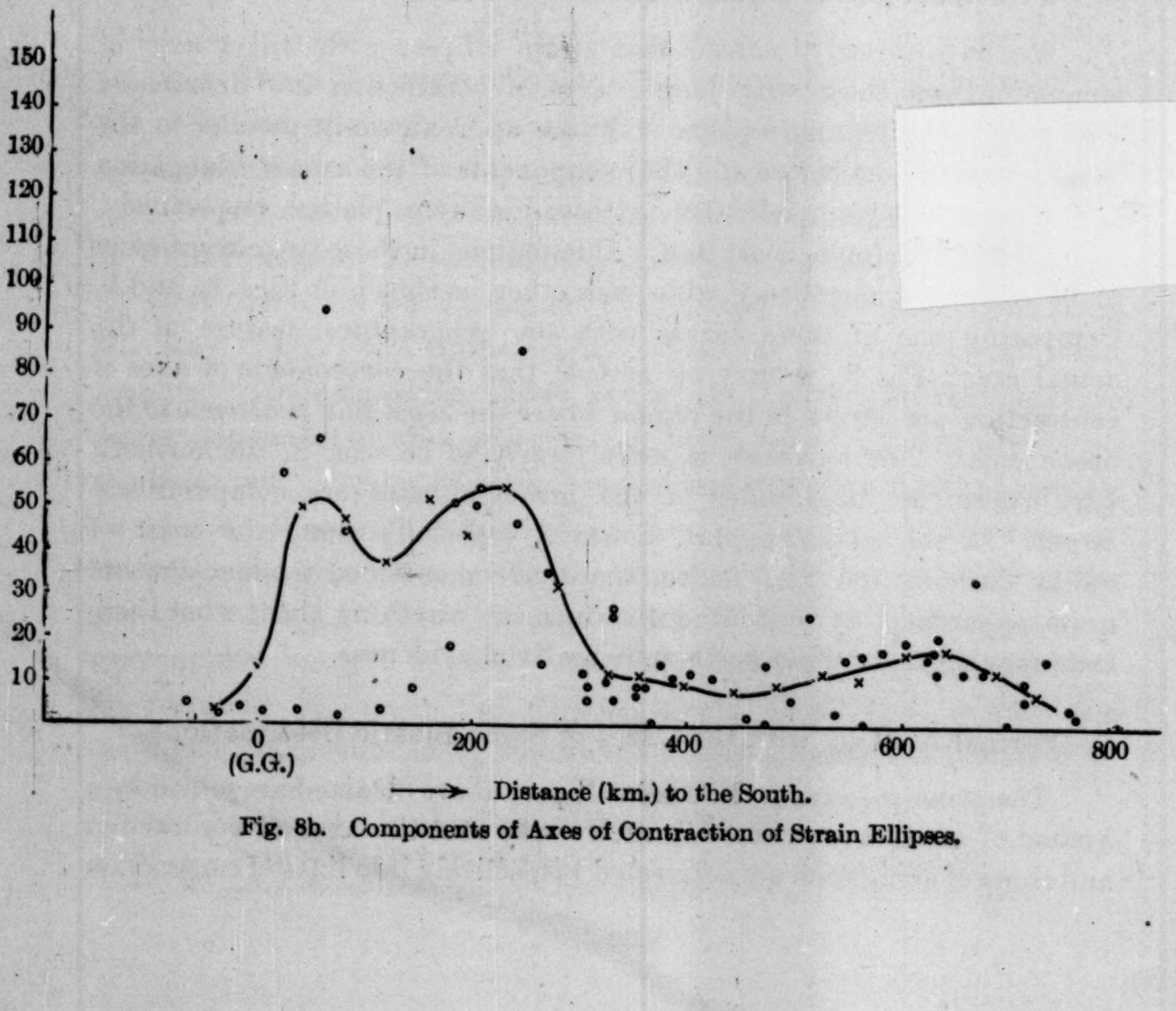

Fig. 8b. Components of Axes of Contraction of Strain Ellipses.

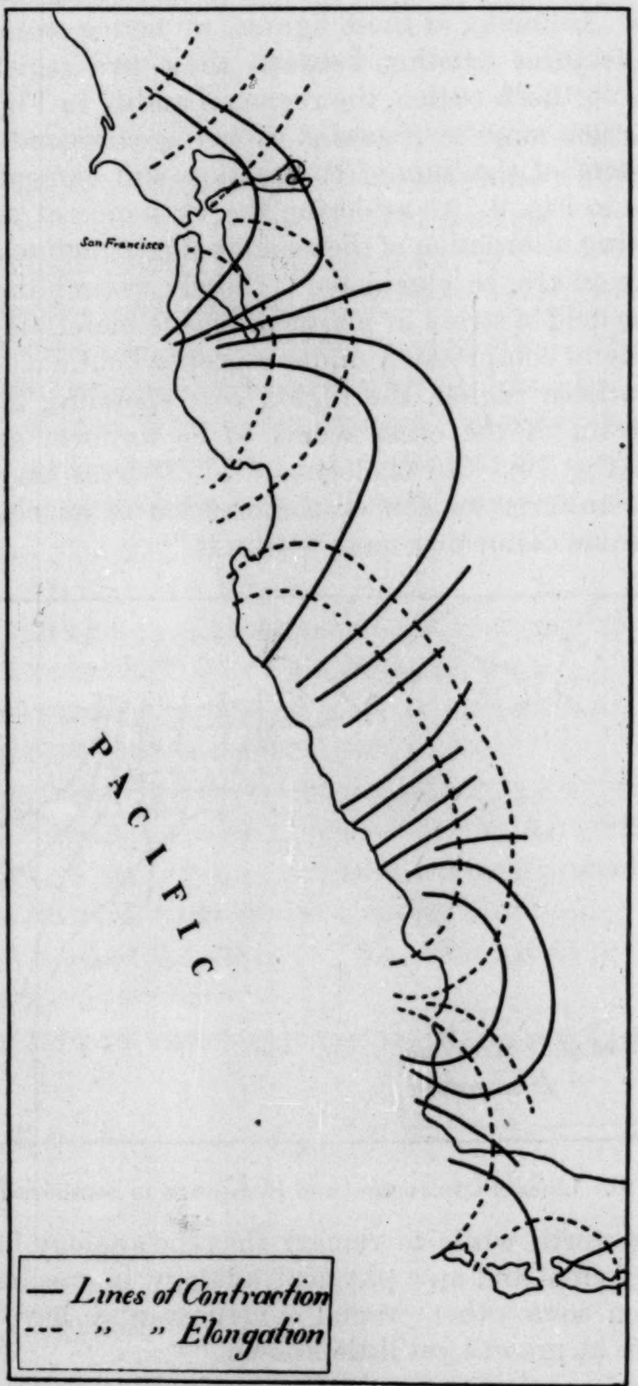

Fig. 9. Lines of Contraction and Elongation in Northern Part.

and elongation, to make up a diagram something like the diagrams of the fields of elastic strain or stress of some deformed materials as shown in Figs. 9 and 10. Glancing at these figures, we notice some characteristic differences of features existing between these two regions, north and south. In the northern region, the regions I and II in Fig. 4, the field of strain of the crust may be regarded as being composed of a coherent orthogonal system of the lines of contraction and elongation, of such a typical form as in Fig. 9. Considering the existence of such system of strain, the existing alternation of the regions of contraction and elongation may, in some measure, be elucidated. Closely resembling features may be shown in the field of stress in plastic or elastic materials when they are exposed to a lateral compression under a proper boundary condition.[10]

In the southern region, the region corresponding to III in Fig. 4, the field of strain of the crust seems to be uniform excepting some disturbed area (Fig. 10). An analogous field of stress may be produced by applying a uniform tension or compression to an elastic or plastic material with some disturbing mass within it.[11]

Fig. 10. Lines of Contraction and Elongation in Southern Part.

It may be worth while to remark that the analogy here mentioned is nothing but formal and any physical analogy in mechanism may be cited only when some other crucial evidences may have been brought forth, which are at present yet little known.

In conclusion, the present writer wishes his sincere thanks to Professor Torahiko Terada for his kind advices and guidance.

10) Some stress diagrams closely resembling to the field of strain of the crust here shown may be found in Th. WYSS's "*Kraftfelder in festen elastischen Körpern*" (1926), Tafel 33.

11) c.f. Tafel 26 of WYSS's "*Kraftfelder* etc."

3. カリフオルニアに於ける地殼の變形

地震研究所 宮部直巳

W. Bowie によつて調査されたカリフオルニアに於ける 1906 A.D. の地震前後の三角點の移動の結果について、著者等が、丹後地震の際の三角點の移動を取扱つたと同様の方法を應用し、Divergence, Rotation, Shear, Strain ellipse の主軸等の諸量を計算してその地理的分布を調べてみた。その結果は取纏めて次の如く約言することが出來る。

i) Divergence と地形との關係は大體に於いて、前と同樣に高い所が正の Divergence, 低い所が負の Divergence の傾向を示してゐる。たゞ San Francisco 附近は、地形の方でもう少し上昇すれば、尙よく一致するのであるが、將來この附近の土地がもう少し上昇して Divergence の示す傾向に追隨すると考へれば、丹後半島が同樣の傾向を示してゐた事と一致し、問題の地震がその附近に起つた事も偶然にも合致する。併し、現にこの地方が上昇しつゝあるといふ、直接の證據は擧げられない。重力殘餘の値の分布も之に負の相關を示す樣に見えるが、之は補正した平衡層の厚さの 113.7 km. といふ値が、(113.7 km. は全米に一樣な値) この地方のみに對しては不適當な爲めの見掛け上のものではないかと思はれる。

ii) Rotation の分布を見ると、左旋と右旋の地域が交互に存在するかの如く見え、嘗て、藤原教授の指摘された地形の渦の形成の途上にあるものの如き感を與へる。

iii) Shear は、三角網中 San Andreas の斷層の過つてゐる地方で大きく、他では小さい傾向を示し、三角點移動の分布より想像される所と大差はない。

iv) Strain ellipse の主軸の海岸線に略々直角なる方向の成分をとつて考へると、その大いさの fluctuation が、elongation の軸のそれと、contraction の軸のそれとで負の相關となる。又、是等と、海岸線の出入とを比較してみると、elongation の軸の成分の比較的大なる處では海岸線が內陸に灣入し、その小なる處では海の方へ突出してゐる傾向が見える。

v) Strain ellipse の分布の狀態は一瞥した所、ある plastic 又は elastic の物質がある歪を受けた場合のその中の力の場に似たものがある。

以上の如き事實が如何なる事を意味するかについては、更に多くの事實が見出されるまでは明かになし得ない。

4. *On the Nature of Destructive Earthquakes.*

By Torahiko TERADA,

Earthquake Research Institute.

(Read Sept. 25, 1928.—Received Dec. 20, 1929.)

From the usual seismometrical point of view, i.e. of an observer equipped with a sensitive seismograph as his exclusive means of observation, an earthquake may appear as a simple phenomenon of propagation of elastic waves originating in a geometrical point. The normal trends of the lines of equal intensities are to be represented by a system of curves more or less resembling concentric circles, and otherwise the cases would be called anomalous. On the other hand, the common people in their civil life are little concerned with such an wave phenomenon as long as it involves no material loss of their properties. What they are interested and afraid of are not the elastic vibration of their houses which leaves no trace when it is over, but a few number of shocks which destroy their belongings before the lapse of a few seconds.

It is, indeed, in the cases of such destructive earthquakes that the usual seismometrical analysis loses its significance and the location of so-called epicentre becomes at once ambiguous and irrevelant. Prof. Imamura, in his recent paper[1], emphasized the multiplicity of the origins of disturbances in the case of the great Kwantô Earthquake of 1923. Such a multiplicity of source may be taken as the common characteristic feature of any destructive earthquake of importance.

Though the Kwantô Earthquake of 1923 and also the Mino-Owari Earthquake of 1891 may be counted among the severest shocks experienced since the dawn of seismology in this country, they are by no means the typical examples of the large-scale earthquakes which have ever been recorded in our history. The formers may rather be regarded as the examples of local destructive earthquakes of remarkable intensities, if we compare them with the cases of Hôei (1707) or Ansei 1, December (1854) which were of so vast scales that we are at a loss to designate them by the names of some definite localities as in the cases of Mino-Owari, Kwantô, or Tango Earthquakes. In these cases of "panseismic" disturbance the usual seismometrical methods will, at the best, be overburdened

1) A. IMAMURA, *Proc. Imp. Acad.*, 5 (1929), 330.

with too large number of unknowns to be deduced from rather scanty and irrevelant materials available, especially because the present seismometrical observatories are poorly equipped with the megaseismic instruments.

For these reasons, it seems plausible and even urgent to attempt to regard the phenomena of destructive earthquakes from a stand point widely different from the usual one of the seismometrical seismologists and more akin to that of a layman concerned only with the gross effect of destruction.

In the "macroscopic" view which ignores the elementary "microscopic" mechanisms, the only *observable* thing is the ultimate effect of destruction, i.e. the irreversible change left after the shocks. Any elastic vibration of the mechanical system, leaving no trace after its passage, entirely escapes the observation of such a macroscopic observer. At present, the macroscopic data in the above sense are mainly afforded by the statistical materials regarding the damage of buildings of different kinds, and, in some cases, supplemented by the records of land-slide, earth fissure etc.

It was, indeed, the frequent usage of seismologists to draw the lines of equal intensities of shocks according to the statistical degree of destruction referred to buildings of some similar type, say ordinary living houses of wooden construction. This method, though encumbered with considerable difficulties in its practical application, is theoretically quite justifiable, and is probably the only possible one for the present in the hand of the macroscopic seismologist above mentioned.

Suppose a building consisting of N mechanical elements which contribute to the strength of the building against its usual modes of loading and some extra-loading such as due to wind pressure. The degree of destruction may then be measured as a suitable function of the ratio r of the number n of those elements which are made ineffective by the earthquake, to the total number N of the elements. On the other hand, the degree of destruction may be assumed to depend on the following quantity with respect to the earthquake motion,

$$S=\int_0^\tau |\alpha-\alpha_0| \cdot dt,$$

where α is the acceleration of the ground, α_0 a constant, t the time and τ the total duration of the earthquake. We may assume that the mean value of the above ratio $r=n/N$ over a large number of similar houses in a certain local area is a definite function of the quantity S as above

defined, though the functional form may vary with the types of building and probably also of earthquake. Thus, if we draw the lines of equal r for successive values suitable chosen, the general trends of these lines will coincide with those of the lines of equal S. Our experiences show that the effective destruction is accomplished by a few number of shocks at the initial stage of the main disturbances. We may, therfore, take S as a definite function of the maximum acceleration α_m of the whole train. Thus,

$$r=\frac{n}{N}=f(S)=\phi(\alpha_m)$$

and

$$\frac{df}{dS}>0, \qquad \frac{d\phi}{d\alpha_m}>0.$$

These considerations, though very crude and essentially of no novelty, may illustrate the theoretical feasibility of taking the lines of equal percent damage of wooden houses as the indicator of the macroscopic distribution of the intensity of seismic disturbance.

The present case is in some measure analogous to the case in which the distribution of the light energy incident upon a photographic dry plate is determined by the photometrical measurement of the " blackening " after developing of the plate. In the latter case, the ratio of the number of the reduced silver grains to the possible total number may be taken as a measure of the time integral of the light energy, provided that the colour of the light is given. Similar consideration of " colour " is wanted in the case of earthquakes, as the same S may give different values of r for different types of earthquake. The local characteristics of the type of building may then correspond to the characteristics of different sensitive plates. Fortunately, the type of building, or the mode of statistical distribution of the different types of building is not much different in the different parts of a district of such an extent as is generally involved in a destructive earthquake. Moreover, the " spectrum " of earthquake disturbances may probably be assumed as largely similar for the area of the maximum destruction, as least for a given earthquake.

2. In order that the investigation of the macroscopic intensity distribution as above defined, may be carried out efficiently, we must be furnished with very exhaustive data. One of the typical examples is afforded in the case of Kwantô Earthquake, by the investigation of Dr. Matuzawa.[2]

2) T. Matuzawa, *Rep. E. I. C.* (Japanese), 100 A (1925), Fig. 7 opposite p. 34 for the Kwanto District, and Fig. 56 facing p. 48 for Tokyo City.

Another beautiful example is shown in the report of Prof. Yamasaki and Dr. Tada[3] on Tango Earthquake. Somewhat earlier cases are illustrated in the papers of Prof. Imamura[4] regarding the Earthquakes of Hamada (1872), Rikuu (1896), Senhoku, Akita (1914) etc.[5] Glancing at the maps given in these papers showing the detailed outlines of the meizoseismal regions, i.e. the areas of greatest S in our sense, they are very far from being of an oval shape as was conceived in the earlier days of seismology. It seems much more plausible to regard the areas to consist of a number of narrow bands, sometimes connected or intersecting with, and sometimes detached from each other. In some of these cases, conspicuous active faults were actually located along the axes of the band-like areas. In other cases, these axes were identified with some remarkable structural lines revealed by geological and topographical observations, or discovered as the results of repeated precise levellings.

The results of the recent investigations in various lines which were and are being pursued by the members of this Institute, seem to conspire in bringing the real seismological significance of the so-called block structure of the crust under an ever-increasing light. The important bearing of such units upon the general crustal movements and the occurrence of earthquakes connected with these movements can scarcely be doubted. Though the idea of "rigid" blocks subjected to rather haphazard motions may be rather artificial and conventional, it is beyond doubt that the deformation of the earthcrust such as is important in geophysical and seismological problems is neither concentrated in a small spherical region nor continuously distributed, even approximately, as in the case of elastic problems of infinitesimal deformations. The well known laboratory experiments of Kârmán, Nadai etc. and also those of Sachs and his collaborators[6] have shown that the *finite* deformation beyond the limit of elasticity occurs *localized* in a system of slip-planes or zones of deformation, while the strains of the other parts are relieved by the formation of such system of maximum strain. The present authors[7] has also shown that the same holds even in the case of the loose mass such as a pile of sand.

3) N. YAMASAKI and F. TADA, *Bull. E. R. I.*, **4** (1927), Pl. 17.

4) A. IMAMURA, *Rep. E. I. C.* (Japanese), **77** (1913) and **82** (1915).

5) For an example of Europea earthquake, see SIEBERG's "*Erdbebenkunde*" (1923), p. 107, Fig. 53 and p. 492.

6) For examples, G. SACHS u. E. SEIDL, *Naturwiss.*, **13** (1925), 1032; E. SEIDL, *ZS. deutsch. Geol. Ges.*, **77** (1925), Nr. 3.

7) T. TERADA and N. MIYABE, *Bull. E.R.I.*, **4** (1928), 33; **6** (1929), 109; **7** (1920), 65.

It is in the immediate vicinity of this slip-plane or zone of maximum deformation that the most energy is consumed in the irreversible non-elastic deformation. The results of the precise levellings in the cases of earthquakes of Oomati, Tango, Kwantô etc. furnish us with many examples in which the vertical displacements show striking *marginal effects* at the points of junction where the levelling route crosses the boundaries of the supposed blocks. The curve of the vertical displacements plotted along the route frequently makes a sudden kick, upward or downward, in the immediate neighbour of an identified fault or a zone of maximum shocks.

In short, from the macroscopic point of view as is here represented, the destructive earthquakes with which we are exclusively concerned in the present paper, are the marginal phenomena of the block motion of the crust and the chief site of the disturbances is localised in a system of narrow zones lining the boundary surfaces of the blocks.

This way of regarding the matter, if of no great novelty,[8] can now be emphasized with the strong support of the material evidences and if once accepted, may have some important bearings upon the interpretation of different facts connected with the phenomena of destructive earthquakes. For example, the data of the historical earthquakes may now be reviewed under a light considerably different from usual.

3. The historical documents of the past severe earthquakes, when reviewed under the new light, seem to present some aspects utterly different from those depicted by our forerunners who were obliged, with right in their days, to be satisfied with drawing more or less oval curves for vaguely marking out the meizoseismal areas. One of the few examples in which the complicated branched form of the meizoseismal area is shown for a historical earthquake, is the case of Kôkwa or Zenkôzi Earthquake of 1847, investigated by Prof. Omori.[9] In this case the number of reliable documents is very large so that he was able to construct a map for the area of maximum destruction with a degree of accuracy somewhat akin to the cases of the recent great earthquakes. Another examples may be shown from the results of the valuable inves-

---

8) The idea of the seismotectonic lines or *Erdlineamente* as the boundary lines of the block structure is by no means new (see, for example, Hobbs-Ruska's "Erdbeben" Cap. VI), but it seems to revive with entirely fresh aspects under the light of the recent strong evidences, especially those afforded by the results of the repeated precise levellings in different regions of this country. What was scarcely more than a suggestive hypothesis appears now as an established fact.

9) F. Omori, *Rep. E. I. C.* **68** B (1913); *Bull. E. I. C.*, 2_2 (1908), 136.

tigations by Prof. Imamura for the case of the "Summer Earthquake of Ansei" and also the cases of more recent earthquakes of Hamada etc. already cited.

Before entering into the investigation of the other historical earthquakes, the Zenkôzi Earthquake of 1847 above cited was chosen for our first example to see if any modification was possible of the map of Omori when reviewed from the present point of view. The data were mainly taken from Dainihon-Disin-Siryô[10] and supplemented by a few others, among which may be mentioned some old wood-cut prints showing the distribution of damaged areas. The percentage values of totally or half destroyed houses could be estimated, very satisfactorily in some districts but only very roughly in the others, from the abundunt documents both official and private. The records are insomuch reliable as any severe damage is recorded in more than one documents however remote and secluded the locality be and, moreover, the localities with no great damage are particularly named in this or that document.

The results of investigation are shown in Fig. 1 in which the area

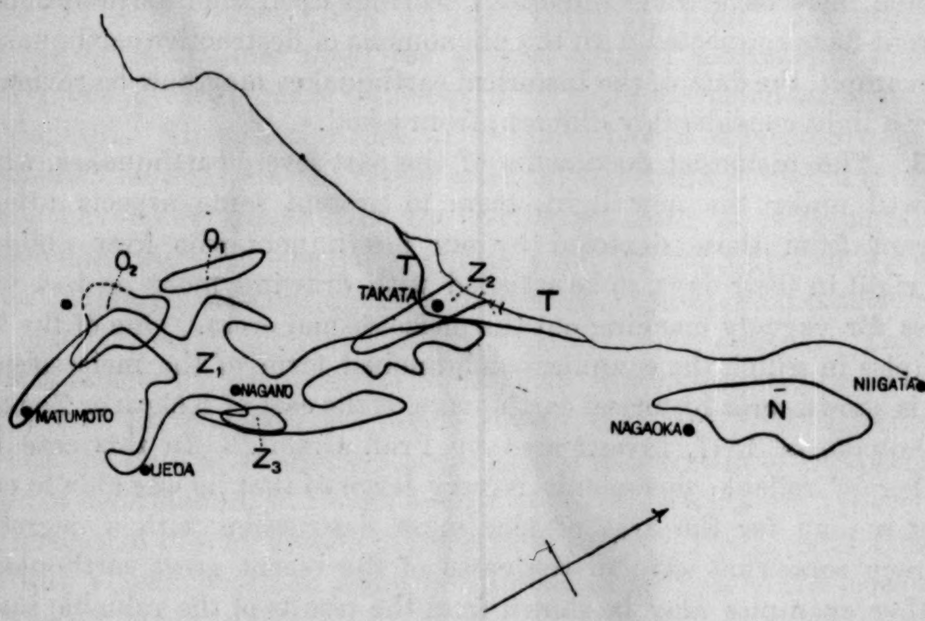

Fig. 1.

with above 50% destruction is outlined by the contour Z_1. The area marked with Z_2 corresponds to the earthquake which shook Takata district on the next day, 9 May, of the Zenkôzi Earthquake 8 May, 1847. It will be seen that our result agrees with Omori's in general features,

10) *Rep. E. I. C.*, 46A and 46B (1904).

though differing in many minor details. The peculiarly branched shape of the disturbed area, reminding us something like the outline of Celebes Island is noteworthy, and gives us a vivid mental picture of the block system of the district. It seems difficult to explain such a form of the meizoseismal area without assuming the block structure or something like that.

Though in Fig. 1 the topographical contour lines are dispensed with, it will be remarked that the meizoseismal area agrees by no means with the area of the densest population or with the topographical depression zone as might be expected from a superficial consideration. Some of the branches of the destructive zone run across the mountainous regions with only sparse population, while some parts of the low alluvial land with dense populations fall in with the safty zone lying between the adjacent destructive zones.

In Fig. 1 are also drawn the outlines of some remarkable destructive earthquakes recorded in the region covered by this map. O_1 refers to the so-called Oomati Earthquake of Syôtoku (1714) and O_2 to the more recent Oomati Earthquake of 1918. T is the Hôreki (1751) Earthquake in Takata district in which case the destructive zone is seen to coincide with the coast line, suggesting, as in many other cases, that the coast line forms here a conspicuous block boundary.[11] For the Nagaoka or Sandyô Earthquake of Bunsei (1828), denoted by N in the same Fig., the materials taken from Dainihon-Disin-Siryô could be supplemented by a very valuable documents in possession of Viscount Mizoguchi which was placed at my disposal by the kind intervention of Viscount Ōkochi. The demarcation of the meizoseismal zone in this case may be regarded as particularly accurat on this account. The recent Sekihara Earthquake (1927), which was of very limited extent, occurred just at the SW extremity of this elliptic zone N. The networks formed by these different destructive zones will give a general trend of the seismically active structural lines of this region.

For the next example, the most notorious case of Ansei Earthquake of 23–24, 25 December 1854, was taken. The disturbance of the earth crust on this occasion was of so wide an extent that the gross outline of the area affected in the course of the three successive days covers about ten degrees of longitude, involving about half length of the main island, Honsyû. Fig. 2 shows the distribution of the area of destruction estimated similarly as in the case of the Zenkôzi Earthquake, Fig. 1. The

11) Similar examples are also seen in Fig. 4.

different modes of hatching are used for distinguishing the days on which the respective zones were disturbed. Such a picture of zonal distribution of destruction as is here depicted might scarcely have been accepted by the seismologists of the earlier days, but will appear more natural in our days than the traditional oval distribution.

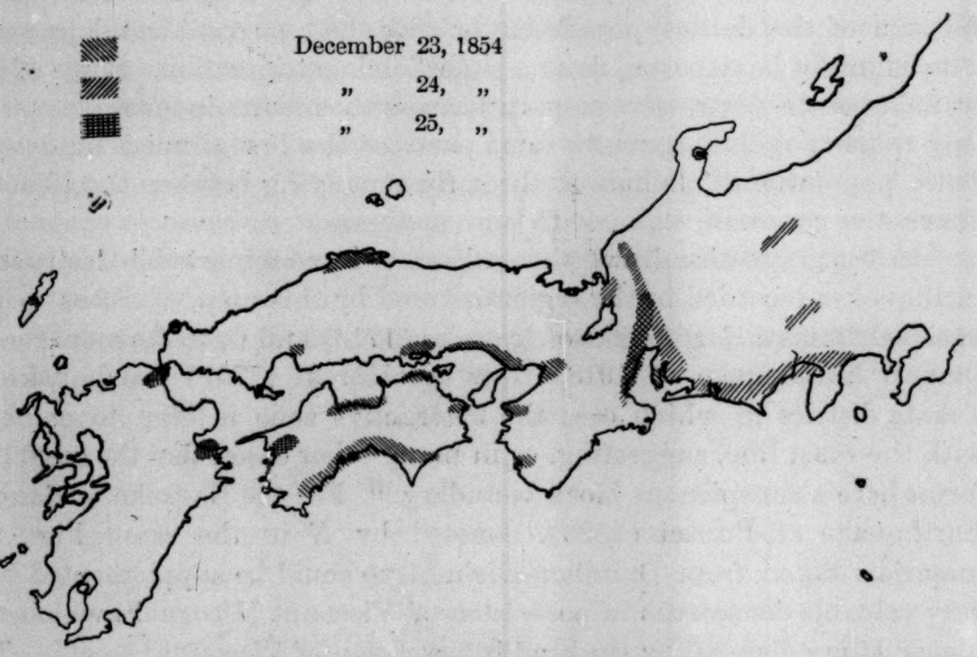

Fig. 2. Ansei Earthquake.

Among the rest of examples, one may cite the Kwanbun Earthquake of 16 June 1662 which shook the entire Kinai Districts. As shown in Fig. 3 by the shaded areas, I, II, III, IV, the destructive zones of this earthquake appear in a characteristic *échélon* form. As the region affected is in the vicinity of the metropolis of that age, the absence of records over any wide area with considerable population situated in the interspace between the destructive zones here depicted may probably be taken as an evidence of the comparative weakness of shocks in the corresponding area. Moreover, for the region separating the second and third destructive areas from the right (II and III), there are four local records of evidences for weakness of shocks. Again, it is interesting to observe that an isolated local spot of destruction is recorded in the Province of Mikawa, which is shown as an detached shaded area I to the right of Fig. 3. This

record was discarded by Prof. OMORI as doubtful, probably by the very

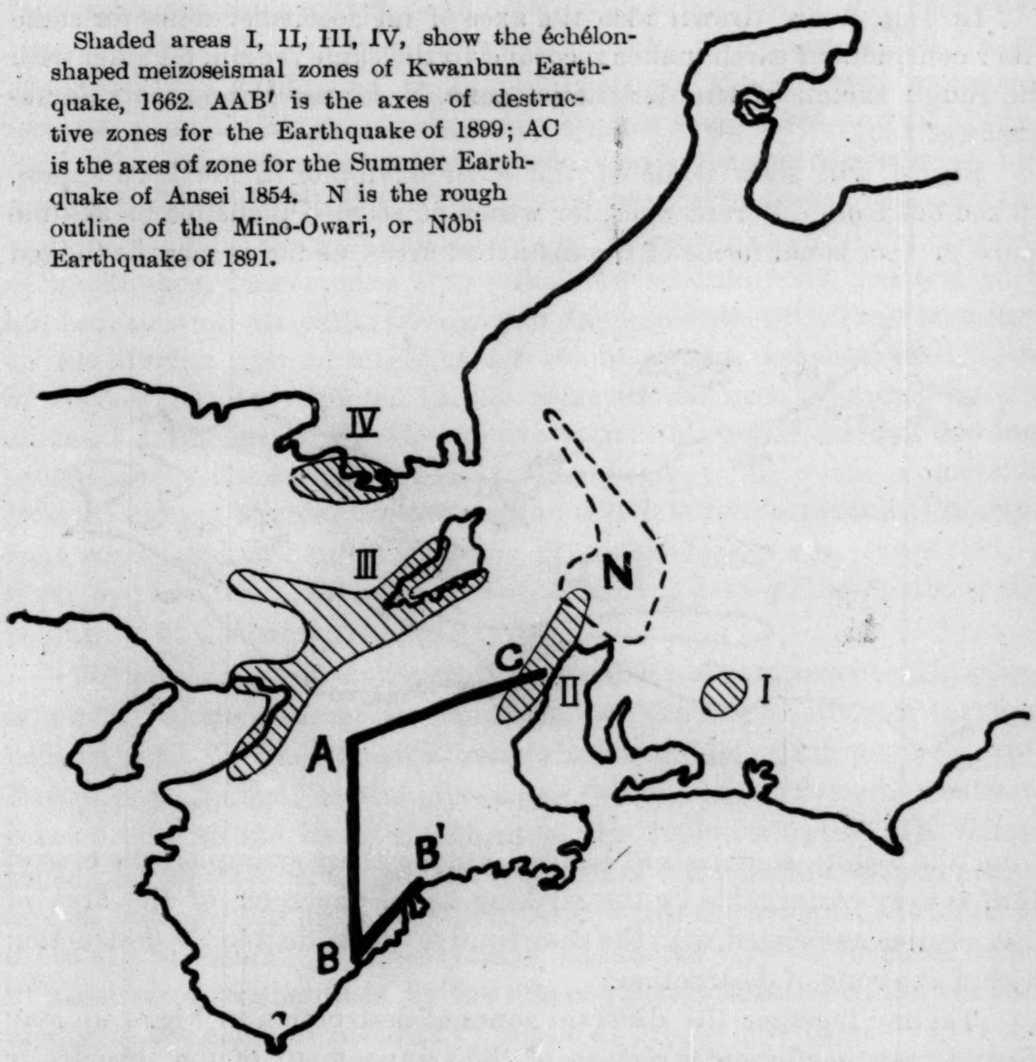

Fig. 3.

reason that it is isolated, but under the light of our present knowledge this singular spot seems to just supply the missed last step of the échélon.[12] Indeed, such an échélon form may also be seen in the case of Ansei

12) The traditional idea that a meizoseismal region should consist of a more or less oval singly-connected area, seems to have given rise to a tendency to neglect the isolated records. In view of the present author, however, it becomes especially important to search after the records of these detached areas of destruction, in order to locate the system of blocks involved in the crustal disturbances, which make up the entire macroscopic phenomena of the earthquake in question.

Earthquake shown in Fig. 2. and may be assumed as a common form in the cases of large-scale earthquakes.

In Fig. 3 are drawn also the axes of meizoseismal zones for some other conspicuous earthquakes recorded in the same region, together with the rough sketch of the destructive zone, N, for the Mino-Owari Earthquake of 1891.

Fig. 4 will show some of the other examples in Northern Japan, picked out from different ages, for which it seemed plausible to assume more or less zonal forms of the disturbed areas, as far as may be judged

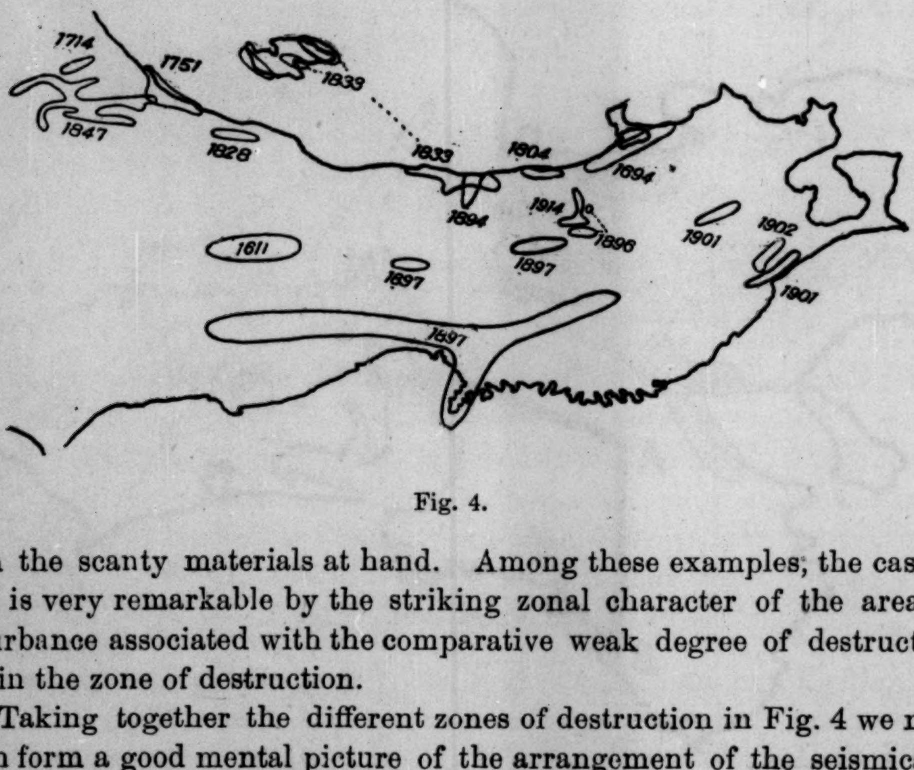

Fig. 4.

from the scanty materials at hand. Among these examples, the case of 1897 is very remarkable by the striking zonal character of the area of disturbance associated with the comparative weak degree of destruction within the zone of destruction.

Taking together the different zones of destruction in Fig. 4 we may again form a good mental picture of the arrangement of the seismically active lines in the Northern Japan.

4. It cannot be denied that in the majority of cases above cited the zone of damage coincides in some measure with the zone of depression in the topographical map. This fact has long since been generally recognized and usually disposed of by a superficial explanation either based on the weakness of the alluvial ground or on the density of population characterizing such depressed areas, and the deeper physical significance of this remarkable fact has rarely been inquired, except by late Prof. Kusakabe who in his very original but forgotten paper, "An illustration of seismic wave conductivity in forming past Japanese towns", pointed

out a possible physical connection between the geographical conditions favourable for the development of a town and the geophysical conditions favourable for the occurrence of destructive earthquakes. His explanation of the relation was essentially based on the difference of the "wave conductivity", as defined by himself, between the different geological formations, and, though may be partly true in some cases, cannot always hold, since there are examples in which no difference of geological formation is discernible between the zone of maximum destruction and the neighbouring district with small damage. Moreover, the striking example of the Zenkôzi Earthquake shows that the mountainous districts with hard substratum can suffer the severest damage while the village standing on an alluvial ground might escape the maximum destruction, in spite of the fact that it is situated in the midst of an area bounded by the adjacent branches of the destructive zone. Moreover, in his "conductivity theory" the damage is considered to be due to the waves propagated from a distant source, an assumption which is fundamentally different from what is taken here as the basis of consideration and supported, I hope, by the substantial evidences of the recent dates as mentioned at the beginning of the present paper.

Without denying, however, the possibility of some eventual application of Kusakabe's theory we can formulate the explanation of the fact pointed out by his keen insight somewhat in the following manner: (a) Destructive effects of earthquakes are localised along a system of narrow zones proper to the block structure of the region affected. (b) These zones generally coincide with the boundaries between the adjacent blocks and on that account agree most frequently with the conspicuous faults or zones of depression. (c) These active boundaries may be detected, even in absence of earthquakes, by the marked discontinuities in the vertical motion of the earth as revealed by repeated precise levellings. (d) If the topographical zones of depression are favourable for the development of dense populations, a locality to which a number of such zones is confluent is, on one hand, the point to which the highways of the local communication converge and, on the other hand, the very spot which is most frequently threatened by destructive earthquakes.

5) The modification in the concept of the nature of destructive earthquakes, as was here dwelt upon at some length, seems to bring with it a demand of applying some revision to our traditonal idea concerning the so-called seismic zones.

A seismic zone is usually considered as an ideal lines connecting the

positions of the possible epicentres which are arranged on a continuous line with its radius of curvature not very small compared with the earth's radius. This conventional way of regarding the matter was, it cannot be denied, very fertile in the early stage of development of seismology. It seems, however, that we may now break off from this traditional way and adopt another which, though perhaps equally conventional, may far better conform with the recent status of our knowledge.

To quote only the results of Dr. Nasu's investigations,[13] the entire system of possible origins of the minor earthquakes recorded in Tango District seems to be arranged on a system of intersecting planes or surfaces which strikingly resembles to the system of slip-planes formed in some plastic bodies strained above the limits of strength.

If the small earthquakes as investigated by Nasu are associated with small blocks with a linear dimension of a few km., the phenomena of the earth-sound, as frequently observed in the vicinity of Mt. Tukuba, are probably connected with still much smaller blocks of the granitic rock. On the other extremity of the *scale* may then be placed those large blocks associated with the destructive earthquakes of considerable extent as are here concerned.

It may, indeed, be shown in different ways at least qualitatively that the total energy flux near the epicentre as measured by the time integral of the kinetic energy obtained from the seismogram must increase with the linear dimensions of the blocks concerned, whether the energy be due to the liberation of the gravitational or elastic potential energy.

Thus, the site of the strong earthquakes may better be associated with a coupled system of active blocks, instead of a locus of points. It is pertinent to study the spatial distribution as well as the modes of mutual linkage of these active blocks. Some studies in this direction have already been effectively carried out by the members of our Institute. As, however, the great-scale earthquakes such as those of Ansei are fortunately, or unfortunately, very rare, it seems worth while to attempt to reconstruct the distribution of such active blocks for the cases of the historical earthquakes as is here attempted. Though the task may in some cases be akin to that of a palæontologist trying to reconstruct a prehistoric mammals by means of a jaw-bone and some teeth. For this purpose, therefore, the accumulation of as large number as possible of the historical documents is highly desirable. It was one of the chief aim of the present note to

13) N. NASU, *Proc. Imp. Acad.*, (1929), 164; *Bull. Earthq. Res. Inst.*, 6 (1929), 245; *Journ. Fac. Sci.*, Tokyo, 3 (1929), 29-129.

demonstrate that these documents may be utilized quite effectively for the macroscopic study of the block structures, provided the ample materials could be obtained and those materials be treated properly according to some sound guiding principles based on our recent substantial knowledges.

To provide for the future destructive earthquakes of Ansei type, we may also propose the installation of some macroscopic or megaseismic instruments as urgent, which are able to record the quantity corresponding to r above defined somewhat better than the wooden houses. If such an instrument be distributed among the stations forming a sufficiently close net, we will not fail to obtain a far better macroscopic view of the phenomena than is just sheerly possible at present.

---

4. 破壊的地震に就て

地震研究所 寺 田 寅 彦

大規模の破壊的地震に際して家屋等の破損の最も著しい地域が帶狀の部分の集合から成るやうに見える。さうして此等帶狀地域の軸線が丁度地殼構造上の地塊の境界線に當る場合が多い。それで此の考を基として歴史的の大地震に關する史料を見直した。此等地震の場合の强震地帶の輪廓を畫いて見ると、そのやうにして求めた帶軸は矢張顯著な構造線と一致し、又或ものは現在でも活動して居ることが分かる。

大規模地震は稀にしか起らないから、將來に備へる爲には、過去の史料を出來るだけ蒐集し此れを現在の知識に照して研究することが可成大事な仕事の一つであらうといふので、玆には、唯その一つの試みを提出したのである。

此論文の見地からすれば、從來の大地震の震源地帶と稱するものゝ觀念に若干の變更を加へるのが便宜であると考へられる。

又さういふ大規模地震に就ては從來の驗震學的方法は余り有効でなくなると思はれるから、將來に備える爲に特別な驗震器を配置して置きたいといふ希望をもつて居る。

---

5. *On the Effect of Ocean Current, "Kurosiwo", upon Sea Level. Effect of Waves.*

By Seiti YAMAGUTI,

(Read Oct. 15, 1929.—Received Dec. 20, 1929.)

Effect of Ocean current.

In a previous paper,[1] the report was given of the result of the comparison of two curves of the monthly mean sea level for Aburatubo and Hososima corrected for the cyclonic factor=10 and 15 respectively, and it was shown that a parallelism may be observed between the two curves, at least for some months. This result may probably be due to the parallelism of the variations of water density in the two stations, which we may expect from the fact that the two stations are under the direct influence of the ocean current, "Kurosiwo."

To test this idea, a statistical investigation was made availing of the data comprising the values of the temperature and salinity of sea water at various depths, at a station 10 miles off Sionomisaki, in Kii, as well as another station 10 miles off Aburatubo, in Sagami, which were kindly placed at my disposal by Prof. M. Tauti of the Imperial Japanese Fishery Institute, Tokyo.

Firstly, the monthly mean temperature of sea water at the depth of 25 metres, 10 miles off Aburatubo, was directly compared with the monthly mean sea level at Aburatubo, corrected for the cyclonic factor=10, for the five years 1923–1927. Both the deviation of the temperature and the sea level, from the five year means of each month, were taken respectively and plotted in $\Delta T-\Delta L$ diagram as shown in Fig. 1.

Secondly, the density[2] of the sea water, reduced from the temperature and salinity at the depth of 25 metres, 10 miles off Aburatubo, was taken and similarly treated as shown in Fig. 2.

Thirdly, the values of the mean density of sea water reduced from the temperature and salinity at the surface and at the depth of 200 metres respectively, 10 miles off Sionomisaki, in Kii, were taken and compared with the sea level at Aburatubo. The data for the densities and the sea level, were quite similarly treated as in the preceeding two cases, as shown in Fig. 3.

Among 60 months taken, the observations of the temperature and salinity of sea water, were wanting in fifteen months, so that we were

1) S. YAMAGUTI, *Bull. Earthq. Res. Inst.*, 7 (1927), Part 3.
2) The effect of pressure in situ is neglected.

obliged to put 12 months out of account, though a few months could be approximately replaced by the data off Nozimasaki, in Awa.

In Fig. 1, 2, 3, the centres of gravity of the points, distributed

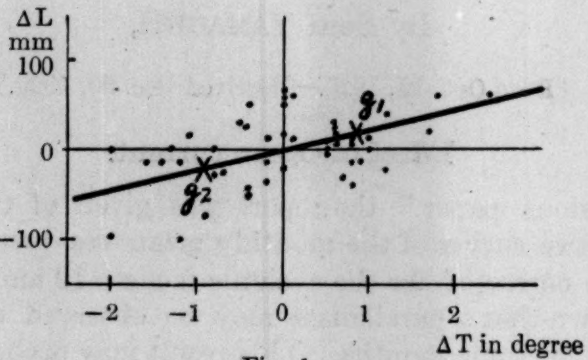

Fig. 1.

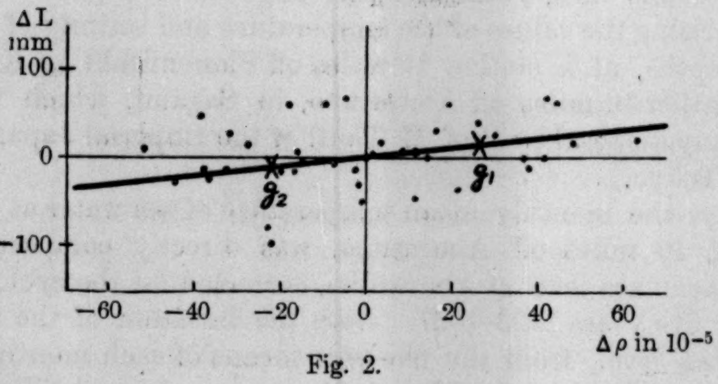

Fig. 2.

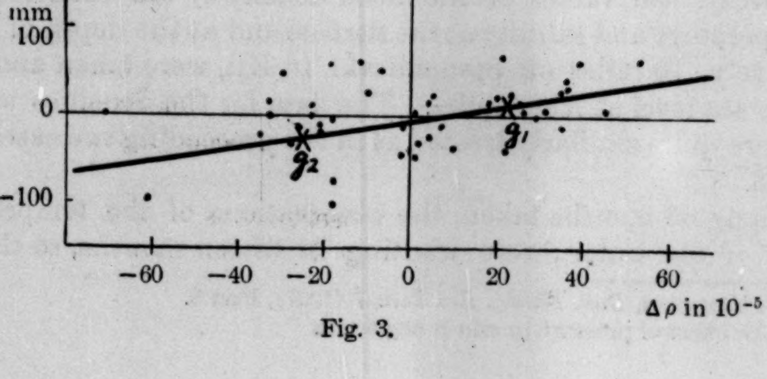

Fig. 3.

respectively in the right-hand side and in the left-hand side of the axis $\Delta\rho=0$, are denoted by g_1 and g_2, respectively. Drawing a straight line connecting g_1 and g_2, it is inclined to the axis of abscissa at a certain angle, and the points show a tendency to be rather widely distributed along this line on both sides. The straight line may be considered to show the effects of the anomaly in the oceanographical condition of sea water upon the sea level, as the effect of the regular annual variation of the density caused by the annual change of the meteorological conditions is considered to be eliminated already in the process of the above treatment. From the inclination of the line, we may obtain a ratio $\Delta L/\Delta\rho$, which may be called the "density factor" with respect to the monthly value. The factor thus determined roughly is 75, where ΔL is measured is millimetre and $\Delta\rho$ in 10^{-3}. If, on the other hand, we take the value of $\Delta\rho$ at Sionomisaki, instead of that at Aburatubo, we obtain a value of this factor still amounting to 50, which fact will suggest the effect of ocean current, "Kurosiwo", in govorning the anomaly of oceanographical condition along the Pacific Coast. The values of $\Delta L/\Delta T$ is estimated as 23, ΔT being measured in degree centigrade.

Though it is our ultimate aim to obtain the small residual values of the anomalies of monthly mean sea level after being corrected for the pressure, wind, cyclone and moreover for the temperature and salinity of water, we are at present obliged to give up the correction for the latter, as the data are wanting in 12 months among 60 months (1923–1927).

Next, we calculated the probable error, r, of the observed values of the monthly mean sea level, taking their deviations from the mean values for the five years above cited, and obtained the value of $r=52$ mm. We also calculated the value of r, taking the deviations from the 24 year mean for each month, and obtained the value of $r=32$ mm. Lastly, we calculated the probable error of the residual value of the monthly mean sea level after being corrected firstly for the cyclonic factor, and secondly corrected graphically for the density factor above explained, and obtained $r=23$mm.

These results show that, if we apply the corrections for the cyclone and for the density effect deduced from the scanty data for only five years, we may be able to get a decidedly smaller value of the probable error of the monthly mean sea level than that of the observed value, corrected merely for the average monthly variation deduced from the 24 year mean for each month. It will also be seen that the former value is less than half the value of the probable error of the observed value referred to the mean monthly values for the five years, with no correction for the

cyclonic and density effect. This will show the important significance of the said corrections.

Effect of Waves.

A recent investigation[3] of the present author regarding the abnormal rise of sea level in the Japan Sea Coasts of Etizen, Etigo and Ugo, on Jan. 2, 1929, has shown that at the time of the maximum rise of the sea level in the above region, the centre of cyclone had already passed over the Japan Sea area and was travelling on the Pacific Ocean near Hanasaki, in Nemuro, and that the change of the sea level could not be explained well by the direct influence of winds, and also that the effect of waves due to the cyclonic winds must be considered as one of the most important factors governing the variation of the sea level.

In connection with a further study of this latter effect, we tried to investigate the variation of the monthly mean sea level at Wazima, in Noto, comparing it with the corresponding barometer differences at various stations.

Before entering into this investigation, it was tested, if there might exist some sensible relation between the sea level at Wazima and the cyclone situated in the Pacific Ocean off the coast of Hanasaki, ignoring its direction of progress. The number, n, of the cyclonic days in the said region, was counted for each month from the Daily Weather Charts of the North Pacific Ocean, published by the Imperial Marine Observatory, Kôbe, for the five years (1923–1927). The doviation of n from the five year mean for each month was denoted by Δn. On plotting the deviation, ΔL, of the monthly mean sea level from the 25 year mean of each month, as ordinates, against Δn taken as abscissa, no systematic distribution of the points can be observed, though treated in the similar way as usual, showing no trace of sensible correlation suspected. Therefore, the cyclone in the Pacific Ocean off Hokkaidô affects the sea level at Wazima not merely by its position, but by the effect of its passage over the Japan Sea area.

Next, the diagrams were drawn with ΔL, above cited, as ordinates and the barometer differences, Δb, between (a) Sionomisaki, in Kii, and Aomori, (b) Genzan, in Korea, and Aomori, (e) Hamada, in Iwami and Akita, (d) Fuzan, in Korea, and Maoka, in Saghalien, respectively, taken from the Monthly Summary Report of the Central Meteorological Observatory in Japan, as abscissa, as shown in Fig. 4. In the diagram, the

3) S. YAMAGUTI, *Bull. Earthq. Res. Inst.*, 7 (1929), Part 3.

points, g_1 and g_2 are the centres of gravity of the points distributed in the right-hand side and in the left-hand side respectively of the axis of

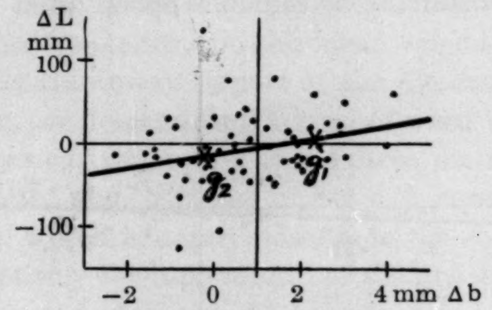

Sionomisaki and Aomori

Fig. 4a.

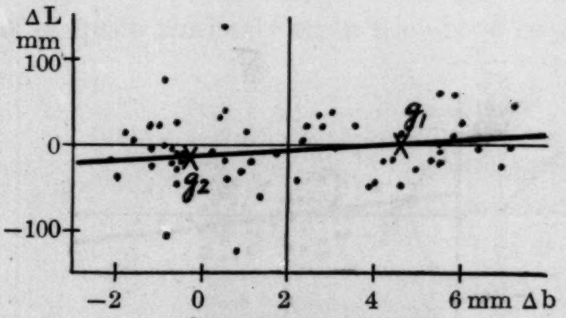

Genzan and Aomori

Fig. 4b.

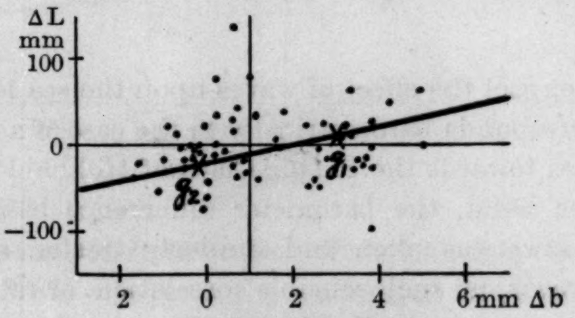

Hamada and Akita

Fig. 4c.

ordinates. The straight line, connecting the above two points, g_1 and g_2 is inclined to the axis of abscissa at a certain angle, of which the tangent is

considered to show the correlation factor between the sea level and the barometer differences.

When the barometric pressure in the region of Kinai and Tyûgoku is decidely higher during a sensible epoch than that in the region of

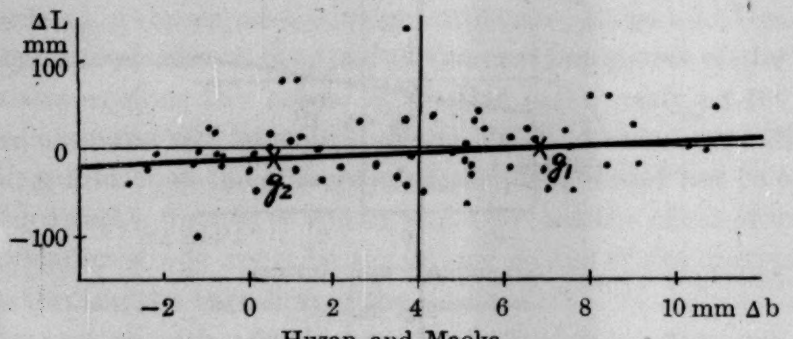

Fig. 4d.

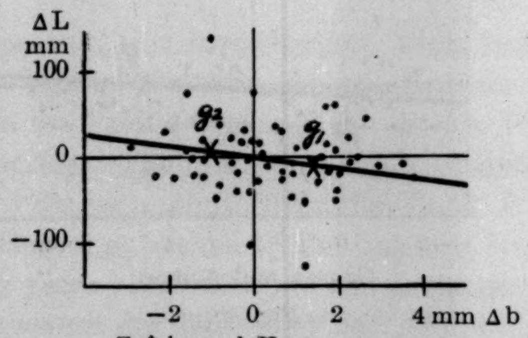

Fig. 4e.

Aomori, we may expect the effect of waves upon the sea level at Wazima, since the case corresponds barometrically to the case of a cyclone passing over the Japan Sea towards the Pacific Coast of Hokkaidô.

On the other hand, the barometer differrence between Zyôsin, in China, and Kanazawa was taken and similarly treated as before. The result shows, however, no such sensible correlation, or rather the straight line connecting g_1 and g_2, is inclined to the negative direction of the axis of abscissa at some angle as shown in Fig. 4e.

Unfortunately, the variation of the amplitudes of surface waves cannot be traced from the mareograms of Wazima, due to the ample damping of the tide-gauge, so that we were not able to undertake the direct

comparison of the amplitude of waves with the sea level of this station, and were obliged to take the data for the winds, instead of waves, under the assumption that the amplitude of waves at a station is a definite function of the wind velocity at a neighbouring station. Taking the direction of maximum frequency and the mean velocity of wind, which is given in the Monthly Summary Report of the Central Meteorological Observatory in Japan, as determining a kind of wind vector, the vector sum of the three vectors corresponding to the three stations, Miyadu, in Tango, Husiki, in Noto, and Niigata, in Etigo, is constructed and projected on NE-direction, which is nearly parallel to the coast line, and also on SE-direction respectively for each month of the five years (1923–1927). The average NE-component of the wind vector for the district being thus estimated, its deviation from the five year mean of each month was calculated and plotted in the diagram as abscissa, against ΔL above cited taken as ordinates, as shown in Fig. 5a. The straight line connecting the two points, g_1 and g_2 quite similarly as in the above cases, is inclined to

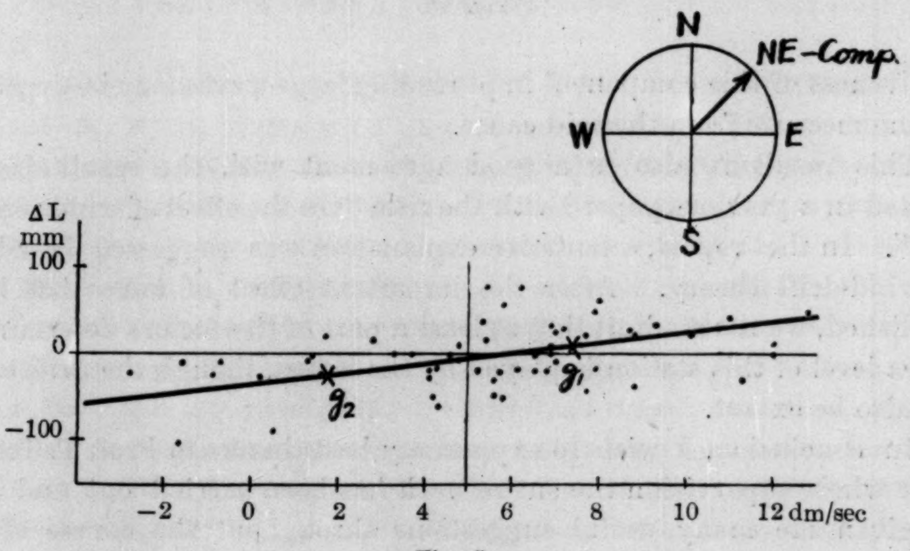

Fig. 5a.

the axis of abscissa at a certain angle. This fact may be considered to show the effect of SW-winds on the sea level at Wazima. On the other hand, the SE-components of the vector sum are taken and similarly treated as shown in Fig. 5b, in which the line connecting g_1 and g_2 nearly coincides with the axis of abscissa. We may, therefore, conclude that the effect of wind, if any, is chiefly determined by its component velocity towards NE.

It will be known that the height of waves caused by winds increases with the extent of open sea area towards the windward direction. As the NE direction roughly coincides with the larger axis of the Japan Sea, the

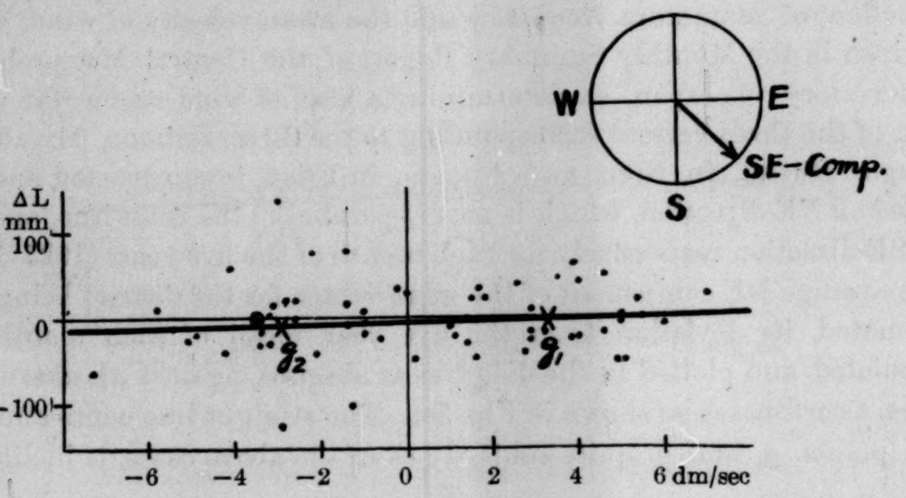

Fig. 5b.

effectiveness of this component in producing large waves may be expected in some measure from the said cause.

This result is also in a good agreement with the result already reported in a previous paper[4] with the title "On the effect of winds on sea level". In that report, a tentative explanation was suggested based on the wind-drift theory. After the important effect of waves has been established, we must admit that at least a part of the factors determining the sea level of this station is played by the waves, though the drift effect may also be extant.

In conclusion, I wish to express my best thanks to Prof. T. Terada under whose supervision the entire work has been carried out and who has given me many useful suggestions throughout the course of my investigation.

---

4) T. TERADA and S. YAMAGUTI, *Jap. J. Astr. Geophys.*, 4, No. 1 (1926).

5. 海水面に及ぼす海流の影響並びに波浪の影響に就て

山 口 生 知

海 流 の 影 響

先に「地震研究所彙報第七號第一册昭和四年六月」の中に於て發表して置いたやうに油壺に於ける月々の平均海水面の觀測値より低氣壓による影響を取り去ると、その殘りは可なり小さな値にはなるけれども、尙未だ不規則な變化が殘つてゐるので參考の爲に細島の觀測値に就いても同樣の修正を加へて之等二ケ所の値を比較して見た。所が或幾月かは海水面の變化の模樣が全く平行に行はれてゐるのを發見した。之は恐らく細島と油壺とは黑潮に對して同じ樣な影響の下にあるから、その黑潮に基因する海水密度の變化によるものではなからうかと推量した。

此推量が果して事實であるか否かを確める爲に次の樣な調査を試みた。卽ち水產講習所の田內博士より潮の岬沖及油壺沖 10 浬の所に於ける種々の深さの海水溫度及鹽分の値の材料を頂戴して、之等の値より誘導した海水密度の月々の變化と海水面の變化との間に相關關係があるかどうかを調べて見た。

兩方の値共各月の平均の値よりの變動量を夫々 ΔL 及 $\Delta\rho$ として $\Delta\rho-\Delta L$ 圖を畫いて見た。それが第一圖、第二圖、第三圖に示さるゝものであつて、これを見れば大體に於て海水密度と海水面との間に或る相關關係のあることが窺はれる。京都帝國大學の野滿教授等は海水面の年變化について海水密度の年變化が大なる影響のあることを指摘して居られるが、その意味に於ける規則正しい海水密度の年變化による影響は上述の取扱方によつて既に消去されて居る故に、結局海流（黑潮）の影響として海洋狀況に變動を與へたものと考ふることが出來る。

次に月々の平均海水面の觀測値の年平均よりの變動量並びに各月 24 年間平均値よりの變動量及び低氣壓並びに海水密度による影響を取り去つた殘りの量について、夫々公算誤差を計算してみると 52mm, 32mm 及び 23mm となる。この事實から吾々は次のことがいはれる。卽ちもしも海水面の月々の平均値に低氣壓及海水密度の變化による適當な修正を加ふる時は、僅か5年間の材料を以てして 25 年間の平均値を以て修正を加へたものよりも小なる公算誤差を得る事が出來、又無修正のものに比較すれば其半分以下の公算誤差を得るのである。これは低氣壓及海水密度による修正が如何に大切なものであるかを示すものである。

波 の 影 響

昭和四年一月二日日本海々水面の異常に關する最近の研究（地震研究所彙報第七號第三册昭和四年十二月）に依つて著者は次の如き結論に到着した。卽ち日本海面の最も高まる時刻には颱風の中心は既に日本海上を通過して北海道の東方太平洋上に在るといふ事、及海水面變化を支配する最も大切な因子の一つは波浪の影響であるといふ事である。

この研究の繼續として、然らば颱風の中心が北海道近くの太平洋上に表はれて居る時には、如

何なる方向より進行して來た颱風でも常に日本海輪島の海水面に影響を與ふるや否やを調べて見た。その結果は輪島の海水面を支配する低氣壓は、矢張り日本海上を通過するといふことが必要な條件であるといふことになつた。

次に輪島の月々の平均海水面と波との關係を直接比較研究して見たかつたのであるが、遺憾ながら輪島の檢潮曲線には、恐らく波が檢潮器の細管の中で衰滅した爲に、その痕跡を止めてゐない故に、止むを得ず波の代りに風を採つて調べることにした。これは波の振幅はその附近の風速の或一定の函數であるといふ假定の下に行つたのである。卽中央氣象臺發行の氣象要覽から宮津、伏木、及び新潟の三ケ所の月々の平均風速及び最多風向を取つてその有向量的の和を作り、更に之を海岸線に殆ど平行なる北東方向及び之に直角なる南東方向に分解して、夫々その分風速度と輪島の月々の平均海水面との關係を調べて見た。その結果は第五圖 a, b に示さるる通り南東の分速度は殆んどその影響を認めることが出來ないが、北東の分速度卽南西の風は相當の影響あることを示してゐる。

一體波の高さは外海洋の面積が風の方向に廣がつて居れば居る程一層増大するものであるが、丁度北東方向は日本海の長軸の方向と殆ぼ一致してゐるからその爲に南西の風が吹く時は大なる波浪を起して輪島の海水面を高めることになるものと考ふることが出來よう。

又この結果は既に寺田博士と共に研究して「海水面に及ぼす風の影響」と題して「日本天文學及地球物理學輯報第四卷第一號大正十五年」に發表して置いた結果とよく一致してゐる。あの時の論文に於ては風の爲に起る皮流の理論を基礎として說明を試みたのであつたが、その後波浪の影響が大切な因子であるといふことが確立された今日に於ては、輪島の海水面を支配する主なる因子は颱風に伴ふ波浪の影響であることを承認せざるを得ないのである。而して前に述べた皮流の影響の現存することは勿論であらふ。

6.　大阪近傍水準測量の結果に就て

陸地測量師　梅　本　豐　吉

（昭和四年十二月二十日受理）

關東及丹後の兩震災後に於ける陸地測量部復舊一等水準測量の結果に就て見るに地震に依る土地の垂直變動は可なり著しいものであると云ふことを認識されたのであるが又同時に土地の經年變化と云ふ事實も忽緒に附することの出來ないと云ふことも經驗されたのである、此の事實は從來の測量に於ても屢々遭遇したことであるが未だ適確に土地の經年變化と云ふ樣な斷定は下されなかつた。土地の經年變化を調ぶるには從來同一地方で水準測量を反復施行せられた結果があるならば此の研究の爲め唯一の好資料を與へることは言を俟たないところである。

現に東京市內に於ける環線水準網は是迄屢々其の測量を反復せられたので此の結果から武藤、熱海兩氏に依り有益な研究を遂げられたことは既に發表せられた通りである。

然るに斯かる有益なる參考資料を與へる測量結果は前記以外日本全國中幾つもあるものでない、唯一つ大阪近傍に於てのみ明治十八年以來今日迄數回水準測量を繰り返されて居る、今此等の古い材料を集めて其の成果を比較して見ることにした。

尤も此の改測途中水準點の異狀を發見して已むなく其の改埋を行つた點が多く此等の成果關係は非常に複雜で其の比較も實は甚だ容易でないのである。

唯茲で斷つて置きたい事は各水準點の成果は其の平均成果を取らず觀測成果を採つて比較したことである。從て各水準點の成果は既に發表されたる陸地測量部の成果と多少の差異のあることは已むを得ない次第である。

尙此の地方に於ける水準點改測の多くは大津市に於ける一等水準點一三〇〇號を不動として實施せられたものであるが特に大阪市內のみの水準點改測は吹田町に於ける一等水準點四七二號を不動として實施された

るものである、依て此等を總て統一して大津市に於ける一等水準點一三〇〇號を不動と假定せるものに改算を施したことを書き加へて置く。

圖に示す樣な沈下狀態は向後尙引續き持續するものか、或は幾年かを經て停止すべきものか、此れは今後の改測結果に待つより外はないが希くは大阪市の如き日本主要都市たる地域では尙水準點を增設し斯かる測量を少なくも五年置き位に實施して其の結果を明かにしたいものである。

---

6. Results of the Repeated Levellings in the Vicinity of Oosaka.

By Toyokiti UMEMOTO,

Land Survey Department.

Since 1885, the precise levelling survey was repeated several times along a system of routes situated in the vicinity of Oosaka and extended to Ootu, province of Oomi. A comparison of the results obtained in different epochs reveals some remarkable features of the vertical displacement of the earth crust in this district, as may be seen from the curves given in the annexed figures.

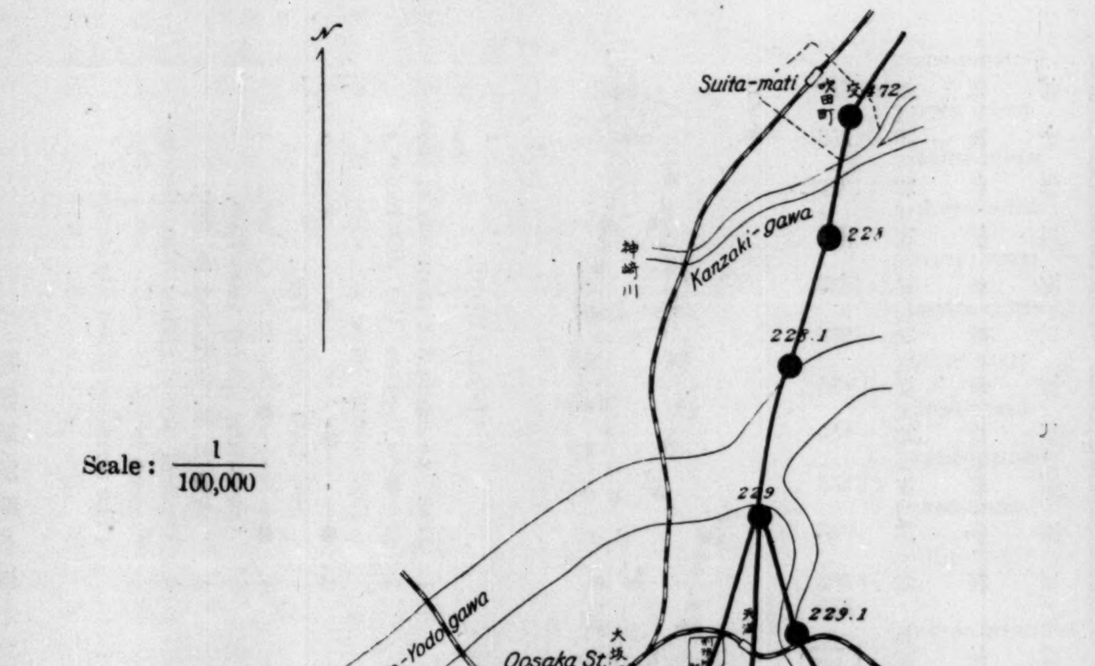

第一圖　大阪市內水準點位置圖

Fig. 1. Positions of the Bench Marks in the Vicinity of Oosaka.

7. *The Effect of Temperature Distribution on the Deformation of a Semi-infinite Elastic Body.*

By Genrokuro NISHIMURA,

Earthquake Research Institute.

(Read Feb. 18, 1930.—Received March 20, 1930.)

1. The problem of the deformation of a semi-infinite elastic solid due to the surface loading was solved by many mathematicians: H. Hertz,[1] H. Nagaoka,[2] K. Terazawa,[3] H. Lamb[4] and others. And recently K. Sezawa[5] studied the case of the deformation of a semi-infinite elastic body due to the internal nuclei of strain. Presumably the results of the investigations of these authorities may give some clue to the questions of the surface deformation and the internal state of the earth.

The recent geophysical researches tell us the incessant variation of the surface form of the earth crust, and although the phenomenon may take place by the action of the crustal force or by the physico-chemical changes in the interior of the earth, we cannot yet neglect the effect of the temperature distribution and variation in the neighbourhood of the surface. Professor K. Sezawa seems to have sticked a long time on his view that the deformation of the crust observed at a local portion is chiefly due to such an effect of the temperature, and he urged the author to solve the problem of this effect. The temperature distribution and variation, of course, depend upon the heat radiated from the sun and also upon other meteorological and topographical circumstances. Even if the above effect should necessarily be diminished towards the interior of the earth crust, we do not yet know in any exact manner how much effects the temperature distribution on the surface of the earth crust as well as in the interior of the same crust may have upon the deformation of the earth.

---

1) H. Hertz, *Ges. Werke*, **1** (1895).
2) H. Nagaoka, *Tokyo Math.-Phys. Soc. Proc.*, **6** (1912), 208.
3) K. Terazawa, *Phil. Trans. Roy. Soc.*, (A), **217** (1916), 35.
4) H. Lamb, *Proc. Roy. Soc.*, London, (A), **93** (1917), 293.
5) K. Sezawa, *Bull. Earthq. Res Inst.*, Tokyo, **7** (1929), 1.

Thus, it will not be useless to study the present problem in order to know the true nature of the deformation of the surface of the earth and to give some step on the advancement of the seismological science.

Recently Dr. R. Takahasi,[6] the assistant professor of the Earthquake Research Institute, Tokyo, using the Michelson tube and the Ishimoto tiltmeter, observed the tilt of the house of the Institute, and found the result that the chief deformation of the house is of the daily and annular variation of the tilt due to the heat of the sun on the surface of the house. The similar nature may be found, when fully examined, in the deformation of the local portion of the actual earth crust.

Although the bending of a relatively long house due to the temperature change is very simply analysed in the manner of the engineering mechanics, yet the theoretical researches concerning to the problem of a semi-infinite body have not been much developed, and the present paper, the author thinks, may throw some lights on the study of this problem.

It is important to bring the problem of the diffusion of heat distributed on the surface of the earth in the interior of the crust in order to deal with the effect of the temperature distribution on the deformation of a semi-infinite elastic solid. But this problem of conduction is not so important on the deformation of the crust. Theoretically Dr. Y. Kodaira[7] at the Central Meteorological Observatory, Tokyo, studied the conduction of heat evolved from magma in the volcano districts, but it is not concerned with the present problem.

The present author has obtained the equations of equilibrium of the solid, in which the case of steady state of heat distribution of some kinds or of a certain instant of non-steady state is taken. The assumption on the temperature distribution is very reasonable, not incoherent with but satisfying the state at an instant of conduction of heat in a solid. From the calculations which will appear presently, the author has obtained the important facts upon the geophysical researches as given in Section 16.

The mathematical parts below are composed of three parts: in the first part the author has obtained the general equations of equilibrium of the elastic solid when the variations of temperature occur, and the second part gives us the two-dimensional problem and the third the three-dimensional problem, and in these last two parts some examples have been solved by using Fourier's double integral formula.

6) R. TAKAHASI, 45th Colloq. Meeting of the Institute (Jan. 21, 1930).
7) Y. KODAIRA, *Geophysical Magazine*, Tokyo, 1 (1926).

Part I. General Theory.

2. The mathematical theory of elasticity shews that when an elastic homogeneous isotropic body is exposed to pressure in the condition of standard temperature, the stress and strain relations are given as follows:

$$\left.\begin{aligned} X_x &= \lambda\left(\frac{\partial u}{\partial x}+\frac{\partial v}{\partial y}+\frac{\partial w}{\partial z}\right)+2\mu\frac{\partial u}{\partial x}, \\ Y_y &= \lambda\left(\frac{\partial u}{\partial x}+\frac{\partial v}{\partial y}+\frac{\partial w}{\partial z}\right)+2\mu\frac{\partial v}{\partial y}, \\ Z_z &= \lambda\left(\frac{\partial u}{\partial x}+\frac{\partial v}{\partial y}+\frac{\partial w}{\partial z}\right)+2\mu\frac{\partial w}{\partial z}, \\ X_y = \mu\left(\frac{\partial v}{\partial x}+\frac{\partial u}{\partial y}\right),\ & X_z = \mu\left(\frac{\partial u}{\partial z}+\frac{\partial w}{\partial x}\right), \ \& \ Y_z = \mu\left(\frac{\partial w}{\partial y}+\frac{\partial v}{\partial z}\right). \end{aligned}\right\} \cdots(1)$$

The meaning of the notations in the above equations are given in Love's text book[8] of elasticity.

When the temperature of the body is raised by T, and no external forces are applied, the strains are given as follows:

$$\left.\begin{aligned} &\frac{\partial u}{\partial x}=\frac{cT}{3},\quad \frac{\partial v}{\partial y}=\frac{cT}{3},\quad \frac{\partial w}{\partial z}=\frac{cT}{3}, \\ \text{and}\quad &\frac{\partial v}{\partial x}=\frac{\partial u}{\partial z}=\ \cdots\cdots\ =0, \end{aligned}\right\} \cdots\cdots(2)$$

where c is the cubical expansion coefficient of the body. Now these strains in (2) are connected with the stresses, when the body is in the standard temperature, in the forms:

$$\left.\begin{aligned} &X_x=\left(\lambda+\frac{2}{3}\mu\right)cT,\quad Y_y=\left(\lambda+\frac{2}{3}\mu\right)cT,\quad Z_z=\left(\lambda+\frac{2}{3}\mu\right)cT, \\ \text{and}\quad &X_y=X_z=Y_z=0. \end{aligned}\right\} \cdots(3)$$

Therefore the general expressions of the stress and strain relations are written in the following forms:

---

8) LOVE, *The Mathematical Theory of Elasticity*, 4th ed., 102.

$$\left.\begin{aligned} X_x &= \lambda\left(\frac{\partial u}{\partial x}+\frac{\partial v}{\partial y}+\frac{\partial w}{\partial z}\right)+2\mu\frac{\partial u}{\partial x}-\left(\lambda+\frac{2}{3}\mu\right)cT,\\ Y_y &= \lambda\left(\frac{\partial u}{\partial x}+\frac{\partial v}{\partial y}+\frac{\partial w}{\partial z}\right)+2\mu\frac{\partial v}{\partial y}-\left(\lambda+\frac{2}{3}\mu\right)cT,\\ Z_z &= \lambda\left(\frac{\partial u}{\partial x}+\frac{\partial v}{\partial y}+\frac{\partial w}{\partial z}\right)+2\mu\frac{\partial w}{\partial z}-\left(\lambda+\frac{2}{3}\mu\right)cT, \end{aligned}\right\}\cdots(4)$$

and

$$X_y = \mu\left(\frac{\partial v}{\partial x}+\frac{\partial u}{\partial y}\right),\quad X_z = \mu\left(\frac{\partial u}{\partial z}+\frac{\partial w}{\partial x}\right),\quad Y_z = \mu\left(\frac{\partial w}{\partial y}+\frac{\partial v}{\partial z}\right).$$

These relations have been given by Professor Love.[9]

Now, the stress-equations of equilibrium of no body forces are

$$\left.\begin{aligned} \frac{\partial X_x}{\partial x}+\frac{\partial X_y}{\partial y}+\frac{\partial Z_x}{\partial z} &= 0,\\ \frac{\partial X_y}{\partial x}+\frac{\partial Y_x}{\partial y}+\frac{\partial Y_z}{\partial z} &= 0,\\ \frac{\partial Z_z}{\partial x}+\frac{\partial Y_z}{\partial y}+\frac{\partial Z_z}{\partial z} &= 0. \end{aligned}\right\}\cdots\cdots(5)$$ [10]

If we put the relations (4) in the stress-equations (5), we get the following equations of equilibrium of an elastic body of the temperature distribution T, after some reduction:

$$\left.\begin{aligned} (\lambda+2\mu)\frac{\partial \Delta}{\partial x}-2\mu\frac{\partial \varpi_z}{\partial y}+2\mu\frac{\partial \varpi_y}{\partial z} &= \alpha\frac{\partial T}{\partial x},\\ (\lambda+2\mu)\frac{\partial \Delta}{\partial y}-2\mu\frac{\partial \varpi_x}{\partial z}+2\mu\frac{\partial \varpi_z}{\partial x} &= \alpha\frac{\partial T}{\partial y},\\ (\lambda+2\mu)\frac{\partial \Delta}{\partial z}-2\mu\frac{\partial \varpi_y}{\partial x}+2\mu\frac{\partial \varpi_x}{\partial y} &= \alpha\frac{\partial T}{\partial z}, \end{aligned}\right\}\cdots\cdots(6)$$

where

$$\left.\begin{aligned} \Delta &= \frac{\partial u}{\partial x}+\frac{\partial v}{\partial y}+\frac{\partial w}{\partial z},\\ 2\varpi_x &= \frac{\partial w}{\partial y}-\frac{\partial v}{\partial z},\\ 2\varpi_y &= \frac{\partial u}{\partial z}-\frac{\partial w}{\partial x},\\ 2\varpi_z &= \frac{\partial v}{\partial x}-\frac{\partial u}{\partial y}, \end{aligned}\right\}\cdots\cdots(7)$$

9) LOVE, *loc. cit.*, 108.
10) LOVE, *loc. cit.*, 85.

and

$$\alpha = \left(\lambda + \frac{2}{3}\mu\right)c. \quad \cdots\cdots(8)$$

In order to determine the form of T in the equations (6), we must first solve the equation of conduction of heat, such that

$$\frac{\partial T}{\partial t} = \varkappa\left(\frac{\partial^2 T}{\partial x^2} + \frac{\partial^2 T}{\partial y^2} + \frac{\partial^2 T}{\partial z^2}\right). \quad \cdots\cdots(9)$$

But, if we select a certain suitable form of T satisfying the condition of conduction at every moment and the conditions of the problem to be solved, we can easily solve the equations (6), and can finally complete our study.

Part II. Two-dimensional Problem.

3. In two-dimensional problem, we use the Cartesian coordinates (x, y). Let the plane $y = 0$ be the surface of the semi-infinite elastic solid, and the axis of y be taken vertically downwards. (Fig. 1.)

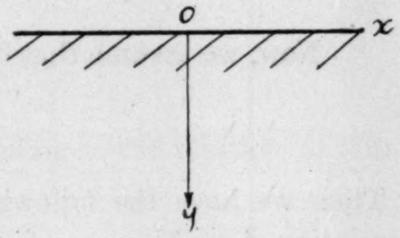

Fig. 1.

The equations of equilibrium, when the temperature distribution T takes place, are given in the forms:

$$\left.\begin{aligned} (\lambda+2\mu)\frac{\partial \Delta}{\partial x} - 2\mu\frac{\partial \varpi}{\partial y} &= \alpha\frac{\partial T}{\partial x}, \\ (\lambda+2\mu)\frac{\partial \Delta}{\partial y} + 2\mu\frac{\partial \varpi}{\partial x} &= \alpha\frac{\partial T}{\partial y}, \end{aligned}\right\} \quad \cdots\cdots(10)$$

where

$$\left.\begin{aligned} \Delta &= \frac{\partial u}{\partial x} + \frac{\partial v}{\partial y}, \\ 2\varpi &= \frac{\partial v}{\partial x} - \frac{\partial u}{\partial y}. \end{aligned}\right\} \quad \cdots\cdots(11)$$

We can, now, construct the following equations from (10),

$$\frac{\partial^2}{\partial x^2}\left[(\lambda+2\mu)\Delta - \alpha T\right] + \frac{\partial^2}{\partial y^2}\left[(\lambda+2\mu)\Delta - \alpha T\right] = 0, \quad \cdots\cdots(12)$$

$$\frac{\partial^2 \varpi}{\partial x^2} + \frac{\partial^2 \varpi}{\partial y^2} = 0. \quad \cdots\cdots(13)$$

Now, in the problems at which we are aiming, the temperature should be gradually small according as the depth of the solid from the free surface $y=0$ is increased, and at $y=\infty$ it must be zero. Therefore, we take the following standard form for the temperature distribution:

$$T = \mathfrak{A}\, e^{-\gamma y} \left.\begin{matrix}\cos\\ \sin\end{matrix}\right\} \beta x, \qquad \cdots\cdots(14)$$

where $\mathfrak{A}$ is an arbitrary constant which is the measurement of the temperature magnitude.

As we have already discussed in Section 2, the equation (14), just we have assumed, should give the temperature distribution at a certain moment in the conduction of heat.

From (12) and (14), we have the following equation,

$$\frac{\partial^2 \varDelta}{\partial x^2} + \frac{\partial^2 \varDelta}{\partial y^2} = \frac{\alpha \mathfrak{A}}{\lambda + 2\mu} (\gamma^2 - \beta^2)\, e^{\gamma y} \left.\begin{matrix}\cos\\ \sin\end{matrix}\right\} \beta x. \qquad \cdots\cdots(15)$$

Now, we assume that the dilatation $\varDelta$ is of the following form:

$$\varDelta = F(y) \left.\begin{matrix}\cos\\ \sin\end{matrix}\right\} \beta x. \qquad \cdots\cdots(16)$$

Then we have the following particular solution $\varDelta_1$ and complementary solution $\varDelta_2$ of (15),

$$\varDelta_1 = \frac{\alpha \mathfrak{A}}{\lambda + 2\mu} e^{-\gamma y} \left.\begin{matrix}\cos\\ \sin\end{matrix}\right\} \beta x, \qquad \cdots\cdots(17)$$

$$\varDelta_2 = B e^{-\beta y} \left.\begin{matrix}\cos\\ \sin\end{matrix}\right\} \beta x. \qquad \cdots\cdots(18)$$

As the complementary solution, we have another form of $e^{\beta y} \left.\begin{matrix}\cos\\ \sin\end{matrix}\right\} \beta x$, but it is omitted in our case. When $\gamma = \beta$, $\varDelta_1 = 0$.

The solution of (13) which is suitable to the present purpose is

$$2\varpi = D e^{-\beta y} \left.\begin{matrix}\sin\\ \cos\end{matrix}\right\} \beta x. \qquad \cdots\cdots(19)$$

If we put these dilatations and rotation in the equation (10), we have the following relation between the constants B and D;

$$\left.\begin{matrix}(\lambda + 2\mu) B + \mu D = 0, & [\gamma \neq \beta] \\ (\lambda + 2\mu) B + \mu D = \alpha \mathfrak{A}. & [\gamma = \beta]\end{matrix}\right\} \qquad \cdots\cdots(20)$$

Now we must have the displacement (u, v) from the equations (17), (18) and (19). Following the analytical method[11] of Professor K. Sezawa, we obtain the following system of displacements.

If we assume that the displacement (u_1, v_1) satisfies Δ_1 of the equation (17) and $2\varpi = 0$,

then

$$\left.\begin{aligned} u_1 &= \frac{\alpha\mathfrak{A}}{\lambda+2\mu}\frac{\beta}{\beta^2-\gamma^2}e^{-\gamma y}\begin{matrix}\sin\\ -\cos\end{matrix}\Big\}\beta x,\\ v_1 &= \frac{\alpha\mathfrak{A}}{\lambda+2\mu}\frac{\gamma}{\beta^2-\gamma^2}e^{-\gamma y}\begin{matrix}\cos\\ \sin\end{matrix}\Big\}\beta x.\end{aligned}\right\} \quad \cdots\cdots\cdots\cdots\cdots\cdots(21)$$

When $\gamma = \beta$, $u_1 = v_1 = 0$.

The displacement (u_2, v_2) satisfying Δ_2 expressed by (18), and $2\varpi = 0$, is written by

$$\left.\begin{aligned} u_2 &= \frac{1}{2}By\,e^{-\beta y}\begin{matrix}\sin\\ -\cos\end{matrix}\Big\}\beta x,\\ v_2 &= -\frac{B}{2\beta}(1-\beta y)\,e^{-\beta y}\begin{matrix}\cos\\ \sin\end{matrix}\Big\}\beta x.\end{aligned}\right\} \quad \cdots\cdots\cdots\cdots\cdots\cdots(22)$$

If (u_3, v_3) is the displacement corresponding to the rotation of (19) and satisfying $\Delta_1 + \Delta_2 = 0$,

then

$$\left.\begin{aligned} u_3 &= -\frac{D}{2\beta}(1-\beta y)\,e^{-\beta y}\begin{matrix}\sin\\ -\cos\end{matrix}\Big\}\beta x,\\ v_3 &= \frac{D}{2}y\,e^{-\beta y}\begin{matrix}\cos\\ \sin\end{matrix}\Big\}\beta x,\end{aligned}\right\} \quad \cdots\cdots\cdots\cdots\cdots\cdots(23)$$

and if we assume that the displacement (u_4, v_4) is to satisfy the condition $\Delta_1 + \Delta_2 = 2\varpi = 0$, we can write

$$\left.\begin{aligned} u_4 &= F\,e^{-\beta y}\begin{matrix}\sin\\ -\cos\end{matrix}\Big\}\beta x,\\ v_4 &= F\,e^{-\beta y}\begin{matrix}\cos\\ \sin\end{matrix}\Big\}\beta x.\end{aligned}\right\} \quad \cdots\cdots\cdots\cdots\cdots\cdots(24)$$

Therefore the general expressions of the displacement (u, v) are of the following forms:

11) K. Sezawa. *Bull. Earthq. Res. Inst.*, Tokyo, **2** (1927), **3** (1927), **4** (1928), **5** (1928), **6** (1929), **7** (1929).

$$
\left.\begin{aligned}
u &= \left[\left\{\frac{B}{2}\,y - \frac{D}{2\beta}\,(1-\beta y) + F\right\} e^{-\beta y} + \frac{\alpha\mathfrak{A}}{\lambda+2\mu}\,\frac{\beta}{\beta^2-\gamma^2}\,e^{-\gamma y}\right] \begin{matrix}\sin\\ -\cos\end{matrix}\Big\}\,\beta x,\\
v &= \left[\left\{-\frac{B}{2\beta}\,(1-\beta y) + \frac{D}{2}\,y + F\right\} e^{-\beta y} + \frac{\alpha\mathfrak{A}}{\lambda+2\mu}\,\frac{\gamma}{\beta^2-\gamma^2}\,e^{-\gamma y}\right] \begin{matrix}\cos\\ \sin\end{matrix}\Big\}\,\beta x.
\end{aligned}\right\} \quad \text{......(25)}
$$

When $\beta=\gamma$,

$$
\left.\begin{aligned}
u &= \left[\frac{B}{2}\,y - \frac{D}{2\beta}\,(1-\beta y) + F\right] e^{-\beta y} \begin{matrix}\sin\\ -\cos\end{matrix}\Big\}\,\beta x,\\
v &= \left[-\frac{D}{2\beta}\,(1-\beta y) + \frac{D}{2}\,y + F\right] e^{-\beta y} \begin{matrix}\cos\\ \sin\end{matrix}\Big\}\,\beta x,
\end{aligned}\right\} \quad \text{......(26)}
$$

Now the stresses are given as follows:

$$
\left.\begin{aligned}
X_x &= \lambda\Delta + 2\mu\,\frac{\partial u}{\partial x} - \alpha T,\\
Y_y &= \lambda\Delta + 2\mu\,\frac{\partial v}{\partial y} - \alpha T,\\
X_y &= \mu\left(\frac{\partial v}{\partial x} + \frac{\partial u}{\partial y}\right).
\end{aligned}\right\} \quad \text{......(27)}
$$

Therefore we can construct the stresses which are necessary for the present study by using the equations (25) or (26) and (27).

Now the surface $y=0$ of the solid is assumed to be of the temperature distribution of the form of

$$
\mathfrak{A} \begin{matrix}\cos\\ \sin\end{matrix}\Big\}\,\beta x, \quad \text{......(28)}
$$

and no stresses are applied.

From the condition that the surface is free from traction, we can construct the following relations:

$$
y=0, \qquad \widehat{yy} = \widehat{xy} = 0. \quad \text{......(29)}
$$

From these relations and (27), we find the following forms of constants B, D and F:

$$\left.\begin{aligned} &\left.\begin{aligned} B &= \frac{2\alpha\mu\mathfrak{A}}{(\lambda+\mu)(\lambda+2\mu)}\,\frac{\beta}{\beta+\gamma}, \\ D &= -\frac{2\alpha\mathfrak{A}}{\lambda+\mu}\,\frac{\beta}{\beta+\gamma}, \\ F &= -\frac{\alpha\mathfrak{A}}{\lambda+2\mu}\,\frac{\beta}{\beta^2-\gamma^2}, \end{aligned}\right\} \quad [\beta \neq \gamma] \\ &\left.\begin{aligned} B &= \frac{\alpha\mathfrak{A}}{\lambda+\mu}, \quad D = -\frac{\alpha\mathfrak{A}}{\lambda+\mu}, \\ F &= 0. \end{aligned}\right\} \quad [\beta = \gamma] \end{aligned}\right\} \quad \cdots\cdots(30)$$

Putting these relations (30) in (25) and (26), we get the following forms of u and v which are suitable for our purpose.

$$\left.\begin{aligned} u &= -\frac{\alpha\mathfrak{A}}{(\lambda+2\mu)(\beta+\gamma)}\left[\left(\beta y - \frac{\mu\beta-(\lambda+2\mu)\gamma}{(\lambda+\mu)(\beta-\gamma)}\right)e^{-\beta y} - \frac{\beta e^{-\gamma y}}{\beta-\gamma}\right] \begin{matrix}\sin\\ -\cos\end{matrix}\Big\}\,\beta x, \\ v &= -\frac{\alpha\mathfrak{A}}{(\lambda+2\mu)(\beta+\gamma)}\left[\left(\beta y - \frac{\mu\gamma-(\lambda+2\mu)\beta}{(\lambda+\mu)(\beta-\gamma)}\right)e^{-\beta y} - \frac{\gamma e^{-\gamma y}}{\beta-\gamma}\right] \begin{matrix}\cos\\ \sin\end{matrix}\Big\}\,\beta x, \end{aligned}\right\}$$

$$[\beta \neq \gamma] \quad \cdots\cdots(31)$$

$$\left.\begin{aligned} u &= \frac{\alpha\mathfrak{A}}{2(\lambda+\mu)\beta}\,e^{-\beta y} \begin{matrix}\sin\\ -\cos\end{matrix}\Big\}\,\beta x, \\ v &= \frac{\alpha\mathfrak{A}}{2(\lambda+\mu)\beta}\,e^{-\beta y} \begin{matrix}\cos\\ \sin\end{matrix}\Big\}\,\beta x. \end{aligned}\right\} \quad [\beta = \gamma] \quad \cdots\cdots(32)$$

The displacement thus we obtained is merely a elementary solution fulfilling the condition that the temperature distribution in the solid may be assumed to be of the form expressed by (14). Therefore, when the temperature distribution of the surface of the solid is expressed by $f(x)$, we can find the suitable form of the displacement using the above mentioned elementary solutions and Fourier's double integral formula:

$$f(x) = \frac{1}{\pi}\int_0^\infty d\alpha \int_{-\infty}^{\infty} f(\lambda)\cos\alpha(x-\lambda)\,d\lambda \cdots\cdots\cdots\cdots\cdots\cdots(33)$$

Now, from the beginning of this section we have not fully examined the relation of β and γ, but in the following sections we shall consider the relation of β and γ. If not, we cannot proceed our course of study. In the 4th section we assume that β and γ are independent each other, and in the 5th section β and γ are connected by the following relation:

$$\gamma = \gamma'^{n} \beta, \qquad \text{(34)}$$

where γ' is a mere number which is arbitrary, and n is the number of 1, 2, 3……

The above mentioned assumptions on the relation between β and γ do not lose the generality of the problem as will be explained in the following sections.

4. When the temperature distribution of the surface of a semi-infinite elastic body is of the form of $f(x)$, and the surface is free from tractions, we can construct the appropriate forms of the temperature distribution in the body, and the displacement at any point of the body by using the equations of (14) and (31) in the following system.

The temperature distribution in the solid, when the surface distribution is $f(x)$, is expressed in the form:

$$T = \frac{1}{\pi}\int_0^\infty d\beta \int_{-\infty}^{\infty} e^{-\gamma y} f(\varkappa) \cos\beta(x-\varkappa)\, d\varkappa. \qquad \text{(35)}$$

The components of the displacement (u, v) are as follows:

$$\begin{aligned} u = -\frac{\alpha}{\pi(\lambda+2\mu)}\Bigg[& \frac{(\lambda+2\mu)\gamma}{\lambda+\mu}\int_0^\infty d\beta \int_{-\infty}^{\infty} f(\varkappa)\, \frac{e^{-\beta y}}{\beta^2-\gamma^2} \sin\beta(x-\varkappa)\, d\varkappa \\ & -\frac{\mu}{\lambda+\mu}\int_0^\infty d\beta \int_{-\infty}^{\infty} f(\varkappa)\, \frac{e^{-\beta y}}{\beta^2-\gamma^2} \sin\beta(x-\varkappa)\, \beta d\varkappa \\ & + y\int_0^\infty d\beta \int_{-\infty}^{\infty} f(\varkappa)\, \frac{e^{-\beta y}}{\beta+\gamma} \sin\beta(x-\varkappa)\, \beta d\varkappa \\ & - e^{-\gamma y}\int_0^\infty d\beta \int_{-\infty}^{\infty} f(\varkappa)\, \frac{\sin\beta(x-\varkappa)\beta}{\beta^2-\gamma^2}\, d\varkappa\Bigg], \qquad \text{(36)} \end{aligned}$$

$$v = -\frac{\alpha}{\pi(\lambda+2\mu)}\Big[\frac{\lambda+2\mu}{\lambda+\mu}\int_0^\infty d\beta\int_{-\infty}^\infty f(x)\frac{e^{-\beta y}}{\beta^2-\gamma^2}\cos\beta(x-x)\beta dx$$

$$-\frac{\mu\gamma}{\lambda+\mu}\int_0^\infty d\beta\int_{-\infty}^\infty f(x)\frac{e^{-\beta y}}{\beta^2-\gamma^2}\cos\beta(x-x)\,dx$$

$$+y\int_0^\infty d\beta\int_{-\infty}^\infty f(x)\frac{e^{-\beta y}}{\beta+\gamma}\cos\beta(x-x)\beta dx$$

$$-\gamma e^{-\gamma y}\int_0^\infty d\beta\int_{-\infty}^\infty f(x)\frac{\cos\beta(x-x)}{\beta^2-\gamma^2}dx\Big]. \quad\cdots\cdots\cdots(37)$$

The inclination $\frac{\partial v}{\partial x}$ can easily be written such that

$$\frac{\partial v}{\partial x} = \frac{\alpha}{\pi(\lambda+2\mu)}\Big[\frac{\lambda+2\mu}{\lambda+\mu}\int_0^\infty d\beta\int_{-\infty}^\infty f(x)\frac{e^{-\beta y}}{\beta^2-\gamma^2}\sin\beta(x-x)\beta^2 dx$$

$$-\frac{\mu\gamma}{\lambda+\mu}\int_0^\infty d\beta\int_{-\infty}^\infty f(x)\frac{e^{-\beta y}}{\beta^2-\gamma^2}\sin\beta(x-x)\beta dx$$

$$+y\int_0^\infty d\beta\int_{-\infty}^\infty f(x)\frac{e^{-\beta y}}{\beta+\gamma}\sin\beta(x-x)\beta^2 dx$$

$$-\gamma e^{-\gamma y}\int_0^\infty d\beta\int_{-\infty}^\infty f(x)\frac{\sin\beta(x-x)}{\beta^2-\gamma^2}\beta dx\Big]. \quad\cdots\cdots\cdots(38)$$

The stresses X_x, Y_y and X_y can easily be determined similarly, but as these are not needed in our study, these formulae are omitted in this paper.

5. In this section we take the example of the 4th section, that the temperature distribution of the surface of the body is limitted by the following form :

$$f(x) = B, \quad a > x > -a. \quad\cdots\cdots\cdots\cdots\cdots\cdots\cdots\cdots\cdots(39)$$

Then the temperature distribution in the body is formed by using the formula (35):

$$
\left.\begin{aligned}
t &= \frac{B}{\pi} e^{-\gamma y} \int_0^\infty \frac{1}{\beta} \left\{ \sin\beta(x+a) - \sin\beta(x-a) \right\} d\beta \\
&= B e^{-\gamma y}, \quad \text{for} \quad a > x > -a, \\
&= 0, \quad x > a \quad \text{and} \quad x < -a.
\end{aligned}\right\} \qquad \cdots\cdots\cdots(40)
$$

From the formulae (37) and (38), we can find the following forms of displacement v and inclination $\frac{\partial v}{\partial x}$:

$$
\begin{aligned}
v = -\frac{\alpha B}{\pi(\lambda+2\mu)} \Bigg[& \frac{\lambda+2\mu}{\lambda+\mu} \int_0^\infty \frac{e^{-\beta y}}{\beta^2-\lambda^2} \left\{ \sin\beta(x+a) - \sin\beta(x-a) \right\} d\beta \\
& - \frac{\mu\gamma}{\lambda+\mu} \int_0^\infty \frac{e^{-\beta y}}{\beta^2-\gamma^2} \left\{ \sin\beta(x+a) - \sin\beta(x-a) \right\} \frac{d\beta}{\beta} \\
& + y \int_0^\infty \frac{e^{-\beta y}}{\beta+\gamma} \left\{ \sin\beta(x+a) - \sin\beta(x-a) \right\} d\beta \\
& - \gamma e^{-\gamma y} \int_0^\infty \frac{\sin\beta(x+a) - \sin\beta(x-a)}{\beta^2-\gamma^2} \frac{d\beta}{\beta} \Bigg], \qquad \cdots\cdots(41)
\end{aligned}
$$

$$
\begin{aligned}
\frac{\partial v}{\partial x} = \frac{\alpha B}{\pi(\lambda+2\mu)} \Bigg[& \frac{\lambda+2\mu}{\lambda+\mu} \int_0^\infty \frac{e^{-\beta y}}{\beta^2-\gamma^2} \left\{ \cos\beta(x-a) - \cos\beta(x+a) \right\} \beta d\beta \\
& - \frac{\mu\gamma}{\lambda+\mu} \int_0^\infty \frac{e^{-\beta y}}{\beta^2-\gamma^2} \left\{ \cos\beta(x-a) - \cos\beta(x+a) \right\} d\beta \\
& + y \int_0^\infty \frac{e^{-\beta y}}{\beta+\gamma} \left\{ \cos\beta(x-a) - \cos\beta(x+a) \right\} \beta d\beta \\
& - \gamma e^{-\gamma y} \int_0^\infty \frac{\cos\beta(x-a) - \cos\beta(x+a)}{\beta^2-\gamma^2} d\beta \Bigg]. \qquad \cdots(42)
\end{aligned}
$$

Now, to find the surface displacement and the surface inclination, we must first construct the following integral formulae[12]:

---

12) These formulae are easily obtained from the integral formulae obtained by Prof. K. Sezawa.

K. SEZAWA, "Some Problems of Shocks transmitted in Bars and in Plate," *Report of Aeron. Res. Inst.*, Tokyo, 4, No. 4 (1928).

K. SEZAWA, "On the Propagation of the Leading & Trailing Parts of a Train of Elastic Waves," *Bull. Earthq. Res. Inst.*, Tokyo, 4 (1928).

for $a > 0$,

$$\left.\begin{aligned}
\int_0^\infty \frac{\cos ax}{x-k}\,dx &= -\frac{\pi}{2}\sin ka - Cika\cos ka - Sika\sin ka,\\
\int_0^\infty \frac{\sin ax}{x-k}\,dx &= \frac{\pi}{2}\cos ka - Cika\sin ka + Sika\cos ka,\\
\int_0^\infty \frac{\cos ax}{x+k}\,dx &= -Cika\cos ka + \left(\frac{\pi}{2} - Sika\right)\sin ka,\\
\int_0^\infty \frac{\sin ax}{x+k}\,dx &= \left(\frac{\pi}{2} - Sika\right)\cos ka + Cika\sin ka,
\end{aligned}\right\}\quad\cdots\cdots(43)$$

and for $a < 0$,

$$\left.\begin{aligned}
\int_0^\infty \frac{\cos ax}{x-k}\,dx &= \frac{\pi}{2}\sin ka - Cika\cos ka - Sika\sin ka,\\
\int_0^\infty \frac{\sin ax}{x-k}\,dx &= -\frac{\pi}{2}\cos ka - Cika\sin ka + Sika\cos ka,\\
\int_0^\infty \frac{\cos ax}{x+k}\,dx &= -Cika\cos ka - \left(\frac{\pi}{2} + Sika\right)\sin ka,\\
\int_0^\infty \frac{\sin ax}{x+k}\,dx &= -\left(\frac{\pi}{2} + Sika\right)\cos ka + Cika\sin ka,
\end{aligned}\right\}\quad\cdots\cdots(44)$$

where Cix and Six are the integralcosine and integralsine in the form of $\int_0^\infty \frac{\cos u}{u}\,du$, $\int_x^\infty \frac{\sin u}{u}\,du$.

By using the equations (43) and (44), we can evaluate the integrals in (41) and (42) when $y = 0$ as follows:

$x < -a$:—

$$\begin{aligned}
v = -\frac{\alpha B}{\gamma\pi(\lambda+\mu)}\Big[&\frac{\pi}{2}\left\{\cos\gamma(x+a) - \cos\gamma(x-a)\right\}\\
&+ Si\,\gamma(x+a)\cos\gamma(x+a) + Ci\,\gamma(x-a)\sin\gamma(x-a)\\
&- Ci\,\gamma(x+a)\sin\gamma(x+a) - Si\,\gamma(x-a)\cos\gamma(x-a)\Big],
\end{aligned}\quad\cdots\cdots\cdots(45)$$

$-a < x < a$:—

$$v = -\frac{\alpha B}{\gamma\pi(\lambda+\mu)}\Big[\pi - \Big\{\frac{\pi}{2} - Si\,\gamma(x+a)\Big\}\cos\gamma(x+a)$$

$$-Ci\,\gamma(x+a)\sin\gamma(x+a) - \Big\{\frac{\pi}{2} + Si\,\gamma(x-a)\Big\}\cos\gamma(x-a)$$

$$+Ci\,\gamma(x-a)\sin\gamma(x-a)\Big]. \quad \cdots\cdots(46)$$

and $x > a$:—

$$v = -\frac{\alpha B}{\gamma\pi(\lambda+\mu)}\Big[\frac{\pi}{2}\Big\{\cos\gamma(x-a) - \cos\gamma(x+a)\Big\}$$

$$+Si\,\gamma(x+a)\cos\gamma(x+a) + Ci\,\gamma(x-a)\sin\gamma(x-a)$$

$$-Ci\,\gamma(x+a)\sin\gamma(x+a) - Si\,\gamma(x-a)\cos\gamma(x-a)\Big]. \quad \cdots\cdots(47)$$

Similarly we can construct the displacement u and the inclination $\frac{\partial v}{\partial x}$. But we omit these operations in this section. From the results expressed by (45), (46) and (47), it may be noticed that the displacement of the surface of the body depends extraordinarily upon the tendency of the temperature distribution, and the surface form of the deformation is somewhat similar to the form of temperature distribution of the surface. The magnitude of the displacement at any point of the body is proportional to the temperature at that point, and also the distribution of the displacement is much affected by the temperature distribution in the vertical direction of the solid. When the temperature distribution of the surface of the body is constant but that of the interior of the body is variable according to the law of $e^{-\gamma y}$ in which γ is variable, the surface displacement is much affected by the temperature distribution in the interior of the body. When γ is very small, namely the temperature effect in the interior of the solid is not so small, the surface displacement is large. But, if γ is large, the surface displacement is less. The magnitude of γ changes the temperature distribution in the interior of the body, i.e, for larger γ the temperature distribution is more concentrated in the neighbourhood of the surface of the body. We know that large γ corresponds to the daily variation, and small γ the annular variation of the temperature distribution in the interior of the earth.

When we compile the result of (40), we get the curves in Figs. 2a & 2b. We shall perhaps understand from the figure what we have discussed in the above paragraph.

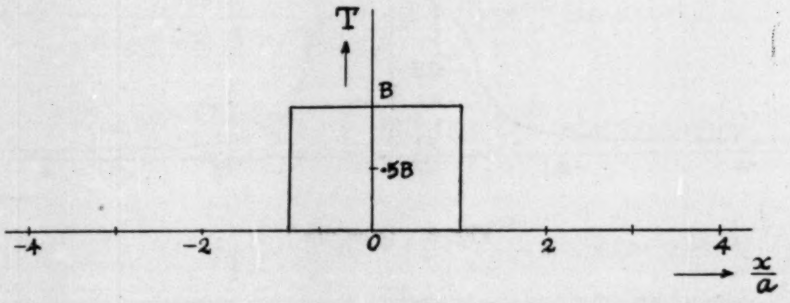

Fig. 2a. Temperature distribution of the surface of the solid.

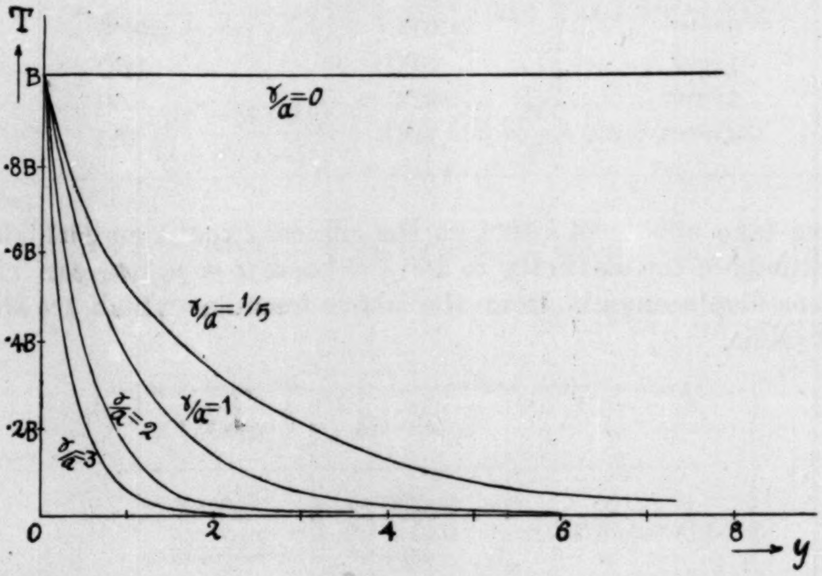

Fig. 2b. $\left[\frac{x}{a}=0.\right]$

The surface displacement is drawn in Figure 3 which is obtained from (45), (46) and (47), when $\gamma = \frac{2}{a}$.

As actual examples, we take the following two cases in which the temperature of 100°C is distributed over the surface of the body about 20 meters long, and γ/a is taken 1/5 and 2; namely the effects of the surface temperature in the earth at $x = 0$ are given by the following table. (next page)

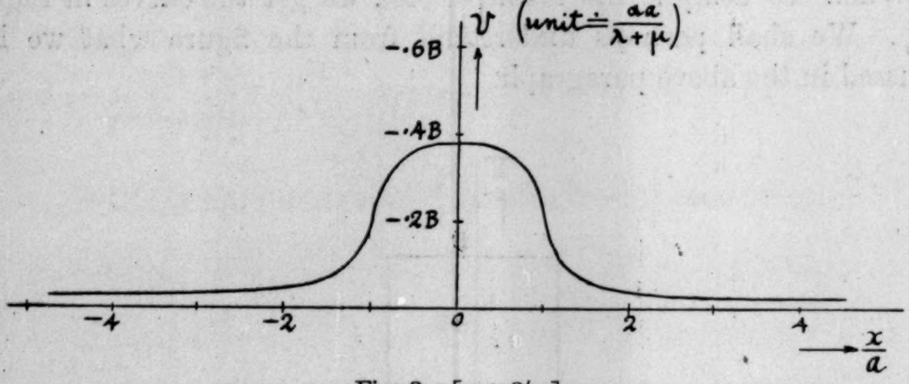

Fig. 3. [$\gamma = 2/a.$]

distance from the surface (y)	γ/a = 1/5 (1st example)	γ/a = 2 (2nd example)
0 meter	100°C	100°C
1 meter	50°C	14°C
2 meters	32°C	2°C
4 meters	14°C	0°C

If we take about $\cdot 24\times 10^{-4}$ as the cubical expansion coefficient and the conditions of the elasticity to be $\lambda=\infty$ & $\lambda=\mu$, we can calculate the surface displacements from the above formulae which are shown in the next table:

λ	$\gamma/a = 1/5$	$\gamma/a = 2$
∞	$-\cdot 0332$ cm	$-\cdot 00896$ cm
μ	$-\cdot 0279$ cm	$-\cdot 00748$ cm

6. In the same manner as we mentioned in Section 3, we shall proceed to the case that γ is a function of β, namely $\gamma=\gamma'\beta^n$, $[n=1, 2, 3\cdots]$. For the sake of simplicity, we take $n=1$, i.e. $\gamma=\gamma'\beta$, where γ' is a mere number.

When $\gamma=\gamma'\beta$, we can easily get the temperature distribution, displacement and inclination by the same method described in Section 4.

The temperature distribution, being expressed by

$$T=\frac{1}{\pi}\int_0^\infty d\beta\int_{-\infty}^{\infty} f(\varkappa)\, e^{-\gamma'\beta y}\cos\beta\,(x-\varkappa)\, d\varkappa, \quad\cdots\cdots\cdots\cdots\cdots\cdots(48)$$

the components of displacement (u, v) and the inclination $\dfrac{\partial v}{\partial x}$ are of the following expressions:

$$u = -\frac{\alpha}{\pi(\lambda+2\mu)(1+\gamma')}\Big[y\int_0^\infty d\beta\int_{-\infty}^\infty f(\varkappa)\,e^{-\beta y}\sin\beta(x-\varkappa)\,d\varkappa$$

$$-\frac{\mu-(\lambda+2\mu)\gamma'}{(\lambda+\mu)(1-\gamma')}\int_0^\infty d\beta\int_{-\infty}^\infty f(\varkappa)\frac{e^{-\beta y}}{\beta}\sin\beta(x-\varkappa)\,d\varkappa$$

$$-\frac{1}{1-\gamma'}\int_0^\infty d\beta\int_{-\infty}^\infty f(\varkappa)\frac{e^{-\gamma'\beta y}}{\beta}\sin\beta(x-\varkappa)\,d\varkappa\Big],\quad [\gamma'\neq 1]$$

..................(49)

$$v = -\frac{\alpha}{\pi(\lambda+2\mu)(1+\gamma')}\Big[y\int_0^\infty d\beta\int_{-\infty}^\infty f(\varkappa)\,e^{-\beta y}\cos\beta(x-\varkappa)\,d\varkappa$$

$$-\frac{\mu\gamma'-(\lambda+2\mu)}{(\lambda+\mu)(1-\gamma')}\int_0^\infty d\beta\int_{-\infty}^\infty f(\varkappa)\frac{e^{-\beta y}}{\beta}\cos\beta(x-\varkappa)\,d\varkappa$$

$$-\frac{1}{1-\gamma'}\int_0^\infty d\beta\int_{-\infty}^\infty f(\varkappa)\frac{e^{-\gamma'\beta y}}{\beta}\cos\beta(x-\varkappa)\,d\varkappa\Big],\quad [\gamma'\neq 1]$$

..................(50)

$$\left.\begin{aligned} u &= \frac{\alpha}{2\pi(\lambda+\mu)}\int_0^\infty d\beta\int_{-\infty}^\infty f(\varkappa)\frac{e^{-\beta y}}{\beta}\sin\beta(x-\varkappa)\,d\varkappa,\\ v &= -\frac{\alpha}{2\pi(\lambda+\mu)}\int_0^\infty d\beta\int_{-\infty}^\infty f(\varkappa)\frac{e^{-\beta y}}{\beta}\cos\beta(x-\varkappa)\,d\varkappa,\end{aligned}\right\}\quad[\gamma'=1]$$

..................(51)

and

$$\frac{\partial v}{\partial x} = \frac{\alpha}{\pi(\lambda+2\mu)(1+\gamma')}\Big[y\int_0^\infty d\beta\int_{-\infty}^\infty f(\varkappa)\,e^{-\beta y}\sin\beta(x-\varkappa)\,\beta d\varkappa$$

$$-\frac{\mu\gamma'-(\lambda+2\mu)}{(\lambda+\mu)(1-\gamma')}\int_0^\infty d\beta\int_{-\infty}^\infty f(\varkappa)\,e^{-\beta y}\sin\beta(x-\varkappa)\,d\varkappa$$

$$-\frac{1}{1-\gamma'}\int_0^\infty d\beta\int_{-\infty}^\infty f(\varkappa)\,e^{-\gamma'\beta y}\sin\beta(x-\varkappa)\,d\varkappa\Big],\quad[\gamma'\neq 1]$$

..................(52)

$$\frac{\partial v}{\partial x} = \frac{\alpha}{2\pi(\lambda+\mu)}\int_0^\infty d\beta \int_{-\infty}^{\infty} f(\chi)\, e^{-\beta y} \sin\beta(x-\chi)\, d\chi.$$

$$[\gamma' = 1] \quad \cdots\cdots(53)$$

7. As an example of the section 8 just we have studied, we shall take the temperature distribution of the following form on the surface of the body:

$$f(x) = \frac{Ba^2}{b^2+x^2}, \quad \cdots\cdots(54)$$

where a and b are the constants which can be adjusted to obey to the distribution of the surface temperature to a wide range, and B is the measurement of temperature, having no dimension.

Then from (48), we can find the following form of temperature distribution:

$$T = \frac{Ba^2}{b}\int_0^\infty e^{-(\gamma' y+b)\beta} \cos\beta x\, d\beta, \quad \cdots\cdots(55)$$

by the aid of

$$\int_0^\infty \frac{\cos\alpha x}{1+x^2}\, dx = \frac{\pi}{2} e^{-\alpha}. \quad \cdots\cdots(56)$$

Now we can easily evaluate the integral of (55), using the integral formula

$$\int_0^\infty e^{-bf} \cos fx\, df = \frac{b}{b^2+x^2}, \quad \cdots\cdots(57)$$

in the form of

$$T = \frac{Ba^2}{b} \times \frac{b+\gamma' y}{x^2+(b+\gamma' y)^2}. \quad \cdots\cdots(58)$$

Now, the inclination $\frac{\partial v}{\partial x}$ due to the temperature distribution expressed by the equation (58) is written from (52) in the following form:

$$\frac{\partial v}{\partial x} = \frac{\alpha B a^2}{b(\lambda+2\mu)(1+\gamma')}\Big[y\frac{\partial}{\partial x}\int_0^\infty e^{-(b+y)\beta}\cos\beta x\,d\beta$$

$$-\frac{\mu\gamma'-(\lambda+2\mu)}{(\lambda+\mu)(1-\gamma')}\int_0^\infty e^{-(b+y)\beta}\sin\beta x\,d\beta$$

$$-\frac{\gamma'}{1-\gamma'}\int_0^\infty e^{-(b+\gamma' y)\beta}\sin\beta x\,d\beta\Big]$$

$$=\frac{\alpha B a^2}{b(\lambda+2\mu)(1+\gamma')}\Big[\frac{\lambda+(2-\gamma')\mu}{(\lambda+\mu)(1-\gamma')}\,\frac{x}{x^2+(b+y)^2}$$

$$-\frac{2xy(b+y)}{\{x^2+(b+y)^2\}^2}-\frac{\gamma'}{1-\gamma'}\,\frac{x}{x^2+(b+\gamma' y)^2}\Big],$$

$$[\gamma' \neq 1] \quad \cdots\cdots(59)$$

$$\frac{\partial v}{\partial x} = \frac{\alpha B a^2}{2(\lambda+\mu)b}\int_0^\infty e^{-(b+y)\beta}\sin\beta x\,d\beta$$

$$=\frac{\alpha B a^2}{2b(\lambda+\mu)}\,\frac{x}{x^2+(b+y)^2}. \quad [\gamma' = 1] \quad \cdots\cdots\cdots\cdots(60)$$

The surface tilt due to temperature distribution of (58) is expressed by

$$\frac{\partial v}{\partial x} = \frac{\alpha B a^2}{b(\lambda+\mu)(1+\gamma')}\,\frac{x}{(b^2+x^2)}. \quad \cdots\cdots\cdots\cdots\cdots\cdots\cdots\cdots(61)$$

We can see from the above formula that the inclination of the surface is extraordinarily affected by the number of γ', namely the inclination $\frac{\partial v}{\partial x}_{y=0}$ is inversely proportional to $(1+\gamma')$. The value of γ', as we have discussed in the above section, changes the temperature distribution in the interior of the solid, and the larger the value of γ' is, the more intensively diminishes the effect of the surface distribution of the temperature in the interior of the solid. Hence we may suppose that the large value of γ' corresponds to the daily variation of the temperature, and the small value of γ' to the annular variation of the

temperature in the interior of the earth. These relations are given in Figures 4a, 4b, which are compiled from the equation of (58).

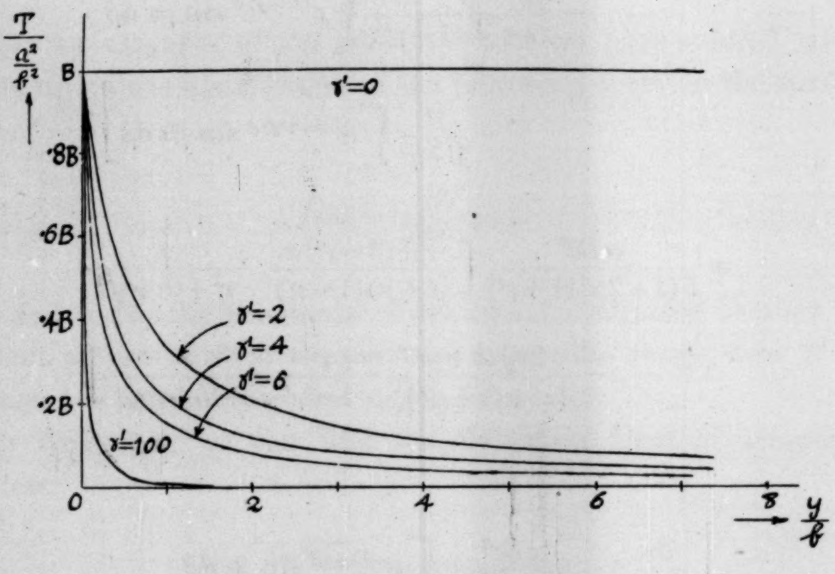

Fig. 4a. $\left[\frac{x}{b}=0.\right]$

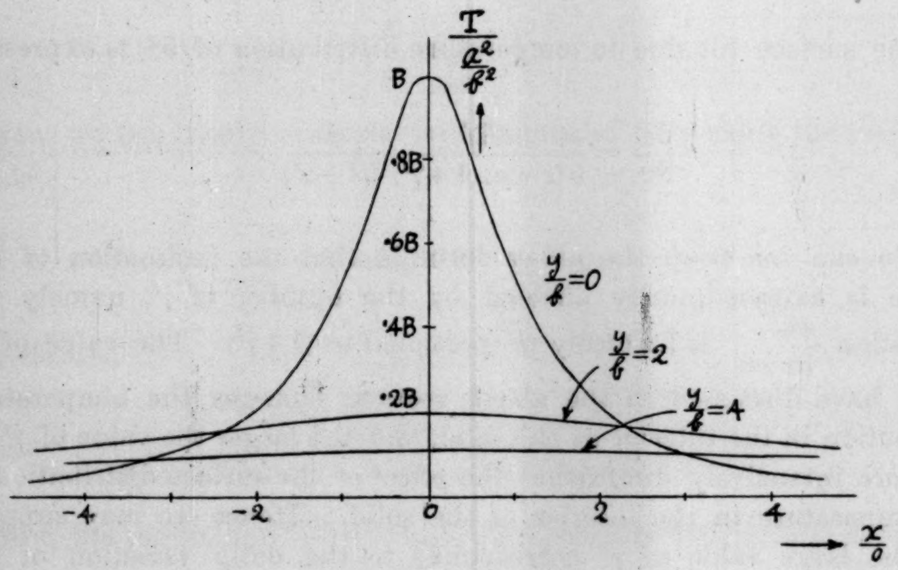

Fig. 4b. $[\gamma' = 2.]$

From the above figures, we can easily understand the above mentioned facts. In Fig. 4a the temperature distributions in the interior of the solid are compiled, when $x/a=0$ and $\gamma'=0$, 2, 4, 6 & 100, and Fig. 4b shews the temperature distribution when $y/b=0$, 2 & 4, and we can see that the effect of the surface distribution in the interior of the solid is extraordinarily small when the value of γ' is large.

Now, from the equations (59), (61) we can easily see that the surface tilt is limited by the value of γ', namely the maximum inclination occurs when γ' is zero, that is the case of the constant temperature distribution at all depth in the interior of the solid. These relations will be seen in Figure 5.

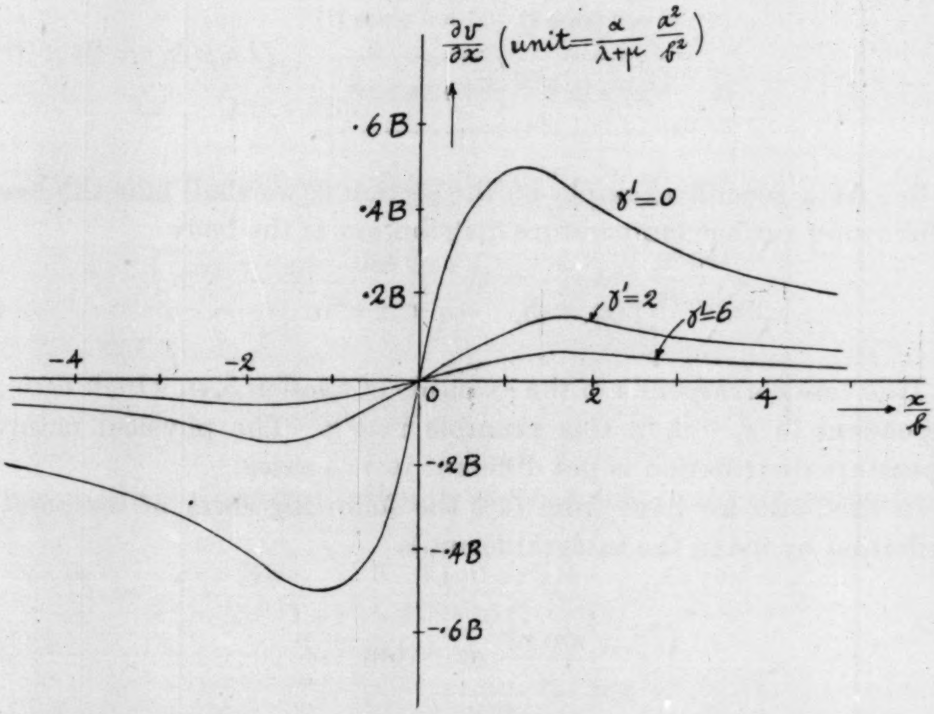

Fig. 5.

In the following two examples, we assume that γ' shall be taken 2 and 6, and the surface temperature distribution is given in Table I, and the effects of these surface temperature distribution in the interior of the solid at $x=0$ are written in Table II.

Table I.

distance from the origin (x)	surface temperature
0 meter	100°C
1 meter	50°C
2 meters	20°C
4 meters	5°C
6 meters	3°C

Table II.

distance from the surface (y)	$\gamma' = 2$ (1st example)	$\gamma' = 6$ (2nd example)
0 meter	100°C	100°C
1 meter	33°C	15°C
2 meters	22°C	7°C
4 meters	11°C	4°C
6 meters	8°C	3°C
8 meters	6°C	2°C

When we take these two cases, we have the following surface tilt at the point 2 meters far from the center, as given in the following table.

$\gamma' = 2$ (case I)	$\gamma' = 6$ (case II)
$2{\cdot}7 \times 10^{-4}$	$1{\cdot}3 \times 10^{-4}$

$[\lambda=\mu \;\&\; c={\cdot}24\times10^{-4}.]$

8. As a second example of the section 6, we shall take the case of the following surface temperature distribution of the body:

$$f(x) = B, \quad -a < x < a. \qquad \cdots\cdots(62)$$

This case corresponds to the example of Section 5, in which case γ is independent to β, but in this example $\gamma=\gamma'\beta$. The physical nature of temperature distribution is not different in two cases.

In this case we have from (48) the following form of temperature distribution by using the integral formula

$$\int_0^\infty e^{-ax} \frac{\sin px}{x} dx = \tan^{-1} \frac{p}{a}, \qquad \cdots\cdots(63)$$

$$\begin{aligned} T &= \frac{2B}{\pi} \int_0^\infty \frac{e^{-\gamma'\beta y}}{\beta} \cos \beta x \sin \beta a \, d\beta \\ &= \frac{B}{\pi} \left[\tan^{-1} \frac{x+a}{\gamma' y} + \tan^{-1} \frac{a-x}{\gamma' y} \right] \quad -a < x < a \\ &= 0. \qquad a < x, \quad -a > x \qquad \cdots\cdots(64) \end{aligned}$$

In Section 5 we have studied the surface deformation, but in this section we shall discuss the inclinations at all depth of the body due to the surface temperature distribution represented by (62).

Then from the formula expressed by (52), we have the following formula of inclination at all depth of the body:

$$\frac{\partial v}{\partial x}=\frac{2B\alpha}{\pi(\lambda+2\mu)(1+\gamma')}\Big[y\int_0^\infty e^{-\beta y}\sin\beta x\sin\beta a\,d\beta$$

$$-\frac{\mu\gamma'-(\lambda+2\mu)}{(\lambda+\mu)(1-\gamma')}\int_0^\infty\frac{e^{-\beta y}}{\beta}\sin\beta x\sin\beta a\,d\beta$$

$$-\frac{\gamma'}{1-\gamma'}\int_0^\infty\frac{e^{-\gamma'\beta y}}{\beta}\sin\beta x\sin\beta a\,d\beta\Big],\ [\gamma'\neq 1]\cdots(65)$$

$$\frac{\partial v}{\partial x}=\frac{B\alpha}{\pi(\lambda+\mu)}\int_0^\infty\frac{e^{-\beta y}}{\beta}\sin\beta x\sin\beta a\,d\beta.\quad[\gamma'=1]\ \cdots\cdots\cdots(66)$$

Now using the following formulae,

$$\left.\begin{aligned}&\int_0^\infty e^{-\beta x}\frac{\cos\alpha x-\cos\xi x}{x}\,dx=\frac{1}{2}\log\frac{\beta^2+\xi^2}{\beta^2+\alpha^2},\\&\int_0^\infty e^{-ax}\cos cx\,dx=\frac{a}{a^2+c^2},\end{aligned}\right\}\ \cdots\cdots\cdots\cdots(67)$$

we can easily evaluate the integrals of (65) & (66) in the following forms:

$$\frac{\partial v}{\partial x}=\frac{B\alpha}{\pi(\lambda+2\mu)(1+\gamma')}\Big[\frac{\lambda+(2-\gamma')\mu}{2(\lambda+\mu)(1-\gamma')}\log\frac{(x+a)^2+y^2}{(x-a)^2+y^2}$$

$$-\frac{\gamma'}{2(1-\gamma')}\log\frac{(x+a)^2+\gamma'^2y^2}{(x-a)^2+\gamma'^2y^2}$$

$$+\frac{4axy^2}{\{(x+a)^2+y^2\}\{(x-a)^2+y^2\}}\Big],$$

$$[\gamma'\neq 1]\ \cdots\cdots(68)$$

$$\frac{\partial v}{\partial x}=\frac{B\alpha}{4\pi(\lambda+\mu)}\log\frac{(x+a)^2+y^2}{(x-a)^2+y^2},\quad[\gamma'=1]\ \cdots\cdots\cdots\cdots\cdots\cdots\cdots\cdots(69)$$

and the surface tilt is of the form of

$$\frac{\partial v}{\partial x_{y=0}} = \frac{B\alpha}{2\pi(\lambda+\mu)(1+\gamma')} \log \frac{(x+a)^2}{(x-a)^2}. \qquad \text{(68)}'$$

From the equation (64), we can see that the temperature effect in the interior of the body is more decreased as larger the value of γ' becomes. This nature is shown in Figure 6b which is compiled from (64) at $x=0$.

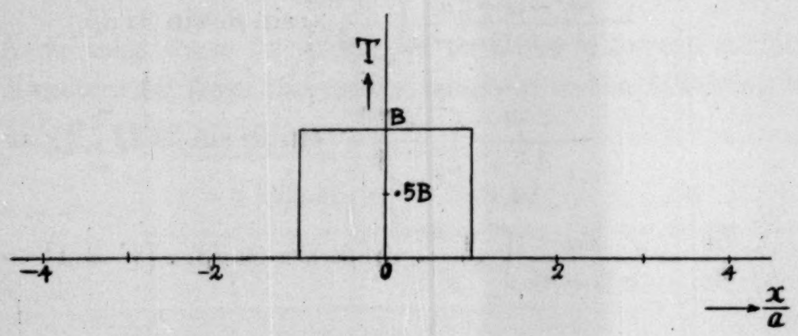

Fig. 6a. [$y = 0.$]

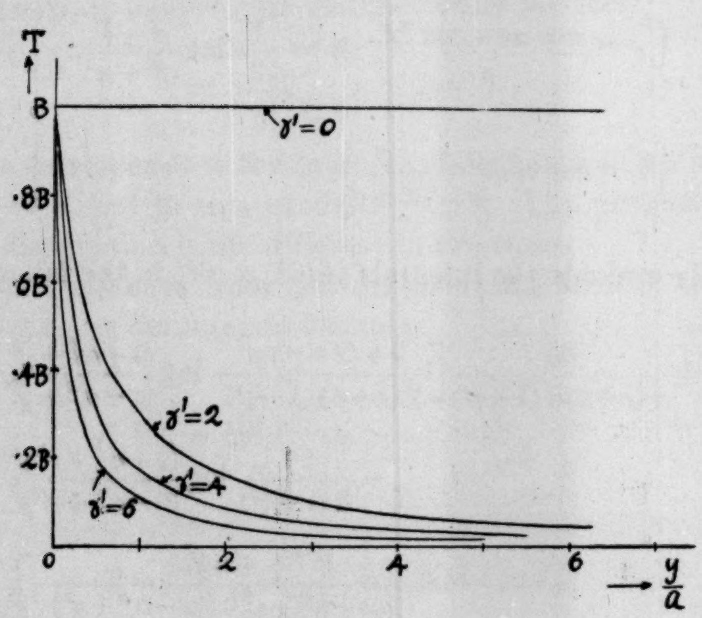

Fig. 6b. [$x = 0.$]

The equations (68), (69) teach us that for any temperature of the surface of the solid the inclination at a large depth is very small,

and the inclination of the surface is extraordinarily affected by the number of γ', namely it is inversely proportional to $(1+\gamma')$. These natures have been shown in Section 5.

If we compile the inclination at the surface when $\gamma'=0$, 1, 2 & 4, we have Figure 7 from the formulae (68) & (69).

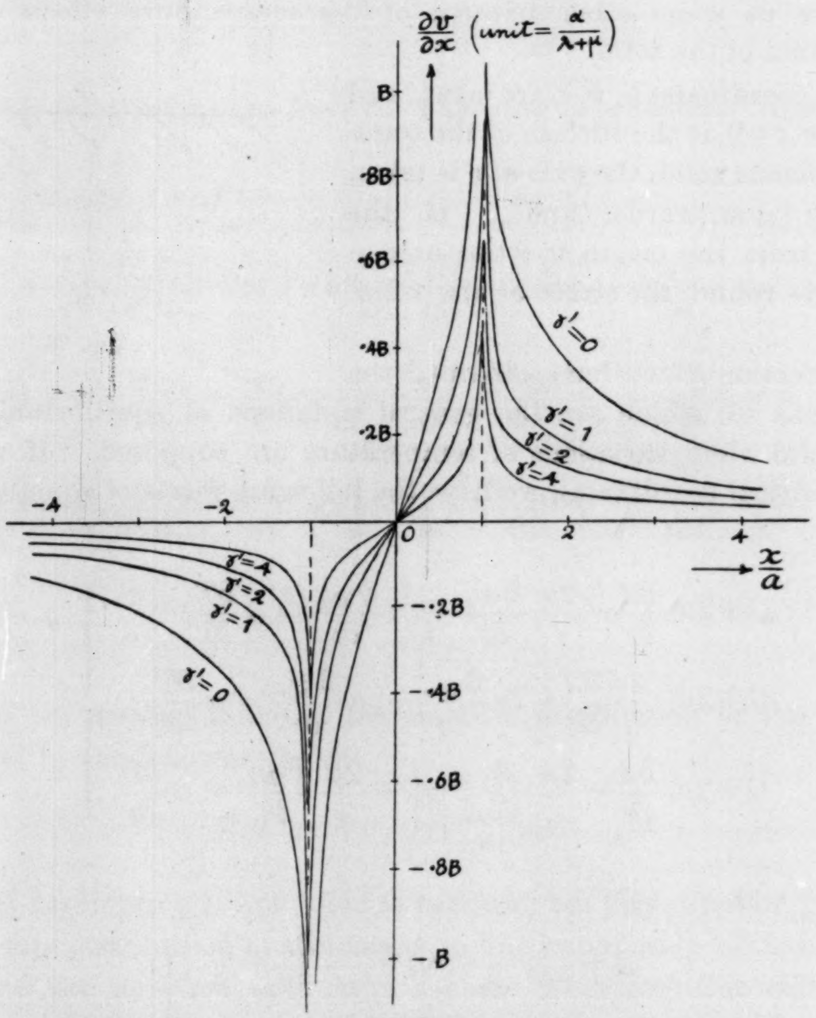

Fig. 7. [$y=0$.]

At the point of $x=\pm a$, the inclination of the surface is infinite. This nature is not violent when we know the temperature distribution of the surface of the solid.

Part III. Three-dimensional Problem.

9. In the above sections we have studied the two-dimentional problem, and we have many valuable natures at the study of the effects of temperature distribution of the surface on the deformation of the solid. In the present and succeeding sections we shall take the threedimensional problems using the cylindrical coordinates, which may give us some other natures of the temperature effects on the deformation of the solid.

The coordinates (r, θ, z) are taken, and the plane $z=0$ is the surface of the semi-infinite elastic solid, the axis of z is taken vertically downwards and r is the distance from the origin 0, θ the azimuthal angle round the z-axis of the solid. (Fig. 8)

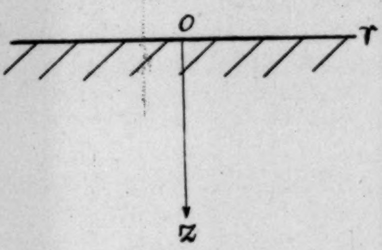

Fig. 8.

In Section 2 we have obtained the expressions (6) which are the general equations of equilibrium of an elastic solid when variations of temperature are supposed. If we take the cylindrical coordinates, we have the following forms of equations:

$$\left.\begin{aligned}
(\lambda+2\mu)\frac{\partial \Delta}{\partial r} - \frac{2\mu}{r}\frac{\partial \varpi_z}{\partial \theta} + 2\mu\frac{\partial \varpi_\theta}{\partial z} &= \alpha\frac{\partial T}{\partial r},\\
(\lambda+2\mu)\frac{1}{r}\frac{\partial \Delta}{\partial \theta} - 2\mu\frac{\partial \varpi_r}{\partial z} + 2\mu\frac{\partial \varpi_z}{\partial r} &= \alpha\frac{\partial T}{r\partial \theta},\\
(\lambda+2\mu)\frac{\partial \Delta}{\partial r} - \frac{2\mu}{r}\frac{\partial}{\partial r}(r\varpi_\theta) + \frac{2\mu}{r}\frac{\partial \varpi_r}{\partial \theta} &= \alpha\frac{\partial T}{\partial z},
\end{aligned}\right\}\quad\cdots\cdots\cdots\cdots(70)$$

where

$$\left.\begin{aligned}
\Delta &= \frac{1}{r}\frac{\partial}{\partial r}(ru) + \frac{1}{r}\frac{\partial v}{\partial \theta} + \frac{\partial w}{\partial z},\\
2\varpi_r &= \frac{1}{r}\frac{\partial w}{\partial \theta} - \frac{\partial v}{\partial z},\\
2\varpi_\theta &= \frac{\partial u}{\partial z} - \frac{\partial w}{\partial r},\\
2\varpi_z &= \frac{1}{r}\frac{\partial (rv)}{\partial r} - \frac{1}{r}\frac{\partial u}{\partial \theta},
\end{aligned}\right\}\quad\cdots\cdots\cdots\cdots\cdots\cdots(71)$$

and T is the difference of the temperature, and

$$\alpha = \left(\lambda + \frac{2}{3}\mu\right)c. \qquad \cdots\cdots(72)$$

Now we know that there is the following identical relation between ϖ_r, ϖ_θ and ϖ_z:

$$\frac{1}{r}\frac{\partial(r\varpi_r)}{\partial r} + \frac{1}{r}\frac{\partial\varpi_\theta}{\partial\theta} + \frac{\partial\varpi_z}{\partial z} = 0. \qquad \cdots\cdots(73)$$

Using this relation, we can have the following expressions[13] from (70):

$$\frac{\partial^2}{\partial r^2}\Big[(\lambda+2\mu)\,\Delta - \alpha T\Big] + \frac{1}{r}\frac{\partial}{\partial r}\Big[(\lambda+2\mu)\,\Delta - \alpha T\Big] + \frac{1}{r^2}\frac{\partial^2}{\partial\theta^2}\Big[(\lambda+2\mu)\,\Delta - \alpha T\Big] + \frac{\partial^2}{\partial z^2}\Big[(\lambda+2\mu)\,\Delta - \alpha T\Big] = 0, \qquad \cdots\cdots(74)$$

$$\frac{\partial^2\varpi_r}{\partial r^2} + \frac{3}{r}\frac{\partial\varpi_r}{\partial r} + \frac{\varpi_r}{r^2} + \frac{1}{r^2}\frac{\partial^2\varpi_r}{\partial\theta^2} + \frac{\partial^2\varpi_r}{\partial z^2} + \frac{2}{r}\frac{\partial\varpi_z}{\partial z} = 0, \qquad \cdots\cdots(75)$$

$$\frac{\partial^2\varpi_\theta}{\partial r^2} + \frac{1}{r}\frac{\partial\varpi_\theta}{\partial r} - \frac{\varpi_\theta}{r^2} + \frac{1}{r^2}\frac{\partial^2\varpi_\theta}{\partial\theta^2} + \frac{\partial^2\varpi_\theta}{\partial z^2} + \frac{2}{r^2}\frac{\partial\varpi_r}{\partial\theta} = 0, \qquad \cdots\cdots(76)$$

$$\frac{\partial^2\varpi_z}{\partial r^2} + \frac{1}{r}\frac{\partial\varpi_z}{\partial r} + \frac{1}{r^2}\frac{\partial^2\varpi_z}{\partial\theta^2} + \frac{\partial^2\varpi_z}{\partial z^2} = 0. \qquad \cdots\cdots(77)$$

Now we assume that the temperature distribution of the body is expressed by the following form:

$$T = \mathfrak{A}e^{-\beta z} J_m(kr) \left.\begin{matrix}\sin\\ \cos\end{matrix}\right\} m\theta. \qquad \cdots\cdots(78)$$

This assumption is not made at randum, but this equation gives the temperature distribution at a moment in the conduction of heat in the body, and the zero temperature at $z = \infty$. Therefore this equation is very favourable for our study. In (78) $\mathfrak{A}$ is any constant, and a measurement of the magnitude of temperature, and m, k and β are any constants not defined in this section.

---

13) The reductions of these equations when $T = 0$ have been made by Prof. K. Sezawa.

K. Sezawa, *Bull. Earthq. Res. Inst.*, **6** (1929), 1.

Then, from the equation (74), we have

$$\frac{\partial^2 \Delta}{\partial r^2}+\frac{1}{r}\frac{\partial \Delta}{\partial r}+\frac{1}{r^2}\frac{\partial^2 \Delta}{\partial \theta^2}+\frac{\partial^2 \Delta}{\partial z^2}=\frac{\alpha\mathfrak{A}}{\lambda+2\mu}e^{-\beta z}J_m(kr)\left.\begin{matrix}\sin\\ \cos\end{matrix}\right\} m\theta. \cdots\cdots(79)$$

The particular solution of this equation is of the following form:

$$\Delta_1 = \alpha\mathfrak{A}\frac{e^{-\beta z}}{\lambda+2\mu}J_m(kr)\left.\begin{matrix}\sin\\ \cos\end{matrix}\right\} m\theta, \cdots\cdots(80)$$

and the complementary solution, which is useful for our study, is

$$\Delta_2 = A_m e^{-kz} J_m(kr)\left.\begin{matrix}\sin\\ \cos\end{matrix}\right\} m\theta. \cdots\cdots(81)$$

The solution of (77), which is suitable to this case, is of the form of

$$2\varpi_z = B_m e^{-kz} J_m(kr)\left.\begin{matrix}-\cos\\ \sin\end{matrix}\right\} m\theta. \cdots\cdots(82)$$

We have thus the following expressions of ϖ_r and ϖ_θ from the equations (75) and (76):

$$2\varpi_r = \left[C_m\frac{J_m(kr)}{r} - B_m\frac{1}{k}\frac{\partial J_m(kr)}{\partial r}\right]e^{-kz}\left.\begin{matrix}-\cos\\ \sin\end{matrix}\right\} m\theta, \cdots\cdots(83)$$

$$2\varpi_\theta = \left[C_m\frac{1}{m}\frac{\partial J_m(kr)}{\partial r} - B_m\frac{m}{k}\frac{J_m(kr)}{r}\right]e^{-kz}\left.\begin{matrix}\sin\\ \cos\end{matrix}\right\} m\theta. \cdots\cdots(84)$$

In the above expressions of Δ, ϖ_r, ϖ_θ and ϖ_z, A_m, B_m, C_m are arbitrary constants. From the equilibrium equations expressed by (70), we can find the relation between A_m and C_m:

$$A_m/C_m = \frac{k}{m}\frac{\mu}{\lambda+2\mu}, \cdots\cdots(85)$$

when $\beta = k$,

$$(\lambda+2\mu)A_m - \frac{\mu k}{m}C_m = \alpha\mathfrak{A}. \cdots\cdots(86)$$

As we know the relations among the displacement (u, v, w), the dilatations (Δ_1, Δ_2) and the rotations $(\varpi_r, \varpi_\theta, \varpi_z)$ as seen in (71), we can find the displacements from Δ_1, Δ_2, ϖ_r, ϖ_θ, ϖ_z expressed by (80), (81), (82), (83) and (84) as the following system.[14)]

14) Prof. K. Sezawa devised this analytical method of obtaining the displancements except (u_1, v_1, w_1) *Bull. Earthq. Res. Inst.*, 6 (1929), 1. Even though the expressions of the displacement can also be obtained in the manner as Prof. K. Terazawa employed in his paper on the problem of tidal loading, *Jour. Coll. Soc.*, Tokyo, 37 (1916), his method of deduction is too complex to introduce in this analytical calculation.

Now the displacement (u_1, v_1, w_1) satisfying Δ_1 expressed by (80) and $\varpi_r=\varpi_\theta=\varpi_z=0$, is expressed by

$$\left.\begin{aligned} u_1 &= \frac{\alpha\mathfrak{A}}{\lambda+2\mu}\,\frac{e^{-\beta z}}{\beta^2-k^2}\,\frac{\partial J_m(kr)}{\partial r}\,\begin{matrix}\sin\\ \cos\end{matrix}\Big\}\,m\theta, \\ v_1 &= -\frac{\alpha\mathfrak{A}}{\lambda+2\mu}\,\frac{me^{-\beta z}}{\beta^2-k^2}\,\frac{J_m(kr)}{r}\,\begin{matrix}-\cos\\ \sin\end{matrix}\Big\}\,m\theta, \\ w_1 &= -\frac{\alpha\mathfrak{A}}{\lambda+2\mu}\,\frac{\beta e^{-\beta z}}{\beta^2-k^2}\,J_m(kr)\,\begin{matrix}\sin\\ \cos\end{matrix}\Big\}\,m\theta. \end{aligned}\right\} \quad \cdots\cdots\cdots\cdots(86)$$

The displacement (u_2, v_2, w_2) satisfying Δ_2 expressed by (81), and $\varpi_z=\varpi_\theta=\varpi_z=0$ is written by

$$\left.\begin{aligned} u_2 &= -\frac{A_m}{2k}\,ze^{-kz}\,\frac{\partial J_m(kr)}{\partial r}\,\begin{matrix}\sin\\ \cos\end{matrix}\Big\}\,m\theta, \\ v_2 &= \frac{mA_m}{2k}\,ze^{-kz}\,\frac{J_m(kr)}{r}\,\begin{matrix}-\cos\\ \sin\end{matrix}\Big\}\,m\theta, \\ w_2 &= -\frac{A_m}{2k}\,(1-kz)\,e^{-kz}\,J_m(kr)\,\begin{matrix}\sin\\ \cos\end{matrix}\Big\}\,m\theta. \end{aligned}\right\} \quad \cdots\cdots\cdots\cdots(87)$$

The displacement (u_3, v_3, w_3) answering to $\Delta=\Delta_1+\Delta_2=0$ and satisfying $2\varpi_z$ expressed by (82), and the second term of ϖ_r and ϖ_θ expressed by (83) and (84) is of the form of

$$\left.\begin{aligned} u_3 &= B_m\,\frac{m}{k}\,e^{-kz}\,\frac{J_m(kr)}{r}\,\begin{matrix}\sin\\ \cos\end{matrix}\Big\}\,m\theta, \\ v_3 &= -B_m\,\frac{1}{k^2}\,e^{-kz}\,\frac{\partial J_m(kr)}{\partial r}\,\begin{matrix}-\cos\\ \sin\end{matrix}\Big\}\,m\theta, \\ w_3 &= 0. \end{aligned}\right\} \quad \cdots\cdots\cdots\cdots(88)$$

The displacement (u_4, v_4, w_4) answering to $\Delta=2\varpi_z=0$, and fulfilling the relations of the first of $2\varpi_r$ and $2\varpi_\theta$ expressed by (83) and (84) is expressed by

$$\left.\begin{aligned} u_4 &= \frac{1}{2m}\,C_m\,ze^{-kz}\,\frac{\partial J_m(kr)}{\partial r}\,\begin{matrix}\sin\\ \cos\end{matrix}\Big\}\,m\theta, \\ v_4 &= -\frac{C_m}{2}\,ze^{-kz}\,\frac{J_m(kr)}{r}\,\begin{matrix}-\cos\\ \sin\end{matrix}\Big\}\,m\theta, \\ w_4 &= -\frac{C_m}{2m}\,(1+kz)\,e^{-kz}\,J_m(kr)\,\begin{matrix}\sin\\ \cos\end{matrix}\Big\}\,m\theta. \end{aligned}\right\} \quad \cdots\cdots\cdots\cdots(89)$$

Now the displacement to fulfill the condition that $\Delta=\varpi_r=\varpi_\theta=\varpi_z=0$ is of the following form:

$$\left.\begin{aligned} u_5 &= E_m\, e^{-kz} \frac{\partial J_m(kr)}{\partial r} \begin{Bmatrix}\sin\\ \cos\end{Bmatrix} m\theta, \\ v_5 &= -mE_m\, e^{-kz} \frac{J_m(kr)}{r} \begin{Bmatrix}-\cos\\ \sin\end{Bmatrix} m\theta, \\ w_5 &= -kE_m\, e^{-kz} J_m(kr) \begin{Bmatrix}\sin\\ \cos\end{Bmatrix} m\theta. \end{aligned}\right\} \qquad \text{(90)}$$

The general expressions of the components of displacement favourable in our study are of the form of

$$\left.\begin{aligned} u &= u_1+u_2+u_3+u_4+u_5, \\ v &= v_1+v_2+v_3+v_4+v_5, \\ w &= w_1+w_2+w_3+w_4+w_5, \end{aligned}\right\} \qquad \text{(91)}$$

where u_1, v_1, w_1, u_2,...... are expressed by the equations (86), (87), (88), (89) and (90). When $\beta=k$, $u_1=v_1=w_1=0$. We must, however, remember that there is a relation between A_m and C_m expressed by (85) or (86).

As the stresses are given by

$$\left.\begin{aligned} \widehat{rr} &= \lambda\Delta+2\mu\frac{\partial u}{\partial r}-\alpha T, & \widehat{\theta\theta} &= \lambda\Delta+2\mu\left(\frac{u}{r}+\frac{1}{r}\frac{\partial v}{\partial\theta}\right)-\alpha T, \\ \widehat{zz} &= \lambda\Delta+2\mu\frac{\partial w}{\partial z}-\alpha T, & \widehat{r\theta} &= \mu\left(\frac{\partial v}{\partial r}-\frac{v}{r}+\frac{1}{r}\frac{\partial u}{\partial\theta}\right), \\ \widehat{\theta z} &= \mu\left(\frac{1}{r}\frac{\partial w}{\partial\theta}+\frac{\partial v}{\partial z}\right), & \widehat{rz} &= \mu\left(\frac{\partial u}{\partial z}+\frac{\partial w}{\partial r}\right), \end{aligned}\right\} \qquad \text{(92)}$$

we can find the stresses which are necessary for our study by using the equations (78), (80), (81) and (91).

Now the surface ($z=0$) of the solid is assumed to be free from tractions, so that we have the following conditions on the surface $z=0$:

$$\widehat{zz}=\widehat{\theta z}=\widehat{rz}=0. \qquad \text{(93)}$$

From these relations we can find the following forms of constants A_m, C_m, E_m and B_m:

$$\left.\begin{aligned} A_m &= \frac{2\alpha\mu\mathfrak{A}}{(\lambda+\mu)(\lambda+2\mu)}\frac{k}{\beta+k}, \\ C_m &= \frac{2m\alpha\mathfrak{A}}{\lambda+\mu}\frac{1}{\beta+k}, \\ E_m &= -\frac{\alpha\mathfrak{A}}{(\lambda+\mu)(\lambda+2\mu)}\frac{(\lambda+2\mu)\beta-\mu k}{k(\beta^2-k^2)}, \\ B_m &= 0, \end{aligned}\right\} \quad [\beta \neq k] \quad \cdots\cdots\cdots(94)$$

$$\left.\begin{aligned} A_m &= \frac{\alpha\mathfrak{A}}{\lambda+\mu}, \qquad B_m = 0, \\ C_m &= \frac{m}{k}\frac{\alpha\mathfrak{A}}{\lambda+\mu}, \qquad E_m = -\frac{\alpha\mathfrak{A}}{2(\lambda+\mu)k^2}. \end{aligned}\right\} \quad [\beta = k] \quad \cdots\cdots\cdots(95)$$

Then, from (91), (92), (94) and (95), we get the following forms of u, v and w:

$$\left.\begin{aligned} u &= -\frac{\alpha\mathfrak{A}}{\lambda+2\mu}\left[\frac{(\lambda+2\mu)\beta-\mu k}{(\lambda+\mu)k(\beta^2-k^2)}e^{-kz}-\frac{ze^{-kz}}{\beta+k}-\frac{e^{-\beta z}}{\beta^2-k^2}\right]\frac{\partial J_m(kr)}{\partial r}\begin{matrix}\sin\\ \cos\end{matrix}\Big\}\, m\theta, \\ v &= \frac{\alpha\mathfrak{A}m}{\lambda+2\mu}\left[\frac{(\lambda+2\mu)\beta-\mu k}{(\lambda+\mu)k(\beta^2-k^2)}.e^{-kz}-\frac{ze^{-kz}}{\beta+k}-\frac{e^{-\beta z}}{\beta^2-k^2}\right]\frac{J_m(kr)}{r}\begin{matrix}-\cos\\ \sin\end{matrix}\Big\}\, m\theta, \\ w &= -\frac{\alpha\mathfrak{A}}{\lambda+2\mu}\left[\frac{\mu\beta-(\lambda+2\mu)k}{(\lambda+\mu)(\beta^2-k^2)}e^{-kz}+\frac{kze^{-kz}}{\beta+k}+\frac{\beta e^{-\beta z}}{\beta^2-k^2}\right]J_m(kr)\begin{matrix}\sin\\ \cos\end{matrix}\Big\}\, m\theta, \end{aligned}\right\}$$

$$[\beta \neq k] \quad \cdots\cdots\cdots(96)$$

$$\left.\begin{aligned} u &= -\frac{\alpha\mathfrak{A}}{2(\lambda+\mu)}e^{-kz}\frac{\partial J_m(kr)}{k^2\partial r}\begin{matrix}\sin\\ \cos\end{matrix}\Big\}\, m\theta, \\ v &= \frac{\alpha\mathfrak{A}m}{2(\lambda+\mu)}e^{-kz}\frac{J_m(kr)}{k^2 r}\begin{matrix}-\cos\\ \sin\end{matrix}\Big\}\, m\theta, \\ w &= -\frac{\alpha\mathfrak{A}}{2(\lambda+\mu)}e^{-kz}\frac{J_m(kr)}{k}\begin{matrix}\sin\\ \cos\end{matrix}\Big\}\, m\theta. \end{aligned}\right\} \quad [\beta = k] \quad \cdots\cdots\cdots(97)$$

The displacements thus we obtained are merely the elementary solutions satisfying the condition that the temperature distribution of the body is assumed to be of the type expressed by (78).

When the temperature distribution of the surface of the solid is expressed by $f(r, \theta)$, we can construct the favourable form of displacement by summing up the above elementary solutions by the aid of Fourier's series and the Fourier's Bessel double integral formula.

10. The temperature distribution at any point in the body, when the surface distribution is given by $f(r, \theta)$, is easily formulated by using (78) in the following form:

$$T = \sum_m \left\{ \int_0^\infty J_m(kr)\, e^{-\beta z}\, kdk \int_0^\infty f_m(\xi)\, J_m(k\xi)\, \xi d\xi \right\} \begin{matrix}\sin\\ \cos\end{matrix}\Big\} m\theta, \quad \cdots\cdots\cdots(98)$$

in which we assume that $f(r, \theta)$ can be expanded into a trigonometrical series of the form of

$$f(r,\theta) = \sum_m f_m(r) \begin{matrix}\sin\\ \cos\end{matrix}\Big\} m\theta, \quad \cdots\cdots\cdots(99)$$

where $f_m(r)$ is supposed to satisfy the theorem expressed by the following form:

$$f_m(r) = \int_0^\infty J_m(kr)\, kdk \int_0^\infty f_m(\xi)\, J_m(k\xi)\, \xi d\xi. \quad \cdots\cdots\cdots(100)$$

And the components of displacement (u, v, w) due to the temperature distribution above mentioned are easily written by

$$\begin{aligned} u = -\frac{\alpha}{(\lambda+2\mu)} \sum_m \Bigg[\frac{1}{\lambda+\mu} \int_0^\infty \frac{(\lambda+2\mu)\beta - \mu k}{\beta^2 - k^2}\, e^{-kz}\, \frac{\partial J_m(kr)}{\partial r}\, dk \int_0^\infty f_m(\xi)\, J_m(k\xi)\, \xi d\xi \\ - z \int_0^\infty \frac{e^{-kz}}{\beta + k}\, \frac{\partial J_m(kr)}{\partial r}\, kdk \int_0^\infty f_m(\xi)\, J_m(k\xi)\, \xi d\xi \\ - \int_0^\infty \frac{e^{-\beta z}}{\beta^2 - k^2}\, \frac{\partial J_m(kr)}{\partial r}\, kdk \int_0^\infty f_m(\xi)\, J_m(k\xi)\, \xi d\xi \Bigg] \begin{matrix}\sin\\ \cos\end{matrix}\Big\} m\theta, \end{aligned}$$

$$[\beta \neq k] \quad \cdots\cdots(101)$$

$$v=\frac{\alpha}{(\lambda+2\mu)}\sum_m m\Big[\frac{1}{\lambda+\mu}\int_0^\infty\frac{(\lambda+2\mu)\beta-\mu k}{\beta^2-k^2}\,e^{-kz}\,\frac{J_m(kr)}{r}\,dk\int_0^\infty f_m(\xi)\,J_m(k\xi)\,\xi d\xi$$

$$-z\int_0^\infty\frac{e^{-kz}}{\beta+k}\,\frac{J_m(kr)}{r}\,kdk\int_0^\infty f_m(\xi)\,J_m(k\xi)\,\xi d\xi$$

$$-\int_0^\infty\frac{e^{-\beta z}}{\beta^2-k^2}\,\frac{J_m(kr)}{r}\,kdk\int_0^\infty f_m(\xi)\,J_m(k\xi)\,\xi d\xi\Big]\begin{matrix}-\cos\\ \sin\end{matrix}\Big\}\,m\theta,$$

$$[\beta\neq k]\quad\cdots\cdots(102)$$

$$w=-\frac{\alpha}{(\lambda+2\mu)}\sum_m\Big[\frac{1}{\lambda+\mu}\int_0^\infty\frac{\mu\beta-(\lambda+2\mu)k}{\beta^2-k^2}\,e^{-kz}\,J_m(kr)\,kdk\int_0^\infty f_m(\xi)\,J_m(k\xi)\,\xi d\xi$$

$$+z\int_0^\infty\frac{e^{-kz}}{\beta+k}\,J_m(kr)\,k^2dk\int_0^\infty f_m(\xi)\,J_m(k\xi)\,\xi d\xi$$

$$+\int_0^\infty\frac{\beta e^{-\beta z}}{\beta^2-k^2}\,J_m(kr)\,kdk\int_0^\infty f_m(\xi)\,J_m(k\xi)\,\xi d\xi\Big]\begin{matrix}\sin\\ \cos\end{matrix}\Big\}\,m\theta,$$

$$[\beta\neq k]\quad\cdots\cdots(103)$$

and when $\beta=k$,

$$u=-\frac{\alpha}{2(\lambda+\mu)}\sum_m\Big[\Big]\int_0^\infty e^{-kz}\,\frac{\partial J_m(kr)}{k\partial r}\,dk\int_0^\infty f_m(\xi)\,J_m(k\xi)\,\xi d\xi\Big]\begin{matrix}\sin\\ \cos\end{matrix}\Big\}\,m\theta,\qquad[\beta=k]$$

$$\cdots\cdots\cdots(104)$$

$$v=\frac{\alpha}{2(\lambda+\mu)}\sum_m m\Big[\Big]\int_0^\infty e^{-kz}\,\frac{J_m(kr)}{kr}\,dk\int_0^\infty f_m(\xi)\,J_m(k\xi)\,\xi d\xi\Big]\begin{matrix}-\cos\\ \sin\end{matrix}\Big\}\,m\theta,\quad[\beta=k]$$

$$\cdots\cdots\cdots(105)$$

$$w=-\frac{\alpha}{2(\lambda+\mu)}\sum_m\Big[\Big]\int_0^\infty e^{-kz}\,J_m(kr)\,dk\int_0^\infty f_m(\xi)\,J_m(k\xi)\,\xi d\xi\Big]\begin{matrix}\sin\\ \cos\end{matrix}\Big\}\,m\theta.\qquad[\beta=k]$$

$$\cdots\cdots\cdots(106)$$

In the above equations (101), (102), (103), (104), (105) & (106), we assume that the temperature distribution $f(r,\theta)$ of the surface of the solid is of the following form:

$$f(r,\theta) = \sum_m f_m(r) \left.\begin{matrix}\sin\\ \cos\end{matrix}\right\} m\theta,$$

and $f_m(r)$ is supposed to satisfy the theorem of (100).

We can easily formulate the thermal stresses $\widehat{rr}, \widehat{\theta\theta}, \widehat{zz}, \cdots\cdots$ due to the heat distribution expressed by (98) by the aid of above mentioned method, but in our study we have omitted this procedure.

In this section, we have obtained the general expressions of temperature distribution in the body and the displacement (u, v, w) due to the surface temperature of which distribution is of the type of $f(r, \theta)$. In the actual cases, too, the temperature distribution having the azimuthal variation is most probable, but the equations thus we obtained are very complicated and it is sufficient to study the symmetrical cases to know the effect of the temperature distribution in the three-dimensional problem. Moreover this case is more simple than the case having the azimuthal variation.

11. When the temperature distribution in the body has no azimuthal variation, and the temperature distribution of the surface is given by the form of

$$T = f(r), \qquad z = 0, \qquad \cdots\cdots\cdots\cdots\cdots\cdots\cdots\cdots\cdots(107)$$

we have the following temperature distribution instead of (98):

$$T = \int_0^\infty J_0(kr)\, e^{-\beta z}\, kdk \int_0^\infty f(\xi)\, J_0(k\xi)\, \xi d\xi, \qquad \cdots\cdots\cdots\cdots\cdots\cdots(108)$$

and the components of the displacement (u, v, w) have the following forms instead of (101), (102), (103), (104), (105), (106):

$$u = -\frac{\alpha}{\lambda+2\mu}\left[\frac{1}{\lambda+\mu}\int_0^\infty \frac{(\lambda+2\mu)\beta-\mu k}{\beta^2-k^2}\, e^{-kz}\, \frac{\partial J_0(kr)}{\partial r}\, dk \int_0^\infty f(\xi)\, J_0(k\xi)\, \xi d\xi \right.$$
$$-z\int_0^\infty \frac{e^{-kz}}{\beta+k}\, \frac{\partial J_0(kr)}{\partial r}\, kdk \int_0^\infty f(\xi)\, J_0(k\xi)\, \xi d\xi$$
$$\left. -\int_0^\infty \frac{e^{-\beta z}}{\beta^2-k^2}\, \frac{\partial J_0(kr)}{\partial r}\, kdk \int_0^\infty f(\xi)\, J_0(k\xi)\, \xi d\xi \right],$$
$$[\beta \neq k] \quad \cdots\cdots(109)$$

$$w = -\frac{\alpha}{(\lambda+2\mu)}\left[\frac{1}{\lambda+\mu}\int_0^\infty \frac{\mu\beta-(\lambda+2\mu)k}{\beta^2-k^2}\, e^{-kz} J_0(kr)\, kdk \int_0^\infty f(\xi)\, J_0(k\xi)\, \xi d\xi\right.$$

$$+ z\int_0^\infty \frac{e^{-kz}}{\beta+k} J_0(kr)\, k^2dk \int_0^\infty f(\xi)\, J_0(k\xi)\, \xi d\xi$$

$$\left.+\int_0^\infty \frac{\beta e^{-kz}}{\beta^2-k^2} J_0(kr)\, kdk \int_0^\infty f(\xi)\, J_0(k\xi)\, \xi d\xi\right],$$

$$[\beta \neq k] \quad \cdots\cdots(110)$$

$$u = -\frac{\alpha}{2(\lambda+\mu)}\int_0^\infty e^{-kz}\frac{\partial J_0(kr)}{k\partial r}\, dk \int_0^\infty f(\xi)\, J_0(k\xi)\, \xi d\xi,$$

$$[\beta = k] \quad \cdots\cdots(111)$$

$$w = -\frac{\alpha}{2(\lambda+\mu)}\int_0^\infty e^{-kz} J_0(kr)\, dk \int_0^\infty f(\xi)\, J_0(k\xi)\, \xi d\xi.$$

$$[\beta = k] \quad \cdots\cdots(112)$$

We can easily find the tilt $\frac{\partial w}{\partial r}$ in the following form:

$$\frac{\partial w}{\partial r} = \frac{\alpha}{\lambda+2\mu}\left[\frac{1}{\lambda+\mu}\int_0^\infty \frac{\mu\beta-(\lambda+2\mu)k}{\beta^2-k^2}\, e^{-kz} J_1(kr)\, k^2dk \int_0^\infty f(\xi)\, J_0(k\xi)\, \xi d\xi\right.$$

$$+ z\int_0^\infty \frac{e^{-kz}}{\beta+k} J_1(kr)\, k^3dk \int_0^\infty f(\xi)\, J_0(k\xi)\, \xi d\xi$$

$$\left.+\int_0^\infty \frac{\beta e^{-\beta z}}{\beta^2-k^2} J_1(kr)\, k^2dk \int_0^\infty f(\xi)\, J_0(k\xi)\, \xi d\xi\right],$$

$$[\beta \neq k] \quad \cdots\cdots(113)$$

$$\frac{\partial w}{\partial r} = \frac{\alpha}{2(\lambda+\mu)}\int_0^\infty e^{-kz} J_0(kr)\, kdk \int_0^\infty f(\xi)\, J_0(k\xi)\, \xi d\xi. \quad [\beta = k] \quad \cdots\cdots(114)$$

12. In the last section we have not fully examined the relation of β and k, and when β is a arbitrary constant, not a function of k, it is not easy to evaluate the integrals; thus we assume that β is a function of k such that

$$\beta = \beta' k^n, \quad \cdots\cdots\cdots\cdots\cdots\cdots\cdots\cdots\cdots\cdots\cdots (115)$$

where β' and n are mere numbers. This assumption does not lose the generality of our study as we have seen in the two-dimensional problems.

Now in our study of the following sections we shall consider only the case of $n=1$, namely $\beta=\beta' k$, for the sake of simplicity. Then we have the following form of temperature distribution when the surface distribution is of the form of $f(r)$ from (108):

$$T = \int_0^\infty e^{-\beta' kz} J_0(kr)\, k dk \int_0^\infty f(\xi)\, J_0(k\xi)\, \xi d\xi, \quad \cdots\cdots\cdots\cdots\cdots\cdots (116)$$

and from (109) and (110), we have

$$u = -\frac{\alpha}{(\lambda+2\mu)(\beta'^2-1)} \Big[\frac{(\lambda+2\mu)\beta' - \mu}{\lambda+\mu} \int_0^\infty e^{-kz} \frac{\partial J_0(kr)}{k\partial r}\, dk \int_0^\infty f(\xi)\, J_0(k\xi)\, \xi d\xi$$

$$- z(\beta'-1) \int_0^\infty e^{-kz} \frac{\partial J_0(kr)}{\partial r}\, dk \int_0^\infty f(\xi)\, J_0(k\xi)\, \xi d\xi$$

$$- \int_0^\infty e^{-\beta' kz} \frac{\partial J_0(kr)}{k\partial r}\, dk \int_0^\infty f(\xi)\, J_0(k\xi)\, \xi d\xi \Big],$$

$$[\beta' \neq 1] \quad \cdots\cdots (117)$$

$$w = -\frac{\alpha}{(\lambda+2\mu)(\beta'^2-1)} \Big[\frac{\mu\beta' - (\lambda+2\mu)}{\lambda+\mu} \int_0^\infty e^{-kz} J_0(kr)\, dk \int_0^\infty f(\xi)\, J_0(k\xi)\, \xi d\xi$$

$$+ z(\beta'-1) \int_0^\infty e^{-kz} J_0(kr)\, k dk \int_0^\infty f(\xi)\, J_0(k\xi)\, \xi d\xi$$

$$+ \beta' \int_0^\infty e^{-\beta' kz} J_0(kr)\, dk \int_0^\infty f(\xi)\, J_0(k\xi)\, \xi d\xi \Big],$$

$$[\beta' \neq 1] \quad \cdots\cdots (118)$$

and from (111) and (112),

$$u = -\frac{\alpha}{(\lambda+\mu)}\int_0^\infty e^{-kz}\frac{\partial J_0(kr)}{k\partial r}\,dk\int_0^\infty f(\xi)\,J_0(k\xi)\,\xi d\xi,\quad [\beta'=1]\quad \cdots\cdots(119)$$

$$w = -\frac{\alpha}{2(\lambda+\mu)}\int_0^\infty e^{-kz}\,J_0(kr)\,dk\int_0^\infty f(\xi)\,J_0(k\xi)\,\xi d\xi,\qquad [\beta'=1]\quad \cdots\cdots(120)$$

and the tilt $\frac{\partial w}{\partial r}$ is easily formulated, namely from the equation (113), (114), we have

$$\begin{aligned}\frac{\partial w}{\partial r} = \frac{\alpha}{(\lambda+2\mu)(\beta'^2-1)}\Big[\frac{\mu\beta'-(\lambda+2\mu)}{\lambda+\mu}&\int_0^\infty e^{-kz}\,J_1(kr)\,kdk\int_0^\infty f(\xi)\,J_0(k\xi)\,\xi d\xi\\ &+z(\beta'-1)\int_0^\infty e^{-kz}\,J_1(kr)\,k^2dk\int_0^\infty f(\xi)\,J_0(k\xi)\,\xi d\xi\\ &+\beta'\int_0^\infty e^{-\beta' kz}\,J_1(kr)\,kdk\int_0^\infty f(\xi)\,J_0(k\xi)\,\xi d\xi\Big],\\ &[\beta'\neq 1]\quad \cdots\cdots(121)\end{aligned}$$

$$\frac{\partial w}{\partial r} = \frac{\alpha}{2(\lambda+\mu)}\int_0^\infty e^{-kz}\,J_1(kr)\,kdk\int_0^\infty f(\xi)\,J_0(k\xi)\,\xi d\xi.\quad [\beta'=1]\quad \cdots\cdots(122)$$

13. For the example of Section 14, we shall take the temperature distribution of the following form on the surface of the solid:

$$f(r) = \frac{Ab}{\sqrt{b^2+r^2}},\quad b>0,\quad \cdots\cdots\cdots\cdots\cdots\cdots(123)$$

where b is the constant which can be adjusted to obey the distribution and A is the constant to express the measurement of temperature.

Then, by the aid of

$$\int_0^\infty \frac{J_0(kx)}{\sqrt{b^2+x^2}}\,dx = \frac{e^{-bk}}{k},\quad b>0\cdots\cdots\cdots\cdots\cdots\cdots(124)^{15)}$$

15) This formula is obtained by Prof. K. Terazawa and others.
K. Terazawa, "On Deep Sea Water Waves caused by a Local Disturbance on or beneath the Surface," *Proc. Roy. Soc.*, London, A **82** (1916).

we have the following temperature distribution from (116):

$$T = Ab\int_0^\infty e^{-(\beta' z+b)k} J_0(kr)\,dk. \quad\cdots\cdots(125)$$

The evaluation of the integral of (125) is very easy, and we have the following form of the temperature distribution of the solid:

$$T = A\frac{b}{\sqrt{r^2+(\beta' z+b)^2}}. \quad\cdots\cdots(126)$$

The Figures 9 and 10 are compiled from the expression of (126).

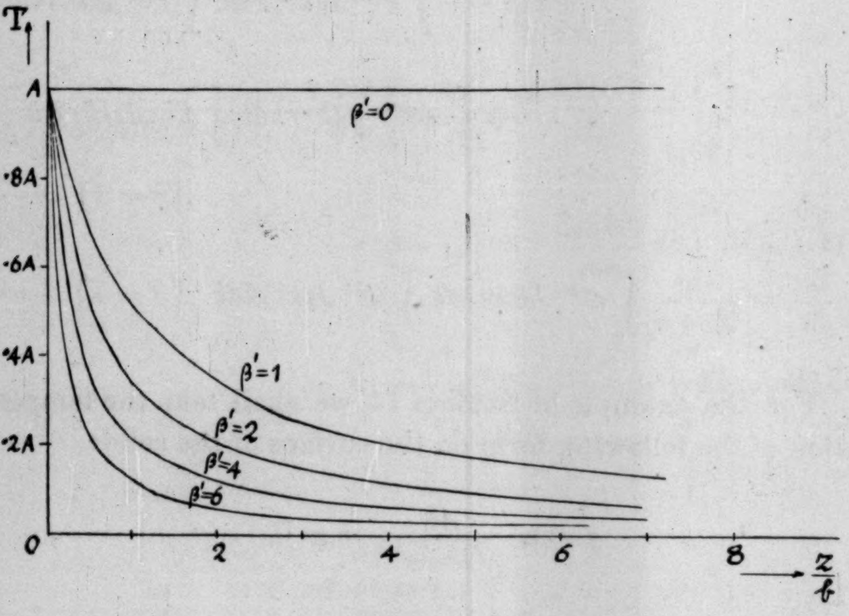

Fig. 9. $\left[\frac{r}{b}=0.\right]$

Fig. 9 indicates the temperature distribution in the solid on the plane $r/b=0$ when $\beta'=0, 1, 2, 4$ & 6. When $\beta'=2$, the temperature distributions on the planes $z/b=0, 1, 2$ are compiled in Fig. 10. From these two figures we can easily understand that the greater the number of β' is, the more intensively decreases the effect of temperature in the solid, namely the effect is localised only on the surface.

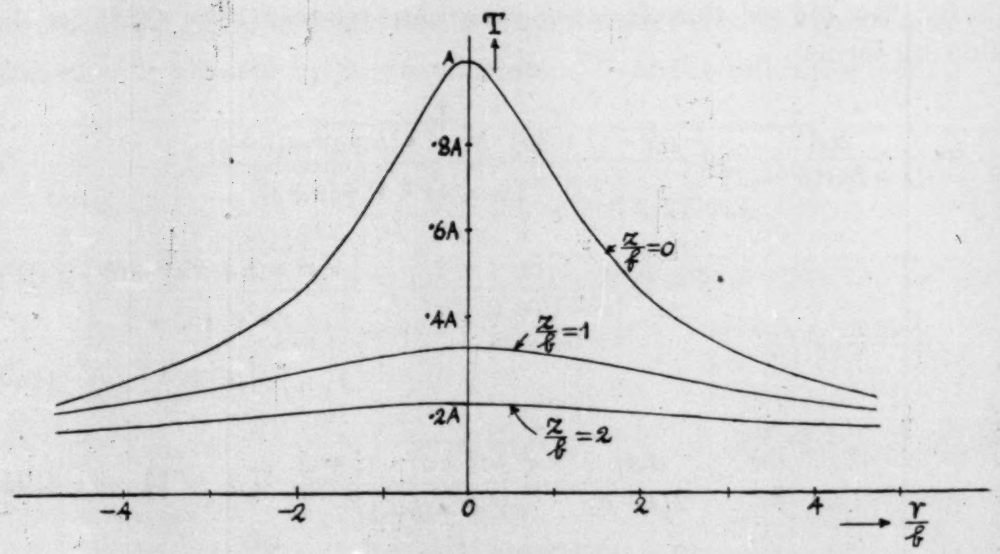

Fig. 10. $[\beta' = 2.]$

We have the following expression of the inclination of the solid :

$$\frac{\partial w}{\partial r} = \frac{\alpha A b}{(\lambda+2\mu)(\beta'^2-1)}\Big[\frac{\mu\beta'-(\lambda+2\mu)}{\lambda+\mu}\int_0^\infty e^{-(z+b)k} J_1(kr)\,dk$$
$$+(\beta'-1)\,z\int_0^\infty e^{-(z+b)k} J_1(kr)\,kdk$$
$$+\beta'\int_0^\infty e^{-(\beta'z+b)k} J_1(kr)\,dk\Big], \quad [\beta' \neq 1] \qquad \cdots\cdots\cdots(127)$$

$$\frac{\partial w}{\partial r} = \frac{\alpha A b}{2(\lambda+\mu)}\int_0^\infty e^{-(b+z)k} J_1(kr)\,dk. \quad [\beta' = 1] \qquad \cdots\cdots(128)$$

by the above formula of (124).

Now we know the following relations :

$$\left.\begin{aligned} \int_0^\infty J_1(tx)\,e^{-ty}\,tdt &= \frac{x}{(x^2+y^2)^{3/2}}, \\ \int_0^\infty J_1(tx)\,e^{-ty}\,dt &= \frac{\sqrt{x^2+y^2}-y}{x\sqrt{x^2+y^2}}. \end{aligned}\right\} \qquad \cdots\cdots\cdots\cdots\cdots\cdots\cdots\cdots(129)$$

By the aid of this equation, we can reduce (127), (128) in the following forms:

$$\frac{\partial w}{\partial r}=\frac{\alpha Ab}{(\lambda+2\mu)(\beta'^2-1)}\left[\frac{\mu\beta'-(\lambda+2\mu)}{\lambda+\mu}\frac{\sqrt{r^2+(b+z)^2}-(b+z)}{r\sqrt{r^2+(b+z)^2}}\right.$$

$$\left.+(\beta'-1)\frac{rz}{\{r^2+(b+z)^2\}^{3/2}}+\beta'\frac{\{\sqrt{r^2+(b+\beta'z)^2}-(b+\beta'z)\}}{r\sqrt{r^2+(b+\beta'z)^2}}\right],$$

$$[\beta'\neq 1] \quad \cdots\cdots(130)$$

$$\frac{\partial w}{\partial r}=\frac{\alpha Ab}{2(\lambda+\mu)}\frac{\sqrt{r^2+(b+z)^2}-(b+z)}{r\sqrt{r^2+(b+z)^2}}, \quad [\beta'=1] \quad \cdots\cdots(131)$$

and the surface tilt is of the form of

$$\frac{\partial w}{\partial r}=\frac{\alpha Ab}{(\lambda+\mu)(1+\beta')}\frac{\sqrt{r^2+b^2}-b}{r\sqrt{r^2+b^2}}. \quad \cdots\cdots\ \cdots\cdots\cdots(130)$$

From the annexed Figure 11, in which we have compiled $\frac{\partial w}{\partial r}$ on the surface $z=0$ when $\beta'=2$ and 4, the surface inclination of the solid is much affected by the value of β', and inversely proportional to $(1+\beta')$, i.e. the more the effect of the surface temperature distribution in the solid diminishes, the smaller the amount of the surface inclination becomes, in spite of a constant surface temperature distribution.

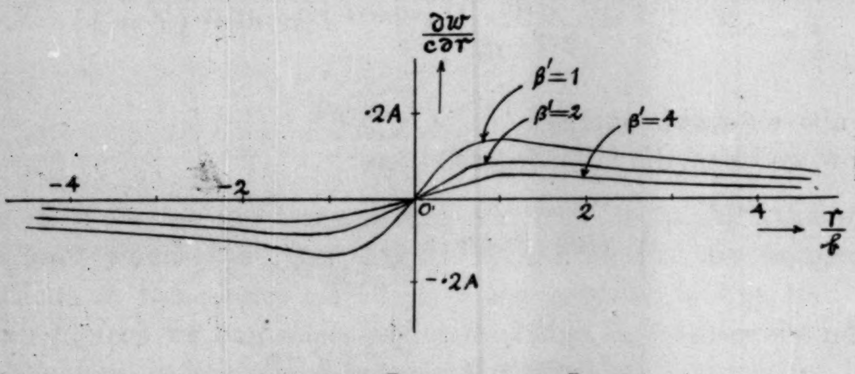

Fig. 11. $\left[\frac{z}{b}=0 \quad \lambda=\mu.\right]$

To understand how much the displacement w in the interior of the earth may be affected by β', we calculate $\frac{\partial w}{\partial z}$ in the following form:

$$\frac{\partial w}{\partial z} = -\frac{\alpha A b}{(\lambda+2\mu)(\beta'^2-1)}\Big[\frac{\lambda\beta'+\mu}{\lambda+\mu}\int_0^\infty e^{-(z+b)k} J_0(kr)\,dk$$

$$-(\beta'-1)z\int_0^\infty e^{-(z+b)k} J_0(kr)\,kdk-\beta'^2\int_0^\infty e^{-(\beta'z+b)k} J_0(kr)\,dk\Big],$$

$$[\beta' \neq 1] \quad \cdots\cdots(132)$$

$$\frac{\partial w}{\partial z} = \frac{\alpha A b}{2(\lambda+\mu)}\int_0^\infty e^{-(z+b)k} J_0(kr)\,dk. \quad [\beta' = 1] \quad \cdots\cdots(133)$$

By means of the formulae,

$$\left.\begin{aligned} \int_0^\infty J_0(tx)\,e^{-ty}\,tdt &= \frac{y}{(x^2+y^2)^{3/2}}, \\ \int_0^\infty J_0(tx)\,e^{-ty}\,dt &= \frac{1}{\sqrt{x^2+y^2}}, \end{aligned}\right\} \quad \cdots\cdots\cdots\cdots\cdots\cdots\cdots(134)$$

we get finally

$$\frac{\partial w}{\partial z} = -\frac{\alpha A b}{(\lambda+2\mu)(\beta'^2-1)}\Big[\frac{\lambda\beta'+\mu}{\lambda+\mu}\frac{1}{\sqrt{r^2+(b+z)^2}}$$

$$-(\beta'-1)\frac{z(z+b)}{\{r^2+(b+z)^2\}^{3/2}}-\frac{\beta'^2}{\sqrt{r^2+(\beta'z+b)^2}}\Big],$$

$$[\beta' \neq 1] \quad \cdots\cdots(135)$$

$$\frac{\partial w}{\partial z} = \frac{\alpha A b}{2(\lambda+\mu)}\frac{1}{\sqrt{r^2+(b+z)^2}}. \quad [\beta' = 1] \quad \cdots\cdots(136)$$

When $r=0$,

$$\frac{\partial w}{\partial z}=-\frac{\alpha Ab}{(\lambda+2\mu)(\beta'^2-1)}\left[\frac{\lambda\beta'+\mu}{\lambda+\mu}\frac{1}{(b+z)}-\frac{(\beta'-1)z}{(b+z)^2}-\frac{\beta'^2}{(b+\beta'z)}\right],$$

$$[\beta'\neq 1] \quad \cdots\cdots(137)$$

$$\frac{\partial w}{\partial z}=\frac{\alpha Ab}{2(\lambda+\mu)}\frac{1}{b+z}. \quad [\beta'=1] \quad \cdots\cdots\cdots\cdots(138)$$

The compiled results of the normal strain $\frac{\partial w}{\partial z}$ on the plane $\frac{r}{b}=0$ of the solid is shown in Fig. 12.

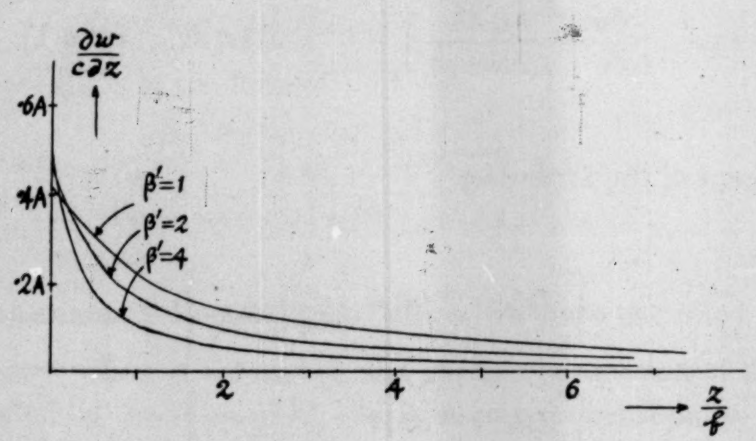

Fig. 12. $\left[\frac{r}{b}=0,\ \lambda=\mu.\right]$

This figure shews that the magnitude of the surface normal strain $\frac{\partial w}{\partial z}$ is the greatest of all the normal strains in the solid, and that the more the effect of the temperature distribution is concentrated in the neighbourhood of the surface of the solid, the larger the magnitude of the surface normal strain $\frac{\partial w}{\partial z}$ becomes, and the smaller becomes the normal strain $\frac{\partial w}{\partial z}$ in the interior of the solid.

14. If the surface temperature distribution is given by the form of

$$f(x)=\frac{Aa^2}{b^2+r^2}, \quad \cdots\cdots\cdots\cdots\cdots\cdots\cdots\cdots(139)$$

where the physical meanings of constants a, b and A are same in the above sections.

Then we have the following forms of temperature and displacement:

$$T=\frac{Aa^2\pi i}{2}\int_0^\infty e^{-\beta' kz}\,H_{1,0}(kbi)\,J_0(kr)\,kdk, \qquad \cdots\cdots(140)$$

$$\begin{aligned} u=\frac{Aa^2\alpha\pi i}{2(\lambda+2\mu)(\beta'^2-1)}\Big[&\frac{(\lambda+2\mu)\,\beta'-\mu}{\lambda+\mu}\int_0^\infty H_{1,0}(kbi)\,J_1(kr)\,e^{-kz}\,dk \\ &-(\beta'-1)\,z\int_0^\infty H_{1,0}(kbi)\,J_1(kr)\,e^{-kz}\,kdk \\ &-\int_0^\infty H_{1,0}(kbi)\,J_1(kr)\,e^{-\beta' kz}\,dk\Big], \end{aligned}$$

$$[\beta'\neq 1] \qquad \cdots\cdots(141)$$

$$\begin{aligned} w=-\frac{Aa^2\alpha\pi i}{2(\lambda+2\mu)(\beta'^2-1)}\Big[&\frac{\mu\beta'-(\lambda+2\mu)}{\lambda+\mu}\int_0^\infty H_{1,0}(kbi)\,J_0(kr)\,e^{-kz}\,dk \\ &+(\beta'-1)\,z\int_0^\infty H_{1,0}(kbi)\,J_0(kr)\,e^{-kz}\,kdk \\ &+\beta'\int_0^\infty H_{1,0}(kbi)\,J_0(kr)\,e^{-\beta' kz}\,dk\Big] \end{aligned}$$

$$[\beta'\neq 1] \qquad \cdots\cdots(142)$$

$$u=\frac{Aa^2\alpha\pi i}{4(\lambda+\mu)}\int_0^\infty H_{1,0}(kbi)\,J_1(kr)\,e^{-kz}\,dk, \qquad [\beta'=1] \qquad \cdots\cdots(143)$$

$$w=-\frac{Aa^2\alpha\pi i}{4(\lambda+\mu)}\int_0^\infty H_{1,0}(kbi)\,J_0(kr)\,e^{-kz}\,dk, \qquad [\beta'=1] \qquad \cdots\cdots(144)$$

by means of

$$\int_0^\infty \frac{J_0(k\xi)}{b^2+\xi^2}\,\xi d\xi=\frac{i\pi}{2}\,H_{1,0}(kbi). \qquad \cdots\cdots(145)$$

Using the following formula

$$\int_0^\infty H_{1,\nu}(ty)\, J_\rho(tx)\, t^\sigma dt = e^{\frac{\rho+\sigma-\nu}{2}\pi i} \frac{2^\sigma x^\rho}{\pi y^{\rho+\sigma+1}} \frac{\Gamma\left(\frac{\rho+\sigma+\nu+1}{2}\right)\Gamma\left(\frac{\rho+\sigma-\nu+1}{2}\right)}{\Gamma(\rho+1)} \times$$

$$F\left(\frac{\rho+\sigma+\nu+1}{2},\ \frac{\rho+\sigma-\nu+1}{2},\ \rho+1,\ \frac{x^2}{y^2}\right), \quad \cdots\cdots\cdots(146)$$

we can easily find the following forms of surface displacement by (143), (144):

$$u_{z=0} = \frac{Aa^2\alpha i}{2(\lambda+\mu)(\beta'+1)} e^{\frac{\pi i}{2}} \frac{r}{b^2 i^2} F\left(1, 1, 2, -\frac{r^2}{b^2}\right), \quad \cdots\cdots\cdots(147)$$

$$w_{z=0} = -\frac{Aa^2\alpha\pi}{2b(\lambda+\mu)(\beta'+1)} F\left(\frac{1}{2}, \frac{1}{2}, 1, -\frac{r^2}{b^2}\right). \quad \cdots\cdots\cdots\cdots(148)$$

When $r=0$, we have the following form of displacement:

$$\left.\begin{aligned} u_{\substack{z=0\\r=0}} &= 0, \\ w_{\substack{z=0\\r=0}} &= -\frac{Aa^2\alpha\pi}{2(\lambda+\mu)(\beta'+1)b}. \end{aligned}\right\} \quad \cdots\cdots\cdots\cdots\cdots\cdots\cdots\cdots(149)$$

15. When the surface temperature distribution is given by the form of

$$f(r) = \frac{Aa^3}{(a^2+r^2)^{3/2}}, \quad \cdots\cdots\cdots\cdots\cdots\cdots\cdots\cdots\cdots\cdots(150)$$

where the constants A, a are determined by experiments as in the above examples. Then we have the following forms of temperature distribution in the body and the displacement and its delivatives using the formulae (116), (117), (118), (119) and (120).

Applying the relation employed by Prof. K. Terazawa,[16] namely

16) K. Terazawa, *Phil. Trans. Roy. Soc.*, London, (A) 217 (1916) and *J. Coll. Sci.*, Tokyo, 37 (1916).

$$\int_0^\infty \frac{aJ_0(f\lambda)\,\lambda d\lambda}{(a^2+\lambda^2)^{3/2}} = e^{-fa}, \quad \cdots\cdots(151)$$

we find

$$T = a^2 A \int_0^\infty e^{-(a+\beta' z)k} J_0(kr)\,kdk, \quad \cdots\cdots(152)$$

$$u = \frac{Aa^2\alpha}{(\lambda+2\mu)(\beta'^2-1)}\Big[\frac{(\lambda+2\mu)\beta'-\mu}{\lambda+\mu}\int_0^\infty e^{-(a+z)k} J_1(kr)\,dk$$

$$-(\beta'-1)\,z\int_0^\infty e^{-(a+z)k} J_1(kr)\,kdk - \int_0^\infty e^{-(a+\beta' z)k} J_1(kr)\,dk\Big],$$

$$[\beta' \neq 1] \quad \cdots\cdots(153)$$

$$w = -\frac{Aa^2\alpha}{(\lambda+2\mu)(\beta'^2-1)}\Big[\frac{\mu\beta'-(\lambda+2\mu)}{\lambda+\mu}\int_0^\infty e^{-(a+z)k} J_0(kr)\,dk$$

$$+(\beta'-1)\,z\int_0^\infty e^{-(a+z)k} J_0(kr)\,kdk + \beta'\int_0^\infty e^{-(a+\beta' z)k} J_0(kr)\,dk\Big],$$

$$[\beta' \neq 1] \quad \cdots\cdots(154)$$

$$u = \frac{\alpha a^2 A}{2(\lambda+\mu)}\int_0^\infty e^{-(a+z)k} J_1(kr)\,dk, \quad [\beta'=1] \quad \cdots\cdots(155)$$

$$w = -\frac{\alpha a^2 A}{2(\lambda+\mu)}\int_0^\infty e^{-(a+z)k} J_0(kr)\,dk. \quad [\beta'=1] \quad \cdots\cdots(156)$$

Now we can easily evaluate the integrals in the above mentioned formulae by using

$$\left.\begin{aligned}
&\int_0^\infty J_1(tx)\, e^{-ty}\, dt = \frac{\sqrt{x^2+y^2}-y}{x\sqrt{x^2+y^2}}, \\
&\int_0^\infty J_\nu(tx)\, e^{-ty}\, t^\nu dt = \frac{\Gamma(\nu+{}^1/_2)}{\sqrt{\pi}}\, \frac{(2x)^\nu}{(x^2+y^2)^{\nu+{}^1/_2}}, \\
&\int_0^\infty J_\nu(tx)\, e^{-ty}\, t^{\nu+1}\, dt = \frac{2\Gamma(\nu+{}^3/_2)}{\sqrt{\pi}}\, \frac{y\,(2x)^\nu}{(x^2+y^2)^{\nu+{}^3/_2}},
\end{aligned}\right\} \quad \cdots\cdots\cdots\cdots(157)$$

in the following forms :

$$T = Aa^2 \frac{(a+\beta' z)}{\{r^2+(a+\beta' z)^2\}^{3/2}}, \quad \cdots\cdots\cdots\cdots(158)$$

$$u = \frac{Aa^2\alpha}{(\lambda+2\mu)(\beta'^2-1)}\left[\frac{(\lambda+2\mu)\beta'-\mu}{\lambda+\mu}\,\frac{\sqrt{r^2+(a+z)^2}-(a+z)}{r\sqrt{r^2+(a+z)^2}}\right.$$

$$\left. -(\beta'-1)\frac{rz}{\{r^2+(a+z)^2\}^{3/2}} - \frac{\sqrt{r^2+(a+\beta' z)^2}-(a+\beta' z)}{r\sqrt{r^2+(a+\beta' z)^2}}\right],$$

$$[\beta' \neq 1] \quad \cdots\cdots(159)$$

$$w = -\frac{Aa^2\alpha}{(\lambda+2\mu)(\beta'^2-1)}\left[\frac{\mu\beta'-(\lambda+2\mu)}{\lambda+\mu}\,\frac{1}{\sqrt{r^2+(a+z)^2}}\right.$$

$$\left. +(\beta'-1)\frac{z(a+z)}{\{r^2+(a+z)^2\}^{3/2}} + \frac{\beta'}{\sqrt{r^2+(a+\beta' z)^2}}\right],$$

$$[\beta' \neq 1] \quad \cdots\cdots(160)$$

$$u = \frac{Aa^2\alpha}{2(\lambda+\mu)}\,\frac{\sqrt{r^2+(a+z)^2}-(a+z)}{r\sqrt{r^2+(a+z)^2}}, \quad [\beta' = 1] \quad \cdots\cdots(161)$$

$$w = -\frac{Aa^2\alpha}{2(\lambda+\mu)}\,\frac{1}{\sqrt{r^2+(a+z)^2}}. \quad [\beta' = 1] \quad \cdots\cdots(162)$$

The temperature distribution in the solid when $\frac{r}{a} = 0$ is shown in Figure 13 where $\beta' = 2$, 4 & 6. Figure 14 gives the temperature distribution on the planes $\frac{z}{b} = 0$, 1 & 2 when $\beta' = 2$.

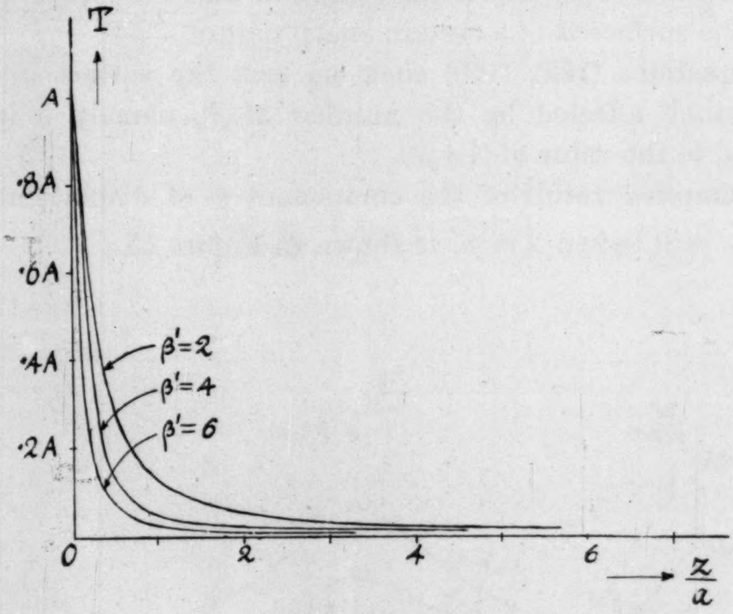

Fig. 13. $\left[\frac{r}{a} = 0.\right]$

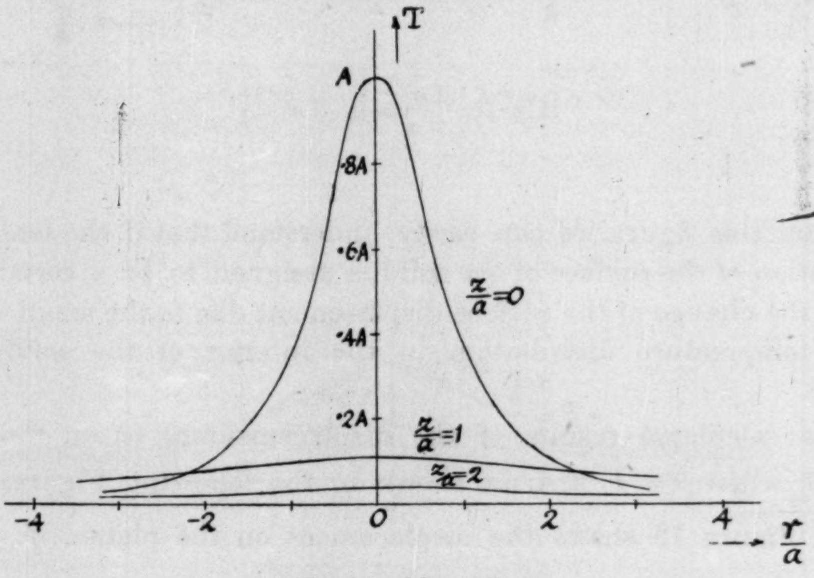

Fig. 14. $[\beta' = 2.]$

It may be seen from the above figures that the value of β' specifies the temperature distribution in the interior of the solid as we have already discussed in Section 13.

We will now study more fully how much effects the variation of the temperature distribution in the interior of the solid may have upon the deformation of the solid under the condition that the temperature distribution on the surface is of a certain sharp nature.

The equations (159), (160) shew us that the surface displacement (u, w) is much affected by the number of β', namely it is inversely proportional to the value of $(1+\beta')$.

The compiled result of the component w of displacement on the surface $\frac{r}{a}=0$, when $\lambda=\mu$, is shown in Figure 15.

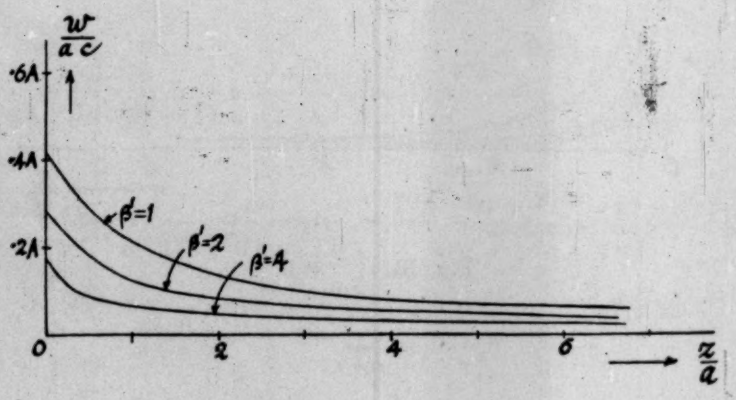

Fig. 15. $\left[\frac{r}{a}=0, \ \lambda=\mu.\right]$

From this figure we can easily understand that if the temperature distribution of the surface of the solid is assigned to be a certain sharp nature, the change of the surface displacement due to the small variation of the temperature distribution in the interior of the solid is very sensible.

The calculated results of the displacement (u, w) on the surface $\frac{z}{a}=0$, when $\beta'=1, 2, 4$, are shown in the following Figures 16 and 17 and Figure 18 shews the displacement on the planes of $\frac{z}{a}=0$, 1 and 2 when $\beta'=2$.

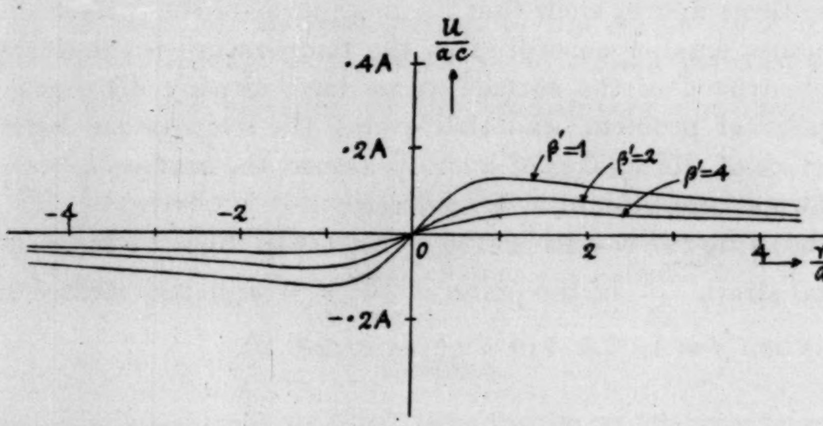

Fig. 16. $\left[\frac{z}{a} = 0, \quad \lambda = \mu.\right]$

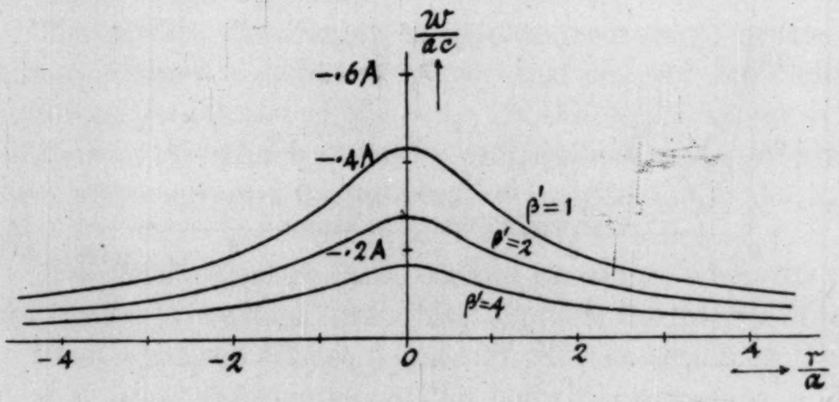

Fig. 17. $\left[\frac{z}{a} = 0, \quad \lambda = \mu.\right]$

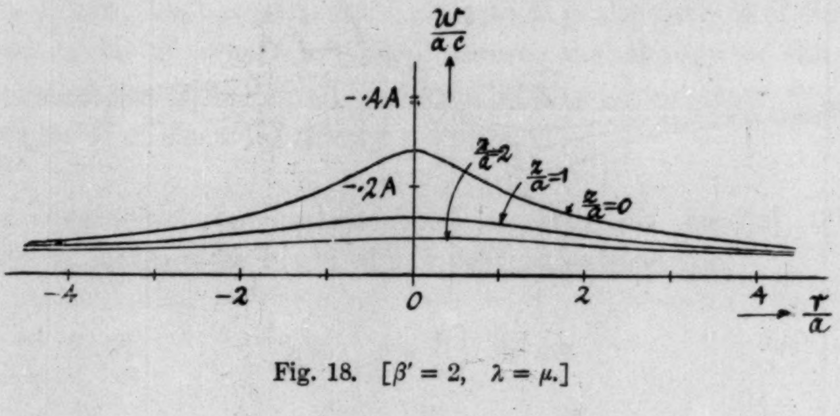

Fig. 18. $[\beta' = 2, \quad \lambda = \mu.]$

These three figures shew that the magnitude of the surface displacement becomes smaller according as the temperature is concentrated in the neighbourhood of the surface as we have already discussed in the two-dimensional problem, and that even if the temperature distribution of the surface of the solid is of a sharp nature, the surface as well as the inner deformation of the solid is moderate.

Again, using the results of (159), (160), (161), (162), we have compiled the normal strain $\frac{\partial w}{\partial z}$ of the plane of $\frac{r}{a}=0$ and the surface inclination $\frac{\partial w}{\partial r}$ when $\beta'=1$, 2 & 4 in Figures 19 and 20.

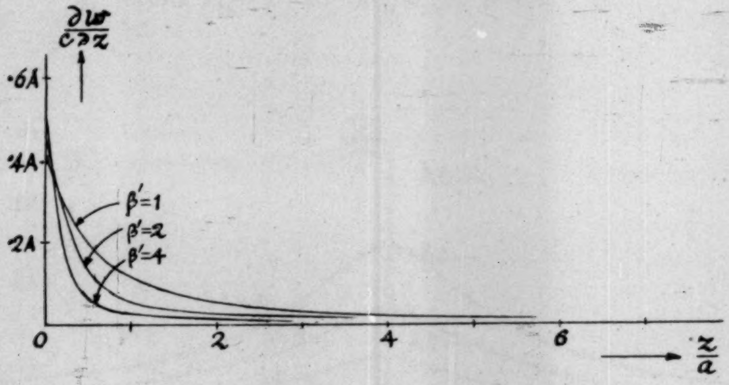

Fig. 19. $\left[\frac{r}{a}=0,\quad \lambda=\mu.\right]$

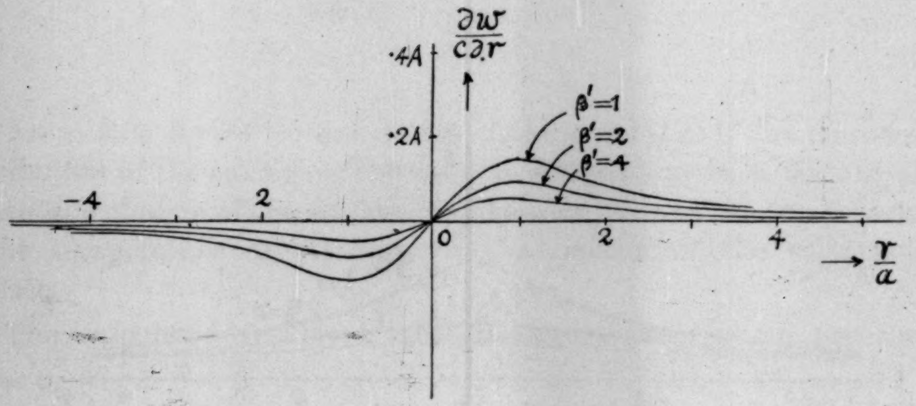

Fig. 20. $\left[\frac{z}{a}=0,\quad \lambda=\mu.\right]$

Fig. 19 indicates the reliableness of the result[17] which we have obtained in the section 13 concerning the relation between the normal strain $\frac{\partial w}{\partial z}$ and the variation of the temperature distribution in the interior of the solid. Also we confirm, from Fig. 11[18] and Fig. 20, that when the temperature distribution of the surface is of a certain sharp nature, the surface tilt is sharper than that when the temperature distribution of the surface is of a moderate nature.

Résumé.

16. We have now obtained some results which may be interesting on the geophysical problems, and of which the principal facts are enumerated as below:

1. The magnitude of the displacement at a given point in the solid is proportional to the temperature at that point.

2. The surface distribution of displacements is, of course, affected by the temperature distribution of the surface, and especially by the distribution in the interior of the body, i.e. the displacement or the tilt of the surface of the solid is inversely proportional to $(1+\beta')$ where β' is a constant which specifies the temperature distribution in the interior of the solid.

3. The surface displacement becomes maximum when the temperature distribution is constant through all depth in the interior of the solid.

4. Even when the surface temperature is discontinuous, the surface as well as internal deformation of the body is continuous, and in this case the portion of no temperature change is also deformed.

5. Even if the temperature distribution of the surface of the solid is of a sharp nature, the surface deformation of the solid has a moderate nature.

6. When the temperature distribution of the surface of the solid is assigned to be of a certain sharp nature, the change of the surface displacement due to the small variation of the temperature distribution in the interior of the solid is very sensible.

In conclusion the author must express his cordial thanks to Professor K. Sezawa for his kind advices and supervision.

17) *loc. cit.*, 132.
18) *loc. cit.*, 130.

7. 温度分布が半無限彈性體の變形に及ぼす影響

地震研究所 西 村 源 六 郎

地球表面の絶えざる變形を起す原因は色々あるであらうが我々は決して温度分布による影響も見逃す理にはゆかない。地球表面に壓力の加はる場合や、地球內部に歪核のある場合に生ずる地表の變形は寺澤先生や妹澤先生によつて研究されてあるが、表面の溫度分布による影響はまだ解いてない樣である。この問題は種々地形變化觀測の方面に關係がある樣に思はれるが、これ等の事に就て多少でも參考になる事があれば幸と思つてゐる。

研究の方法は、溫度の影響を含んだ一般彈性體平衡方程式の解から出發して、二次元の問題と三次元の問題を二三の例に就て解いてみただけである。たゞ計算中、表面から地球內部へかけて溫度が種々變つた場合に地殼の變形がどの樣に變化されるかをみる爲め、この方面に主として力を入れた。

計算中所々から得た結果を擧げてみると，

1. 地殼中のある點の變位量はその點の溫度に比例する。
2. 地表の變形は勿論地表の溫度分布の狀態の變化によつて支配されるが特に溫度の地球內部に變る割合によつて非常に影響を受ける。即ち地表の變形或は傾斜は $(1+\beta')$ の價に逆比例する事がわかる。但し β' は溫度の地球內部に變る割合を支配する或る常數である。
3. 地表面上の變位は地中深く溫度が變る時に、特にその量が多い。
4. 表面の溫度分布に不連續點があつても地表面及び內部に於ける變形には不連續點はないばかりか、溫度變化のない所でも或る程度まで變形をうける。
5. 地表の溫度分布が集中性の時でも地表變形の分布は緩漫性を帶びる。
6. 地表の溫度分布が集中性を帶びてゐる時には地球內部での溫度分布が少し變つても地表面の變位の量は非常に變化される。

8. *Preliminary Report on the Observation of the Tilting of the Earth's Crust with a Pair of Water Pipes.*

By Ryutaro TAKAHASI,

Earthquake Research Institute.

(Read Jan. 21, 1930.—Received March 20, 1930.)

The instrument used in the present observation is based on the same principle with that used by A. Michelson in 1914 in his observation of the earth tide.[1] It consists essentially of a pair of pipes which are buried horizontally in the ground perpendicular to each other and halfly filled with water. The present observation was planned before the time of construction of the main building of the Earthquake Research Institute, and the pipes and the observing chambers were constructed in parallel with the main building of the Institute.

Observations of the tilt of the ground with this instrument has already been made for nearly one year. The results obtained will now be given in the following, together with some descriptions of the pipes and the observing chambers.

1. The observing chambers are situated at the corners of the site of the main building of the Institute as shown in Fig. 1. The distance

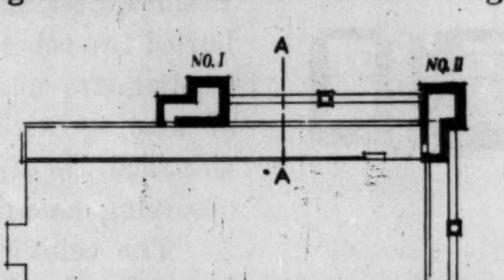

Fig. 1.

between two chambers is 17·5 m. The two end chambers are 2·5 m. × 2 m.

1) A. A. Michelson, *Astrophys. Journ.*, 39 (1914), 105.

in dimension, while the central one is 2·5 m. × 2·5 m. In Fig. 2 is given the section of an end chamber as an example to show the construction of the observing chambers. Each wall of the chamber is 80 cm. thick including an air space of the thickness of 15 cm. The floor is 100 cm. thick. The cielings, walls and floors are all of reinforced concrete and are lined with white mortar. Each chamber is provided with an electric fan for ventilation, a switch-board and a double door.

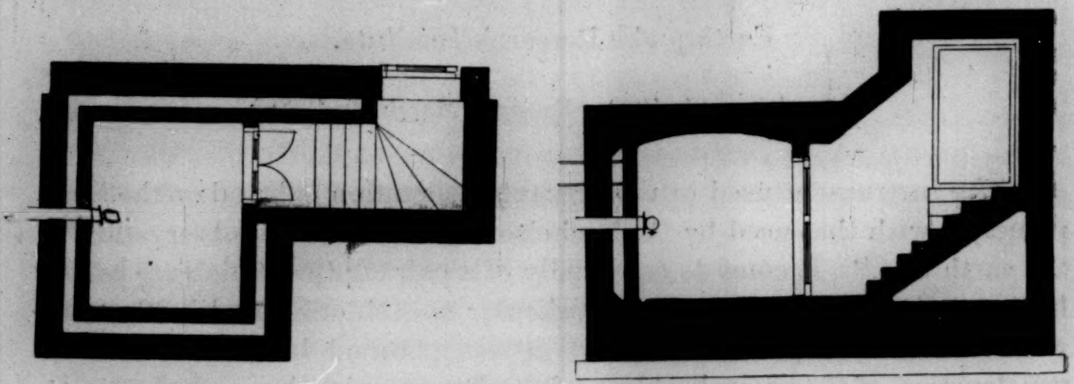

Fig. 2.

The chambers are connected with an under-ditch having a manhole at the middle point. The water pipe is placed in this ditch. Details of the construction of the ditch and the manner of fixing the pipe in it are to be seen in Fig. 3. The pipes are made of iron, 6 inches in diameter, 18 metres in length and are lined with enamel to prevent the water contained in it from staining. Besides these main pipes there are buried two other pipes each 1 inch in diametre to serve as the pass of leading wires connecting the electrical equipments in each observing chamber.

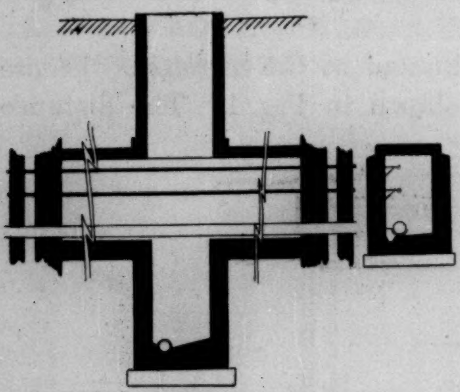

Fig. 3.

The ceiling of each chamber is at the depth of 2·4 m. under the surface of the ground.

Temperature condition of the observing chambers and the ditches are thus held pretty good. A recording thermograph inserted in the ditch showed practically no variations in temperature in a period of a week.

2. Now if the ground tilts to the direction of a pipe, the water in the

pipe changes its level relatively to the pipe. The amount of the change of the level is just proportional to the amount of tilt of the ground, if there is no condensation or evaporation of the water or an asymmetrical bending of the pipe. The effect of the condensation or evaporation of the water in the pipe can be eliminated by taking the algebraic difference of the variation of the level of the water at the both ends of a pipe. There are three kinds of the methods of measuring the variation of water level which have already used for this purpose; namely the micrometer method, the optical lever method and the interference method. In the present observation the first method was adopted. The second method is recently used by J. Egedal[2] in his niveauvariometer observation. In his instrument the displacement of a float on the water surface in the pipe was magnified by an optical lever. This method is not free from objections, though it has its own merit in the simplicity of the apparatus. The third method seems to be most accurate and perfect one, but for certain purpose such a highly accurate method is not fitted.

The apparatus used in the micrometer method consists essentially of a micrometer screw with a sharp point under the surface of the water, the level of which is to be measured. The sharp point and its image reflected at the surface of the water are brought into contact by turning the screw. The number of turns of the screw shows the height of the water surface measured from an arbitrary zero. The details of the instrument used in the present observation can be seen in Fig. 4. The

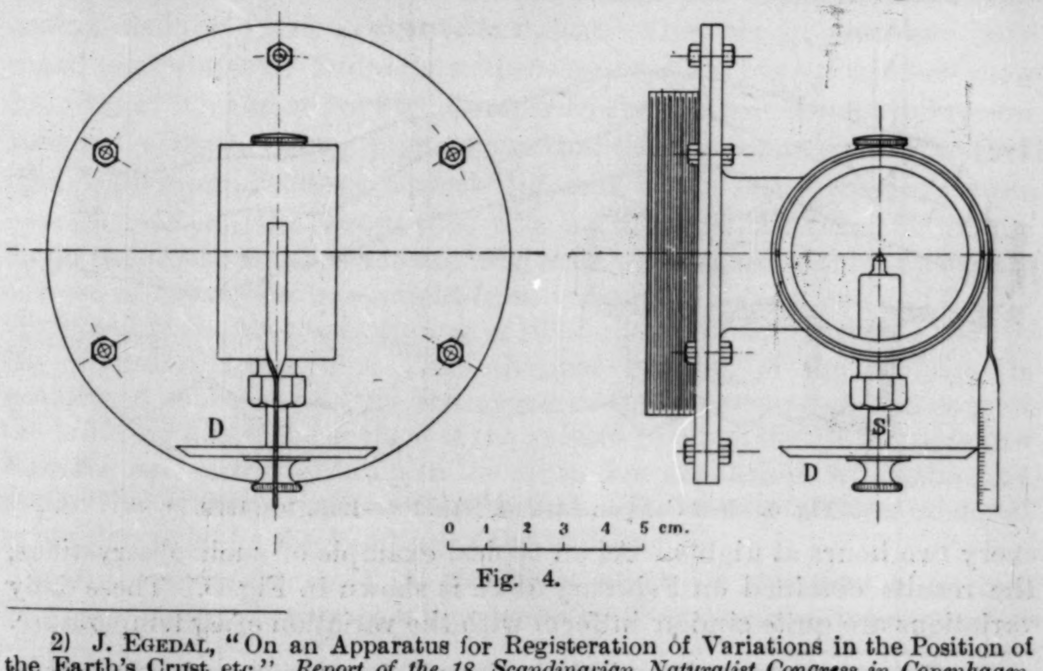

Fig. 4.

2) J. Egedal, "On an Apparatus for Registeration of Variations in the Position of the Earth's Crust etc.", *Report of the 18. Scandinavian Naturalist Congress in Copenhagen, 26-31, Aug., 1929.*

micrometer screw S is made of stainless steel and the pitch of the srew is 0·5 mm. This stainless steel proved to be quite satisfactory in that it did not grow rusty during the period of the observation for a year. The micrometer screw is provided at its lowest end a dial D which is graduated in 250 divisions, so that the smallest division of the dial corresponds to $2\,\mu$. It is easy to set the screw S into contact with its image within the error of 2 divisions of the dial without using a microscope or a magnifying glass, because a slight clearance between the screw and its image becomes visible when they are illuminated from behind.

By the pipe of 18 metres in length, a tilt of the ground of the amount of $1''$ produces the elevation of the water surface corresponding to 22·5 dial divisions at one end of the pipe and the depression of the same amount at the other end. Therefore the difference of the variations of the water level at both ends becomes 45 divisions which can be measured within the error of 4 divisions.

In the neck part of the instrument which connect the main part to the flange, a buffer is provided to minimize mechanical disturbances in the water. 1 gram of HgCl was solved in the water contained in the pipe to prevent the water from corruption.

3. Results of Observation.[3] In the first place, we will describe about the daily tilt of the ground. Readings of the values of the water level at both ends of a pipe were taken at every one hour in days and at

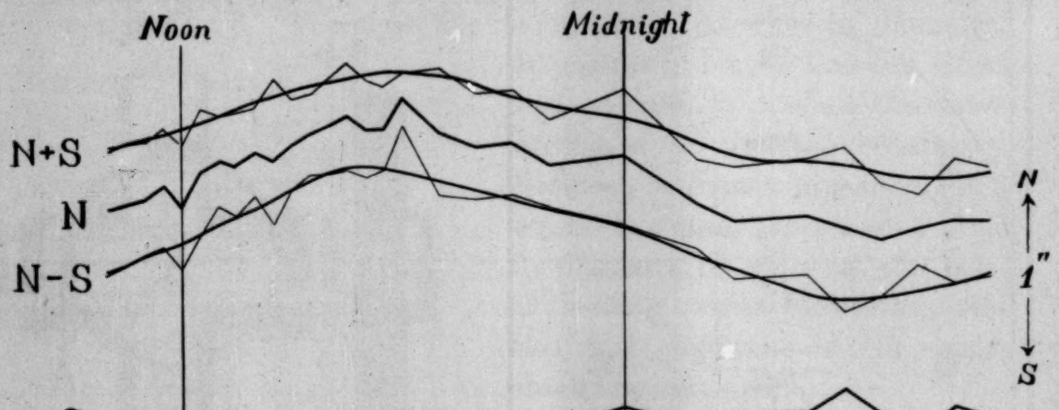

Fig. 5. N-S Component, Feb. 18th. 10h—19th. 10h, 1929.

every two hours at nights. As an typical example of such observations, the results obtained on February 18th. is shown in Fig. 5. These daily variations are quite similar in form with the variation of air temperature.

3) The present observation is limited only to N-S component, as the apparatus for E-W component, which is based on the interference mothod, is yet under preparation.

The amplitude of the daily variation is generally less than or equal to 1″ and the maximum northward tilt occurs at about 18 h. The ground tilts northwards with rising temperature and tilts southwards with lowering temperature. It shows a phase lag of about 4 hours relatively to the air temperature.

The value of the tilt at noon coincides roughly with the mean value of the daily tilt curve. It is therefore enough to take the reading of the level of the water once a day at noon for the purpose of detecting a secular or cumulative tilting of the ground. In Fig. 6 is shown a tilt curve for the period from February to December of the year 1929 obtained by such simplified method of observation. In the same figure a curve showing the atmospheric temperature variation for the same period is also inserted. The annual variation of the inclination of the ground is clearly seen from the figure. In the annual variation, the ground tilts also northwards with the rising temperature. The amplitude of the annual variation amounts to about 15″ and the maximum northward tilt occurs in August.

The period of the observation is not yet long enough to detect the cumulative or secular tilt of the ground.

In the under-cellar observation room of the Institute which is at the southern end of the building of the Institute, a pair of the Ishimoto[4] tiltmeters made of fused quartz is installed. They are in principle horizontal pendulums of Zöllner's suspension type. These tiltmeters show daily tilt of the amount of 8″. Comparison of this record with the record obtained with the water pipe, shows that they are quite similar in form though their amplitudes are much different, but in sense they are quite opposite. When the water pipe tilts northwards, the tiltmeter in the under-cellar tilts southwards and *vice versa*. The cause of this apparently curious phenomenon was sought from various points of views and finally attributed to the thermal bending of the building of the Institute and of the ground adjacent to it. The thermal bending of the building is concidered to be caused by the excess of the expansion of the part of the building above the surface of the ground. When the air temperature rises the part of the building in the air makes expansion, while the part under the ground remains as original. The result of this unequal expansion must be the bending of the building.

If the upper part of the building which is 10 metres high and 30 metres long, is higher in temperature by 2° C than the lower part of

---

4) M. Ishimoto, *Bull. Earthq. Res. Inst.*, 2 (1927), 1; *Jap. Journ. Astro. Geophys*, 4 (1928), 83.

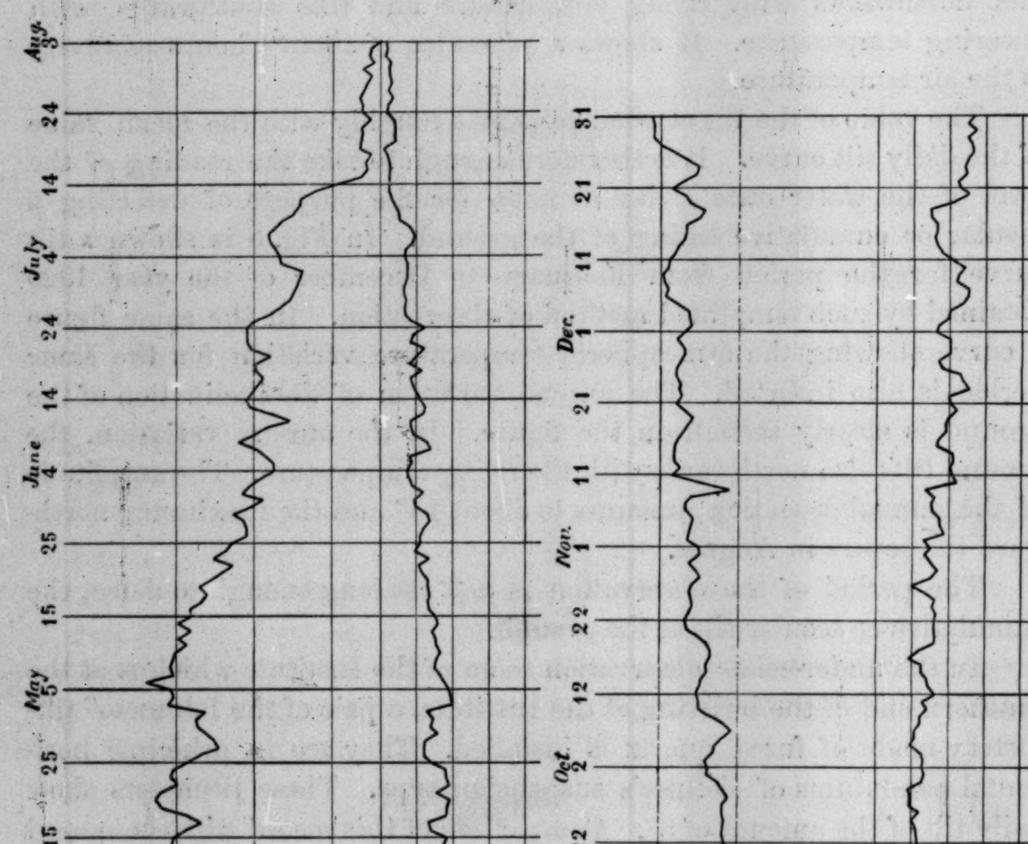
(1929)
Feb. 25
Mar. 6
16
26
Apr. 5
15
25
May 5
15
25
June 4
14
24
July 4
14
24
Aug. 3
Sep. 2
13
23
Oct. 2
12
22
Nov. 1
11
21
Dec. 1
11
21
31
Tilt
Air Temp.
5"
0"
-5"
30°
20°
10°
0°
-10°

Fig. 6

the building, then the difference of the length of the building caused by the unequal expansion is

$$dl = 30\,\text{m} \times (2\times10^{-5}) = 0{\cdot}6\,\text{mm},$$

taking the expansion coefficient of concrete to be the same with that of iron. With this difference of length between the upper and lower parts of the building, we have for the radius of curvature of the bending

$$R = 30\,\text{m} \times \frac{10\,\text{m}}{dl} = 5 \times 10^5\,\text{m},$$

therefore for the distance of 18 m., which is the distance between No. I and No. II chambers, the difference of the tilt will be

$$\theta = \frac{18}{5} \times 10^{-5}\ \text{radian} = 7''{\cdot}2.$$

The tilt measured by the pipe is, however, the difference of the level of the water in the pipe divided by the length of the pipe. In the present case of the bending of the building of the Institute, the vertex point of the bending where no thermal tilt is produced coincides roughly with the line A–A in Fig. 1, as is stated in the later pages of this paper. The distance between the line A–A and No. I chamber is about 6 metres. We have therefore as the tilt observed by the pipe

$$\theta = \frac{\frac{1}{2}\left(\frac{2}{3}L - \frac{1}{3}L\right)}{R} = \frac{3}{5\times10^5} = 1''{\cdot}2,$$

which is almost in the same order with the actually observed value.

For the purpose to ascertain more clearly the mode of this thermal bending of the building, two tiltmeters were installed in No. I and No. II chambers respectively in N–S direction. In Fig. 7 are shown the record of tiltmeter installed in No. II chamber and that of the tiltmeter installed in the under-cellar for the same period. The tiltmeter installed in No. I chamber showed daily tilt of only 1″ or less and the tilt was in the same sense with that of the under-cellar. This is very reasonable, because No. I chamber is situated at about the middle point of the building of the Institute and is hence near to the minimum point of the tilt caused by the bending.

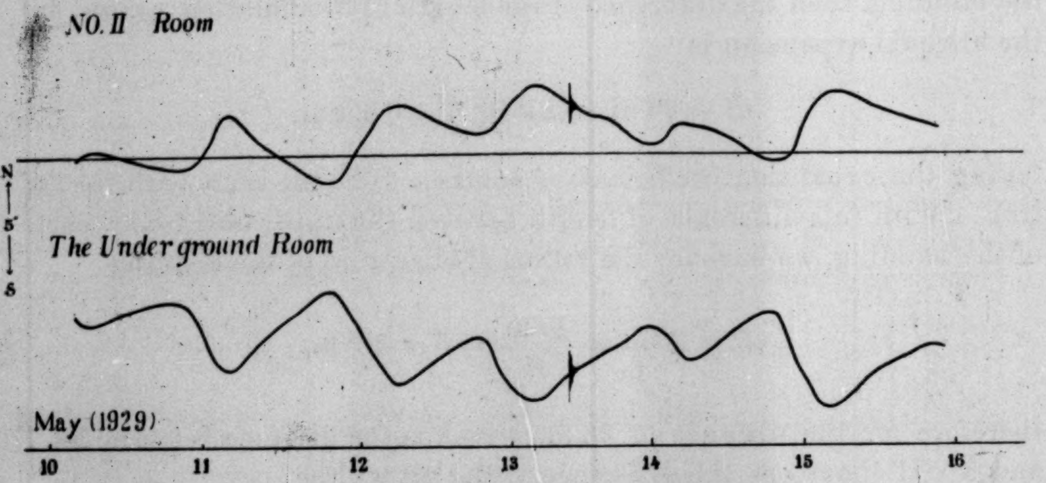

Fig. 7.

Now if the water pipe bends, the rise of the water level at one end of the pipe is not equal in amount to the depression of the level at the other end. The algebraic sum of the amount of the variation of the level at both ends is not constant. In such cases, the algebraic difference of the values of the water level at both ends does not represent the amount of tilt of the ground and we must make some calculations to obtain the true tilts.

Taking the origin of coordinate at the highest point of the bended tube which was initially straight and horizontal, and using the following notations:

ζ the variation of the level of the water in the pipe,

ζ_0 the variation of the level of the water in the pipe at the origin,

R the radius of curvature of the bent pipe,

L the length of the pipe,

x the coordinate taken along the pipe,

we have

$$\zeta = \frac{x^2}{2R} - \zeta_0,$$

and that

$$\int_{-l_1}^{l_2} \zeta \, dx \equiv 0 \; ^{5)},$$

5) In this case, the effect of condensation or evaporation of the water in the pipe was neglected. In the present observation, the temperature of the chambers and ditches, and of the water in the pipe was practically constant and there is, if any, only an insignificant effect caused from this origin.

where l_1 and l_2 are the coordinates of the ends of the pipe. Then we have for ζ at l_1 and l_2,

$$\zeta_{l_1} = \frac{1}{6R}(2l_1^2 + l_1 l_2 - l_2^2),$$

$$\zeta_{l_2} = \frac{1}{6R}(-l_1^2 + l_1 l_2 + 2l_2^2),$$

from which we obtain

$$l_1 = \frac{L}{2} + \frac{L}{6}(\zeta_{l_1} - \zeta_{l_2})/(\zeta_{l_1} + \zeta_{l_2}),$$

$$l_2 = \frac{L}{2} - \frac{L}{6}(\zeta_{l_1} - \zeta_{l_2})/(\zeta_{l_1} + \zeta_{l_2}).$$

These l_1 and l_2 give almost constant values when there is no true tilting of the ground, and the value of l_1 is a little larger than $L/3$ in our case. Denoting by $\bar{l}_1$ and $\bar{l}_2$ the mean values of l_1 and l_2, we have for a case when there is a true tilt of the ground of the amount of θ,

$$\zeta_1 = \zeta_{\bar{l}_1} - \frac{L\theta}{2},$$

$$\zeta_2 = \zeta_{\bar{l}_2} + \frac{L\theta}{2},$$

where ζ_1 and ζ_2 are the observed values of the variation of the level of the water at both ends of the pipe. From these relations we get for the value of the true tilt

$$\theta = \frac{1}{L}\left\{\lambda(\zeta_1 + \zeta_2) - (\zeta_1 - \zeta_2)\right\},$$

where

$$\lambda = \frac{3}{L}(\bar{l}_1 - \bar{l}_2).$$

By these analysis we could find that in our case the highest point of the bending of the building of the Institute or the point where there is no thermal tilt coincides with the position indicated by the line A–A in Fig. 1. The distances from this A–A line to the tiltmeters installed in the under-cellar, in No. I chamber and in No. II chamber are about 17 m., 6 m. and 12 m. respectively. These distances are approxomately proportional to the amount of tilt of each tiltmeter.

As to the true tilt of the ground, it will be given in near future after the accomplishment of the calculation which is now going on.

In conclusion the author wishes to express his most cordial thanks to Professor Mishio Ishimoto for his valuable critiques and discussions.

---

8. 十八米突の鐵管による地表傾斜變化の觀測（豫報）

地震研究所　高橋龍太郎

此の觀測に用ひた裝置は 1914 年に A. A. Michelson が地殼の潮汐現象の觀測に用ひたものと同じ原理に基づくものである。今、地中に水平に、東西及南北の方向に、鐵管を埋め、其の中に水を半ば容して置く。地表の傾斜に若し變化を生ずれば、管中の水は管に對して其の水位を變へる。卽一端に於ては水位は高くなり他端に於ては水位は低下する。其の水位の變化を精密に測定すれば、傾斜變化を知りうるのである。水位の變化を測定するには色々の方法があるが、現裝置に於ては測微螺子を用ひてゐる。此の方法に依つて約十分の一秒迄の傾斜變化を測定しうるのである。

此の裝置によつて約十ケ月間の觀測を行つた結果、此の器械に現れる變化の主なるものは、氣溫の變化に依つて本研究所の建物が膨脹收縮する爲に生ずる建物の彎曲であつて眞正の地表の傾斜變化は觀測の結果に或る計算を施さねばならぬ事が判明したのである。眞の地表の傾斜變化に就ては計算の完了を待つて發表する豫定である。

---

9. *Investigation on the Deformation of the Earth's Crust in the Tango District connected with the Tango Earthquake of 1927. (Part I.)*

By Chûji TSUBOI,

Earthquake Research Institute.

(Received March 20, 1930.)

Contents.

		Page
1.	Introduction	153
2.	Data of Precise Levellings	160
3.	Study on the Results of Precise Levellings	172
4.	Comparison of the Results of Triangulations Before and After the Earthquake	190
5.	Study on the Results of Triangulations	194
6.	The Relation between the Vertical Displacements and the Divergence	203
7.	Postseismic Displacements of Secondary Triangulation Points	206
8.	Movements along the Gômura and Yamada Faults	215
9.	Concluding Remarks	218

1. Introduction.

On March 7th of 1927, about 30 minutes past 6 o'clock in the evening, a great earthquake occurred in the Tango district of northern Central Japan.[1] The people in this district were suddenly attacked by this unexpected catastrophe when they were mostly enjoying their evening meals. The shocks of the earthquake were extremely severe and entirely destroyed no less than 30% of houses in the meizoseismal area. The oscillations due to this earthquake were strong enough to be felt even in Tokyo which is situated as far as some 400 km. from the epicentre of the earthquake. The motion felt in Tokyo at that time was very long in its period and according to the author's own experience in

1) According to A. Imamura, the accurate time of initial occurrence of this earthquake at the origin is March 7th, 1927, 18 h, 27·6 m. The epicentre was at 135° 1′ E and 35° 39′ N.

Tokyo, the personal feeling was not so much like that of a periodic oscillation as of a slight giddiness. This may be because the seismic oscillations with shorter periods which were originally produced at the origin of the earthquake damped quickly with distance from the epicentre and only those with longer periods survived or less damped to be propagated into some distant places from the epicentre than the former.

Instrumentally the motions of this earthquake were recorded by most seismographs distributed on the globe.[2] The earthquake may be thus ranked as a "world-shaker" and among the earthquakes recently occurred in this country this was indeed next to the Kwantô great earthquake of Sept. 1st of 1923 in its magnitude.

A number of reports regarding this Tango earthquake have already been published from seismometrical, geological, geophysical and many other points of view. It will therefore be needless to give a detailed accounts about this earthquake in this paper, but the writer may be allowed to give a short sketch on it, for this is necessary for the proper understanding of what will be described in the following pages.

Almost at the same time of the outburst of the earthquake, fires occurred from many houses and factories in the towns and villages in the meizoseismal area and spread almost entirely over them which literally multiplied the fatal and economic loss than otherwise. According to the official report regarding this earthquake, 15,594 houses were entirely destroyed or burnt out of 21,600 in the meizoseismal area, and out of 96,615 of population, 3,017 fell victims of the catastrophe. Economic losses produced by this earthquake were tremendous. The district of Tango has long been known for the activity of the silk industry especially for the production of crapes commonly known by the name of "Tango Tirimen." The direct economic losses produced by this earthquake were estimated to amount more than 53,000,000 yen.

Geographically, the district of Tango lies on the northern coast of Central Japan and faces to the Sea of Japan. (Fig. 1.) Oku-Tango Peninsula, roughly rectangular in its shape, protrudes north-eastwards into the bay of Wakasa which is a remarkable depression embayment in the north coast of the main island of Japan. The mountains within the peninsula are almost of a uniform height of about 500–700 m., making a feature of a remarkable plateau. The west side of

2) O. HECKER, "Das Erdbeben in Japan am 7 März 1927," (Jena, 1928), and other seismological reports.

F. KISHINOUYE, *Earthquake*, 1 (1929), 723.

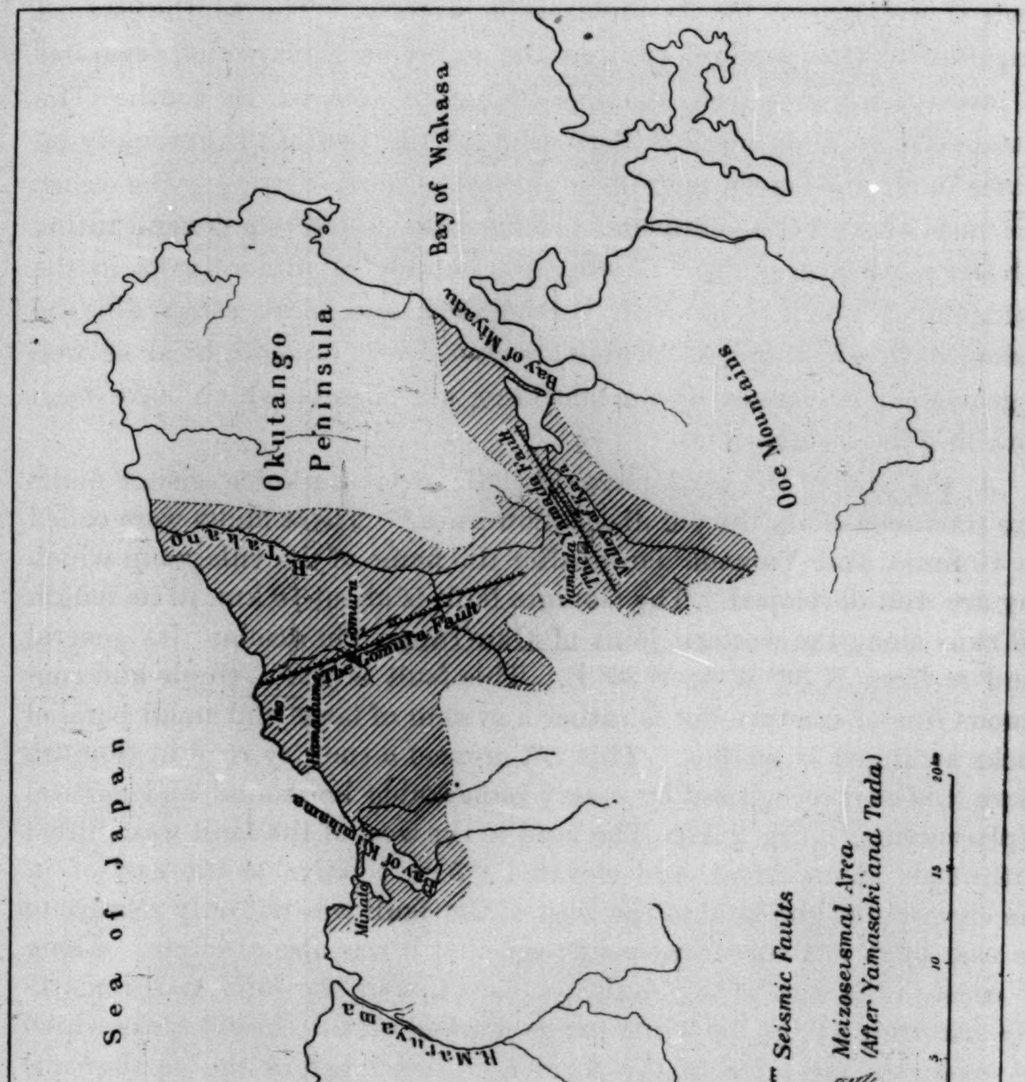

Fig 1 General Reference Map of the Tango District.

this central plateau faces to a belt of hill land across the fault valley of the river Takano which separates the above two areas quite distinctly. On its southern side, Oku-Tango Peninsula embraces the inlet of Miyadu which is well-known for its picturesque scenery. The southwestward elongation of this lowland runs as the valley of Kaya which separates the peninsular block from the Ooe mountain area on its south. The coastal terrace along the northern edge of the peninsula gradually increases in altitude as we go from southwest to northeast along the coast. This implies that the peninsular block was subjected to a general tilting with the southwestern dip. There are a number of minor faults in the peninsula of which those with northeastern and southeastern dips are predominating in number. There are thus every topographical as well as geological evidences of the blocking movements which have been prevailing in this district.[3)]

At the time of the earthquake of 1927, two remarkable seismic faults were produced along the old dislocation lines.[4)] These faults were called the Gômura and Yamada faults after the name of the villages in which they are well developed. The Gômura fault is about 18 km. in its length and runs along the western joint of Oku-Tango Peninsula. Its general trend is from N 30° W to S 30° E. This fault is not a single and continuous line of fracture but is rather a system of large and small parallel cracks arranged *en échelon*. This rift crossed a country road in Gômura where it is well recognised by a very remarkable horizontal and vertical displacements. (Fig. 2 A.) The land to the west of the fault was shifted southwards about 2·5 m. and elevated 0·5 m. relative to the east of it. The elevation of the land to the west of the fault was not only relative to the east of it but there are evidences that it was also absolute. Along the coast to the west of this fault, the elevation of the land was remarkably ascertained by the white bands marked on the coastal rocks which are evidently the trace of the former sea-level before the earthquake. (Fig. 2 B.) The elevation thus estimated is at its maximum at Hamadume being some 60 cm. and thence it decreases gradually westwards till

3) N. YAMASAKI and F. TADA, *Bull. Earthq. Res. Inst.*, 4 (1928), 159.
H. TSUYA, *ibid.*, 4 (1928), 139.
F. TADA, *ibid.*, 5 (1928), 111.
R. TAYAMA, *Rep. Saito Gratitude Foundation*, No. 6 (1928).

4) N. YAMASAKI and F. TADA, *Proc. Imp. Acad.*, 3 (1927), 223; *Bull. Earthq. Res. Inst.*, 4 (1928), 159.

Fig. 2 A. The Gômura Fault.

Fig. 2 B. The Elevation of the Coast at Iso.

Minato at the Bay of Kumihama where the elevation is scarcely to be recognised.[5]

The other Yamada fault was produced along the southern scarp of Oku-Tango Peninsula. Its general trend was from S 55° W to N 55° E. Across a country road near the village of Yamada, this fault is well developed in a form of a remarkable flexure. The land to the south of it was depressed about 0·7 m. relative to that to its north. The horizontal shifting along the fault was estimated to be 0·8 m., the land to its south being shifted westwards.

These two faults were no doubt produced along the old dislocation lines. Geological examination of the district ascertained this, and the earthquake of 1927 was thus regarded as nothing but an episode of the blocking movements which have long been prevailing in this district.[6]

Immediately after this earthquake, some of the staffs of our Institute were despatched to the disturbed district where they began their field and instrumental observations regarding this earthquake. At the same time, a deep hope was expressed by the staffs of our Institute to have precise data concerning the deformations of the earth's crust connected with the earthquake. For this purpose, it is necessary to make revisions of triangulations and precise levellings over the disturbed area and to repeat them successively with time. This hope was fortunately realised through the effort of Prof. K. Suyehiro, the Director of our Institute, who asked the Land Survey Department of the Imperial Japanese Army to execute these contemplated surveys. This request was willingly accepted by the later authority. Up to the present, in the interval of about two year and a half after the earthquake, both the triangulation and precise levellings were repeated as much as four times. In Table I is given the program in which these surveys were executed. Fig. 3 represents the same graphically.

Table I.

Date of the Earthquake	March 7, 1927.
First Levelling	April 13–June 16, 1927.
Second Levelling	June 17–July 31, 1927.
Third Levelling	March 3–April 20, 1928.
Fourth Levelling	August 7–Oct. 10, 1929.
First Triangulation	May-June, 1927.
Second Triangulation	August-Sept., 1927.
Third Triangulation	Oct.-Nov., 1927.
Fourth Triangulation	April-Sept., 1928.

5) S. T. Nakamura, *Sci. Rep. Tohoku Imp. Univ.*, **18** (1929), 419; *Rep. Saito Gratitude Foundation*, No. 5 (1928).

6) H. Tsuya, *Bull. Earthq. Res. Inst.*, **4** (1928), 139.

The results of these surveys were published from time to time in this Bulletin.[7] They are extremely interesting and have naturally been subjected to much discussions.

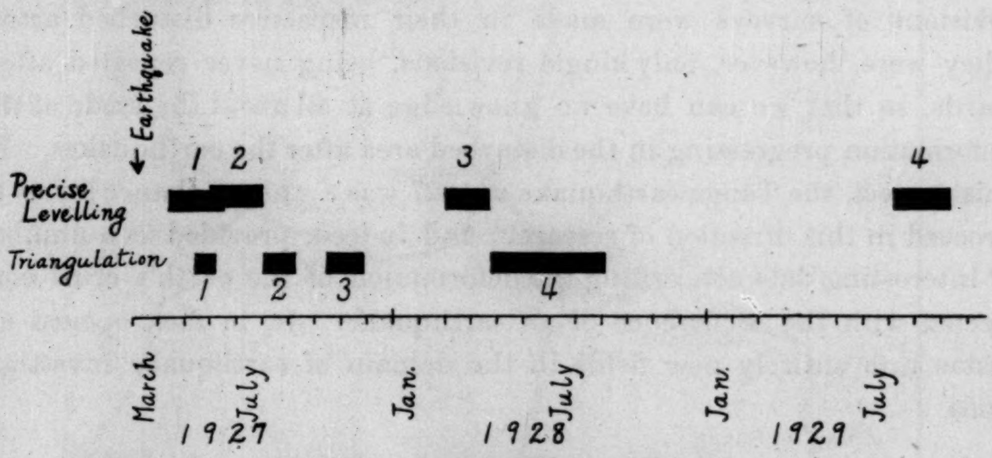

Fig. 3. The Program of the Surveys.

It was T. Terada and N. Miyabe[8] who intiated to make an analytical treatment of the results of these surveys. They studied the relations between the horizontal and vertical displacements of the earth's crust produced by the earthquake. They later extended the investigation to study the relations between the horizontal displacements and present topographical relief of the district concerned. On the other hand, the present author[9] examined the results of precise levellings and showed that the positive evidences of the occurrence of the blocking movements in the earth's crust of this district are involved in these results. Accumulation of data of these surveys after these papers were published enabled the writer not only to treat them in a similar way of analysis as was described in the former works but also to get some new informations regarding the deformation of the earth's crust in this district. It is the object of the present paper to described the results of some detailed examinations made on these results and to discuss their significance from the seismo-tectonic point of view.

So far as the writer knows, such exaustive revisions of surveys examining the deformation of the earth's crust connected with an earth-

7) *Bull. Earthq. Res. Inst.*, 3 (1927) 163; 4 (1928), 223, 225, 227; 5 (1928), 165; 7 (1929), 587.

A. Imamura, *Pub. Earthq. Inv. Comm.*, No. 25 (1930).

8) *Bull. Earthq. Res. Inst.*, 7 (1929), 223. *Proc. Imp. Acad.*, 4 (1928), 211, 215, 218, 296.

9) *Bull. Earthq. Res. Inst.*, 6 (1929), 71. *Proc. Imp. Acad.*, 4 (1928), 529.

quake has never been attempted in the world. It is true that in the California earthquake of 1906,[10] the Kwanto earthquake of 1923, and in a number of other earthquakes and volcanic eruptions,[11] a series of revisions of surveys were made in their respective disturbed areas. They were, however, only single revisions, being never repeated afterwards, so that we can have no knowledge at all about the mode of the deformation progressing in the disturbed area after the earthquakes. In this respect, the Tango earthquake of 1927 was a unique chance for us to proceed in this direction of research, and indeed, provided us a number of interesting data concerning the deformation of the earth's crust connected with the occurrence of an earthquake. It, in fact, opened up vistas into entirely new fields in the domain of earthquake investigations.

2. Data of Precise Levellings.

Through the district of Tango, a levelling route runs approximately in E–W direction. This route is shown in Fig. 4 in a full line. It starts at Ebara in its west extremity, passes through Kumihama, Mineyama, Kutiôno, Miyadu and terminates at Maiduru, its total length being 98 km., including 48 bench marks. Along this route, a levelling was once executed in 1888, some 40 years before the earthquake of 1927. Immediately after the earthquake, a levelling survey was carried out along this same route. The differences of the heights of the bench marks determined by these two levellings, the former in 1888 and the latter immediately after the earthquake of 1927, give the vertical displacements of the bench marks on this route, most part of which were produced at the time of the earthquake of 1927. These differences seem to include, not only these changes directly produced by the Tango earthquake, but also those produced as the effect of accumulation of chronic deformation of the earth's crust.[12] This is again superposed by the effect produced by the Tazima severe earthquake of 1925[13] which

10) W. BOWIE, *Spec. Pub. U. S. Coast Geod. Survey*, No. 151 (1928).

11) C. TSUBOI, *Bull. Earthq. Res. Inst.*, 7 (1929), 103.
A. IMAMURA, *Pub. Earthq. Inv. Comm.*, No. 25 (1930).

12) N. YAMASAKI, *Proc. Imp. Acad.*, 4 (1928), 60.

13) N. YAMASAKI, *Bull. Imp. Earthq. Inv. Comm.*, 10 (1928), 109.
A. IMAMURA, *ibid.*, 10 (1928), 71.
B. KOTO, *Journ. Fac. Sci. Imp. Univ. Tokyo*, Sec. II, 2 (1926), 1.

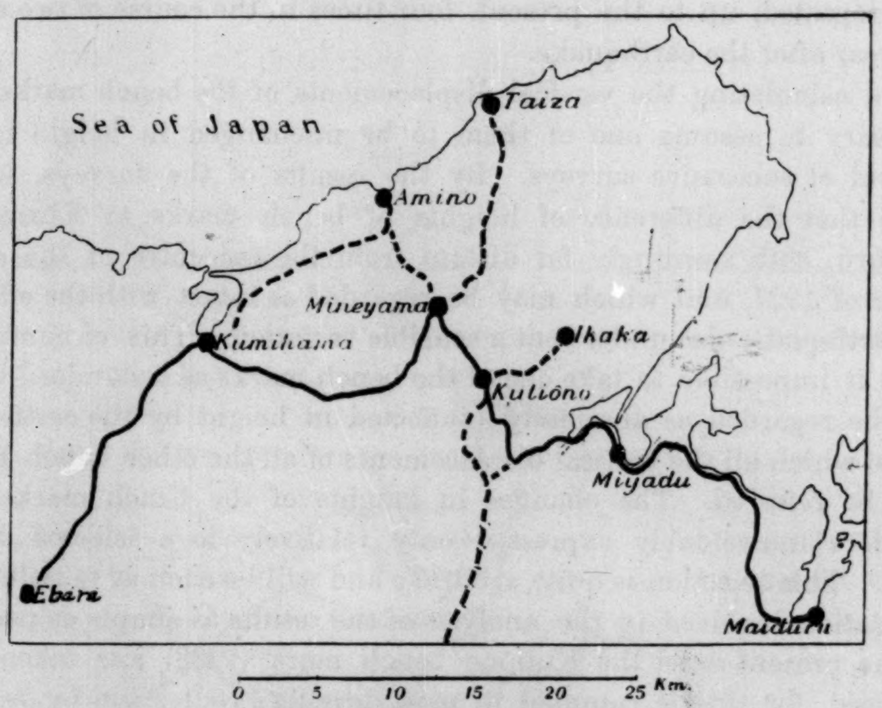

Fig. 4. Levelling Routes.

occured in the district of Tazima with its epicentre some 8 km. north-west of Kumihama.

Besides this old levelling route from Ebara to Maiduru, a series of new routes was established in this district after the earthquake, in order to get some informations regarding the spatial distribution of the deformations of the earth's crust caused by the earthquake. These new routes are shown by dotted lines in Fig. 4. They are as follows;

Table II.

	Length	Number of B. M.
Kumihama-Amino Station	18 km.	10
Mineyama-Amino	10	6
Mineyama-Taiza	16	9
Kutiono-Ikaka	8	5
Kutiono-Hukutiyama	44	21
Total	96	51

After the Tango earthquake, these old and new routes have been examined by means of precise levellings. These surveys have since

been repeated, up to the present, four times in the course of two and a half year after the earthquake.

In calculating the vertical displacements of the bench marks, it is necessary to assume one of them to be unchanged in height in the interval of successive surveys. By the results of the surveys, it was found that the difference of heights of bench marks at Ebara and Maiduru, both seemingly far distant from the epicentre of the earthquake of 1927, and which may be regarded as intact with the effect of the earthquake also underwent a sensible variation. This circumstance made it impossible to take one of the bench marks as a standard which may be regarded as absolutely unaffected in height by the earthquake and to which all the vertical displacements of all the other bench marks may be referred. The changes in heights of the bench marks were therefore unavoidably expressed only relatively to a selected one of them. This selection is quite arbitrary and will be such as to reduce the calculation involved in the analysis of the results as simple as possible. In the present case, the Kutiôno bench mark (1232) was taken as a standard, for this is common in most levelling routes and by doing so we can simplify the calculation. The levelling instrument used in these surveys was "Zeiss Level No. III" with an optical variation plate. The levelling scale was made of invar to get rid of the effect of atmospheric temperature which will otherwise affect its length. By this equipment, it is possible to make a direct reading of 1/20 mm. in the difference of heights of bench marks. The closing error is limited within 3 mm. The results of the surveys are given in Tables III–VIII. For the sake of simplicity, the following abbreviations are adopted in these tables.

P···The date of the preseismic levelling
I···The date of the first postseismic levelling
II···The date of the second postseismic levelling
III···The date of the third postseismic levelling
IV···The date of the fourth postseismic levelling

I–P···The change of height of a bench mark in the interval between the preseismic and the first postseismic levellings.

II–I···The change of height of a bench mark in the interval between the first and the second postseismic levellings.

etc.

The geographical positions and numbers of the bench marks are shown in Fig. 5.

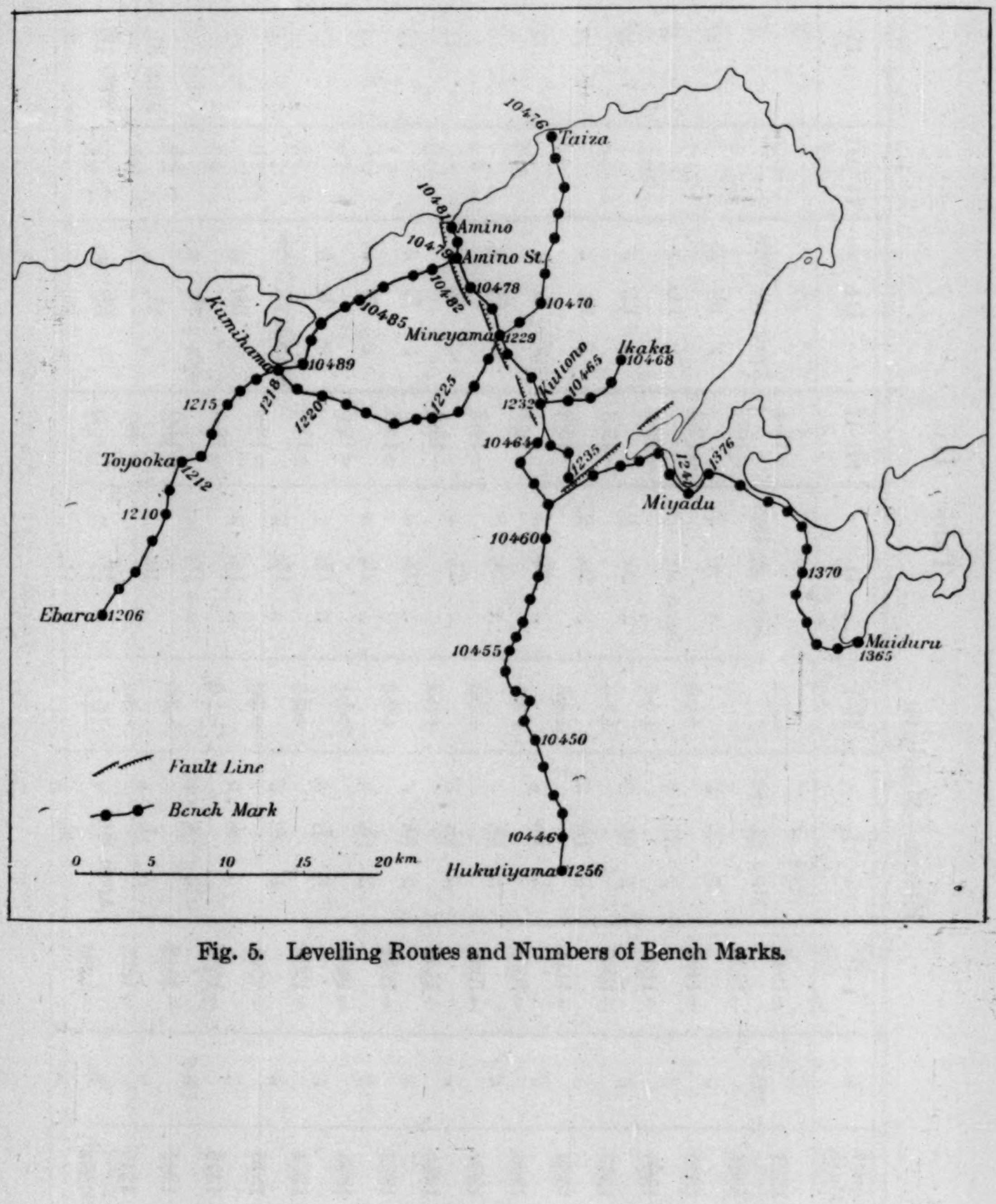

Fig. 5. Levelling Routes and Numbers of Bench Marks.

Table III.

Ebara—Maiduru

Bench-Mark	$\overline{P}$	I-$\overline{P}$	I	II-I	II	III-II	III	IV-III	IV	III-I	IV-I
1363		−1042				−17·4					
	1888		May 22, 1927		July 8, 1927		April 15, 1928				
1364		−1128				−18·0					
	”		” 21, ”		” 4, ”		” 13, ”				
1365		−1457		+8·5		−17·3				− 8·8	
	”		” 20, ”		June 30, ”		” 14, ”				
1366		−1104		+6·2		−19·1				−12·9	
	”		” 19, ”		” 29, ”		” 12, ”				
1367		−1068		+5·0		−19·3				−14·3	
	”		” 17, ”		” 28, ”		” 10, ”				
1368		−1111		+4·9		−15·8				−10·9	
	”		” 15, ”		” 25, ”		” 8, ”				
1369		−1063		+3·5		−16·1				−12·6	
	”		” 13, ”		” 24, ”		” 3, ”				
1370		−1027		+2·3		−14·7				−12·4	
	”		” 11, ”		” 23, ”		” 6, ”				
1371		−1152		+0·3		−15·0				−14·7	
	”		” 10, ”		” 22, ”		” 5, ”				
1372		−1251		+0·2		−14·2				−14·0	
	”		” 8, ”		” 21, ”		” 2, ”				
1373		−1009		−1·1		−14·6				−13·5	
	”		” 7, ”		” 17, ”		” 1, ”				
1374		−1209		−0·5		−15·6				−16·1	
	”		” 5, ”		” 15, ”		March 27, 1928				
1375		−1091		−2·0		−13·0				−15·0	
	”		” 4, ”		” 14, ”		” 28, ”				
1376		−1608		−1·0		−13·0				−14·0	
	”		” 3, ”		” 13, ”		” 25, ”				
1241		−1518		−3·5		−11·0		− 2·6		−14·5	−17·1
	”		” 1, ”		” 12, ”		” 25, ”		Aug. 31, 1929		
1240		−1273		−3·2		− 8·7		− 3·6		−11·9	−15·5
	”		April 30, ”		” 11, ”		” 24, ”		Sept. 5, ”		
1239		−1286		−1·2		− 8·7		− 3·3		− 9·9	−13·2
	”		” 28, ”		” 11, ”		” 23, ”		” 3, ”		

(to be continued.)

Table III. (*continued.*)

Bench-Mark	$\overline{P}$	I–$\overline{P}$	I	II–I	II	III–II	III	IV–III	IV	III–I	IV–I
1238		−2107		−2·2		−10·2		− 5·0		−12·4	−17·4
	1888		April 27, 1927		June 10, 1927		March 22, 1928		Sept. 2, 1929		
1237		−2777		−3·6		−15·8		− 6·2		−19·4	−25·6
	"		" 24, "		" 8, "		" 21, "		" 11, "		
1236		−3530		−2·8		−11·1		− 4·0		−13·9	−17·9
	"		" 23, "		" 5, "		" 13, "		" 8, "		
1235		+7848		−0·1		+ 1·2		+ 7·3		+ 1·1	+ 8·4
	"		" 22, "		" 5, "		" 10, "		" 13, "		
1234		+4682		−2·7		+ 2·8		+ 4·8		+ 0·1	+ 4·9
	"		" 20, "		" 4, "		" 6, "		" 14, "		
1233		+2634		−1·4		− 1·3		+ 1·7		− 2·7	− 1·0
	"		" 19, "		" 2, "		" 5, "		" 15, "		
1232		0		0·0		0·0		0·0		0·0	0·0
	"		" 20, "		" 2, "		" 4, "		" 17, "		
1231		− 764		−5·8		− 2·2		− 4·8		− 8·0	−12·8
	"		" 22, "		" 3, "		" 5, "		" 19, "		
1230		−2528		−5·2		− 6·3		−18·2		−11·5	−29·7
	"		" 23, "		" 4, "		" 8, "		" 11, "		
1229		−4410		−3·1		− 2·4		−16·0		− 5·5	−21·5
	"		" 24, "		" 5, "		" 9, "		" 12, "		
1228		+3081		+2·5		+ 7·6		−15·8		+10·1	− 5·7
	"		" 25, "		" 6, "		" 17, "		" 15, "		
1227		+1354		−2·5		+ 5·0		−20·7		+ 2·5	−18·2
	"		" 27, "		" 9, "		" 16, "		" 8, "		
1226		+1003		−8·0		+ 4·6		−21·4		− 3·4	−24·8
	"		" 29, "		" 10, "		" 15, "		" 6, "		
1225		+ 317		−9·0		+ 2·8		−27·1		− 6·2	−33·3
	"		" 30, "		" 12, "		" 18, "		" 5, "		
1224		+ 22		−7·0		+ 1·0		−25·5		− 6·0	−31·5
	"		May 4, "		" 14, "		" 20, "		" 2, "		
1223		− 546		−2·5		+ 0·5		−30·4		− 2·0	−32·4
	"		" 5, "		" 16, "		" 21, "		Aug. 31, "		
1222		− 843		−5·6		+ 2·5		−34·4		− 3·1	−37·5
	"		" 7, "		" 17, "		" 23, "		Sept. 1, "		

(*to be continued.*)

Table III. (*continued.*)

Bench-Mark	$\overline{P}$	I–$\overline{P}$	I	II–I	II	III–II	III	IV–III	IV	III–I	IV–I
1221	1888	− 906	May 8, 1927	−7·8	June 19, 1927	+ 4·3	March 24, 1928	−37·7	Aug. 25, 1929	− 3·5	−41·2
1220	"	−1949	" 9, "	−6·0	" 20, "	− 4·0	" 25, "	−37·5	" 23, "	−10·0	−47·5
1219	"	−1415	" 10, "	−5·1	" 21, "	− 2·2	" 27, "	−36·5	" 21, "	− 7·3	−43·8
1218	"	−1738	" 12, "	−8·5	" 22, "	+ 0·2	" 28, "	−39·3	" 19, "	− 8·3	−47·6
1217	"	−1563	" 13, "	−7·1	" 23, "	+ 1·9	" 29, "	−38·9	" 20, "	− 5·2	−44·1
1216	"	−1629	" 15, "	−3·6	" 26, "	+ 2·6	" 30, "	−42·0	" 17, "	− 1·0	−43·0
1215	"	−1622	" 19, "	−3·5	" 29, "	+ 2·4	April 4, "	−47·7	" 15, "	− 1·1	−48·8
1214	"	−1743	" 20, "	−1·1	" 30, "	− 0·4	" 5, "	−44·5	" 16, "	− 1·5	−46·0
1213	"	−2219	" 21, "	+0·4	July 2, "	− 7·3	" 6, "	−43·0	" 14, "	− 6·5	−49·9
1212	"	−8323	" 22, "	−3·0	" 4, "	−23·5	" 7, "	−57·8	" 7, "	−26·5	−84·3
1211	"	−4677	" 23, "	−2·4	" 6, "	−22·2	" 8, "	−54·4	" 8, "	−24·6	−79·0
1210	"	−3753	" 24, "	−1·2	" 8, "	−16·9	" 9, "	−47·4	" 10, "	−18·1	−65·5
1209	"	−2663	" 26, "	−1·8	" 11, "	−17·7	" 13, "	−37·5	" 9, "	−19·5	−57·0
1208	"	−2542	" 27, "	−0·2	" 12, "	−20·9	" 14, "	−37·6	" 11, "	−21·1	−58·8
1207	"	−1960	" 28, "	+0·1	" 10, "	−22·7	" 14, "	−32·5	" 13, "	−22·6	−55·1
1206	"	−1970	" 29, "	+1·4		−22·4		−32·0		−21·0	−53·0
1205	"	−2015	" 30, "								
1204		−1977									

Table IV.

Kumihama—Amino St.

Bench-Mark			I	II–I	II	III–II	III	IV–III	IV	III–I	IV–I
1218				−5·4		+ 0·2		−39·3		− 5·2	−44·5
			May 30, 1927		June 28, 1927		March 27, 1928		Aug. 27, 1929		
10489				−6·8		+ 0·9		−34·2		− 5·8	−40·0
			„ 29, „		„ 29, „		April 10, „		„ 26, „		
10488				−6·8		− 0·1		−37·8		− 6·9	−44·7
			„ 28, „		„ 27, „		„ 9, „		„ 29, „		
10487				−3·5		− 1·6		−43·5		− 5·1	−48·6
			„ 27, „		„ 26, „		„ 8, „		Oct. 3, „		
10486				−2·9		− 0·3		−39·3		− 3·2	−42·5
			„ 25, „		„ 23, „		„ 6, „		„ 1, „		
10485				−2·2		− 1·5		−35·0		− 3·7	−38·7
			„ 24, „		„ 22, „		„ 4, „		„ 4, „		
10484				−1·3		− 2·6		−28·1		− 3·9	−32·0
			„ 22, „		„ 21, „		„ 5, „		„ 5, „		
10483				−1·3		+ 4·1		−26·6		+ 2·8	−23·8
			„ 21, „		„ 20, „		„ 1, „		„ 9, „		
10482				+2·7		+ 6·6		−16·0		+ 9·3	− 6·7
			„ 19, „		„ 18, „		March 29, „		„ 10, „		
10479				+5·1		+12·4		−24·0		+17·5	− 6·5

Table V.

Kutiono—Ikaka

Bench-Mark	$\overline{P}$	I-$\overline{P}$	I	II-I	II	III-II	III	IV-III	IV	III-I	IV-I
1232		0·0		0·0		0·0				0·0	
			April 25, 1927		June 10, 1927		March 1, 1928				
10465				−0·8		−4·9				−5·7	
			„ 27, „		„ 12, „		„ 16, „				
10466				−1·4		−3·3				−4·7	
			„ 28, „		„ 14, „		„ 17, „				
10467				+2·4		−4·4				−2·0	
			„ 29, „		„ 15, „		„ 18, „				
10468				−1·6		−1·4				−3·0	

Table VI.

Kutiono—Hukutiyama

Bench-Mark	$\overline{P}$	I-P	I	II-I	II	III-II	III	IV-III	IV	III-I	IV-I
1232		0·0		0·0		0·0		0·0		0·0	0·0
			May 2, 1927		June 19, 1927		April 3; 1928		Sept. 20, 1929		
10464				+ 2·5		+ 6·4		+ 2·7		+ 8·9	+11·6
			„ 5, „		„ 21, „		„ 4, „		„ 19, „		
10463				− 1·1		− [illegible]0		+ 1·2		− 6·1	− 4·9
			„ 7, „		„ 23, „		„ 5, „		„ 18, „		
10462				− 3·4		+ 6·8		+10·1		+ 3·4	+13·5
			„ 9, „		„ 26, „		„ 7, „		„ 23, „		
10461				− 2·6		−23·8		+ 2·2		−26·4	--24·2
			„ 11, „		„ 27, „		„ 10, „		„ 25, „		
10460				− 2·4		−11·6		+ 0·7		−14·0	−13·3
			„ 16, „		July 1, „		, 6, „		„ 30, „		

(*to be continued.*)

Table VI. (*continued.*)

Bench-Mark	$\overline{P}$	I−$\overline{P}$	I	II−I	II	III−II	III	IV−III	IV	III−I	IV−I
10459				+ 0·2		−14·0		+ 2·7		−13·8	−11·1
			May 18, 1927		July 7, 1927		April 7, 1928		Sept. 27, 1929		
10458				− 0·8		−18·1		− 0·2		−18·9	−19·1
			„ 19, „		„ 9, „		„ 8, „		„ 29, „		
10457				+ 0·8		−17·8		+ 3·7		−17·8	−14·1
			„ 23, „		„ 11, „		„ 9, „		Oct. 3, „		
10456				− 4·0		−19·7		+ 5·1		−23·7	−18·6
			„ 25, „		„ 13, „		„ 10, „		„ 6, „		
10455				− 5·2		−25·3		+ 5·2		−30·5	−25·3
			„ 27, „		„ 15, „		March 28, „				
10454				− 2·1		−31·0				−33·1	
			„ 29, „		„ 17, „		„ 26, „				
10453				+ 6·1		−35·8				−29·7	
			June 1, „		„ 18, „		„ 24, „				
10452				+ 4·4		−33·5				−29·1	
			„ 3, „		„ 20, „		„ 21, „				
10451				+ 5·8		−32·7				−26·9	
			„ 6, „		„ 23, „		„ 19, „				
10450				+10·7		−33·7				−23·0	
			„ 7, „		„ 24, „		„ 17, „				
10449				+ 9·2		−37·7				−28·5	
			„ 8, „		„ 25, „		„ 16, „				
10448				+ 9·2		−41·0				−31·8	
			„ 12, „		„ 27, „		„ 12, „				
10447				+ 5·7		−39·3				−33·6	
			„ 14, „		„ 29, „		„ 9, „				
10446				+ 4·7		−38·0				−33·3	
			„ 16, „		„ 31, „		„ 7, „				
1256				+ 3·0		−38·8				−35·8	

Table VII.

Amino—Mineyama

Bench-Mark	$\overline{P}$	$\overline{P}$-I	I	II-I	II	III-II	III	IV-III	IV	III-I	IV-I
10481			May 17, 1927	+3·9	June 17, 1927	+24·0	March 31, 1928	−18·6	Oct. 7, 1929	+27·9	+ 9·3
10480			„ 16, „	−0·5	„ 16, „	+ 9·0	„ 30, „	−30·8	„ 6, „	+ 8·5	−22·3
10479			„ 15, „	+5·1	„ 13, „	+12·4	„ 29, „	−24·0	„ 16, „	+17·5	− 6·5
10478			„ 12, „	+3·7	„ 12, „	+10·0	„ 18, „	−16·1	„ 17, „	+13·7	− 2·4
10477			„ 11, „	−2·2	„ 11, „	+ 4·7	„ 16, „	−17·1	Sept. 13, „	+ 2·5	−14·6
1229				−3·1		− 2·4		−16·0		− 5·5	−21·5

Table VIII.

Mineyama—Taiza

Bench-Mark	$\overline{P}$	$\overline{P}$-1	I	II-I	II	III-II	III	IV-III	IV	III-I	IV-I
1229				−3·1		−2·4		−16·0		−5·5	−21·5
			April 30, 1927		June 2, 1927		March 24, 1928		Sept. 20, 1929		
10469				−2·7		−2·5		−16·9		−5·2	−22·1
			May 2, „		„ 3, „		„ 23, „		„ 19, „		
10470				−2·0		−3·0		−11·9		−5·0	−16·9
			„ 4, „		„ 4, „		„ 26, „		„ 18, „		
10471				−0·5		−4·7		−22·3		−5·2	−27·5
			„ 5, „		„ 4, „		„ 27, „		„ 23, „		
10472				+0·1		−0·1		−18·0		0	−18·0
			„ 6, „		„ 5, „		„ 22, „		„ 22, „		
10473				+2·1		−1·9		−11·2		+0·2	−11·0
			„ 7, „		„ 7, „		„ 21, „		„ 24, „		
10474				+2·0		−2·5		−11·4		−0·5	−11·9
			„ 9, „		„ 8, „		„ 19, „		„ 25, „		
10475				+3·8		−2·8		−22·6		+1·0	−21·6
			„ 10, „		„ 9, „		„ 18, „		„ 27, „		
10476				+3·2		−1·4		−13·5		+1·8	−11·7

3. Study on the Results of Precise Levellings.

In order to make clear the vertical displacements of the bench marks between P and I, Fig. 6 was constructed. In this figure, the horizontal distance along the levelling route from Ebara to Maiduru is taken in abscissa and the change of heights of bench marks in this interval was taken in ordinate. In constructing Fig. 6, zero of vertical displacement was taken tentatively at Kutiôno (1232). The distance between the successive bench marks measured along the levelling route is roughly constant being about 2 km. In constructing Fig. 6, the successive distance between the bench marks was therefore taken throughout constant for the sake of simplicity. The levelling route crosses the Gômura fault between the bench marks 1228 and 1229 with the fall of 79·41 cm. It also crosses the Yamada fault between the bench marks 1235 and 1236 with the fall of 113·78 cm. The ground west to the Gômura fault may be seen to have generally been subjected to western tilting. The curve I–P is concave upward in this part of the route, but this does not necessarily imply that the ground was deformed with upward curvature. As may be seen in Fig. 5, the levelling route itself is concave northwards. Even if the ground was tilted to southwestward direction with no relative deformation in itself, it will give essentially the similar graph of vertical displacements as the case with the curved deformation. In the present case, we cannot decide whether the case in Tango is due to the former circumstance or to the latter. From the bench mark 1229 to 1235, the vertical displacements sharply increase. This is evidently due to the northward tilting of the land block which is bounded by the Gômura and Yamada fault at its west and south sides respectively. The angle of tilting of this block amounts as much as 20″. The land to the east of the Yamada fault was not deformed very much except in its immediate neighbourhood. Thus the general feature of the vertical deformation of the ground may be somewhat like that shown in Fig. 7.

In Figs. 8 and 9 are represented the successive (II–I, III–II, IV–III), and cumulative (II–I, III–I, IV–I) vertical displacements of the bench marks after the earthquake of 1927 along the same route. III–I, which means the change of height of a bench mark between the third and the first levellings after the earthquake is obtained by taking the algebraic sum of the changes of heights of a bench mark between the second and first levelling (II–I) plus that between the third and the second (III–II).

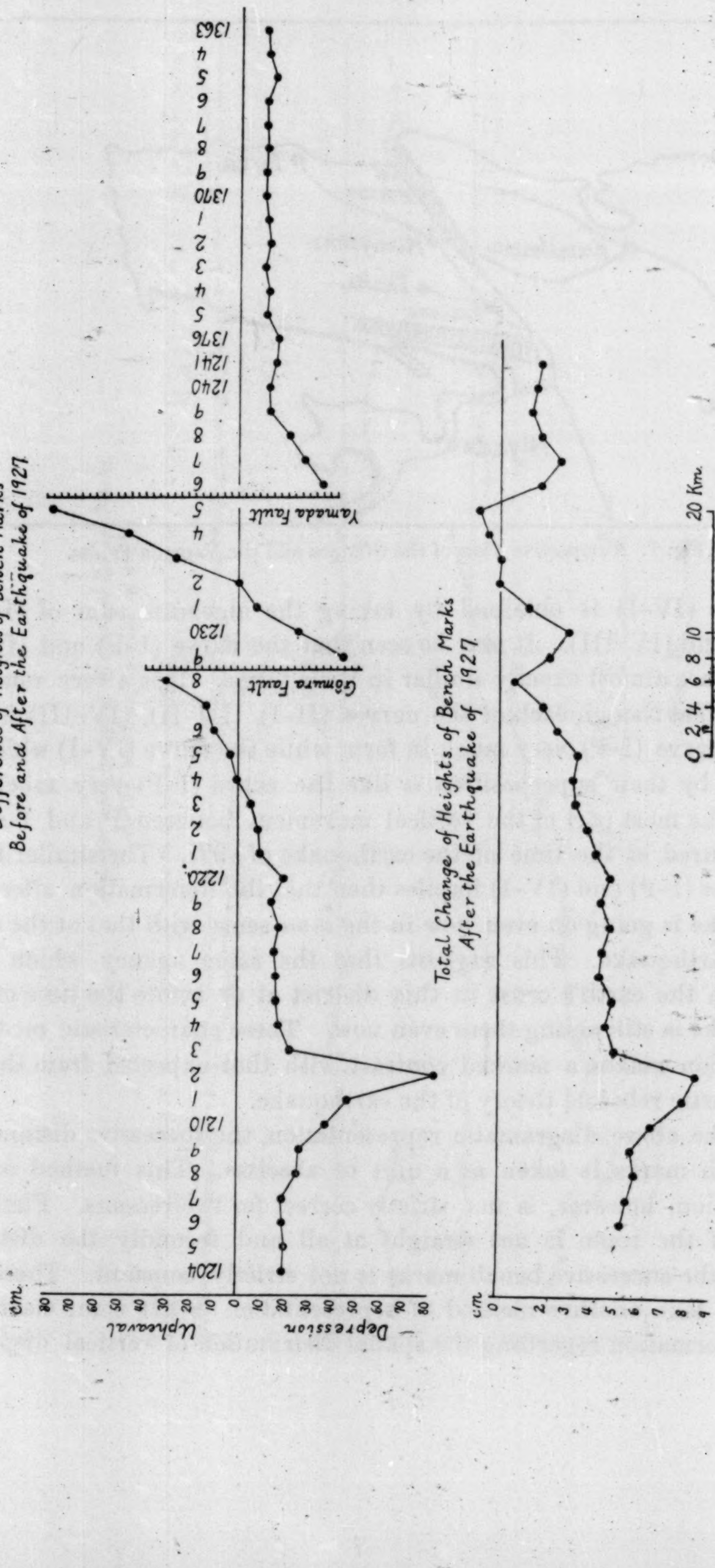
Difference of Heights of Bench Marks
Before and After the Earthquake of 1927
Upheaval
– Depression
cm
Gōmura fault
Yamada fault
Total Change of Heights of Bench Marks
After the Earthquake of 1927
cm
0 2 4 6 8 10 20 Km

Fig. 6.

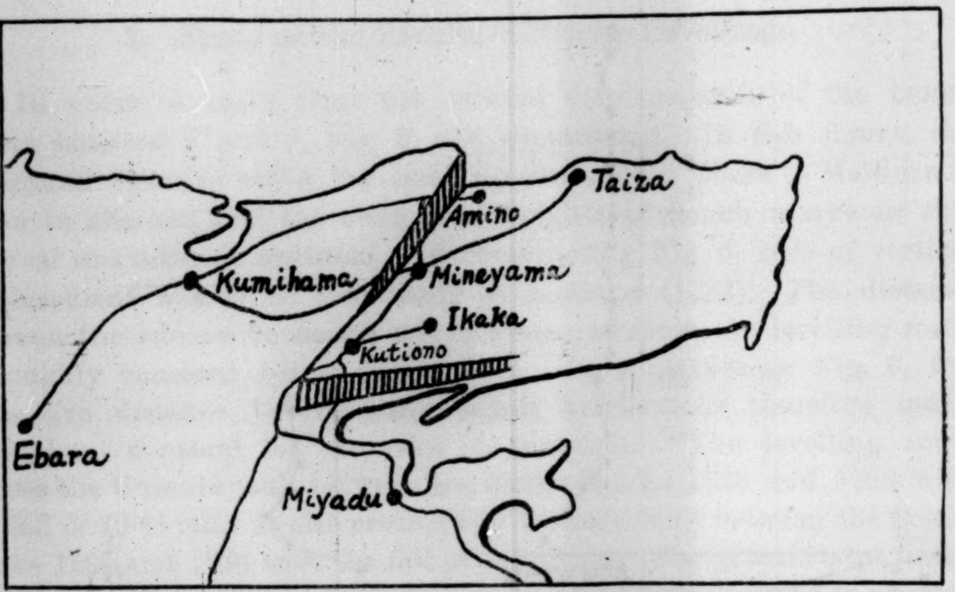

Fig. 7. Perspective View of the Gômura and the Yamada Faults.

Similarly (IV–I) is obtained by taking the algebraic sum of (II–I), (III–II) and (IV–III). It may be seen that the curve (I–P) and (IV–I) in Fig. 6 are almost exactly similar in their forms. It is a very remarkable fact that though each of the curves (II–I), (III–II), (IV–III) is *not* like the curve (I–P) very much in form while the curve (IV–I) which is obtained by their superposition *is* like the curve (I–P) very much in form. The most part of the vertical movement between P and I must have occured at the time of the earthquake of 1927. The similarity of the curves (I–P) and (IV–I) implies then that the deformation after the earthquake is going on even now in the *same* sense with that at the time of the earthquake. This suggests that the same agency which was acting on the earth's crust in this district at or before the time of the earthquake is still acting there even now. These characteristic mode of deformation makes a marked contrast with that expected from the so-called elastic rebound theory of the earthquake.

In the above diagramatic representation, the successive distance of the bench marks is taken as a unit of abscissa. This method of representation, however, is not strictly correct for two reasons. First the course of the route is not straight at all and secondly the distance between the successive bench marks is not strictly constant. Therefore we must take another method of representation to get some clear and strict information regarding the spatial distribution of vertical displace-

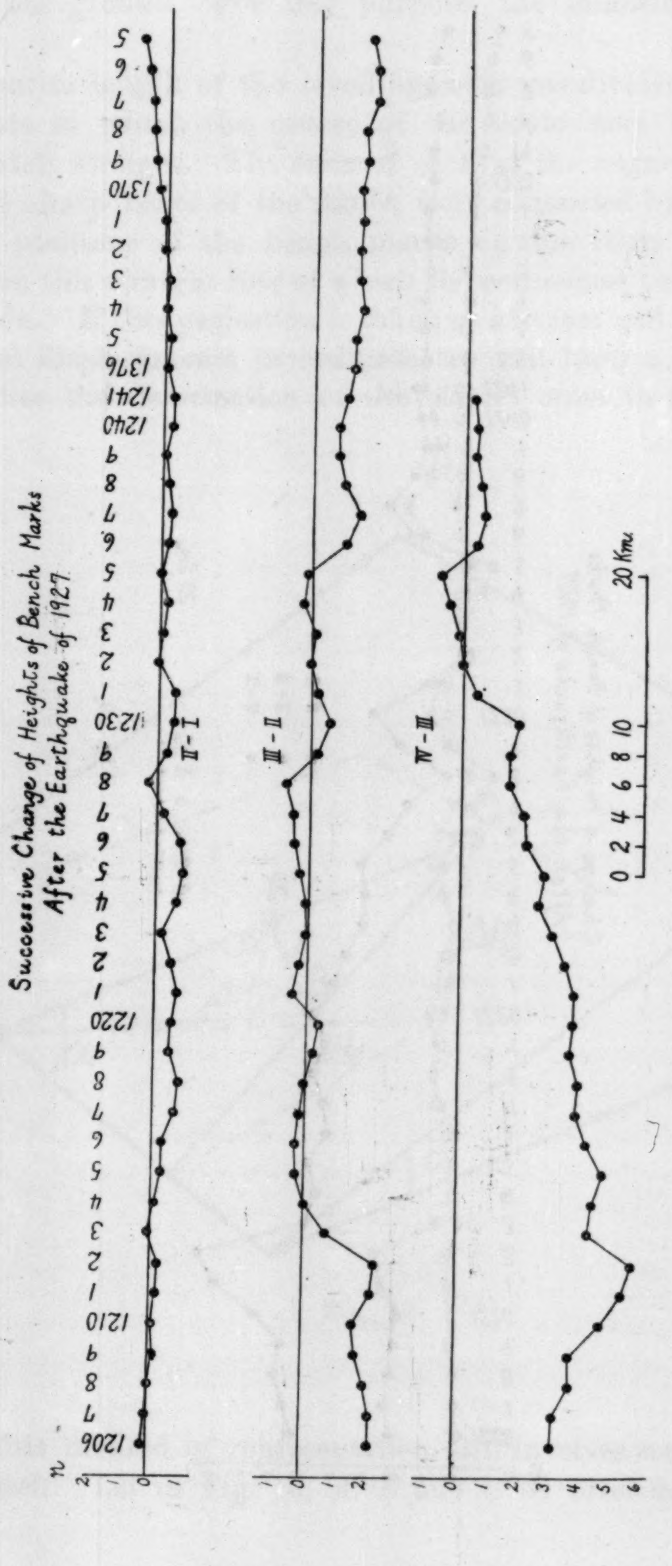
Successive Change of Heights of Bench Marks
After the Earthquake of 1927.
II - I
III - II
IV - III
20 Km
0 2 4 6 8 10

Fig. 8.

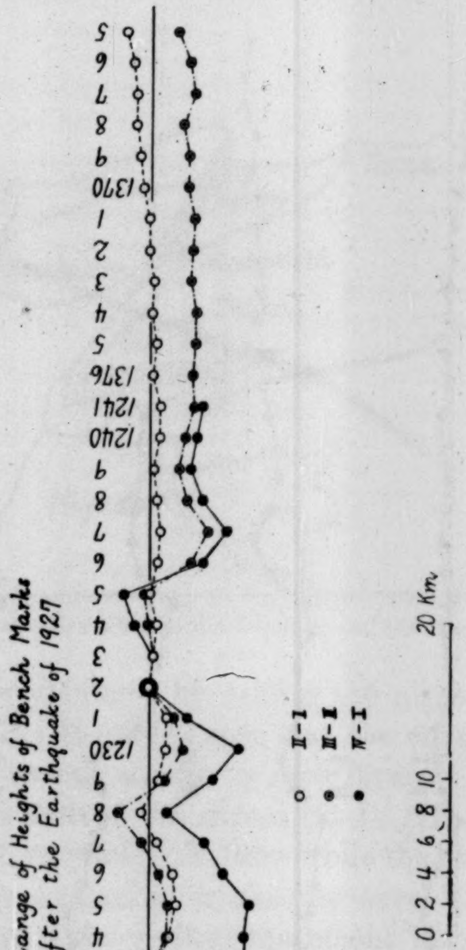
Change of Heights of Bench Marks
After the Earthquake of 1927
cm
II-I
III-I
IV-I
20 Km

Fig. 9.

ments of the ground. For this purpose, the following method was adopted.

The entire length of the levelling route was divided into a number of segments in which the course of the route may be regarded as approximately straight. The ends of each of the segments, which are situated at sharp bents of the routes, were connected by a straight line. Then the positions of the bench marks on the route were normally projected on this straight line of which the connected two bench marks are the ends. If this projection is taken as abscissa and the corresponding vertical displacements in ordinate, we will have a diagram which will visualise the deformation of the earth's crust in the region con-

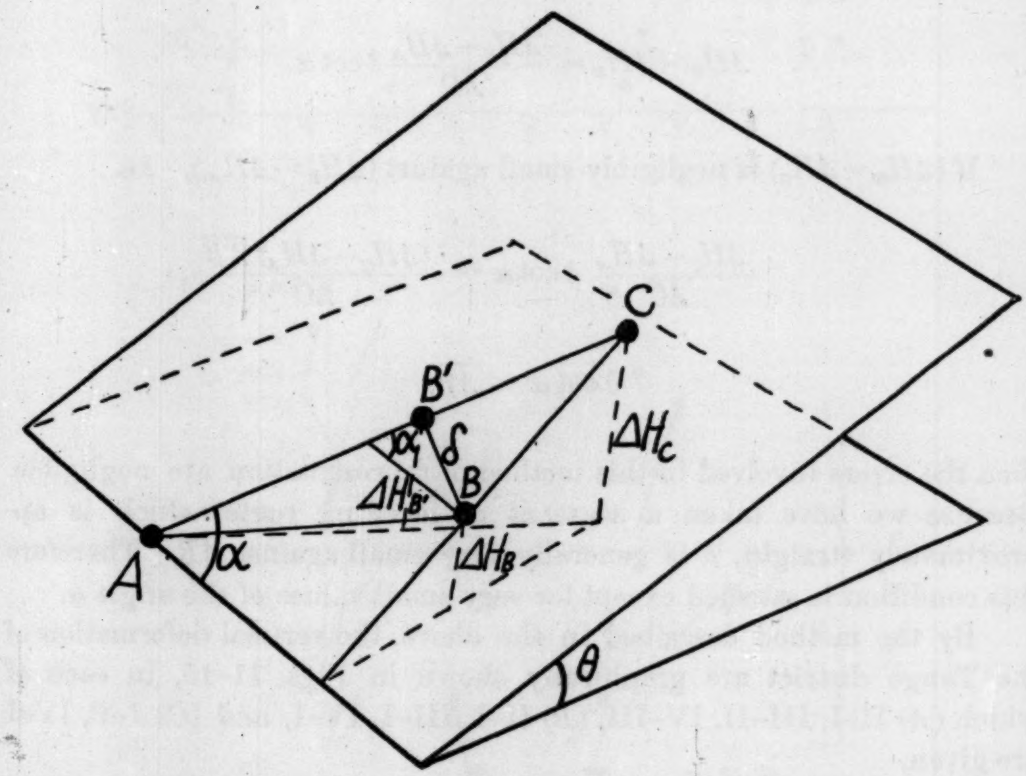

Fig. 10.

cerned. This method of representation still involves some unavoidable errors in itself. Let in Fig. 10, *A*, *B* and *C* be three successive bench

marks. Let B' be the foot of the perpendicular drawn from B on the straight line AC, and δ be the distance of BB'. Suppose the plane ABC was subjected to a tilting of θ with the axis PP' which makes an angle α with the straight line AC. Let further the vertical displacements of A, B, B' and C produced by this tilting be represented by ΔH_A, ΔH_B, $\Delta H_{B'}$ and ΔH_C respectively. In the above method of representation, ΔH_B and $\Delta H_{B'}$ are taken as equal. This is not strictly correct. We have

$$\Delta H_{B'} = \frac{(\Delta H_C - \Delta H_A)\,\overline{AB'}}{\overline{AC}} + \Delta H_A,$$

$$\Delta H_B = (\Delta H_C - \Delta H_A)\,\frac{\overline{AB'} - \delta \cot\alpha}{\overline{AC}} + \Delta H_A .$$

$$\therefore \quad \Delta H_{B'} - \Delta H_B = \frac{\Delta H_C - \Delta H_A}{\overline{AC}}\,\delta \cot\alpha .$$

If $(\Delta H_{B'} - \Delta H_B)$ is negligibly small against $(\Delta H_{B'} - \Delta H_A)$, i.e.

$$\frac{\Delta H_C - \Delta H_A}{\overline{AC}}\,\delta \cot\alpha \ll \frac{(\Delta H_C - \Delta H_A)\,\overline{AB}}{\overline{AC}},$$

$$\delta \cot\alpha \ll \overline{AB},$$

then the errors involved in this method of representation are negligible. Because we have taken a segment of levelling route which is approximately straight, δ is generally very small against AB. Therefore this condition is satisfied except for very small values of the angle α.

By the method described in the above, the vertical deformation of the Tango district are graphically shown in Figs. 11–15, in each of which (*A*) II–I, III–II, IV–III, (*B*) II–I, III–I, IV–I, and (*C*) I–P, IV–I are given.

In A of each of these figures, the distribution of the points is more or less systematic. The points representing the vertical displacements of the bench marks are distributed, not on an irregular or continuous curve, but systematically on a number of broken segments of straight lines. The end of these broken segments lie on the same or very closely near abscissa for all of the graphs II–I, III–II, and IV–III. These facts

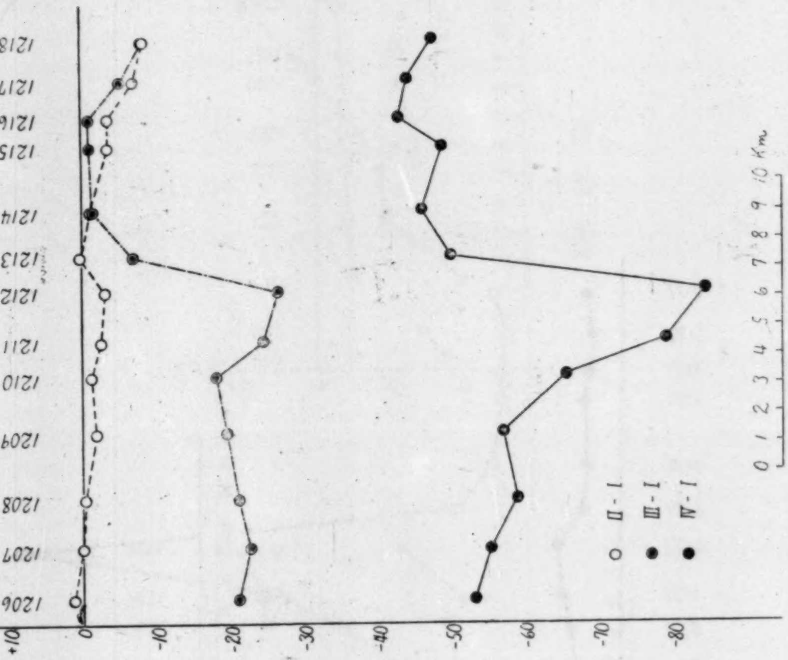

Fig. 11. B.

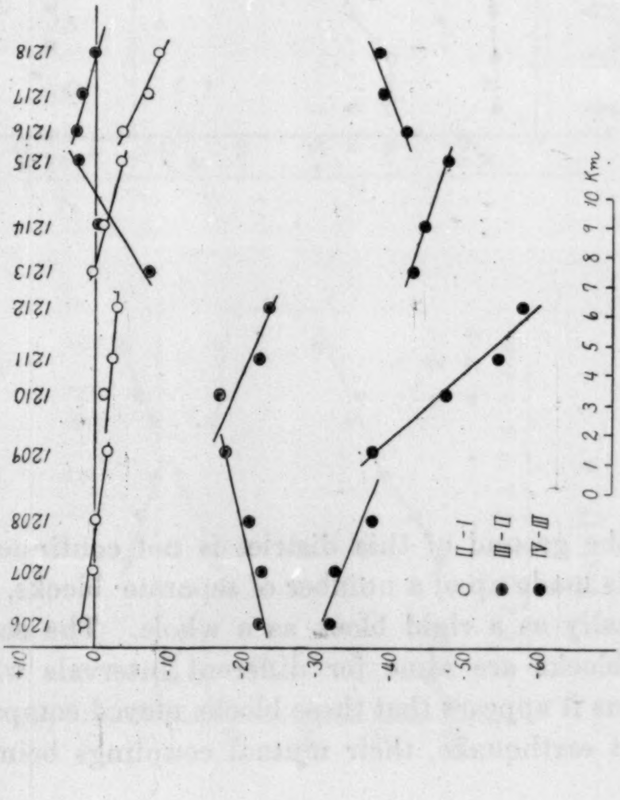

Fig. 11. A

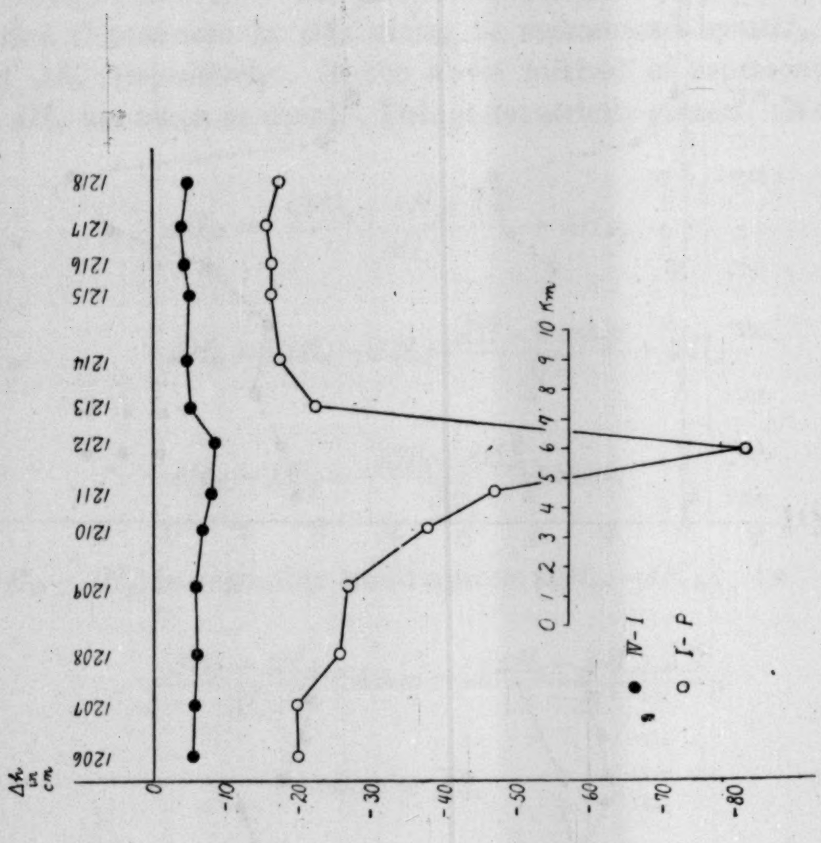

Fig. 11. C

suggest that the ground of this district is not continuous at all in its structure but is made up of a number of separate blocks, each of which moved practically as a rigid block as a whole. The sense of tilting of some of the blocks are same for different intervals while others are reversed. Thus it appears that these blocks moved comparatively easily after the great earthquake, their mutual couplings being considerably

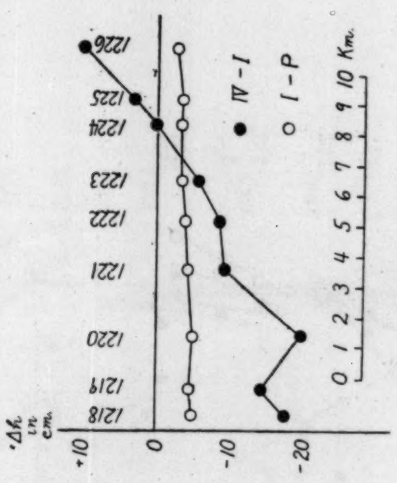

Fig. 12. C.

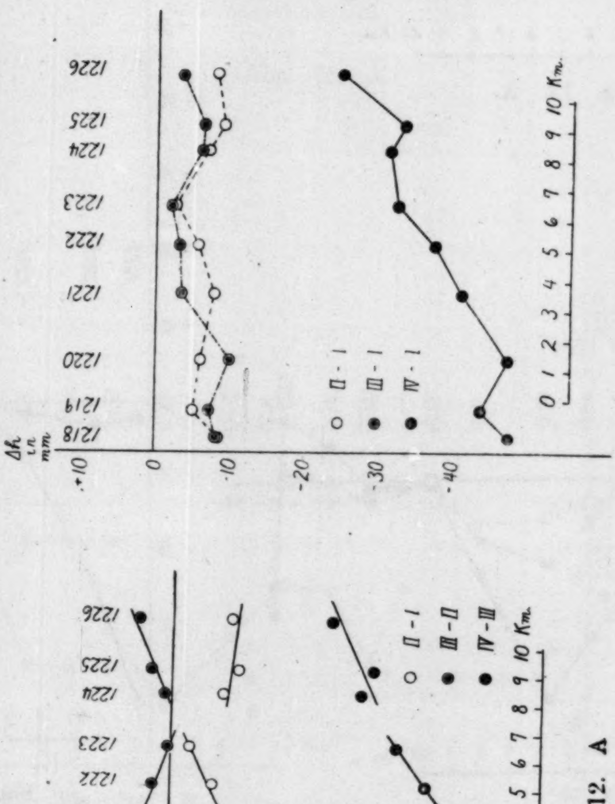

Fig. 12. B.

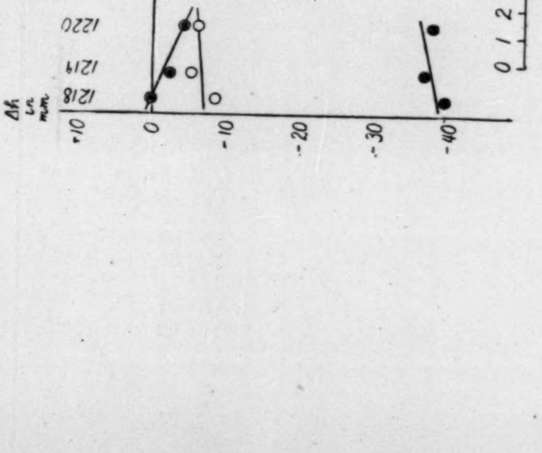

Fig. 12. A

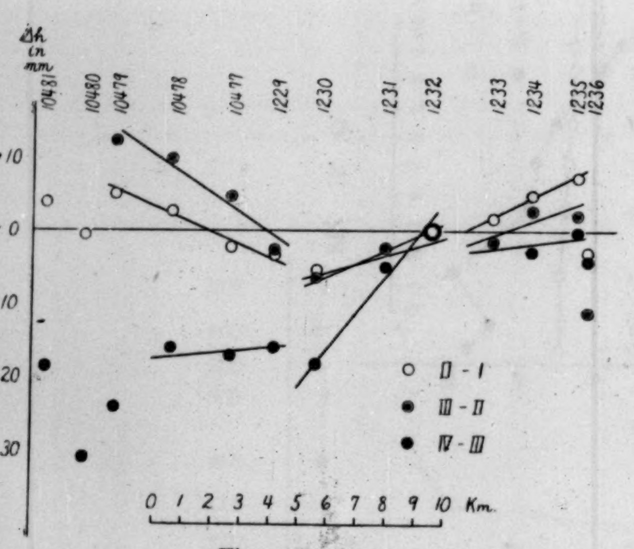

Fig. 13. A.

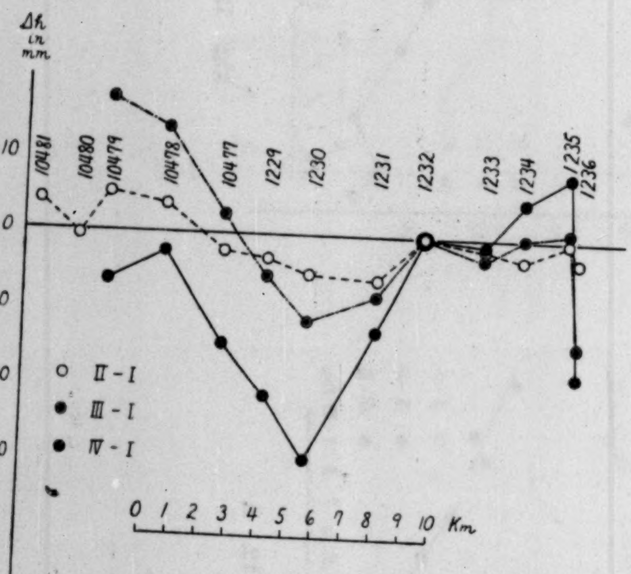

Fig. 13. B.

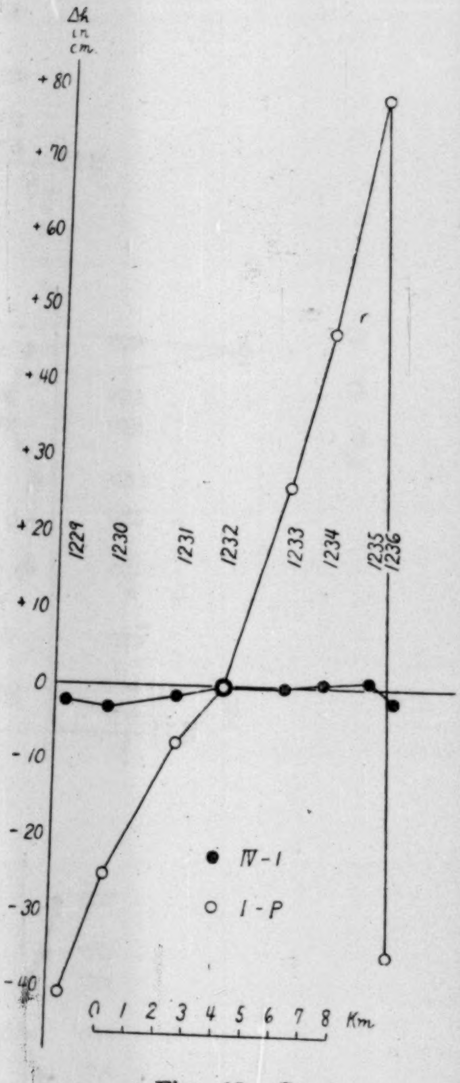

Fig. 13. C.

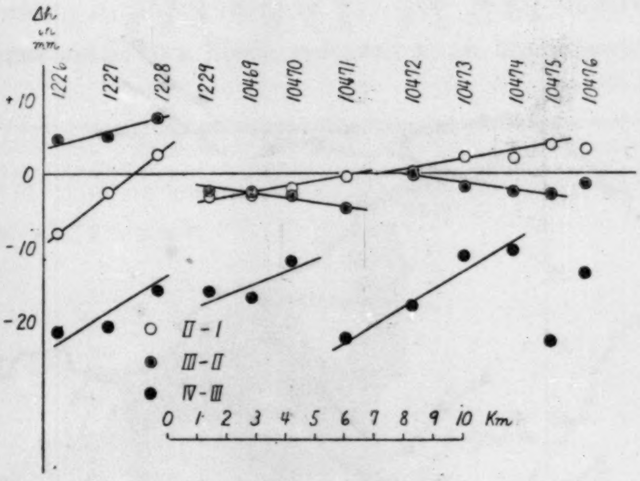

Fig. 14. A.

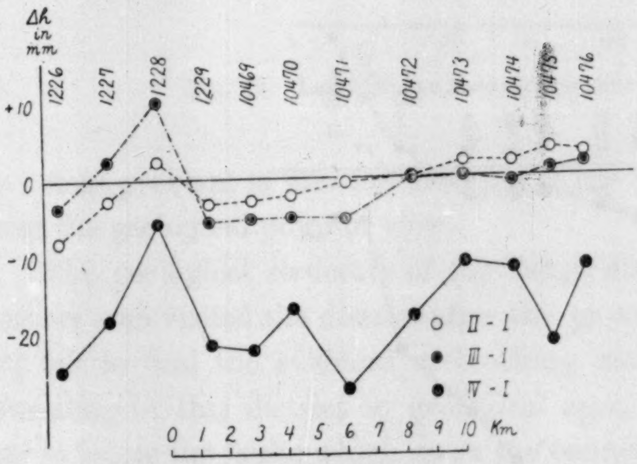

Fig. 14 B.

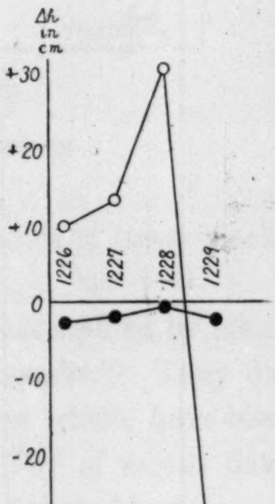

Fig. 14. C.

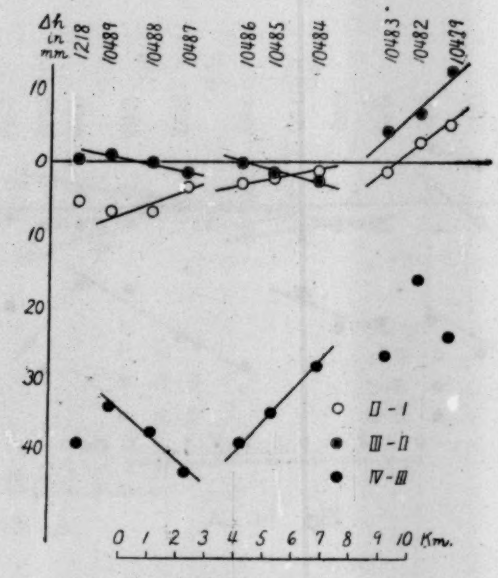

Fig. 15. A.

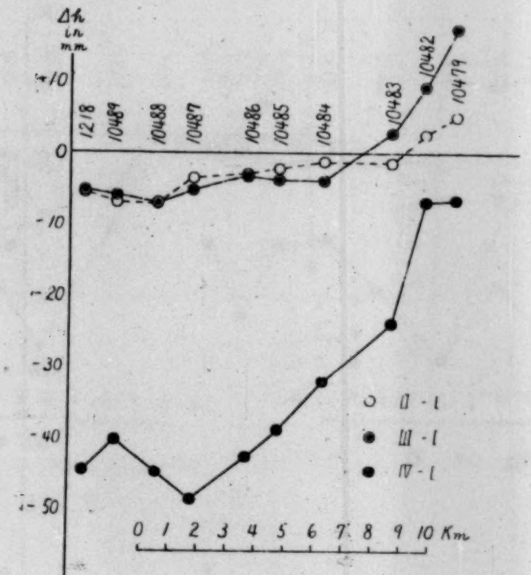

Fig. 15. B.

loose. This stands in a striking contrast with the concept of the continuous and elastic earth's crust. The boundaries of these blocks thus revealed are shown by thick lines in Fig. 16. Each shaded part between these lines corresponds to a block referred to in the above. It will now

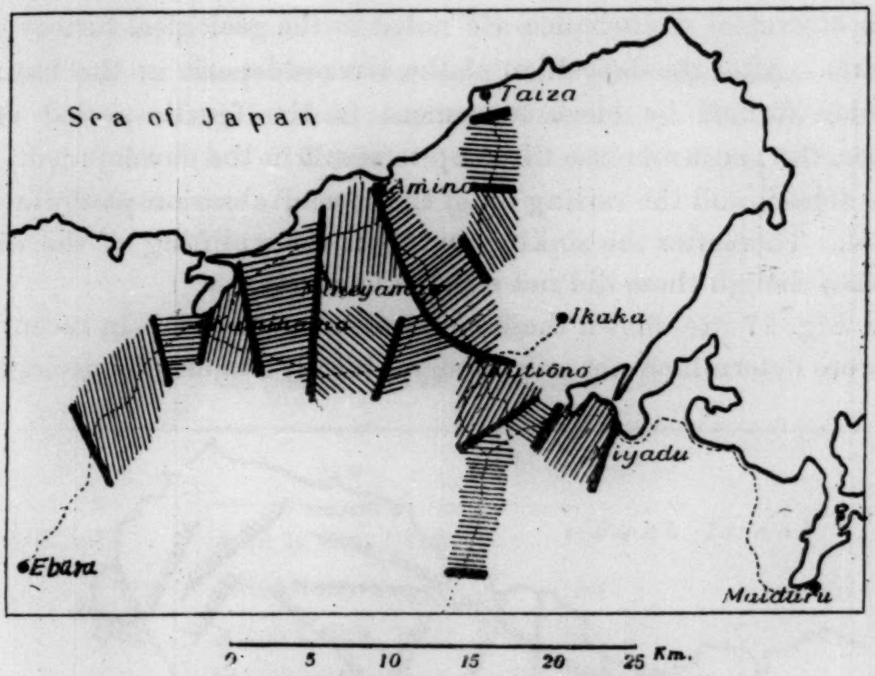

Fig. 16. Land Blocks Revealed by Precise Levellings.

be a next problem to find the meaning of the boundaries of these blocks from the geological point of view.

The geological structure of the Tango district was studied by many authors who visited the district after the great earthquake.[14] They did not fail to find the evidence of blocking movements which have been prevailing in this district in geological ages, especially of recent date, and to locate the faults which mark the boundaries of these blocks.

---

14) H. TSUYA, *Bull. Earthq. Res. Inst.*, 4 (1928), 139.
F. TADA, *ibid.*, 5 (1928), 111.
T. TAYAMA, *Rep. Saito Gratitude Foundation*, No. 6 (1928).
K. WATANABE and H. SATO, *Rep. Imp. Geol. Surv.*, No. 100 (1928).
B. KOTO, *Journ. Fac. Sci., Imp. Univ. Tokyo*, Sec. II, 2 (1928), 265.

According to the thorough study of H. Tsuya of our Institute on the geological structure of this district, "the peninsula of Tango is built up of granite, quartz porphyry, paleo-andesite, lower Neogene strata, various andesite, upper Neogene strata, and liparite, besides recent terrace deposits, enumerating in the order of formation. ...... At least four periods of crustal disturbance are noted in the geological history of the peninsula. After the deposition of the terrace-deposit in the basin-like depression formed by block movement in the fourth period of disturbance, the peninsula was tilted up to result in the development of the terrace deposit and the raising up of the coastal abrasion platform above sea level. Thereafter the sinking and then the uplifting of the district took place though these did not effect extensively."

In Fig. 17 are shown these faults which were active in recent date. They were determined not only topographically but also by geologically.

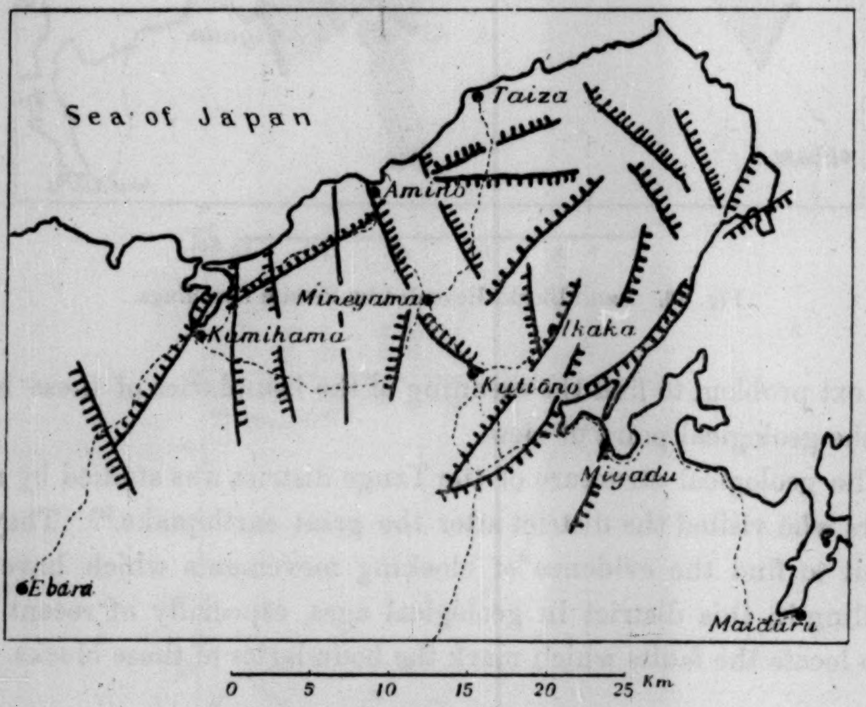

Fig. 17. Geological Faults.

When Figs. 16 and 17 are compared, it will be at once found that the boundaries of the land blocks of the ground as located by means of the analysis of the results of precise levellings coincide very closely with

the geological faults. This suggests that these geological faults are sensibly active after the great earthquake.

The difference of the heights of the neighbouring bench marks on both sides of these active lines varied gradually with time. This represents the differential movements at these faults and can be calculated from the data of precise levellings. These values are given in Table IX, with the date on which they were measured. The difference of heights in the first levelling is taken as zero for reference. The number in the bracket in the column of the date is the number of days from the first day of 1927 to the day of the levelling.

Table IX.

1228–1229 (The Gomura Fault).

Date	Dif. of Heights.
April 24, 1927. (114)	mm. 0
June 5, 1927. (156)	5·6
March 9, 1928. (434)	15·6
Sept. 2, 1929. (975)	15·8

1235–1236 (The Yamada Fault).

Date	Dif. of Heights.
April 23, 1927. (113)	0
June 5, 1927. (156)	1·7
March 13, 1928. (438)	14·0
Sept. 11, 1929. (984)	25·3

1209–1210

Date	Dif.
May 24, 1927. (144)	0
July 8, 1927. (189)	−0·6
April 9, 1928. (465)	−1·4
Aug. 10, 1929. (952)	+8·5

1223–1224

Date	Dif.
May 5, 1927. (124)	0
June 14, 1927. (165)	+4·5
March 20, 1928. (445)	+4·0
Sept. 5, 1929. (978)	−0·9

1212–1213

Date	Dif.
May 21, 1927. (141)	0
July 2, 1927. (183)	− 3·4
April 6, 1928. (462)	−19·6
Aug. 16, 1929. (958)	−33·4

1218–10489

Date	Dif.
May 10, 1927. (130)	0
June 29, 1927. (180)	+1·4
March 27, 1928. (452)	+0·7
Aug. 27, 1929. (969)	−4·4

1215–1216

Date	Dif.
May 15, 1927. (135)	0
June 26, 1927. (177)	+0·1
March 31, 1928. (456)	−0·1
Aug. 20, 1929. (962)	−5·8

10487–10486

Date	Dif.
May 27, 1927. (147)	0
June 26, 1927. (177)	−0·6
April 9, 1928. (465)	−1·9
Oct. 3, 1929. (1006)	−6·1

1220–1221

Date	Dif.
May 8, 1927. (128)	0
June 19, 1927. (170)	+1·8
March 24, 1928. (449)	−6·5
Sept. 1, 1929. (974)	−6·3

10484–10483

Date	Dif.
May 22, 1927. (142)	0
June 21, 1927. (173)	0
April 5, 1928. (461)	−6·7
Oct. 5, 1929. (1008)	−8·2

These results are graphically shown in Fig. 18 and 19. The cases with the Gômura and Yamada faults are specially interesting. The line corresponding to the Yamada fault is seen to have constantly been

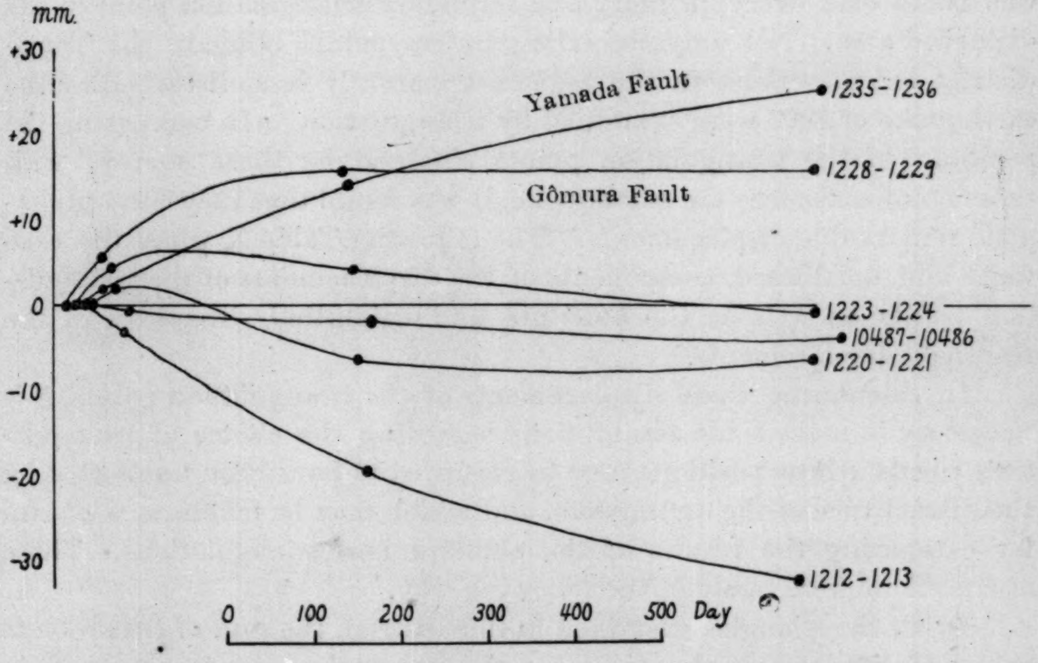

Fig. 18. Relative Vertical Movements along the Boundaries of Land Blocks.

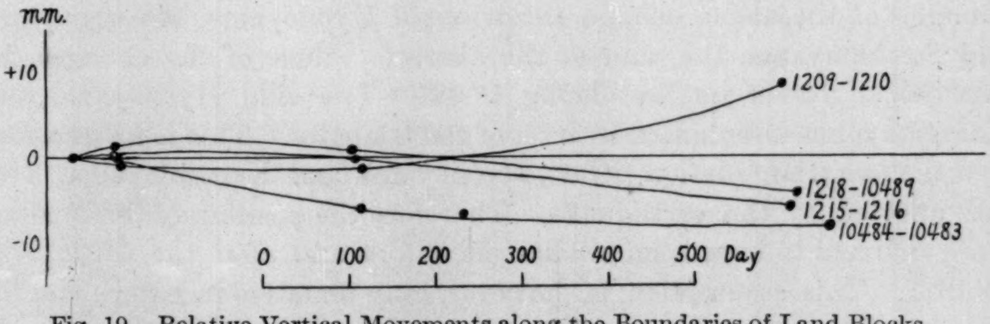

Fig. 19. Relative Vertical Movements along the Boundaries of Land Blocks.

active, the fall of the fault still increasing approximately in a uniform rate. On the other hand, the case is somewhat different with the Gômura fault. The fall of the fault increased in a rapid rate immediately after the earthquake, but the rate gradually decreased until at present the fault shows no sensible activity. We will later come back again to study of the activity of these two faults.

4. Comparison of the Results of Triangulation Before and After the Earthquake.

After the earthquake of 1927, The revision of triangulation survey was made over every primary and secondary triangulation point in the disturbed area. Not only the triangulation points lying in the Tango district but also those in the regions apparently less disturbed by the earthquake of 1927 were examined by triangulation. In comparing the positions of the triangulation points obtained by these surveys with those obtained before the earthquake, it was found that they have undergone remarkable displacements. The following Table X gives the eastward and northward components of the displacements of the triangulation points as well as the amounts and azimuthal directions of the resultant displacements.

In calculating these displacements of the triangulation points, it is necessary to make some assumptions regarding the choice of triangulation points whose positions may be regarded to have been unaffected by the disturbance of the earthquake, and which may be taken as a datum for comparing the results of the old and new triangulations. These assumptions were made in the following way.

Of all the triangles examined in this district, the sum of the absolute values of difference in the corresponding internal angles in a triangle in the old and new triangulations is the least in the triangle of Hyônoyama, Kasagatayama and Tokonooyama being $0''{\cdot}298$. Of all the adjoining triangles of the above one, in the triangle Hyônoyama, Kasagatayama and Sirahatayama, the sum of the absolute values of the changes the internal angles is smallest being $1''{\cdot}924$. The side Hyônoyama and Kasagatayama is common in both of the triangles. This is an evidence that the two triangulation points, Hyônoyama and Kasagatayama, were less affected by the earthquake. Therefore the position of these points were assumed to have been unchanged before and after the earthquake of 1927. This assumption is, however, only tentative in nature and the triangulation survey must be extended to a sufficiently distant district so as to get a base which may be regarded as absolutly unaffected by the earthquake. It seems to the writer, however, that this is after all impossible in this country in which the earth's crust is very unstable and literally mobile. It may thus be rather reasonable to take a tentative assumption regarding the base and to develope the discussion of the results of the surveys concerning alone the *relative* displacements of the triangulation points.

Table X.

The Displacement of Triangulation Points between P and IV.

Δx ....Eastward Displacement.
Δy ....Northward Displacement.
$\sqrt{\Delta x^2 + \Delta y^2}$ ....Resultant Displacement.
α ....Direction of Displacement (Measured clockwise from North.)

Triangulation Point	Δx	Δy	$\sqrt{\Delta x^2+\Delta y^2}$	α
	m	m	m	
Isikawa	−0·408	+0·425	0·589	316° 10′
Yuragatake	−0·393	+0·296	0·492	306 59
Kayaoku	−0·151	−0·009	0·151	266 35
Sengenzi	−0·219	+0·265	0·344	320 26
Hurudera	+0·066	−0·169	0·182	158 40
Higasimitumatu	−0·035	+0·243	0·245	351 48
Amauti	−0·242	+0·136	0·278	299 20
Sendyôgatake	−0·182	+0·253	0·312	324 16
Iza	+0·020	−0·151	0·152	172 27
Okadanakamura	−0·272	+0·320	0·420	319 38
Yôrôgatake	−0·116	+0·154	0·193	323 1
Osa	0·000	−0·068	0·068	180 0
Yabegatake	−0·124	+0·317	0·340	338 38
Noboriotôge	−0·124	+0·043	0·131	289 8
Kutami	−0·101	+0·210	0·233	334 19
Mutuyori	−0·111	+0·154	0·190	324 13
Notaoe	0·000	+0·265	0·265	0 0
Naomi	−0·045	+0·037	0·058	309 26
Okumedi	−0·050	+0·080	0·094	328 0
Hirotani	+0·101	−0·034	0·107	108 36
Higasihatta	−0·048	+0·136	0·144	340 34
Kamikagu	−0·157	+0·065	0·170	292 29
Hosihara	−0·036	+0·126	0·142	332 21
Kamanowa	+0·015	+0·049	0·051	17 1
Oda	−0·056	+0·037	0·067	303 27
Kamikawai	+0·013	+0 040	0·042	18 0
Simotakeda	−0·094	+0·031	0·099	288 15
Mitôgeyama	−0·008	+0·065	0·066	352 59
Onoderayama	+0·061	+0·105	0·121	30 9
Hosodani	+0·033	+0·139	0·143	13 21

(*to be continued.*)

Table X. (*continued.*)

Triangulation Point	Δx	Δy	$\sqrt{\Delta x^2+\Delta y^2}$	α
	m	m	m	
Myôkôzan	−0·035	+0·099	0·105	340° 32′
Wasiomiyama	+0·020	+0·166	0·167	6 52
Hyônoyama	—	—	—	—
Kasagatayama	—	—	—	—
Kuruhiyama	+0·106	−0·197	0·224	151 43
Isogoyama	+0·018	−0·484	0·484	177 52
Taneziyama	−0·204	+0·259	0·330	321 46
Tokonooyama	−0·033	−0·006	0·033	259 42
Karasugatake	−0·088	+0·169	0·190	332 30
Mitakesan	−0·028	+0·099	0·103	344 12
Taikoyama	−0·473	+0·339	0·582	305 38
Sobutakiyama	+0·078	+0·031	0·084	68 20
Tyôrôgatake	−0·040	+0·018	0·044	294 14
Awakayama	−0·035	+0·074	0·082	334 41
Nomura	−0·432	+0·376	0·573	311 2
Itigao	−0·869	+0·626	1·071	305 46
Oohara	−0·588	+0·327	0·673	299 5
Osima	−0·287	+0·404	0·496	324 37
Simooka	+0·531	−1·128	1·247	154 48
Kwannonzan	−0·023	−0·068	0·072	198 41
Minato	+0·078	−0·364	0·372	167 54
Yosizawa	−0·745	+0·804	1·096	317 11
Kutoyama	+0·171	−0·046	0·177	105 3
Tudumigatake	−0·524	+0·524	0·741	315 0
Mehu	−0·070	−0·807	0·810	184 57
Motomiduka	−0·083	−0·151	0·172	208 48
Kurosaki	−0·556	+0·487	0·739	311 13
Sakai	−0·217	+0·092	0·236	292 59
Mitani	+0·126	−0·308	0·333	157 45
Mie	+0·116	+0·918	0·925	7 12
Ooyama	−0·139	+0·243	0·280	330 14
Sibo	+0·015	−0·182	0·183	175 17
Hatidyô	+0·003	−0·247	0·247	179 18
Ookadera	−0·136	−0·277	0·309	206 9

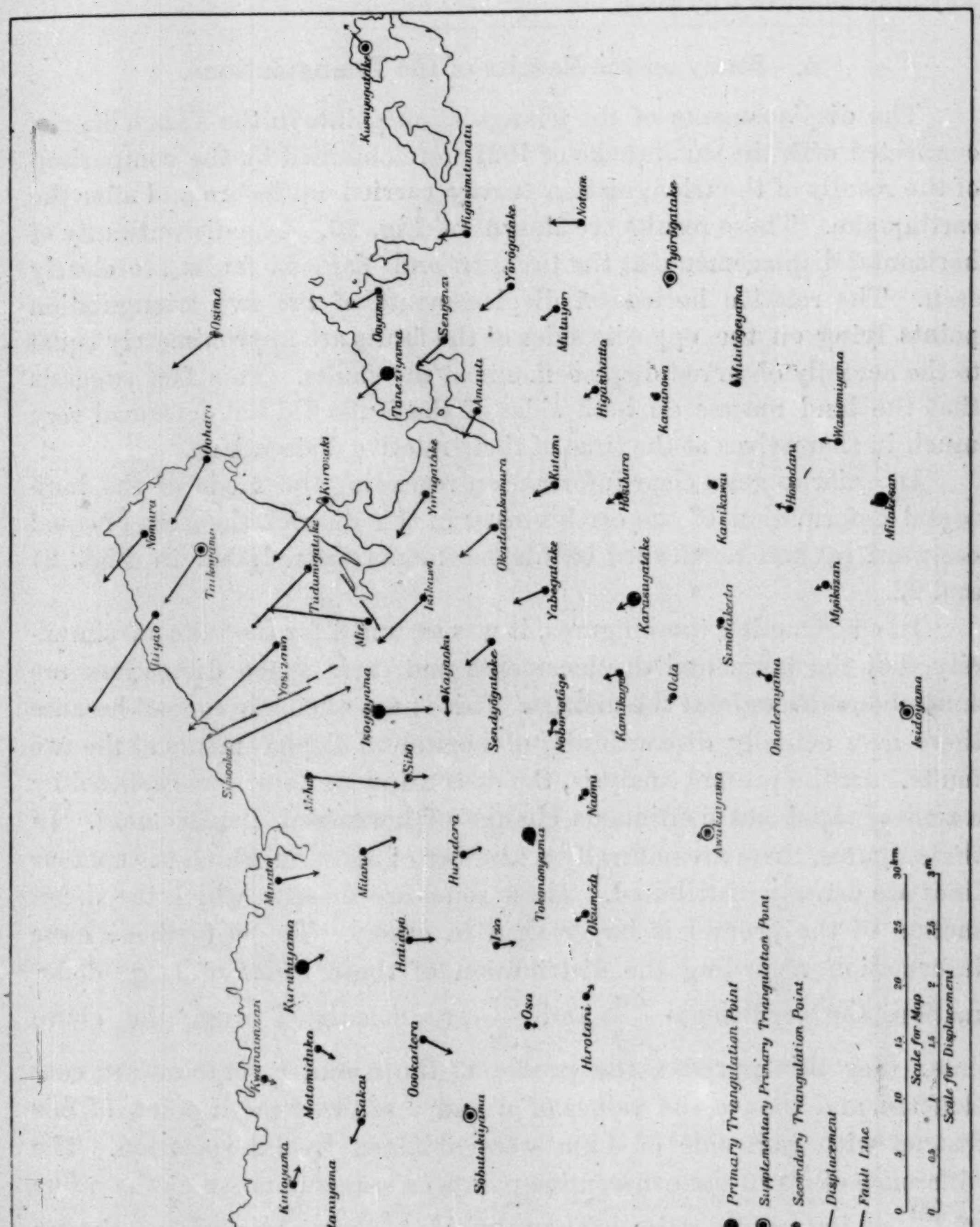

Fig. 20. Horizontal Displacements of Secondary Triangulation Points.

The displacements of the triangulation points determined in this way are shown in Fig. 20.

5. Study on the Results of the Triangulations.

The displacements of the triangulation points in the Tango district connected with the earthquake of 1927 were obtained by the comparison of the results of the triangulation survey carried out before and after the earthquake. These results are shown in Fig. 20. The discontinuity of horizontal displacements at the Gômura and Yamada faults are clearly seen. The relative horizontal displacements of the two triangulation points lying on the opposite sides of the faults are approximately equal to the actually observed displacements at the faults. This fact suggests that the land masses on both sides of the faults did not deformed very much in themselves at the time of their relative dislocations.

In order to get a clear information regarding the mode of the horizontal deformation of the earth's crust in this district, the lines of equal eastward (u) and northward (v) displacements were drawn in Figs. 21 and 22.

In constructing these figures, it was assumed for the sake of simplicity that the horizontal displacements and their space derivatives are continuous throughout the district. This is not of course correct because there *were* actually discontinuity of horizontal displacements at the two faults. In the present analysis, the discontinuous fault was replaced by a zone of rapid but continuous change of horizontal displacement. In these figures, there are naturally a number of zones in which the contour lines are densely distributed. These zones are those in which the deformation of the ground is larger than in others. To get further a clear information regarding the distribution of these zones of large deformation, the coefficients $\frac{\partial u}{\partial y}$ and $\frac{\partial v}{\partial x}$ are calculated from the above data. For this purpose, the profile of the u and v contours are constructed and thence the values of u and v at every mesh points of this district with unit side of 4 km were obtained by interpolation. The difference of u's in the consecutive points on y-axis is taken as the value of $\frac{\partial u}{\partial y}$ at its middle point. The value of $\frac{\partial v}{\partial x}$ was obtained in a similar manner. They give the magnitudes of shearing deformation along x- and y-axis respectively. The lines of equal $\frac{\partial u}{\partial y}$ and $\frac{\partial v}{\partial x}$ thus obtained are shown in Figs. 23 and 24.

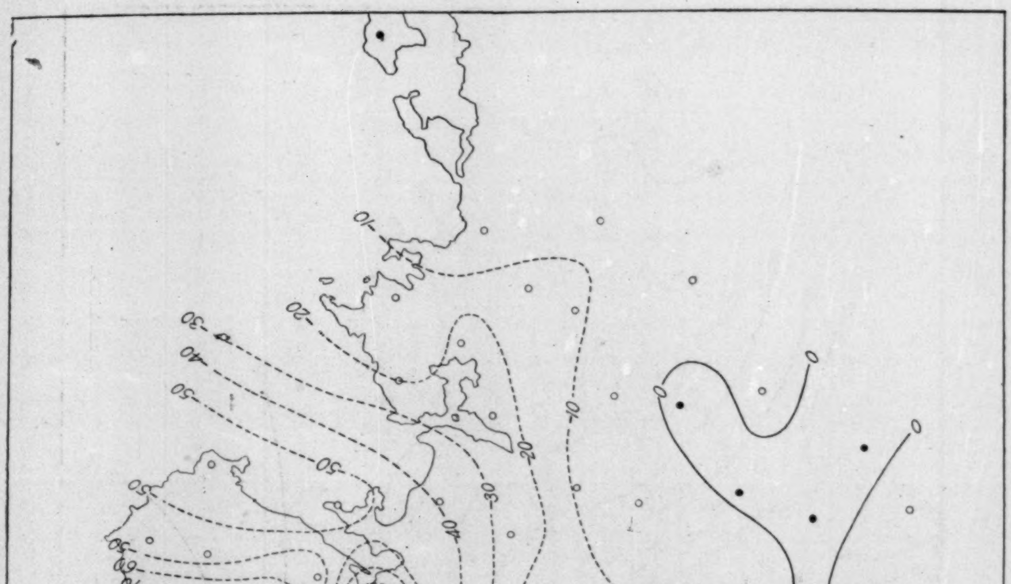

Lines of Equal Eastward Displacement u in cm.

Fig. 21

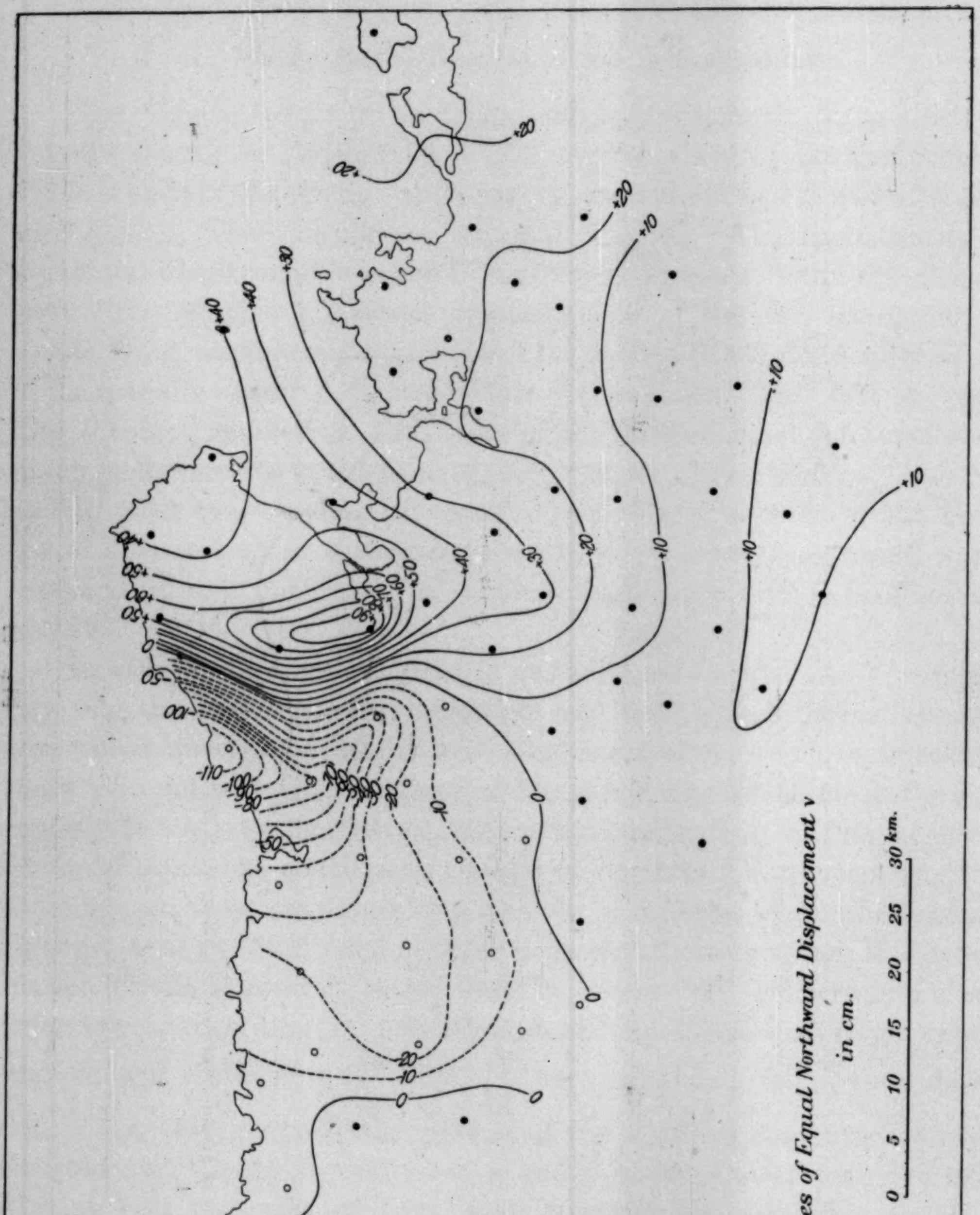
Lines of Equal Northward Displacement v
in cm.
0 5 10 15 20 25 30 km.

Fig. 22

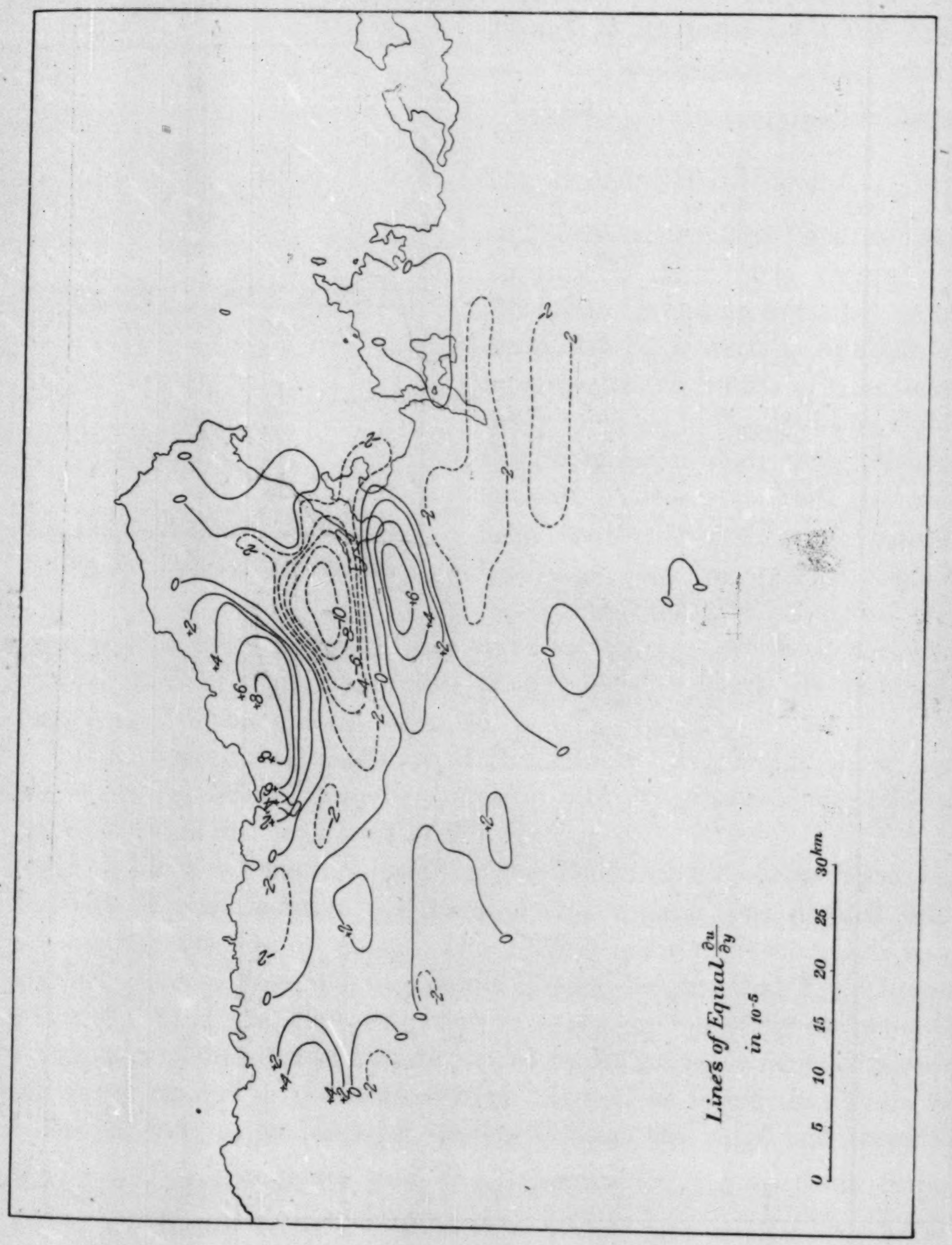
Lines of Equal $\frac{\partial u}{\partial y}$
in 10^{-5}
0 5 10 15 20 25 30km

Fig. 23.

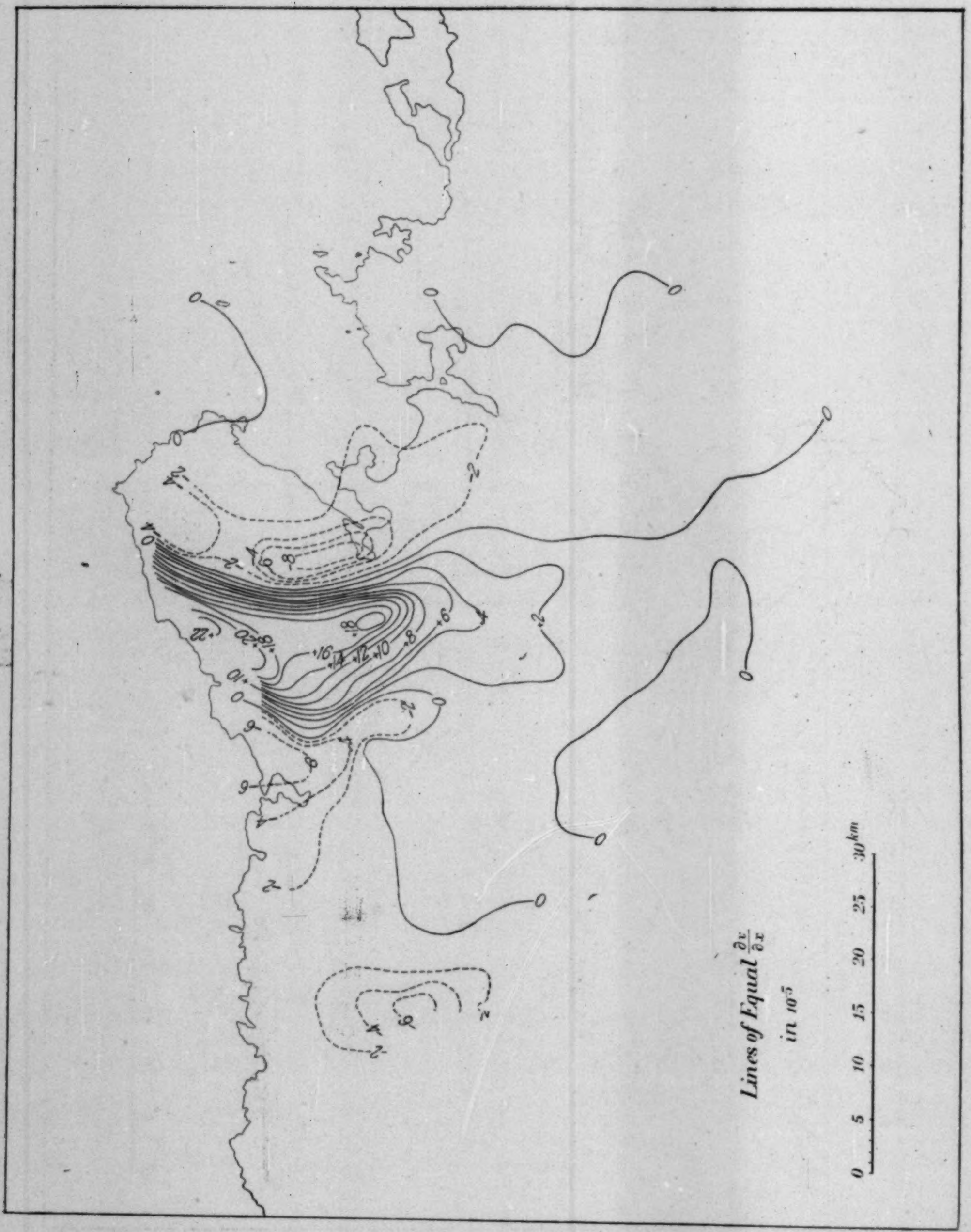
Lines of Equal $\frac{\partial v}{\partial x}$
in 10^{5}
0 5 10 15 20 25 30km

Fig. 24

In these figures, the zones of maximum shearing correspond in position to the ridge and trough of contours. It will be seen that the ground is traversed by a few lines in x and y directions along which $\frac{\partial v}{\partial x}$ and $\frac{\partial u}{\partial y}$ are remarkably large. The contours of $\frac{\partial u}{\partial x}$ and $\frac{\partial v}{\partial y}$ show no such remarkable distribution. To explain these facts reasonably, the ground must be regarded to be composed of a certain number of separate blocks, which are far more easily movable in the direction along their boundaries than perpendicular to them. These hypothesis also conform with the results of precise levellings described in the preceding chapter. As a model of the ground with these structure may serve an aggregate of wooden blocks between each of which a number of deformable spheres are inserted, something like that shown in Fig. 25.

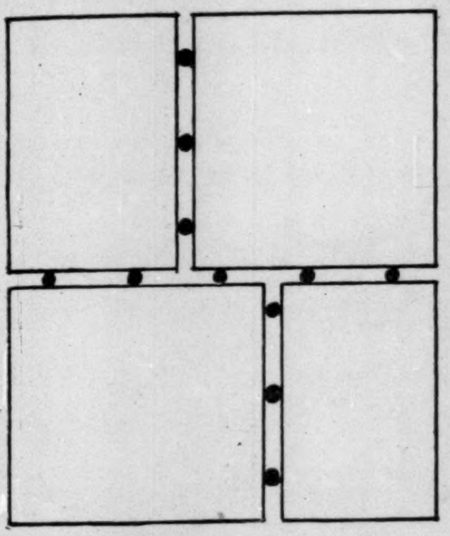

Fig. 25. Model of Land Blocks.

The geographical positions of the zones of maximum shear are shown in Fig. 26 and may be compared with the general topographical features of this district shown in Fig. 27.

Fig. 27 is a "summit level" of the Tango district constructed by F. Tada of our Institute. A map of this district was divided into rectangular meshes of $\overline{2\text{ km.}}^2$ The highest point in each mesh was marked. It was by connecting points of equal heights that Fig. 27 was obtained. This was done to get an information regarding the general topography of this district mainly formed by crustal movements eliminating minor topographies due to erosion. It will be found that there is a very striking coincidence of position between the ridge and troughs of $\frac{\partial u}{\partial y}$ and $\frac{\partial v}{\partial x}$ contours and the topographically important lines, which are mostly active in geologically recent date, at least after lower Neogene. Some of these lines are also recognised in the results of precise levellings described in the preceding chapter.

From these facts, it is reasonably concluded that some of the tectonic lines in this district are still active. The relation between the sense or

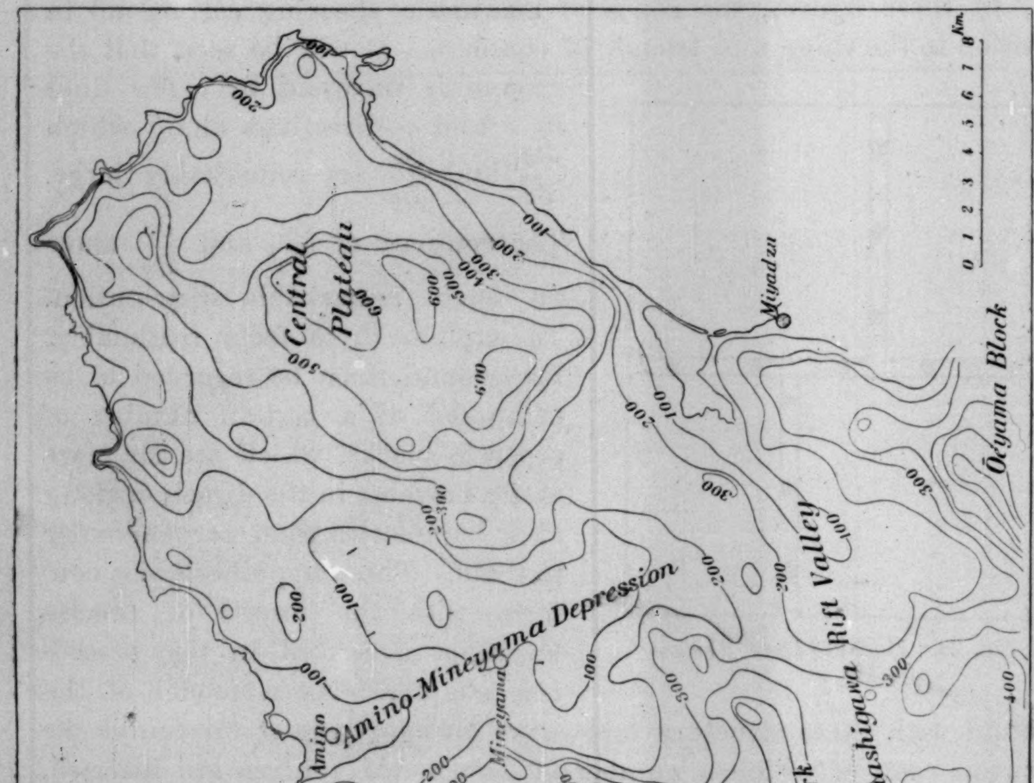
Central Plateau
Amino-Mineyama Depression
Rift Valley
Kurahashigawa
Isogoyama Block
Kumihama Lowland
Maruyamagawa Depression
Ōeyama Block
Miyadzu
Amino
Mineyama
Kumihama
Toyooka
0 1 2 3 4 5 6 7 8 Km.

Fig. 27.

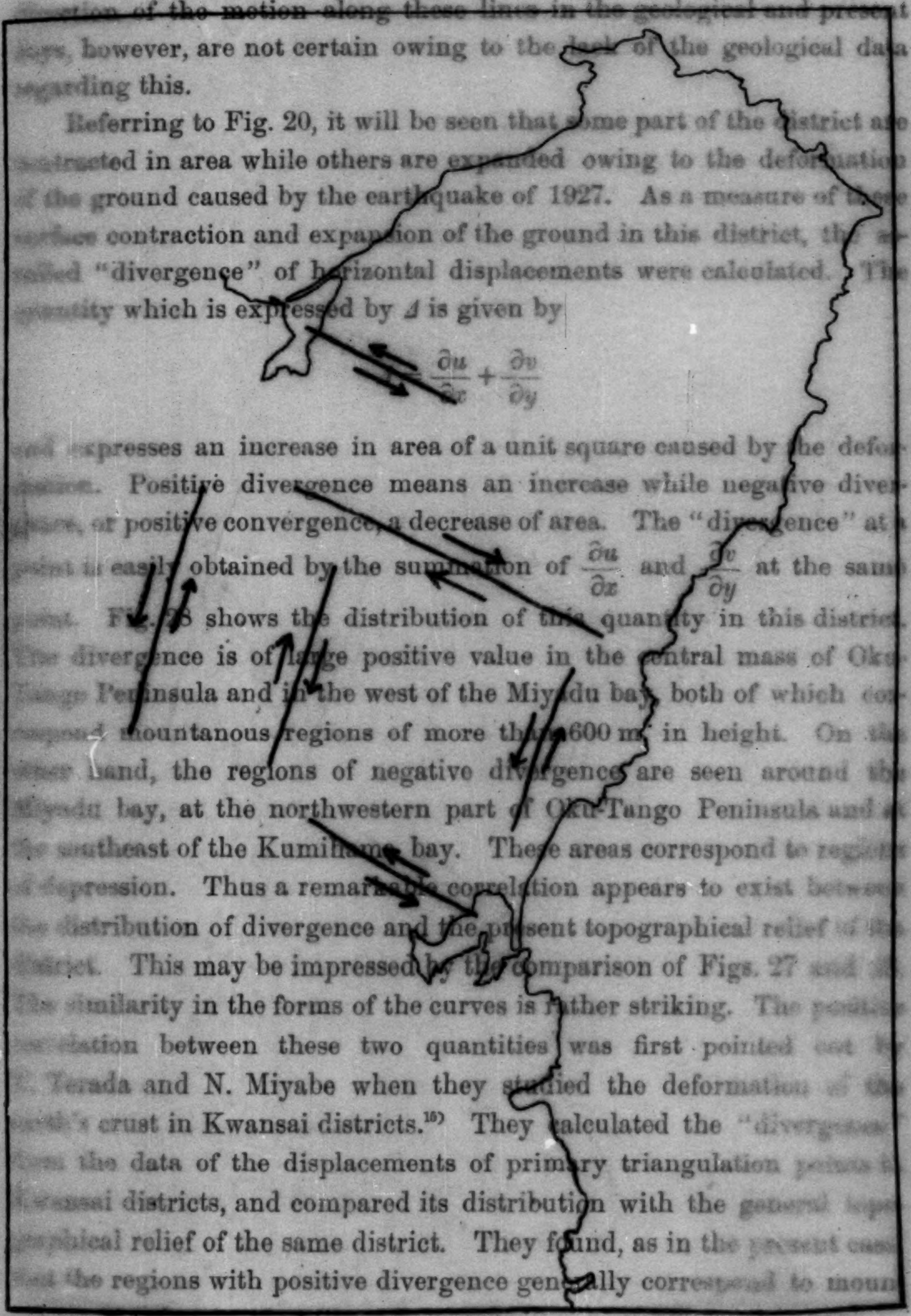

direction of the motion along these lines in the geological and present days, however, are not certain owing to the lack of the geological data regarding this.

Referring to Fig. 20, it will be seen that some part of the district are contracted in area while others are expanded owing to the deformation of the ground caused by the earthquake of 1927. As a measure of these surface contraction and expansion of the ground in this district, the so-called "divergence" of horizontal displacements were calculated. The quantity which is expressed by Δ is given by

$$\Delta = \frac{\partial u}{\partial x} + \frac{\partial v}{\partial y}$$

and expresses an increase in area of a unit square caused by the deformation. Positive divergence means an increase while negative divergence, or positive convergence, a decrease of area. The "divergence" at a point is easily obtained by the summation of $\frac{\partial u}{\partial x}$ and $\frac{\partial v}{\partial y}$ at the same point. Fig. 28 shows the distribution of this quantity in this district. The divergence is of large positive value in the central mass of Oku-Tango Peninsula and in the west of the Miyadu bay, both of which correspond mountanous regions of more than 600 m. in height. On the other hand, the regions of negative divergence are seen around the Miyadu bay, at the northwestern part of Oku-Tango Peninsula and at the southeast of the Kumihama bay. These areas correspond to regions of depression. Thus a remarkable correlation appears to exist between the distribution of divergence and the present topographical relief of the district. This may be impressed by the comparison of Figs. 27 and 28. The similarity in the forms of the curves is rather striking. The positive correlation between these two quantities was first pointed out by T. Terada and N. Miyabe when they studied the deformation of the earth's crust in Kwansai districts.[15] They calculated the "divergence" from the data of the displacements of primary triangulation points in Kwansai districts, and compared its distribution with the general topographical relief of the same district. They found, as in the present case, that the regions with positive divergence generally correspond to moun-

15) *Bull. Earthq. Res. Inst.*, 7 (1929), 223.

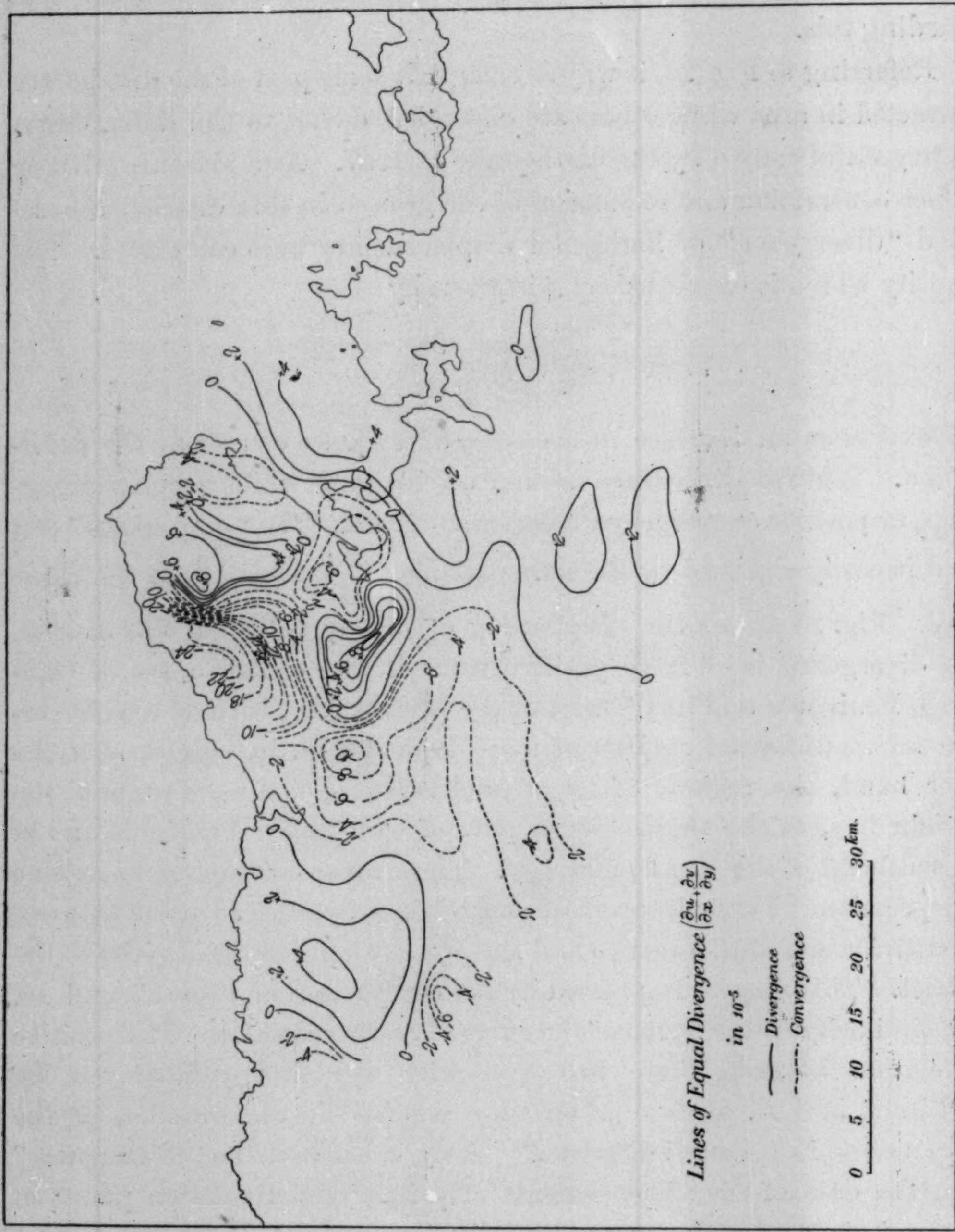
Lines of Equal Divergence $\left(\frac{\partial u}{\partial x}+\frac{\partial v}{\partial y}\right)$
in 10^{-5}
Divergence
Convergence
0 5 10 15 20 25 30 km.

Fig. 28.

tains, and the regions with negative divergence to low-lands. The correspondence found in the present case is similar with that found by Terada and Miyabe, but it is far much closer than that found by them.

The divergence calculated in the above is that of *area*, but not a divergence of *volume* of the earth's upper crust, because the term of vertical deformation $\frac{\partial w}{\partial z}$ is omitted in the calculation. The term $\frac{\partial w}{\partial z}$ cannot be obtained in the present results of the surveys alone. The remarkable correlation between the horizontal divergence and the present topographical features seems to imply, however, that the former has really a physical meaning or that the term $\frac{\partial w}{\partial z}$ is negligibly small against $\left(\frac{\partial u}{\partial x}+\frac{\partial v}{\partial y}\right)$.

The calculation of the quantity "rotation" was done similarly. This quantity is defined as $\left(\frac{\partial u}{\partial y}-\frac{\partial v}{\partial x}\right)$ and it is positive when the sense of rotation is clockwise and negative when counterclockwise. The distribution of this quantity in this district is shown in Fig. 29.

6. The Relation between the Vertical Displacements and the Divergence.

The vertical displacements along the levelling route from Ebara to Miyadu passing through Toyooka, Kumihama, Mineyama and Kutiono were already discussed. The distribution of divergence along the same route, on the other hand, can be obtained from Fig. 28. The dotted line in Fig. 30 was obtained in this way. The full line in the same figure represents the vertical displacements I–P along the same route. Except in the neighbourhood of Toyooka, these two curves are generally quite similar in their forms, the positive divergence corresponding to crustal elevation and the negative divergence to depression at the time of the earthquake.

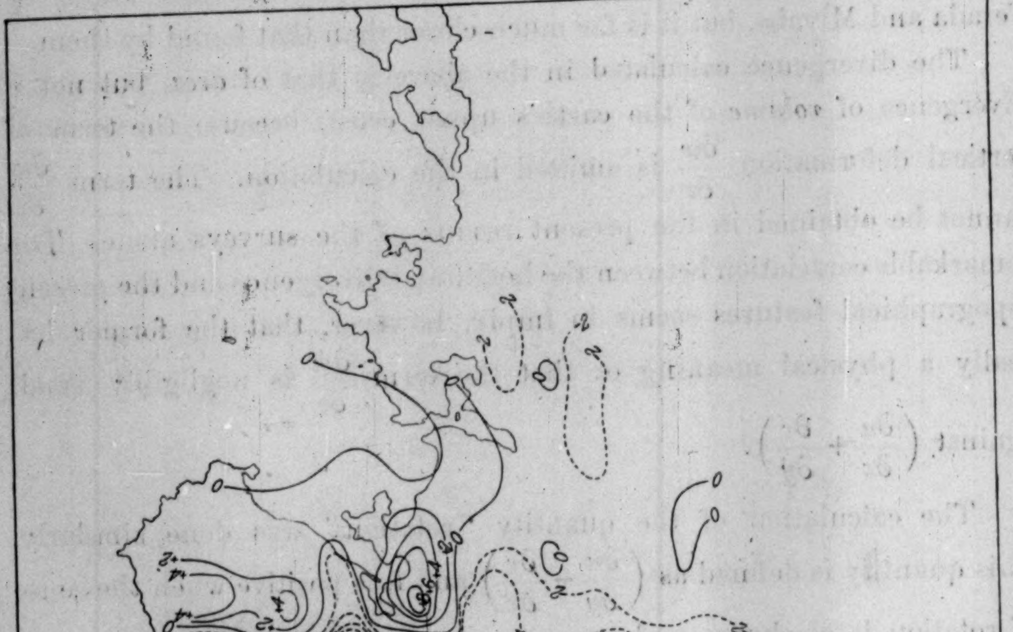
Lines of Equal Rotation $\left(\frac{\partial u}{\partial y}-\frac{\partial v}{\partial x}\right)$ in 10^{-5}
Clockwise
Counter-clockwise
0 5 10 15 20 25 30 km.

Fig. 29.

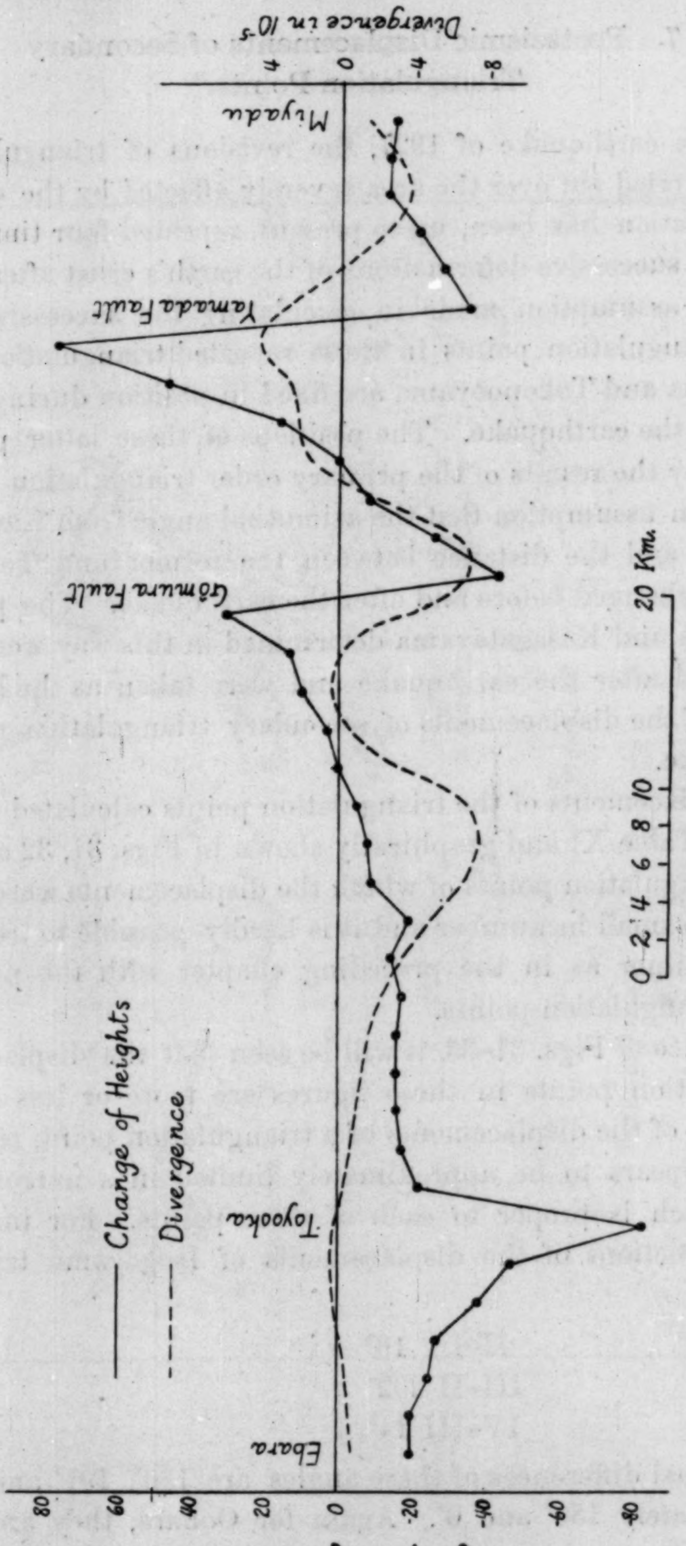

Divergence in 10^{-5}
4
0
-4
-8
Miyadu
Yamada Fault
Gômura Fault
20 Km.
0 2 4 6 8 10
Change of Heights
Divergence
Toyooka
Ebara
80
60
40
20
0
-20
-40
-60
-80
Change of Heights in cm.

Fig. 30.

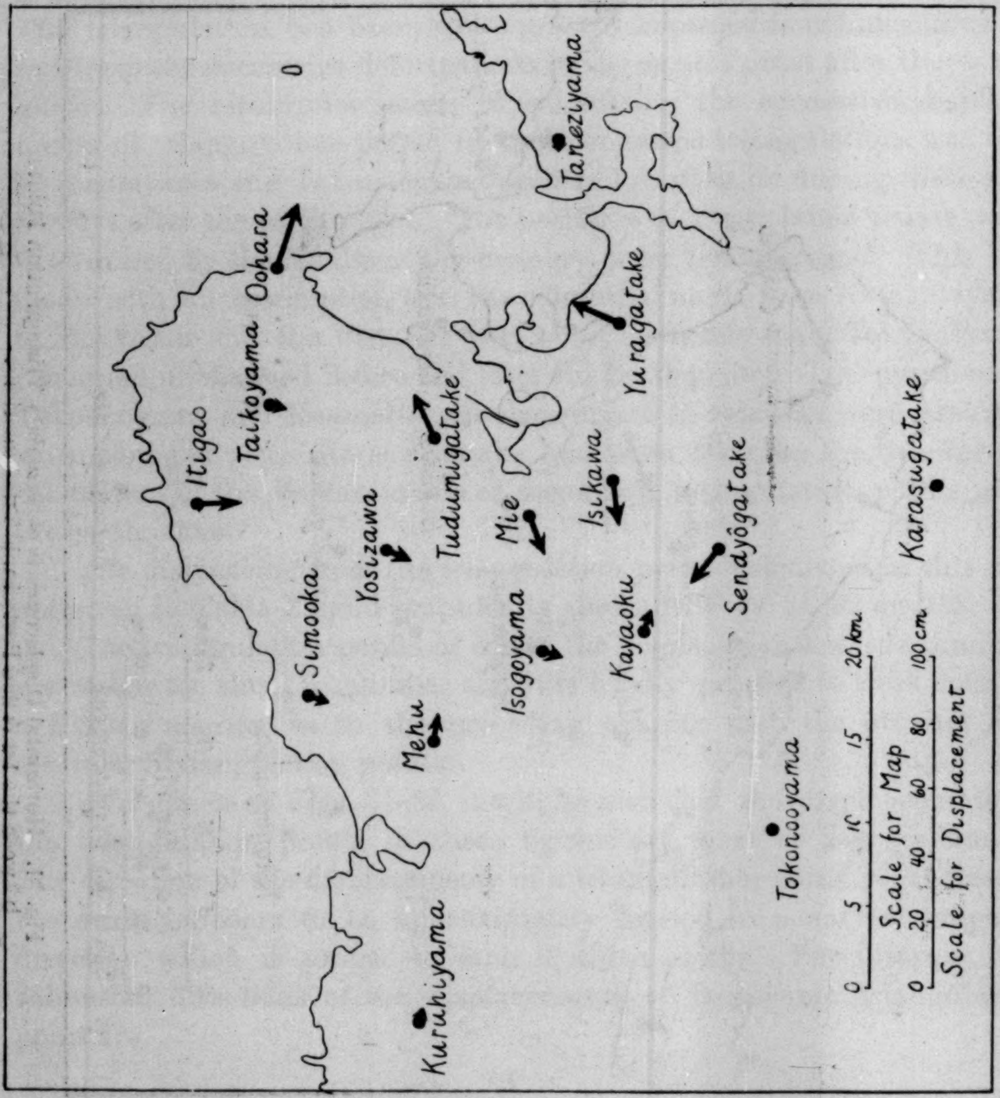

Fig. 32. Horizontal Displacements of Secondary Triangulation Points between the 2nd and 3rd Postseismic Triangulations.

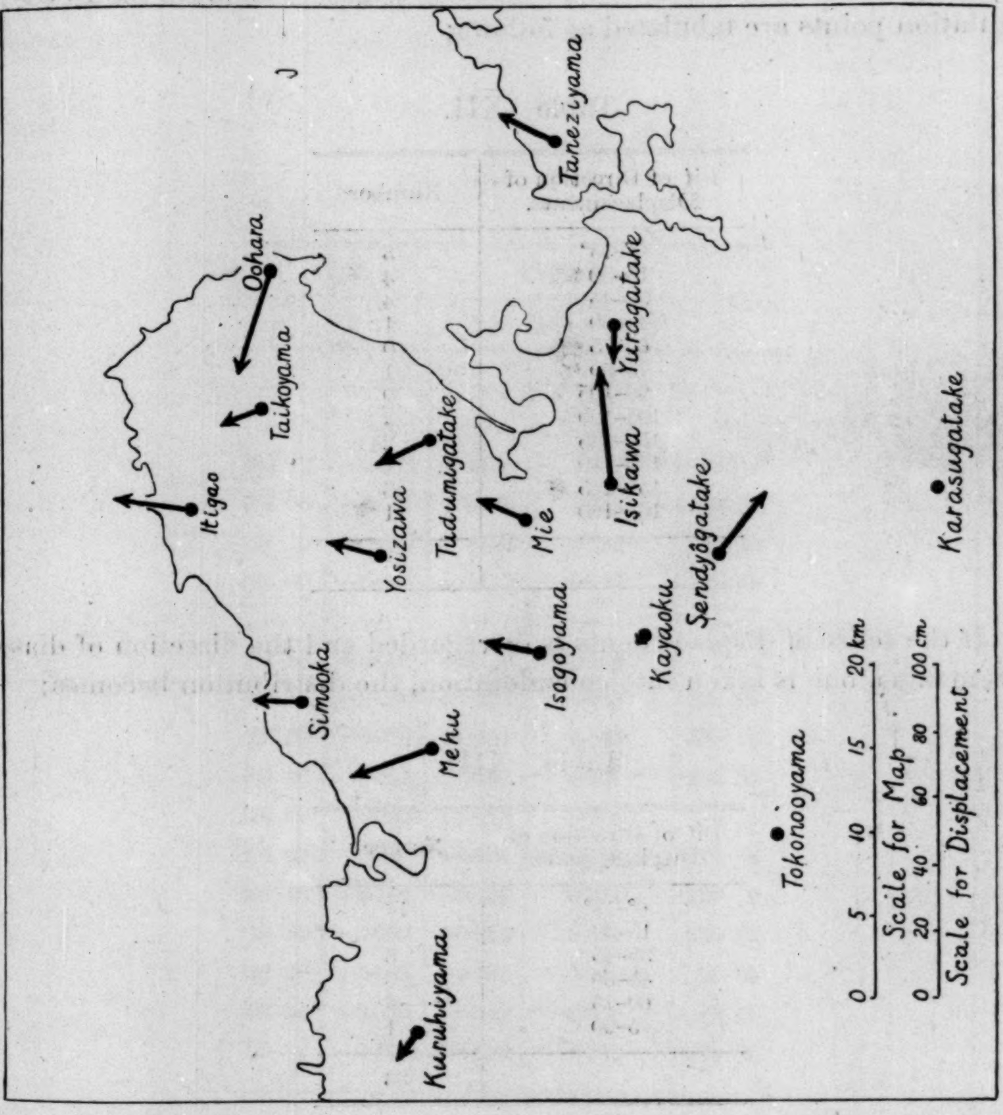

Fig. 33. Horizontal Displacements of Secondary Triangulation Points between the 3rd and 4th Postseismic Triangulations.

7. Postseismic Displacements of Secondary Triangulation Points.[16)]

After the earthquake of 1927, the revisions of triangulation were repeatedly carried out over the area severely affected by the earthquake. The triangulation has been, up to present, repeated four times, thus we can trace the successive deformations of the earth's crust after the earthquake. The assumption made in calculating the successive displacements of triangulation points in these repeated triangulations was that Kasagatayama and Tokonooyama are fixed in position during these four surveys after the earthquake. The positions of these latter points were determined by the results of the primary order triangulation. This was made with an assumption that the azimuthal angle from Kasagatayama to Rokkôsan and the distance between the former and Tokonooyama remained unchanged before and after the earthquake. The positions of Tokonooyama and Kasagatayama determined in this way were assumed as unchanged after the earthquake and were taken as the base for the calculation of the displacements of secondary triangulation points after the earthquake.

The displacements of the triangulation points calculated in this way are given in Table XI and graphically shown in Figs. 31, 32 and 33.

The triangulation points of which the displacements were examined are rather too small in number and it is hardly possible to treat them in a similar manner as in the preceding chapter with the primary and secondary triangulation points.

At a glance of Figs. 31–33, it will be seen that the displacements of the triangulation points in these figures are more or less systematic. The direction of the displacements of a triangulation point, regardless to the sense, appears to be approximately limited in a narrow range of direction which is proper to each of these points. For instance, the azimuthal directions of the displacements of Isogoyama triangulation point are,

II–I 16°
III–II 202°
IV–III 11°

The mutual differences of these angles are 186°, 191° and 5° which are approximately 180° and 0°. Again for Oohara, they are 192°, 183°

16) C. Tsuboi, *Proc. Imp. Acad.*, 6 (1930), 56.

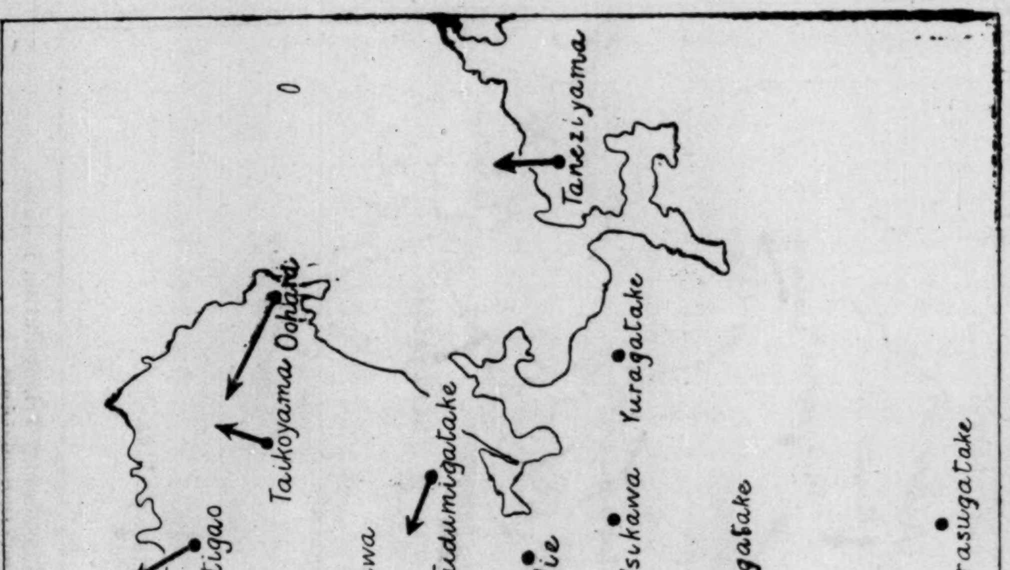

Fig. 31. Horizontal Displacements of Secondary Triangulation Points between the 1st & 2nd Postseismic Triangulations.

and 9° which are also nearly 180° and 0°. On the other hand, there are also a few points whose displacements show no such regularity at all, for instance, Tudumigatake with azimuthal difference 50′, 92° and 42°. The frequency distribution of these differential angles of azimuth for 15 triangulation points are tabulated as follows;

Table XII.

Dif. of Direction of Displacements.	Number
0°–15°	3
15–30	4
30–45	4
45–60	1
60–75	0
75–90	1
90–105	0
105–120	2
120–135	2
135–150	2
150–165	3
165–180	11
	33

If the sense of displacements is disregarded and the direction of displacements alone is taken into consideration, the distribution becomes;

Table XIII.

Dif. of Direction of Displacements.	Number
0°–15°	14
15–30	7
30–45	6
45–60	3
60–75	2
75–90	1
	33

The distributions are graphically shown in Figs. 34 and 35. They are evidently similar to that of Gaussian distribution and thus it is suggested that each triangulation point has *statistically* its own direction of displacements. The azimuthal differences between the displacements in P–I and in each of the intervals II–I, III–II and IV–III show no such regularity at all, as may be seen in the following table.

Table XI. The Displacements of S

Δx ....Eastward
Δy ....Northward
$\sqrt{\Delta x^2 + \Delta y^2}$ ....Resultant
α ....Direction o
clockwise f

Triangulation Point	I–P				II–P					
	Δx	Δy	$\sqrt{\Delta x^2 + \Delta y^2}$	α	Δx	Δy	$\sqrt{\Delta x^2 + \Delta y^2}$	α	Δx	Δ
Karasugatake	m −0·146	m +0·142	m 0·204	314° 12′					—	—
Tokonooyama	+0·045	−0·009	0·046	101 19					—	—
Isogoyama	+0·083	−0·752	0·757	173 42					m +0·023	m +0·0
Kuruhiyama	+0·317	−0·324	0·453	135 38					−0·018	+0·0
Taneziyama	−0·348	−0·228	0·416	236 46					−0·010	+0·1
Taikoyama	−0·410	−0·080	0·418	258 58					+0·050	+0·1
Kasagatayama	—	—	—	—					—	—
Simooka	+0·616	−1·593	1·708	158 52					+0·050	+0·1
Mehu	+0·277	−1·076	1·111	165 34					+0·025	−0·0
Tudumigatake	−0·425	+0·092	0·435	282 13					−0·171	+0·0
Oohara	−0·010	−0·111	0·112	185 9					−0·282	+0·1
Itigao	−0·508	+0·031	0·509	273 30					−0·108	+0·1
Yosizawa					m −0·428	m +0·549	m 0·696	322° 4′		
Sendyôgatake					−0·131	−0·012	0·132	264 46		
Kayaoku					−0·123	−0·216	0·249	209 40		
Mie					+0·358	+0·773	0·852	24 51		
Isikawa					−0·297	+0·247	0·386	309 45		
Yuragatake					−0·403	−0·055	0·407	262 14		

of Secondary Triangulation Points.

ard Displacement.
ward Displacement.
ant Displacement.
ion of Displacement (Measured
vise from North.)

III–1			III–11				IV–111			
Δy	$\sqrt{\Delta x^2+\Delta y^2}$	α	Δx	Δy	$\sqrt{\Delta x^2+\Delta y^2}$	α	Δx	Δy	$\sqrt{\Delta x^2+\Delta y^2}$	α
—	—	—	—	—	—	—	—	—	—	—
—	—	—	—	—	—	—	—	—	—	—
m	m		m	m	m		m	m	m	
+0·086	0·089	14°58′	−0·020	−0·049	0·053	202°12′	+0·030	+0·154	0·157	11° 1′
+0·074	0·076	346 20	+0·035	−0·012	0·036	108 55	−0·101	+0·068	0·122	303 57
+0·197	0·197	357 6	−0·018	0·000	0·018	27 0	+0·086	+0·160	0·182	28 15
+0·145	0·153	19 2	−0·013	−0·043	0·045	196 49	−0·043	+0·117	0·124	339 49
—	—	—	—	—	—	—	—	—	—	—
+0·157	0·165	17 40	−0·023	−0·059	0·063	201 18	+0·005	+0·139	0·139	2 4
-0·012	0·026	115 38	+0·093	−0·015	0·094	99 10	−0·086	+0·231	0·247	339 35
+0·071	0·185	292 33	+0·121	+0·062	0·136	62 52	−0·070	+0·151	0·166	335 8
+0·148	0·318	297 41	+0·196	−0·055	0·204	105 40	−0·304	+0·102	0·321	288 33
+0·191	0·220	330 31	+0·008	−0·120	0·120	176 11	+0·030	+0·213	0·215	8 1
			−0·030	−0·062	0·068	205 49	+0·040	+0·154	0·159	14 3
			−0·096	+0·080	0·125	309 48	+0·187	−0·136	0·231	126 2
			+0·050	−0·025	0·056	116 34	−0·010	+0·012	0·014	320 12
			−0·111	−0·046	0·120	247 29	+0·065	+0·136	0·151	25 33
			−0·141	−0·018	0·142	262 44	+0·320	+0·043	0·323	82 21
			+0·060	+0·136	0·149	23 48	−0·106	+0·009	0·106	274 52

(Facing p. 210)

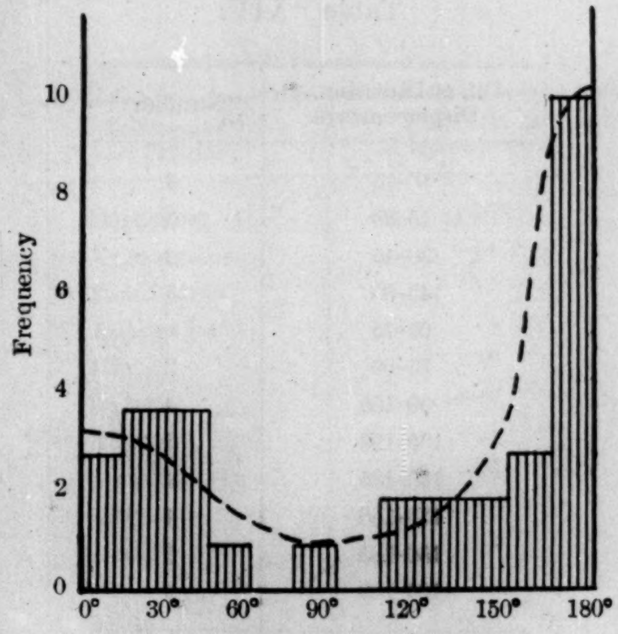

Fig. 34. Direction of Displacement.

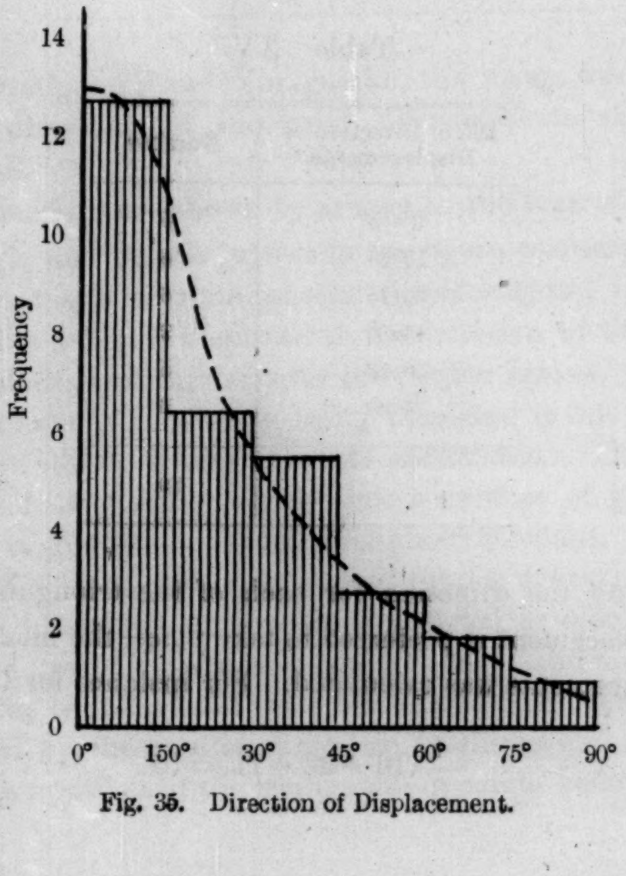

Fig. 35. Direction of Displacement.

Table XIV.

Dif. of Direction of Displacements.	Number
0°-15°	3
15-30	2
30-45	2
45-60	5
60-75	2
75-90	2
90-105	4
105-120	3
120-135	4
135-150	4
150-165	6
165-180	2
	39

Table XV.

Dif. of Direction of Displacements.	Number
0°-15°	5
15-30	8
30-45	6
45-60	9
60-75	5
75-90	6
	39

For finding the direction for each of the triangulation points in which its displacement is preferred to take place, the mean of the directions of displacements was calculated. For instance for Isogoyama,

$$\frac{1}{3}(16^\circ+22^\circ+11^\circ)=16^\circ.$$

The results of the calculations are shown in Table XVI.

Table XVI.

Triangulation Points.	Direction of Displacements.
Isogoyama	16°
Kuruhiyama	−64
Taneziyama	17
Taikoyama	18
Mie	26
Itigao	− 8
Yosizawa	20
Sendyôgatake	−52
Kayaoku	−52
Isikawa	83
Simooka	14
Mehu	−73
Tudumigatake	—
Oohara	−71
Yuragatake	—

For Tudumigatake and Yuragatake, the mean was not calculated, because the directions of successive displacements show no regular tendency at all.

These directions are shown by arrows on the map of Fig. 36.

The single and double arrows in the figure correspond respectively to two different sets of simultaneous displacements; in other words, when one of the points is displaced in the direction of the single arrow, all the other do so, and similarly for the double arrows. The triangulation point Oohara is constantly being displaced in one direction. The distribution of these arrows is quite systematic. The triangulation points in this district can be divided into a number of groups in which the direction of displacements are throughout constant. This again corresponds to the block structure of the district concerned. The boundaries of the blocks are apparently contracted or elongated when the displacements are of direction shown by single and double arrows respectively. The boundaries of these blocks also coincident with some of those revealed by the results of precise levellings and also by the comparison of the positions of the triangulation points before and after the

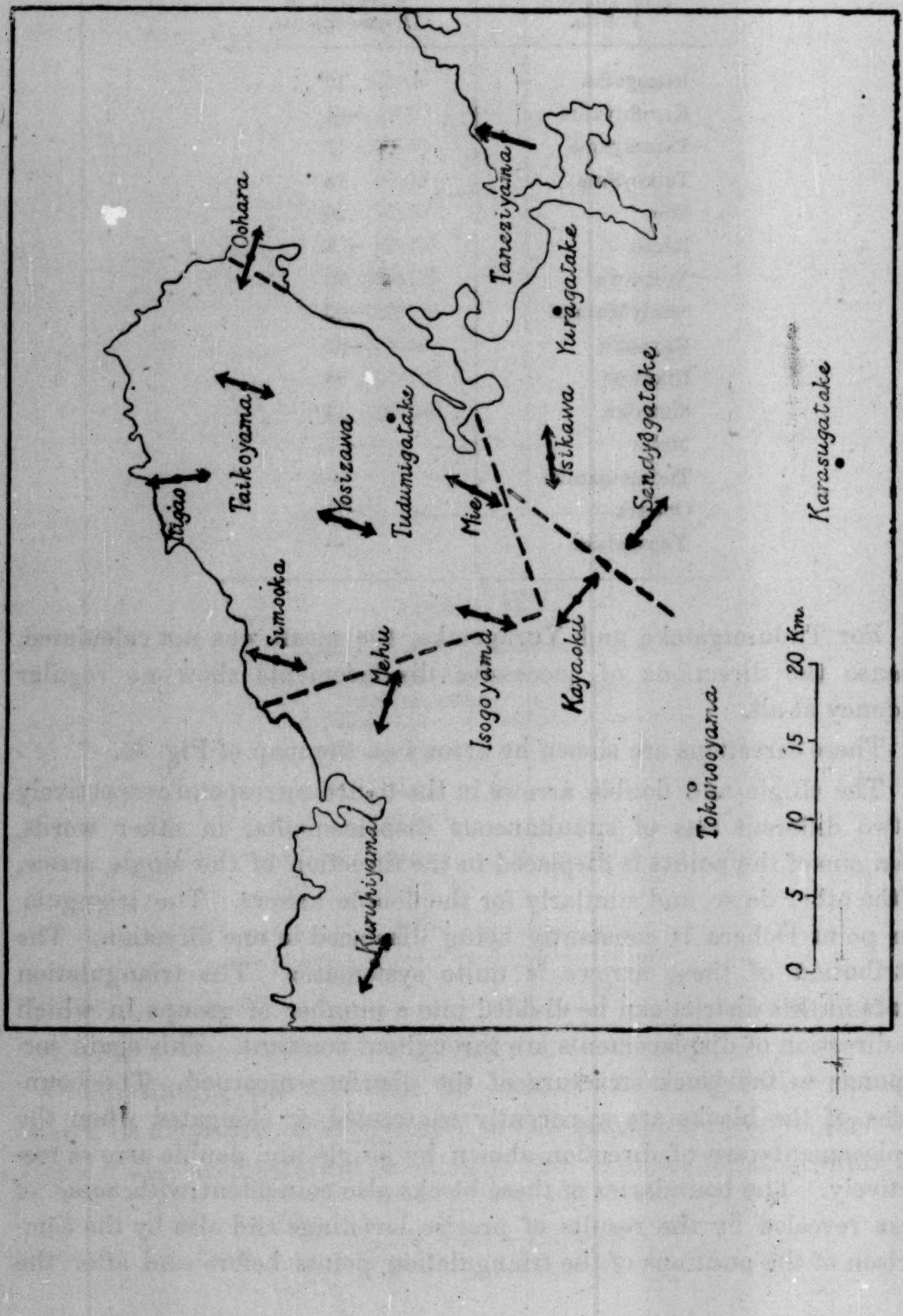

Fig. 36. Direction of Displacements of Secondary Triangulation Points.

earthquake. One of these boundaries coincides with the Yamada fault, while the Gomura fault no longer is recognised in the distribution of horizontal displacements. It appears, as it were, to have healed altogether. This again well conforms with the results of the precise levellings.

It will be seen that the pentagonal area, with Mie, Isikawa, Isogoyama, Kayaoku and Sendyogatake at its vertices are contracted in III–II and expanded in IV–III. The mobility of ther ground is rather astonishing. As was pointed out by T. Terada,[17] the apparent horizontal displacements of triangulation points may be produced by the tilting of the block on which they lie. We have at present no means to determine whether the horizontal displacements revealed by the triangulations are really such or only apparent ones produced by the tilting of the ground. In either case, the blocks in this district must be regarded as extremely loose in their mutual couplings.

8. Movements along the Gômura and Yamada Faults.

According to the comparison of the triangulations before and after the earthquake of 1927, the triangulation points Simooka and Yosizawa which are situated upon both sides of and close to the Gômura fault were subjected to a remarkable relative dislocations. According to the calculation, the components of the relative movement in parallel and perpendicular direction of the fault are 232 cm. and 36 cm. respectively. The change of level at the fault is, according to the precise levellings, 75 cm. Thus the motion at the fault may be schemetically represented in the Fig. 37.

This appears to be a thrust of angle 64°. The west side of the fault seems to have got on top of the east side. On the other hand, F. Tada[18] of our Institute, based on his field observations, estimated the dip of this plane of fault to be 60°–80° westward. A. Imamura and N. Nasu,[19] based on their observation of the distribution of the after-shocks accompanying the great earthquake, estimated it to be 70°. These values obtained in three independent ways are in good accord with each other.

17) *Proc. Imp. Acad.*, 6 (1930).
Bull. Earthq. Res. Inst., 7 (1929), 237.
18) *Bull. Earthq. Res. Inst.*, 4 (1928), 170.
19) *ibid.*, 6 (1929) 245; 7 (1929), 133.
Journ. Fac. Sci., Imp. Univ. Tokyo, Sec. II, 3 (1929), 29.

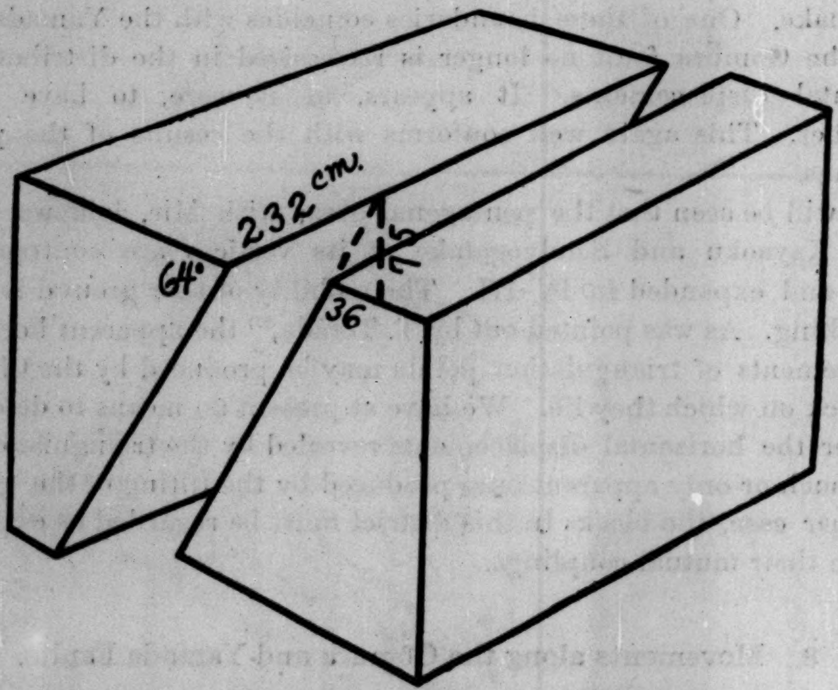

Fig. 37. Movement along the Gômura Fault.

After the earthquake, no sensible displacement took place along the fault as was described elsewhere.

With the Yamada fault, the case is somewhat different from the Gômura fault. According to the calculation, the horizontal components of the relative displacements parallel and perpendicular to the fault are 71 cm. and 11 cm. respectively. The vertical displacement at the fault is, according to the results of precise levellings, 114 cm. The displacement at the Yamada fault at the time of the earthquake can therefore be schematically represented as in Fig. 38.

This is evidently of a type of a normal fault, the plane of the fault dipping southward by an angle of 84°. According to H. Tsuya, there developed in the neighbourhood of the Yamada fault, a number of joints in granitic mass which are dipping northwards by about 40°-50°. The study of the distribution of the orgins of the after-shocks connected with the Yamada fault also shows that the plane of this fault is dipping northwards. The dip of the fault thus determined in these ways differs decidedly from each other.

As was described elsewhere, the displacements along the Yamada fault have been still active after the earthquake of 1927, while that along

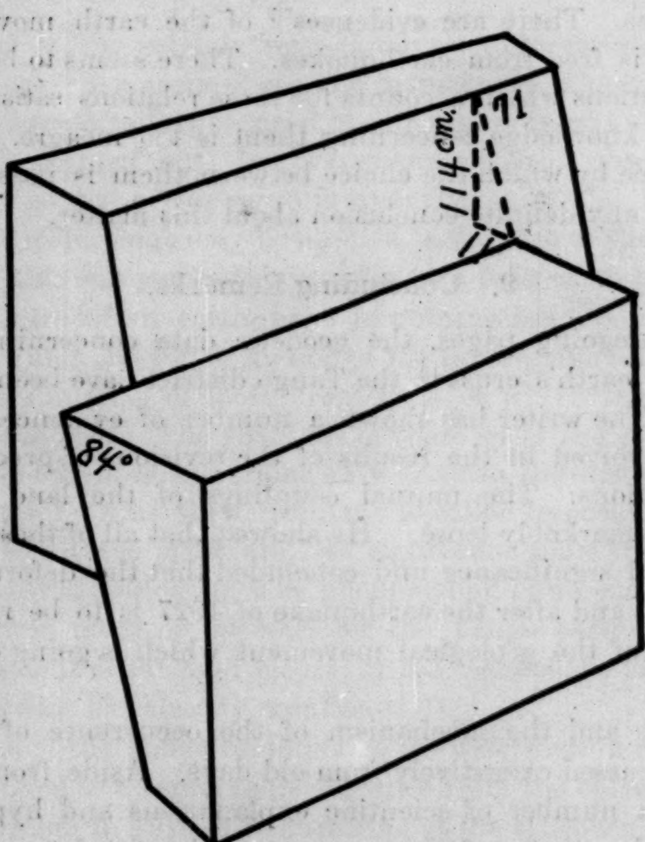

Fig. 38. Movement along the Yamada Fault.

the Gômura fault have entirely ceases away. According to the results of the study of the three dimensional distribution of the after-shocks, the decrease in number of after-shocks originating along the Gomura and Yamada faults did not differ very much. The two facts may seem to contradict at first sight with each other, but it is true that we have no reason to expect that the occurence of after-shocks and the differential blocking movements must take place simultaneously. We have further a remarkable example. In Fig. 14 A, there was no differential movement between the bench marks 10471 and 10472 in the interval of II–I while there *was* in the interval of III–II. At the boundary of these two blocks, no earthquake was observed in the interval of III–II. Thus it appears as if the seismic activity and the differential blocking movements are entirely independent phenomena. N. Yamasaki[20] pointed out the existence of chronic tilting of land blocks which is not accompanied

20) *Proc. Imp. Acad.*, 4 (1928), 60.

by earthquakes. There are evidences[21] of the earth movements in a region which is free from earthquakes. There seems to be many alternative explanations which accounts for these relations satisfactorily, but at present our knowledge concerning them is too meagre. We have no crucial evidence by which the choice between them is possible. It will safe to reserve any definite conclusion about this matter.

9. Concluding Remarks.

In the foregoing pages, the geodetic data concerning the deformation of the earth's crust in the Tango district have been discussed in some detail. The writer has shown a number of evidences of blocking movements involved in the results of the revisions of precise levellings and triangulations. The mutual couplings of the land blocks were proved to be remarkably loose. He showed that all of these land blocks have geological significance and concluded that the deformation of the earth's crust at and after the earthquake of 1927 is to be regarded as a manifestation of the geological movement which is going on in present days.

The cause and the mechanism of the occurrence of earthquakes have been discussed exaustively from old days. Aside from the absurd speculations, a number of scientific explanations and hypotheses have been proposed. Each of them seems to be fitted to elucidate the phenomena concerning a special earthquake to which the explanation owes its birth. But this generally fails to cover the phenomena of other earthquakes. Considering that there are a number of different types of earthquakes, it seems natural that there are a number of explanations as much. Most of them are, however, similar to each other in that they regard the earthquake to start from a single point or from a single plane of fracture. They are far from explaining the case of the Tango earthquake. As the writer has emphasised throughout this paper, there are a number of evidences of the blocking movements in the Tango district and that the mutual couplings of the land blocks are remarkably loose. In this respect, the Tango earthquake proved to have provided an example of a new type of the earthquake. The ground must be regarded to be an aggregate of more or less rigid blocks. If the physical behaviors of the earth's crust are to be regarded as such, what will happen in it at the time of the earthquake?

21) W. KRANZ, *Petermann's Mitt.*, 68 (1922).
W. WOLFF, *ZS. d. Ges. f. Erdk. Berlin*, (1929), 241.

According to the seismic wave analyser observation by K. Suyehiro,[22] there are, in a train of seismic disturbance, a number of groups of waves which seem to be produced at different points at different times. A. Imamura[23] pointed out, by his seismometrical observations, the multiplicity of source of the seismic disturbance of the Kwantô earthquake of 1923. The same may be applied to the case of the Tango earthquake though this was generally regarded as a twin earthquake.

The epicentre of an earthquake is nothing but a point right above the spot from which the initial motion of the earthquake happens to start. There must be a number of spots, from each of which the train of disturbances is produced. The positions of these spots are generally hard to be determined from seismograms only because the disturbances start from them later in time than from the so-called hypocenter. But this never implies that these spots are less significant than the hypocentre. They are equally significant. The phenomenon of an earthquake in its meizoseismal area must be, at least for the Tango earthquake, a complicated adjustment of the land blocks, or the *chaos* of the blocking movements as the writer has already mentioned.[24]

In the case of the Tango earthquake, the deformation of the earth's crust was extended to a remarkable distance from the epicentre. In the case of the eruption in 1914 of Sakurazima at the southern extremity of Kyûsyû, the deformation of the earth's crust was observed within the whole area of southern Kyûsyû.[25] As some experiments show,[26] a force applied on one side of an aggregate of solid is not transmitted to the other side of it. This may be still valid for the case of an aggregate of land blocks. It is evident that in such an aggregate of land blocks, there can exist no statical elastic stress which has been too often referred to in the explanation of the earthquake occurrence.

The writer[27] pointed out that there is a close correlation between the geographical distribution of gravitational anomalies and that of the epicentres of earthquakes in this country. The districts most frequented by earthquakes were found to be those in which the gravitational anomalies

---

22) *Bull. Earthq. Res. Inst.*, **7** (1929), 467.

23) *Proc. Imp. Acad.*, **5** (1929), 330.

24) C. Tsuboi, *Bull. Earthq. Res. Inst.*, **7** (1929), 113.

25) F. Omori, *Bull. Imp. Earthq. Inv. Comm.*, **8** (1914–1922), 50.

26) T. Terada and N. Miyabe, *Bull. Earthq. Res. Inst.*, **4** (1928), 33; **6** (1929), 109; **7** (1929), 65.

27) C. Tsuboi, *Proc. Imp. Acad.*, **5** (1929), 326.

are remarkably negative. This suggests that the generation of earthquakes, or rather of the *chaos* of blocking movements, is due to some peculiar circumstances of the physical or chemical state of the portion of the earth's crust in the immediate neighbourhood of, or right beneath, the earthquake district, but not to any force working from distant places.

After these views were expressed in the former paper, the writer came aware of the paper of W. H. Hobbs,[28] in which he expressed his view on the occurrence of earthquake. His view seems to be essentially similar to the writer's.

Acknowledgements.

In concluding this paper, it is a happy duty for the writer to record his high appreciation of the constant helps he has received from many quarters during this work.

Above all the writer highly appreciates the efforts of the experts of the Land Survey Department who made the actual observations in the surveys of the Tango district. The value of the results obtained is hard to be overestimated.

The writer expresses his sincere thanks to Professor T. Terada for his helpful criticism during this work and to Messrs F. Tada and H. Tsuya for their advices in the geological side of the present work. The writer's thanks are also due to Messrs. K. Yasumuro, S. Kawasima and Y. Kosaka for their kind assistance in preparing this paper. Lastly, but not least, thanks must be expressed to Mr. S. Iwanami for his kind help in the execution of the surveys.

Earthquake Research Institute,
Tokyo Imperial University.

---

28) W. H. Hobbs, *Smithonian Rep. f. 1926* (1927), 257.
The writer thanks Prof. W. H. Hobbs for his private communication.

9. 昭和二年丹後地震に關聯せる丹後地方の地殼の變形に關する研究（第一報）

地震研究所　坪　井　忠　二

昭和二年の丹後地震後には、同地方に三角測量及水準測量の改測が實施された。此の論文は其の結果を整理して、丹後地方の地殼に如何なる變形が生じたかを調べたものである。主な結果は、

(1) 水準測量の結果から此の地方の地塊運動が見られる。

(2) 地震前後の三角測量を比較して見ると、地殼の水平移動がやはり地質學上の重要な線を境にして急に變化してゐる事が解る。

(3) 三角點の移動から地殼の展縮を計算して、之を地殼の垂直移動と比較して見ると、面積のひろがつた所が上昇し、縮まつた所が沈降した事が解る。

(4) 面積のひろがつた所は現在の地形で高い所であり、縮まつた所は低地である。

(5) 二等三角點の地震後の移動を見ると、地塊運動の證據が明瞭に認められる。

(6) 測量の結果だけから見ると、郷村斷層は 64° の thrust であり、山田斷層は 84° の normal fault である。

最後に、此の樣にして明になつた地殼の物理的性質から見て一般に地震發生の現象について若干の考察を加へた。

10. Observations sur les variations de l'inclinaison de la surface terrestre (deuxième rapport). Résultats obtenus dans la région épicentrale du tremblement de terre de Sekihara

par **Mishio ISHIMOTO,**

Institut de Recherches sur les Tremblements de terre.

(Lu le 17 Décembre 1929.—Reçu le 20 Mars 1930.)

1. Après avoir constaté que les variations de l'inclinaison de la surface terrestre précédent le tremblement de terre, nous venons d'installer un certain nombre de clinographes de quartz dans les régions en question. Parmi les lieux d'observation nous distinguons d'une part les stations en sous-sol, dont les conditions thermiques demeurent constantes, et qui sont considérées comme propres aux observations permanentes; d'autre part les stations au niveau du sol, dont les perturbations thermiques sont énormes, et qui ne permettent d'observations que dans la région aussitôt après un tremblement de terre.

Nous avons trois stations permanentes dans la région de Kwantô; l'une à Mitaka (à l'Observatoire Astronomique de Tôkyô), la deuxième à Tukuba (à l'Observatoire Sismique de Tukuba, qui depend de notre Institut), et la troisième à Aburatubo (à la Station Marine Biologique de Misaki). Nous constatons des perturbations thermiques surtout à Mitaka, tandis qu'elles sont très faibles à Aburatubo. Nous constatons d'ailleurs à Aburatubo que les variations périodiques de l'inclinaison sont produites suivant l'exhaussement de l'eau dans la baie.[1] Mais à Tukuba, nous distinguons certaines variations de l'inclinaison précédant les tremblements de terre[2] dont les épicentres se placent dans la région de Kwantô. Ce phénomène nous conduit à penser, d'une part que le bloc de Tukuba est particulièrement sensible à l'apparition des séismes et d'autre part que le domaine efficace d'un séisme est assez grand pour pouvoir donner certaines variations de l'inclinaison de blocs situés à plus de 50 km. de distance.

1) R. Takahasi, *Bull. Earthq. Res. Inst.*, 6 (1929), 85.
2) W. Inouye, *Proc. Imp. Acad.*, 5 (1921), 457.

L'étude des variations de l'inclinaison dans la région qui vient d'être troublée par un grand tremblement de terre, nous oblige quelquefois à construire une cabine provisoire au niveau du sol pour les observations. Bien que nous disposions l'appareil sur des fondations de grande masse, les variations fondamentales d'un bloc sont souvent masquées par des perturbations thermiques, ainsi que par l'approche des opérateurs. Cependant comme les mouvements du bloc de terrain dans la région troublée sont comparativement énormes vis à vis des perturbations locales, nous pouvons en général négliger ces dernières. Comme nous l'avons signalé pour les l'observations faites[3] à Miyadu juste après le tremblement de terre de Tango, il y a certaines variations de l'inclinaison qui précédent la plupart des grandes répliques malgré les perturbations thermiques. De plus par ces observations, nous avons été conduits à imaginer l'existence du bloc à la suite de la détermination des positions hypocentrales.[4] D'autre part, suivant les résultats obtenus par le jalonnement exécuté dans cette région, nous inclinons à supposer l'existence d'un groupe de blocs ayant des mouvements individuels, sans aucun couplage entre eux[5]: par suite il est certain que la plupart des variations de l'inclinaison observées dans une station ne sont autres que les variations du bloc.

De toute façon, nous avons fait assez d'observations sur les variations de l'inclinaison pour pouvoir établir les conclusions suivantes :

1° Il y a certaines variations de l'inclinaison précédant les tremblements de terre.

2° La plupart des variations observées sont considérées comme celles de l'inclinaison du bloc sur lequel se trouve la station.

3° Pour éviter des perturbations locales, il vaut mieux installer les appareils dans une cave creusée au sein de la masse rocheuse.

4° Dans une région qui vient d'être troublée par un grand tremblement de terre, nous pouvons nous contenter d'exécuter les observations dans une cabine au niveau du sol pour la raison que les mouvements individuels des blocs sont comparativement plus grands que les perturbations locales.

---

3) M. Ishimoto, *Bull. Earthq. Res. Inst.* 4, (1928), 203. *Jap. Journ. Astron. & Geophys* 6 (1928), 83.

4) N. Nasu, *Bull. Earthq. Res. Inst.*, 6 (1929), 245; 7 (1929), 133.

5) C. Tsuboi, *Bull. Earthq. Res. Inst.*, 6 (1929), 71.

C'est à partir de ces principes que nous avons décidé de commencer nos observations à Sekihara, région troublée récemment par un fort tremblement de terre.

2. Le tremblement de terre de Sekihara s'est produit le 27 Octobre 1927. Comme les secousses n'ont pas été très fortes, il n'y a pas eu de victime, ni de maison complètement détruite: dans les quatre villages situés dans la région épicentrale, les dommages suivants ont été causés[6]:

à Sekihara:	fissures au mur; cinq maisons à moitié détruites; une maison s'est déplacée vers l'Est; chute de lanternes de pierre situées devant de temple Simmei; crevasses dans les rues; jaillissements de boues.
à Miyamoto:	6 maisons à moitié détruites; 40 maisons endommagées; crevasses dans les rues; jaillissements de gaz.
à Hiyosi:	excoriations aux murs de magasins; 9 maisons à moitié détruites; crevasses dans les rues et dans les rizières; éboulement sur la grande route.
à Hikosi:	fissures au mur; petites crevasses dans les rues.

En tout cas les dommages sont demeurés légers et la séismicité maxima est du neuvième degré dans l'échelle de Mercalli. Cependant comme nous avons en des éboulements sur la grande route par suite des secousses, l'importance des dommages a été plus ou moins exagerée dans les informations.

Il y a deux mémoires sur ce tremblement de terre, l'un par M. T. Matuzawa[7], Professeur à l'Institut Sismologique, et l'autre par M. S. Kunitomi[8], Ingénieur de l'Observatoire Central de Météorologie. Dans le deuxième, l'auteur fait une discussion sur la nature des directions initiales des ondes sismiques enregistrées par les sismographes distribués dans tout le Japon. Cette méthode de recherche a été développée particulièrement dans notre pays, car nous pensons que nous pourrions relever certaines indications sur le mécanisme de la production des ondes sismiques autrement dit qu'il y aurait production d'une faille pouvant rayonner des ondes sismiques. Pourtant il est certain, *a priori*, que cette méthode de recherche est développée suivant une hypothèse sur le mécanisme du foyer, c'est-à-dire la production d'une faille; conséquemment cela ne prouve pas que l'origine du séisme soit une faille. En tout

6) d'après M. T. FUJIWARA, à l'Ecole primaire de Sekihara.
7) T. MATUZAWA, *Bull. Earthq. Res. Inst.*, 5 (1928), 29.
8) S. KUNITOMI, *Geophys. Mag.*, 1 (1928), 238.

cas ce que nous ne pouvons qu'imaginer d'après la carte représentant les mouvements initiaux des ondes sismiques, c'est le mode de vibrations au foyer.

Suivant le point de vue topographique nous distinguons, d'ailleurs, trois chaînes de montagnes dans cette région situées parallèlement les unes aux autres. Elles sont toutes formées par des couches de la fin du tertiaire et les exhaussements ont probablement eu lieu au commencement de l'époque suivante ; par conséquent il nous semble que les mêmes exhaussements se manifestent partiellement jusqu'aujourd'hui encore. Du fait que cette région contient un des champs pétrolifères, des recherches géologiques ont été exécutées avec assez de précision pour nous faire apercevoir trois failles remarquables entre ces trois chaînes et il nous semble que les mouvements individuels ont été réalisés d'après la croissance des failles.

La position du foyer de ce tremblement de terre se trouvera dans la partie superficielle de la croûte qui continue ses mouvements depuis les temps géologiques. Nous avons relevé certains changements d'altitude de repères dus à ce tremblement de terre ; ces changements s'accordent bien avec ceux qui apparaissent généralement aux grands tremblements de terre surtout dans la région épicentrale. Par conséquent, quand nous voulons discuter le mécanisme de la production d'un séisme, il est nécessaire de faire attention avant tout à ces changements topographiques.

Le regretté Professeur N. Yamasaki[9] a constaté, d'après les résultats obtenus par le nivellement de précision exécuté dans la région littorale de la province d'Etigo, qu'il y a des changements chroniques de l'inclinaison des blocs sans accompagnement de tremblement de terre. Grâce à la répétition du nivellement de précision en plusieurs endroits, soit dans la région montagneuse soit dans la région plaine, nous pouvons remarquer des changements chroniques d'altitude de repères. De ces faits nous pouvons conclure que des mouvements imperceptibles de blocs existent toujours dans certaines régions tandis que les mouvements brusques de blocs sont accompagnés de forts tremblements de terre. En tout cas il n'est pas possible de discuter le phénomène sismique sans tenir compte des conditions d'équilibre des blocs, c'est-à-dire de l'état de la matière sous le bloc.

C'est au mois d'Août que le deuxième jalonnement fut terminé. Mais à la suite du tremblement de terre du mois d'Octobre, un troisième

9) N. Yamasaki, *Proc. Imp. Acad.*, 4 (1928), 60.

jalonnement a été répété tout de suite dans la région épicentrale, supposant que nous pourrions constater quelques changements d'altitude de repère accompagnés par ce tremblement de terre. D'après les résultats obtenus à la répétition du jalonnement, nous constatons un exhaussement remarquablement grand pour deux repères situés tout près de Sekihara. Comme il n'y a qu'une direction de route de jalonnement, il est impossible de décider le sens ainsi que la valeur de l'inclinaison du bloc. Mais avant tout, il est remarquable que nous ayons pu constater un tel exhaussement brusque de terrain accompagné par un tremblement de terre de pareil ordre. Quant à la détermination des limites du bloc en question, les résultats du jalonnement ne nous donnent rien mais les études géologiques et topographiques nous font connaitre les limites présumées, représentées sur la figure 1.

3. Les observations sur les variations de l'inclinaison à Sekihara ont duré presque 2 ans, du 12 Janvier 1928 au 31 Décembre 1929. Nous avons installé une paire de pendules de quartz, signalés déja dans ce Bulletin[10], qui sont employés partout pour les même observations. Bien qu'une cabine provisoire destinée à contenir nos appareils eût été construite au niveau du sol, les variations thermiques de l'intérieur n'étaient autres que celles du plein air.

Comme nous l'avons remarqué, les observation faites avec un appareil situé au niveau du sol sont toujours troublées par des perturbations thermiques, car quoique nous maintenions la température de l'intérieur de la cabine à peu près constante, la température du plein air fait plus ou moins varier l'inclinaison de la portion superficielle du sol. De plus, pendant l'hiver, il y a une grande accumulation de neige surtout dans cette partie du Japon et il est certain qu'elle cause des perturbations considérables à nos observations.

Or, comme éléments d'un séisme, il faut généralement compter a) le temps de l'occurence, b) l'intensité des secousses et c) l'épicentre. Comme nous n'avions pas installé un seul sismographe dans cette région, il était difficile de déterminer ces trois éléments pour toutes les répliques. Pour notre but, néanmoins, il est suffisant de connaître au moins la date pour le temps de l'occurence. Quant à l'intensité des secousses, nous les avons classées en deux catégories, secousses légères et secousses faibles[11];

---

10) M. Ishimoto, *Bull. Earthq. Res. Inst.*, 2 (1927), 1.

11) Sur la figure 2, le grand point noir pour les secousses légères, le petit point noir pour les secousses faibles.

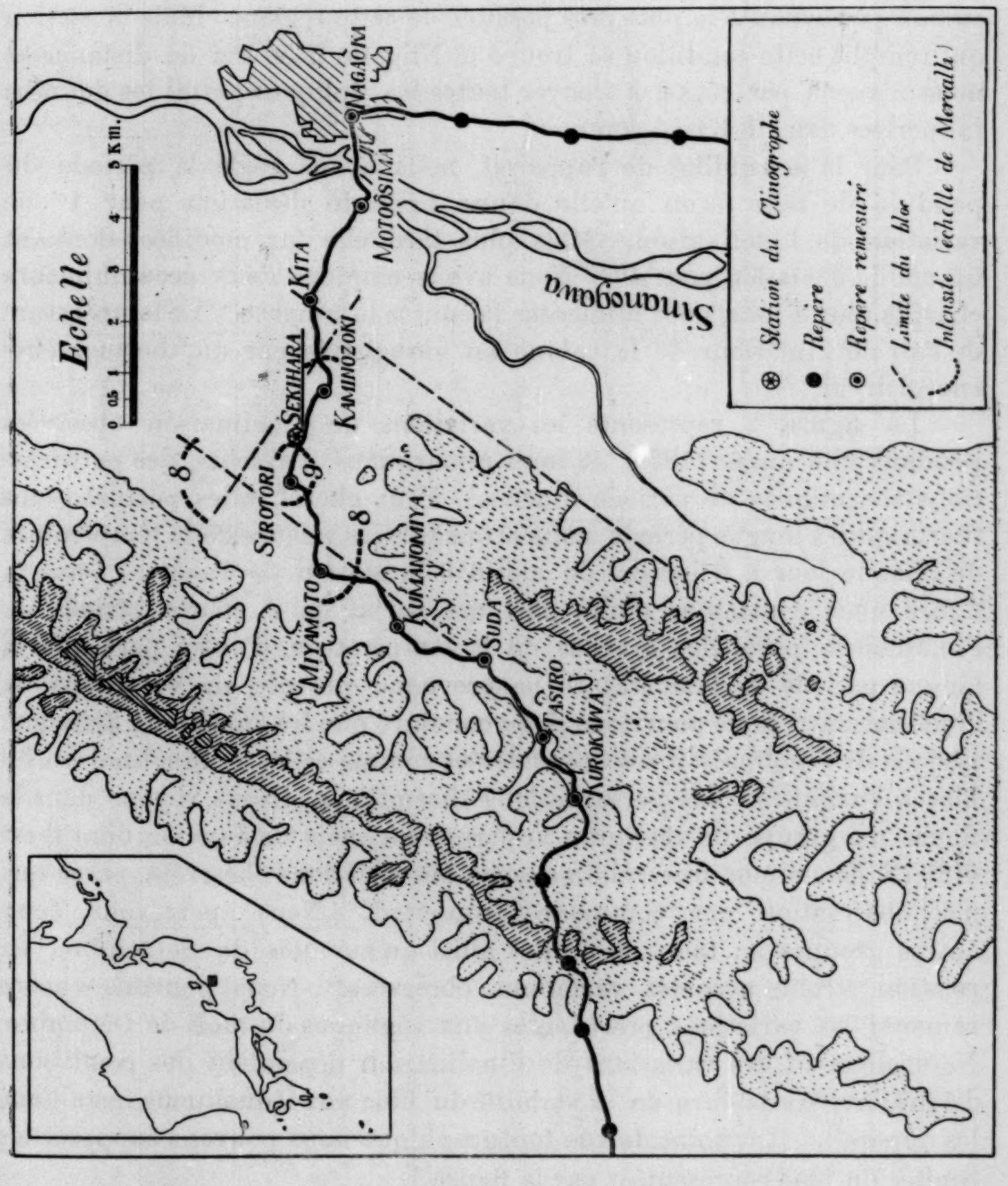
Echelle
0 0.5 1 2 3 4 5 Km.
Sinanogawa
NAGAOKA
MOTOOSIMA
KITA
SEKIHARA
SIROTORI
MIYAMOTO
KUMANOMIYA
SUDA
TASIRO
KUROKAWA
Station du Clinographe
Repère
Repère remesuré
Limite du bloc
Intensité (échelle de Mercalli)

Fig. 1.

mais comme on est habitué à exagérer plus ou moins l'importance des secousses les estimations seront en général trop hautes. Pour déterminer les positions épicentrales, nous avons essayé de chercher une station permanante le plus près possible de cette région. Mais la station qui remplit cette condition se trouve (à Niigata) à 50 km de distance et nous n'avons pas réussi à trouver toutes les répliques parmi les données rapportées dans le Kisyô-yôran.

Pour la sensibilité de l'appareil, nous avons réglé la période du pendule de telle façon qu'elle donne 1 cm de déviation pour 1″ de variation de l'inclinaison. Mais plus tard elle fut modifiée, donnant 0,5 cm de déviation pour 1″. Nous avons employé deux accumulateurs chargés tour à tour, pour alimenter la source lumineuse. La température de l'air de l'intérieur de la cabine est enregistrée par un thermomètre-enregistreur.

La figure 2 représente les variations de l'inclinaison observées pendant une année (1928), et nous remarquons, d'ailleurs, des perturbations thermiques de période diurnes. Pour chercher les perturbations thermiques à longue période, nous avons pris les valeurs de la température de chaque jour à 6 heures du matin à la station de Takata. Dans la figure nous constatons d'une part des variations à courte période de l'inclinaison parallèles à celles de la température, d'autre part que la longue période de température ne provoque que peu de variations de l'inclinaison. Nous pourrions donc conclure que les variations à longue période de l'inclinaison sont considérées comme celles de l'inclinaison du bloc à l'exclusion des perturbations thermiques. Nous voyons dans la figure un groupe de répliques apparues au mois de Janvier, dont il est difficile de donner une relation avec les variations observées, parce que nos observation ont commencé trop tard. Nous apercevons deux autres groupes au mois de Juillet ainsi qu'au mois de Septembre, en relation étroite avec les variations observées. Nous pouvons encore ramener les variations précédentes aux répliques du mois de Décembre. Naturellement ces variations de l'inclinaison dépendent des conditions d'équilibre, c'est-à-dire de la stabilité du bloc sur lequel nous installions les appareil. Du point de vue topographique nous pouvons supposer les limites du bloc representées par la figure 1.

Suivant la figure 2 nous pouvons déterminer le sens de variations prédominées avant les occurences de groupes. Il y a le sens SO au mois de Juillet, SE au mois de Septembre et SO au mois de Décembre. Ce sont les sens naturels de l'inclinaison du bloc en question et il sera

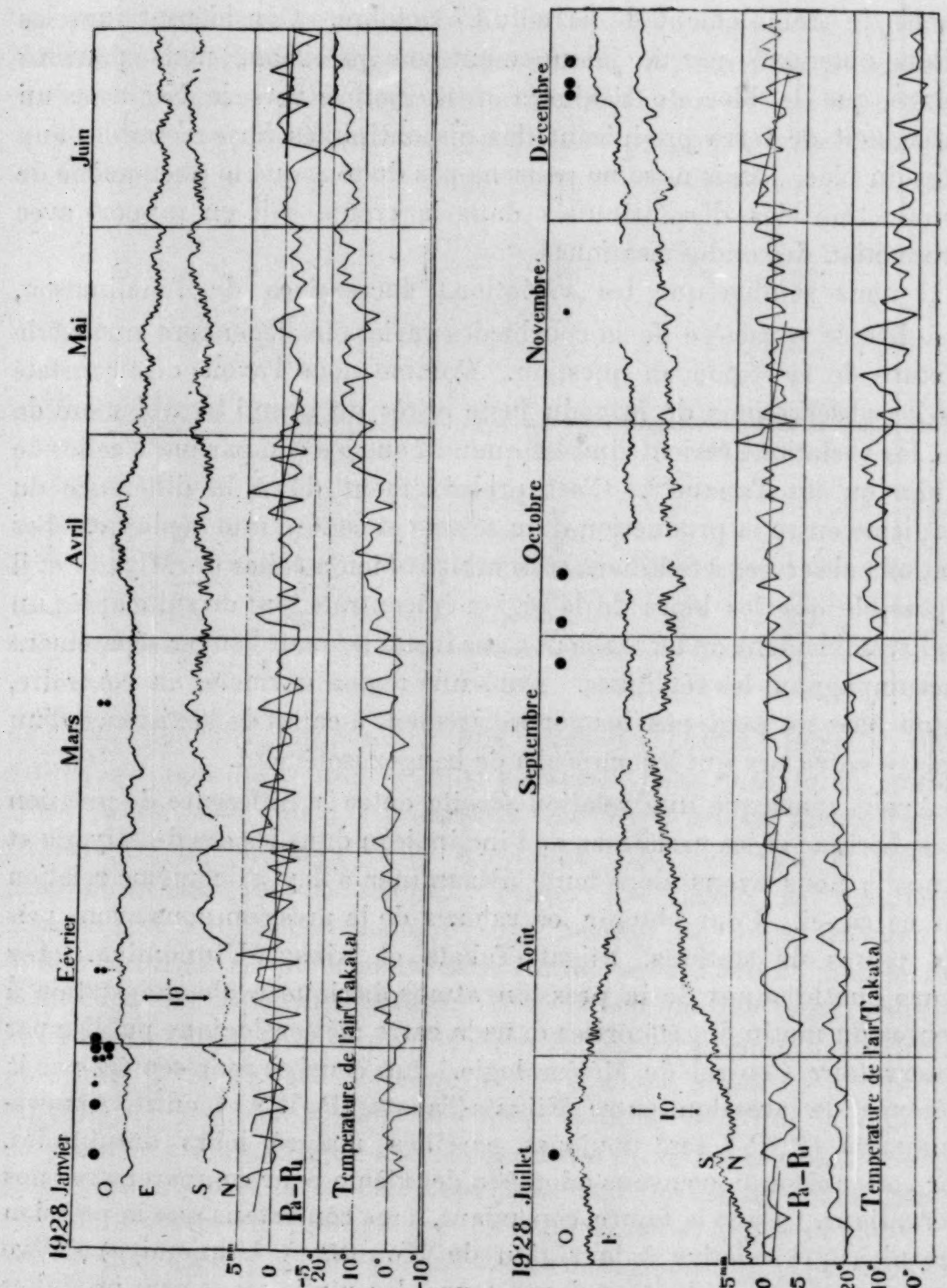
1928 Janvier
Février
Mars
Avril
Mai
Juin
O
E
S
N
10'
Ra–Ru
Température de l'air (Takata)
1928 Juillet
Août
Septembre
Octobre
Novembre
Décembre
O
E
S
N
10'
Ra–Ru
Température de l'air (Takata)

Fig. 2

donc permis de présumer le sens des variations de l'inclinaison au moment du tremblement de terre du 27 Octobre. Considérant aussi les résultats obtenus[12] par le jalonnement de précision, nous pouvons conclure que le bloc de Sekihara s'est incliné vers le NO avec un tremblement de terre produisant des discontinuités imperceptibles aux limites du bloc. Mais nous ne pensons pas du tout que le phénomène de la production des discontinuités dans la croûte soit en rapport avec la production des ondes sismiques.

Il nous semble que les variations successives de l'inclinaison, c'est-à-dire le caractère de la courbe des variations dépendent surtout de la nature de la région en question. Comme nous l'avons déja constaté dans les observations de Miyadu juste après un grand tremblement de terre, les variations étaient simples quand nous les comparions à celles de Tukuba ou de Tanabe[13]. C'est probablement dû à la différence du mécanisme entre la production d'un séisme et celle d'une réplique. Les variations observées à Sekihara ressemblent bien a celles de Miyadu et il est possible que les blocs de la région épicentrale tout de suite après un grand tremblement de terre soient assez instables pour bouger séparément en accompagnant les répliques. Dans une région normale, au contraire, chaque bloc ne peut pas bouger séparément à cause de l'existence d'un couplage entre eux qui les empêche de bouger isolément.

Ayant remarqué une relation étroite entre la différence de pression atmosphérique et les variations de l'inclinaison dans les cas de Miyadu et Tukuba[14], nous avons alors tenté d'examiner s'il y a la même relation dans ce cas-ci. Pour obtenir les valeurs de la pression nous avons pris deux paires de stations, Niigata-Takata et Aikawa-Utunomiya. Les valeurs quotidiennes de la pression atmosphérique à chaque station à 6 heures du matin ont été prises dans la carte météorologique publiée par l'Observatoire Central de Météorologie. Les courbes représentées par la différence de pression entre Niigata-Takata (P_N-P_T) et entre Aikawa-Utunomiya (P_A-P_U) sont toujours pareilles malgré leurs amplitudes. Pour cette raison nous avons adopté la deuxième pour comparer avec nos observations. Dans la figure, cependant, nous constatons que la pression atmosphérique relative à la région de Kwantô (à Utunomiya) s'élève progressivement pendant quelques jours, les répliques se sont produites

12) Voir la figure 3.
13) A. Imamura, *Proc. Imp. Acad.*, 5 (1929), 460.
14) *loc. cit.*

dans la région épicentrale. Bien que nous ne puissions pas faire correspondre toutes les variations de l'inclinaison du bloc à celles de la différence de pression, il est certain que la différence de pression joue un rôle important dans l'apparition des répliques. Il est bien naturel que la croûte terrestre ait une propriété analogue à celle d'une sorte

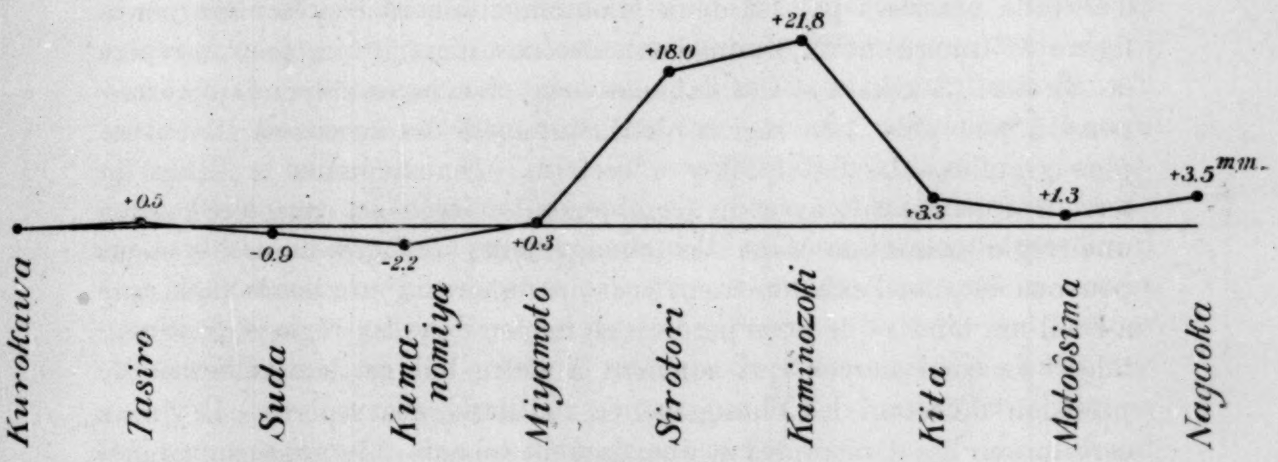

Fig. 3.

de brai, pouvant s'opposer à une force de courte période tandis qu'elle se manifeste tout à fait plastique pour une force statique. D'un autre côté, nous connaissons les expériences faites par les Professeurs H. Nagaoka et S. Kusakabe[15] qui ont tiré au clair les propriétés élastiques des roches. Toutes les roches se manifestent comme une substance élastique sous l'action de forces momentales tandis qu'elles se déforment sans limite sous l'action d'une force statique d'une certaine grandeur. Il nous semble que telles propriétés s'appliquent aussi à la croûte où la pression est présumée très grande. Par suite à la surface terrestre nous pouvons observer d'une part l'inclinaison du bloc suivant une force statique telle que la différence de pression atmosphérique exercée dans une direction pendant quelques jours; d'autre part la croûte s'opposera aux forces de courte période et nous n'observons presque pas de mouvements forcés de bloc. Il est certain qu'il y a des perturbations thermiques qui gènent toujours nos observations et conséquemment les variations dues à la pression atmosphérique demeurent obscures. C'est parce que la station se

15) H. Nagaoka, *Pub. Earthq. Inv. Comm.*, **4** (1900); S. Kusakabe, *ibid.*, **14** (1903), **17** (1904).

place juste à la surface du sol et il n'y a aucun moyen d'éviter les perturbations thermiques.

Certainement ce tremblement de terre s'est produit juste après l'exécution du jalonnement fait dans cette région et les mesures ont été reprises tout de suite afin de mettre en évidence des changements d'altitude accompagnés par ce tremblement de terre. Les différences d'altitude obtenues par les deux jalonnements sont représentées par la figure 3[16] montrant 21,8 mm d'exhaussement maxinum, pour le repère de Sirotori (Sekihara). Cet exhaussement maximum cependant correspond à peu près à la région où les intensité des secousses étaient les plus grandes. Le fait qu'il y a certains exhaussements brusques du terrain apparaissant avec un tremblement de terre est considéré comme une règle commune dans les changements topographiques[17]: nous pouvons détecter l'exhaussement brusque de terrain aux bords de la mer à l'oeil nu, tandis que nous perdons ce moyen dans les régions continentales. Le seul moyen qui convient à notre but est le nivellement de présision détectant les changements d'altitude des repères. Il y a un certain nombre d'exemples de changement topographiques accompagnés par le tremblement de terre[18] que nous partageons en deux catégories: dans la première, nous comptons les tremblement de terre de Kwantô, Tango etc. et dans la seconde ceux de Nôbi (Mino-Owari), Oomati etc. En tout cas c'est une remarquable découverte que d'avoir pu mettre en évidence de si faibles exhaussements de terrain, produits par de petits tremblements de terre. Naturellement nous sommes obligés de tenir compte dans nos conceptions des causes des tremblements de terre de cette règle générale des changements topographiques.

---

16) le repère de Kurokawa est présumé fixe.

17) Les exhaussements de terrain accompagnés par les tremblements de terre historiques du Japon ont été signalés depuis 1331 A.D. à l'occasion du tremblement de terre de Senri-ga-hama. D'autre part nous pouvons facilement remarquer l'exhaussement de terrain relatif au niveau de la mer surtout sur la côte de la mer du Japon, où les variations du niveau suivant la marée sont assez petites. Le Prof. A. Imamura rapporte de tels exhaussements de terrain dans ce Bulletin 4 (1928) 173.

En Europe, cependant, R. Mallet a déja remarqué l'exhaussement du terrain au bord de la mer et de suite il est arrivé à croire que les phénomènes sismiques seront expliqués par un exhaussement brusque du terrain. D'autre part E. Seuss donne son opinion dans son ouvrage "Antlitz der Erde" sur l'exhaussement du terrain accompagné par les tremblements de terre catastrophiques de Chili, où il refuse même les témoignages oculaires. Quoiqu'il veiulle nier ces faits les tremblements de terre apparaissent les uns après les autres accompagnant les exhaussements dans la région épicentrale, soit au bord de la mer, soit dant la région continentale.

18) A. IMAMURA, *Pub. Earthq. Inv. Comm.*, No. 25 (1930).

Quant à l'exhaussement ou l'affaisement de la surface terrestre, nous sommes habitués à considérer l'équilibre vertical de l'écorce superficielle rapportée à la couche souterraine c'est-à-dire l'équilibre isostatique. Néanmoins, il est difficile d'accepter que tel exhaussement est celui qui est du à la compensation verticale de la force statique suivant la condition d'équilibre de l'écorce : parce que l'écorce n'est pas considérée surtout au point de vue géologique, comme étant de structure simple. D'après les travaux géologiques, nous voulons considérer la déformation locale de la surface terrestre comme le résultat de l'injection magmatique dans la croûte. Certainement il est possible que ces deux sortes d'explication (l'équilibre isostatique et l'injection magmatique) indiquent quelquefois le même phénomène regardé de deux côtés différents ; mais puisque nous discutons principalement les déformations superficielles, il est plus naturel d'introduire le transport du magma que les forces produites par l'équilibre hydrostatique de l'écorce. Nous ne voulons pas discuter maintenant la question générale du flottement des continents mais nous voulons expliquer le phénomène de l'exhaussement brusque de terrain plus ou moins limité dans une petite région. De plus, quand nous supposons l'intrusion magmatique comme cause de la déformation de la surface terrestre, la production des ondes sismiques sera ainsi expliquée par l'arrêt brusque d'une masse de magma ayant un moment cinétique très grand ; nous pourrons dire autrement que le remplissement d'un vide par le magma donne un choc à la croûte et lui fait rayonner des ondes sismiques.

La profondeur du foyer de ce tremblement de terre a été déterminée à 8 km et il est possible qu'il se soit produit dans la masse de sial. M. S. Kunitomi nous l'a montré par ses études sur les directions initiales des ondes sismiques enregistrées par les sismographes distribués par tout au Japon. Pour expliquer le mécanisme de la production des ondes sismiques de ce tremblement de terre, il a supposé une naissance de faille à la position hypocentrale, la faille inclinée vers le NO, étant produite par une force de compression. Supposant que la trace superficielle de cette faille corresponde à la vallée de Miyamoto, nous nous heurtons à des difficultés qui nous empêchent d'expliquer l'exhaussement apparu dans la région de Sekihara. Mais en supposant que le bloc situé au NO de la vallée de Miyamoto s'est exhaussé plus que celui de Sekihara, les distributions de l'intensité des secousses ne s'accordent point même dans la région en question. Encore, si nous supposons la vallée de Kita comme correspondant à la faille superficielle, les changements

topographiques s'accordent bien à cette hypothèse, tandis que la distribution des intensités n'est pas élucidée du tout. D'après ces résultats nous considérons plutôt que la production des ondes sismiques est indifférente à l'apparition de la faille. Nous voulons donc croire qu'en général le phénomène sismique est celui qui accompagne l'exhaussement local de terrain en produisant les ondes sismiques, indépandamment de la production d'une faille. Le fait que nous voyens souvent la production de faille à la surface terrestre au moment d'un tremblement de terre sera une simple discontinuité du bord de l'exhaussement local du terrain.

Quant à la distribution des mouvements initiaux des ondes sismiques, nous supposons que la croûte a tendance à s'ébranler suivant la structure locale du foyer par le choc de l'injection. De ce que la production des ondes sismiques est due à l'injection du magma dans la croûte, il est bien possible que son moment cinétique soit assez grand pour produire des fissures autour du foyer surtout vers les directions inférieures. Le phénomène de l'injection remlissant des fissures produites explique aussi que nous ayons un grand nombre de répliques accompagnant un fort tremblement de terre.

Nous ne voulons pas nier l'existence de la force horizontale qui peut accompagner les plissements ou les failles horizontales, néanmoins la production des failles n'est pas considérée comme étant l'origine directe de la production des ondes sismiques. Les forces horizontales peuvent donner certains déplacements suivant la destruction produite par le choc de l'injection dans la croûte terrestre.

Nous supposons ainsi les formations du batholithe ou du laccolithe comme les causes fondamentales de la production des ondes sismiques ainssi que les changements topographiques. Pour comprendre le tremblement de terre de Sekihara, nous ne pouvons pas rester indifférents d'une part aux observations de l'inclinaison du bloc, d'autre part au jalonnement exécuté tout de suite après ce tremblement de terre. Afin de discuter le phénomène des variations de l'inclinaison du bloc, il faut considérer les conditions de la matière sous le bloc ou surtout la pression de vapeur dans le magma qui augmente suivant l'abaissement de la température[19], Il y aura un état critique quand la pression de vapeur arrivera justement à la valeur de la pression extérieure. Par suite de

19) Sur ce sujet, il y a une étude très connue faite par G. W. MOREY, [*Journ. Wash. Acad. Sci.*, 12 (1922), 219].

l'injection du magma dans la croûte, l'abaissement de la pression sera réalisée en dirigeant le bloc vers la condition stable. Nous avons déja adopté cette explication à l'occasion de l'observation faite à Miyadu et maintenant nous sommes également arrivés à la même conclusion.

4. Il est vrai que les résultats obtenus à Sekihara ne donnent aucune nouvelle conclusion ; c'est parce que les perturbations thermiques demeuraient considérables. Mais ce que nous pouvons constater c'est qu'il y a eu certaines variations de l'inclinaison précédant les répliques. Pour avoir des résultats précis, il faut faire les observations avant tout dans une cave à l'abri des perturbations thermiques.

Pour terminer, nous tenons à exprimer nos vifs remercîments à Messieurs T. Fujiwara et K. Soné, maîtres de l'école primaire de Sekihara, qui ont exécuté des observations qui nous ont été infiniment précieuses.

---

10. 地表の傾斜の變化に就て（第二報）
關原における地震後の観測

地震研究所　石本巳四雄

1.　水晶傾斜計を使用して地表傾斜變化を觀測する事は其の後各地において行はれて居るが、地表においては氣温變化の影響が可成り大であるため、地下室特に自然岩中に觀測室を選ぶ事が最も適して居る事は論を俟たない。但し大地震後觀測を直ちに開始する必要ある場合においては、地塊運動が烈しいと云ふ理由の下に地表に建設した一時的小屋を使用する事も出來る。

關東における常時觀測所は三點あり各〻特長を有して居る。丹後地震直後宮津において試みられた觀測の結果からは地塊の存在を推定し得べき結果が得られ、地震發生と傾斜變化との間には密接の關係ある事が判明した。

2.　一九二七年十月二十七日に發生した關原地震は其の震動が比較的弱かつた爲め、倒壞家屋、人畜の死傷は皆無であつた。此の地方は油田地方に相當する關係上地質調査が行き屆いて居り、互に平行した三山脈の間には明かに斷層の存在が認められ、今回の地震に從つても之等斷層位置において多少の運動が行はれたと推定される。而して此の場合問題となる事は地塊の平衡が如何にして保たれるかと云ふ事であつて、震央附近における地塊の大いさは地形及び水準測量の結果等から推定して圖中破線を以て示してある。

3.　關原における傾斜變化は一九二八年一月十二日より開始され、一九二九年十二月卅一日に終つて居るが、一時的の小屋の中にて觀測した爲め氣温の影響が充分認められる。餘震は可成り頻々發生して居るが、其の發震時、震度、震央については正確な事は不明である。然し乍ら吾々の目的上甚だしい正確さは必要としない。器械の感度は一秒角の傾斜變化に對して1cm（後に0·5cm）

の振れを記錄する樣に整正した。一九二八年間に得た觀測結果は第二圖に示してある。氣溫變化が傾斜變化に如何に影響を與へるかを見るために高田における每日午前六時の値を天氣圖から得て圖に表はした。氣溫の小變化に對して傾斜は見えるが極めて徐々に變化する傾斜變化は氣溫では說明出來ず、從つて此れは地塊の運動によるものと見做し得る。而して此の徐々の變化に對して餘震群の發生ある事も充分明かである。即ち地塊の不安定と云ふ事が餘震發生に關係するのである。

第二圖の餘震前に傾斜する方向は假定地塊の最も自然的運動を意味するものであり、水準測量の結果と合せ考へるならば十月二十七日の地震時において此の地塊は北西の方向に傾いたと推定出來る。關原における傾斜變化は宮津において觀測し得たものと類似である事から此の型の變化は餘震發生に關係する特長と見る事が出來る。

此の地方における一定方向の氣壓差が餘震發生と關係を持つであらうと云ふ考へから相川——宇都宮の氣壓差 (P_A-P_U) を圖に示した。即ち關東方面において數日間に亘つて氣壓の上昇が相對的に行はれる場合には餘震の發生を見るのであつて、此の事實から地殼の流動性が想像される。

地震直後行はれた水準測量の結果からは震央地域において土地隆起の事實が判明したが此れは大地震の場合に發生する地形變動の一般法則に一致するものであり、此の地形變動によつて地震發生の機巧も說明されなければならない。即ち一局部の土地が相當短時間に隆起すると云ふ現象は地殼內における貫入岩成生を想像するのが最も便宜であらう。國富技師によつて爲された地震初動の硏究から斷層の存在を假定する事は、此の場合地形變動及び震度分布の事實とは一致しない。即ち地塊運動其のものが地震波を發生せしめるのではなくて、岩漿の貫入が地殼內に行はれ地形變動を生ぜしめると同時に其の運動量變化が地震波を發生すると爲す事が地震現象を最も容易に說明し得るものとなる。

4. 傾斜變化觀測は地下室內において行はない限りは氣溫變化の影響があつて充分よい結果は得られないから、今後は地下室を觀測室として撰ぶ事が是非必要である。

11. The Eruption of Komagatake, Hokkaidô, in 1929.

On June 17, 1929, there occurred an eruption of Komagatake in southern Hokkaidô. After the eruption, some members of our Institute visited the scene of activity to study the volcanic phenomena from geological, seismological, geodetic, gravitational and other sides. The papers presented by them embodying the results of their investigations are compiled here. They are:

Part	I.	The Volcano Komagatake, Hokkaidô, its Geology, Activity, and Petrography. . . .	Hiromichi Tsuya.
Part	II.	On the Temperature of the Pumiceous Ejecta of Komagatake, Hokkaidô, as inferred from their Modes of Oxidation.	Seitarô Tsuboi and Hiromichi Tsuya.
Part	III.	Meteorological and Seismological Observations.	Fuyuhiko Kishinouye.
Part	IV.	Observations of the Tilt of the Ground accompanying the Eruption.	Ryutaro Takahasi.
Part	V.	Precise Levellings around the Volcano. . .	Chûji Tsuboi.
Part	VI.	Observation with Gravity Variometer. . .	Chûji Tsuboi.
Part	VII.	Electrical Phenomena caused by the Eruption of Komagatake.	Kin'ichi Nakata.
Part	VIII.	Observation on Komagatake.	Naomi Miyabe.

The writers of the papers jointly take this occasion to express their sincere thanks to Professors B. Kotô, K. Suyehiro, T. Terada, S. Fujiwhara, M. Ishimoto and F. Tada of our University for their interest throughout the course of the present investigations. They are also indebted to Messrs. M. Ootuka, S. Kawasima and M. Iwasita for the assistance in the instrumental observations, to Mr. H. Nemoto and other members of the Hakodate Meteorological Station for giving facilities in many respects and to Mr. Z. Sato of Sahara for granting the use of his cottage for our instrumental observations. Thanks are also due to many other gentlemen, whose assistance in various ways is acknowledged in the following papers.

Part I. The Volcano Komagatake, Hokkaidô, its Geology, Activity, and Petrography.

By Hiromichi TSUYA,

Earthquake Research Institute.

(Received March 20, 1930.)

Contents.

I. Morphology and Structure.
- General topography.
- Foundation.
- General structure.
- Craters.
- Geologic history.

II. Recorded History of Eruption.

III. The Eruption of 1929.
- The course of eruption.
- Craters.
- Fissures.
- Solid ejecta.
- Solfataras.

IV. Petrography of the Ejecta of 1929.
- A. Juvenile ejecta.
- B. Accessory ejecta.
- C. Accidental ejecta.
- D. Xenoliths.

V. Summary and Conclusions.

I. Morphology and Structure.

General Topography.—The volcano Komagatake, Hokkaidô, is a *homate* truncated at its top with the ring-wall surrounding a horseshoe-shaped caldera. The sides of the volcano show generally the natural slope of a volcanic cone. They are steep, 30-40°, near the top, decreasing in slope downwards. The northern and western sides are steeper than the other sides. On the flanks there are several knobs, Kakaruma-Maruyama, Sahara-Maruyama, Akahageyama, etc., elevated 30-50 m. from the general slope. The north and west skirts are gentle as well as extensive; while the east and south skirts are undulated with numerous hills, less than 20 m. in height.

The volcano is not much dissected. The northern, western and southern flanks are dissected by numerous radial valleys, V-shaped in the upper courses, but U-shaped in the lower, finally disappearing at the skirts. These valleys are empty, for the rain-water that falls on the upper slope of the volcano is soaked into the deposits of clastic ejecta with which the entire slope is loosely covered. The eastern half of the northern flank is dissected by several valleys that open to the sea (Hunkwa Wan or Volcano Bay). Some of them have the permanent streams. The eastern flank is rather gentle up to the summit and is dissected by numerous gulches.

The river Oridogawa runs east through the southern skirt. This is the passage of the lakes Oonuma, Konuma, and Junsainuma, all of which are dammed with mud-flows of the volcano.

The northern skirt is subjected to marine-erosion, being cut into

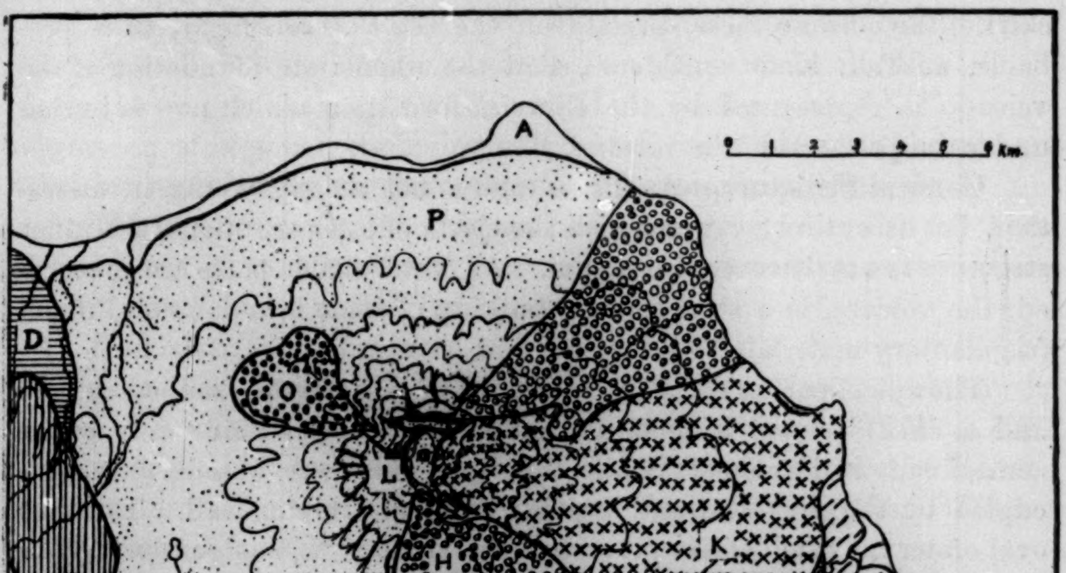

Fig. 1. Geologic sketch-map of Komagatake and its environs, based on Kato's geologic map.

A—Alluvium; O-Osidasizawa mud-flow; K—Kurumizaka mud-flow; H—Horseshoe-shaped crater mud-flow; F—Flowed mound region; P—Pumiceous ejecta; L—Lavas; D—Diluvial terrace-deposits; Y—Yokotudake volcanics; R—Rhyolitic rocks; T—Tertiary.

precipitous sea-cliffs. The elevation of the sea-cliff varies in different parts, generally increasing eastwards. It is especially high in the eastern half of the northern coast, where the thick deposits of mud-flows are subjected to the marine-erosion.

Foundation.—The immediate foundation, on which the volcano has been constructed, may be conjectured from the geology of the neighbouring districts (Fig. 1). The districts adjacent to the volcano are built up of younger volcanics such as rhyolite, andesite, basalt, and allied rocks, along with the Tertiary and Quaternary formations. The volcanics cover the wide areas, southeast as well as southwest of the volcano. The Tertiary formation develops in a narrow zone adjacent to the west, consisting of clayey rocks and tuffs. The Diluvial formation occurs as coastal terraces along the shore outside the area, in which the volcano is situated, and consists of gravel-and pumice-beds; while they are entirely absent along the shore between Sikabe and Mori, where the northern skirt of the volcano faces directly on the sea. Accordingly, it is probable, as Tak. Kato considers[1], that the immediate foundation of the volcano is represented by the Diluvial formation which now is buried under the products of the volcano.

General Structure.—As the volcano is not merely young in dissection, but is entirely covered with the ejecta of later eruptions, the inner structure is not discovered in detail. As far as visible parts are concerned, the volcano is a stratified one built up of some lava-flows and much fragmentary materials.

The apical part of the volcano consists of a horseshoe-shaped caldera and a small central cone in the latter. The eastern side only of the central cone is developed; while the other sides are absent, being occupied by the northern and western parts of the ring-wall. Thus, an oval crater in which active pit-craters are situated, is surrounded by the ring-wall and the crest of the central cone.

On the northwestern flank, there is a knob, Kakaruma-Maruyama, whose outer form suggests it to be a parasitic cone; while nothing is known of its inner structure and building materials, as it is covered with later ejecta. The knobs, Sahara-Maruyama, Akahageyama, etc., on the southeastern flank and numerous hills at the east and south skirts are the mounds composed of lava-blocks and ash-materials, being resulted from accumulation of mud-flows.

1) Tak. Kato, "Geology of Komagatake Volcano (Hokkaidô)," *Report Earthq. Inv. Comm.*, 62 (1909), 1-64, (in Japanese).

Craters.—*Caldera.* The caldera is surrounded on its north, west, and south sides with the ring-wall represented by ridges, viz. Saharadake, Komanose, Komagatake proper, Umanose, and Sumidamori; while on its east side there is a great gap in the ring-wall (Fig. 2, p. 242).

The northern wall, Saharadake, has an unbroken stretch from E. to W. of one thousand meters. Its highest point is 1115·1 m.[2] above sea level. The northwestern wall forms a saddle, Komanose, between the northern and western walls, stretching from N.N.E. to S.S.W., with an uniform crest-line for a length of 500 m. This saddle is the result of a side explosion, by which the upper part of the northwestern wall has been blown away. The western wall culminates in a rocky pinnacle, Komagatake proper, attaining 1140 m. above sea level. The southern wall runs from N.W. to S.E., its highest point, Sumidamori, attaining 880 m. above sea level. There is a saddle, Umanose, between the highest points, Sumidamori and Komagatake proper, on the southern and western walls. The crest-line of this saddle is elevated gradually toward N.W. Thus, the ring-wall is lower on the south than on the north in altitude.

The ring-wall, except for the part of the southern saddle, Umanose, forms an almost perpendicular cliff toward the inside. On the cliff are exposed repeated layers of lava-flows and fragmentary materials.

The eastern gap in the ring-wall has a meridional width of 2 km. from the eastern end of the northern wall, Saharadake, to the eastern end of the southern wall, Sumidamori.

Oval crater. The northern and western parts of the ring-wall and the crest, Namakoyama, of the central cone surround an oval crater, the major and minor axes of which are 1 km. from N.N.E. to S.S.W. and 0.7 km. from W.N.W. to E.S.E. respectively. The configuration of the area within this oval crater has been changed from time to time. During half a century past, it was:

In 1872, when Captain Bridgford[3] visited the volcano, there were six small craters, one of which was then active.

In 1877, according to John Milne[4], there was a pit-crater, 100 m. across and 20 m. deep, from which steam was issuing. There were fissures running to the pit-crater.

In 1889, according to K. Jimbo[5], there were two pit-craters, one of

2) The heights of the ridges above sea level are those read on the topographic map 1:50000, sheet Komagatake, Land Survey Department, 1915.

3) Bridgford, R.M.A., *Transactions of the Asiatic Society*, Tokyo, 2 (1874), 80.

4) J. Milne, "The Volcanoes of Japan," *Transactions of the Seismological Society of Japan*, 9 (1886), 121–122.

5) K. Jimbo, Report on the Geology of Hokkaidô, 2 (Hokkaidô, 1892), 128–129.

which was formed by an eruption in 1856 and the other by an eruption in 1889. The former, 350 m. by 290 m. in size and 100 m. in depth, was situated at the center of the oval crater. The latter, 270 m. across, was situated on the northwest side of the former. Its inside was screened by dense vapor issuing vigorously.

In 1906, a year after an eruption took place, Tak. Kato[6] made a general geological survey of the volcano. Fig. 2 is a crater-map based on the geologic map he made. According to him, the configuration of the area within the oval crater was: A, the pit-crater of 1856, 200 m. across and 30 m. deep, with a central dome from which a little solfataric vapor was issuing. K, a rift-crater of 1905, 200 m. long and 20 m. wide, running northeast. In this rift-crater there were active solfataric vents steaming vigorously. F, a large carter-like depression, the southern part of which was studded with numerous solfataric vents. L, a pit-crater, extinct. Besides these, there were numerous rifts, on which steaming vents were arranged, running from east to west.

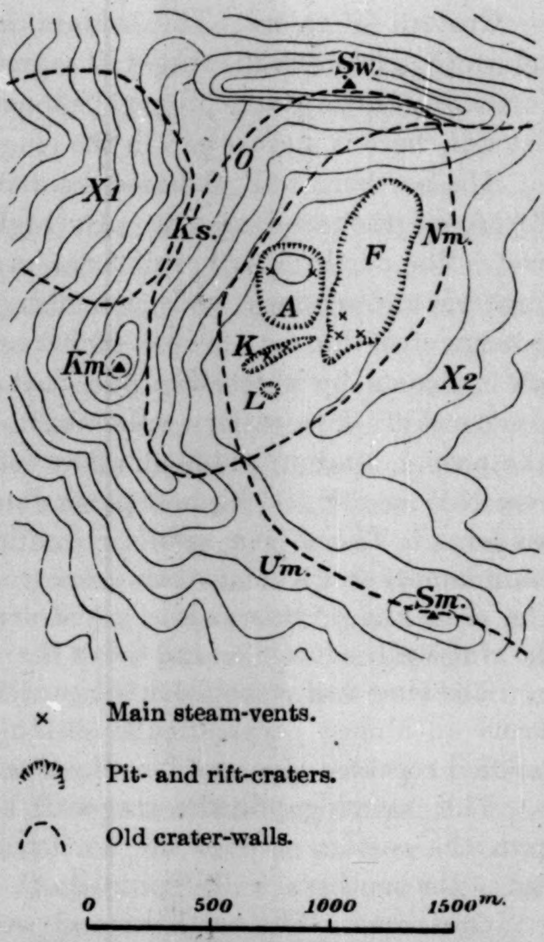

Fig. 2. Sketch-map showing the state of the inside of the caldera in 1906. (After Tak. Kato).

Ridges: Sw—Saharadake; Ks—Komanose; Km—Komagatake; Um—Umanose; Sm—Sumidamori; Nm—Namakoyama.

Craters: X_1—Osidasizawa explosion-crater; X_2—Horseshoe-shaped explosion-caldera; O—Oval crater; A—Crater of 1856; K—Crater of 1905; L—Crater extinct; F—Crater ?

In 1907, C. E. Bruce Mitford[7] visited the volcano. He considered

6) Tak. KATO, *loc. cit.*

7) C. E. B. MITFORD, "Notes on the Physiography of Certain Volcanoes in Northern Japan," *The Geographical Journal*, 31 (1908), 187-198.

the cone, Namakoyama (Nm. in Fig. 3), to be a new one thrown up near the eastern gap of the caldera, for no mention of this cone had been made either by Captain Bridgford or John Milne. K in Fig. 3 was then jointed further east by several longer rifts, which ran parallel to the former, to the flank of Namakoyama. A in Fig. 3 was then 40 m. across and 10–15 m. deep.

In 1909, when I. Friedländer[8] visited the volcano, the western wall, Komagatake proper, of the caldera was passed through by a fissure running toward A in Fig. 3, which was then 50 m. deep. Steam was issuing from this fissure.

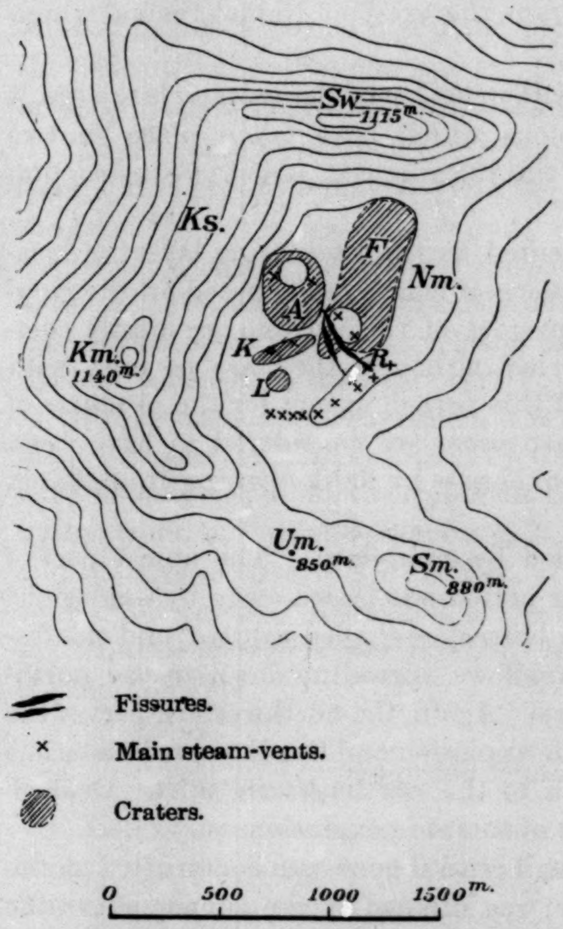

Fig. 3. Sketch-map showing the state of the inside of the caldera in 1918–20. (After A. Imamura).

Sw, Ks, Km, Um, Sm, Nm, A, K, L, and F correspond to those in Fig. 2. R: rift appeared in 1918.

In 1918–20, A. Imamura[9] observed thrice the state of the crater before and after a slight activity displayed in 1919. Fig. 3 is based on the crater-map he made. A, K, L, and F in the figure correspond to those in Fig. 2. According to him, A was then 350 m. by 270 m. in size and 60 m. in depth, with a central cone, somewhat to the north of the center of the crater-floor, from which steam was issuing. Of two vents in K, one at the east was discharging steam most vigorously till 1919 when a slight activity was displayed; while the other at the west was filled with water. There were several steam vents, somewhat to the south of L, on a line running east toward Namako-

8) I. Friedländer, "Über einige japanische Vulkane," *Mitteilungen der Deutschen Gesellschaft für Natur- und Völkerkunde Ostasiens*, 12 (1910), 144–148.

9) A. Imamura, *Report Earthq. Inv. Comm.*, 95 (1921), 92–99, (in Japanese).

yama. In the southern corner of F, there was a mound, 30 m. high and 15 m. across, with solfataric vents on its east, west, and south sides. A rift, R in Fig. 4, 280 m. long and 20–30 m. wide, ran southeast toward Namakoyama through the mound. The activity in 1919 was displayed in this rift.

The bottom of this oval crater was about 300 m. in depth from the top of Komagatake proper and about 130 m. from the crest of Komanose; while it was only 50 m. in depth from the crest of Namakoyama which was about 870 m. above sea level.

Geologic History.—The present structure of the volcano is the result of repeated eruptions and explosions which have taken place in two periods in the geologic history of the volcano, viz. period of construction and period of destruction.[10]

The former period is represented by the alternating layers of lava-flows and fragmentary materials, some of which are exposed on the ring-wall. The northern and western sides of the volcano are mostly composed of the materials of this period, although they are covered with later ejecta. All the materials of this period, except for the products of the parasitic knob, Kakaruma-Maruyama, are considered to have been ejected from the apical crater, for there is no flank opening from which they may have been discharged.

The latter period is represented by mud-flows. The apical part of the cone constructed in the former period was blown away by explosions to result in the formation of the horseshoe-shaped caldera, and the disrupted cone-materials caused mud-flows spreading down to the northeastern, eastern, and southern skirts. Again, the northwestern part of the ring-wall was blown away by a side explosion and the disrupted materials caused a mud-flow spreading down to the northwestern skirt. Osidasizawa explosion-crater is the result of this side explosion.

By subsequent eruptions a small central cone was constructed in the caldera. As its crater (oval crater) was situated by the inner side of the ring-wall, the eastern side only of the cone was developed and the products, agglomerate-lava and mud-flows, discharged from the crater descended the eastern side through the eastern gap of the ring-wall.

It is recognized that volcanic eruption often accompanies either upheaval or depression of the land on which the eruption has taken place. However its cause may be, relative depression of the land occupied by the volcano Komagatake is confirmed by evidences:

10) Tak. KATO, *loc. cit.*

Near sea level of the sea-cliff, 2·5 m. high, at Kakaruma, west of Sahara, is exposed a black soil-bed, 0·3 m. thick, overlain by an ash-bed, 0·2 m. thick, containing fossil plants (stalks and blades) that take roots in the underlying black soil-bed. The ash-bed is then overlain by a pumice-bed, 1 m. thick, which passes upwards into a bed, 1 m. thick, composed of volcanic ashes mingled with pumice-blocks. These succession of beds shows that an ancient land-surface represented by the black soil-bed has been buried under the products of subsequent eruptions of the volcano, and that the ancient land-surface has been brought to sea level by relative depression of the land.

In the lakes Oonuma and Konuma are found numerous submerged trees. It is probable that they are the result of depression of the land by the lakes.[11]

By comparing the result of precise levelling done after the eruption, June 17, 1929, with that previously done, it is confirmed that the land at the northwestern foot of the volcano has been depressed relatively from the land adjacent to the west (Part V, p. 298).

From what has been stated, it is suggested that a differential movement between the land occupied by the volcano and adjacent land may have taken place along the conjugate lines, probably tectonic, represented by the trend of low land extending, N.N.W.-S.S.E., from Mori to Oonuma and the river-course, S.S.W.-E.N.E., of the Oridogawa; and it may be answered by relative depression of the land occupied by the volcano, why the Diluvial terrace is seen nowhere on that land; while it develops on the land outside.

II. Recorded History of Eruption.

The volcano seems to have been active for untold ages, but nothing about its eruption has been recorded but the eruptions since 1640, A. D. The eruptions on record are:

1640 (*17th year of Kwan'ei era*). On June 13, 1640, a great eruption took place. It was accompanied by tunamis and earthquakes. At noon on the same day, the southern coast of the Volcano Bay was visited by tunamis. Ships more than one hundred were wrecked and people more than seven hundreds drowned. During the following three days, the ash fell in the districts, southwest of the volcano.

---

11) F. Omori, "Eruption of Komagatake and the Submerged Trees of Oonuma," *Journal of Geography*, **34** (1922), 133–136, (in Japanese).

1765 (*2nd year of Meiwa era*). A slight eruption took place in 1765.

1784 (*4th year of Temmei era*). On February 8, 1784, an eruption took place.

1856 (*3rd year of Ansei era*). At daybreak on August 26, 1856, earthquakes were felt at the southeastern foot of the volcano. At about 9 a.m., roarings were heard from the volcano and ash-clouds were seen ascending from the summit. Pumices were ejected and fell in the southeastern districts. A large number of houses were destructed by fire started from the hot ejecta. A new pit-crater, A in Fig. 4, was formed by this eruption.

1888 (*21st year of Meidi era*). A small eruption took place. A new pit-crater was formed on the northwest side of the crater of 1856.

1905 (*38th year of Meidi era*). Roarings were heard from the volcano on August 16-17, 1905. In the morning on August 19, the first eruption took place from a newly opened crater, K in Fig. 4. The activity culminated during the next four days. On August 22, a mud-flow caused by rain-fall ran northeast toward Osiranai.

1919 (*8th year of Taisyô era*). On June, 17, 1919, a small eruption took place. A new rift, R in Fig. 4, from which the activity was displayed, was formed. On June 24, another eruption occurred.

1922 and **1924** (*11th year and 13th year of Taisyô era*). In these years, slight activities were displayed.

III. The Eruption of 1929.

The Course of Eruption.—On June 17, 1929, a great eruption of the volcano took place. Taking the accounts by eyewitnesses and by people who live in the neighbourhood, the course of eruption was as follows:

It was about 0:30 a.m., June 17, when rumblings from the volcano were heard at Oonuma. About an hour later rumblings were also heard at Sikabe. Some people there found the volcanic ashes falling at about 3 a.m. Then, rumblings were of frequent occurrence.

During the early morning, the top of the volcano was hidden from view by a dense fog, and it was past 9 a.m., when the top was seen for the first time, discharging dark volutes of ash-cloud.

Simultaneously with heavy rumblings came great explosions at about 10 a.m. In the meantime, volcanic ashes and lapilli began to fall heavily in Sikabe district. Emission of dark ash-cloud increased in

violence, with ejection of incandescent pumice-blocks. Following the violent emissions of dark ash-cloud, flashes of lightning appeared in the midst of the cloud, being accompanied by thunders (Part VII, p. 302). In Sikabe district, the rain of ejecta was steady.

It was past noon when a mass of pumice-blocks ran for the first time over the northwestern saddle, Komanose, in the ring-wall, flowing into the valley Osidasizawa.

At about 1 p.m. or a little later, the ejecta began to fall in Tomenoyu near the mouth of the lake Oonuma.

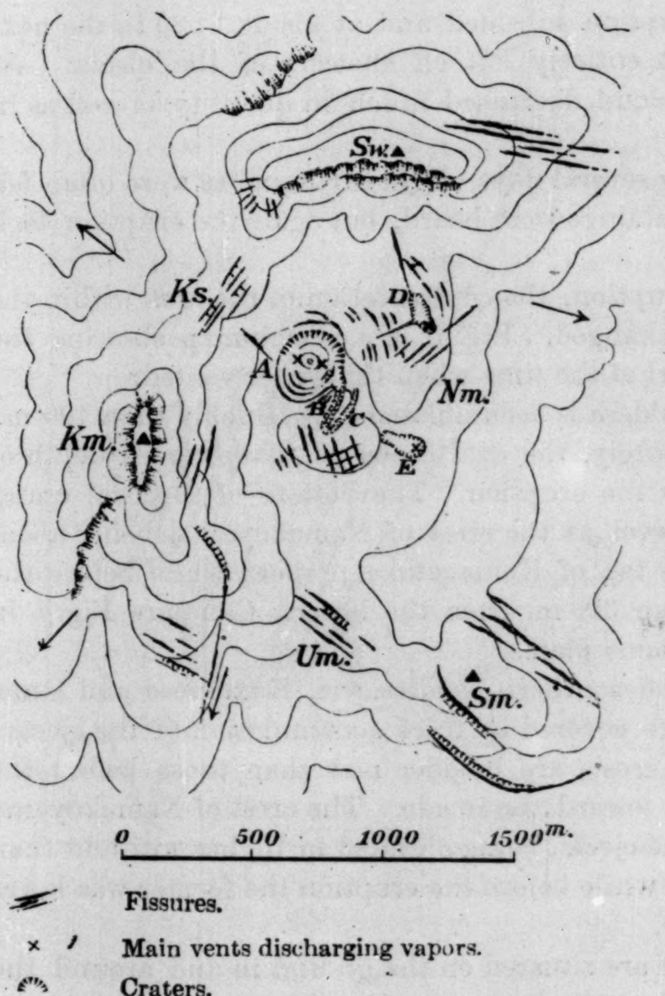

Fig. 4. Sketch-map showing the state of the inside of the caldera after the eruption, June 17, 1929.

The ash-laden cloud was ejected to an enormous height (PL. I, Fig. 1). At 2 p.m., its height measured by a sextant at Hakodate Meteorological station attained about 13000 m. (Part III, p. 275). The cloud expanded outwardly in the cauliflower-shape against the surrounding air (PL. I, Fig. 2). Dispersion through the air of the ejecta was mainly controlled by the prevailing wind (PL. I, Fig. 3). Thus, ashes and sands were borne far into the Pacific in the direction of the upper atmospheric current (Fig. 5); while lapilli and bombs fell in showers from the ash-cloud on the ground within a short distance to the southeast.

After 3 p.m. on, great masses of pumice-blocks were not only projected through the air, but dis-

charged intermittently over Komanose, Umanose, and Namakoyama, toward northwest, southwest, and southeast and descended the mountain-slope (PL. I, Fig. 4). At about 5 p.m., they were also discharged northwards over Saharadake.

The eruption continued through the day into the evening hours. When the night fell, a red look near the crater of the ejecting materials was observed.

At about 7 p.m., the eruption culminated in discharging products, in lightning, and in thundering, and it was almost steady till about 11 : 30 p.m. on the same day.

Thenceforth, the eruption subsided and at about 1 : 30 in the next morning, Sikabe district entirely left off showers of the ejecta. At the same time, the ash-cloud decreased much in quantity as well as in height.

During the following several days, slight earthquakes were often felt (Part III, p. 275) and rumblings were heard, but again no eruption took place.

Craters.—By the eruption, the configuration of the area within the caldera has remarkably changed. Fig. 5 is a sketch-map showing the feature of the crateral part at the time when the writer visited.

The inside of the caldera is accumulated more thickly than 100 m., with the ejecta. Accordingly, the oval crater is shallower in depth of its floor than that before the eruption. The bottom of the oval crater is almost in the same level as the crest of Namakoyama, being about 200 m. in depth from the top of Komagatake proper; while before the eruption it was more than 300 m. from the latter. Compare Fig. 1 in Pl. II with Fig. 2 in the same plate.

The northwestern and southern saddles, viz. Komanose and Umanose, in the ring-wall are covered by thick accumulation of the ejecta; and the grounds of their crests are broader now than those before the eruption, sloping gently toward the inside. The crest of Namakoyama is also accumulated by the ejecta, being elevated to higher altitude than the top of Sumidamori; while before the eruption the former was lower in altitude than the latter.

The active pit-craters are situated on the ground in and around the oval crater. In the oval crater there is a circular pit-crater A, 150 m. across and 50 m. deep, which is successor to the crater formed by an eruption in 1856, A in Fig. 3. The southern wall of this pit-crater slopes gently toward the crater-bottom; while the northern wall is an almost

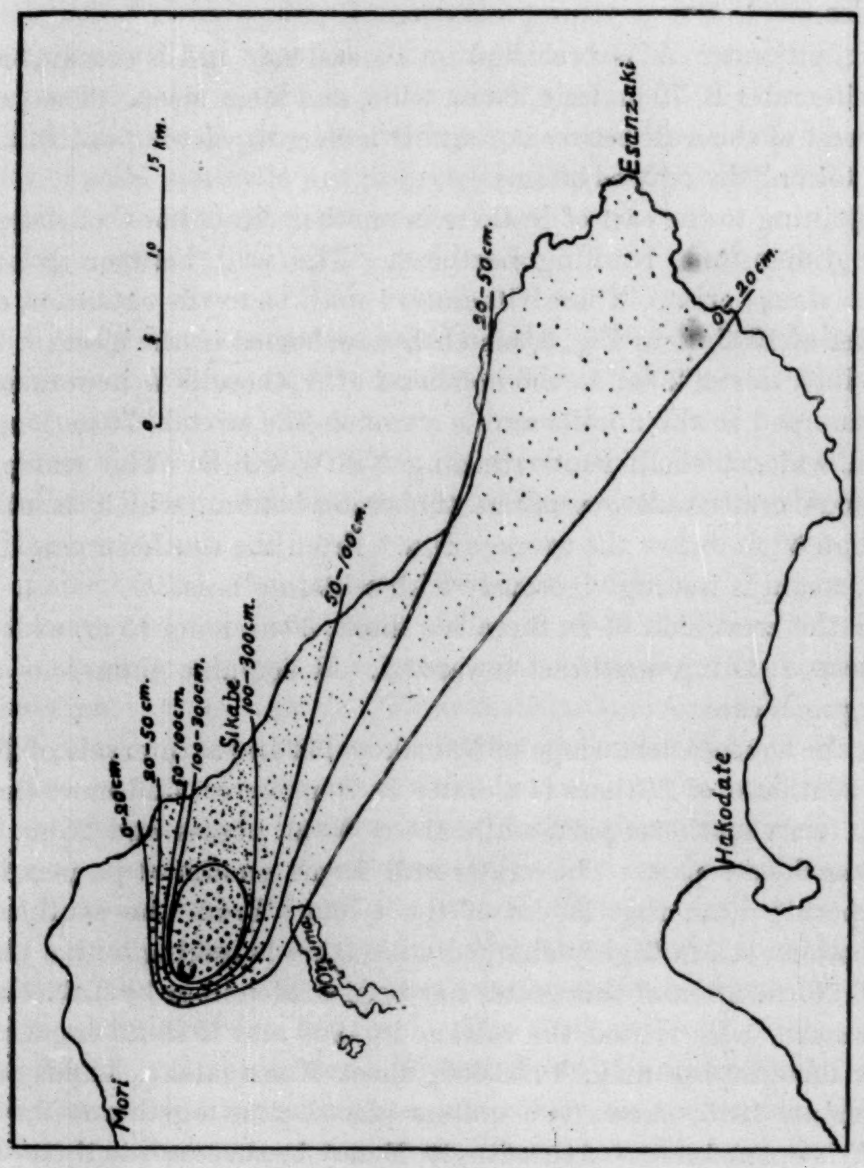

Fig. 5. Map showing the zones of equal thickness of ejecta distributed in the eastern Osima.

perpendicular cliff exposing numerous layers of the ejecta. The crater-bottom is occupied by an ash-covered cone, 20 m. across and 5 m. high, issuing much vapor charged with ashes from the crevices on its east and west sides.

The pit-crater A is breached on its east side and is communicated with a rift-crater B, 70 m. long, 30 m. wide, and 20 m. deep. The ground of the crest of the wall between A and B is narrow, sloping on both sides steeply toward the crater-bottoms.

Adjoining to the east of B, there is another rift-crater C of somewhat smaller dimensions, running northeast. The wall between B and C forms a sharp crest. These rift-craters may be in the extension of the rift-crater of 1905, K in Fig. 3, which is now buried in the ejecta.

At intervals of 20 m. to the northeast of A, there is a new crater D. It is crumped in the middle and is a trench-like stretch, 70 m. long and 20–25 m. wide, of small vents running N.N.W.-S.S.E. The rim of the precipitous crater-wall overhangs the crater-bottom, which is at least more than 30 m. below the average rim. From the southernmost crater-bottom, steam is issuing vigorously with a hissing noise.

On the west side of D, there is a ditch, 30 m. long, 15 m. wide, and 10 m. deep, running southeast toward A. It contains numerous vents discharging steam.

On the southeastern slope of Namakoyama and at intervals of 200 m. to the southeast of A, there is a crater E, 70 m. across and more than 50 m. deep in its southeast part, while about 30 m. across and 25 m. deep in its northwest part. The crater-wall forms an almost perpendicular cliff exposing numerous layers of the ejecta. From the southeastern crater-bottom, steam highly charged with ashes is issuing with a roaring sound. No mention of this crater has been made either by Tak. Kato or A. Imamura, who visited the volcano in 1906 and 1918–20 respectively. But the topographic map, 1 : 50 000, sheet Komagatake, Land Survey Department, 1915, shows two craters placed close together at the place where E is opened now. Accordingly, E may be successor to these shown in the topographic map.

Fissures.—Numerous fissures traverse the ground within the caldera (see Fig. 4). Among them prevail the radial and concentric fissures on the ground around the central pit-crater, A in Fig. 4. In this connection, it is noted that the crater D is situated at an intersecting point of fissures of these two systems and that the crater E consists of two vents arranged in a line running southeast radially from A.

There are also numerous fissures on the internal wall of the caldera. On the flat ground of the crests Komanose and Umanose, the fissures often form trench-like depression along the crests; while on the steep inner slopes of Saharadake, Komagatake proper, and Sumidamori, they form step-faults along which the hanging sides of the grounds slip down, causing occasional avalanches of the tali of ejecta.

Solid Ejecta.—During the paroxysmal phase of the activity, a large quantity of solid materials was projected. The map[12] in PL. VIII shows the distributions of these ejecta on the volcano.

Volcanic ashes, sands, lapilli, and bombs. These cover a large area, southeast of the volcano. Their deposit is the thickest in a zone running from the crater-bowl southeast toward Sikabe, where it attains about 1 m. in thickness, and thins rapidly on both sides of that zone; while there is no accumulation on the western foot of the volcano. Toward the crater, these ejecta naturally increase in thickness of their deposit as well as in individual size. A large quantity of these ejecta fell in the Volcano Bay (Hunkwa Wan) and was washed up by the waves, forming a new beach at about 50 m. off shore along the coast at Sikabe.

Flows of pumice-blocks. These occupy most of the lower slope of the volcano, running through the gaps, viz. Umanose, Komanose, and Namakoyama, in the ring-wall. Their distributions are as follows:

The pumice blocks, which descended the outer slope of Umanose, accumulate on the southwestern skirt between 200 m. and 400 m. in altitude above sea level, forming an extensive elevated ground. Their flows are counted by more than seven. The farthest front of these flows reaches Yakeyama, 6 km. off the crater. The pumice-blocks, which, running over the northwestern saddle, Komanose, flowed into the valley Osidasizawa, accumulate on the northwestern skirt between 100 m. and 400 m. in altitude above sea level. The farthest front of these flows reaches 6·5 km. off the crater. Several flows of pumice-blocks, which ran over Namakoyama, accumulate extensively on the eastern skirt, up to 500 m. in altitude above sea level. The front of one of these flows reaches the shore, north of the cape Dekimazaki. In this area, however, they are overlapped with the deposit of volcanic ashes, sands, lapilli, and bombs. Several flows, which are however less extensive, accumulate on the western and northern skirts.

When descended the steep slopes near the summit of the volcano,

12) For the preparation of the map, the writer is indebted to Mr. K. Yasumuro, the cartographer of this Institute.

the pumice-blocks eroded the surface of the ground to form frequent scars (see Fig. 1 in PL. IV). Accordingly, in the subterminal parts of the flows of pumice-blocks are found occasionally old materials swept by ths flows. At the skirts where the slopes are gentle, the flows stretched in the fan-shape, accumulating thickly upon one another (see Fig. 2 in PL. IV). Earlier flows were pushed aside by later ones, being thrown up like a lateral morain. At places where their courses turn sharply to either side, the flows branched off laterally, even over high ridges. Near the fronts of the flows, pumice-blocks formed numerous mounds elevated 5–30 m. from the general slope.

The pumice-blocks are of all grade of size, up to 1 m. in diameter, and are rounded due to the mutual friction on flowing. They are mingled with fine ash-materials resulted from smashing themselves on flowing. Flowing like a fluidal liquid, the ash-materials are often locally collected.

Temperatures of the solid ejecta. There are several evidences that the solid ejecta were fairly high in temperature when they were projected:

(1) In a large area, southeast of the volcano, where the ejecta fell in quantity, the foliage of trees was entirely scorched and the grasses pinned under the bombs were blackened. At Tomenoyu, about 6 km. from the crater, fire was started by heat from the ejecta, and all houses were burned down.

In the area where the flows of pumice-blocks accumulated, trees buried in the flows were burned, and for several weeks the fire was being smothered with them.

(2) Temperatures of the flows of pumice-blocks were measured by a thermometer and an electric pyrometer with the following results:

Table I.

	Temp. (C)	Date	Loc.
1	180	June 22, 1929	Yakeyama
2	335	June 22, 1929	Yakeyama
3	426	July 2, 1929	Osidasizawa

1. At 25 cm. below the surface of a flow of pumice-blocks.
2. At 51 cm. below the surface of a flow of ash-materials.
3. At 70 cm. below the surface of a flow of ash-materials.

(3) The pumice that flew through the air has a reddish zone inside. On the other hand, there is a reddish zone at a depth below the surface of the flows of pumice-blocks. These facts indicate that the outer crust of pumice-bomb and the surfacial part of the flow of pumice-blocks were rapidly cooled; while the zones inside retained for a sufficient length of time at a sufficiently high temperature to be oxidized by circulating air.

In order to ascertain the temperature at which oxidation took place, some laboratory study was made of the pumice. The results are discussed in the next paper (see p. 271).

(4) The temperature, at which the pumice had ever been, was ascertained from the microscopic study of the xenoliths found in the bread-crust bombs. A xenolith is of hornfels structure, and is similar in component minerals to some contact metamorphosed rocks, consisting of quartz, plagioclase, pyroxene, wollastonite, and accessory minerals (accidental xenolith, see p. 267). Among the component minerals of the xenolith, quartz occur in aggregates at the contact between the xenolith and the host rock (see Fig. 6). This fact indicates that the quartz was formed after the xenolith had been caught by the lava in which it occurs. Accordingly, the quartz is useful as a geologic thermometer in ascertaining the temperature, at which the lava might have been before it was ejected as the bread-crust bombs.

Fig. 6. An accidental xenolith in a piece of bread-crust bomb.

There are evidences that the quartz in the xenolith has suffered the

high-low inversion. On the other hand, it is certain that the quartz is not that which has changed from tridymite. Therefore, it may be said that the quartz has ever been at a temperature above the high-low quartz inversion point (573°C. at one atmosphere pressure); but that it has not been retained for a sufficient length of time at a temperature above the quartz-tridymite inversion point (870°C. at one atmosphere pressure) to be transformed to tridymite. The high-low quartz inversion point is raised about 23°C for 1000 megabaryes of pressure, and the quartz-tridymite inversion point about 100°C. for 1000 megabaryes of pressure. But, practically, the influence of pressure on these inversion points may be negligible in near-surface conditions in which the quartz in the xenolith may have been formed.

From what has been stated, it may be concluded that the lava, in which the xenolith occurs, was at a temperature above 573°C., but it was not retained for a sufficient length of time at a sufficiently high temperature above 870°C. to transform the quartz in the xenolith to tridymite.

The same xenolith contains low-wollastonite. Accordingly, it may be said that the lava, in which the xenolith occur, did not heat the xenolith at a temperature above 1180°C. (high—low wollastonite inversion point) for a time sufficiently long for inversion of the wollastonite. But, unless its chemical composition is known, wollastonite is uninstructive as the geologic thermometer, for its inversion temperature is highly effected by the presence of $MgSiO_3$ which the wollastonite may take into solid solution.

Secondary mud-flows. Dark ashes that fell during the days after the activity cover the deposits of ejecta, June 17, 1929, on the east slope and the eastern half of the northern slope of the volcano. The temporary drainages caused by the rain-water furrowed the slopes covered with the ashes, and carried the materials down. In the lower courses they cut gulches through the deposits of ejecta. Thus, the ashes and pumice-fragments conmingled with rain-water formed the secondary mud-flows that devastated the areas along the valleys on the eastern half of the northern slope.

Solfataras.—There are two kinds of solfataras, viz. primary solfatara and secondary solfatara. The primary solfataras are those in which the water-vapor and gas may be directly fed from the main source of activity. The secondary solfataras are those which develop upon the flows of pumice-blocks (see Fig. 3 in PL. IV). Far more active and longer-lived are the primary solfataras formed upon a series of fissure on the ground around the active craters.

The secondary solfataras are relatively short-lived, for their sources are limited to the volatile substances occluded in the flows of pumice-blocks. They follow either cracks, with which the flows of pumice-blocks are traversed, or zone of contact of one flow of pumice-blocks with other. They apparently fluctuate in number according to the weather, for in fine weather heated gas is emitting without visible condensation of water-vapor. But, as time passes, they decrease in number and show declining activity in temperature as well as in emanation.

The gas from the solfataras may be uninstructive in its composition, for it is liable not only to contain extraneous matter derived from the terranes it traverses, but also to mix with air when it passes through crevices. According to incomplete analyses by S. Tanaka, the gases collected (air-displacement method) at solfataras on the ground near the active craters and on a flow of pumice-blocks consist, except for the water-vapor, mainly of sulphur dioxide, with carbon dioxide, oxygen, and much nitrogen. A larger amount of carbon dioxide was detected in the gas from a solfatara on the flow of pumice-blocks. It may be due to burning of trees buried under the flow of pumice-blocks, through which the gas traverses.

The solfataras are incrusted with sublimates, white, yellow, red, and brown in color. In accompany with ash-materials, the sublimates at a solfatara on the ground near the active crater A were collected in a flask, which after collection of the sublimates was sealed by fusing its mouth. The analyses by S. Tanaka[13] of the sample are as follows:

Composition of mixture

Insoluble matter	59·80
Soluble matter	14·50
S	3·70
H_2O	22·00

Composition of soluble matter

SO_4	29·38
Cl	44·52
Fe″	1·01
Fe‴	6·00
Al	8·38
Ca	7·52
Mg	1·63
Na	1·56
Total	100·00

13) For the chemical analyses published in this paper, the writer is indebted to Mr. S. Tanaka, the analyst of our Institute.

The soluble matter may be in the forms of salts as follows:

$FeSO_4$	2·75
$Fe_2(SO_4)_3$	21·48
$Al_2(SO_4)_3$	14·43
$AlCl_3$	30·16
$MgCl_2$	6·38
$CaCl_2$	20·83
NaCl	3·97
Total	100·00

Among the sublimates formed by the solfataras on the flows of pumice-blocks, ammonium chloride is also found. Sometimes, these sublimates are sooted by carbon probably derived from trees buried under the flows of pumice-blocks. In the ashes are detected metallic sulphides even at places where solfataras are absent. In accompany with the ash-materials, they might be ejected from the craters in which the primary solfataras were depositing them.

The temperatures of the solfataras, primary as well as secondary, are variable from time to time and from one to other. They also depend on the depths from the mouths of the solfataric vents, where they are measured. In Table 3 are shown some data as to the temperatures at various solfataras on the ring-wall.

Table II.

	Temp. (C)	Date	Loc.
1	73	July 1, 1929	Sumidamori
2	170	"	"
3	340	"	"
4	275	July 1, 1929	Saharadake
5	375	"	"

1, 2. On solfataric vents.
3. On fissure discharging solfataric gas.
4, 5. On fissures discharging solfataric gas.

IV. Petrography of the Ejecta of 1929.

There are three kinds of the ejecta of 1929, viz. juvenile ejecta, accessory, and accidental ones. Besides these, some of the juvenile ejecta have xenoliths. Petrographic descriptions of these ejecta and xenoliths will be given below.

A. Juvenile Ejecta.

Pumice (*Two-pyroxene-andesite*). (Figs. 1, 2, & 3, PL. VI).

Mode of Occurrence.—There are three different modes of occurrence of the pumice: (1) Pumice occurs as a thick deposit that covers a large area, southeast of the volcano; (2) It occurs as the bread-crust bombs scattering on the deposit in a limited area, southeast side of the volcano; (3) it occurs as numerous flows occupying most of the lower slope of the volcano.

Megascopic Characters.—The pumice of the first category is angular and is of three grades—sands, lapilli, and bombs—in size. The pumice of sands-and lapilli-grades are white; while the pumice of bomb-grade is white on its surface, with a reddish zone inside, representing probably the zone of oxidation on cooling (see p. 253)

The pumice of the second category has a denser bread-crusted surface surrounding the pumiceous interior. It is white inside and ash-gray outside. In this pumice, the effect of oxidation is generally absent.

The pumice of the third category is rounded due to the mutual friction on descending the slope, and is up to about 1 m. in diameter. Each piece of pumice that is exposed to the air is generally white; while its bottom-side is red, representing probably the zone of oxidation on cooling.

In hand-specimens of any pumice above mentioned, phenocrysts of plagioclase (1·5 mm. by 1·0 mm. in size) and pyroxene (1·5 mm. by 1·0 mm. in size) are scattered through the vitreous groundmass. Grouped phenocrysts of these minerals are often enclosed in vesicles.

Microscopic Characters.—Phenocrysts seen under the microscope are plagioclase, hypersthene, augite, in the decreasing order of amount.

Plagioclase phenocryst in the pumice of the first and third categories is euhedral and prismatic. Albite twin, often combined with the Carlsbad twin, is common, but the pericline twin is rare. Faint zoning of less and more calcic plagioclases is exhibited. Extinction angles on a zoned crystal are: $X \wedge (010) = 43{\cdot}5°$, $X \wedge (010) = 34{\cdot}5°$. $n_{1D} = 1{\cdot}564(3)$. Optic

character: positive. Accordingly, the plagioclase phenocryst was identified as a calcic labradorite Ab_{31} An_{69}. It contains numerous inclusions of brown glass and rare inclusions of pyroxene.

Plagioclase phenocryst in the pumice of the second category is euhedral, but occasionally is broken into pieces. It is not zonally built. Albite and Carlsbad twins are common. Extinction angles are: $Z \wedge (001)=42°$, $Y \wedge (001)=47°$. $n_{1D}=1{\cdot}561(8)$, $n_{2D}=1{\cdot}569(3)$. Optic character: positive. Thus, the plagioclase phenocryst was identified as a labradorite Ab_{38} An_{62}.

Pyroxene phenocrysts in the pumice of all categories are identical. Hypersthene is euhedral and prismatic parallel to c-axis. It is moderately pleochroic with the axial colors: Z—light green, Y—yellowish brown, X—light brown. Optic plane is parallel to c-axis. $n_{1D}=1{\cdot}700(5)$. The mineral contains, as inclusions, plagioclase and glass. Augite is euhedral and is in a short prismatic form with (100), (010), (110), and (111). Twinning after (100) is often developed. Extinction angle: $c \wedge Z=50°$. $n_{1D}=1{\cdot}693(5)$. The mineral contains inclusions of plagioclase, magnetite, and glass.

Groundmass is a colorless glass. It is very vesicular, flow-structure being well marked. $n_D=1{\cdot}493(5)$.

Chemical Compositions.—The chemical analyses of the pumices were made by S. Tanaka, the analyst of our Institute, with the following results.

Table III.

	Wt. %		Norms		
	1	2		1	2
SiO_2	59·15	59·35	Q	16·10	16·33
Al_2O_3	17·00	16·42	Or	5·56	5·00
Fe_2O_3	2·68	3·38	Ab	28·31	27·26
FeO	4·74	5·54	An	28·65	28·09
MgO	2·84	2·96	Di	2·97	5·51
CaO	7·21	7·17	Hy	11·37	11·33
Na_2O	3·34	3·25	Mt	3·94	4·86
			Il	1·22	1·21
			Ap	0·31	0·31

(*to bo continued.*)

Table III. (*continued.*)

	Wt. %			Ratios	
K_2O	0·93	0·88		1	2
H_2O^{+}	0·72	0·28	$\frac{Sal}{Fem}$	3·9	3·3
H_2O^{-}	0·09	0·02			
TiO_2	0·64	0·67	$\frac{Q}{F}$	0·25	0·27
P_2O_5	0·21	0·20	$\frac{K_2O'+Na_2O'}{CaO'}$	0·62	0·60
MnO	0·18	0·20			
Total	99·73	100·32	$\frac{K_2O'}{Na_2O'}$	0· 8	0·17

1. Pumice-block of 1929 flowing down the slope into Yakeyama.
2. Bread-crust bomb of 1929, from Sumidamori. Includes S 0.34.

According to the C. I. P. W. quantitative system of classification, the pumice-block from Yakeyama belongs to Tonalose (II. 4. 3(4). 4) and the bread-crust bomb from Sumidamori to Tonalose (II. 4. 3(4) 4(5)).

Comparison with the Old Rocks.—According to Tak. Kato,[14] the rocks of the volcano are of the types:

1. Two-pyroxene-andesite.
2. Olivine-bearing two-pyroxene-andesite.
3. Quartz-hypersthene-andesite.

Lavas and pyroclastic products of which the volcano is built are mostly two-pyroxene-andesite. Olivine-bearing two-pyroxene-andesite occurs locally among the rocks exposed at Saharadake. Quartz-hypersthene-andesite occurs as a dike (1 m. thick) at Kakaruma-Maruyama. Some of the phenocrysts contained in these rocks were examined optically by the writer. The results are shown in Table IV, with those of the pumice of 1929.

14) Tak. Kato, *loc. cit.*

Table IV.

	Plagioclase (n_{1D})	Hypersthene (n_{1D})	Augite (n_{1D})
1	1·562(3)	n. d.	1·6940
2	1·5630	n. d.	1·6940
3	1·565(1)	n. d.	1·693(5)
4	1·562(7)	n. d.	1·693(2)
5	1·563(3)	n. d.	1·6940
6	1·544(9)	1·699(3)	—
7	1·564(3)	1·700(5)	1·693(5)
8	1·561(8)	1·700(5)	1·693(3)

1. Olivine-bearing two-pyroxene-andesite···Komagatake lava.
2. Two-pyroxene-andesite···Basal lava.
3. Two-pyroxene-andesite···Komagatake lava.
4. Two-pyroxene-andesite···Umanose mud-flow.
5. Two-pyroxene-andesite···Kurumizaka mud-flow.
6. Quartz-hypersthene-andesite···Dike at Kakaruma-Maruyama.
7. Two-pyroxene-andesite···Pumice of 1929.
8. Two-pyroxene-andesite···Bread-crust bomb of 1929.

The above table shows that the rocks of Komagatake, except the rock occurring as dike, vary within a very limited range of composition of plagioclase. The phenocrysts in the pumices of 1929 do not differ much in composition from those in the rocks which build the visible parts of the volcano. From this fact, it is inferred that the volcanic history, from the ejection of the visible oldest products to the recent day, is limited to a relatively short interval in the cooling history of the magma.

2) *Ashes and Sands.* These are found abundantly in accompany with the lapilli and bombs. Ashes and sands are white in color, consisting under the microscope mainly of splinters of colorless glass and fragments of minerals (plagioclase, augite, and hypersthene) that occur as phenocrysts in the pumice, with a negligible amount of magnetite grains. Accordingly, it is probable that they were derived from subdivision due to explosions of the pumice.

Ash-materials also occur in the flows of pumice-blocks. They are white; but sometimes red, having been oxidized on cooling. The ash-materials are composed, under the microscope, of comminuted glass, with fragments of plagioclase, augite, and hypersthene. The glass fragments in the reddish ash-materials are stained under the microscope with reddish dusts, probably microcrypt particles of oxidized magnetite. The ash-materials may be considered to have been derived from smashing of the pumice-blocks on flowing.

B. Accessory Ejecta.

Accessory ejecta occur as fragments of two grades, lapilli and bombs. They are found on the southeast slope of the volcano, in accompany with the juvenile ejecta. Principal types of the accessory ejecta will be described in the order: 1) scoriaceous ejecta; 2) glassy ejecta; 3) porphyritic ejecta; and 4) crystalline ejecta.

1) *Scoriaceous Ejecta* (*Two-pyroxene-andesite*). (Fig. 4, PL. VI).

Megascopic Characters.—These are dark gray; sometimes banded with white pumiceous base. They are vesicular, porphyritic, and are crowded, especially in the vesicles, with megacrysts, 0·5 mm. in average diameter, of plagioclase and pyroxene. Occasionally, they enclose fragments of foreign materials.

Microscopic Characters.—Phenocrysts seen under the microscope are: plagioclase, augite, and hypersthene.

Plagioclase phenocryst is euhedral, and is twinned in simple and polysynthetic lamellae according to the Carlsbad and albite laws. Faint zoning of less and more calcic plagioclases is exhibited. $c \wedge Y'$ (on 010)= 24·5°. $n_{1D}=1{\cdot}5610$, $n_{2D}=1{\cdot}565(2)$. Optic character: positive. Accordingly, the plagioclase phenocryst was identified as labradorite $Ab_{38}An_{62}$. The mineral has numerous inclusions of brown glass.

Augite phenocryst is euhedral, of staut prism, 0·1–2 mm. in length, and is greenish brown in color. Lamellar twinning on (100) is often exhibited. $c \wedge Z$ (on 010)=50°. $n_{1D}=1{\cdot}692(7)$. Inclusions are: plagioclase and magnetite.

Hypersthene is euhedral, 0·5 mm. by 0·2 mm. in size, and pleochroic with the axial colors: Z–green, Y–yellowish brown, X–light brown. Optic plane is parallel to c-axis. $n_{1D}=1{\cdot}7010$.

Groundmass is hyalopilitic, with plagioclase laths, 0·1 mm. in length, augite and magnetite. The glass base is brown and vesicular.

Microscopic inclusions of foreign materials are often found. One of them is angular, 1 mm. across, porphyritic, and holocrystalline, consisting of plagioclase, augite, hypersthene and magnetite, with biotite developed around the pyroxene crystals.

Chemical Composition.—A specimen of the scoriaceous ejecta was chemically analysed by S. Tanaka, with the following result.

Table V.

	Wt. %		Norm		Ratios
SiO_2	58·03	Q	13·80	$\frac{Sal}{Fem}$	3·4
Al_2O_3	18·04	Or	4·45		
Fe_2O_3	2·63	Ab	25·15	$\frac{Q}{F}$	0·21
FeO	5·36	An	33·64		
MgO	3·17	Di	12·44	$\frac{K_2O'+Na_2O'}{CaO'}$	0·4
CaO	7·95	Hy	4·79	$\frac{K_2O'}{Na_2O'}$	0·16
Na_2O	2·99	Mt	3·71		
K_2O	0·65	Il	1·22		
$H_2O^{+}_{-}$	0·19 0·04	Ap	tr.		
TiO_2	0·61				
P_2O_5	0·18				
MnO	0·18				
Total	100·02				

According to the C. I. P. W. quantitative system of classification, it belongs to Bandose (II. 4′. 4. 4 (5)).

2) *Glassy Ejecta* (*Two-pyroxene-andesite*). (Fig. I, PL. VII).

Megascopic Characters.—These are angular, black or dark brown, and compact. Phenocrysts of plagioclase (1 mm. by 0·7 mm. in size) and pyroxene (2 mm. by 0·5 mm. in size) are scattered through the glass base.

Microscopic Characters.—Phenocrysts seen under the microscope are: plagioclase, augite, and hypersthene.

Plagioclase phenocryst is euhedral and is twinned according to the albite, Carlsbad, and rarely pericline laws. Faint zoning of less and more calcic plagioclases is exhibited. $n_{1D}=1{\cdot}564(3)$, $n_{2D}=1{\cdot}5720$. Optic character: positive. Accordingly, the plagioclase phenocryst was identified as a calcic labradorite $Ab_{31}An_{69}$. Inclusions are: plagioclase, pyroxene, and brown glass.

Augite is euhedral, of staut prism, and is greenish brown in color. Twinning on (100) is common in either simple or polysynthetic lamellae. $n_{1D}=1{\cdot}693(2)$.

Hypersthene is euhedral and pleochroic, with the axial colors: Z – green, Y – yellowish brown, and X – light brown. Optic plane is parallel to c–axis. $n_{1D}=1{\cdot}703(6)$.

Accessory minerals are magnetite and apatite. Magnetite occurs as subhedral or euhedral isometric crystals, about 0·2 mm. across. Apatite is 0·05 mm. long and occurs either as inclusions in the phenocrysts or isolated crystals.

Groundmass is a glass, colorless or brown. The brown part of the glass shows a sinuous flow-structure, with slender laths of plagioclase microlite. The colorless part of the glass is: $n_D=1{\cdot}494$. Vesicles are not common.

Chemical Composition.—A chemical analysis of the glassy ejecta was made by S. Tanaka, with the following result.

Table VI.

	Wt. %		Norm		Ratios
SiO_2	58·25	Q	13·19	$\frac{Sal}{Fem}$	3·23
Al_2O_3	17·50	Or	5·56	$\frac{Q}{F}$	0·22
Fe_2O_3	2·68	Ab	25·15	$\frac{K_2O'+Na_2O'}{CaO'}$	0·50
FeO	5·45	An	31·69	$\frac{K_2O'}{Na_2O'}$	0·21
MgO	3·40	Di	12·61		
CaO	7·79	Hy	5·69		
Na_2O	3·04	Mt	3·94		
K_2O	0·77	Il	1·37		
H_2O^+	0·25				
H_2O^-	0·06				
TiO_2	0·71				
P_2O_5	0·16				
MnO	0·20				
Total	100·26				

According to the C. I. P. W. quantitative system of classification, it belongs to Bandose (II. 4'. '4. 4').

3) *Porphyritic Ejecta* (*Two-pyroxene-andesite*).

Megascopic Characters.—These are angular, compact, and dark gray. Phenocrysts of plagioclase (1 mm. by 2 mm. in size) and pyroxene (1 mm. by 0·5 mm. in size) are scattered through an aphanitic groundmass.

Microscopic Characters.—Microscopically these are dopatic in texture, with phenocrysts of plagioclase, augite, and hypersthene.

Plagioclase phenocryst is euhedral and is twinned according to the albite and Carlsbad laws. Faint zoning of less and more calcic plagioclases is exhibited. $n_{1D}=1{\cdot}564(5)$. Accordingly, the plagioclase phenocryst was identified as a calcic labradorite $Ab_{31}An_{69}$. Inclusions are: plagioclase, pyroxene, and brown glass.

Augite phenocryst is euhedral, prismatic, and light greenish. Simple and lamellar twinning on (100) are present. $c \wedge Z=48.°$ $n_{1D}=1{\cdot}693(4)$. Plagioclase inclusions are commonly observed.

Hypersthene is euhedral, prismatic, and pleochroic, with the axial colors: Z—clear green, Y—pale yellow, and X—light brown. Penetration twinning is rarely developed. Optic plane is parallel to c–axis. $n_{1D}=1{\cdot}702(2)$. Inclusions are: plagioclase, apatite, and glass.

Augite and hypersthene are usually altered to an uralitic hornblende. The alteration occurs along the borders or the cleavage planes of the pyroxenes. The hornblende is fibrous or is in the forms of the pyroxenes. It is green and weakly pleochroic. Optic character: negative. Elongation: positive. $n_{1D}=1{\cdot}640$.

4) *Crystalline Ejecta* (*Two-pyroxene-porphyrite*).

Megascopic Characters.—These are light gray, holocrystalline, and porphyritic. Phenocrysts (1–1·5 mm. in diameter) of plagioclase, pyroxene, and rarely of hornblende are seen with the naked eyes.

Microscopic Characters.—Microscopically, these are persemic or dosemic in texture, consisting of plagioclase, augite, hypersthene, and hornblende, with the groundmass composed of feldspar, biotite, quartz, magnetite, and apatite.

Plagioclase phenocryst is euhedral and is twinned according to the albite, Carlsbad, and pericline laws. Zoning of less and more calcic plagioclases is strongly exhibited. Extinction angles in a crystal cut normal to X are: $Y \wedge (010)=33°$ in the core part of the crystal, and $Y \wedge (010)=27°$ in the shell part. Accordingly, the plagioclase varies in composition

from $Ab_{25}An_{75}$ in its core part to $Ab_{40}An_{60}$ in its shell part. Optic character: negative. A cleavage piece showed $n_{1D}=1{\cdot}5640$. Inclusions are: plagioclase, pyroxene, and glass.

Augite is euhedral and light brownish. Twinning is present in lamellae parallel to (100). $n_{1D}=1{\cdot}693(7)$.

Hypersthene is euhedral and moderately pleochroic, with the axial colors: Z—green, Y—light yellow, and X—brown. Contact and penetration twinnings are developed. Optic plane is parallel to c-axis. $n_{1D}=1{\cdot}700$.

Hornblende is euhedral and green. $c \wedge Z'=16°$. $n_{1D}=1{\cdot}662$, $n_{2D}=1{\cdot}673-1{\cdot}678(5)$.

Feldspars in the groundmass are both plagioclase (andesine) and orthoclase which is however negligible in amount.

Biotite occurs as isolated flakes (0·15 mm. in length) or as rims surrounding the pyroxene crystals.

Quartz is anhedral, filling the interstices of other minerals.

C. Accidental Ejecta.

The accidental ejecta are of two types:

1) *Accidental Ejecta—α-type.* These are gray, aphanitic, and show sometimes a perlitic luster on their surfaces. Microscopically, they are holocrystalline, millimeter-grained, and somewhat of hornfels structure, consisting of quartz, orthoclase, plagioclase, magnetite, rutile, together with vein-like swarms of quartz, magnetite, biotite, and rhombic pyroxene.

2) *Accidental Ejecta—β-type.* (Fig. 2, PL VII).

Megascopic Characters.—These are light gray in color, holocrystalline, and fine-grained. Minerals seen with the naked eyes are plagioclase and pyroxene.

Microscopic Characters.—Under the microscope these are decimillimeter-grained, of hornfels structure, but sometimes of poikilitic texture, consisting of plagioclase, orthoclase, hypersthene, quartz, magnetite, and apatite.

Plagioclase is subhedral or anhedral, and 0·05–0·7 mm. across. It is twinned according to the albite and Carlsbad laws. Zoning of less and more calcic plagioclases is absent. $n_{1D}=1{\cdot}550(3)$. Optic character: positive. Accordingly, the plagioclase was identified as a calcic andesine $Ab_{56}An_{44}$.

Orthoclase occurs as an interstitial matter or oikocryst for plagioclase and hypersthene. It also occurs as small anhedral crystals, often arranged in parallel extinction, in plagioclase.

Hypersthene is subhedral or anhedral, and 0·01–0·2 mm. long. It is moderately pleochroic, with the axial colors: Z—green, Y—yellowish green, X—brown. Optic plane is parallel to c–axis. $n_{1D}=1{\cdot}701(3)$. The hypersthene crystals are sometimes set in lines, exhibiting parallel extinction.

D. Xenoliths.

Xenoliths, accessory and accidental, are found almost always in the bread-crust bombs. They occur as nucli in voids within the bombs, there being either attached to the walls of the voids, or detached from the latter. Occasionally, they are coated with thin crust of the material of the bomb. These xenoliths are:

1) *Accessory Xenolith* (*Two-pyroxene-andesite*).

Megascopic Characters.—This is compact, angular or rounded, and is dark or light gray in color. Phenocrysts (2 mm. by 1 mm. in size) of plagioclase and pyroxene are scattered through an aphanitic groundmass.

Microscopic Characters.—This is markedly porphyritic and sempatic. Phenocrysts seen under the microscope are plagioclase, augite, and hypersthene.

Plagioclase phenocryst occurs as simple euhedral crystals or glomeroporphyritic groups. Albite and Carlsbad twins are common, and penetration twinning is rarely exhibited. Faint zoning of less and more calcic plagioclases is developed. $n_{1D}=1{\cdot}5650$, $n_{2D}=1{\cdot}568(4)$. Optic character: positive. Accordingly, the plagioclase phenocryst was identified as a calcic labradorite $Ab_{31}An_{69}$. Inclusions are: plagioclase, pyroxene, and brown glass.

Augite phenocryst is euhedral, of staut prismoid, and light greenish. Lamellar twinning on (100) is often developed. $c\wedge Z=48°$. $n_{1D}=1{\cdot}693(5)$. Inclusions are: plagioclase, hypersthene, and brown glass.

Hypersthene is euhedral and prismatic. It is moderately pleochroic, with the axial colors: Z—light green, Y—light yellow, X—light yellowish brown. Penetration twinning is often developed, there $c\wedge c$ being about 60°. Optic plane is parallel to c-axis. $n_{1D}=1{\cdot}701(5)$. Inclusions are: plagioclase and brown glass.

Groundmass is intersertal in texture and percrystalline or docrystalline, consisting of plagioclase laths (0·1 mm. long), augite grains (0·01 mm. across), magnetite, and glass.

2) *Accidental Xenolith.* (Fig. 3, PL. VII).

Megascopic Characters.—This is compact, angular, about 3 cm. across, and is light gray in color. It is microcrystalline and only mineral seen with the naked eyes is quartz. Quartz grains (1–0·3 mm. across,) occur in irregular pathes or are scattered through the mass. Besides these, quartz crystals occur in aggregates at the boundary between the xenolith and the host rock.

Microscopic Characters.—Microscopically, this is holocrystalline, seriate homoid but sometimes poikilitic in fabric, consisting of about 45 parts quartz, 20 parts plagioclase, 15 parts pyroxene, 10 parts wollastonite, and 10 parts magnetite, titanite, and zoisite.

Quartz is anhedral, and forms a mosaic in which the grains of quartz and plagioclase lie in contact with each other. Again, it occurs as oikocrysts for other minerals. It is very clear, and is traversed uniformly by irregular cracks, sometimes showing a distinct biaxiality. These facts indicate that the quartz underwent the high-low inversion (p. 253).

Plagioclase occurs either as chadacrysts for the quartz or a mosaic of subhedral crystal grains, less than 0·1 mm. in diameter. Albite twin is common. $n_{1D}=1{\cdot}5750$, $n_{2D}=1{\cdot}581(7)$. Accordingly, the plagioclase was identified as bytownite-anorthite $Ab_{10}An_{90}$.

Augite is subhedral or anhedral, 0·05 mm. across, and is greenish brown in color. Lamellar twinning is often developed. n_{1D} and n_{2D} are larger than 1·701.

Wollastonite occurs as anhedral crystal grains (0·05–0·1 mm. across) arranged in parallel extinction, or as long-continued crystals filling the interstices of other minerals. Lamellar twinning is developed. Optic character: positive. Optic plane is perpendicular to b-axis, that is, elongation: positive or negative. In sections perpendicular either to X or Y are developed two systems of cleavage cracks, one parallel and the other normal to the optic plane. Optic angle is small. Double refraction (γ-α) is fairly high, green color of the second order being exhibited on a section, about $20\mu\mu$ thick.

Among the accessory minerals, magnetite is isometric and 0·05–0·1 mm. across. Titanite is euhedral, 0·05 mm. across, and light yellowish, exhibiting distinct pleochroism. Zoisite, which is however rare, is 0·1 mm. across. Its optic character is positive and elongation negative.

V. Summary and Conclusions.

Komagatake is a homate composed of repeated layers of lava-flows and fragmentary materials of two-pyroxene-andesite. As far as the visible parts are concerned, lavas are quite inferior in amount to fragmentary materials. This fact suggests probably the explosive nature of the activity which has been displayed at the volcano. The apical part of the volcano has been blown away by explosions to result in the formation of a caldera, from which mud-flows spread down eastwards through the eastern gap in the ring-wall. The products of later eruptions build up a cone occupying the inside of the caldera. This cone, together with the northern and western parts of the ring-wall, embrace an oval crater in which several pit-craters are opened.

In historic times the activity has been frequently displayed in the oval crater. Accordingly, the configuration of the area within the oval crater has changed from time to time, probably in the courses of eruptions that took place in the years: 1640, 1765, 1784, 1856, 1888, 1905, and 1919.

In recent years the volcano had continued its activity in discharging solfataric gas, but no surface manifestation of the activity, which might be a preliminary symptom of coming of the eruption on June 17, 1929, was observed at the volcano.

The activity began with an earthquake and rumbling noises at about 0:30 a.m., June 17, 1929. Thenceforth, the activity had gradually increased in discharging volcanic ashes and in rumblings till about 10 a.m., when a great explosion came in accompany with an earthquake. Since then, emission of ash-laden cloud, ejection of pumice, and earth-tremor had been done almost without interruption. In the afternoon of the same day, a large amount of pumice-blocks was projected over the ring-wall, still retaining hot gas, and spreaded down to the skirts of the volcano. The eruption continued through the day into the evening hours. At about 11:30 p.m. on the same day, it subsided; while violent emission of ash-laden cloud continued for the following several days.

The configuration of the area within the oval crater was remarkably changed by the eruption. The inside of the oval crater was filled with the deposit of the newly ejected materials; and three groups of pit-craters, two of which are successor to those before the eruption, are formed on the deposit.

A large quantity of fragmentary materials of all grades—volcanic

ashes, sands, lapilli, and bombs—covers not only the ground around the crater but also the wide area, southeast of the volcano. Numerous flows of pumice-blocks occupy most of the lower slope of the volcano.

Numerous solfataras, primary and secondary, develop on the ground around the pit-craters and on the flows of pumice-blocks. Among the sublimates, metallic sulphates, metallic chlorides and free sulphur are predominant.

The ejecta were so high in temperature at the time when they were ejected that fires were started on trees and houses at places where they deposited. On July 2, 1929, with an electric pyrometer, the writer observed the temperatures, as high as 415°C. in a flow of pumice-blocks. From the effect of oxidation which the juvenile pumice underwent by air circulating through its deposit, it was confirmed that the juvenile pumice had probably been at a temperature above 700°C. On the other hand, the bread-crust bomb of juvenile pumice was certainly at such a temperature for such a length of time as an accidental xenolith within it might be thermally metamorphosed to result in the formation of high-quartz and α-wollastonite, which under one atmosphere pressure are stable at temperatures between 573° and 870°C., and below 1180°C. respectively.

Accordingly, the temperature of the lava, in which the xenolith occurred, was certainly higher than 573°C. But it might not be higher than 1180°C., or probably it might not approach to that temperature, at least just before the ejection of the lava in the form of bread-crust bomb. By all means, it was not sufficiently higher than 870°C. for a sufficient length of time to allow the high-quartz in the xenolith to be transformed into tridymite.

The ejecta are, except for a small quantity of the accessory and accidental ones, fairly uniform (pumice) in characters, megascopical as well as microscopical, petrographically belonging to two-pyroxene-andesite. Accordingly, they might be derived from a subcrateral magma-reservoir.

The volcano has probably been born in late Diluvium. Since the time when the visible oldest products were ejected, however, the subcrateral magma appears to have been maintained within a narrow range of temperature, as may be inferred from the petrological evidences. Consequently, evolution and accumulation of gases, which are occluded in the magma, have constantly been done, leading to occasional outbursts without prolonged period of quietude. In this way, the gas-content in

the subcrateral magma-conduit had increased till it was released with the violent explosions, June 17, 1929. The course of the eruption, June 17, 1929, may be analysed as follows.

Several hours in the early morning were passed in ejecting the materials of the old crater-floor, in rumblings, and in earthquakes. When the load of the conduit had been removed to some extent by blowing-away of the materials of the old crater-floor, the gas-content began to be released with violent explosions, along with ejection of juvenile lava from the magma-conduit highly charged with free gas.

The early explosions were so powerful that the lava was subdivided into pumice-fragments of all grades—volcanic ashes, sands, lapilli, and bombs. These fragments were projected in the air and landed on the ground not only around the crater, but also in a distance, southeast of the volcano.

When the gas-content had been partially spended on the early powerful explosions, less powerful explosions were set in. In this case the lava might not be subdivided into fragments and might not be projected highly in the air, as in the former. Accordingly, a large quantity of pumice-blocks was projected over the ring-wall still retaining hot gases, and descended the slope of the volcano. At a later phase, a small quantity of bread-crust bombs was projected. Such mode of activity as has been stated may be one of the Vulcanian type of eruption.

The results of precise levelling show that the land occupied by the northwestern half of the volcano has been relatively depressed from the land outside. There are also geological evidences that the land occupied by the volcano has relatively sunk. Thus, depression of the land, on which volcanic activity has been displayed, may have a causal relationship to the volcanic activity.

The Eruption of Komagatake.

Fig. 1. Komagatake at a paroxysmal phase of eruption, as seen from Hakodate. About 5:30 p.m., June 17, 1929. (Hakodate Meteor. St.)

Fig. 2. Komagatake at a paroxysmal phase of eruption, as seen from Mori. About 7 p.m, June 17, 1929. (Photo Kagaya)

Fig. 3. Ash-cloud veering toward southeast, as seen from Oonuma. About 5 p.m., June 17. 1929. (Photo Sasako)

Fig. 4. A flow of pumice-blocks descending the southwestern slope of the volcano. About 5:30 p.m., June 17, 1929. (Photo Tomoe)

[Bull. Earthq. Res. Inst., Vol. VIII, Pl. II.]

(震研彙報第八號、圖版、津屋)

The Eruption of Komagatake.

Fig. 1. View of the inside of the caldera after the eruption in 1929, as seen northwards from Umanose. Km–Komagatake; Sw–Saharadake; Nm–Namakoyama; Ks–Komanose; Um–Umanose. A and E—Vapor-clouds issuing from the respective pit-craters. See Fig. 4, p. 247.

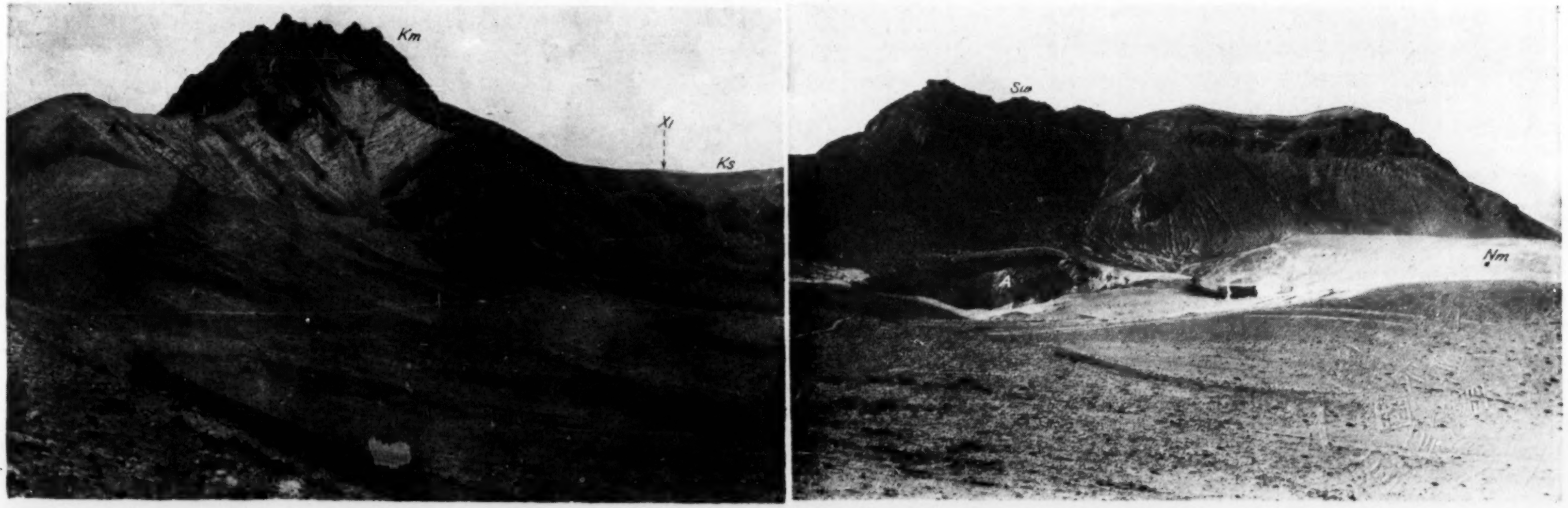

Fig. 2. View of the inside of the caldera before the eruption in 1929, as seen northwards from Umanose. Km–Komagatake; Sw–Saharadake; Nm–Namakoyama; Ks–Komanose; Um–Umanose; A—Crater in 1856.

([illegible])

The Eruption of Komagatake.

Fig. 1. Northern view of the volcano prior to the eruption in 1929, as seen from Oonuma Km–Komagatake; Sw–Saharadake; Um–Umanose; Sm–Smidamori; Ak–Akahageyama; O–Oonuma

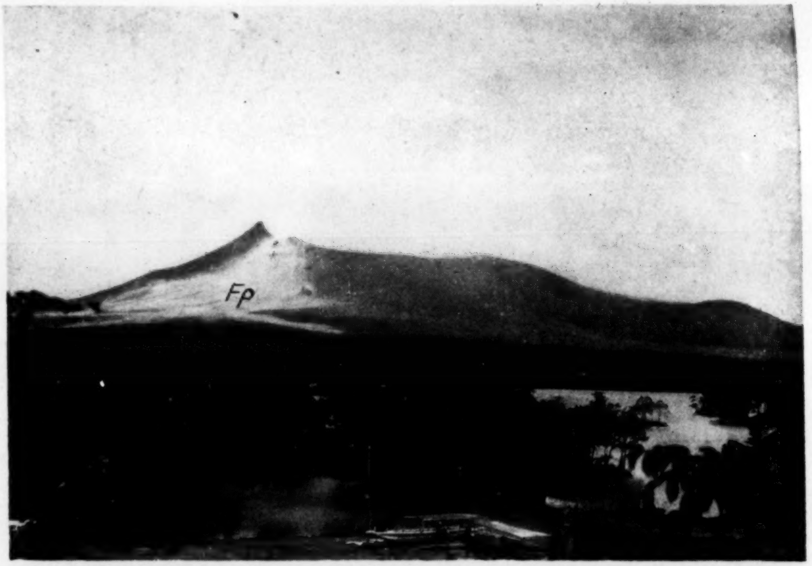

Fig. 2. Northern view of the volcano after the eruption in 1929, as seen from Oonuma. Fp–Flows of pumice-blocks. The crest of Saharadake can slightly be seen above that of Umanose. Compare with the le t figure.

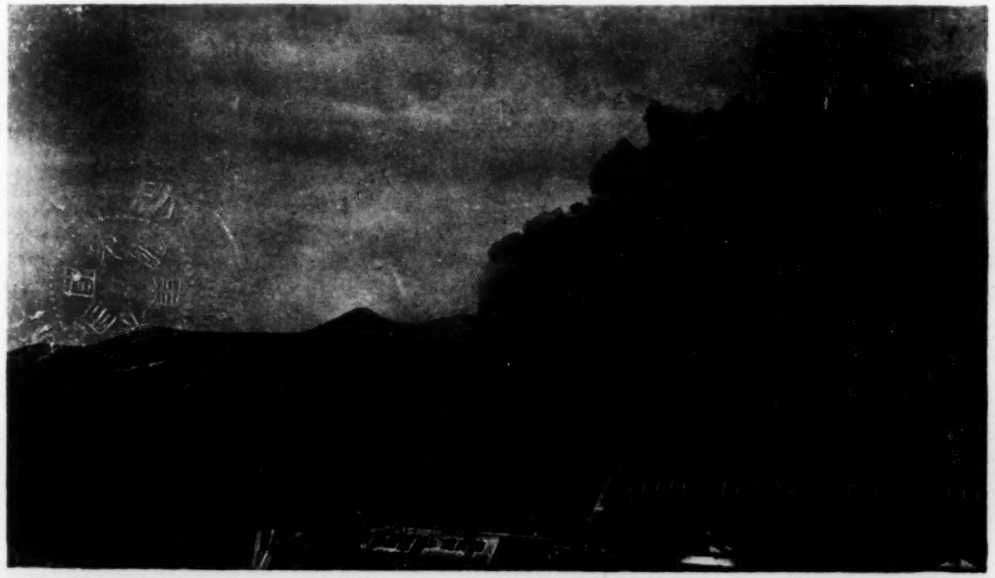

Fig. 3. Northwestern view of the volcano after the eruption in 1929, as seen from Orido near Sikabe. Sm–Sumidamori; Nm–Namakoyama; Sw–Saharadake; E–crater on the east side of Namakoyama.

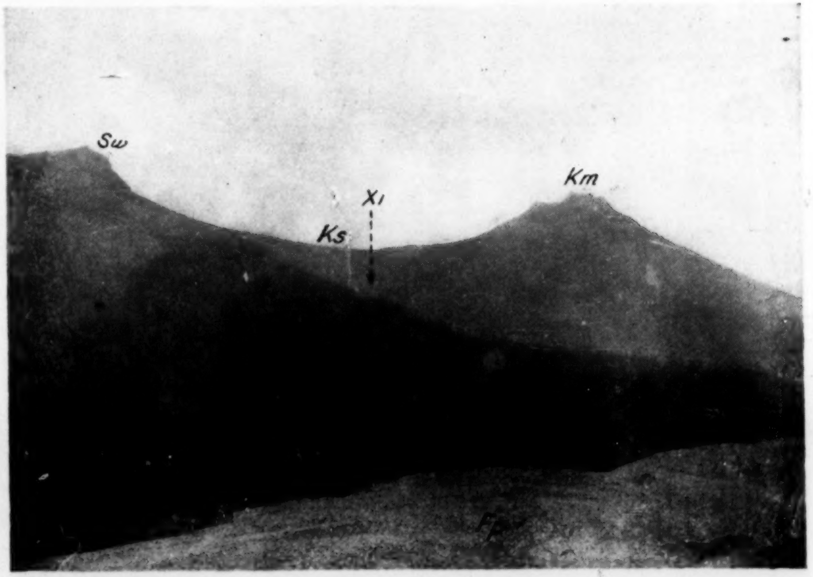

Fig. 4. Southern view of the apical part of the volcano after the eruption in 1929, as seen from the Tentozawa, a northern tributary of the Osidasizawa. Km–Komagatake; Sw–Saharadake; Ks–Komanose; X_1–Osidasizawa explosion-crater; Fp–Flows of pumice-blocks.

(震研彙報第八號、圖版、津屋)

The Eruption of Komagatake.

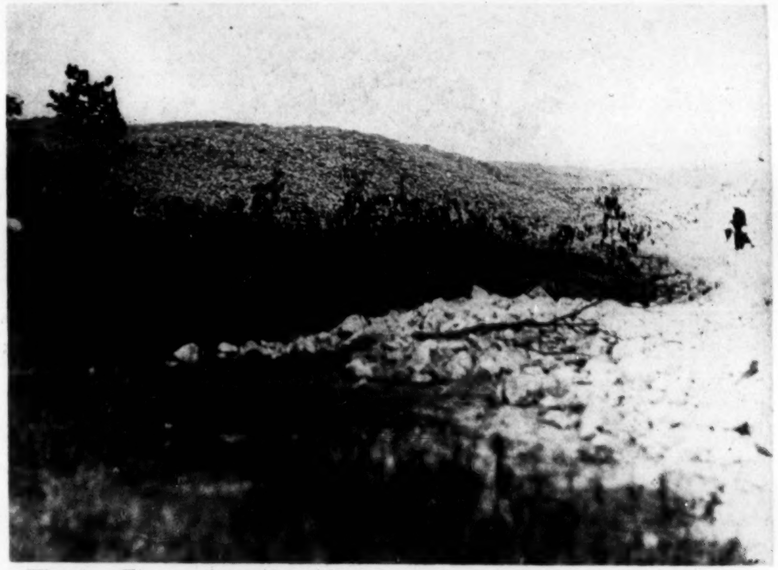

Fig. 1. Flows of pumice-blocks on the northwestern skirt of the volcano. See p. 251.

Fig. 2. A scar produced by the flows of pumice-blocks on the northwestern side of Saharadake. See p. 252.

Fig. 3. Ash-field of the east side of Saharadake, eroded by drainages of rain-water. Solfataric vapors are issuing from the underlying deposit of pumice ejected by the eruption in 1929. See p. 253.

The Eruption of Komagatake.

Fig. 1. Houses in Orido near Sikabe buried in the deposit of volcanic ashes, sands, and lapilli.

Fig. 2. Houses in Sikabe damaged by the ejecta.

(震研彙報第八號、圖版、津屋)

(震研彙報第八號、圖版、津屋)

Microphotographs of the Ejecta of Komagatake.

Fig. 1. Two-pyroxene-andesite. Pumice (lapilli) of 1929, from Saharadake. See p. 257. ×28

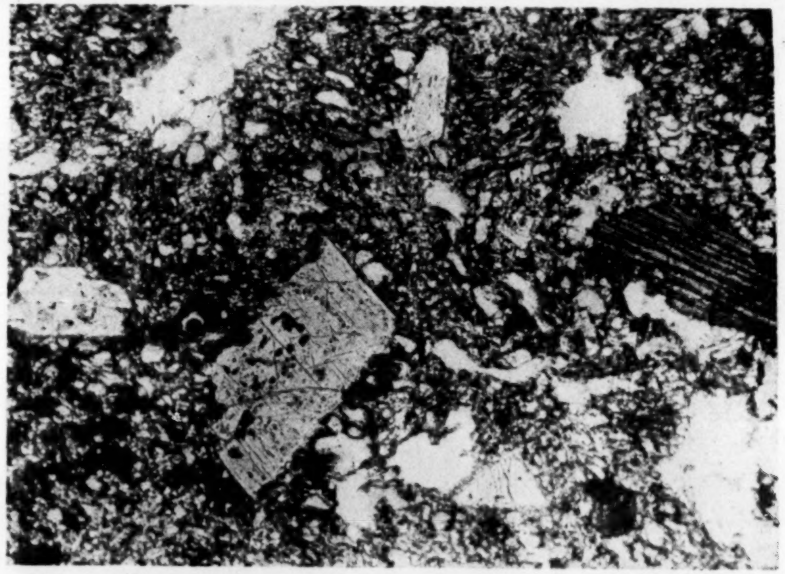

Fig. 2. Two-pyroxene-andesite. Pumice-blocks of 1929, flowing down the mountain-slope. See p. 257. ×28.

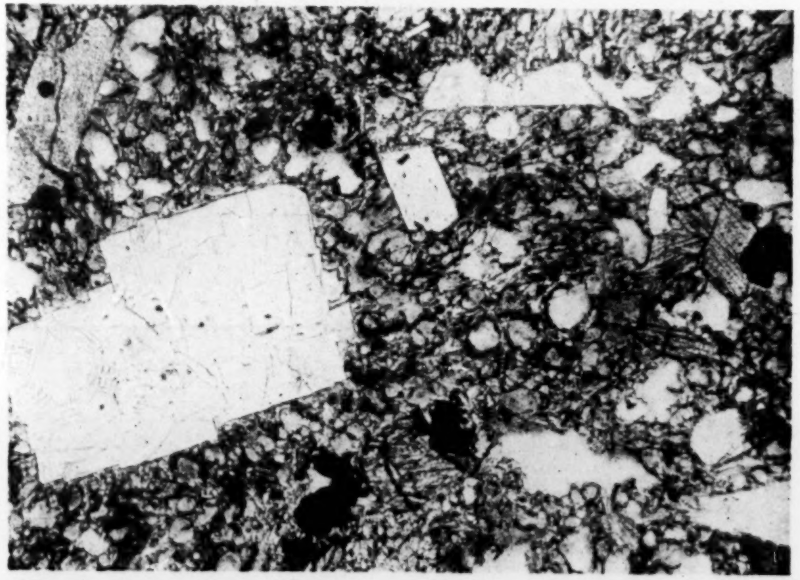

Fig. 3. Two-pyroxene-andesite. Bread-crust bombs of 1929. See p. 257. ×28

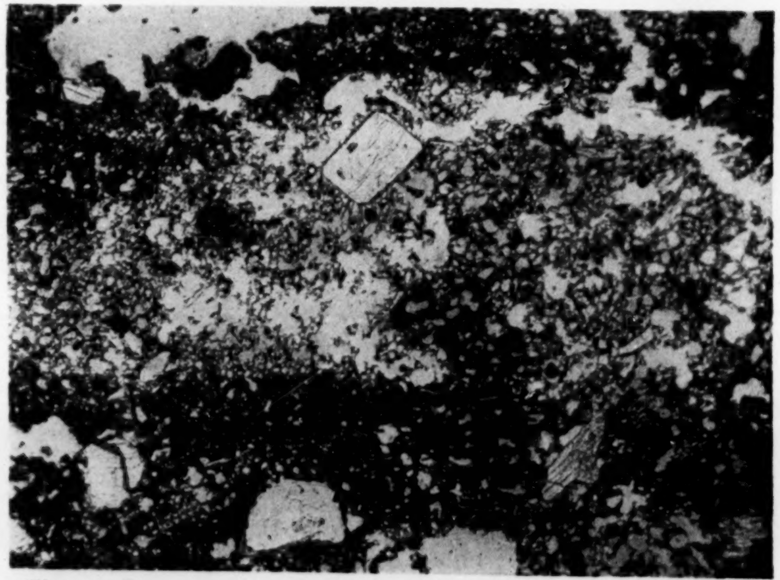

Fig. 4. Two-pyroxene-andesite. Accessory ejecta (1). See p. 261. ×28

（震研彙報第八號、圖版、津屋）

Microphotographs of the Ejecta of Komagatake.

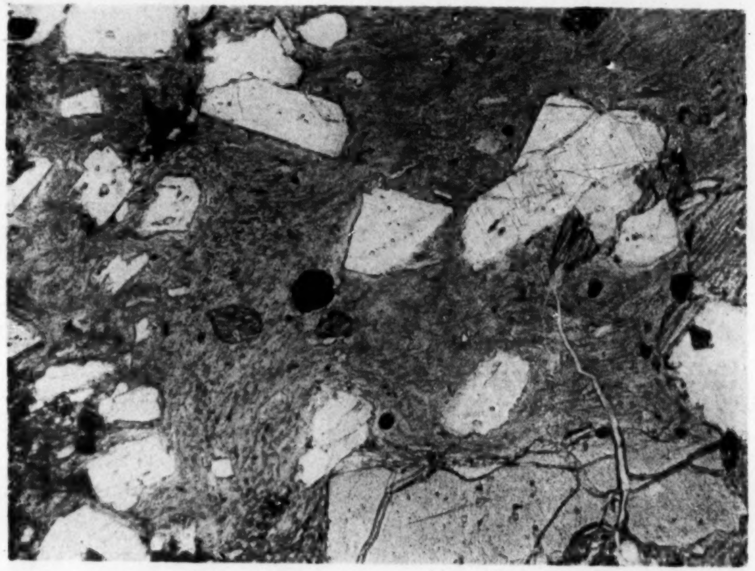

Fig. 1. Two-pyroxene-andesite. Accessory ejecta (2). See p. 261. × 28

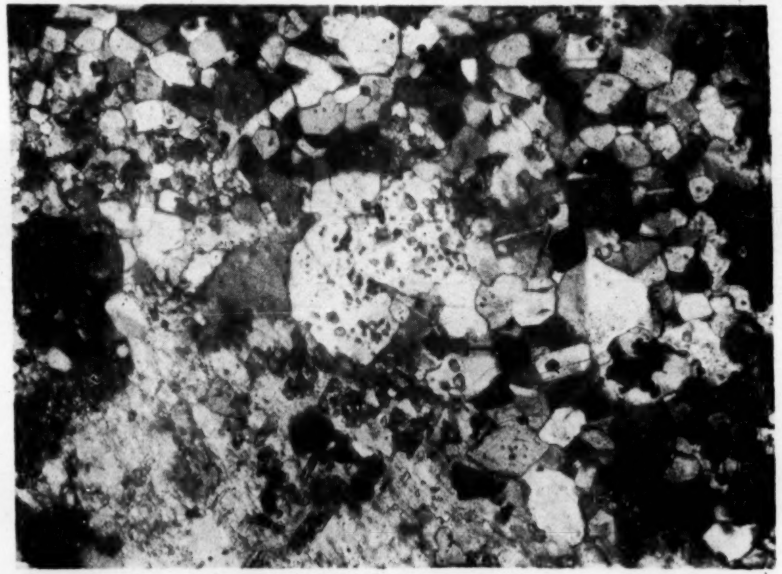

Fig. 2. Hypersthene-orthoclase-plagioclase-rock. Accidental ejecta (β-type). See p. 265. Crossed nicols. × 60

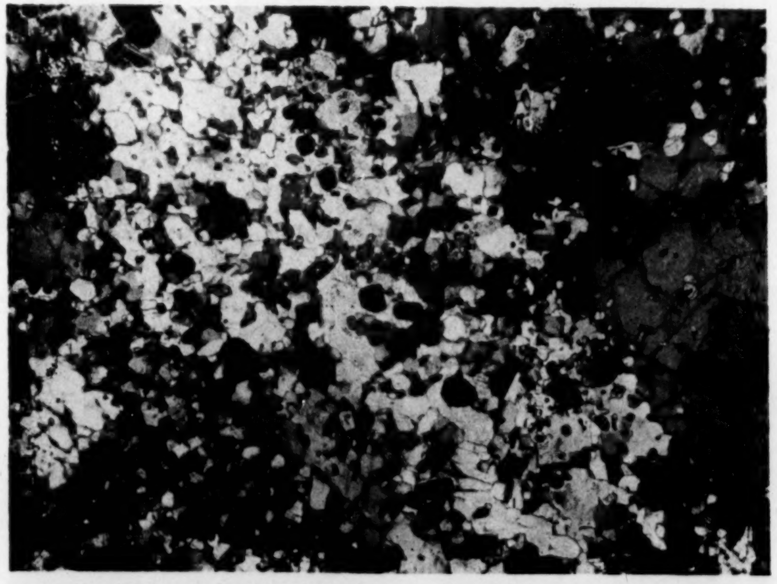

Fig. 3. Quartz-augite-plagioclase-wollastonite-rock. Accidental xenolith. See p. 267. Crossed nicols. × 60

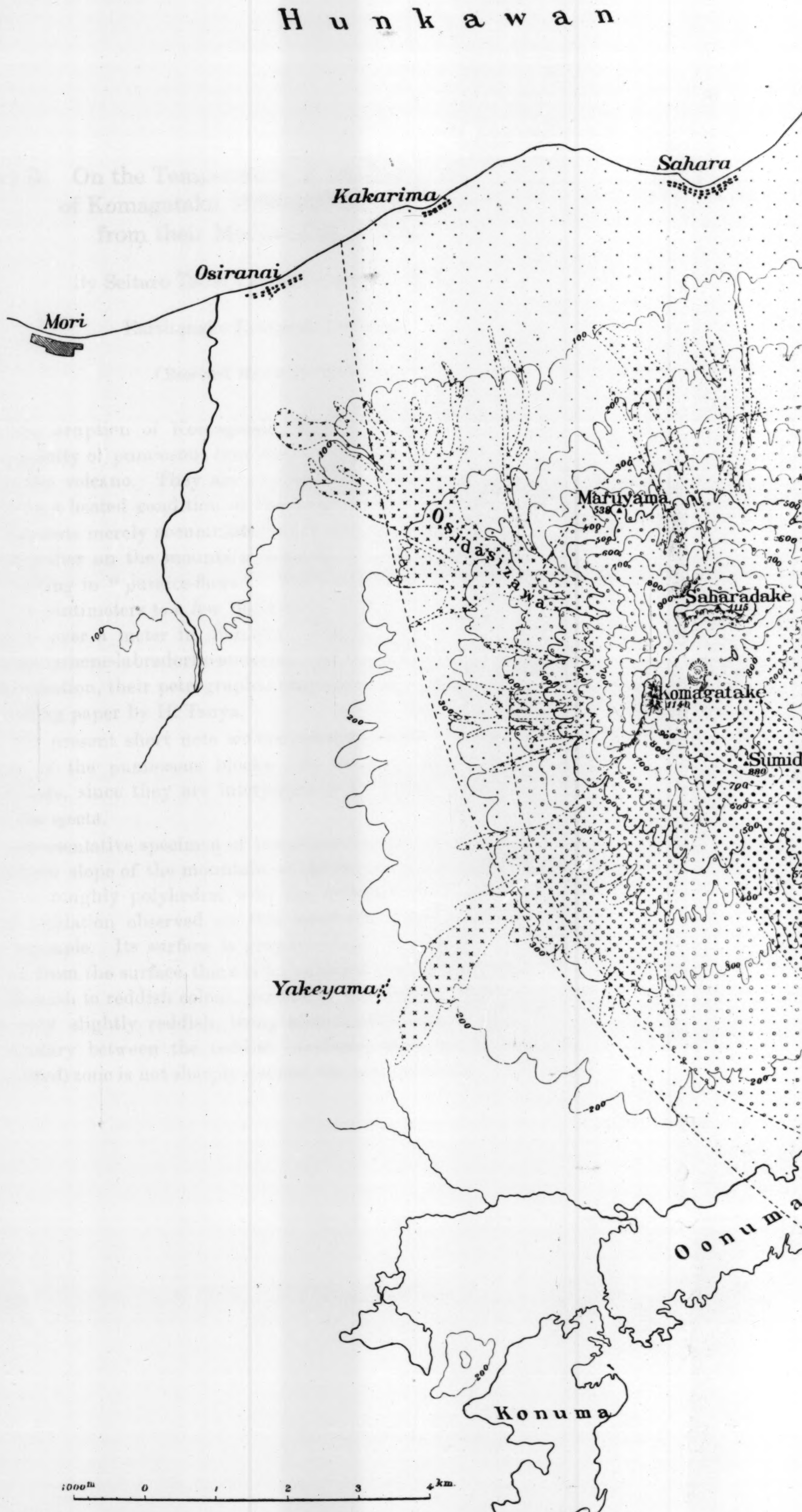

（震研彙報第八號、圖版、津屋）

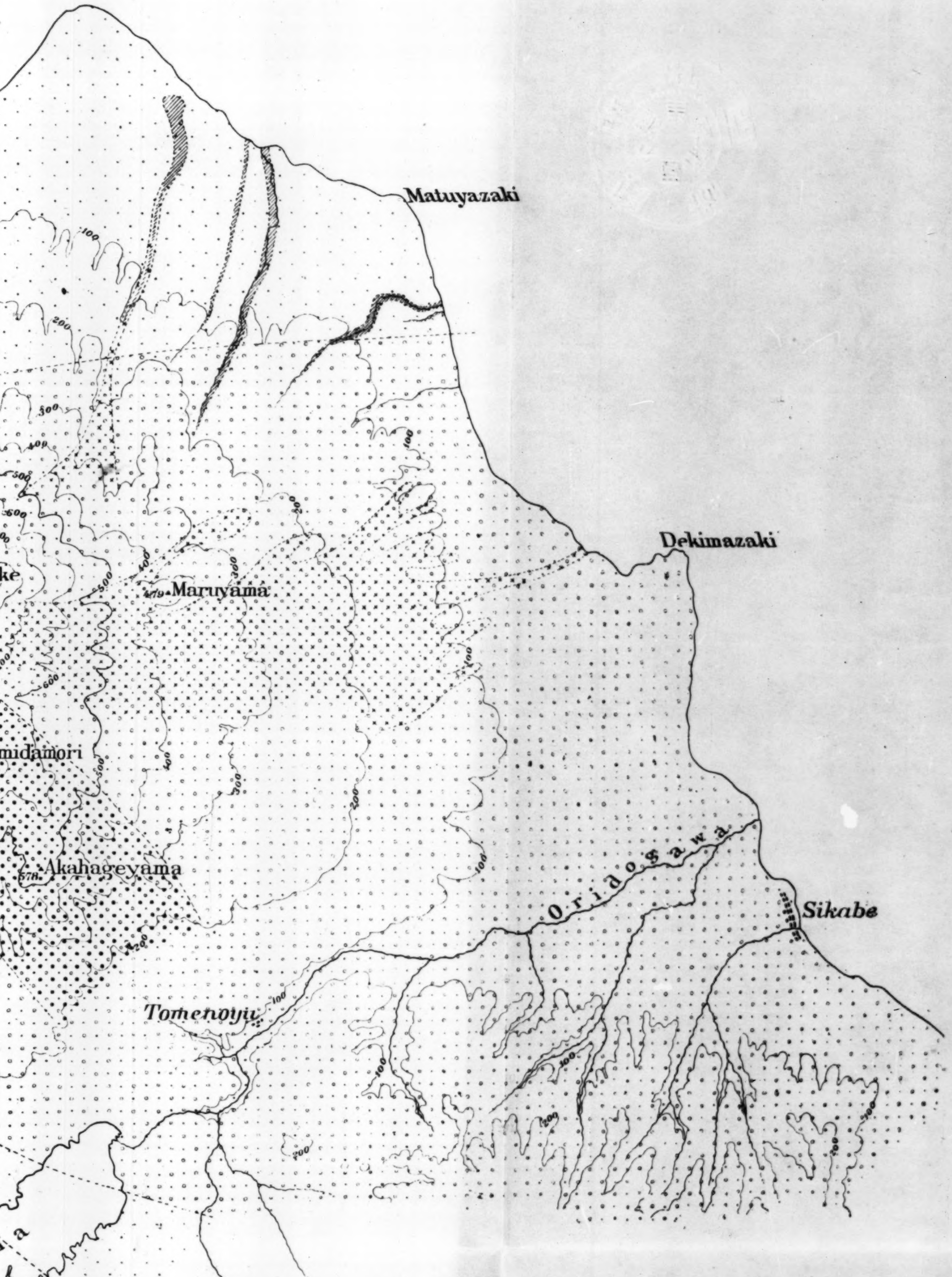
Matuyazaki
Dekimazaki
Maruyama
Akahageyama
Oridosawa
Sikabe
Tomenoyu
Crater
Secondary mud-flow.
Volcanic ashes.
Bread-crust bombs.
Pumice.
Flow of pumice-blocks.

Part II. On the Temperature of the Pumiceous Ejecta of Komagatake, Hokkaidô, as inferred from their Modes of Oxidation.

By Seitarô TSUBOI and Hiromichi TSUYA,

Earthquake Research Institute.

(Received March 20, 1930.)

By the eruption of Komagatake, Hokkaidô, on June 17th, 1929, a large quantity of pumiceous lava-blocks were ejected from the summit-crater of the volcano. They are exploded fragments of molten magma, and were in a heated condition at the time of their ejection. Some of these fragments merely accumulated on the ground; while others, being dashed together on the mountain slope, flowed subsequently like fluent lavas, resulting in "pumice-flows". The fragments vary in size mostly from a few centimeters to a few decimeters across, but sometimes reach as large as over a meter in diameter. Petrographically they belong to augite-hypersthene-labradorite-andesite. As to their modes of ejection, their distribution, their petrographic characters, etc., details are given in the preceding paper by H. Tsuya.

In the present short note we are concerned only with the modes of oxidation of the pumiceous blocks. To these a special attention is directed here, since they are interpreted as giving a clue to the temperature of the ejecta.

A representative specimen of the pumiceous lava-block, collected on the southern slope of the mountain at the height of about 300 m. above sea-level is roughly polyhedral with the diameter of some 25 cm. The mode of oxidation observed on this specimen may be described as a typical example. Its surface is gray in colour, but inside, at a depth of 1 to 2 cm. from the surface, there is an oxidized zone, about 1 cm. wide, of light yellowish to reddish colour, parallel to the surface. Still inner part is only very slightly reddish, being almost unoxidized. (See Fig. 1.) The boundary between the reddish (oxidized) zone and the outer gray (non-oxidized) zone is not sharply defined, the two zones being transitional

to each other; while that between the reddish zone and the inner gray zone is rather sharp and abrupt. Under the microscope, the reddish zone is found to contain oxidized magnetite dusts finely disseminated through the glassy base.

The mode of oxidation as described in the above is very common, especially among the blocks that fell to deposit. A probable cause for this zonal oxidation is as follows: Fragmented pieces of molten magma were ejected from the crater still in a heated condition. Then, on contact with the cool air the surficial part of each block was quenched, while the inner part retaining still a high temperature. For oxidation of a pumiceous block, a sufficient supply of air and a sufficiently high temperature are combiningly needed. On the surface of each block which is exposed directly to the air, the air supply was of course sufficient, but there the temperature became soon too low for oxidation. In the inner portion of the block the temperature must have been high enough for oxidation, but there the supply of the air being insufficient, it was left unoxidized. The oxidized zone which lies at the depth of about 1 to 2 cm. from the surface corresponds to the zone where the supply of air was enough and the temperature was sufficiently high for oxidation.

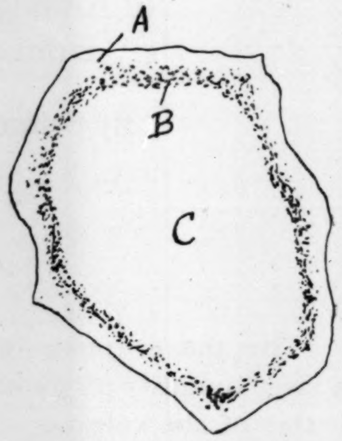

Fig. 1. Zonal oxidation of pumiceous block.
A...Surficical non-oxidized zone
B...Oxidized zone
C...Inner non-oxidized zone

In connection with the above inference it was attempted to determine the temperature necessary to produce the same degree of oxidation effect as that in the oxidized zone of the pumiceous block. For this purpose, a series of experiments were carried out as follows: Pieces of non-oxidized part (gray-coloured part) of pumice were put in an open crucible and were kept at different temperatures under an ample supply of air for different lengths of time. The samples were then compared with the naturally oxidized pumices as to their colour. In these experiments the temperatures at which the samples were kept were determined by means of a Pt-Pt-Rh thermocouple connected to a millivoltmeter.

It has been found from these experiments that:

(1) The sample is oxidized to the same degree as in the oxidized zone of the pumiceous block, when it is kept at 730°C. for 1–4 hours.

(2) At lower temperatures the degree of oxidation of the sample is much lower. For example the sample kept at 660°C. for 2 hours shows but a very slight oxidation effect; while that kept at 530°C. practically none, even after such a prolonged heating as for 8 hours.

From what have been stated in the above, an inference may now be made as to the temperature of the pumiceous lava-blocks at the time of their ejection. It is evident that their temperature was *at least as high as 730°C.*, as is indicated by the existence of the oxidized zone; *but not very much higher than this,* for they must have cooled on their surface below 730°C. too soon to be oxidized, as is inferred from their non-oxidized surface.

Some of the pumiceous blocks which constitute the pumice-flows are peculiar as to the mode of oxidation. For example, the pumiceous blocks, constituting the Akaigawa pumice-flow on the western flank of the volcano, show not infrequently oxidation effect even on the surface. This may be interpreted as indicating that these blocks retained temperatures above 730°C. for a period sufficiently long for oxidation. It is probable that this is due to the peculiar mode of ejection of the pumiceous blocks, which favoured their flowing down like fluent lava.

Part III. Meteorological and Seismological Observations.

By Fuyuhiko KISHINOUYE,

Earthquake Researth Institute.

(Received March 20, 1930.)

1. Meteorological and Seismological Conditions of the Volcano Komagatake at the time of its Eruption.

The nearest meteorological and seismological station to Komagatake is the Hakodate Meteorological Station in the city of Hakodate, about 33 km. south of the crater. Oonuma Forestry Meteorological Station in the Oonuma Park at the south-western foot of the volcano is nearer than Hakodate, but there merely meteorological observation is taken once a day. On the other hand, at Hakodate meteorological observations are made hourly, and continuous recording of seismometers are kept. Then the results of the Hakodate Meteorological Station were mostly used for the investigation.

Hakodate is moderately far from the volcano, and moreover mountain range lies between the two. So the meterological conditions near the volcano may be different from those at Hakodate, but their general features will be equal at the both places.

The great change of atmospheric pressure is said as one of causes of volcanic eruption by many authors. In this case, the pressure was depressing at the time of the eruption since June 13 from 762 mm. to 748 mm. (Fig. 1) The centre of low pressure would have passed near the volcano at the time of the eruption from south to north, and the pressure gradually reduced to 736 mm. till 18h. on June 17.

It was no precipitation for ten days before the eruption, but on the previous day it rained as much as 19·3 mm. The precipitation of water is sometimes thought as the source of the vapour, the chief constituent of the volcanic smoke, and then the vapour-pressure make the volcano erupt.

Consequently passing of the low pressure and the precipitation of the previous day may be regarded as the secondary causes in this case.

On June 17. moderate breeze blew from south before 6h., from east since 6h. till 12h., and gradually changed to south. After 16h. till 22h. wind-direction was NW, and early on that day the western villages from the volcano, Mori, Sahara, and so on, were suffered from volcanic ashes. In the afternoon, the direction of wind changed to north-west, and on the other hand eruption became vigorous, Sikabe and its neighbouring villages were thickly covered with ashes and small pumice-stones. The damages of farms and pastures were generally depend upon the wind-direction when the eruption was energetic.

The volcanic smoke containing much ashes and small pumice-stones went vertically in the air, and its summit sustained an angle of elevation of 22° from Hakodate Meteorological Station at 14h. 17m. on the day of the eruption. Its height was calculated as about 13000m. above the sea level under simple assumptions that the smoke column was vertical and narrow. The angle became 10°—its height about 6000m.—at 15h. on the next day. A photograph taken at 17h. on June 17. from Mori (see Fig. 2 in Pl. I), shows the smoke as a typical example of cauliflower shape, and at the middle height of it vortex of air and skirf-cloud are seen.

No sign of eruption was found on seismograms at Hakodate, before the eruption. But on June 17. at 0h. 23m. 43s., the seismometer registered the earth-vibrations like earth-pulsations which last for about eight minutes, and it was thought as the volcanic disturbances recorded at the first time. The vibration of the same type was recorded again at 8h. 0m. 30s., and an earthquake of ordinary type at 9h. 53m. 37·5s. on the seismogram. These vibrations were not felt by men. The vibrations of long period similar type as occurred at 0h. were recorded incessantly since 11h. on that day, till 0h. of the next day, and during that time houses in the city of Hakodate were frequently shaken and their doors rattled. According to the observations at the Oonuma Forestry Meteorological Station (Table I), the eruption was violent at that time. From this fact, the vibrations recorded at 0h. will be the first record of the eruption, though the activities of the volcano were not recognized by people till the early morning. The period of the vibration was about 3 sec. and the maximum double amplitude 185 microns.

2. Seismological Observations at Sahara.

The eruption of the volcano Komagatake attracted attentions of all who have interest in the volcano. From several institutes, men were

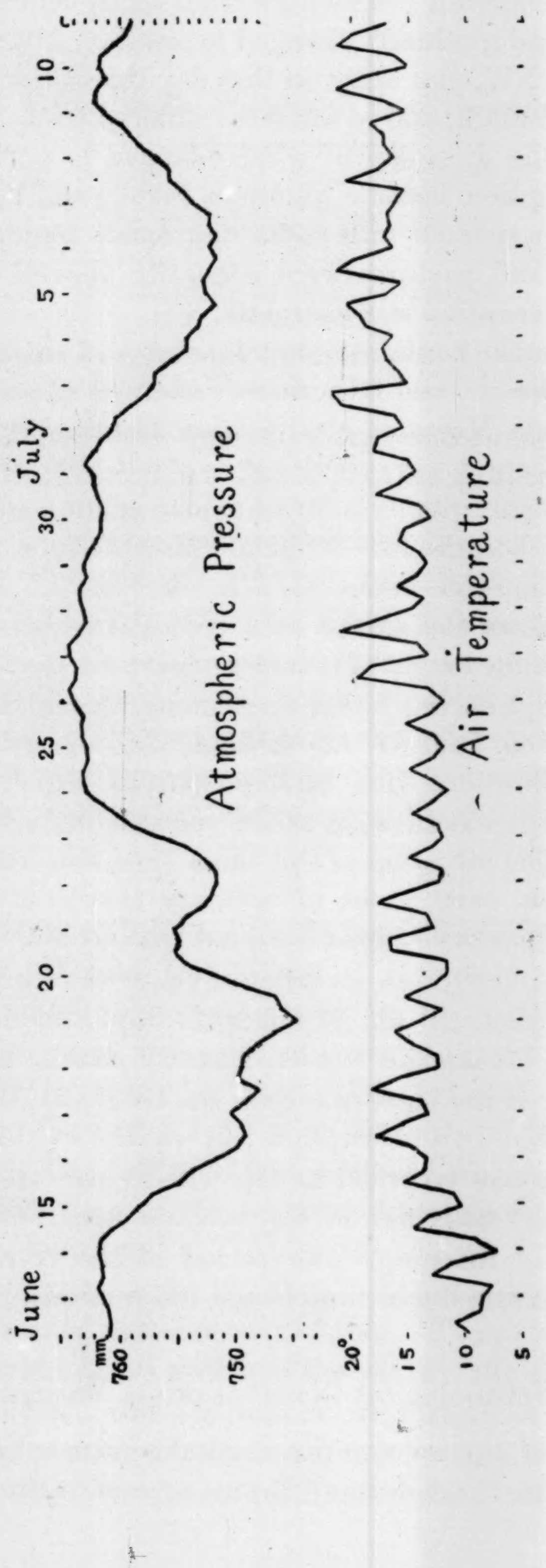

Fig. 1. Observations at Hakodate Meteorological Station.

Table I.

Observations at the Oonuma Forestry Meteorological Station.
(Observed by Mr. Sentaro Mito.)

Date (1929)	Air temperature			Wind (10^h)		Precipitation	Cloudiness (10^h)	Weather (10^h)	Remark
	10^h	Max.	Min.	Direction	Force				
June 15	16·5	20·0	11·0	N	light breeze	25·3	10	cloudy	rain from midnight.
16	15·5	25·0	10·0	W	"	1·4	10	rainy	rain continued till 11^h. (strong on morning).
17	16·5	22·0	10·5	NE	"	—	10	cloudy	1^h—$1^h 30^m$ Komagatake erupted. $10^h 04^m$ erupted again, continued furiously till 24^h. 10^h 20^m—24^h thunder 22^h—$22^h 30^m$ volcanic ash fell.
18	13·0	22·0	8·0	W	moderate breeze	1·3	10	cloudy	18^h—20^h foggy. 20^h rain. after 1^h eruption became calm. $3^h 45^m$ slight shock. (duration 5 sec.).
19	13·0	17·0	11·5	W	light breeze	4·5	10	rainy	11^h heavy rain. $17^h 30^m$ rain stopped.
20	16·0	20·0	9·0	W	"	—	7	clear	23^h slight shock (duration 4 sec.).
21	19·5	21·0	12·5	W	"	2·2	10	cloudy	$8^h 40^m$ slight shock (duration 3 sec.). from $16^h 30^m$ rain. $16^h 30^m$ slight shock (dur. 5 sec.).
22	14·5	16·5	11·0	N	"	2·5	10	rainy	$12^h 15^m$ shock (dur. 2 sec.).
23	15·0	16·5	11·5	NE	"	—	10	cloudy	4^h shock (dur. 2 sec.). $4^h 30^m$ shock (dur. 3 sec.).
24	11·5	15·5	9·5	N	"	—	10	foggy	
25	15·0	21·0	10·0	N	"	0·9	7	clear	
26	20·0	25·5	11·5	SW	"	—	1	fine	
27	22·5	25·0	9·0	W	"	—	5	clear	
28	12·5	14·5	10·0	E	moderate breeze	—	10	cloudy	$18^h 50^m$ shock (dur. 3 sec.).
29	12·0	16·5	10·5	N	light breeze	—	10	cloudy	
30	16·5	20·0	11·0	N	"	—	10	cloudy	

sent to observe the eruption, and from the Earthquake Research Institute five observers were ordered to go to the volcano and they started at the midday on June 20.

Two men of the party took charge of geological and topographical survey, and the others instrumental observations of the volcanic activity. The instruments brought were an one-component microseismometer, a pair of the Ishimoto's tiltometer, a pair of Tsuboi's gravity-variometer. Besides these, Dr. Nakata who joined the party carried two galvanometers, with which he observed earth-current and potential of atmospheric electricity.

In the afternoon on 21., they arrived at Oonuma, a village at the south-western foot of Komagatake, and soon sought a place to set the instruments. The conditions of the place suitable for observation are as follows: the volcanic activities are directly observed, in other words, the observing station is not on the different block of the earth's crust from that of the volcano; the location is handy to means of trancit for observers; natural bed of hard rock is best as the floor of the station, but if such place could not be found, stable hard rock or concrete floor must be provided; the room for the observation is dark and supply of electric current is near at hand, for all instruments brought were optical self-recording on the bromide papers and use electric lamp lighted by six volt secondary batteries.

The instruments were equipped in one of the storehouses of the Maruyama marine products factory which has concrete floor and also meet all the other conditions required, on 22. at Sahara ($\varphi=42°07'$, $\lambda=140°41'$), about 8 km. north of the crater.

The writer took charge of seismometrical observation with an one-component microseismometer stated above, which had been invented by Proffesor Ishimoto[1] and Dr. Takahasi, and details of its construction would be omitted here for that is written in the previous volume of this Bulletin. But now the constants of the seismometer are to be mentioned. The recording magnification was made 500, period of self-vibration 1.5 sec., and oil-damper was attached to the insutrument. The period may be rather small for recording of ordinary earthquakes, but that of volcanic earthquakes is so small that the seismometer has no difficulties in

1) M. ISHIMOTO et R. TAKAHASI, *Bull. Earthq. Res. Inst.*, 7 (1929), 176-178.

resonance. To make sure of this supposition, the writer set the seismometer on the ground-floor of the institute to compare with the ordinary horizontal pendulum seismometers after he returned to Tokyo. Of course the former did not record the long period vibrations as theoretically known, but vibrations of small period were well recorded.

The recording was photographical on bromide paper. The weak point of this means of recording is bromide paper is not sensitive to the image of fast motions. On seismograms P phase is registered in many cases, but S phase of earthquake is hardly recorded. This fact tells that the vibration of S phase is fairly faster than that of P phase. But by use of photographic film, good records of both phases were obtained.

According to Omori's investigation[2] at the volcano Asamayama, the initial movement of volcanic earthquakes is sharp in the radial direction from the crater. So the writer set the seismometer to record NS-component of the earthquake motions, that is nearly radial direction at Sahara.

The recording was begun at 1h. on June 23., and continued till July 10. Though the recording was broken accidentally, more than three hundred earthquakes were recorded during eighteen days.

The seismograms are divided in four classes: the first class includes impulsive earthquakes, amplitudes of which become suddenly large and decrease exponentially in a few seconds (denoted I in Table II, see Pl. IX, Fig. 2); the second very near earthquakes of ordinary type, (II, Figs. 3 and 4) preliminary tremors are seen distinctly; and the third cluster of the small earthquakes (III, Fig. 5); the fourth comparatively distant earthquakes (IV in Table II, Fig. 1); Omori[3] classified the earthquakes of Asamayama in two, non-eruptive and eruptive. The former is impulsive, the later somewhat long in duration. These may be correspond to the first and second class of Table II. But unfortunately it was mostly cloudy while the writer stayed in Hokkaidô, and the volcanic smoke could not be seen, so the volcanic activities were known only through the instrumental records. Under such state, the writer can not say about

---

2) F. Omori, *Bull. Earthq. Inv. Comm.*, 7 (1914).

3) *ditto.*

the relation between the seismographical types of the earthquakes and the volcanic activities.

The recorded amplitude of the earthquakes was mostly less than 1 mm., and even the greatest 6 cm. These earthquakes were local and hardly felt by men. For instance, on July 4. several moderate shocks occurred at Oonuma, but the instrument at Sahara did not record it. The writer felt a shock at about 17h 57m, on June 23. in a house of Osiranai, a village 6 km. apart from the station. Then the writer soon went to see the seismogram, but he could not find record of the shock. Only one earthquake was felt by him, which belongs to the impulsive class, and its velocity of motion was too fast to be recorded on bromide paper, so its record was not photographed. Mr. Iwasita, who stayed for the observation at Sahara till July 10 after the writer returned to Tokyo, felt an earthquake which occurred at 17h 28m on July 10. Its record shown in Fig. 4 on Pl. IX was obtained in a good chance when the vibration was recorded on photographic films, and driving rate of recording-drum made as fast as 26·1 cm./min. That was the only one record with which the vibration-period of principal portion of the earthquake could be measured. Its period obtained was about 0·2 sec. The more accurate measurement of the duration of the preliminary tremours are also got with it.

It is known as mentioned before that the small period seismometer does not record the true motion of earthquake, but resonances with the motion of the period equal to that of the self-vibration. If measurement of only preliminary tremours were required, for at present it is the most important factor in practical seismometry, small-period seismometer may serve for the purpose in some cases. For example, on the seismogram of an earthquake occurred on June 24. off the coast of Iwaki is shown in Fig. 1 on Pl. IX, P phase and S phase of it are distinguished by vibration-period and amplitude as in the case usual seismometers. But the amplitude of both phases are very small, and amplitude difference is little.

The Hakodate Meteorological Station is the nearest place where continuous meteorological and seismometrical observations are done as before mentioned. The writer called at the station and was allowed by the director of the station to inspect the records. There is an

Omori's portable seismometer, its magnification is 10, and its self-vibration period of EW and NS components are 6·1 sec., 4·5 sec. respectively.

Its magnification is too small to recognize the local volcanic earthquakes at about 30 km. distant, for seismic waves soon damped away in the vicinity of the volcano because of its amplitude and period of vibration is very small, and then the shaken area is small. Mainly by such reason only three earthquakes which took place at 18h 48m on June 28., 3h 07m and 11h 05m on July 4., were measured their duration of preliminary tremors at both Hakodate and Sahara.

The duration of preliminary tremours had been measured, and the focus was found under the assumption that the focal distance from each station is proportional to its duration of preliminary tremours. Then by Appolonius theorem in geometry, the locus of the earthquake-foci whose distances from two stations are in the constant ratio of the durations of the preliminary tremors is a sphere, the centre of which lies on the straight line joining the two observing points. The circles in Fig. 2 show the section of the above-mentioned spheres. All cireles passes near the crater, and morever the disturbed area was very small in these cases, then it would be natural to think that the earthquakes have their foci near of the crater. Simply assuming as the stations and the foci are on one plane, the velocity of the virtual wave S—P was calculated as from 2·4 km./sec. to 3·2 km./sec. and in the average 2·9 km./sec. This value, commonly said as k by seismologists, is remarkably small as compared with Omori's value, 7·42 km./sec. But it may be natural result, for Proffesor Imamura[4] and others stated that in upper layer of the earth's crust, the value of k is very small. For instance, it is 3·0 in the case of earthquakes which occur in the neighbourhood of Wakayama City, 5·0 in some district of Kwantô. The earthquakes of Komagatake have their origin very near the earth's surface, and seismic waves pass through rocks that has been less firmly consolidated. So the value of k will be smaller than usual cases.

4) A. Imamura, F. Kishinouye and K. Kodaira, *Bull. Earthq. Res. Inst.*, 7 (1929), 471.

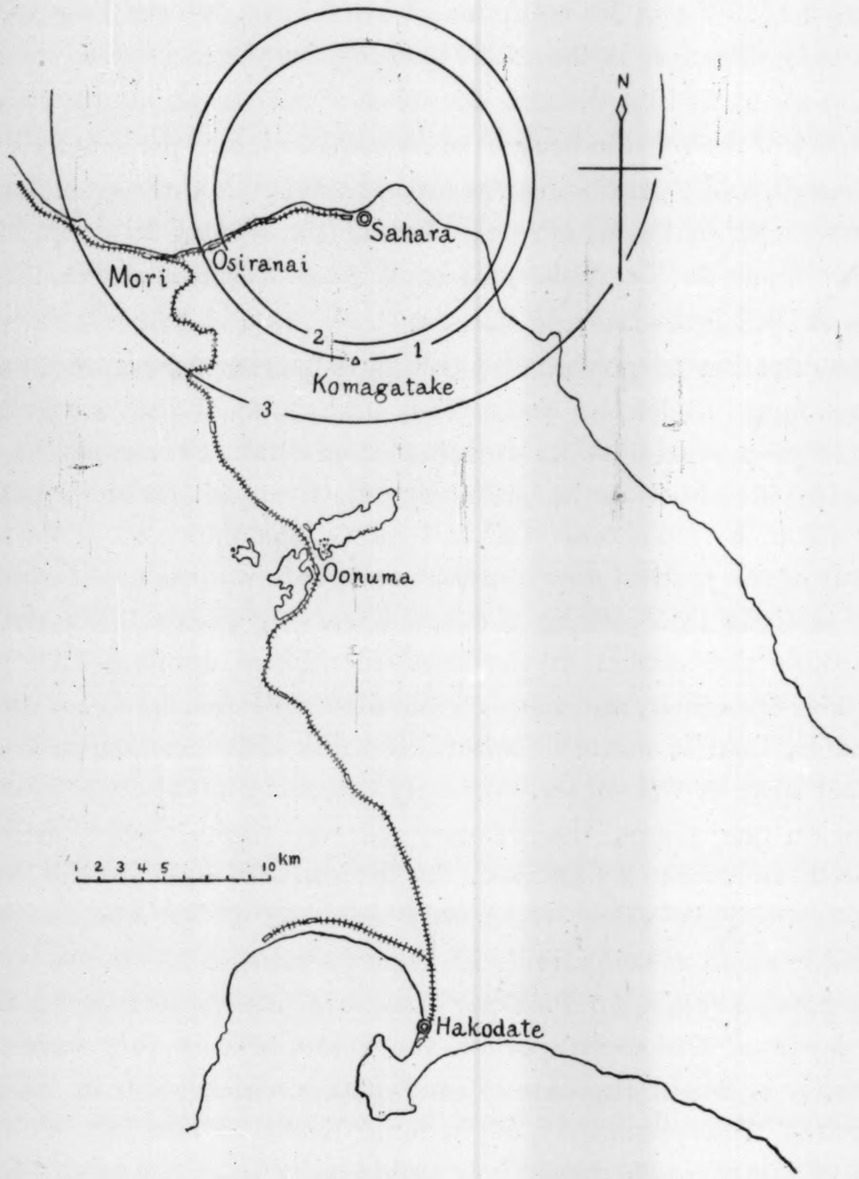

Fig. 2.

No. 1. June 28, 18h 48m
No. 2. July 4, 3 07
No. 3. July 4, 11 05

Table II.

Seismometrical Observations at Sahara from June 23 to July 10, 1929.

D.P.T. = Duration of preliminary tremours.
T.D. = Total duration of earthquake.
Cl. = Class (see p. 279).
M.A. = maximum double amplitude in mm. on the seismogram.

No.	Date	Arrival time	D.P.T.	T. D.	Cl.	M. A.	Remark
		h m	s	s			
1	VI 23	21 44·5		2	II	2	$11^h 37^m$ recording began.
2		21 44·6		2	I	2	$12^h 30^m$—$21^h 30^m$ recording drum stopped.
3		22 22	1·1	13	II	1·6	
4		23 23	0·9	16	II	1	Till VI 24. 0^h no time mark.
5		23 27	1·2	19	II	1·3	
6		23 50	1·9	7	II	1·5	
7	24	1 13	1·5	10	II	1·5	
8		2 15	0·7	1	II	2	
9		8 54·7	1·8	15	II	1	
10		8 55·0	2·7	11	II	1	
11		9 29		120	III	1·5	
12		9 46		60	III	0	
13		10 07·7	0·9	2	I	1	
14		10 08·3	3·3	6	I	1	
15		10 55	0·6	6	II	2·6	
16		11 04	60·0	300	IV	1	
17		11 59		80	III	0	
18		12 19·2		10	II	0	
19		12 19·9	1·4	10	II	1·5	
20		16 05		300	III	1	$15^h 30^m$—$22^h 10^m$ no time mark.
21		16 19		150	III	1	
22		16 23		50	III	1	
23		16 24	0·7	16	II	1·5	
24		16 33		300	III	1	
25		17 14		150	III	1	
26		17 17		15	III	1	
27		20 52	2·5	40	II	1	
28		21 50	12·0	20	II	1·4	
29	25	4 03			II		Records overlapped, and unmeasurable.
30		4 30			II	56	Then the arrival-times are due to the
31		5 48			II		Hakodate Meteorological Station.
32		9 52	2·4	10	II	1·5	
33		11 51		20	II	1·5	
34		11 55	3·1	10	I	2·0	
35		11 57	3·0	10	I	1·5	
36		12 30	2·9	25	I	4·0	
37		14 05		70	III	1·2	
38		14 49		90	III	0	
39		15 40		5	I	1	
40		15 47		90	III	1·4	
41		15 52		2	I	1·5	
42		15 59		2	I	1·4	
43		16 00	2·3	20	I	8·5	
44		16 04		25	II	1·2	
45		16 08		10	II	1	
46		16 22		5	II	0	
47		16 25		40	III	0	

(*to be continued.*)

Table II. *(continued.)*

No.	Date	Arrival time	D.P.T.	T. D.	Cl.	M. A.	Remark
		h m	s	s			
48	VI 25	16 44		60	III	1	
49		17 16		20	II	2.5	
50		17 35		10	II	1·5	
55		18 00		60	III	1·2	
56		18 25		15	I	0	
57		19 47		10	I	1·2	
58		20 06		10	II	1	
59		20 21		25	I	2·6	
60		20 22		20	I	2·5	
61		21 02	4·3	30	II	2·1	
62		21 04	4·2	50	II	3·0	
63		22 25		25	III	1	
64		22 26		5	I	1·6	
65		23 23		30	II	1	
66	26	0 02	2·1	30	I	4	
67		1 58		15	II	1	
68		2 24		1	I	0	
69		8 40		180	III	1	
70		9 00		30	II	1	8h 20m—14h 50m development of recording
71		9 45·5		15	II	1	bromide paper was failed, and measur-
72		9 45·9		10	II	1	ing is very hard.
73		12 08		15	II	1	
74		14 53		20			
75		15 40		5	I	1·5	
76		15 55		25	II	1	
77		16 01	5	25	II	1·4	
78		16 09		20	II	1	
79		16 14		80	III	1	
80		16 18		50	III	1·2	
81		16 27		60	III	1	
82		16 28		10	II	0	
83		16 53		100	III	1	
84		17 12		50	III	1	
85		17 32	3·6	40	II	3·5	
86		19 21		70	III	0	
87		20 07		30	II	1	
88		22 04		50	II	0	
89		23 13	2·0	50	I	4·0	
90		23 47		10	II	1·2	
91		23 53	1·8	30	II	2·5	
92	27	1 29		30	II	1·2	
93		1 47	71	600	IV	1·0	
94		5 05		15	I	3·5	
95		6 35		10	I	3·4	
96		7 33		3	I	1	
97		8 09	3·6	50	II	3·2	8h 50m—10h 17m records overlapped.
98		16 48		100			12h 20m—15h 10m filament of electric lamp
99		16 51		50			was broken, and no record.
100		19 16		20	II	1·5	
101		21 58		1	I	1·2	
102		22 17		1	I	1·4	
103		22 26		20	III	0	
104		22 27		40	III	0	
105		22 28		30	III	1	
106		22 32		20	II	1	

(to be continued.)

Table II. (*continued.*)

No.	Date	Arrival time	D.P.T.	T. D.	Cl.	M. A.	Remark
		h m	s	s			
107	VI 27	22 38		3	II	0	
108		22 40		50	III	0	
109		22 42		30	III	0	
110		22 46		40	III	0	
111		22 48		30	III	0	
112		22 56		50	III	0	
113		23 02		50	III	0	
114		23 04		60	III	0	
115		23 07		10	II	0	
116		23 12		25	III	0	
117		23 13		40	III	0	
118		23 24		2	I	0	
119		23 26		40	III	0	
120		23 28		30	III	0	
121		23 30·5		30	III	0	
122		23 31·0		20	III	0	
123		23 40		40	III	0	
124		23 42		10	II	0	
125		23 44		40	III	0	
126		23 48		15	III	0	
127		23 50		15	II	0	
128		23 51		30	III	1	
129		23 52		30	III	0	
130		23 56		20	II	0	
131		23 59		15	II	0	
132	28	0 04		10	II	0	
133		0 07		35	III	0	
134		0 10		60	II	0	
135		0 12		240	III	1	
136		0 33		80	III	0	
137		0 35		10	II	0	
138		0 37		20	III	0	
139		0 40		15	II	0	
140		0 41		10	III	0	
141		0 42·0		15	III	0	
142		0 42·5		10	II	0	
143		0 46		20	II	0	
144		0 48		10	I	0	
145		0 59		10	II	0	
146		1 14	1·6	20	I	20	
147		1 36		20	II	0	
148		1 44		10	II	0	
149		1 45		60	III	0	
150		1 47		30	III	0	
151		1 53		30	III	0	
152		1 55		20	II	0	
153		2 18		80	III	1	
154		2 27		80	III	1	
155		2 35		50	III	0	
156		2 50		10	II	1	
157		2 58		10	II	0	
158		3 58		15	III	0	
159		4 01		250	III	0	
160		4 05		250	III	0	
161		4 21		20	III	1	

(*to be continued.*)

Table II. *(continued.)*

No.	Date	Arrival time	D.P.T.	T. D.	Cl.	M. A.	Remark
		h m	s	s			
162	VI 28	5 39	2·4	30	II	1·5	
163		6 47		45	III	1·4	
164		7 14		540	IV		Period of vibration is long.
165		7 23	3·0	60	II	1·2	
166		12 00	1·1	30	I	1	
167		14 17	1·6	20	I	1	
168		14 32		60	II	1	
169		14 41		10	I	0	
170		18 48	2·6	80	I	2	D.P.T. of Hakodate = 12·8^{s}.
171		19 12		10	II	0	
172		20 02		20	II	0	
173		20 17		30	II	1	
174		20 36		30	II	0	
175		20 46		20	II	0	
176		21 20		140	III	1·2	
177		22 03		20	II	0	
178		22 37		10	II	1	22^{h} 45^{m}—VI 29. 12^{h} 30^{m} voltage of electric
179	29	12 39	1·5	40	I	1	cells dropped, and light gave out.
180		12 47	1·4	30	II	1·7	
181		12 53		20	III	1	
182		13 05		10	II	1	
183		13 25		15	III	1	
184		14 00		110	II	0	
185		14 11		100	III	1	
186		14 32		15	II	1·6	
187		14 59		25	II	0	
188		18 50		15	II	0	
189		19 11		20	II	1	
190		19 42	2·0	25	II	2·0	
191		21 56		50			Felt.
192		23 29		10	II	0	
193	30	4 41		15	II	1	
194		7 25		20	II	0	
195		8 25		50	I	1	
196		8 47		20	II	1·5	
197		9 05		30	II	0	
198		10 17·7		15	III	1	
199		10 18·5		5	I	1·2	
200		11 14		50	III	1	
201		11 16		20	III	0	
202		11 57		20	III	1	
203		11 58		40	III	1	
204		12 25		60	II	0	
205		13 00		10	II	0	
206		13 29		10	II	0	
207		15 33		80	III	0	
208		16 14		100	III	1	
209		16 31		15	II	1	16^{h} 50^{m}—21^{h} 08^{m} records overlapped.
210	VII 1	1 16		15	II	0	
211		8 06		10	II	0	
212		8 09		40	III	0	20^{h} 40^{m}—22^{h} 25^{m} drum stopped.
213		8 12		40	III	0	
214		9 04		20	III	1	
215		10 47		20	II	1	
216		10 56		20	II	1	

(to be continued.)

Table II. (*continued.*)

No.	Date	Arrival time	D.P.T.	T. D.	Cl.	M. A.	Remark
		h m	s	s			
217	VII 1	11 15		10	II	1	
218		12 22		20	II	0	VII 2. $6^h 00^m$—$21^h 40^m$ drum did not
219		17 18		15	II	0	rotate, and records overlapped.
220		17 23		15	III	0	
221		20 17		10	II	0	D.P.T. of Hakodate = 11^s.
222	3	2 08		40	II		$2^h 00^m$—$9^h 30^m$ record is faint.
223		12 18		180		1	
224		12 43	2·2	30	II	1·5	
225		12 57		20	II	1	
226		15 03		90	II	1	
227		18 00		50	II	0	
228		18 01		60	II	0	
229	4	0 16		30	II	1	
230		3 07	1·9	60	II	2	D.P.T. of Hakodate = 11^s.
231		3 34	1·8	30	II	1·5	
232		5 35		180	II	0	
233		5 39		60	II	0	
234		9 27		110	III	1·0	
235		9 30		60	II	0	
236		9 34		30	II	1·5	
237		10 02		70	II	1	
238		10 11		20	II	0	
239		10 19		5	I	1·5	
240		10 57		90	II	1	
241		11 02		50	II	2	
242		11 05	3·0	130	II	2	D.P.T. of Hakodate = $9·0^s$.
243		11 18		50	II	1	
244		11 33		50	II	3	D.P.T. of Hakodate = $10·0^s$.
245		11 36	1·4	30	II	2	D.P.T. of Hakodate = $9·0^s$.
246		12 08		40	II	1	
247		12 27		10	II	1	
248		12 40		10	II	0	
249		12 41		15	III	1	
250		12 50		30	II	1·2	
251		14 33		20	II	0	$15^h 00^m$—$16^h 40^m$ records overlapped.
252		17 33		5	I	0	
253		17 51		5	I	0	
254		18 37		25	III	0	
255		18 55		5	II	0	
256	5	5 03		180	III	0	
257		6 56		150	III	1·2	
258		8 24		5	II	1	
259		8 29		40	II	0	
260		8 49		30	II	1	
261		8 55		10	I	1	
262		8 59		60	II	1	
263		9 08		25	II	1	
264		9 10		20	II	0	
265		10 07		30	II	0	
266		10 43		150	II	1	
267		11 52		40	II	1	
268		12 27		60	III	1	
269		14 08		40	II	0	
270		14 19		20	II	0	
271		15 09		20	II	0	

(*to be continued.*)

Table II. (*continued.*)

No.	Date	Arrival time	D.P.T.	T. D.	Cl.	M. A.	Remark
		h m	s	s			
272	VII 5	15 18		50	III	1	
273		15 29	4·0	30	I	3	$14^h\,40^m$ – $16^h\,06^m$ records overlapped.
274		17 57		100	III	1	
275		18 39		20	II	1	
276		19 25		10	II	0	
277		20 12		15	II	0	
278		22 00		40	II	1	
279		22 07		25	II	1	
280		23 25		40	II	0	
281		23 32		40	II	0	
282	6	2 10		30	II	1	
283		8 17		80	IV	0	
284		8 51		10	II	0	
285		9 29		20	II	1	
286		10 04		15	II	0	
287		10 06·5		50	II	0	
288		10 07·2		50	II	0	
289		10 08·0		30	II	1	
290		10 08·7		180	III	1	
291		16		100	III	1·1	$11^h\,22^m$—$14^h\,59^m$ records overlapped, and no time-mark.
292		16 30		60	II	1	
293		19		40	III	0	
294		20		40	III	1·2	
295	7	3 22		10	II	2·0	D.P.T. of Hakodate = $9{\cdot}5^s$.
296				60	II	5	records overlapped, and the arrival-time is unmeasurable.
297		9 00		170	III	1	
298		15 45	8·9	150	II	20·	$11^h\,45^m$—16^h records are indistinct.
299		18 14		20	II	1	$16^h\,00^m$—$16^h\,30^m$ records overlapped.
300		18 24	2·1	20	II	4·4	
301		18 47		30	III	1·4	
302		19 02		60	III	1·5	
303		20 16		50	III	1·7	
304		22 34		20	III	1·4	
305		22 38		20	III	1·8	
306		22 48		10	III	1·2	
307		22 49		10	III	1·2	
308		22 50		40	III	1·6	
309		23 47	2·1	50	II	2·4	
310	8	0 06		45	III	1	
311		0 22		160	IV?	0	
312		0 42		50	III	1	
313		4 48		60	III	1·6	
314		5 18		5	II	0	
315		5 21		40	III	1	
316		5 24		50	III	0	
317		5 31		60	III	1·4	
318		6 07		40	III	0	
319		6 29	2·5	80	II	12·	
320		6 38		50	III	0	
321		6 41·0		60	III	0	
322		6 41·5		10	II	1	
323		6 42·0		10	II	1·2	
324		6 43·0		15	II	1·4	
325		6 43·6		15	II	1	
326		6 45		60	III	0	

(*to be continued.*)

Seismograms recorded at Sahara.

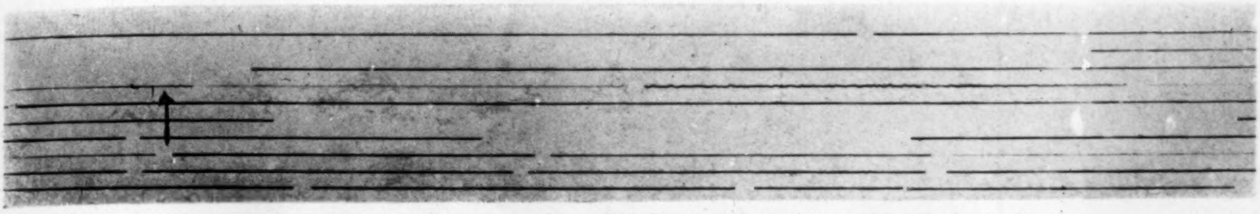

Fig. 1. June 24, $11^h 04^m$. Class IV. Reduced photographically in half. (see P. 280)

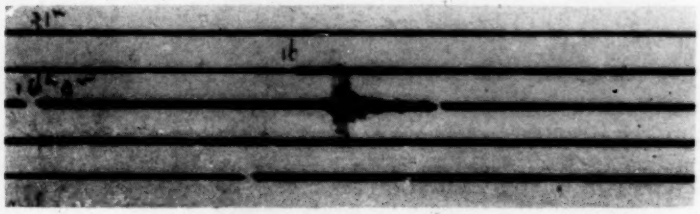

Fig. 2. June 25, $16^h 00^m$. Class I

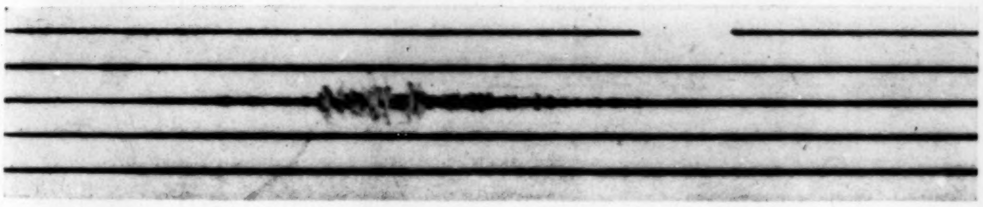

Fig. 3. July 10, $3^h 10^m$ Class II. 1 min. = 132 mm.

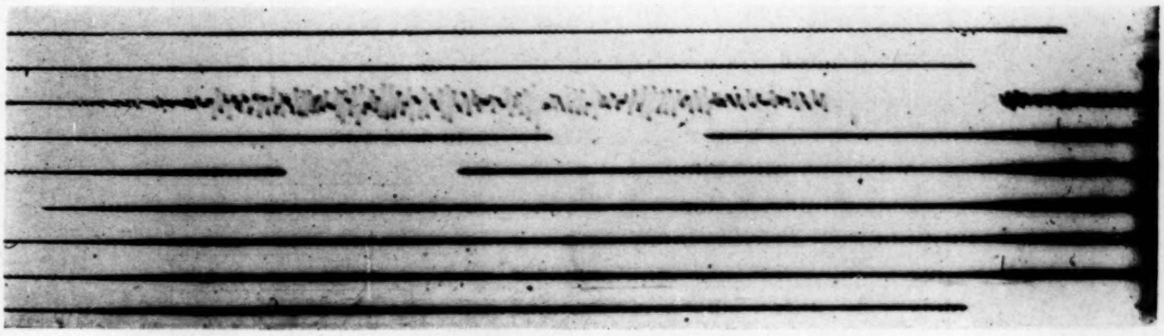

Fig. 4. July 10, $17^h 28^m$. Class II. Recorded on film. 1 min. = 261 mm. (see P. 280)

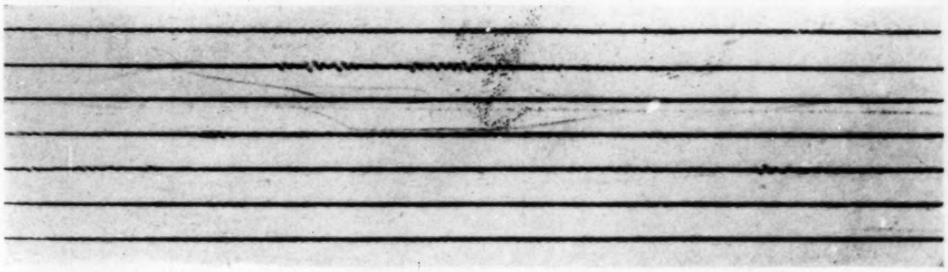

Fig. 5. July 8, about $6^h 40^m$. Class III. 1 min. = 236 mm. Many small earthquakes are seen.

（震研彙報第八號、圖版、岸上）

Table II. (*continued.*)

No.	Date	Arrival time	D.P.T.	T. D.	Cl.	M. A.	Remark
		h m	s	s			
327	VII 8	6 46		70	II	1	
328		6 49		60	III	1	
329		6 56		15	II	1·4	
330		6 57		25	III	1	
331		6 58		25	II	1·8	
332		6 59		60	II	1·4	
333		7 11		40			
334		7					$7^h 30^m$—$9^h 30^m$ records overlapped.
335		7					
336		9 43		30	II	1	
337		9 44		60	III	1·4	
338		9 45	1·1	10	I	2·0	
339		10 23		30	II	1	
340		10 47		120	III	1	
341		11 05		10	III	0	
342		11 15		10	I	1·2	
343		11 30		60	III	0	12^h—15^h records overlapped.
345		17 30	3	180	III	1	
346		18		30	II	1·4	
347		21 32	2·3	40	I	11	$21^h 17^m$—VII 9. $6^h 01^m$ recorded on film.
348		23 03	1·0	30	I	3	
349	9	0 53	1·4	50	I	3·8	
350		0 59		30	II	1	
351		2 31		30	III	0	
352		3 07		10	I	1	
353		3 18		180	III	0	
354		3 26		230	III	0	
355		3 30		250	III	0	
356		3 42		80	III	0	
357		3 44		120	III	1	
358		3 47		80	III	0	
359		4 01		140	III	0	
360		4 13		70	III	0	$4^h 30^m$—$7^h 00^m$ incessant microseisms.
361		4 54		60	III	0	
362		6 55	2·3	25	II	1	
363		7 57		20	III	1	$8^h 07^m$—$19^h 30^m$ records overlapped.
364	10	3 10	13	40	II	5·2	$14^h 04^m$ small earthquake-sounds.
365		3 20	2·3	30	II	2	$20^h 30^m$—VII 10. 0^h drum stopped.
366		4	3·4	60	II	12	$19^h 40^m$—VII 10. 0^h recorded on film.
367		7 04		40	II	1	
368		8 27		130	III	0	
369		9 08		70	III	1	
370		11 51		20	III	2·5	
371		12 05	7·2	50	II	2·0	$12^h 25^m$—14^h microseisms.
372		12 32		35	III	1·8	
373		12 34		10	III	1·4	$12^h 40^m$—$14^h 15^m$ records overlapped.
374		15 49		40	III	1·2	$15^h 47^m$—22^h 30 recorded on film.
375		15 55		30	III	1·6	
376		16 15		40	II	1·4	$22^h 50^m$—VII 11. 0^h recorded on film.
377		17 28	3·7	40	II	5·2	$23^h 30^m$—VII 11. 0^h drum stopped.

Part IV. Observations of the Tilt of the Ground accompanying the Eruption. (*With one figure.*)

By Ryutaro TAKAHASI,

Earthquake Research Institute.

(Read March 18, 1930.—Received March 20, 1930.)

1. An eruption of a volcano is often accompanied by the depression or the upheaval of the volcanic mass itself or of the region surrounding it. As one of the typical example of such phenomena, we can point out those in the case of the eruption of the volcano Sakurazima in Kagosima Bay in 1914[1]. Precise levellings along the coast of Kagosima Bay were repeated twice after this eruption. The first levelling was executed in 1914 and the second in 1915. By the comparison of the results of these levellings with those before the eruption, it was found that the circumferential region of the volcano was depressed by an amount of ca. 50 cm. and that the depressed area extended to the distance of more than 30 km. from the volcano, though the amount of the depression diminished with the increasing distance. Another example was furnished by the eruption of Usu volcano in 1910[2], but the case is more complicated. In this case the volcanic region made an upheaval of an amount as large as 2 metres, while its surrounding regions a depression on the contrary. Moreover, it was revealed in this case by the second levellings carried out in 1911, that the disturbed area made a small amont of recovery within a year after the eruption.

Recently a report of observations for thirteen years of the tilt of the ground of Hawaii Island was given by T. A. Jaggar[3]. In his report we can notice a very close relation between the tilt of the ground and the activity of the Kilauea volcano.

Is it not possible to observe such depression or upheaval accompanying the eruption of a volcano, not only after but also before or during the

1) F. Omori, *Bull. Imp. Earthq. Inv. Comm.*, 8 (1916), 152–179.
2) F. Omori, *Bull. Imp. Earthq. Inv. Comm.*, 5 (1911), 1–38.
3) T. A. Jagger and R. H. Finch, *Bull. Seism. Soc. Amer.*, 19 (1929), 38–51.

event? For the purpose of doing this, it will be a short way to make a continuous observation of the tilt of the ground at a point at the foot of the mountain, as it is practically impossible to carry out precise levellings continually over the area including the volcano.

In these views, we have made a series of continuous observations of the tilt of the ground in the case of the recent eruption of Komagatake. The results of the observation will be described in the following pages.

2. The instrument used in this observation is a pair of Ishimoto's tiltmeters[4]. It is a small horizontal pendulum of Zöllner's suspension type, of which the frame work, the movable horizontal rod and two suspension fibres are all made of fused silica. The quartz suspension fibres are directly fused to the frame work and horizontal rod. No use was made of other materials than fused quartz in the essential part of the pendulum. It is therefore entirely free from elastic after-effect, thermal deformations of the instrument and any kind of frictional resistances. The deflection of the horizontal rod is recorded optically on sensitized photographic paper wound on a drum which make revolutions once a week by a clock work contained in it. The sensitivity of the tiltmeter can easily be adjusted by regulating its period of free oscillations. A 6-volt electric lamp fed by a portable storage battery serves as the light source of the optical system of the instrument.

The tiltmeters were installed, together with a microseismograph and a gravity variometer as described in other part of this report, in a hut at Sahara, a lonely fishing village at the northern skirt of Komagatake. The hut is built on a terrace and is about 250 metres apart from the sea. The soil near the hut is of old mud-flow of Komagatake, composed of sands and gravels. The hut has a concrete floor 15 cm. thick and the instruments were installed directly on this floor. The tiltmeters were set up in such directions as to record N-S component and E-W component of tilt respectively. N-S direction coincides roughly with the radial and E-W with the circumferential direction with regard to the volcano. The sensitivity of the tiltmeters was adjusted to be such that a tilt of 1 second of arc will produce a deflection of 0·5 cm. on the record. It was necessary to protect the glass bell-jar containing the quartz part of the tiltmeter with cotten wool to minimize the convection of air in it.

The observation was commenced at 22 h. on 22nd. of June, the next day of our arrival at Hokkaidô. After two weeks' observation made by ourselves, the managements of the instruments were left to Mr. Z. Sato, the owner of the hut.

3. Fig. 1 shows the north-south and east-west component curves of the tilt of the ground obtained at Sahara, starting from an arbitrary zero,

4) M. Ishimoto, *Bull. Earthq. Res. Inst.*, 2 (1927), 1–12.

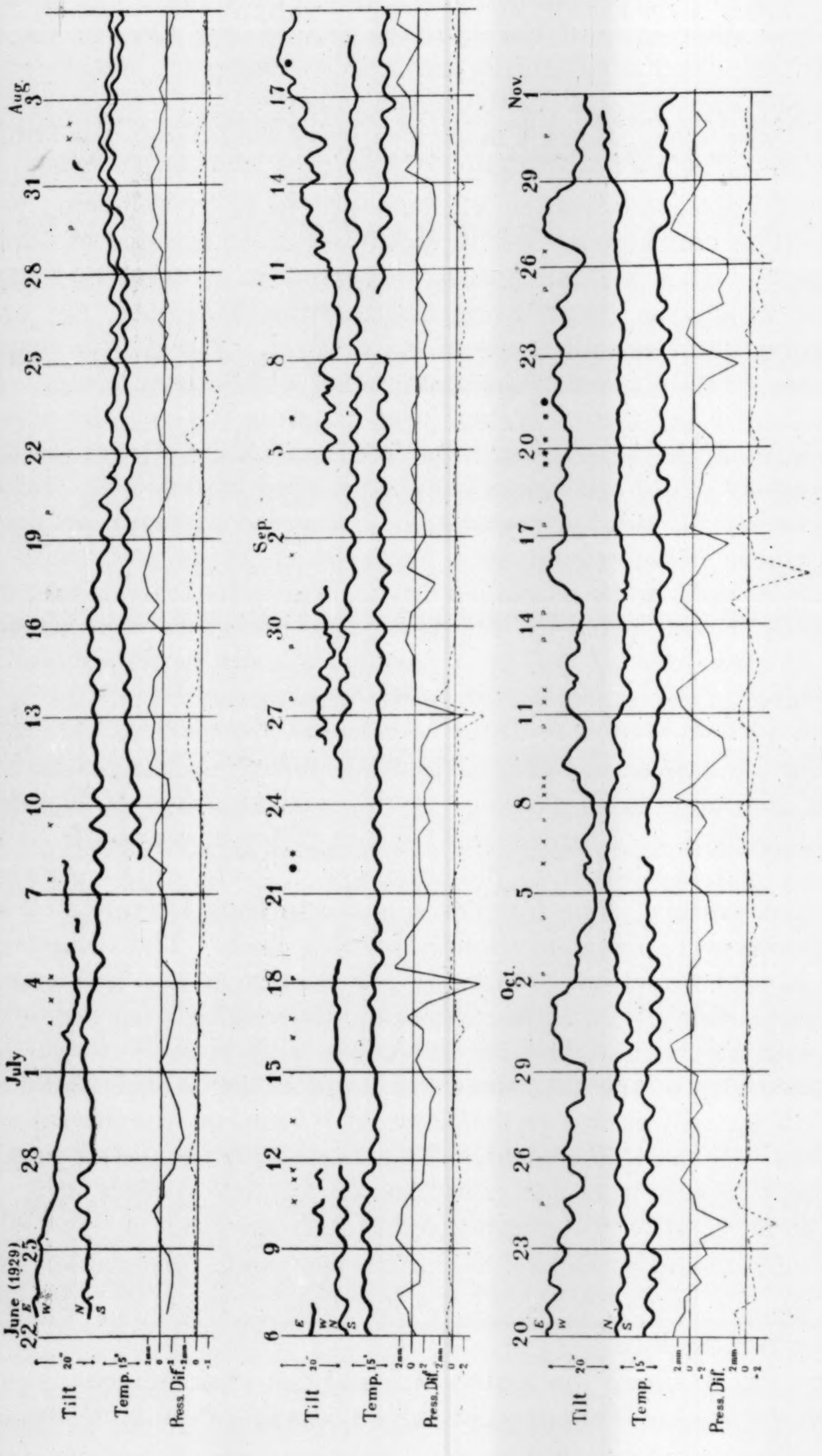

Fig. 1.

together with a curve of atmospheric temperature at Sahara recorded by a Richard thermograph and two curves showing the difference in atmospheric pressure Hakodate-Obihiro and Hakodate-Sapporo. In the former half of the period of observation, the observation was often interrupted, in times by instrumental troubles and in other times by the uncostumnedness of the manager to the manipulation of the instrument.

Superimposed on the tilt curve in Fig. 1, small indentations with daily period are to be seen. These indentations are common in district having a weak superficial layer of soil. They are generally small in amplitude when it is rainy of cloudy. They are almost in phase with the atmospheric temperature variation. The cause of these indentations is already ascertained by the tilt observations at Mitaka, Tukuba, Misaki, Tokyo etc., and is attributed to the effect of thermal strain in the ground.

In addition to these daily variations, there are tilt of the period of several days. Some of these tilt correspond to the long period variation of the atmospheric temperature, but there are others which do not.

Daily tilt in N-S and E-W components do not differ much in amplitude, so that their resultant tilt is directed to N-W when the temperature rises, while E-W tilt of longer period is about two times as large as that of N-S, so that their resultant is directed to NWW, differing from that of the daily variation.

Besides these thermal tilt there are tilts which do not correspond to the variation of temperature. For instance, E-W component of tilt has made a marked variation towards west at the beginning of the observation and continued till July 4th., as can be seen in Fig. 1. From September 10th. to 23th. of the same month E-W component made a large variation than can be expected from the temperature variation. Such variations which do not correspond in amount to the temperature variation can also be seen in N-S component. From October 17th. N-S component ceased to follow the temperature variation and remained in a state inclined to the north for some ten days. It will be worthwhile to notice here that the daily variation in N-S component of tilt becomes small in amplitude when there is non-thermal eastward tilt in E-W component curve.

Correlations of these abnormal tilt with the activity of the mountain and with other meteorological factors will be studied in the next.

4. In Fig. 1 the atmospheric pressure differences between Hakodate and Obihiro and that between Hakodate and Sapporo are shown by full thin line and dotted thin line respectively. Both differences are taken as positive when Hakodate is higher in pressure than others. The

values of the atmospheric pressure are those at 6h. and 18h. of every day taken from the weather map issued from the Central Meteorological Observatory. As can be seen in the figure, there exists a remarkable correlation between these pressure differences and the tilt of the ground observed at Sahara.

Of course there is also a correlation between the atmospheric pressure difference and the atmospheric temperature.

When the pressure at Hakodate is higher than those at two other stations, the ground tilts to the directions south and west, against the expectation of common sense but suggesting some mechanisms of the volcanic action and the block movements. In the earlier part of the period of observation, or in the period soon after the eruption, N-S component of tilt seems to have followed very easily to the variation in pressure difference, while in the later period it has become not to follow the pressure difference variations so easily. As to E-W component of tilt, westward tilt which is independent of pressure and temperature has been very remarkable soon after the eruption and after that the tilt has become oscillatory, controlled by the temperature and pressure.

The tilt seems not to reply the short period variation of the atmospheric pressure difference such as caused by the passage of a cyclone.

In connection with the sharp westward tilt stated above of the ground at Sahara soon after the eruption, we must point out the results of the precise levellings carried out by C. Tuboi and by the Land Survey Department over the route Sahara-Mori-Onuma. According to the results of these surveys, the ground at Sahara tilted towards west, in agreement with the results of our tiltmeter observation. As to the detail of the levellings, readers are requested to refer the part of this report written by C. Tsuboi.

Next we will proceed to describe the relations between the tilt of the ground and the volcanic activity of the mountain. As the measure of the activity of the volcano we will take the frequency of the earthquakes of volcanic character observed at Sahara, the rumbling of the mountain and the pulsation of the ground which is recorded by the tiltmeters. The quantity of the smoke exausted from the crater may serve as another measure of the activity of the volcano. But in our case, there being collected few data concerning this point, we cannot, to our regret, utilize this phenomenon. The tremors of the ground called here as pulsation are of different nature from the ordinary pulsation. It seems to continue only for a short time interval of half a day or less with the mean

amplitude diminishing with the time. It occurs in successsion in an active period of the mountain.

In addition to these data, the earthquakes of inland character observed at Hakodate Meteorological Station were taken into consideration. Some of these earthquakes can be regarded to have their origins at Komagatake.

In Fig. 1 the earthquakes observed at Sahara are shown by black dotts, the rumblings of the mountain by stars, the pulsation of the ground by the letter *p* and the earthquakes observed at Hakodate by small crosses. Of course it must be remembered that the earthquakes, the rumblings of the mountain and the pulsations of the ground listed here are only a few percentage of the whole, and there must be great many of them that have escaped our attension. From the figure it can be seen that the pulsation is predominant in the period when the tilt is going on independently of the variation in temperature.

The frequency of the earthquakes seems to be large when the ground is remaining in a state tilted to the direction EEN or in times when it is recovering from the tilted state to the original. In an active period of the volcano, it seems therefore that the tilt of the ground in the direction EEN occurs in the first place with the pulsation of the ground and then the rumbling of the mountain and earthquakes follow. In this later stage of an active period, the tilting of the ground already ceases and is recovering to its natural state.

It will be worthy to notice that these active periods seem to coincide with the time when there is continually for several days a pressure gradient of the constant sign over the mountain, as can be seen in Fig. 1.

It seems that there is no remarkable correlations between tilt and precipitations, humidity etc.

5. There are many alternative explanations by which we can elucidate the correlations between the atmospheric pressure difference, the tilting of the ground, the variation of air temperature and the outburst of a volcano. It cannot easily be determined which is the original cause and how they are connected to each other. It will however provide one explanation of the relations existing among them to think that the pressure differnce is the radical cause of these phenomena provoking the other three. If this assumption be granted, the relations among these phenomena seems to be anyhow explained.

In the first place, an explanation of the relation between the pressure difference and the tilting of the ground will be tried. In volcanic regions

the tilt of the ground is considered to be composed of the general tilt of the block on which the volcano rests and the tilt of the ground caused by the tumescence or the depression of the volcano.

Correlations between the pressure difference or gradient and the tilting of a land block was for the first time verified by M. Ishimoto[5]. M. Ishimoto found some relations among the atmospheric pressure gradient, tilting of Miyadu block and the occurrence of the aftershocks of the Tango Earthquake. He also noticed in one of his paper[6] that the north-south gradient of the atmospheric pressure over the Kwanto district reflects the east-west tilting of the land block containing Mt. Tukuba. W. Inouye[7] gave recently an interesting paper in which he remarked that whenever the tilt of the Tukuba block which is usually monotonous and one-directioned, changes itself into an oscillatory, to and fro tilting, it is always followed by the occurrence of an earthquake.

Of late block movements of the earth's crust in various part of this country were revealed by precise levellings or triangulations. After the Tango Earthquake levellings and triangulations were repeated four times. According to the results of these surveys, the triangulation points and bench marks in the disturbed area have always showed some displacements and they show no sign of stopping the movements[8]. As cited in the introductory part of this paper, the blocks arround the Sakurazima volcano made remarkable tilts and depressions in the case of the eruption of 1914 and the motion of the blocks was proved to have existed even in the interval between the second and third surveys in a reduced amount.

Even in such districts, not distribed by an earthquake nor by an eruption of a volcano, tilting of blocks are to be seen. Levelling surveys executed in Hokuroku district revealed a chronic tilting of the land blocks consisting the district[9].

In these views of the behaviours of land blocks, they must be considered as if they were wood blocks floating side by side on water. In case of the eruption of a volcano or of an earthquake, this substratum of blocks likened above to water may be considered to become by some

5) M. Ishimoto, *Bull. Earthq. Res. Inst.*, **4** (1928), 203–222.

6) M. Ishimoto, *Jap. Journ. Astron. Geophys.*, **6** (1928), 116.

7) W. Inouye and T. Sugiyama, *Proc. Imp. Acad.*, **5** (1929), 457–459.

8) Land Survey Department, *Bull. Earthq. Res. Inst.*, **3** (1927), 167; **4** (1928), 223, 225; **5** (1928), 165; **7** (1929), 185, 381, 587.

9) N. Yamasaki, *Proc. Imp. Acad.*, **4** (1928), 60–63.

effect more easy to move or less viscous, and the thickness as well as the size of blocks become at the same time small. If this consideration be allowed, a change in the pressure distribution over the block system may result in the tilting of each block of the system, because the block system must change its configuration to keep its stability.

In the time of a volcano, the molten lava is raised to the level just beneath the crater, then the volcano must be under a very critical state and a slight variation, physical or chemical, of its external conditions may be able to become a cause to put the volcano into action. It is not impossible that the pressure gradient over the block system around the volcano can be such a cause. The change of the configuration of the block system caused by the variation of the pressure distribution must necessarily provoke the flow of the substratum of the blocks or of the lava in the lava pocket of the volcano. If this flow of lava can accelerate the cooling of the lava, the pressure in the lava may be increased and the explosion of the volcano may follow it.

On the other hand, a tumescence of the mountain must accompany an explosion of the volcano, and the tumescence must necessarily cause the tilting of the ground at the skirt of the mountain.

That the tilt does not answer to the short period variation of pressure may be attributed to the viscosity or plasticity of the substratum and of the crust itself.

Now we will proceed to the explanation of the relation between the pressure difference and the variation of the atmospheric temperature. If there existed for a few days a pressure difference between two districts, the transmission of air masses must naturally arise, and the atmospheric temperature of the district under consideration must suffer variations, provided that the mean temperature of the districts is different in value. It is also able to refer to the favour of this explanation that a high pressure is a mass of cold air, and that the air temperature controlls the density of air and can become a factor to determine the pressure distribution.

It must be remembered, however, that these explanations are nothing but imaginations, not based on any decisive facts. Further studies in various branches of geophysics must be performed for the elucidation of these interesting phenomena.

In conclusion, the author wishes to express his most cordial thanks to Professor Mishio Ishimoto for his valuable advices and discussions which he has constantly given.

Part V. Precise Levellings around the Volcano.

By Chûji TSUBOI,

Earthquake Research Institute.

(Received March 20, 1930.)

In order to find the deformation, if any, of the ground near Komagatake connected with the eruption, precise levellings were carried out around the volcano. There are two series of levelling route around the volcano, the one along its northern skirt, the other along its western skirt. The former was surveyed by the writer, and the latter by the experts of the Land Survey Department of the Imperial Army. The results of the latter series of the levelling were kindly placed at our disposal through the courtesy of Rare Admiral Oomura, the Chief of the Land Survey Department. The results of these surveys after the eruption were compared with those of the old surveys along the same routes. It was found that the ground around the volcano was deformed sensibly. In the following tables are given the changes in heights of the bench marks in the interval between the old and new levellings.

Table I.

Bench Marks	Δh
5967	assumed unchanged
Junction Pt. 19	−22 mm.
7062	—
7061	−81
7060	−83
7059	−82
7058	−61
7057	−71

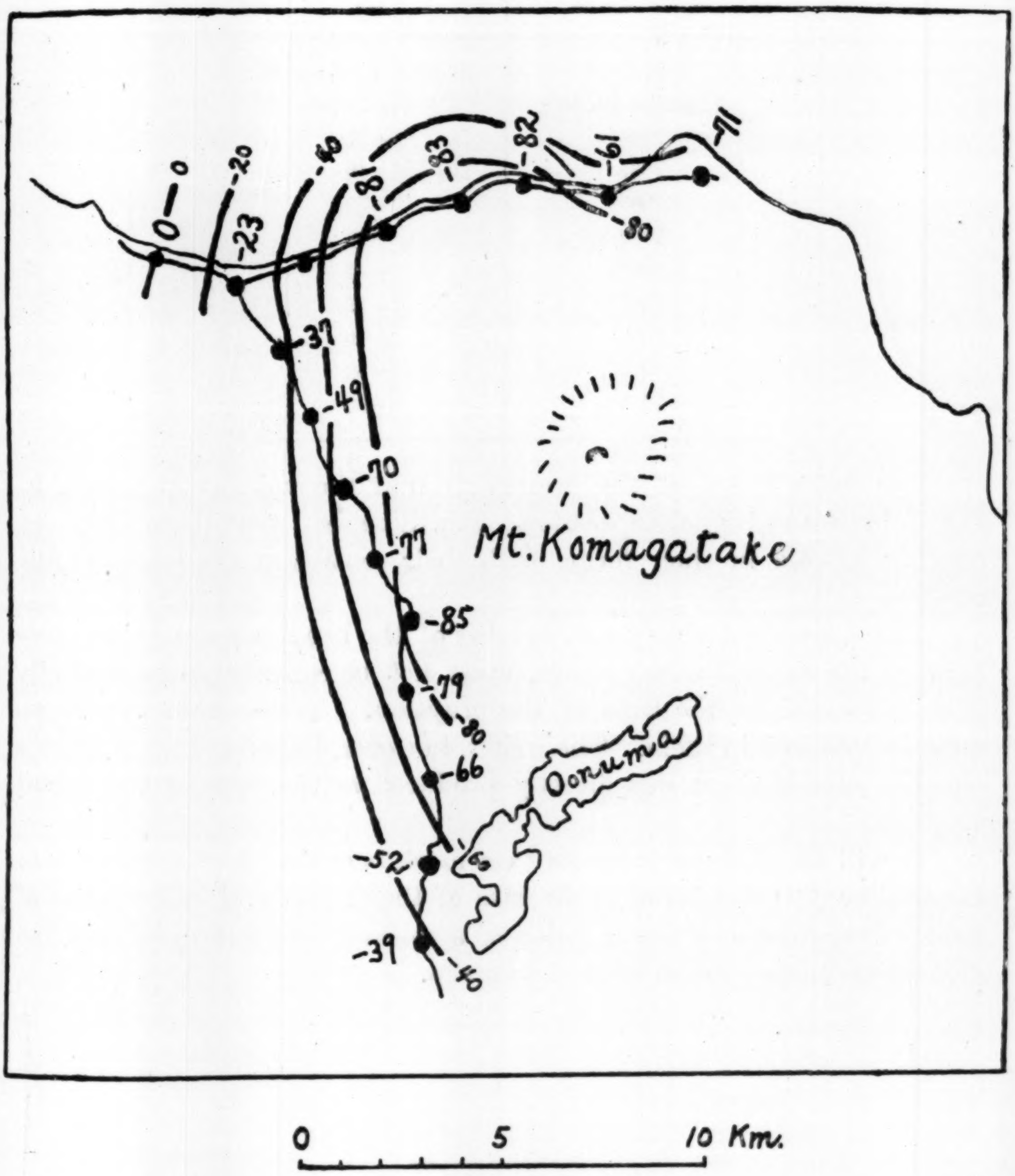

Fig. 1. Lines of Equal Depression in mm.

Table II.

Bench Marks	Δh
5967	assumed unchanged
Junction Pt. 19	−23 mm.
7063	−37
7064	−49
7065	−70
7066	−77
7067	−85
7068	−79
7069	−66
7070	−52
7071	−39

The deformation of the ground around the volcano is shown in Fig. 1. by lines of equal depression. It will be seen that these lines are roughly elliptic in their forms with their centres at the crater of the volcano.

The discovered changes in heights of the bench marks, being those between the old and new surveys, must not be regarded to have wholly been produced at the time of the eruption. Some chronic changes must be involved in them. The writer, however, believes that at least a sensible part of them was directly produced at the time of the recent eruption.

It will be of some interests to remark here that the deformation of the similar type was found in the case of the eruption of Sakurazima of 1914. It appears as if the eruption of a volcano, as a rule, produces the depression in the ground around its scarp.

Part VI. Observation with Gravity Variometer.

By Chûji TSUBOI,

Earthquake Research Institute.

(Received March 20, 1930.)

In view of getting if possible some information regarding the time variation in the subterranean mass distribution in the neighbourhood of the volcano Komagatake, continuous observation was commenced at Sahara with a gravity variometer. This is a kind of torsion balance made of vitreous silica. The theory and the design of this instrument were given by the writer in his previous paper[1]. By this instrument, it is possible to detect some time variation of the order of 10^{-10} c.g.s. in the second space derivatives of the gravitational potential. The instrument was installed at Sahara on 24th of June, 1929, and the observation with it was continued for about half a year. But no trace of change in the gravitational field was detected which was large enough to be recorded by the instrument.

---

1) *Bull. Earthq. Res. Inst.*, 6 (1929), 457.

Part VII. Electrical Phenomena caused by the Eruption of Komagatake.

By Kin'ichi NAKATA.

(Received March 20, 1930.)

Introduction.

The electrical spark discharges caused by the great explosions of volcanoes were recognized by our countrymen from ancient times. A picture of the eruption of Mt. Asama[1] on 5th of July in the third year of Tenmei (1783), illustrating many spark discharges in the cloud of smoke from the crater, still remains. Such phenomena were also recognized when Mt. Sakurajima[2] erupted during the year of An-ei (1779), and an interesting picture of the sparks drawn by Ijichi Kiken, is still in existence. Recently, late Prof. F. Omori[3] gave in his report on the eruption of Mt. Sakurajima in the third year of Taishô, some interesting photographs of spark flashes in the cloud of smoke. But little was studied on these phenomena.

One of the most interesting phenomena caused by the explosion of a volcano is the electrical one which have, as stated above, not been fully studied up to this time. The eruption of Mt. Komagatake in Hokkaidô last year gave us many valuable data in these lines.

This volcano erupted on 17th of June last year, and newspapers reported that furious lightning flashes were observed in the smoke blown up from the crater. I joined the party which was sent from the Earthquake Research Institute to investigate the volcano from every point of view. The object of my investigation was to study the variation of the atomspheric potential gradient and earth current caused by the eruption. In the following, a little note is given on the results of the investigation on these subjects.

1) *Rep. Earthq. Inv. Comm.*, (in Japanese) **73** (1911), Fig. 14.
2) *Pub. Earthq. Inv. Comm.*, **8** (1914), PL. XV.
3) *ibid.*, **8** (1914), PL. V.

Spark discharges on the day of the eruption.

The people near the foot of Mt. Komagatake were astonished at a horrible explosion at about 10 o'clock a. m. on 17th of June, 1929. They were not long in understanding the eruption of the mountain by finding out a tremendous mass of smoke blown out very high from its top. From about 11-30 a.m. they recognized many lightning flashes in the cloud of smoke and thunder claps were incessantly heard. When night came, the sparks increased their brilliancy and vigour and were unceasingly flashing above the fire column ejected from the crater. These flashes were seen not only at Ônuma, Mori and other towns situated near the foot of the mountain but also from Muroran and Hakodate which is situated at the distance of 34 kilometers from the mountain.

These spark discharges continued until about midnight and ceased entirely at about 1-30 a. m. on 18th. Though the intensity of the spark discharges was varied from time to time, the maximum intensity was said to have been experienced during the hours of 7 to 8 o'clock p. m. on 17th.

The wireless engineer on the Shôhô maru, the connecting steamer between Aomori and Hakodate, told us that the disturbance of radio communication caused by atmospherics was first noticed at about noon on 17th, but the transmission and reception of signals was maintained with difficulty until about 3 p. m. Since then the radio communication was completely hindered by the heavy atmospherics and this condition lasted until about 1-30 a. m. next morning. According to his statement, the severest atmospherics were experienced about 7 o'clock p. m. on the day. This corresponds well with the time of the severest lightning flashes observed. The intensity of the atmospherics was not so great as ordinary ones caused by the meteorological lightning discharges, judging from the fact that no spark was observed in a small spark gap connected in parallel with the antenna circuit. It was also pronounced at Hakodate that the JOIK broad casting transmitted from Sapporo was not accepted during these hours.

Many photographs of these spark discharges were taken at Mori, Hakodate, Muroran and other towns near the mountain. They are shown in the following pages. Figure 1 was taken at Mori, situated at 10 kilometers off the north-west of the mountain. The time of exposure was nearly 40 seconds. Figure 2 was taken at Hakodate at about 11 p. m., the time of exposure being nearly one hour. As is seen from these

photographs, the sparks are somewhat different from those of the ordinary lightning flashes. They have no branches and the bending is prominent than in the ordinary ones. The length of the individual spark appears to be a little shorter than usual.

It must be noted that no sparks are to be seen just above the crater though we can see many of them around the crater to a considerably lower position. This might give some light on the mechanism of the generation of the spark discharges in the smoke of a volcano. The spark discharges seen in these photographs must be considered to have been developed in the front side of the dense cloud and the greater number of them must be hidden inside or behind of the smoke, and so, the frequency of spark discharges must be much greater than in the case of ordinary thunder storms.

The mechanism of the accumulation of electric charge in thunderclouds is not yet fully known. It has been ascertained by many observers that electric charge is produced in the case when water drops are blown into small droplets. This is known as Lenard effect. It is also well known that electric sparks are occasionaly observed in the sand or snow storms, when sand or snow particles are driven by strong winds. There are many experimental works dealing with the charge production when solid particls are blown and are collided with each other. In the case of the eruption of a volcano, vast amount of water vapour as well as ashes, sand and rack scraps are blown out furiously. The mechanism of the charge production in the cloud of volcanic smoke may be assumed from the above mentioned phenomena, but it must be borne in mind that the conditions are more complicated in the actual case. Judging from the fact that the spark discharges ceased nearly at the same time when the falling of rock scraps was scarcely recognized although the gush of water vapour and ashes lasted long afterwards, it may be decided that the greater part of the electric charge was produced by the friction between the rock scraps themselves or rock scraps and other materials.

Measurements of atmospheric potential gradient and earth current.

When we arrived at Ônuma (at the southern foot of Mt. Komagatake) on 20th of June, the mountain was seen in the evening light giving a vast amount of grayish smoke and white steam from several places on the upper portion of the mountain. Yet the amount of the smoke was considerably diminished compared with that of the day of explosion.

The spark flashes, of course, could not be seen by our own eyes at that time. At any rate, we had to commence our investigations as soon as possible. I intended, as above mentioned, to study the variation of the atmospheric potential gradient and the earth current in connection with the action of the volcano.

Measuring instruments were set on a flat floor made of concrete about 20 cm thick inside of a wooden warehouse at a village of Sahara. The house was situated at the northern foot of the mountain about 200 meters from the seashore and about 20 meters high above the sea level. Tiltometers, a gravity variometer and a seismometer were also set in the same house.

The measurement of the atmospheric potential gradient was performed after the method adopted by Prof. D. Nukiyama and Mr. H. Noto.[4] A copper wire, the diameter being 0·5 mm, was stretched as an antenna above the ground nearly parallel to the contour line of the mountain (i. e. E-W direction). The length and the height of the antenna were 77·5 and 4·1 meters respectively. A sensitive galvanometer (sens. $4{\cdot}25 \times 10^{-8}$ amp per mm. deflection) was connected to the antenna and the other terminal of the galvanometer was connected to the earth. The insulation of the antenna was prepared by porcelain insulators and the protection from being wetted by rain was done with some specially constructed apparatus which was kindly offered by H. Noto.

The earth plate was made of copper (30×30 cm^2). It was buried surrounded by charcoal at the depth of 1 meter under ground. The deflection of the galvanometer was recorded on a bromide paper rolled aronnd a rotating drum.

The earth current was also measured with a simple method. Many difficulties have been experienced in the measurement of earth current. The problem is how to avoid the contact patential at the electrodes, thermoelectric effect and polarisation. Several methods have been proposed for this purpose but we were in such haste to arrive at the actual place as quickly as possible that I was obliged to adopt the most primitive one.

Two copper rods of the diameter 1·5 cm were driven into the earth and were used as electrodes. A galvanometer was inserted between these electrodes with a high resistance connected in series with it. In this manner the potential difference between two positions was measured.

4) D. NUKIYAMA & H. NOTO, *Japanese Jour. Astr. Geophys*, **4** (1928), 71.

It was obvious that there must arise some ambiguities due to the polarisation and many other sources of errors. As has been already mentioned only the variation of the earth current was necessary, and so, the method adopted was enough to serve the purpose. The distance between these two electrodes was made 150 meters apart, one near the warehouse and the other put in the southern direction (i. e. perpendicular to the contour line) about 5 meters higher than the former. The leading wire connecting these electrodes and the galvanometer was insulated from the earth by small pieces of porcelain.

Results.

At first many unexpected difficultes were met with and the observations were commenced from 11 p. m. on 22nd of June, about 6 days after the first sign of the eruption was recognized.

The records of the atmospheric potential gradient show no special deflection before 26th of June. The record on 26th is characterised by some oscillations of the galvanometer as shown in fig. 5. This disturbance was recorded from about 4-30 a. m. on 26th and lasted about one hour. A smaller disturbance was also recorded about one hour later. The feature of this record is somewhat like that of a distant thunder storm. This can not be considered as due to the instrumental error, for the record of the earth current shows no such a disturbance, while the two galvanometers were set on the same table and the both records were taken on the same bromide paper. The cause of this disturbance must be attributed to a purely meteorological origin or the action of the volcano. As for the meteorological origin, no thunder storm was recognized near that district at that time, while it must be noted that the number of small earthquakes recorded on the seismograph increased from the night of 25th to 26th.

Observations were continued until 10th of July, no other record such as fig. 5 was obtained. The records appeared as smooth straight lines except on rainy days, when, as well known, the oscillations of large amplitudes were recorded. While the records of the seismometer showed that the number of the earthquakes on 28th was more than that on 26th. This seems very unfavourable to the result above obtained, but we must bear it in mind that there is no direct relation between the variation of the atmospheric potential gradient and the earthquake. The number of earthquakes was only considered as a measure of the volcanic

[K. Nakata.]

(震研彙報、第八號、圖版、中田)

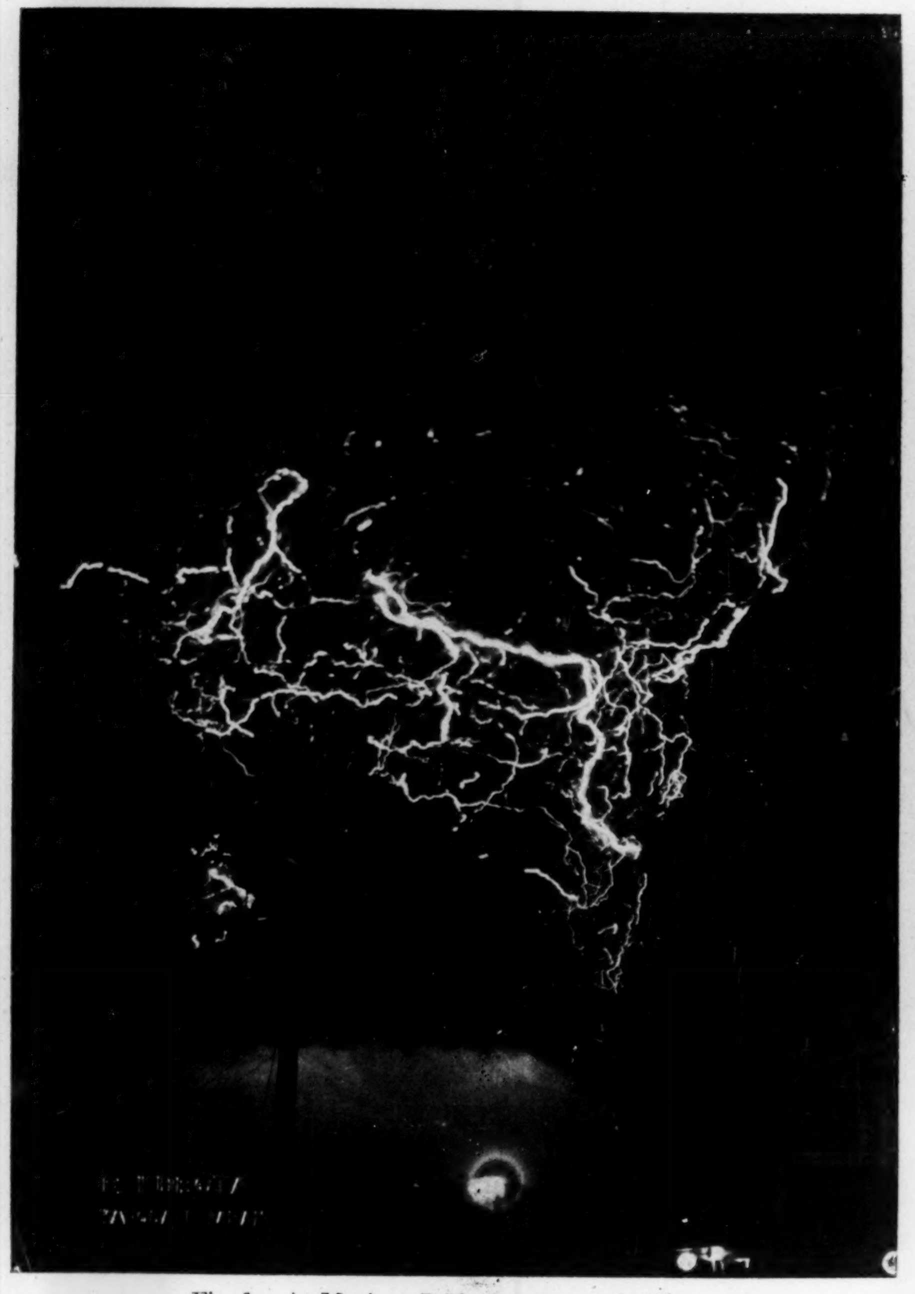

Fig. 1 At Mori, at 7-30 p.m. exposure, 40 sec.

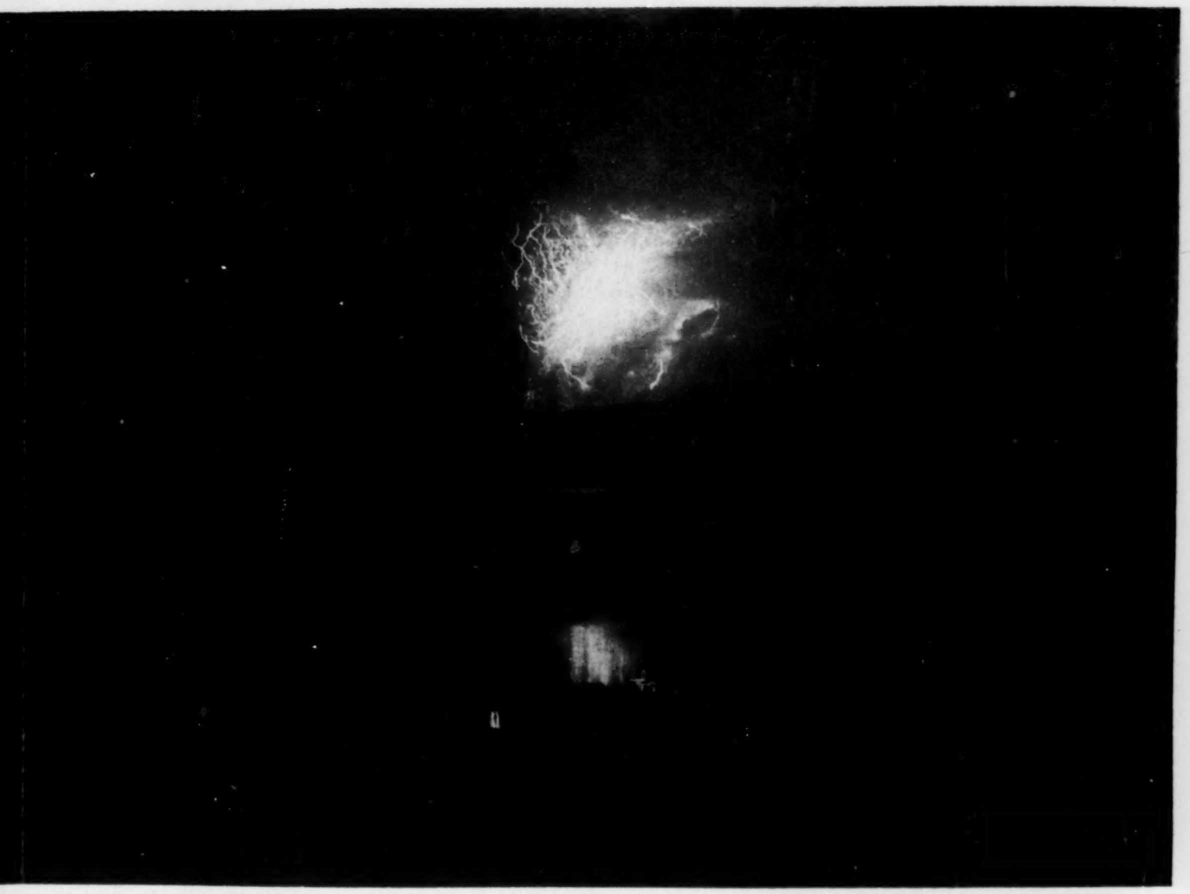

Fig. 2. At Hakodate, at 11 p.m. exposure 1 hour.

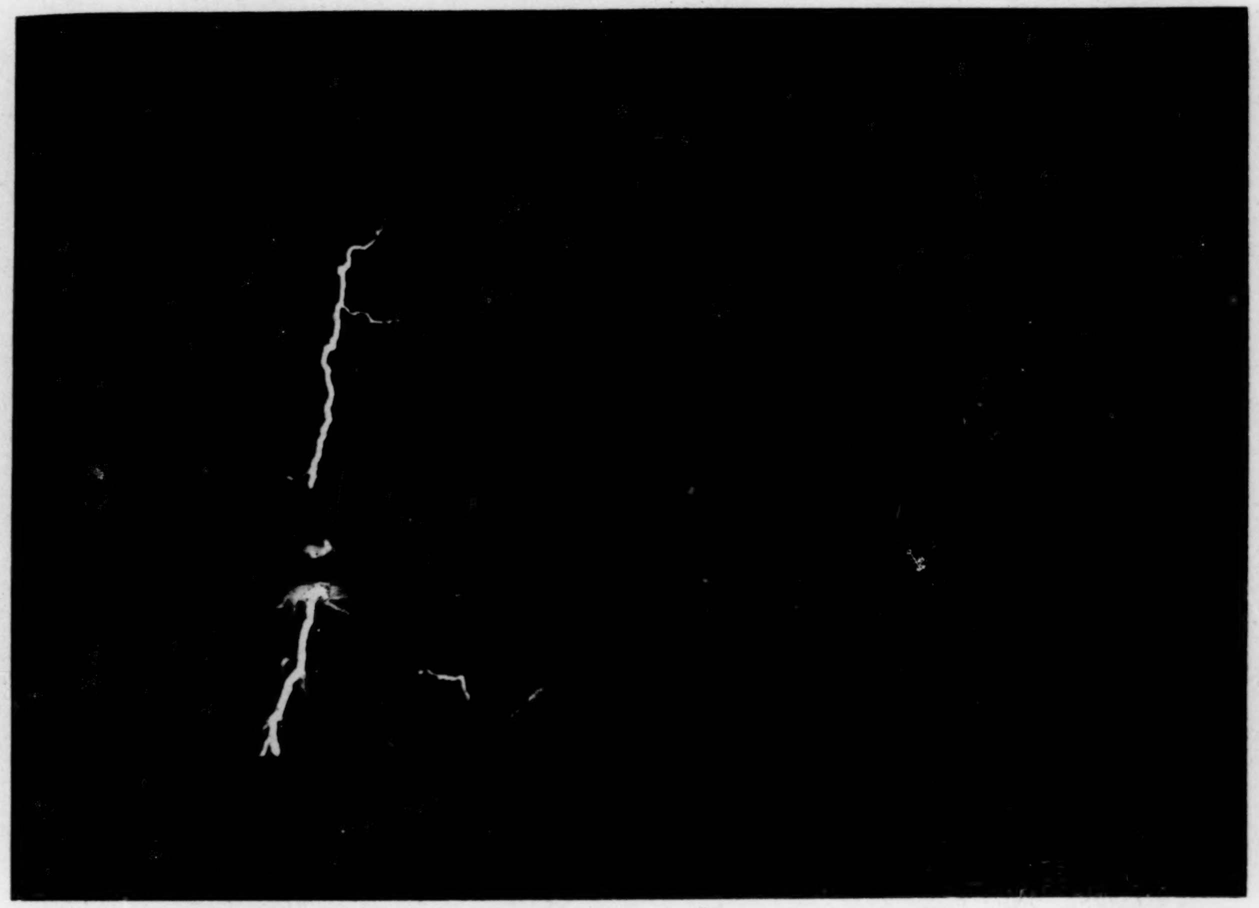

Fig. 3. At Muroran.

Fig. 4. Near Komagatake station, at 8-30 p.m. exposure 1 min.

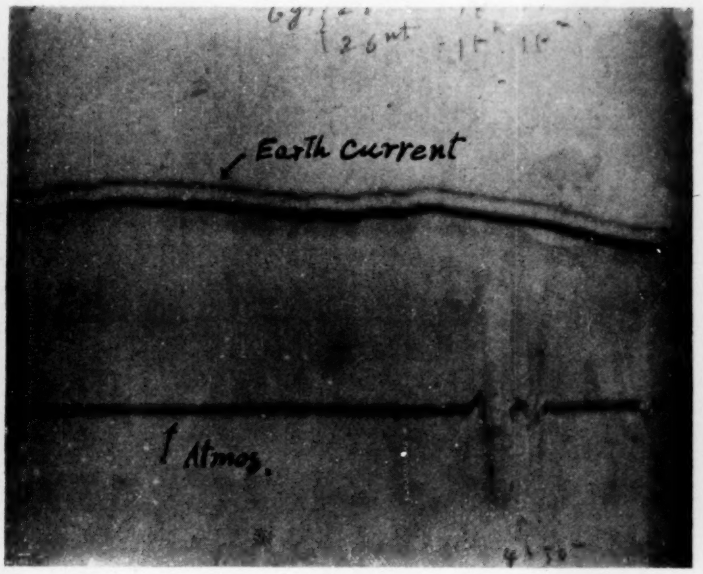

Fig. 5

(震研彙報、第八號、圖版、中田)

activity at the time for convenience. The above results might well be understood as such that they only show the fact that on 26th the action of the volcano was favourable to the change of the atmospheric potential gradient, while on 28th it was unfavourable. At any rate, the result of the present investigation is too poor to give any decided conclusion. I hope many investigations will be made on these lines in the future opportunities.

As for the records of the earth current, no positive result was obtained from such a degree of investigation, owing to the difficulties of its measurements.

In conclusion, I must give my hearty thanks to Prof. M. Ishimoto for his kind invitation to join the party and many facilities he was good enough to give me for the present investigation.

Part VIII. Observations on Komagatake.

By Naomi MIYABE,

Earthquake Research Institute.

(Read Dec. 18, 1929.—Received March 20, 1930.)

1. Immediatly after the recent eruption of Komagatake, which occurred on 17th. June 1929, some members of our Institute were despatched there to make observations of the activity of the volcano from topographical, geological and physical points of view. The results of these observations are given in the preceding reports. It was a month later that the present writer went there with the purpose of observing the subsequent stage of activity and making some supplementary observations if possible. He found, however, no remarkable difference in the general features of the volcanic activity from those described in the preceding reports. Hence, the writer is going to give below the descriptions of some fragmentary facts which he happened to notice during his expedition.

2. The wide area including a number of villages at the foot of Komagatake is covered with pumices and ashes projected from the craters in the recent eruption. Cracks, larger and smaller, are seen everywhere on these piled ejecta. From some of these cracks are being emitted gases smelling of sulphur or its derivatives, while there are found some fissures showing needle-like crystalline incrustations at their openings. A glance from distance on the field with many cracks of this sort reminds us of a green pasture. Cracks observed in these portions are those of smaller scales and are alike to those which are often produced on dried up rice fields.

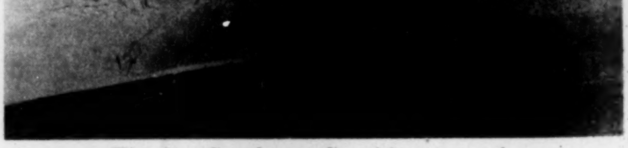

Fig. 1. Cracks on Sumida-no-mori.

Fig. 1 illustrates these cracks produced on the surface of piled ejecta at Sumida-no-mori, as seen from north. These cracks are the larger ones and are continuation of the crack *a* which will be referred to later. Fig. 2 is the schematical sketch. Some of them consist of a numder of cracks arranged *en échelon*. They were probably produced by down-slipping of the part "*B*" relative to the part "*A*".[1)]

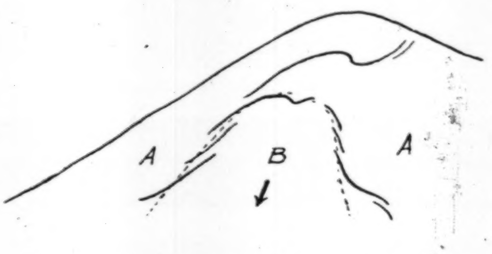

Fig. 2. Schematical Sketch of cracks on Sumida-no-mori.

In the old crater, many cracks are developed in radial and concentric directions with the Ansei Crater (*D*) as their approximate centre. These cracks are shown in Fig. 3 by *a*, *b*, *c*, *d*, *e*, f_1, f_2, *g* and *h*. Among them, *g* is the group of cracks on Sumida-no-mori which was mentioned above. In the region "*H*", there were many radial and concentric cracks, though the writer could not approach them and trace their trend owing to dense fumes emitted out of these cracks.

The largest crack of all was the one that runs southward from the inner side of Sawara-dake along the old crater ridge to Sumida-no-mori, which is denoted by "*a*" in Fig. 3. The breadth of this crack amounts to one metre at Komanose and also at Umanose, and in the neighbourhood of Kengamine it is so wide that we can observe its reddish brown trace from a place several hundred metres apart.

The crack "*b*" is divided into two branches near the Ansei Crater.

f_1, f_2 and the crack nearly perpendicular to "*e*" are recognized by the emission of gases along them.

Some more cracks are observed around the crater *D*.

These cracks, except those of curious shapes observed on Sumida-no-mori, were probably produced by the settling of the piled ejecta in the old crater, as a whole, having the crater *D* as the approximate centre of subsidence. It may be interesting to remark that, in comparing Fig. 3 with Fig. 4 of Dr. Tsuya's report[2)], these cracks appear to have grown sensible in their sizes during the interval of time elapsed between the two observations. For confirming this point, however, some more data will be needed.

---

1) As for the formation of *en échelon* cracks, Prof. Fujiwhara has made some experiments. S. FUJIWHARA, *Jap. Journ. Geophys.*, (1927), No. 2.

2) H. TSUYA, This *Bull.*, p. 238 of this volume.

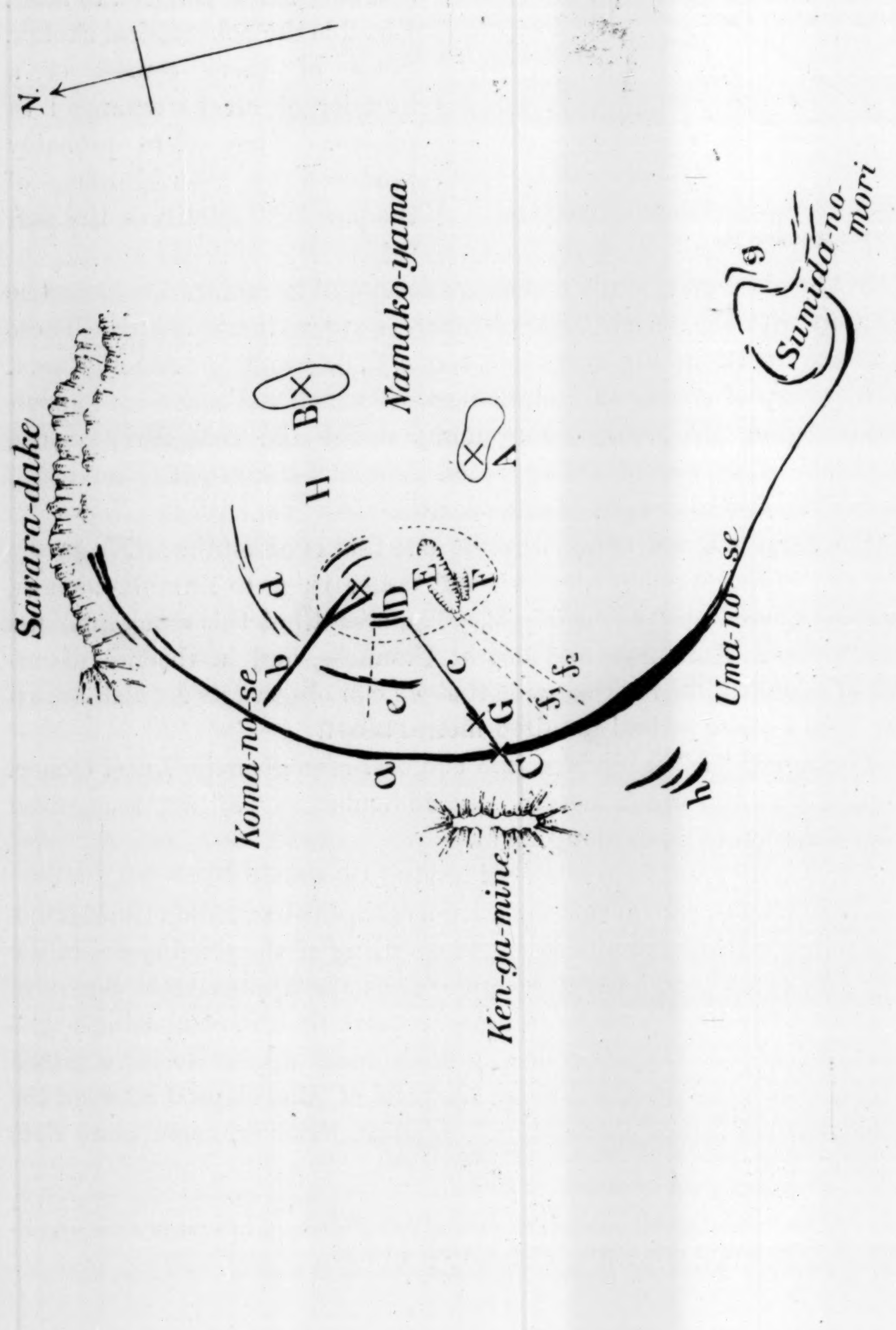

Fig. 3. Cracks and fumaroles in the old crater.

The upper part of the inner side of the cracks "*a*" and "*c*" was reddish in colour, while the lower part was milky white and the exposed surfaces of the deposited layer were covered with ashes. This reddish colouring of the ejecta may be due to the oxidation effected by the high temperature and sufficient supply of air, as will be referred to later. In the neighbourhood of the cracks *b*, *d* and *e*, the surface is covered with dark green ashes in which sulphur is richly contained so that the fresh surface of the inner side of the crack is not exposed.

3. Fumaroles observed are represented by × in Fig. 3, as *A*, *B*, *C* and *D*. Among them, *A* was most active at the time of observation and a rumbling sound was heard every now and then. Activity of *B* was next to that of *A*, but it was without the rumbling sound. From *C* and *D* was being emitted much less quantity of gases than from *A* and *B*. Moreover, as shown in Fig. 4, *C* may not be a crater proper, but only

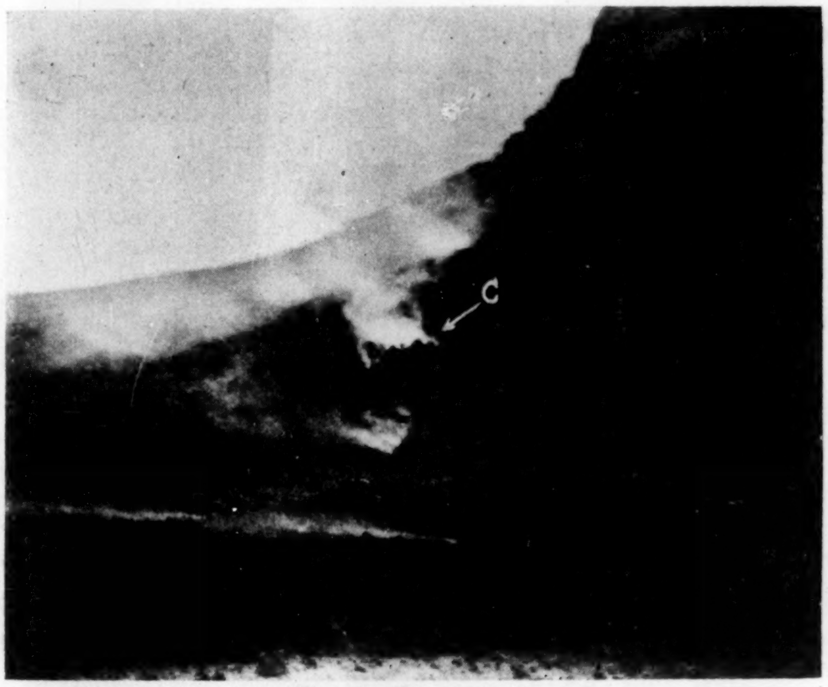

Fig. 4. Fumarole C.

a variety of crack. The gases emitted from it may be supplied from the other fumaroles through the underground channels which may be supposed to exist in the piled ejecta or they may be what was once occluded in the ejecta, and now being released and emitted at last through this crack or vent. *C* was just at the intersection of the cracks "*a*" and "*c*". A halbard-shaped crater adjoining *D* has some fresh

indication on its crater wall that it was destroyed by some eruptions from it, but gas was not being emitted at the time of observation. Emission of gas was also seen faintly on a hill dividing the above mentioned crater from the crater *D*.

A little more detailed sketch of the crater *A* is shown in Fig. 5. Fig. 6 shows the same crater as peeped in from the western edge of it. The Circumference of this crater at its opening was estimated at about

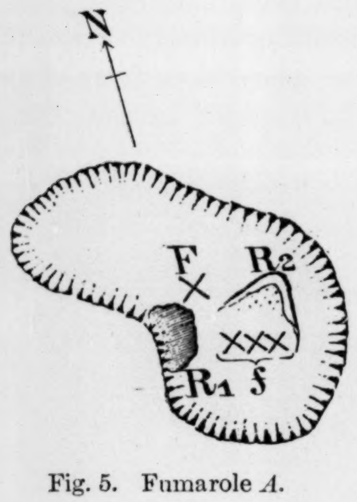

Fig. 5. Fumarole *A*.

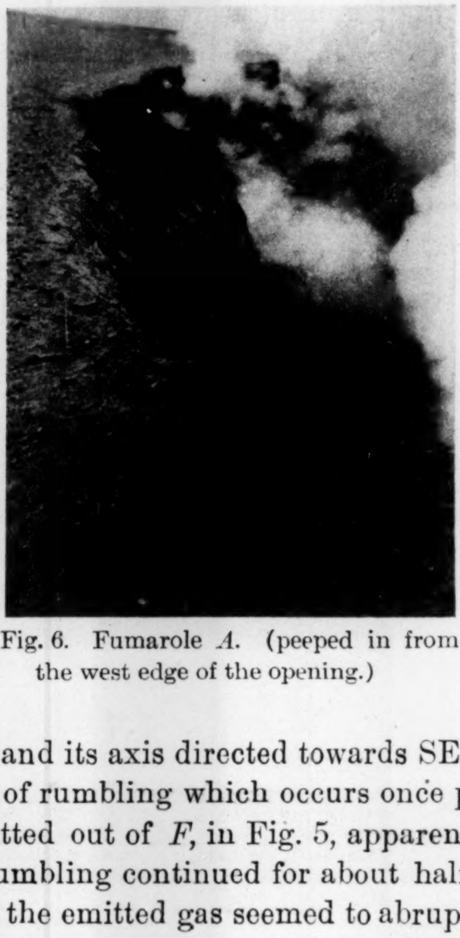

Fig. 6. Fumarole *A*. (peeped in from the west edge of the opening.)

200 m. Its form is just like a gourd and its axis directed towards SE or to the village of Sikabe. At the time of rumbling which occurs once per about five minutes, the gas was emitted out of *F*, in Fig. 5, apparently with a considerable pressure. This rumbling continued for about half a minute, and after that the pressure of the emitted gas seemed to abruptly fall back to its former value. Besides *F*, some more minor fumaroles are seen (f' s) in the crater A. R_1 and R_2 are huge masses of rocks visible through the smoke at the bottom of the crater. R_1 was greyish black in colour, while R_2 was painted with fresh yellow of sulphur at its top and the rest part was reddish black.

The rumbling of this fumarole *A* was heard, from July 18 to July 20, in many villages situated at the foot of Komagatake, except for several

villages such as Mori, Sawara, Osironai, Akaigawa and those in the neighbourhood of the railway station of Komagatake. In these latter villages, the rumbling was scarcely heard or none. These villages are situated mainly in N or NW part of the volcano. On the other hand, the direction of wind then prevailing in this region was NW-SE. Hence, this prevailing wind might probably have affected the sphere of audibility of the rumbling sound of the volcano in the villages surrounding the foot of Komagatake.

4. The piles of pumice covering the area extending from Umanose of the old crater ridge to the northern bank of Lake Oonuma are generally grey in colour. There are also some blocks containing thin white layers. As for their sizes, those of 30–50 cm. in linear dimension are most frequently observed. These pumice piles, at a glance, form a step-like slope somewhat similar to the case which we have demonstrated in the model experiment of deformations of sand mass[3]. A brief description of this pumice pile is as follows. The first step of this slope begins at about one hundered metres down from the ridge of Umanose. The second step succeeds to the first step and so on to the seventh step. The eighth step is more or less deformed and the ninth step was not clearly recognized as it was pushed into the woods on its way. As we have quoted above as "step like", a part with a steeper slopes s_1 and the other part with a more gentle slope s_2 are more or less distinctly recognized (Fig. 7). From the first to the seventh step the distances s_1 and s_2 are roughly the same and so are the height differences at the parts of steeper slopes. The formers are generally

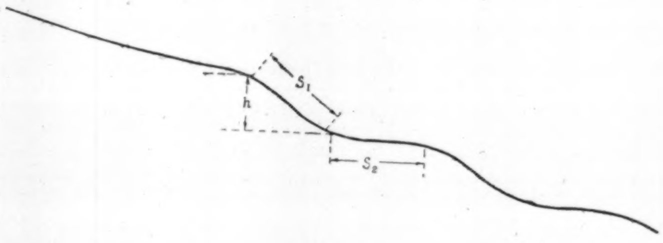

Fig. 7. Supposed slope of pumice pile near Uma-no-se.

20–30 m., while the latters are 15 m. or a little more. Hence, the angle of the slope at the steeper part is about 30° or a little more. As was already mentioned, this step-like pile of pumice is similar to the stepped figure of deformed sand mass experienced in the laboratory experiment. The

3) T. Terada and N. Miyabe, *Bull. Earthq. Res. Inst.*, **4** (1928), 33; **7** (1929), 65.

observed angle of the steep slope in the pile of pumice cannot be identified with the angle of the slip-plane which may be hidden beneath the surface layer. Even when these portions of the steep slope correspond to the slip-planes in the pumice mass, the original slip-planes may not have been maintained. The slope may gradually be deformed, its angle of dip tending to the natural angle of repose of the pumice mass[4]. It may, therefore, be said that the lower limit of the observed angle of the slopes is more significant, being closer to the angle of repose of the pumice mass.

5. Pumice flows are found most remarkable in the neighbourhood of Akaigawa, Osironai and Dekimazaki, while the piles of fallen pumices and ashes are so in the neighbourhood of the villages Sikabe and Honbetu. Descriptions of these pumice flows and piles of pumices and ashes are given in detail in the preceding reports, so that they may be omitted here as superfluous. It is noticeable, however, that these pumice flows contain sometimes reddish coloured blocks while the greatest majority of the blocks are of milky white colour. In an individual block of pumice, we can sometimes find a reddish coloured zone in its outer portion, while the block as a whole looks milky white. The milky white inner portion of the block becomes reddish when it is heated in air. Hence, the reddish coluring of the rocks may be regarded as due to the oxidation resulting from the sufficient supply of air and heat.

The same phenomenon is seen in the pile of ejecta of the former eruptions. Some distances southward of the recent pumice flow of Dekimazaki, an exposure of the pile of a former eruption is seen. Looking at this exposure, we noticed the distinct layers of differently coloured piles of eruptive ejecta: the uppermost layer is of milky white pumice blocks with the thickness of about half a metre; the second is coloured like cinnaber with a thickness of 0·5–1·0 m.; and the lowest consists of the layer of dark yellow materials with a greater thickness. A part of the material from the lowest layer was taken home, and when it was heated for a sufficient time in air, it became reddish or cinnabar-coloured just like that of the second layer. Hence, the existing layers of different colours may be due to the appropriate thickness of the uppermost layer which served in keeping the temperature of the lower layer together with the ventilation of air in the mass just in such a way as to produce the cinnabar-coloured layer within the extent of thickness observed.

4) The term "angle of repose" is used here, if it is allowed, in the sense of the angle of natural slope. The term is used ordinary in civil engineering.

From the observations which we have referred to in preceding pages, we may get a hint on the significant tectonic structures of the region in the vicinity of this volcano. One of the structural lines suggested is the line in the direction of NW-SE along which Osidasizawa, the Craters *D* and *A* lie. Along this line, the eruptive phenomena were comparatively active in recent ages. Another is a line in the direction NE-SW (approximately perpendicular to the former line), along which lie the Fifth-Valley, Crack *c*, Craters *D*, *E* and *B*, fumaroles *C* and *G* and the region *H*. The Fifth-Valley is generally considered as produced by erosion, and yet the grade of erosion of this valley seems to be much more steep compared with the other erosion-valleys of the same mountain. This suggests us that some other primary agency might have been here in action besides the usual erosion to build up such a sharply eroded valley.

The above conjecture regarding the structural lines in the region of the Komagatake is based merely on a scanty number of the facts and phenomena observed in the field. It may, however, be allowed at least to say that the two lines mentioned above are to be considered as something very significant for the tectonic structure in this region and that their existence seems rather natural from the point of view of the theory of elastic deformation.

6. In addition to the above descriptions, the following may be of some interest as it may have some significant bearings on the phenomena of eruption of Komagatake:

a). In the valley of the Kadiyagawa, one of the rivers flowing eastward from Komagatake, we can see a fine exposure of the layers of ejecta as shown in Fig. 8. Notations in the figure means as follows:

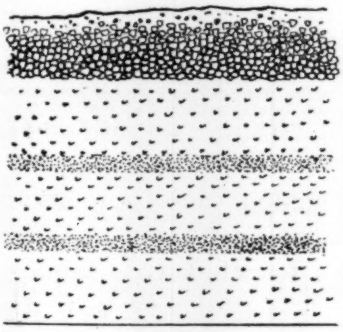

Fig. 8. Strata exposed in the valley of the Kadiyagawa.

- I ······Pumice layer, about 80 cm. thick;
- II, II′, II″······Sand or ash coloured yellowish brown, about 70 cm. thick;
- III, III′ ······Layers of sand which may generally be seen at the bottom of the river or sea shore of this district, about 10 cm. thick.

In the layers II, II′ and II″, blocks of pumice are seen which indicate that these layers consist of the ejecta of earlier eruptions. The layers III and III′ seem to be those which have been deposited in the river bed or sea bottom. As these deposits are seen at the height of about 10 m. above the present sea level, these portions may have been upheaved to a certain amount during the life history of the volcano. This supposition conforms with Professor Kato's opinion[5] that the terraces found in these regions resulted from the upward movement of the coastal zone.

b). Everyone visiting this district will take special notice of the large number of islets scattered in Lake Oonuma and also of the small knolls near the village of Sikabe (called Nagareyama). Larger knolls of this sort are also seen on the slope of Komagatake which are called Maruyama. Moreover, the points on the slope of the mountain where the triangulation points are situated are a little higher than the surrounding portions, or the slopes at these points are more gentle than the other. These so-called Maruyama's and triangulation points seem to be somewhat regularly distributed around the mountain. The regularity is such as shown in the following tables (Tables I and II). In these tables, the radial distances of the points are taken from the crater *D*.

Table I.

	N. Maruyama	E. Maruyama	Butai (Tennenkôsin)
Radial distance	2·4 km.	3·3 km.	2·9 km.
Height above sea level	538·0 m.	479·1 m.	418·2 m.

Table II.

Triangulation point	1	2	3	4	5	6
Radial distance	3·5 km.	5·0 km.	5·2 km.	5·4 km.	3·9 km.	3·4 km.
Height above sea level	283.5 m.	286·6 m.	249·4 m.	210·1 m.	310·8 m.	266·9 m.

We are at present absolutely ignorant as to what this apparent regularity may mean, though it may be due less probably to a mere chance than to some physical or mechanical cause.

5) T. Katô, *Sinsaiyobô-tyôsakai Hôkoku*, No. 62 (1909).

11. 昭和四年六月北海道駒ヶ嶽の噴火

第一部 駒ヶ嶽火山の地質活動狀況及び岩石

地震研究所 津 屋 弘 逵

北海道渡島國駒ヶ嶽火山は「ホマーテ」型の成層火山で、主として複輝石安山岩質の熔岩流とその岩屑とより成る。其頂上には東に開く爆發「カルデラ」があつて、その中に更に楕圓形の火口がある。此楕圓形火口內に從來屢々爆發が繰返されて數個の小火口及び裂罅が出來、夫等から噴氣してゐた。近くは明治三十八年と大正八年とに爆發が起つたが、今回の噴火は安政の噴火以來の大噴火である。

今回の噴火は昭和四年六月十七日の早朝初まつたが、午前十時頃劇くなり、同日午後十一時過まで續いた。その後噴火は漸次鎭まつて、翌朝には最早噴煙のみとなつた。この噴火によつて噴出した多量の輕石は同火山の南東方面に落下堆積したのみでなく、四周の山側を流下して山麓に集積した。是等の輕石は岩石學上複輝石安山岩に屬し、火山體を構成してゐる從來の噴出物と類似してゐる。

第二部 駒ヶ嶽噴出物の酸化狀態より推定せる其の溫度に就て

地震研究所 {坪 井 誠 太 郎
津 屋 弘 逵

昭和四年六月十七日北海道駒ヶ嶽より噴出せる浮石質岩片に於ける酸化狀態を記述し、之より其の噴出當時の溫度を推定し 730°C より高きも是より甚だしく高溫には非ざるべきを論ぜり。

第三部 氣象及び地震觀測

地震研究所 岸 上 冬 彥

1. 駒ヶ嶽火山噴火前後の狀態

噴火の始まつた六月十七日の朝、低氣壓の中心が駒ヶ嶽の附近を南から北に向けて進行中であつた。又十日間程降雨がなかつたのが、噴火の前日、低氣壓に伴つて雨が降つた。南東の麓の鹿部方面に火山灰及び浮石が積つたのは主として當時の風向が北西であつたからであると思はれる。

噴煙の高さは函館測候所の觀測によると十七日の午後二時頃には約 13000 m. であつたが、翌日の午後三時には約 6000 m. に減じた。

函館測候所の地震記象を見ると零時二十三分に週期の長い脈動狀の振動をかいてゐる。同樣な振動が、午前十一時から午後十二時まで絕え間なく續き、丁度その時、大沼森林測候所の報告を見ると、噴火が烈しかつた。この事實から考へると午前零時二十三分の振動も噴火によると考へられる。即ち此の時が噴火の始つた時刻と思はれる。

2. 砂原に於ける地震觀測

本研究所の石本敎授と高橋學士の製作された微動計を駒ケ嶽の北方砂原村に据ゑつけて、六月二十三日から七月十日まで地震觀測をした。その間、時々故障の爲に止つたが、377 回の地震を記錄した。此等の地震を第二表には四種に分けた。I は衝動の樣に急に振幅が大きくなり直に減衰する振動、II は初期微動が明かに見え、次に振幅の大きい主要動となる。III は小さい地震が連續して起るもの、IV とかいてあるのは比較的遠い地震である。

駒ケ嶽の地震の多くは人體に感じなかつたが、感じたものもその有感區域は局部的である。七月四日に大沼方面に弱震程度の大きな地震が多數あつたが、砂原では其の大部分は器械にさへ記錄されなかつた。

第四部　噴火に伴ふ地表傾斜變化の觀測

地震研究所　高橋龍太郎

火山の噴火は屢々其の火山の山麓地域の土地の沈降、隆起を伴ふのである。今回の駒ケ嶽の噴火に際し、此樣な土地の隆起沈降と噴火現象との關係を研究する目的を以て、駒ケ嶽北麓なる砂原村に傾斜計を据付けて、六月二十二日より十二月末日迄地表の傾斜變化の觀測を行つた。其觀測の結果に依れば噴火現象の活動期に於ては砂原村の土地は北東東の方向に傾斜し、同時に土地の脈動を伴ひ、其に次いで地震と鳴動とが起る樣である。土地の傾斜と噴火活動期と，脈の數日間に亙る長週期間の配置と相互に關聯してゐる事も注目に値する事柄である。

第五部　駒ケ嶽噴火に關連せる地盤の垂直變動

地震研究所　坪井忠二

噴火に關連して地盤の垂直變動が起るといふ事は之まで度々經驗された所であつたから、今回の駒ケ嶽噴火に際して、其の北側の水準測量を行つて見た。果してかなり著しい沈降が見出された。尙陸地測量部も駒ケ嶽火山の西側の水準測量を施行され、やはり著しい沈降を見出された。夫等の結果は第一、二表に示した通りで、第一圖は等沈降線のコントルである。

第六部　駒ヶ嶽噴火に關連せる重力の變動

地震研究所　坪　井　忠　二

噴火に關係して若し地下の物質配置の狀況に變動があるならば之を檢出し度いと云ふ目的でシリカ製重力偏差計を砂原に据付けて連續觀測を行つたが、持參した偏差計の精度 (10^{-10}) に現れる位の變動は認められなかつた。

第七部　爆發に伴ふ電氣的現象

中　田　金　市

昭和四年六月十七日に起つた北海道駒ヶ嶽の爆發に伴つて生じた電氣的現象の記述で、火山活動につれて、空中電位、地中電流の變化が起るか否かに就て調べたものである。

第八部　駒ヶ嶽に關する調査報告

地震究研所　宮　部　直　巳

一九二九年六月一七日に爆發した北海道駒ヶ嶽に關する野外調査の報告である。今度の噴火と直接に關係ある噴出物や噴火現象に關しては、津屋氏其他の人々の報告があるから、こゝには舊噴火口内に堆積した新らしい噴出物上に生じた裂罅に關する記載を主とした。尙、筆者の經驗した中、特に印象されたことで、駒ヶ嶽の噴火と關係ある事項についても簡單に記載しておいた。

BULLETIN OF THE EARTHQUAKE RESEARCH INSTITUTE,
TOKYO IMPERIAL UNIVERSITY. Vol. VIII, Part 3, September, 1930.

東京帝國大學
地震研究所彙報

第八號　第三册

昭和五年九月

目　　次

論文及報告　　　　頁

12. 彈性波の反響性及び分散性分散に就て(英文)……………… 妹澤克惟・西村源六郎 321

13. 昭和二年丹後地震に關聯せる丹後地方の地殼の變形に關する研究(第二報)(英文)……………… 坪井忠二 338

14. 筑波山に於ける傾斜變化觀測報告(邦文)……………… 井上宇胤・杉山友紀 346

15. 大地震と太陽黑點との關係に就て(邦文)……………… 高山威雄・鈴木武夫 364

16. 伊豆東海岸に於ける水準測量成果報告(邦文)……………… 375

所　　報

(The titles in occidental languages are given on the back cover.)

本彙報ハ年四回發行ス．但シ第七號ニ限リ三冊トス．（第一號ヨリ第六號マデハ不定期ニ發行セリ．）

本彙報掲載ノ論文及ビ報告ノ内容ニ關シテハ著者ノミニ其責任アルモノトス．

本彙報ニ關スル照會通信ハ東京帝國大學地震研究所長へ宛テラレタシ．

The bulletin is published quarterly, excepting Vol. VII which consists of three parts. (Vols. I–VI were published at irregular intervals.)

The authors of the papers alone are responsible for the statements and opinions contained in their respective papers.

All communications relating to this bulletin should be addressed to the Director of the Earthquake Research Institute, Tokyo Imperial University.

12. *Dispersion of a Shock in Echoing- and Dispersive-Elastic Bodies.**

By **Katsutada SEZAWA** and **Genrokuro NISHIMURA**,

Earthquake Reseach Institute.

(Read May 20 and June 17, 1930.—Received June 20, 1930.)

1. It is well-ascertained fact that the earthquake movement of the ground at a distant station from the seismic origin is oscillatory even when the motion in the neighbourhood of the source is of the type of a single shock. The law that, the farther the epicentral distance, the more increase the repetition of the oscillations and also the duration of the disturbance, appears now to be quite established. Although a certain part of this phenomenon may be caused by the vibratory motion induced in the seismometrical instrument, yet the main motion of the ground itself seems doubtless to obey the above law. Such a law will, of course, be explained from several points of view. The most probable explanation will be that the chief feature of the oscillations is partly due to the ordinary dispersion of elastic waves in the stratified layers of the ground and partly due to the echoing nature of the solid body which has some discontinuities in the distribution of density and elasticity. Professor Terada and Professor Fujiwhara[1] appeared to have long ago somewhat similar views on the above nature of dispersion.

As to the dispersive nature of waves, the problems of Love-waves[2] and Rayleigh-waves[3] propagated along a stratified body are perhaps striking instances. The cases which were considered by the present

---

* The principal calculation contained in this paper has been carried out by G. NISHIMURA. (K. SEZAWA.)

1) For example, Prof. TERADA's & Prof. FUJIWHARA's criticisms on SEZAWA's conception concerning the seismic radiation from multiple sources of land block type, Colloq. Meeting at Seism. Inst., Oct. 1924.

2) A. E. H. LOVE, *Some Problems of Geodynamics* (Cambridge, 1911).

3) K. SEZAWA, "Dispersion of Elastic Waves propagated on the Surface of Stratified Bodies and On Curved Surfaces", *Bull. Earthq. Res. Inst.*, **3** (1927), 1-18.

authors[4] and others,[5] may belong to the similar problems. These problems are, however, connected with the propagation of an infinite train of harmonic waves and the criterion of dispersion in these enquiries has its basis merely upon the velocity of harmonic waves, which is proper to the wave length, but not concerned with the character of the deformation of arbitrary waves progressing towards distant points. A few years ago one of the present authors studied two cases of the deformation of the arbitrary waves in dispersive elastic bodies. One[6] of these deals with the transmission of harmonic disturbances of a limited extent and of the displacement of Rayleigh-type waves when the velocity of propagation in the medium is assumed to vary as wave length in addition to a certain constant, while the other[7] treats of the excitation of periodic Rayleigh-waves due to an arbitrary disturbance in a body in which the velocity of elementary harmonic waves varies as the power series of wave length taken to the second degree. In the present paper the criterion of dispersion has been taken to be based upon the deformation of a single shock with the condition that the elementary harmonic waves satisfy the velocity equations which can be formulated from the curves compiled already by one of the present authors and indicating the exact relation between the velocity and length of Rayleigh-waves on a stratified body.

The phenomenon of apparently dispersive transmission of seismic waves appears to depend also upon the echoing character of the elastic waves when the construction of the crust is heterogeneous in regard to the distribution of density and elasticity. The simplest example of this problem is to take some discontinuous layers which are perpendicular to the direction of propagation of elastic waves. The postulation of a train of harmonic waves of an infinite extent with a constant period cannot indicate any sign of the deformation of the waves, but, when a certain arbitrary shock is applied at an assigned portion of the body, the shock

4) K. SEZAWA & G. NISHIMURA, "Rayleigh-type Waves propagated along an Inner Stratum of a Body", *Bull. Earthq. Res. Inst.*, 5 (1928), 85–96.

5) R. STONELEY, "Elastic Waves at Surface of Separation of Two Bodies", *Proc. Roy. Soc.*, 106 (1924), 416–428.

T. MATUZAWA, "Propagation of Love Waves along a doubly Stratified Layer", *Proc. Phys.-Math. Soc.* Japan, [3], 10 (1928), 25–33.

6) K. SEZAWA, "On the Propagation of the Leading and Trailing Parts of a Train of Elastic Waves", *Bull. Earthq. Res. Inst.*, 4 (1928), 111–116.

7) K. SEZAWA, "Periodic Rayleigh-waves caused by an Arbitrary Disturbance", *Bull. Earthq. Res. Inst.*, 7 (1929), 193–206.

may be deformed into a complex form of waves in transmission through the body and gives us an apparently dispersive nature of elastic waves.

It may be doubted that a clear distinction between the true dispersion of elastic waves and the apparent dispersion of echoed waves can be made from the seismic records. As the result of the present investigation which will appear later enables us to know many facts identifying two cases, the obscurity which attaches to the analysis of seismic records can be avoided to a certain extent. We think that, when a few other cases of examples of the same nature as that in this paper were solved, the determination of the significance of all the seismic records would not necessarily be impossible.

In the first section of this paper the problem of the apparent dispersion of a shock in echoing elastic body is solved, in the second section the true dispersion of a shock in dispersive elastic body is dealt with, while in the remaining section the comparison of the results of both cases is contained.

Dispertion of a Shock in Echoing Elastic Bodies.

2. Let us first consider a simplest case where there is one discontinuous layer perpendicular to the direction of the propagation of waves in an infinitely-extended uniform medium and let the waves be of pure plane-type. Let the axis of x be drawn parallel to the direction of the propagation, the origin being taken at a boundary surface of the layer. The displacements, the density and elastic constants of the outer medium are to be u_0+u_0', u_2, ρ, λ, μ. The similar displacement, density, elastic constants of the layer of thickness H are to be expressed by u_1, ρ', λ', μ'.

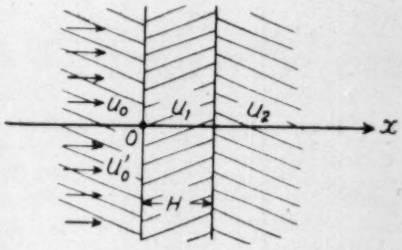

Fig. 1.

The equations of motion of both medium can be written by

$$\rho \frac{\partial^2(u_0+u_0')}{\partial t^2} = (\lambda+2\mu)\frac{\partial^2(u_0+u_0')}{\partial x^2}, \text{(and similarly for } u_2\text{,)} \quad \cdots\cdots(1)$$

$$\rho' \frac{\partial^2 u_1}{\partial t^2} = (\lambda'+2\mu')\frac{\partial^2 u_1}{\partial x^2}. \quad \cdots\cdots\cdots\cdots\cdots\cdots\cdots\cdots(2)$$

The solutions of these equations can be denoted by

$$u_0+u_0' = e^{ih(Vt-x)}+C_0\,e^{ih(Vt+x)}, \quad\cdots\cdots(3)$$

$$u_1 = B_1\,e^{i\beta h(V't-x)}+C_1\,e^{i\beta h(V't+x)}, \quad\cdots\cdots(4)$$

$$u_2 = B_2\,e^{ih(Vt-x)}, \quad\cdots\cdots(5)$$

where C_0, B_1, C_1, B_2 are arbitrary constants to be determined from the boundary conditions and

$$V=\sqrt{\frac{\lambda+2\mu}{\rho}},\quad V'=\sqrt{\frac{\lambda'+2\mu'}{\rho'}},\quad \beta=\sqrt{\frac{\rho'(\lambda+2\mu)}{\rho(\lambda'+2\mu')}}. \quad\cdots\cdots(6)$$

At the boundaries $x=0$ (and H), we have

$$u_0+u_0' = u_1, \qquad (u_1=u_2,) \quad\cdots\cdots(7)$$

$$(\lambda+2\mu)\frac{\partial(u_0+u_0')}{\partial x}=(\lambda'+2\mu')\frac{\partial u_1}{\partial x}. \quad \left[(\lambda'+2\mu')\frac{\partial u_1}{\partial x}=(\lambda+2\mu)\frac{\partial u_2}{\partial x}.\right] \quad (8)$$

From (7) and (8), we can determine C_0, B_1, C_1, B_2 in the forms:

$$\left.\begin{aligned} C_0 &= \frac{(1-\alpha^2)(1-e^{-2i\beta hH})}{(1+\alpha)^2-(1-\alpha)^2\,e^{-2i\beta hH}}, & B_1 &= \frac{2(1+\alpha)}{(1+\alpha)^2-(1-\alpha)^2\,e^{-2i\beta hH}},\\ C_1 &= -\frac{2(1-\alpha)\,e^{-2i\beta hH}}{(1+\alpha)^2-(1-\alpha)^2\,e^{-2i\beta hH}}, & B_2 &= \frac{4\alpha e^{-i(\beta-1)hH}}{(1+\alpha)^2-(1-\alpha)^2\,e^{-2i\beta hH}}.\end{aligned}\right\}\cdots(9)$$

Decomposing (u_0+u_0') in (3) into the primary waves u_0 and the secondary waves u_0' and applying Fourier's formula such that

$$\varphi(x)=\frac{1}{2\pi}\int_{-\infty}^{\infty}dh\int_{-\infty}^{\infty}\varphi(\sigma)\,e^{ih(x-\sigma)}d\sigma, \quad\cdots\cdots(10)$$

we obtain

$$u_0=\frac{1}{2\pi}\int_{-\infty}^{\infty}dh\int_{-\infty}^{\infty}\varphi(\sigma)\,e^{ih(Vt-x+\sigma)}d\sigma, \quad\cdots\cdots(11)$$

$$u_0' = \frac{1}{2\pi}\int_{-\infty}^{\infty}\frac{(1-\alpha^2)(1-e^{-2i\beta hH})\,dh}{(1+\alpha)^2-(1-\alpha)^2\,e^{-2i\beta hH}}\int_{-\infty}^{\infty}\varphi(\sigma)\,e^{ih(Vt+x+\sigma)}d\sigma, \quad \cdots\cdots(12)$$

$$u_1 = \frac{1}{\pi}\int_{-\infty}^{\infty}\frac{(1+\alpha)\,dh}{(1+\alpha)^2-(1-\alpha)^2\,e^{-2i\beta hH}}\int_{-\infty}^{\infty}\varphi(\sigma)\,e^{i\beta h(V't-x+\frac{\sigma}{\beta})}d\sigma$$

$$-\frac{1}{\pi}\int_{-\infty}^{\infty}\frac{(1-\alpha)\,e^{-2i\beta hH}dh}{(1+\alpha)^2-(1-\alpha)^2\,e^{-2i\beta hH}}\int_{-\infty}^{\infty}\varphi(\sigma)\,e^{i\beta h(V't+x+\frac{\sigma}{\beta})}d\sigma, \quad \cdots(13)$$

$$u_2 = \frac{2}{\pi}\int_{-\infty}^{\infty}\frac{\alpha\,e^{-i(\beta-1)hH}dh}{(1+\alpha)^2-(1-\alpha)^2\,e^{-2i\beta hH}}\int_{-\infty}^{\infty}\varphi(\sigma)\,e^{ih(Vt-x+\sigma)}d\sigma. \quad \cdots\cdots\cdots(14)$$

These are the solutions of displacements for a given primary waves of the type

$$t = 0; \qquad u = \varphi(x). \quad \cdots\cdots\cdots\cdots\cdots\cdots\cdots\cdots(15)$$

Again, we know the expressions

$$\frac{1}{(1+\alpha)^2-(1-\alpha)^2\,e^{-2i\beta hH}} = \sum_{m=0}^{\infty}\frac{(1-\alpha)^{2m}}{(1+\alpha)^{2m+2}}\,e^{-2im\beta hH}. \quad \cdots\cdots\cdots(16)$$

Hence (12), (13), (14) reduce to

$$u_0' = \frac{1}{2\pi}\sum_{m=0}^{\infty}\left(\frac{1-\alpha}{1+\alpha}\right)^{2m+1}\int_{-\infty}^{\infty}e^{-2im\beta hH}\,dh\int_{-\infty}^{\infty}\varphi(\sigma)\,e^{ih(Vt+x+\sigma)}d\sigma$$

$$-\frac{1}{2\pi}\sum_{m=0}^{\infty}\left(\frac{1-\alpha}{1+\alpha}\right)^{2m+1}\int_{-\infty}^{\infty}e^{-2i\overline{m+1}\beta hH}dh\int_{-\infty}^{\infty}\varphi(\sigma)\,e^{ih(Vt+x+\sigma)}d\sigma, \quad \cdots\cdots\cdots(12')$$

$$u_1 = \frac{1}{\pi}\sum_{m=0}^{\infty}\frac{(1-\alpha)^{2m}}{(1+\alpha)^{2m+1}}\int_{-\infty}^{\infty}e^{-2im\beta hH}dh\int_{-\infty}^{\infty}\varphi(\sigma)\,e^{i\beta h(V't-x+\frac{\sigma}{\beta})}d\sigma$$

$$-\frac{1}{\pi}\sum_{m=0}^{\infty}\frac{(1-\alpha)^{2m+1}}{(1+\alpha)^{2m+2}}\int_{-\infty}^{\infty}e^{-2i\overline{m+1}\beta hH}dh\int_{-\infty}^{\infty}\varphi(\sigma)\,e^{i\beta h(V't+x+\frac{\sigma}{\beta})}d\sigma, \quad \cdots\cdots(13')$$

$$u_2 = \frac{2}{\pi}\sum_{m=0}^{\infty}\frac{\alpha(1-\alpha)^{2m}}{(1+\alpha)^{2m+2}}\int_{-\infty}^{\infty} e^{i(\overline{2m+1}\beta+1)hH}dh\int_{-\infty}^{\infty}\varphi(\sigma)\,e^{ih(Vt-x+\sigma)}d\sigma. \quad\cdots\cdots(14')$$

3. We may now take a simple case such that

$$t=0, \quad u_0=\varphi(x)=e^{-\frac{x^2}{c^2}}, \quad\cdots\cdots(17)$$

then we find from (11), (12′), (13′), (14′),

$$u_0 = e^{-\frac{(Vt-x)^2}{c^2}}, \quad\cdots\cdots(18)$$

$$u_0' = \sum_{m=0}^{\infty}\left(\frac{1-\alpha}{1+\alpha}\right)^{2m+1} e^{-\frac{(Vt+x-2m\beta H)^2}{c^2}}$$

$$-\sum_{m=0}^{\infty}\left(\frac{1-\alpha}{1+\alpha}\right)^{2m+1} e^{-\frac{(Vt+x-\overline{2m+1}\beta H)^2}{c^2}}, \quad\cdots\cdots(19)$$

$$u_1 = 2\sum_{m=0}^{\infty}\frac{(1-\alpha)^{2m}}{(1+\alpha)^{2m+1}}\, e^{-\frac{\beta^2(Vt-x-2m\beta H)^2}{c^2}}$$

$$-2\sum_{m=0}^{\infty}\left(\frac{1-\alpha}{1+\alpha}\right)^{2m+1} e^{-\frac{\beta^2(Vt+x-\overline{2m+1}H)^2}{c^2}}, \quad\cdots\cdots(20)$$

$$u_2 = 4\sum_{m=0}^{\infty}\frac{\alpha(1-\alpha)^{2m}}{(1+\alpha)^{2m+2}}\, e^{-\frac{[Vt-x-(\overline{2m+1}\beta+1)H]^2}{c^2}}. \quad\cdots\cdots(21)$$

The values of u_0, u_0', u_1, u_2 in a special case $\alpha = \frac{1}{2}$, $\beta = 1$, $2c = H$ are plotted in Fig. 2. The similar values in the case $\alpha = 2$, $\beta = 1$, $2c = H$ are given in Fig. 3.

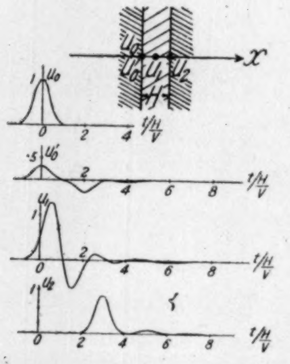

Fig. 2. ($\alpha=\frac{1}{2}$, $\beta=1$, $2c=H$.)

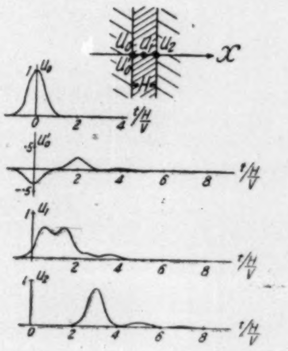

Fig. 3. ($\alpha=2$, $\beta=1$, $2c=H$.)

4. In the same manner of mathematical treatment we can find the solutions of the problem where a number of layers are assumed to reside perpendicular to the direction of propagation. We must, however, notice that, each term of the series of u_2 in (21) is essentially of the like form as that of u_0 in (18), so that it will be rather convenient to suppose that each term of the series of u_2 belonging to the first layer is the primary waves of the second layer and hence we can apply the results in (18), (19), (20), (21) to the problem of this second layer with a small modification in the coefficients of the amplitude equations and the retardation of phases. In this case the reflected waves of the type (19) belonging to the second layer become again primary waves of the first layer, though the direction of their propagation is opposite to that of the first primary waves. In this way the multiple reflection and transmission of elastic waves through and between two layers take place. The same process can be available to obtain the solutions of the problem having any number of layers. Fig. 4 and Fig. 5 give us the case of two layers and Fig. 6 and Fig. 7 indicate that of three layers.

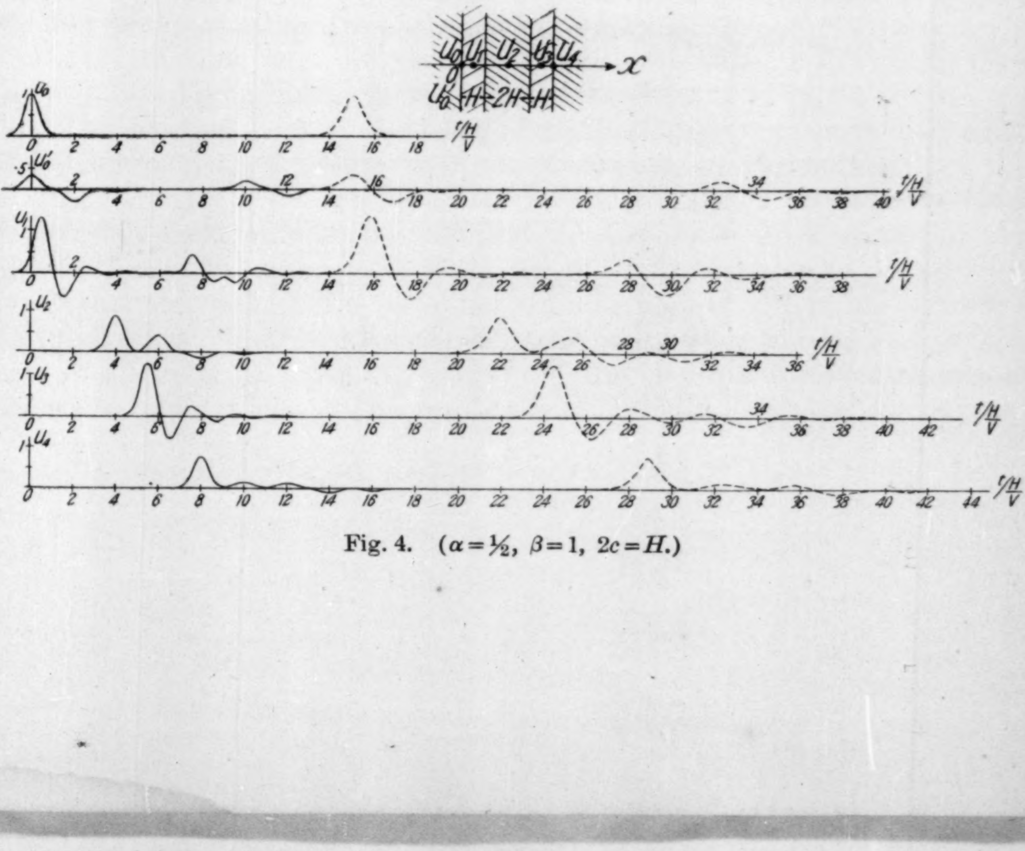

Fig. 4. ($\alpha=\frac{1}{2}$, $\beta=1$, $2c=H$.)

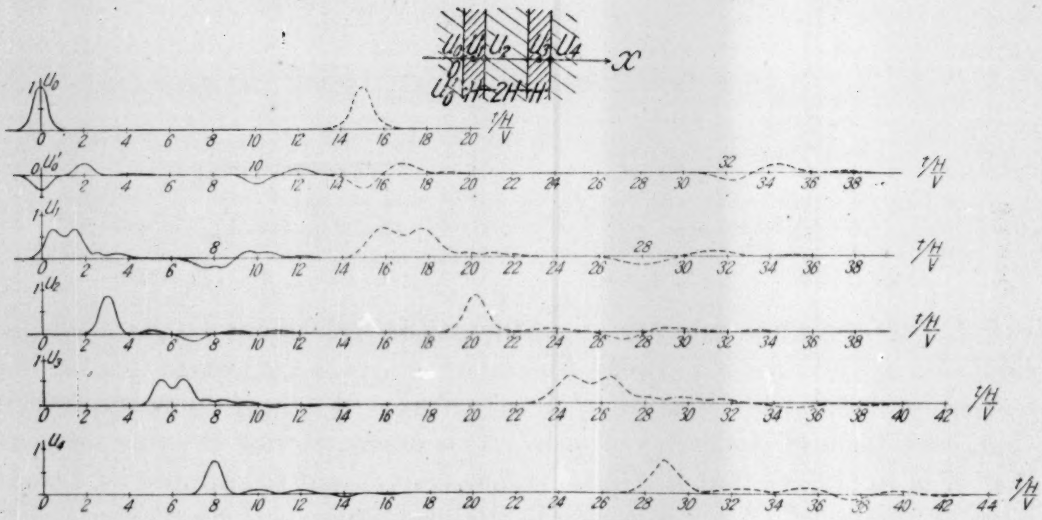

Fig. 5. ($\alpha=2$, $\beta=1$, $2c=H$.)

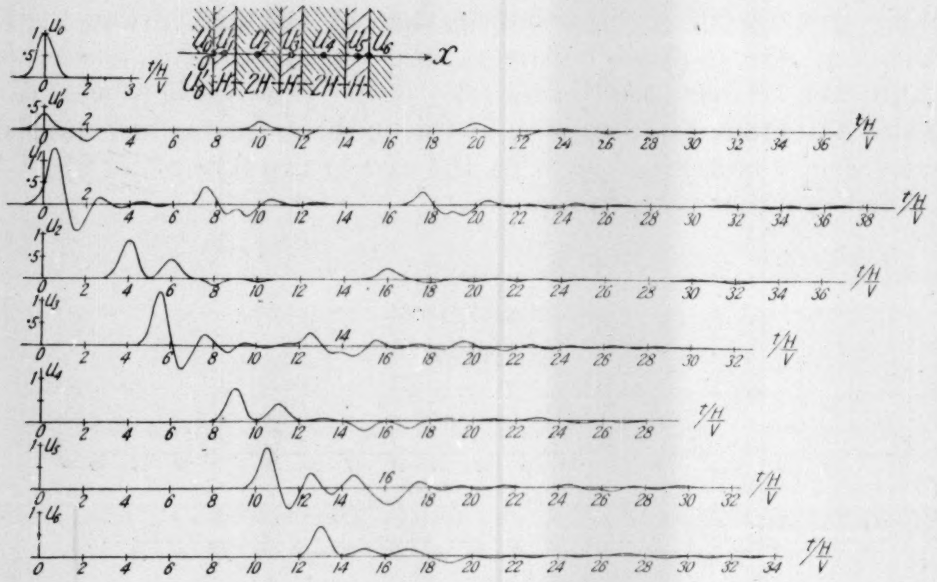

Fig. 6. ($\alpha=\frac{1}{2}$, $\beta=1$, $2c=H$.)

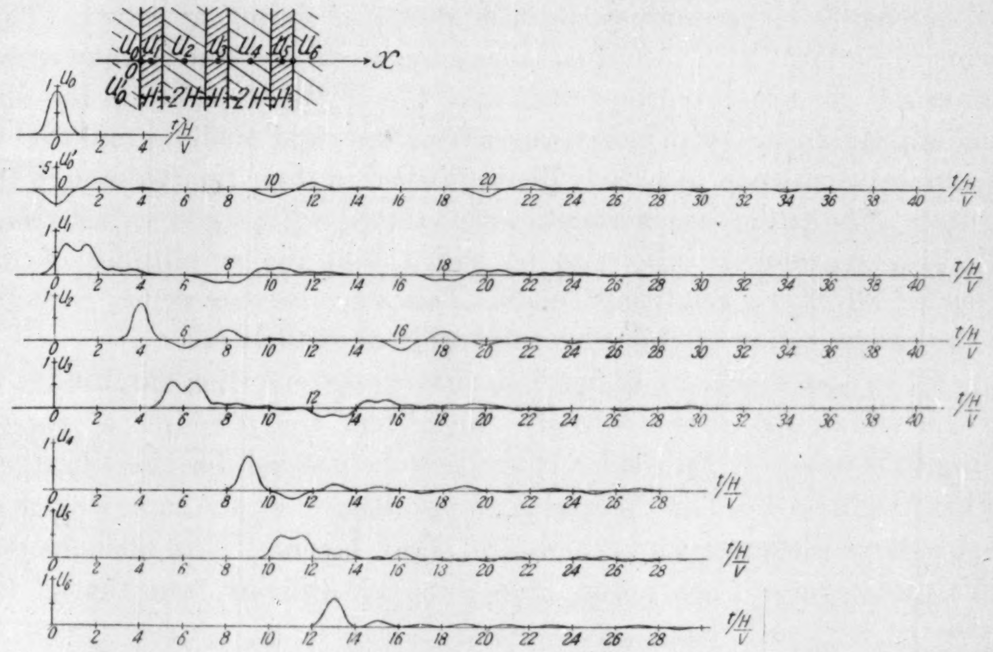

Fig. 7. ($\alpha=2$, $\beta=1$, $2c=H$.)

5. It may be seen from these diagrams that, even when the primary waves are of a type of a single shock, the vibrations in echoing medium or the waves through the echoing layers are oscillatory in general. But when the range of the primary disturbance is wide compared with the thickness of the layers, no periodic oscillation can be produced. The periodicity of the usual pulsatory motion depends on the size of the heterogeneous blocks as well as on their successive arrangement. Again, in the case of one layer the repeated oscillations are purely periodic and have the nature of decaying character, while in the case of more than one layer the vibrations are composed of several groups, each of which is a damped and periodic type. This feature of the problem sometimes obliges us to imagine the seismic waves as if they were radiated from multiple sources.[8)]

The leading part of the train of oscillations is transmitted through the heterogeneous medium with a definite velocity depending upon the effective density and elasticity of the medium. This is perhaps the most favourable fact, unless the medium is dispersive or viscous, for the application of the conception of the time-distance relation to the analysis of seismic records. The phase of leading part of the pulses is always maintained, so that the law of pull-push is justified to hold even in the case of the heterogeneous distribution of the medium in the direction of the wave transmission. The amplitude of the leading part of the train of

8) A. Imamurara, *Proc. Imp. Acad.*, 5 (1929), 330.

oscillations is large compared with those of following waves. This seems to conform with the usual character of all the earthquake movements. It is also important fact that the initial motion in the soft medium caused by the primary waves from the rigid medium and that of the opposite case can be clearly distinguished in their type as seen in the figures. The latter case is sometimes confused with the so-called waves of tilting movements. It is to be added that the amplitudes of the reflected waves are relatively small. This may become some guidance to the recognization of the side of the original disturbance.

When the shocks is diffused in a large extent, the amplitudes of all the vibrations are exceedingly diminished, the principle of energy being thus naturally satisfied. It is also to be noticed that the vibrations in the neighbourhood of the source are oscillatory to the same degree as that at large distances when there are many layers. This phenomenon which is proper to the echoing waves is much different from that of the ordinary dispersed elastic waves.

Dispersion of a Shock in Dispersive Elastic Bodies.

6. We may now proceed to the question of the dispersion of a single shock in a dispersive elastic body. We shall introduce the relation[3] between the wave length of Rayleigh-waves and their velocity, which was obtained by one of the present authors a few years ago.

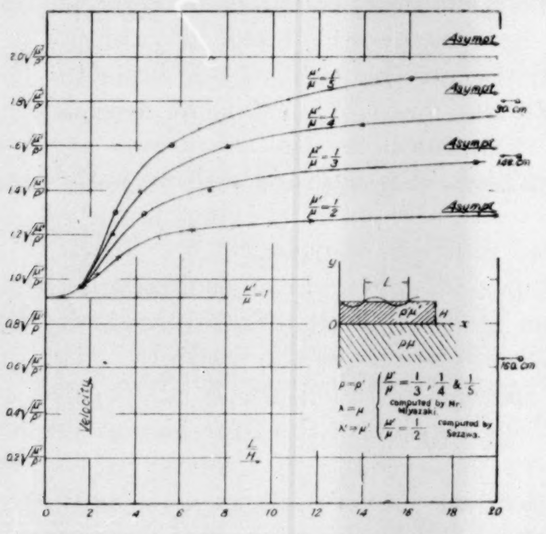

Fig. 8. Dispersion of Reyleigh-waves on Stratified Surface.
[From Bull. Earthq. Res. Inst., **3** (1927), p. 5.]

3) K. SEZAWA, *loc. cit.*, p. 321

Let us formulate the above relation for each μ'/μ in the following form:

$$V = V_1 + \frac{(V_2 - V_1)a^2}{a^2 + f^2}, \quad \cdots\cdots\cdots\cdots\cdots\cdots\cdots\cdots\cdots\cdots(22)$$

where V_1, V_2 are the least and the greatest values of V, a is a constant to be adjusted and $f = 2\pi/\mathrm{L}$.

The vertical and the horizontal components of Rayleigh-waves on the surface can be expressed by

$$v = \frac{1}{\pi}\int_0^\infty \cos fVt\, df \int_{-\infty}^{\infty} \varphi(\sigma) \cos f(x - \sigma)\, d\sigma, \quad \cdots\cdots\cdots\cdots\cdots\cdots(23)$$

$$u = \frac{q}{\pi}\int_0^\infty \cos fVt\, df \int_{-\infty}^{\infty} \varphi(\sigma) \sin f(x - \sigma)\, d\sigma, \quad \cdots\cdots\cdots\cdots\cdots\cdots(24)$$

where V is given by (22), $\varphi(\sigma)$ is the initial vertical disturbance and q is the ratio of horizontal and vertical components of the elementary harmonic waves.

7. Let us take the initial disturbance of the form similar to that in the echoing medium, i.e.

$$\varphi(x) = e^{-\frac{x^2}{c^2}}, \quad \cdots\cdots\cdots\cdots\cdots\cdots\cdots\cdots\cdots\cdots\cdots(25)$$

then, in virtue of this and (22), v and u become

$$v = \frac{c}{2\sqrt{\pi}}\int_0^\infty e^{-\frac{c^2f^2}{4}} \left[\cos f\left\{x + \left(V_1 + \frac{\overline{V_2 - V_1}\,a^2}{a^2 + f^2}\right)t\right\}\right.$$

$$\left. + \cos f\left\{x - \left(V_1 + \frac{\overline{V_2 - V_1}\,a^2}{a^2 + f^2}\right)t\right\}\right] df, \quad \cdots\cdots\cdots(26)$$

$$u = \frac{qc}{2\sqrt{\pi}}\int_0^\infty e^{-\frac{c^2f^2}{4}} \left[\sin f\left\{x + \left(V_1 + \frac{\overline{V_2 - V_1}\,a^2}{a^2 + f^2}\right)t\right\}\right.$$

$$\left. + \sin f\left\{x - \left(V_1 + \frac{\overline{V_2 - V_1}\,a^2}{a^2 + f^2}\right)t\right\}\right] df. \quad \cdots\cdots\cdots(27)$$

To integrate these expressions, we may introduce the idea of stationary point of an oscillating function due to P. Debye[9] and Lord Kelvin[10].

9) P. Debye, *Math. Ann.*, 67, 535.

10) W. Thomson, *Proc. Roy. Soc.*, 42 (1887), 80.

Consider

$$\varDelta = \int_0^\infty e^{-\frac{c^2 f^2}{4}} e^{if\left\{x \pm \left(V_1 + \frac{(V_2 - V_1)a^2}{a^2+f^2}\right)\right\}} df, \quad \cdots\cdots\cdots\cdots\cdots(28)$$

and put

$$\frac{d}{df}\left[fx \pm fV_1 t \pm \frac{fbt}{a^2+f^2}\right] \equiv 0, \quad \cdots\cdots\cdots\cdots\cdots\cdots\cdots\cdots(29)$$

where $b = (V_2 - V_1)a^2$. Then the real possible root f_1 of the equation (29) in f is expressed by

$$f_1 = \sqrt{-\left(a^2 \mp \frac{bt}{2(x \pm V_1 t)}\right) + \sqrt{\left\{a^2 \mp \frac{bt}{2(x \pm V_1 t)}\right\}^2 - \left\{a^4 \pm \frac{a^2 bt}{(x \pm V_1 t)}\right\}}}. \quad \cdots\cdots(30)$$

Again, if we write

$$\frac{d^2}{df^2}\left[fx \pm fV_1 t \pm \frac{fbt}{a^2+f^2}\right]_{f=f_1} = \frac{\mp 2bt\,\{3a^2 - f_1^2\}\, f_1}{(a^2+f_1^2)^3} \left\{\equiv \frac{d^2\phi\,(f_1)}{d\,{}_1^2}\right\}, \quad (31)$$

we have

$$\varDelta = \frac{\sqrt{2\pi}\, e^{-\frac{c^2 f_1^2}{4}}}{\sqrt{\left|\frac{d^2\phi(f_1)}{df_1^2}\right|}}\, e^{i\left[f_1\left\{x \pm \left(V_1 + \frac{b}{a^2+f_1^2}\right)t \pm \frac{\pi}{4}\right]}, \quad \cdots\cdots\cdots\cdots\cdots\cdots(32)$$

provided

$$\frac{d^3\phi(_1)}{df_1^3}\Big/\left[\left|\frac{d^2\phi(f_1)}{df_1^2}\right|\right]^{3/2} \quad \cdots\cdots\cdots\cdots\cdots\cdots\cdots\cdots\cdots(33)$$

is small. In (32), the upper and the lower sign of $\pm\frac{\pi}{4}$ should be taken according as $\frac{d^2\phi(f_1)}{df_1^2}$ is positive or negative.

Now, substituting the result of (32) in (26) and (27), we get

$$v = \frac{c}{\sqrt{2}} \frac{e^{-\frac{c^2 f_1^2}{4}}}{\sqrt{\left|\frac{d^2\phi(f_1)}{df_1^2}\right|}} \left\{\cos\left[f_1\left\{x + \left(V_1 + \frac{V_2 - V_1 a^2}{a^2 + f_1^2}\right)t\right\} \pm \frac{\pi}{4}\right]\right.$$

$$\left. + \cos\left[f_1\left\{x - \left(V_1 + \frac{V_2 - V_1 a^2}{a^2 + f_1^2}\right)t\right\} \pm \frac{\pi}{4}\right]\right\}, \quad \cdots\cdots(34)$$

$$u = \frac{qc}{\sqrt{2}} \frac{e^{-\frac{c^2 f_1^2}{4}}}{\sqrt{\left|\frac{d^2\phi(f_1)}{df_1^2}\right|}} \left\{\sin\left[f_1\left\{x + \left(V_1 + \frac{V_2 - V_1 a^2}{a^2 + f_1^2}\right)t\right\} \pm \frac{\pi}{4}\right]\right.$$

$$\left. + \sin\left[f_1\left\{x - \left(V_1 + \frac{V_2 - V_1 a^2}{a^2 + f_1^2}\right)t\right\} \pm \frac{\pi}{4}\right]\right\}, \quad \cdots(35)$$

together with the value of f_1 in (30).

To find compiled results, we shall take three cases, i.e. i) $\mu'/\mu = 1/2$, ii) $\mu'/\mu = 1/3$, iii) $\mu'/\mu = 1/5$. The original disturbance is assumed to be

$$e^{-\frac{x^2}{H^2}} \quad \cdots\cdots\cdots\cdots\cdots\cdots(36)$$

in each case. From the diagrams in Fig. 8, we find with sufficient approximation the following relations:

TABLE

μ'/μ	1/2	1/3	1/5
V_2/V_1	1·51	1·68	2·10
aH	1·30	1·71	1·48

Applying these relations in (34) and analysing the resulting equation with respect to x/H, V_1t/H. we obtain the vertical component of wave forms of three cases i) $\mu'/\mu = 1/2$, ii) $\mu'/\mu = 1/3$, iii) $\mu'/\mu = 1/5$ as shown in the drawings in Fig. 9, 10 and 11. The value of V_1t/H has been taken to be 50, 75, 100 in all cases. In these figures the mathematical point representing the leading part of the waves should be excluded from consideration owing to the dissatisfaction of the condition (33).

Though the true displacement at this point can be evaluated by a certain exact manner, the process has been omitted here on account of the reason that it is not so important in the present case. Such a calculation will be carried out in some future occasion.

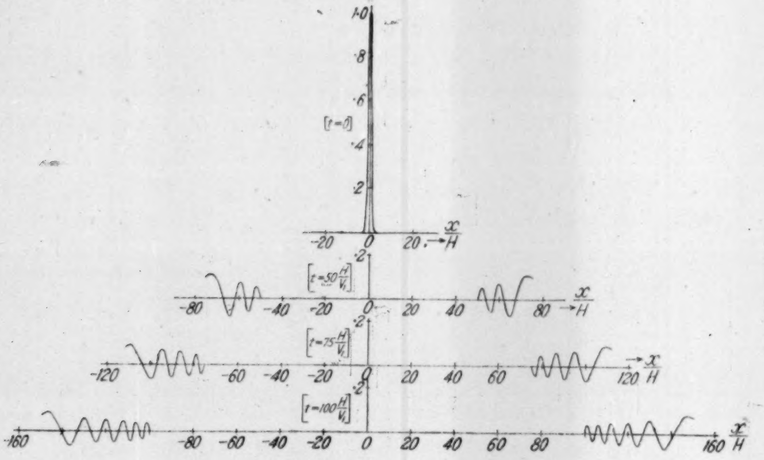

Fig. 9. $[\mu'/\mu = 1/2.]$

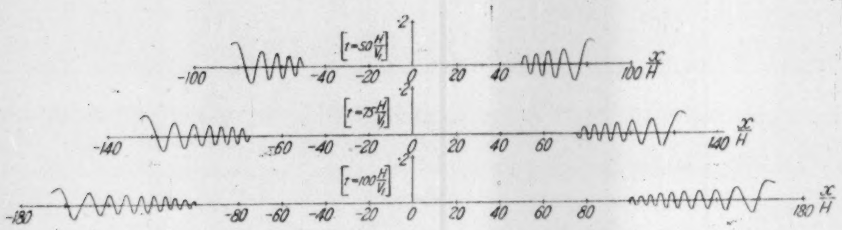

Fig. 10. $[\mu'/\mu = 1/3.]$

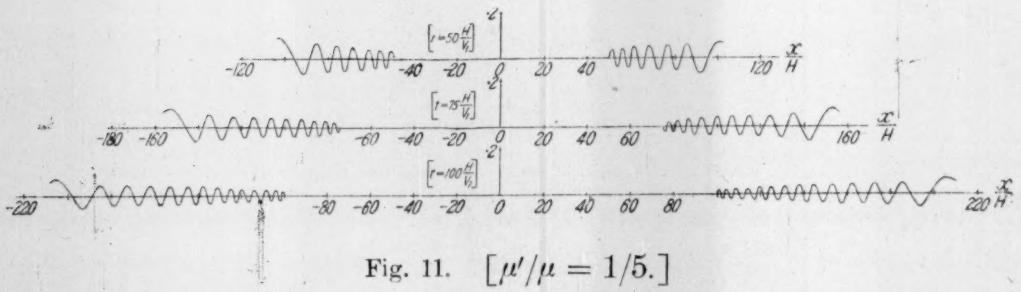

Fig. 11. $[\mu'/\mu = 1/5.]$

8. From these diagrams, it can be seen that, even when the initial disturbance is of the type of a single shock, the transmitted waves at a distance are of oscillatory and continually varying wave length. According as the epicentral distance is farther or nearer, the repetition of oscil-

lations is greater or smaller and the extent of disturbed portion becomes wide or more narrow. The leading and the trailing parts of the disturbed portion take their positions at distances V_2t and V_1t respectively from the origin. The spaces outside the disturbed portion become quiescent on account of the imaginary nature of f_1 in (30) and of some other functions.

It is to be noticed, moreover, that the portion of the longer wave length resides nearer to the leading part, while that of shorter length in the vicinity of the trailing part. This can be easily understood from the physical sense that the longer waves have large velocities in the stratified elastic bodies. The most dominent length of waves in the oscillatory part is controlled by the dispersion-relation of the stratum as shown in the preceding table, but not by the type of the original motion of the source. This may be a very important fact on the problem of the transmission of the seismic waves.

Although the absolute amplitudes of the vibrations depend upon the amplitude of the initial shock and the value of c which defines the sharpness of the shock, yet they are much affected by the dispersion formula already cited. In regard to the sharpness c, there is its certain value which makes the amplitude of waves maximum. The most common feature to be remarked in connection with the dispersed waves is that, the longer the range of the disturbed portion, the more decreases the general amplitudes of the vibratory motion. This phenomenon well conforms with the law of the conservation of the energy of waves.

It appears also that the greater ratio of μ/μ' gives us the wide-spread disturbed portion of transmitted waves and the frequent oscillations of wave forms.

Comparsion of Both Cases of Dispersion.

1. The disturbed portion of the transmitted waves which are dispersed by the echoing nature of the medium is not of a regular form, while in the ordinary dispersed waves the oscillatory part is quite regular and has gradually varying wave length.

2. In the echoed dispersion the leading part of the disturbed portion is distinct and has a large amplitude, while in the ordinary dispersed waves the leading as well as the trailing parts have their own velocities of propagation, the amplitude of the leading part in this case being also large.

3. In the case of echoed dispersion the disturbed portion may be partially of the same wave length and of decaying amplitudes, while in the ordinary dispersed waves even the partial equality of the wave length is impossible.

4. In both cases of dispersion the general amplitudes of the oscillations are diminished as the disturbed portion is diffused in a larger extent.

5. Partial portion of the vibrations in the echoing dispersion is of a gradually decaying type, while in the ordinary dispersion such a nature cannot take place in general.

6. When there are a number of layers, the vibrations due to echoed dispersion are repeated in a great interval of time even in the neighbourhood of the source, though the amplitudes of the succeeding shocks are relatively small compared with the initial shock. In the vibrations due to the ordinary dispersion, the disturbances in the neighbourhood of the source die away in a short time, but the vibratory disturbances at a large epicentral distance do not cease for a long time.

---

12. 彈性波の反響性及び分散性分散に就て

地震研究所 妹澤克惟
西村源六郎

震源の衝擊が極めて單純な場合でも遠方での震動は繰替し的のものであり、而も其の距離が遠ければ遠い程繰替しが長く續くと云ふ事は既に一般に知られて居る事柄である。斯る性質の説明として誰にも想像出來る事は彈性波の反響性と分散性とである。しかしその何れが最も可能的であるかといふ事は勿論の事、其の各の性質さへも未だ餘り研究されて居らぬ様に思はれる。

彈性波の波長によつて其傳播速度が異なるといふ分散の基本的の性質に就ては著者の一人が三四年前に研究した事があるけれども勝手な衝擊が傳播につれて變形して行く性質は充分に手がつけてなかつたのである。但し波動速度を極く簡單な公式に直して取扱ふ事は一二の場合に就てはしらべた事もある。反響性の分散問題は彈性波の場合としては問題が非常に簡單であるにも拘らず未だ手が著けられて居らぬ様に見える。しかし彈性波を分散させるといふ事にはやはり重要な役割をなして居るものである。

兩方の分散性は共に簡單な數學、即ちフーリエの積分や振動函數の定常値を求める方法などで解決が出來さうであつたから其等を適當に應用したのではあるけれども、實際に數値を入れて其結果を出す事は必ずしも容易でなかつた。

反響性の分散で直ちに氣の付く事は、初めの衝擊が單純な場合でも傳播する波動は複雜な波型となつて進み、擾亂部分の所々が週期的の振動となる事である。而して其等の所々が各減衰的の傾向を持つものである。斯くの如く所々が減衰性を持つ事は震源が恰も多數あつて順次に震動勢力を發散したかの如く思はせる。又擾亂部分の先頭は不均一彈性體の效果的速度で傳播される。卽ち彈性體が粘性や速度的分散性がなければ地震の初動によつて震源距離等を確めるが如き事に對して好都合な譯である。又反響性分散をやる場合に初動部は振幅が大きく且つ其位相が保持される。この事も亦驗震學的に重要であらう。特に注意すべき事柄は彈性波が軟い媒體から硬い媒體へ進む時に其初動部が普通と違つた波形を作る事であらう。但しこの場合は媒體が塊狀をなす時であつて一般の反射屈折の時には起らぬ現象である。又、震源の近所で層が變る爲めに第一に反射される波は振幅が非常に小である。之は震源附近の振動型に特別の型を與へるものである。尙反響性分散の爲に擾亂部分が次第に長くなるに從つて一般の振幅が小さくなる事は勢力保持の考にもよく符合して居る事柄である。

分散性の分散で第一に注目すべき事は、初動が單純でも傳播擾亂部分が矢張振動性を帶び、且つ震源からの距離が遠くなればなる程其擾亂部分の長さは長くなり、振動性は益々增大する事である。この部分が長くなればなる程一般の振幅が少くなる事や、其先頭部分が一定の速度を持つ事は反響性分散の場合に似て居る。しかしこの場合には尾部も一定の傳播速度を持つて居る。次に擾亂部分は次第に變化する波長を有し且つその始めの方は長波が占め、終りの方は短波が占めて居るけれども、一般的の波長は或る度合のものになる。この度合は震源の形には殆ど關係がなく、媒體の性質によつて決定されるものである。尙又注意すべきは μ/μ' が大きければ大きい程擾亂部分の長さが非常に速に延び且つ振動の繰替しも割合に多くなる事である。

最後に反響性分散と分散性分散との比較を示して見ると下の如くになる。

1. 反響性媒體中の振動は不規則なのが通例であるが、分散性媒體中の分散波は割合によく規則的になり且つ次第に變化する波長を持つて居る。

2. 反響性分散波は其先頭部だけが明瞭な速度を持つけれども、分散性分散波は先頭部及び尾部共に各一定の速度を持つ。且つ又先頭部は兩方の場合共に大なる振幅になる。

3. 反響性分散では部分的に一定の波長及び減衰性振幅を持つけれども分散性分散では斯る事柄がなく一般に變化する波長を持つのである。

4. 兩方の場合共に擾亂部分の長さが長くなる程一般の振幅が減少して行き、其傾向が波動勢力保持の法則と一致して居る。

5. 反響性分散では層の數が、增大すればする程、振動の繰替しが增加する。しかし其は震源から遠い所のみでなく震源の近所でも多少同じ性質がある。然るに普通の分散性分散では振動源から遠方程擾亂部分の長さと振動の繰替しが增すのであつて、振動源に近い所では擾亂の長さが極めて短く振動の繰替しが非常に少い。

13. *Investigation on the Deformation of the Earth's Crust in the Tango District connected with the Tango Earthquake of 1927. (Part 2.)*

By **Chûji TSUBOI**,

Earthquake Research Institute.

(Received June 20, 1930.)

In the previous paper[1], the writer described the results of the repeated revisions of the triangulations and precise levellings made in the Tango district in which a great earthquake occurred in 1927. In the same paper, he made some detailed discussions on the deformation of the earth's crust of the district connected with the earthquake which were detected by these surveys. The materials upon which the above discussions were based were those derived from the revisions of the precise levellings and the triangulation of primary and secondary orders executed in the Tango district after the earthquake by the hands of the Land Survey Department of the Imperial Army. Since that time, the Department has made further an extensive revisions of third order triangulation over the same district. The field observations have now been wholly completed, and the computation on these results are now in the course of progress. Through the courtesy of Major General E. Isii, the chief of the Land Survey Department, a part of the results was placed at our disposal for which the computation was completed. This part of the examined area covers the whole extent of the Tango peninsula, including 44 triangulation points. It is this part of the results that is specially referred to in the present paper.

In this series of triangulation of third order, not only the horizontal but also the vertical displacements of the triangulation points were examined which may have been produced connected with the earthquake of 1927. The horizontal (u, v) and vertical (h) displacements of the triangulation points revealed by the comparison of the old and new triangulations are tabulated in Table 1. The assumption made in calculating

1) C. TSUBOI, *Bull. Earthq. Res. Inst.*, 8 (1930), 153.

the horizontal displacements of the triangulation points was that the points Hyônoyama and Kasagatayama were undisturbed in position before and after the earthquake.

Table 1.

No.	Name	*u* (cm.)	*v* (cm.)	*h* (cm.)	Resultant Horizontal Displacement (cm.)	Azimuth
1	Taikoyama	− 47·3	+ 33·9	+ 4	58·2	305° 38′
2	Nomura	− 43·2	+ 37·6	− 3	57·3	311 2
3	Itigao	− 86·9	+ 62·6	− 8	107·1	305 46
4	Oohara	− 58·8	+ 32·7	−17	67·3	299 5
5	Yosizawa	− 74·5	+ 80·4	− 9	109·6	317 11
6	Tudumigatake	− 52·4	+ 52·4	−24	74·1	315 0
7	Mie	+ 11·6	+ 91·8	+48	92·5	7 12
8	Isitani	− 47·7	+ 67·8	− 3	82·9	324 52
9	Sarugao	− 45·2	+ 21·6	0	50·1	295 32
10	Taira	− 75·4	+ 61·6	−15	97·4	309 15
11	Hutamatu	− 55·3	+ 43·1	− 1	70·1	307 56
12	Oohira	− 95·5	+ 70·9	−27	118·9	306 35
13	Takinoyama	− 42·7	+ 30·8	+ 7	52·6	305 48
14	Kasayama	− 47·8	+ 40·1	− 4	62·4	310 0
15	Tubo	− 52·8	+ 24·7	−11	58·3	295 4
16	Ooisi	− 90·5	+ 58·6	−17	107·8	302 55
17	Kubo	− 67·9	+ 43·1	−15	80·4	302 24
18	Kohama	− 55·3	+117·1	−16	129·5	334 43
19	Mitinoku	− 95·5	+ 80·1	−20	124·6	309 59
20	Hatakedani	− 47·8	+ 33·9	−15	58·6	305 21
21	Ootani	− 98·1	+ 92·4	−32	134·8	313 17
22	Morigami	− 50·3	+ 43·1	+ 4	66·2	310 36
23	Kamatani	− 75·4	+ 49·3	−24	90·1	303 11
24	Terayama	− 55·3	+ 33·9	− 8	64·9	301 31
25	Inugasira	− 62·9	+ 43·1	−27	76·2	304 25
26	Natani	− 88·0	+ 83·2	−13	121·2	313 24
27	Wasimisaki	− 60·4	+ 24·7	+ 4	65·3	292 14
28	Asago	−125·7	+104·8	−52	163·7	309 49
29	Kadoduki	− 50·3	+ 30·8	−18	59·0	301 29
30	Kongôsan	− 60·4	+ 67·8	−20	90·8	318 18
31	Sengokuyama	− 57·9	+ 37·0	+ 1	68·7	302 35
32	Take	− 60·4	+ 46·2	−31	76·0	307 25
33	Yada	− 93·1	+107·9	−34	142·5	319 13
34	Akasaka	− 88·1	+ 83·2	−25	121·2	313 22
35	Takao	− 73·0	+ 64·7	−21	97·5	311 33
36	Yanahira	− 60·4	+ 55·5	−35	82·0	312 35
37	Yasuke	− 60·4	+ 43·1	− 5	74·2	305 31
38	Mineyama	− 90·6	+123·3	−22	153·0	323 41
39	Takase	− 75·5	+ 95·5	+ 1	121·7	321 40
40	Kidumiyama	− 55·4	+ 80·1	+21	97·4	325 20
41	Nisitani	− 50·3	+ 55·5	−13	74·9	317 49
42	Mititani	− 47·8	+ 67·8	− 4	83·0	324 49
43	Minamidani	− 57·9	+ 52·4	−16	78·1	312 9
44	Misakayama	− 42·8	+ 89·4	+24	99·1	334 25

These horizontal and vertical dispaclements of the points are shown in Figs. 1 and 2 respectively. Fig. 2 was constructed making use not only of the results of the third order triangulation but also of those of the precise levellings. Referring to Fig. 1, the mass of the Tango peninsula is seen to have been displaced into an approximate direction of northwest with no remarkable deformation in itself. Along the west and south side of the peninsula, the displacements of the triangulation points make remarkable discontinuities both in direction and magnitude with those of the points outside of the peninsula, and in fact two seismic faults were produced at these places at the time of the earthquake as were described in the previous paper. Fig. 3 shows the lines of equal eastward deviations from the mean eastward displacements of the triangulation points. These features are of course essentially the same as was deduced from the results of the secondary triangulations. A new information is, however, obtained for this time by the comparison of the horizontal and vertical displacements of the triangulation points.

When Figs. 2 and 3 are compared with each other, it will be seen that the contour lines in these figures are very much similar in their

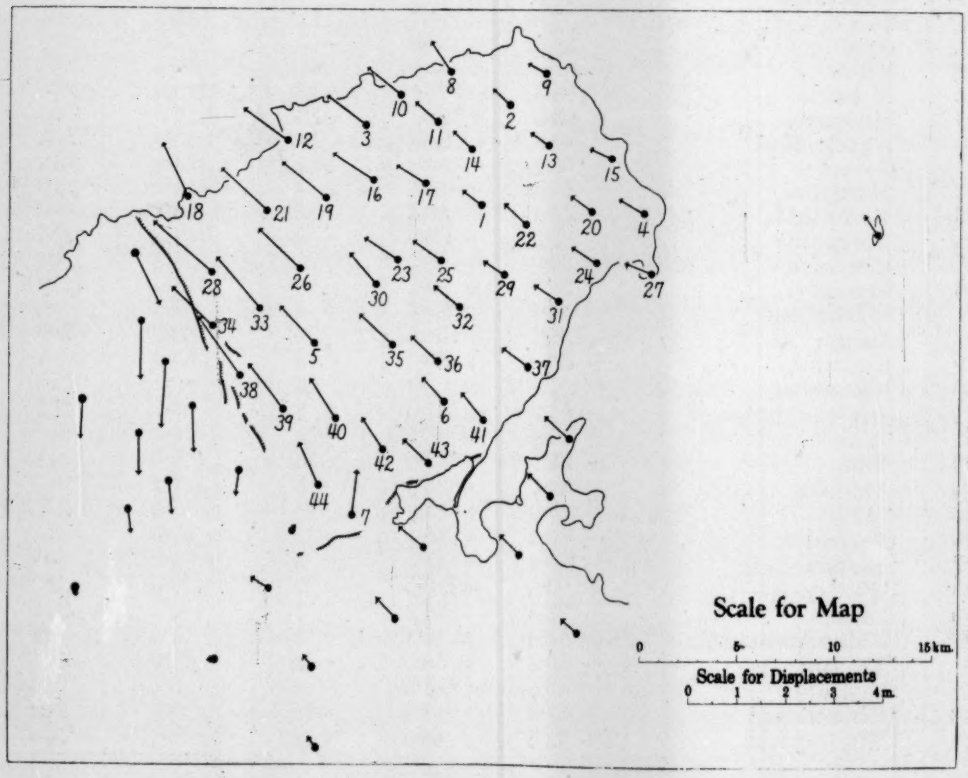

Fig. 1. Horizontal Displacements of Triangulation Points.

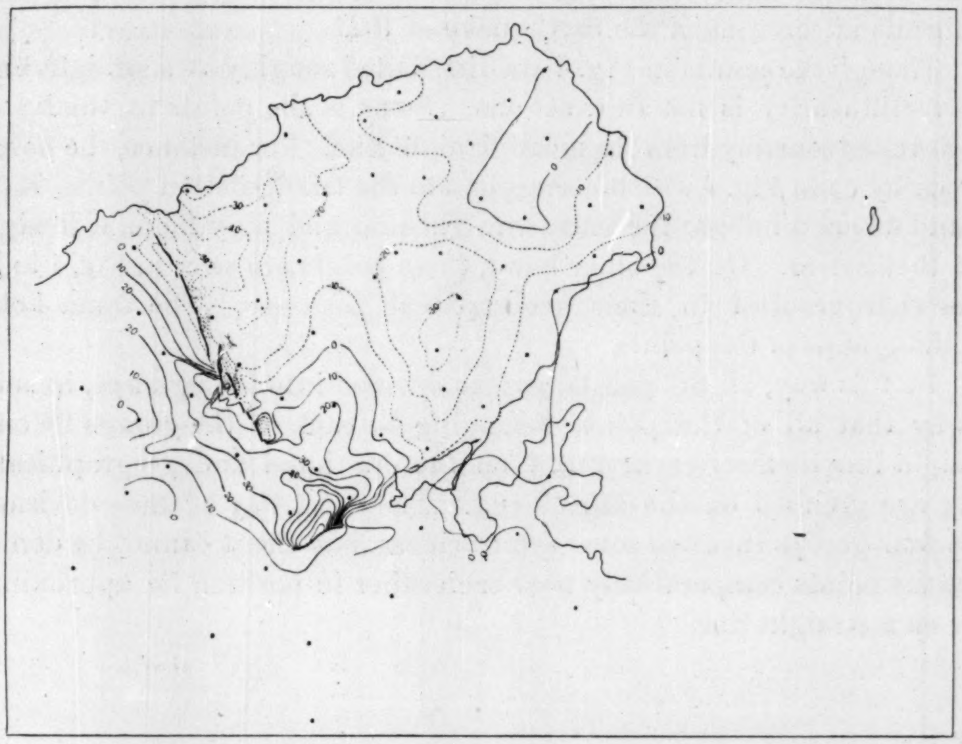

Fig. 2. Lines of Equal Vertical Displacements (cm.).

forms. Most of the triangulation points with positive eastward displacement are seen to have been uplifted at the same time and those with negative eastward displacements depressed. In order to made clear the correlation between these eastward and vertical displacements, Fig. 4 is constructed.

In this figure, the horizontal displacements (deviations from the mean) were taken in abscissa and the vertical displacements (deviation from the mean) in ordinate. If the correlation between these quantities is perfect, the points in the figure must be distributed on a straight line. In the present case, the correlation is not a very good one. The points in the figure lie very roughly on a straight line corresponding to a spatial inclination of about 40° with the hirizontal direction. This is an evidence that all of the triangulation points was displaced at the time of the earthquake along a seires of approximately parallel planes with westward dips, or it may conveniently be said that the movements of the triangulation points were prismatic. The dips of these prisms are toward west and it is interesting that this is of the same direction as that

of the Gomura fault which was formed along the west side of the Tango peninsula at the time of the earthquake of 1927.

Though the points in Fig. 4 are distributed roughly on a straight line, this rectilinearity is not an exact one. Some of the points in the figure are deviated sensibly from the mean straight line. For instance, the points shown by ○ in Fig. 4 which correspond to the triangulation points, 7, 39, 40 and 44 are all above the mean straight line and they lie on a straight line themselves. On the other hand, these points are seen in Fig. 1 to be somewhat grouped in their geographical positions. The same holds for the groups of the points.

In this way, all the points may be devided into four groups, in such a way that all of the points belonging to each of the groups lie on a straight line themselves in Fig. 1 on the one hand and geographically they are grouped on the other hand. The exact way of these devisions into four groups involves some arbitrariness, but the it cannot be denied that the points comparatively near each other in position lie approximately on a straight line.

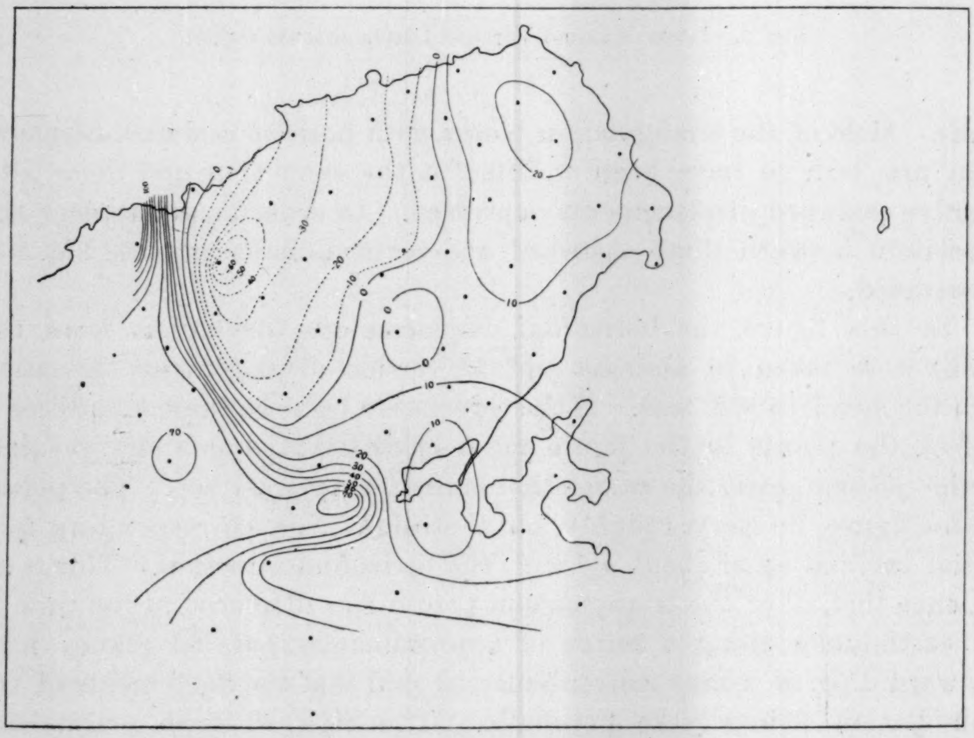

Fig. 3. Lines of Equal Eastward Displacements (cm.).

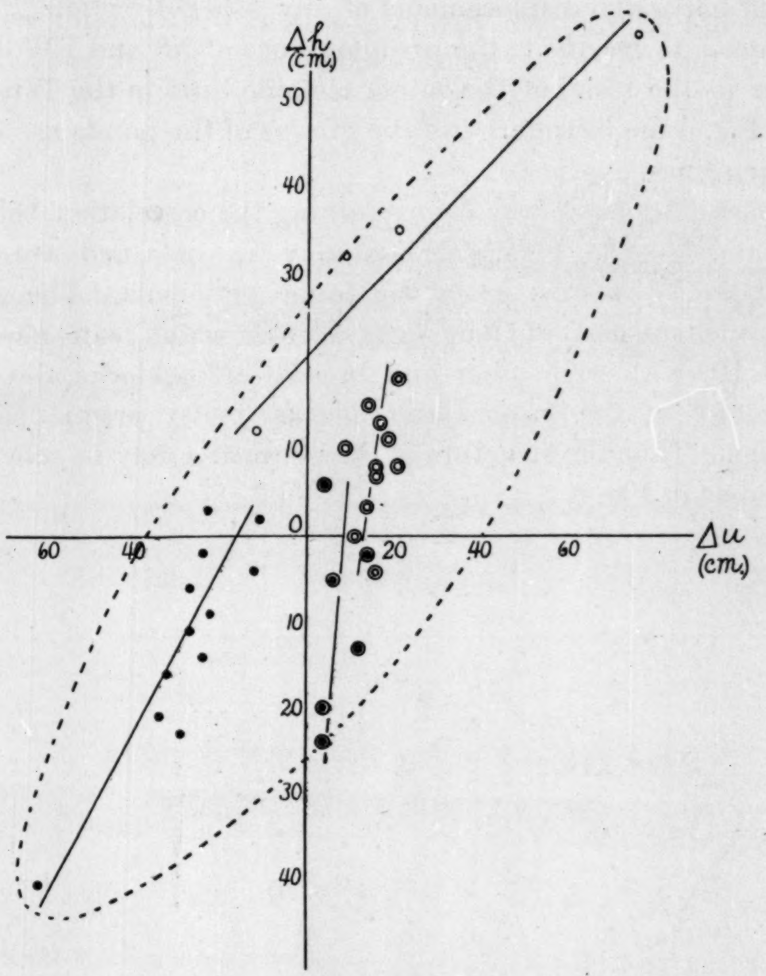

Fig. 4.

In the above the correlation was discussed between the east and vertical displacements. It may be suspected whether there be any other direction than east, the components of displacements of triangulation points in which direction show closer correlation with their vertical displacements. For the purpose of determining this, the components of horizontal displacements in successive directiens α at each 10° intervals were calculated according to the formula

$$w = u \cos \alpha + v \sin \alpha.$$

It was found that the correlation between w and the vertical displacements is after all closest when $\alpha = 0$, in other words the correlation between the east and vertical displacements is closest than between the

vertical and horizontal displacements of any other direction. This may be understood to be due to the predominance of NS and EW directions in number in the trend of the minor tectonic lines in the Tango peninsula. In Fig. 5 the boundaries of the groups of the points are shown by thick broken lines.

The most reasonable way for explaining the correlation between the eastward and vertical displacements may be obtained through the concept of the block structure of the Tango peninsula. The ground of the peninsula consists of four land blocks which can move rather independently with each other and in each of he blocks, the segments of the ground of the minor land blocks move prismatically with western dips. Thus the structure of the peninsula may be schematically represented as in Fig. 6.

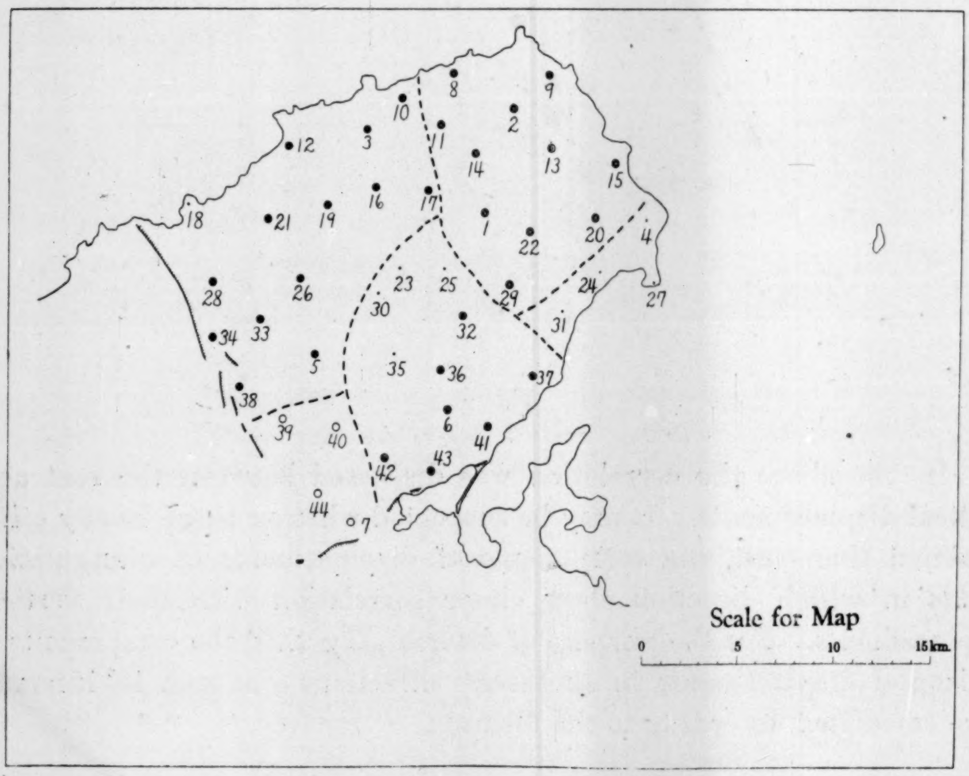

Fig. 5. Land Blocks in the Tango Penrinsula.

The results obtained in this paper are also in good accord with the results described in the previous paper.

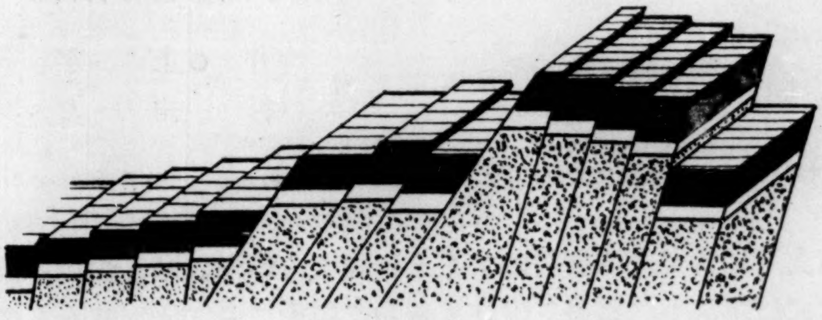

Fig. 6. Schematic Diagram of the Structure of the Tango Peninsula.

---

13. 昭和二年丹後地震に關聯せる丹後地方の地殻の變形に關する研究（第二報）

地震研究所　坪　井　忠　二

丹後地震に關聯した丹後地方の地殻の變形に就いては、彙報第八號(昭和五年)一五三頁に詳しく述べておいた。其の後陸地測量部によつて更に同地方の三等三角測量改測が施行された。本論文は其の結果の一部である丹後半島部の變形に就いて考察を加へたものである。三等三角點の水平移動量の東西成分と垂直移動量とが、かなり密接な相關を示して居る。之は各三角點が略々互に平行で西下りの面内で移動する事を示すものである。此の事實は、丹後半島内の地塊運動として都合よく説明する事が出來る。

---

14. 筑波山に於ける傾斜變化觀測報告

地震研究所 {井上宇胤
杉山友紀

(昭和四年七月九日及昭和五年六月十七日發表－昭和五年六月廿日受理)

筑波山支所に於ては花崗岩のすぐ上に建てられた、殆ど恒溫の觀測室内に石本式傾斜計を二臺据え附けて昭和二年十二月二十三日から傾斜變化を觀測して居ります。機械は室の都合で東北一西南の方向と西北一東南の方向に据えてありますが、此邊の山の斜面は東南へ傾いて居りますので、西北一東南のコンポネントは斜面に沿うた傾斜變化を表はし、東北一西南のコンポネントは斜面に直角の傾斜變化を表はす事に成つて居ります。始めはレコード上で一秒の傾斜が二粍に相當する様に器械を調整して置きましたが、絶えず大きな傾斜變化があつて觀測に不便を感じたので、昭和三年六月廿日から倍率を半分にしました。それで始めは傾斜計の自己振動週期は夫々廿一秒でありましたが、倍率を變へてからは夫々十五秒となつて居ります。觀測の始めから昭和三年二月十五日迄の觀測結果は既に石本教授[1]に依つて報告されてあります。著者等[2]も昭和四年九月廿四日迄の觀測結果を既に報告して置きましたが、此處に更めて觀測の當初から昭和五年六月十日迄約二年半の觀測結果に多少議論を加へて報告致します。

時々故障の爲め觀測が缺けた事があつたり、傾斜變化の二つのコンポネントを組合せてベクトル圖を拵へた時に非常に複雑に成つて來る事があつたので、先づ大勢を見る事にして三日目毎の値を三つづつ平均して拵へた傾斜變化の兩コンポネントの圖は第一圖に、其等を組合せて拵へたベクトル圖は第二圖及び第三圖に示してあります。尙第一圖には參考の爲に筑波山の氣溫を中央氣象臺發行の天氣圖から取つて同樣にスムーズして圖示してあります。此の圖を見ますと、東北一西南のコンポネン

1) M. Ishimoto, *Jap. Journ. Astro. & Geophys.*, 6 (1928), 100.
2) W. Inouye & T. Sugiyama, *Proc. Imp. Acad.*, Japan, 5 (1929), 457.

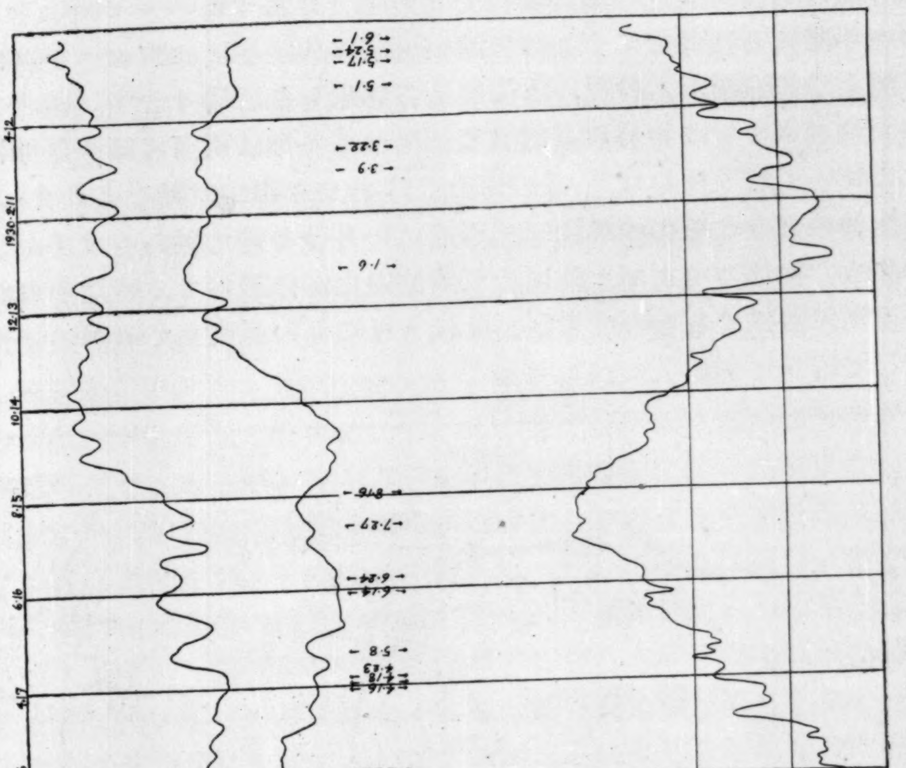

第一圖 Fig. 1.

ト卽ち山の斜面に直角の傾斜變化では東北の方向へ始の一年間に十二秒次の一年間に五秒合せて十七秒程傾いて居る外に冬には東北へ夏期は西南へ傾く二倍振幅が六秒程の季節に依る變化をして居ります。西北一東南のコンポネントは始めの頃は溫度に從つて冬期は東南に傾き夏期には西北に傾いて居りましたが、後の部分ではあまり明かで無くなりました。次に此等の大きな變化の外に二三週或は一月位の變化がありますが、此の變化は、後述のベクトル圖に於て傾斜變化が停滯してる時期の細かな傾斜變化に關係するものですが、此れも可なりの程度まで氣溫の變化に竝行して居ります。

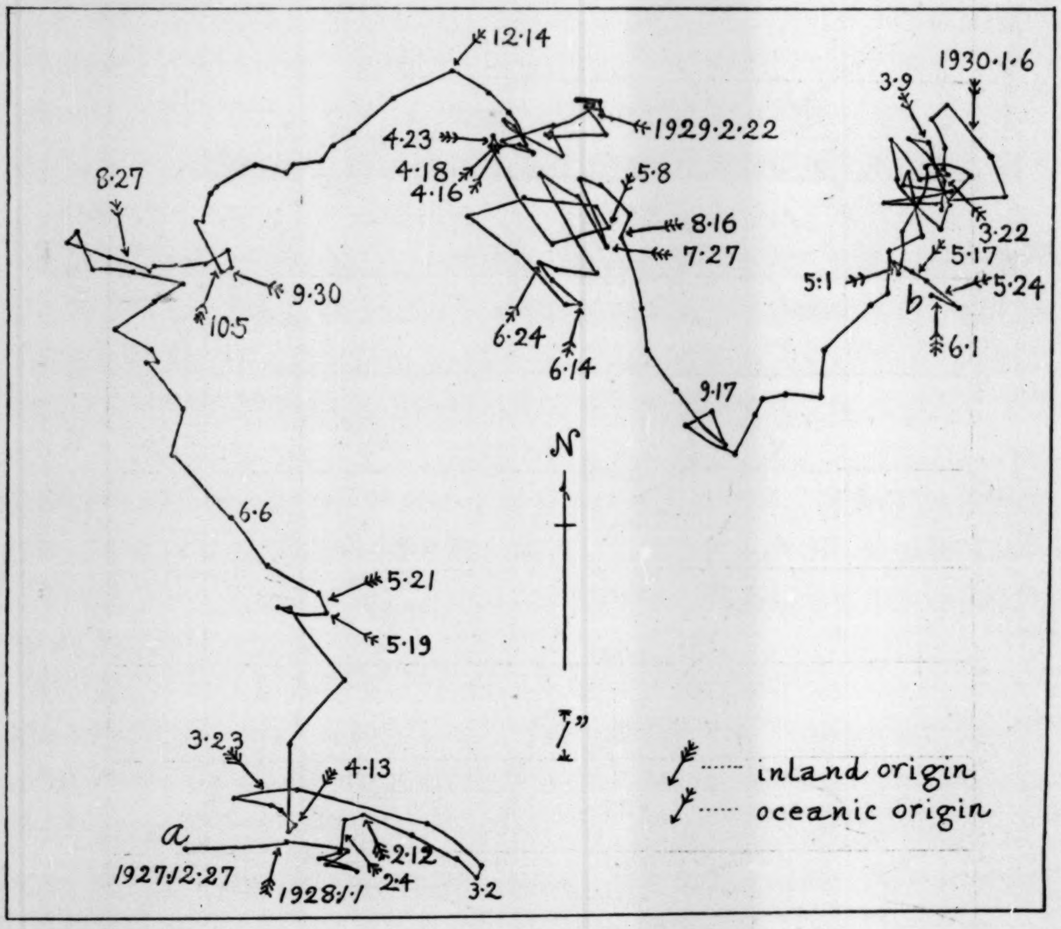

第二圖 Fig. 2.

次に第二圖或は第三圖のベクトル圖を見ますと積年變化が目立ちますが、此れは前述の如く一年目每に元に戾つて來る季節變化だけでは無くて、昭和三年の一月から十月の始め迄は北微西へ十二秒傾き、其れから

其の年の終り迄は東東北へ六秒傾き、昭和四年の一月からは九月の終り迄東南へ七秒程傾き、其れから其年の暮迄東北へ六秒傾き、今年卽ち昭和五年の六月迄は其の邊で停滯して居ります。夫れで今迄の所では、全體として先づ東北の方へ十七秒程傾いて居る事になつてるのは前述の通りです。所で此の積年變化は或は器械のセツトルメントに依るのでは無からうかと云ふ疑はありますが、次の様な此の邊一帶の地盤傾斜に關係を有するものかも知れません。關東震災地の水準再測量の結果を陸地測量部の武藤、熱海[3]兩技師が御調査になつた報告に依ると、土浦から水戸迄の約五十粁のルート及び宇都宮から水戸迄の約六十粁のルートでは共に水戸の方が低下して居りまして、此の邊一帶が極く僅か卽ち角度では一秒足らずではあるが、東北東へ此の數十年の間に傾いた事になつて居ります。此れと上述の筑波地塊の傾斜變化とを直に比較する事は出來無いかも知れませんが、その傾斜の向きが一致してる事は面白い事です。

次に傾斜變化と此の附近の地震とどう云ふ關係があるかを見る爲に、先づ氣象要覽から筑波山から震央距離が約百八十粁以內の顯著地震と稍顯著地震を拾ひ擧げて見ました。其等は第一表に示してあります。其の發生時期は第二圖に矢印で示してあるが、それを見ると此等の地震は皆傾斜變化のベクトル圖に於て積年變化が停滯して短週期の變化をして居る時期に發生して居ります。尙よく注意して見ると其の時期に於ても傾斜の方向が變はる所に發生して居る事に氣附きます。尙地震を海底の地震と陸地の地震とに分けて見ますと、海底地震は傾斜變化の停滯してる時期、假りに傾斜嵐の時期と名附けますと、その時期の始めから終りまでの大部分に發生しますが、陸地地震は傾斜嵐の終る頃に發生して居ると云ふよりも寧ろ傾斜嵐は陸地地震が發生すると共に止むと云つた方が適切な様に思はれます。傾斜嵐の終りでは海底地震があると間も無く陸地地震が發生して居りまして、昭和三年二月四日の海底地震から八日して二月十二日に陸地地震があり、昭和三年五月十九日の海底地震から二日して五月廿一日に陸地地震が發生し、昭和三年九月三十日の海底地震から五日して十月五日の陸地地震があり、昭和四年四月十八日の海底地震から五日して四月廿三日の陸地地震があり、昭和五年五月廿四日の海底地震から八日して六月一日の陸地地震が發生して居ります。

---

3) 武藤勝彥　熱海景良　地震硏究所彙報 7 (1929), 495.

第一表

番號	年	月	日	發表時		震央の位置
1	1928	I	1	1h	16m	鬼怒川下流
2	〃	II	4	3	49	金華山南方沖
3	〃	II	12	6	2	小貝川下流域
4	〃	III	23	10	21	武藏一中川上流
5	〃	IV	13	1	36	小貝川中流域
6	〃	V	19	18	32	鹿島灘
7	〃	V	21	1	29	東京灣北東部
8	〃	VIII	27	3	11	鹿島灘
9	〃	IX	30	6	17	鹽屋崎東南東沖
10	〃	X	5	15	58	荒川中流域
11	〃	XII	14	5	6	九十九里濱沖
12	1929	II	22	13	0	盤城一清戸川河口沖
13	〃	IV	16	9	53	鹿島灘
14	〃	IV	18	3	33	鹿島灘
15	〃	IV	23	23	16	小貝川流域
16	〃	V	8	6	18	鹽屋崎北東沖
17	〃	VI	14	5	23	鹽屋崎東北東沖
18	〃	VI	24	11	4	鹽屋崎東北東沖
19	〃	VII	27	7	48	丹澤山附近
20	〃	VIII	16	22	21	鬼怒川上流域
21	1930	I	6	8	6	鹽屋崎北東沖
22	〃	III	9	19	54	伊東沖
23	〃	III	22	17	50	伊東沖
24	〃	V	1	9	57	鹿島灘
25	〃	V	17	5	14	伊東沖
26	〃	V	24	1	38	伊豆大島附近
27	〃	VI	1	2	58	水戸附近

次に關東地方に發生した小區域地震を第三圖に矢印で示してあります。それに依ると、元來傾斜嵐の時期は他の期間の三倍程長いのですが、小區域地震は傾斜嵐の時期に他の場合の十倍以上も發生して居りますから、まづ顯著、稍顯著地震と同様に傾斜嵐の時期に發生するものと見られます。尙一般に傾斜の方向が變化する所で發生して居る事も顯著地震等の場合と同様ですが、此度は海底地震と陸地地震とで發生時期に區別がありません。次に筑波山で觀測した關東地方の有感無感地震を全部取

つて見ると、昭和三年には幾らか傾斜嵐の時期に餘計發生して居つた様ですが、その後は傾斜嵐に關係なく何時も同じ位發生して居ります。

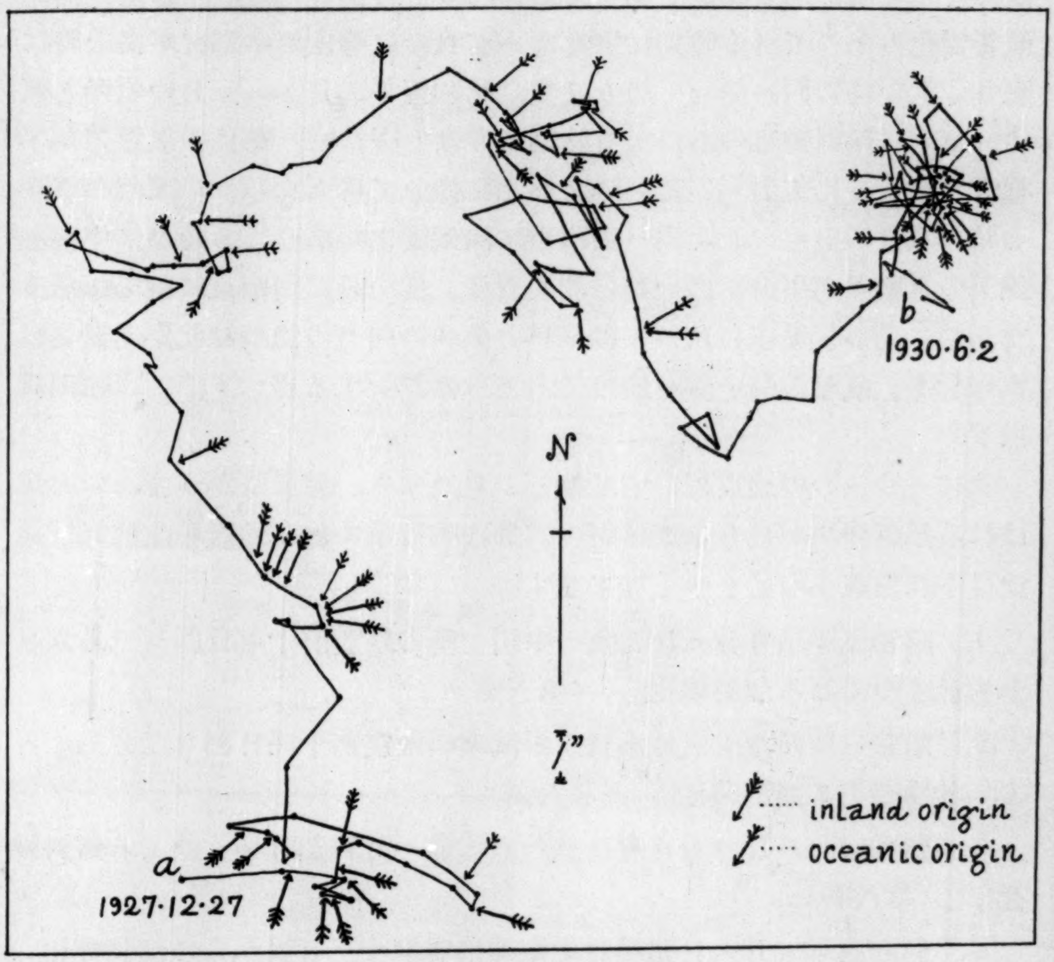

第三圖 Fig. 3.

次に地震前後の日日の傾斜變化と天氣圖から求めた筑波山の氣溫、氣壓、及び宇都宮一布良の氣壓差、甲府一銚子の氣壓差とを比較して見ますと、一般に傾斜變化は氣溫と極めてよく一致して居りまして、西北一東南のコンポネントでは氣溫と殆ど同時に變化して、氣溫が高い頃には北西へ低い頃には東南へ傾いて居ります。東北一西南のコンポネントでは氣溫より少し遲れて氣溫が高いと西南へ低いと東北へ傾きますが、夏期には此の關係が反對に成つてる様です。尙夏期には一般に溫度變化が少いがその割には傾斜變化には影響がある様です。次に氣壓は氣溫と一般

に反對になつて居りますので、從つて傾斜變化とも可成り竝行に行つて居ります。氣壓差の方は一般に餘り傾斜變化と關係がありませんが時に竝行してる事があります。例へば昭和三年一月から二月の半ば迄東西に傾斜變化のあつて居る時期に宇都宮—布良の氣壓差が宇都宮が高い時に東へ、低い時に西へ傾いて居ります。昭和五年二月から三月の頃殆ど西北—東南に傾斜變化のあつてる時期にやはり宇都宮—布良の氣壓差が宇都宮が高い時に東南へ、低い時に西北に傾いて居りました。又昭和四年七月、八月の頃主に北北西—南南東に傾斜變化があつてる時期に甲府—銚子の氣壓差が甲府が高い時に北北西に、低い時に南南東に傾いて居りました。先づ氣壓差に依つては其れと直角の向きの傾斜變化が誘發されるらしく、氣壓の高い方へ向つて右方へ傾斜をする様です。（第四圖以下）

次に一つ一つの地震について精しく見ますと、溫度ばかりでないと思はれる傾斜變化が見られますが、其等は次に示す如く地震發生前二三週或はそれ以前から始まつて居ります。

1. 昭和三年三月廿三日武藏—中川上流の地震前十七日卽ち三月六日から始まつてゐる傾斜變化。（第五圖）

2. 昭和三年四月十三日小貝川中流域の地震前十四日卽ち三月三十日から始まつてる傾斜變化。（第六圖）

3. 昭和三年八月廿七日鹿島灘の地震前一月程から始まつてる傾斜變化。（第八圖）

4. 昭和四年五月八日鹽屋崎北東沖地震前十三日頃からの傾斜變化。（第十二圖）

5. 昭和四年六月廿四日鹽屋崎東北東沖の地震前九日卽ち六月十五日から始まつた傾斜變化。（第十三圖）

6, 7. 昭和四年七月廿七日の丹澤山附近の地震及び昭和四年八月十六日の鬼怒川上流域の地震は共に廿日前から傾斜變化が起つて居ります。（第十四圖）

8. 昭和五年一月六日の鹽屋崎北東沖の地震前十八日からの傾斜變化。（第十五圖）

兎に角全體を通じて此等の地震前の傾斜變化は一方に傾いて次に元に戻り切つた所で地震となつて居ります。

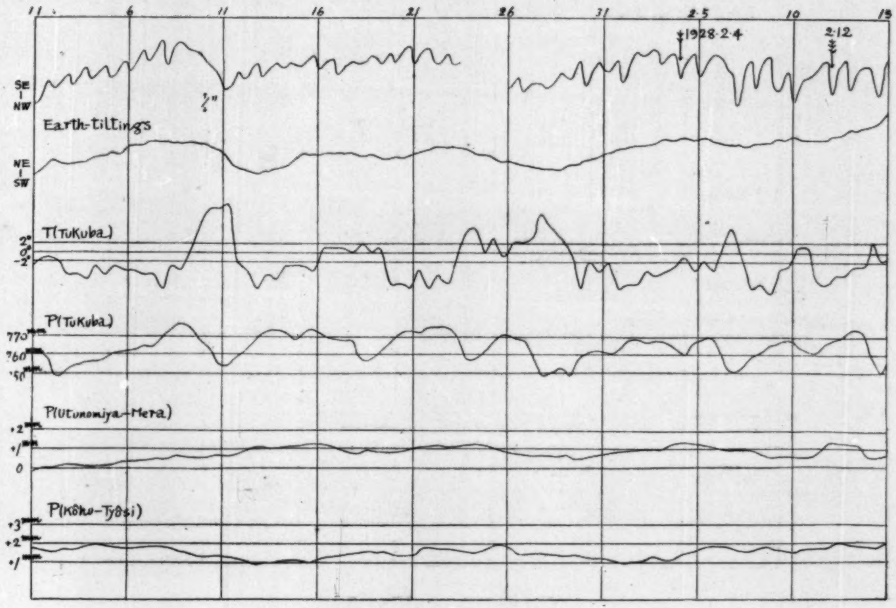

第四圖イ Fig. 4a.

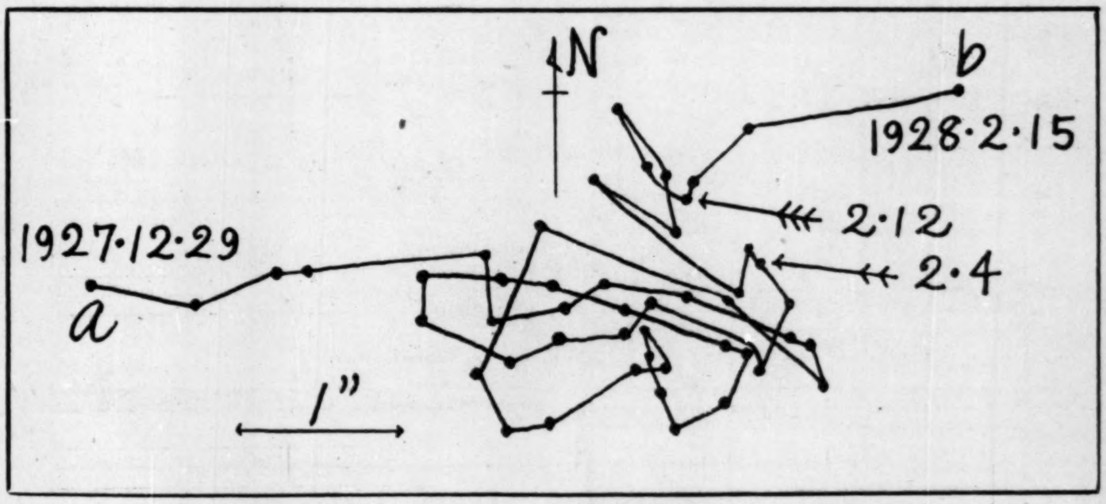

第四圖ロ Fig. 4b. 前圖の傾斜變化のベクトル圖

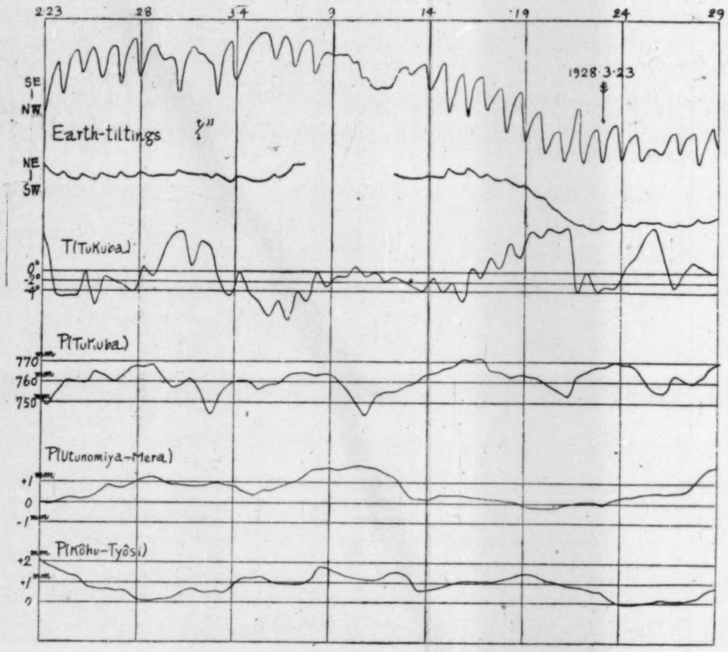

第五圖　Fig. 5.

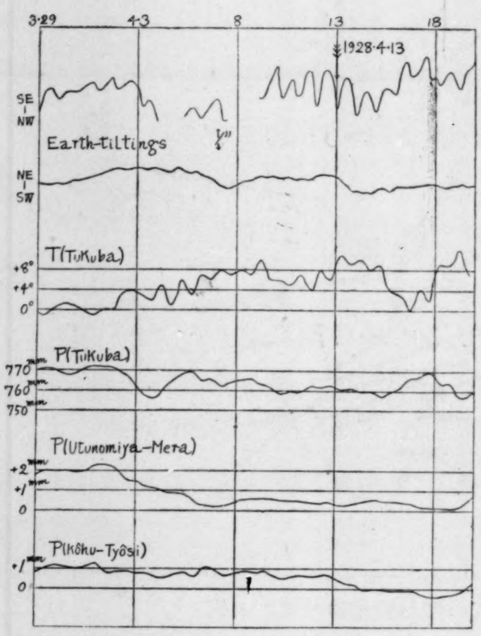

第六圖　Fig. 6.

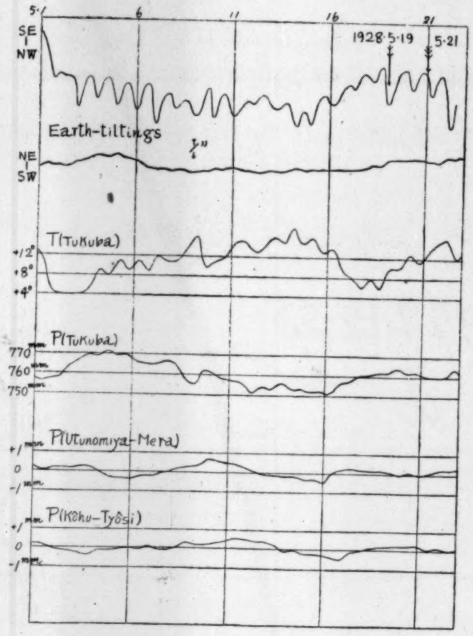

第七圖　Fig. 7.

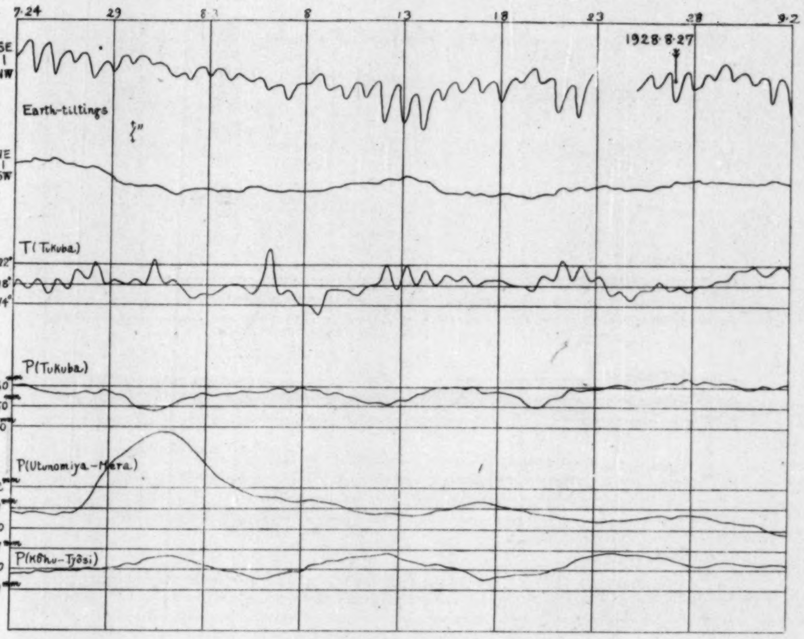

第八圖イ Fig. 8a.

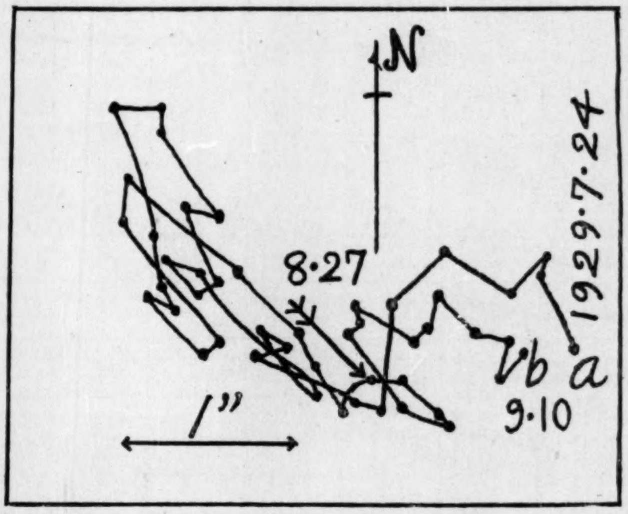

第八圖ロ Fig. 8b. 前圖の傾斜變化のベクトル圖

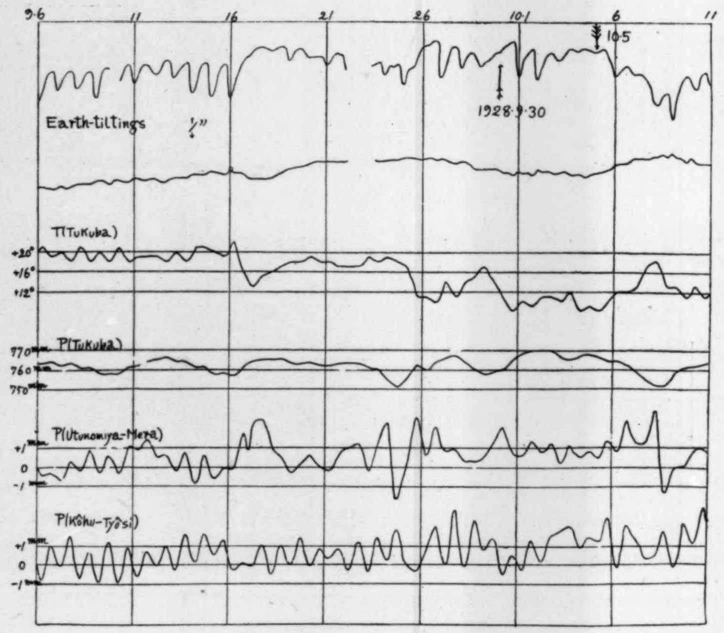

第九圖 Fig. 9

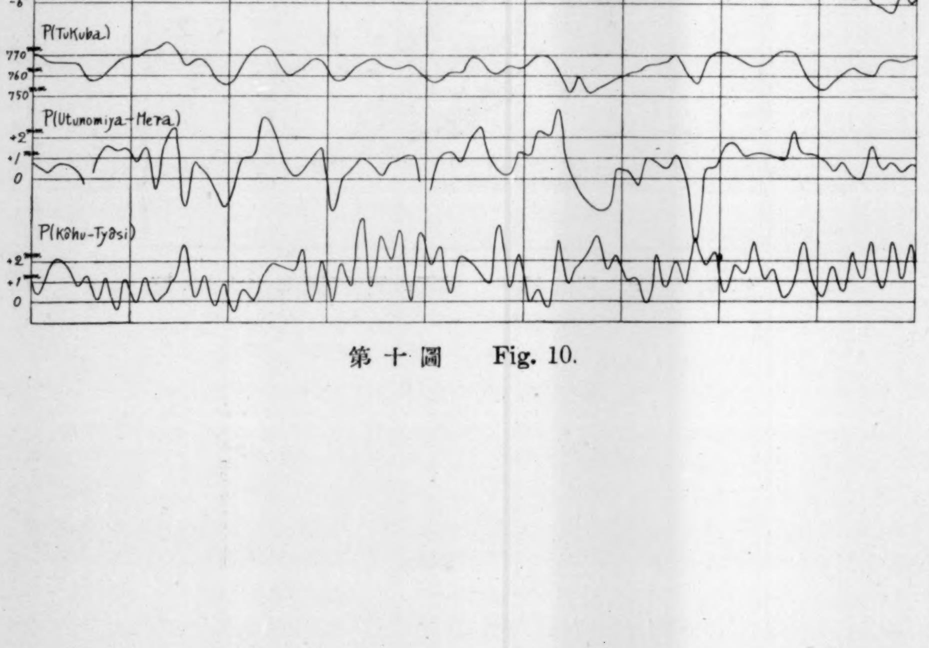

第十圖 Fig. 10.

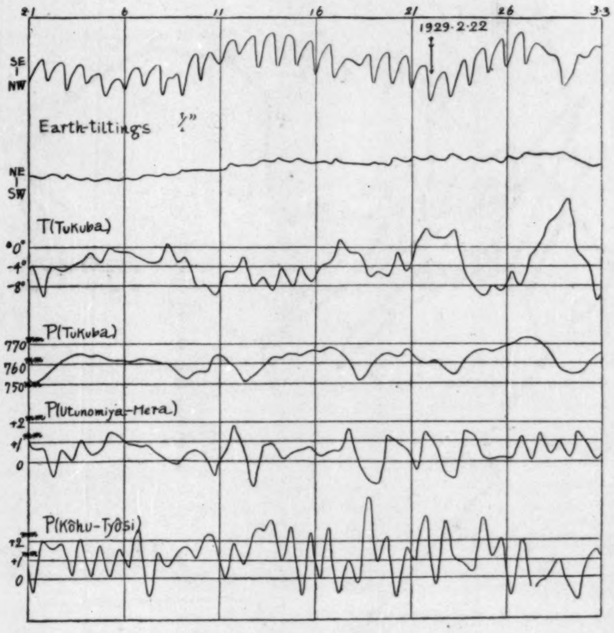

第十一圖 Fig. 11.

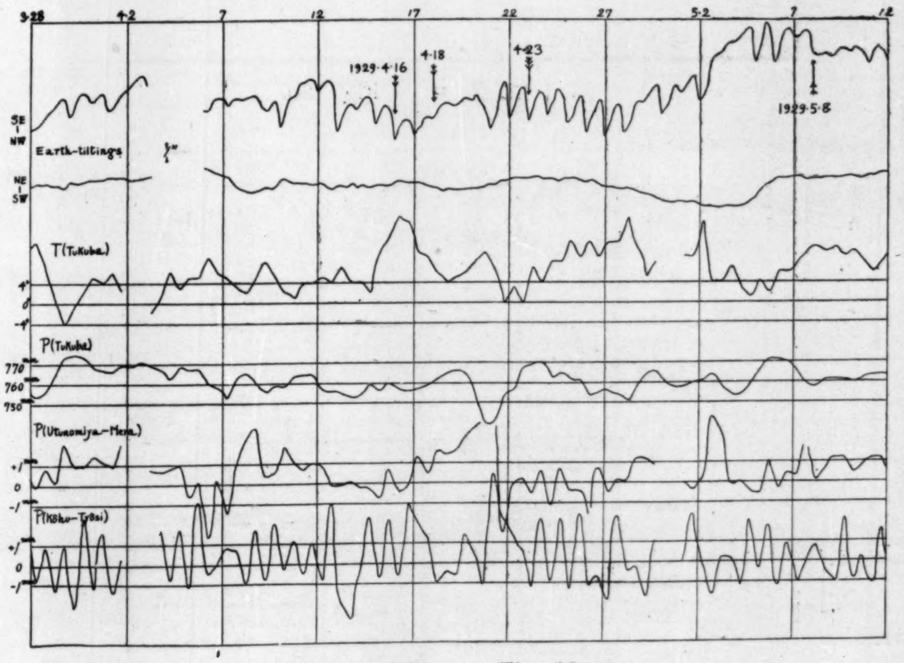

第十二圖イ Fig. 12a.

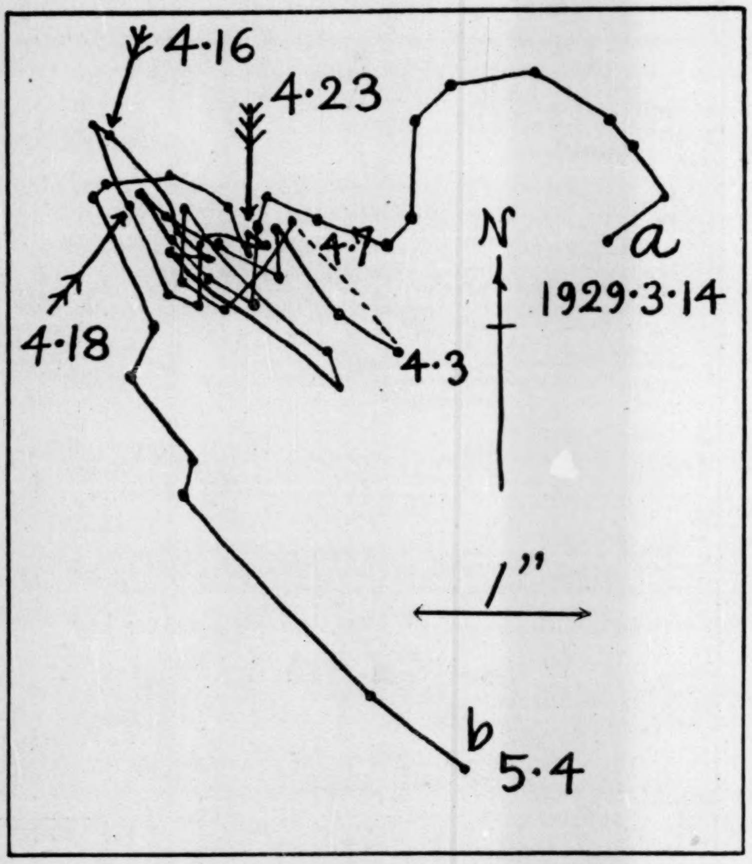

第十二圖 ロ Fig. 12b.

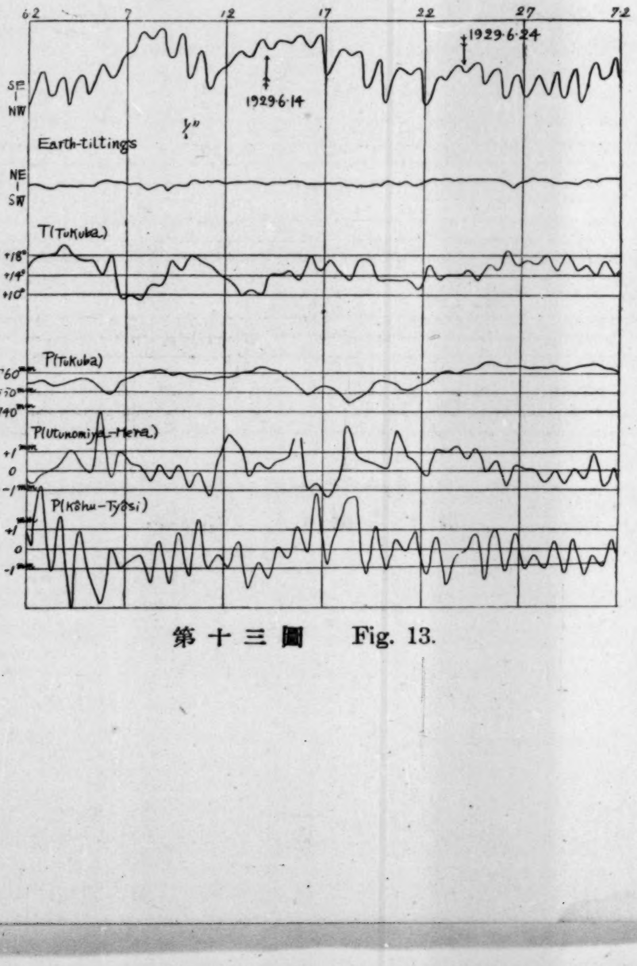

第十三圖 Fig. 13.

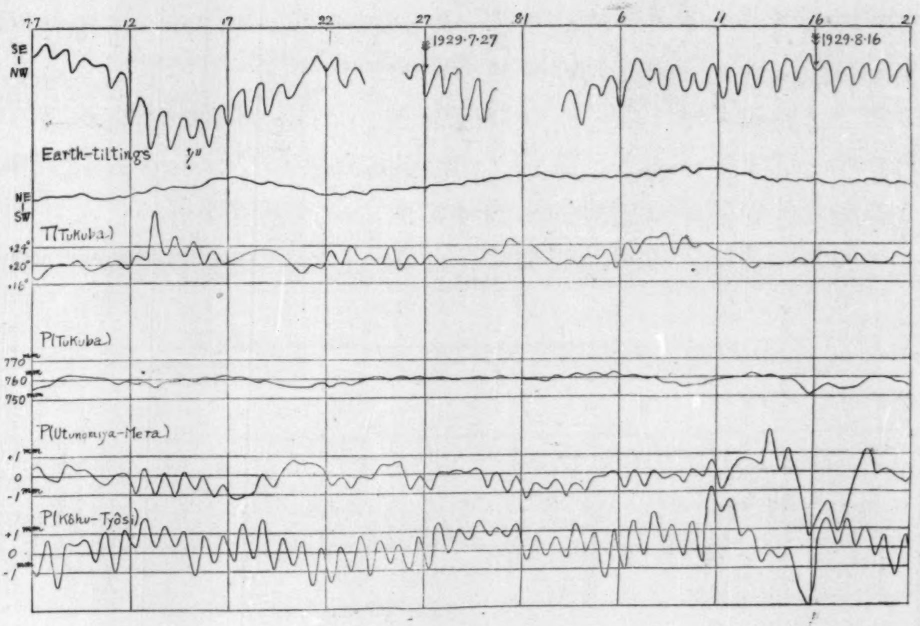

第十四圖 Fig. 14.

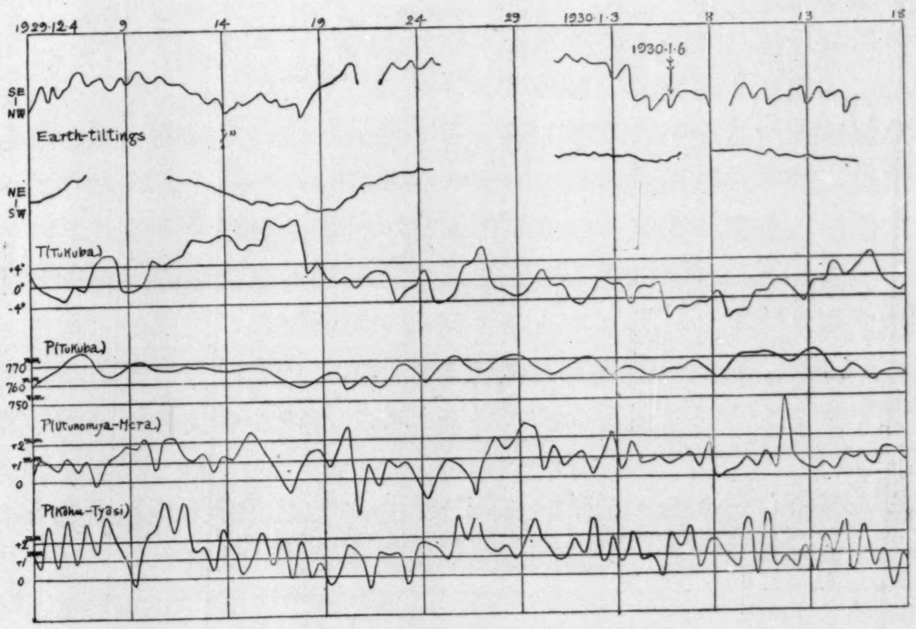

第十五圖 Fig. 15.

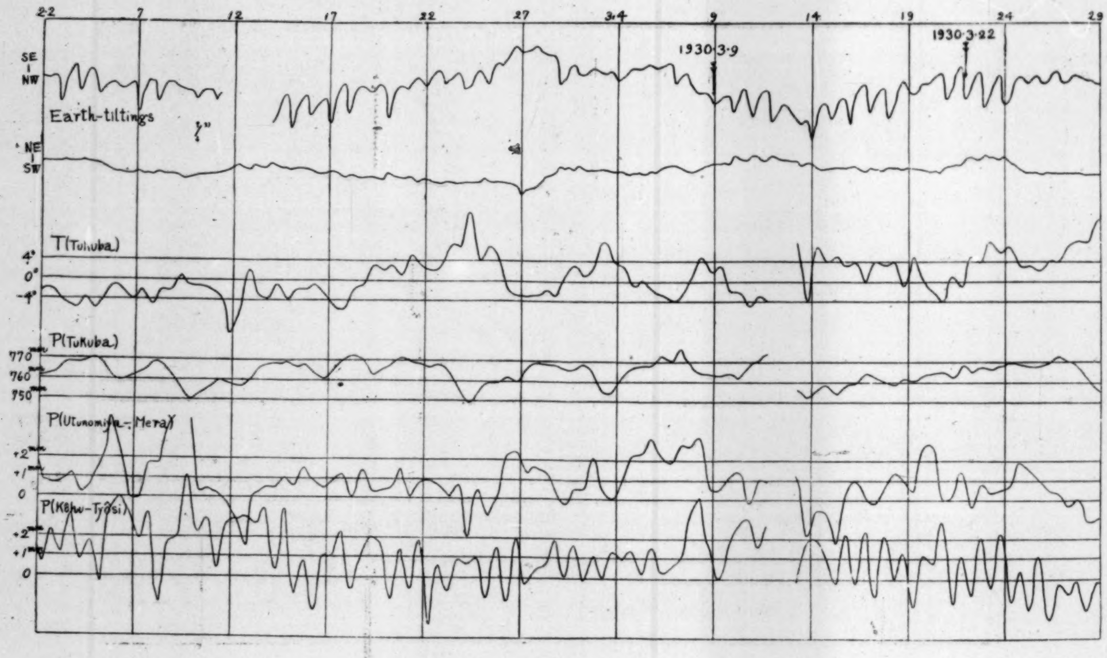

第十六圖 Fig. 16.

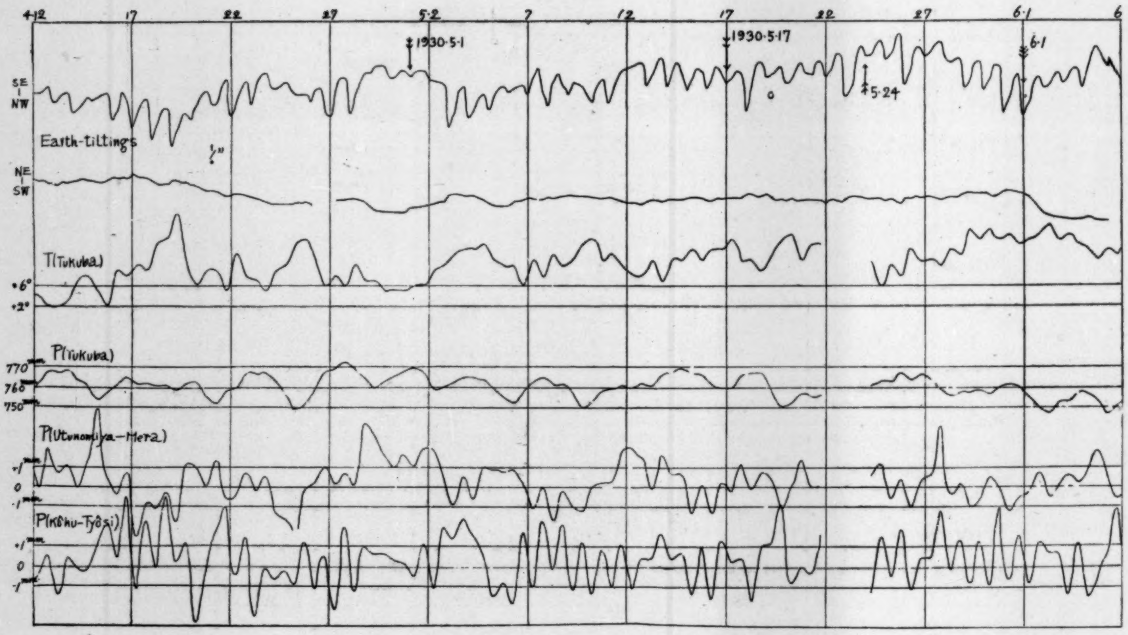

第十七圖 Fig. 17.

次に傾斜變化の日變化は山の斜面に沿うた西北東南の方向の傾斜にだけ表はれて居りまして、朝の六時頃一番東南に行きそれから急に西北に傾いて、十二時頃に一番西北に傾きそれからはゆつくりと東南に傾いて行つて翌日の朝の六時頃に一番東南に傾くと云ふ事を繰返してるのです。西北に傾く時に二つ三つの段が附く事がよくありますが、それは殊に十一月から一月頃が著しい。次に日變化の振幅が季節でどう變るかを見る爲に一週間毎の最大振幅を取つて見たのが第十八圖にでて居ります

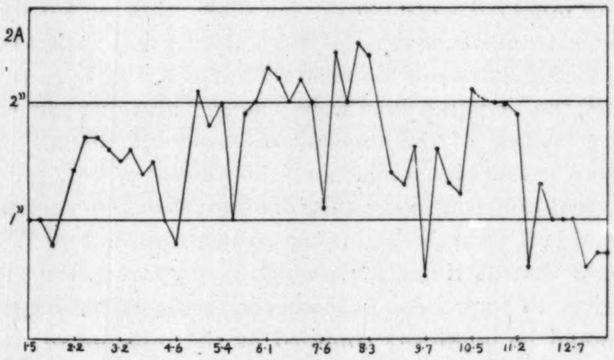

第十八圖 Fig. 18.

が、此れによると夏期は冬期の二倍半程大きくなつて居ります。此等の日變化は勿論日照に依るのでありまして晴天によく現はれ曇天には少いのですが、氣溫より地中溫度に竝行してる現象の様であります。

最後に地震が傾斜嵐の際に發生すると云ふ事は大變面白い事と思ひますが、此れは大きな範圍の氣象狀態の變化の爲の氣溫變化が傾斜變化を起すと共に此の氣象狀態の變化が副原因となつて地震が發生して居るので、丁度傾斜嵐の際に地震が發生する事となるのかも知れませんが、其の中にも地震の原因に直接關係する部もある事と思ひますが遺憾ながら今の所では明瞭に區別する事が出來ません。尙此の様に著しく氣象狀態が地震の副原因に成るものとすると其の方面の研究を充分する事は大切な事と思ひます。

終りに臨み絕えず御指導下さつた石本敎授に深く感謝致します。尙色々御厄介に成つた高橋助敎授及び高山筑波觀測所所長以下觀測員方に厚く感謝します。

14. *On Earth-tiltings observed at Mt. Tukuba.*

By Win INOUYE and Tomonori SUGIYAMA,

Earthquake Research Institute.

A pair of all-silica tiltmeters devised by Professor M. Ishimoto was installed in a room of uniform temperature at the branch station of the Earthquake Research Institute, the station being situated about half-way up Mt. Tukuba. With these instruments, two components of the earth-tiltings were observed continuously since the 23rd of December, 1927. At first, the instruments were so adjusted as to give a deflection of 2 cm. on the photographic record for each second of tilting, but since the 20th of June, 1928, the amplifications were changed into one-half that of the original size because of the constant occurrence of tiltings much larger than had been anticipated for such a rigid granitic mountain block.

The present note contains results of observations continued for about two years and half since the beginning to June 10th, this year. It should be mentioned that at times, for several days running, the photographs would receive no impression whatsoever, while at others the records obtained would be hopelessly confused by the presence of short period fluctuations of the earth-tiltings, so that we have worked out their general features by smoothing out the minute irregularities. This was done, first by taking the daily means, and secondly, by taking the means of three consecutive values, each of which is the daily mean of every third day. The two component earth-tiltings thus smoothed out are shown in Fig. 1. The air temperature at Mt. Tukuba smoothed out by the same process is shown in the same figure for the sake of comparison. Taking the resultant of the two component earth-tiltings, the vector diagram was obtained as illustrated in Fig. 2. As will be seen from the figure, the earth-tiltings exhibit a secular variation disturbed several times by stormy perturbations. As seen from Fig. 1 the secular variation is composed of the NE ward tilting amounting 17 second and the seasonal fluctuations. It may be mentioned that according to the investigation into the results of the new and old measurements of the levelling net in the Kwantô district by Messrs. Katuhiko Muto and Keiryo Atumi of the Land Survey Department of the Army, the region about Mt. Tukuba has tilted NE ward during the period. Next, the stormy perturbations of the tilting are more or less similar to the variation of temperature.

We next tried to find some possible relation between the earth-tiltings and the earthquakes that originated in the vicinity. For this purpose, we selected 27 moderate earthquakes that were reported by the Central Meteorological Observatory as having originated within a distance of about 180 km. It was found that the earthquakes generally occurred when the secular change of earth-tiltings had been undergoing irregular fluctuations of comparatively short period. We may further remark that the earthquakes had a tendency to occur when the sense of the

earth-tiltings had been changing, moreover, the earthquakes of oceanic origin occurred at the beginning and the middle part of the tilt-storms and the tilt-storms ended almost simultaneously with the occurrence of the earthquakes of inland origin.

Next, the daily mean of earth-tiltings before and after these earthquakes was compared with the variation of the air temperature, the barometric pressure at Mt. Tukuba, and the gradient of the barometric pressure in Kwantô district. In general, the tiltings have more or less intimate relation with the air temperature. In several cases, the preseismic earth-tiltings independent on the variations of the air temperature had begun two or three weeks or more before and ended almost simultaneously with the occurrence of the earthquakes. (Figs. 5, 6, 8, 12, 13, 14, 15.)

At last, it may be imagined that the variations of the meteorological condition of rather large extent may cause the tilt storms on the one hand, and act as the triggar or secondary cause of the earthquakes on the other, but we may think that during the tilt-storms there are certain characteristic earth-tiltings due to the instability of the earth's crust prior to an earthquake outbreak as a result of operation of the seismogenic forces in the particular region.

15. 大地震と太陽黑點との關係に就て

地震研究所　高　山　威　雄
地震學室教　鈴　木　武　夫

(昭和五年二月十八日發表――昭和五年六月二十日受理)

太陽黑點の消長が氣象的現象に重大なる影響を及ぼすことは、從來の多くの研究により明らかにされつつある。地震も地殼內に起る地球物理的現象である以上太陽黑點と何等かの關係がありはしないかと思はれる。この問題に就ては著者の知る範圍內では、我が國に於ては殆ど論じられなかつた樣に思ふ。外國に於ては A. Poëy[1] がメキシコ及びアンチル地方に起りたる地震に就て、地震が黑點の極大極小の頃に同じ程度に多く起ることを見出して居る。著者は日本に起つた大地震と太陽黑點との關係の統計的調査を試みた。又地震の頻度の時間的分布についても調べて見た。

I. 大地震と太陽黑點との關係

ここに取り扱つた大地震は、著者の一人(高山)が作成した地震の表(印刷未了)から採つたもので破壞的大地震のみを選んだ。卽ち表中の◎(大震被害甚大)及び◎(大震被害あり)なる記號にて表はされたるものを選んだもので、此の調査に必要な部分だけを Fig. 1 に表はした。太陽黑點としては、每年の「ウォルフ」黑點數を用ひた。「ウォルフ」黑點數の知れているのは 1749 年(以下年代は西曆を以つて表はす)以後で、それ以前は理科年表に太陽黑點の極大及び極小の年代が出ているのでそれを用ひた。又これらの大地震は火山の爆發に伴つて起つた地震(溫泉岳爆發及び櫻島爆發の際の地震)を除いたもので、全部が所謂構造性地震(tectonic earthquake)と考へ得られるものばかりである。かくして或る

1) A. Poëy, "Rapports entre les taches solaires, les tremblements de terre aux Antilles et au Mexique et les éruptions volcaniques sur tout le globe," *C. R.*, 78 (Paris 1874), 51-55.

期間に於て黒點極大の年を中心として前後1年以内の間に起りたる地震回數を算へ、同様に黒點極小の年を中心として前後1年以内に起りたる地震回數を算へる。殘りの場合即ち黒點の極大極小の中間に於て起りたる地震回數を算へる。この様にすれば、極大及び極小の近傍の3ヶ年を取ることとなる。例へば1796年より1886年迄(91年間)では黒點の極大の數が8個、極小の數が8個ある。故に $8\times3=24$ 年が夫々極大及び極小の近くの年數を表はし、殘りの $91-48=43$ 年は極大及び極小の中間の年數を表はす。この間に起つた地震回數を算へ、それを或る共通の年數（例へば30年）のものに引き直したのである。而る後に地震回數に就き%を求めた。この%が太陽黒點の消長と地震頻度即ち地震活動との關係を數量的に示すものと考へ得られるであらう。次ぎに同様に極大及び極小の年を中心として前後2年以内に起りたる地震回數及びそれ以外の年に起りたる地震回數を算へ、それをある共通の年數のものに引き直して%を求めた。此の場合は極大及び極小の近傍の5ヶ年を取ることとなる。例へば上と同じ期間に於ては、$8\times5=40$ 年が夫々極大及び極小の近くの年數を表はすが、この期間で重なる年即ち二重に算へる年が合計6年あるからそれを3年づつ両方から減

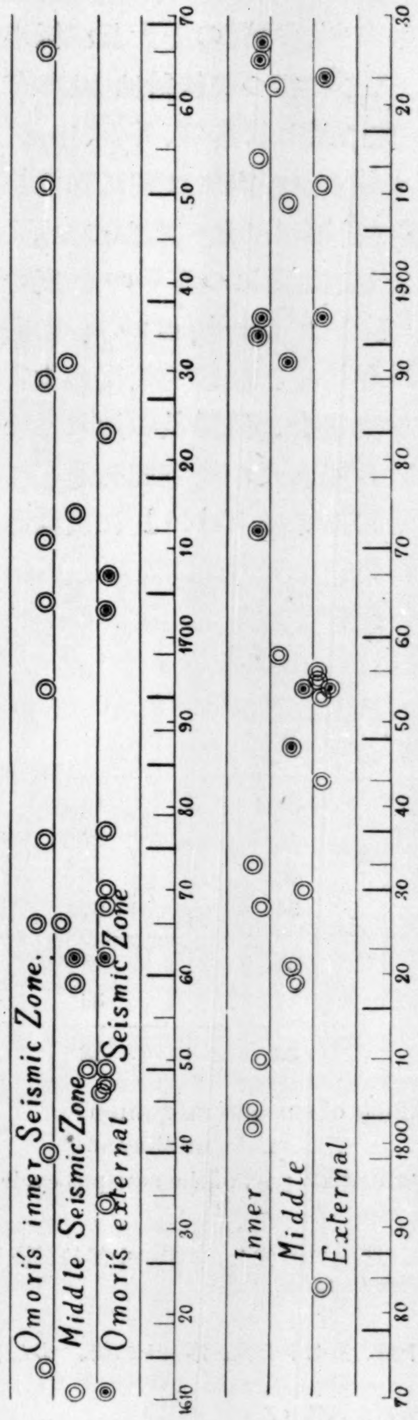

Fig. 1. Time and space distribution of destructive earthquakes in Japan (Formosa excluded)
◉…most destructive. ◎…destructive. | …year of sunspot max. | …year of sunspot min.

じて、極大及び極小の近くの年數として、37年を、極大及び極小の中間の年數として17年を得る。上の二つの場合の％の平均を以つて眞に近い％と見做したのである。

さて大地震の記錄は660年頃から知れてゐるが、黑點の極大及び極小の知れているのは1610年からであるから、ここに行つた統計は1608年から1925年までの318年間のものである。先づ最初に內側、外側、中部[2]の地震帶の區別をつけずに全國に就き調べて見た。臺灣には別に獨立した臺灣地震帶[3]が存在するから、臺灣の地震は計算には加へなかつた。

(1) 全國に就ての統計――別に全國に起つた地震につきその頻度の時間的分布の圖 (Fig. 3) を作つて見ると、それは quasi-periodic の變化を呈するが、この圖から1608年から1925年迄を、比較的頻度の大なる期間及び小なる期間について四期間に分けた場合、黑點數の知れている 1749 年以後とそれ以前との二期間に分けた場合及び全期間を通じての場合と種々の場合に就き統計を取つた。その結果は Table I に表はされた如くなる。

Table I.

Age	Interval in years	A	B	C
1608–1700	93	47%	34%	19%
1701–1795	95	29	44	27
1796–1886	91	32	40	28
1887–1925	39	14	34	52
1608–1747	140	43	34	23
1748–1925	178	25	42	33
1608–1925	318	33	39	28

A… Percentage of earthquake frequency in the vicinity of sunspot maximum.
B… ,, ,, ,, ,, ,, ,, ,, ,, ,, minimum.
C… ,, ,, ,, ,, ,, ,, intermediate part of the sunspot cycle.

2) 內側と外側の中間の本州內陸に存在する地震帶を一括して便宜上ここでは中部地震帶と名づけた。これらの地震帶に就ては大森、今村兩博士の御調査がある。
大森房吉　震災豫防調査會報告　第六十八號 (乙)
今村明恒　震災豫防調査會報告　第五十三號、第七十號、第七十七號、第九十二號、第九十五號

3) 大森房吉　震災豫防調査會報告　第五十四號、第八十八號 (乙)

表に於て A は黒點極大の近くに地震の起る%を、B は黒點極小の近くに地震の起る%を、C は黒點の極大極小の中間に地震の起る%を表はす。四期間に分けた場合では、第一、の期間では最大の%は黒點極大の近くにあり、第二、第三の期間では極小の近くに移る。第四の期間では極大極小の中間の方に移つている。尤も第四の期間は統計年數が短かく、從つて%の數値も左程信用の置けるものではない。二期間に分けた場合でも同じ樣な傾向が見へる。卽ち黒點との關係は何時も同一に規則正しくはなつていない。時とともに變つている。又全期間の場合では、極大極小の方は%は殆ど等しく、中間の方はこれに較べて小しく小さき値を示す。推測を許すならば、ある年代では黒點極大の近くに地震が多く起り、次の年代では逆に黒點極小の近くに多く起り、その次の年代には極大極小の中間に多く起ると云ふが如き輪廻的の變化をなすとも言はれるかも知れないが、假りにその樣なことが存在するとしても 300 年位の統計では決して斷言出來ない。第一表だけの結果からは、太陽黒點と地震とは全國的に見る時は著しい關係は存在しないと云ふ方が寧ろ至當であると思ふ。次に各地震帶別に調べて見た。

(2) 各地震帶に就ての統計——內側、外側、中部の各地震帶について別々に統計した結果は次の如くなる。Table II, III, IV は夫々內側、中部、外側の統計の結果を表はす。

Table II.

Age	Interval in years	A	B	C
1608-1700	93	82%	18%	0%
1701-1795	95	49	45	6
1796-1886	91	54	35	11
1887-1925	39	28	28	44
1608-1747	140	72	24	4
1748-1925	178	42	38	20
1608-1925	318	54	32	14

Table III.

Age	Interval in years	A	B	C
1608–1700	93	54%	39%	7 %
1701–1795	95	0	14	86
1796–1886	91	41	17	42
1887–1925	39	6	36	58
1608–1747	140	38	35	27
1748–1925	178	28	25	47
1608–1925	318	32	29	39

Table IV.

Age	Interval in years	A	B	C
1608–1700	93	22%	42%	36%
1701–1795	95	23	59	18
1796–1886	91	0	68	32
1887–1925	39	0	41	59
1608–1747	140	25	43	32
1748–1925	178	0	64	36
1608–1925	318	13	53	34

内側、中部、外側の地震帯なるものに判然たる境界があるわけではない、從つていづれの地震帶に屬せしむべきか決定に困難な地震も多少はあるが、その爲めに結論を誤る樣なことはないと信ずる。

内側地震帶 (Table II) に就て考ふれば、全期間の統計では A が最大で、二期間に分けた場合では何れの期間に於ても A が最大で、更に四期

間に分けた場合では、最大の%はA, A, A, Cの順序である。四期間に分けた場合は各期間の年數が短かく、又地震回數も少いから（特に最後の期間の1887–1925年はそうである）A, B, C 等の%の數値も fluctuation が大きくなり、從つてそれらの數値の持つ物理的の意味も薄いわけである。二期間に分けた場合の方が、それらの數値の持つ物理的の意味も大なりと考へることが出來るから、大勢がら察すればAが常に最大なりと言つて差支へないであらう。換言すれば內側地震帶では黒點極大の頃により多く地震が起ると云ふことが出來る。Table II から年代を横軸に、A B C 等の値を縱軸にとつて圖に表はしたのが、Fig. 2 の (a) である。

中部地震帶 (Table III) に就て考ふれば、全期間の統計では A, B 共に殆ど等しく 30% で、二期間に分けた場合では、最初の期間では A が最大で次の期間では C が最大となつている。又四期間に分けた場合では最大の%は A, C, C, C の順序になつている。卽ち或る時代には黒點極大の近くに地震が多く起り、他の時代には極大極小の中間の頃に多く地震が起ると云ふ狀態で、常に規則正しさが保たれていない。故に中部地震帶に起る地震と黒點との間には相關はないと云ふことになる。Table III から年代を横軸に、A B C 等の數値を縱軸にとつて圖に表はしたのが Fig. 2 の (b) である。

外測地震帶 (Table IV) に就て考ふれば、これは內側地震帶に就ての場合と同樣の考察によりて、外側ではいつも黒點極小の近傍に地震が多く起るといふ結果になる。前と同樣に圖に表はしたのが、Fig. 2 の (c) である。

(1) に於て全國に就き統計をとつた際に黒點の消長と何等著しい關係を認める事が出來なかつたのは、實は見掛けの上のことで各地震帶に分けて考へることによつて黒點と地震活動との間の關係を知ることが出來たのである。Table I, II, III の何れに於ても表はれておることであるが、C 卽ち極大極小の中間に地震の起る%が 1700 年頃から徐々に增加している。これも 300 年間位の統計ではどうなるか全く知ることが出來ないが、これはどの地震帶でも略ぼ共通に表はれていることであるから內側と外側とにつき上に得られた結果には大した影響はない。內側に於ては黒點極大の時に地震が多く起り、外側では極小の時に多く起るとい

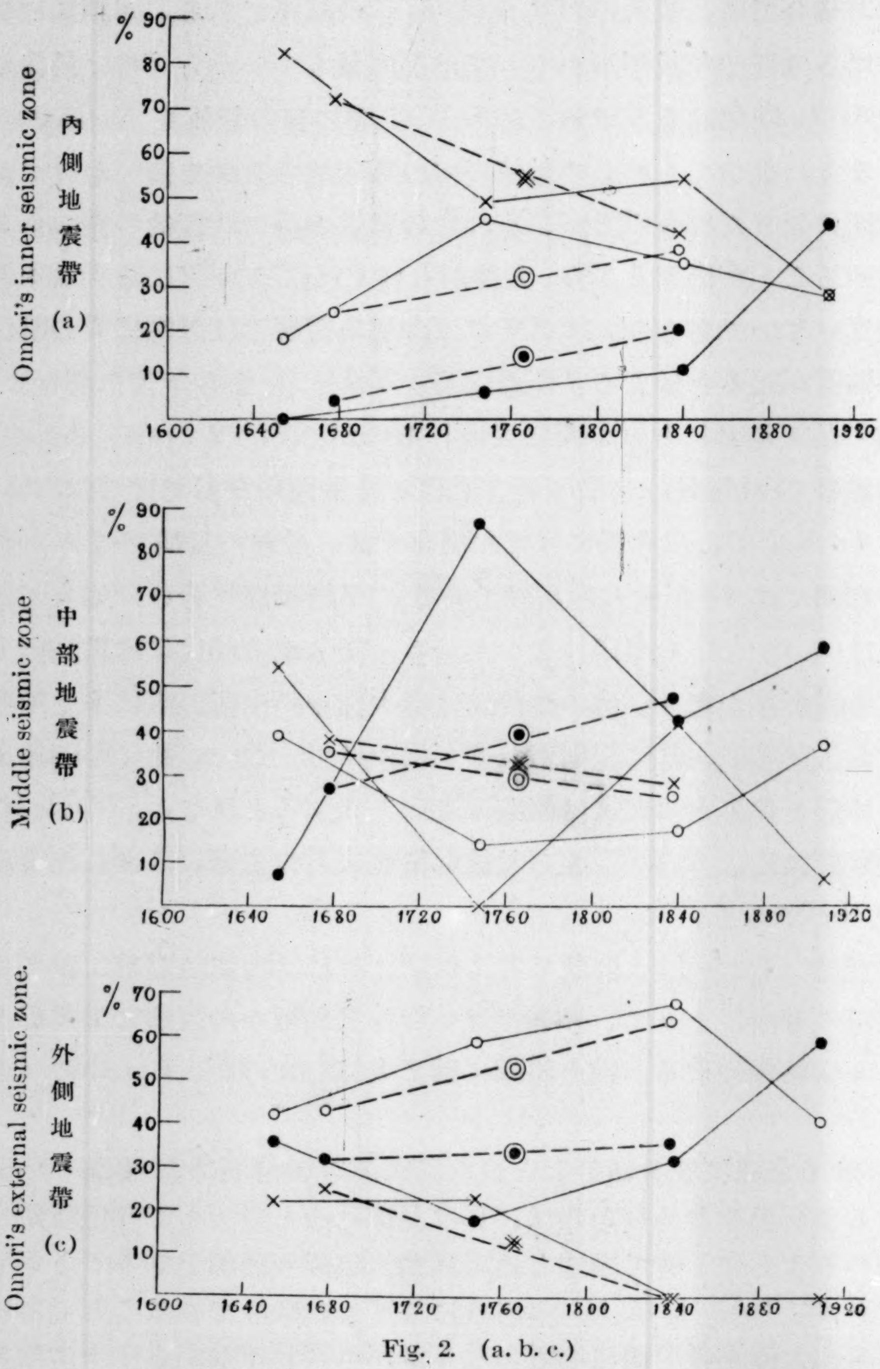

Fig. 2. (a. b. c.)

× shows A. 太陽黑點極大の近傍に地震のおこる百分率 　 復號：全期間の場合

○ 〃 B. 太陽黑點極小の近傍に地震のおこる百分率 　 實線：四期間に分けた場合

● 〃 C. 太陽黑點極大と極小との中間に地震のおこる百分率 　 點線：二期間に分けた場合

The double symbols express the % in the whole period.

The full line expresses the % when the whole interval is divided into 4.

The broken line expresses the % when the whole interval is divided into 2.

ふ結果は、黒點極大の時には高氣壓帶が高緯度に移動し極小の時には低緯度に移動するといふ事實との間の何等かの關係を暗示するのではないかと思はれる。併しこれは唯注意するに留めておく。

II. 大地震の時間的分布

大地震の時間的分布に於て週期とも稱すべきものが存在するや否やの問題に就ては、夙に大森博士[4)]の研究せられた所で、同博士は六世紀頃からの我が國に起りたる大地震の時分布より200年程の週期の存在するらしきことを認められ、又江戸の地震回數につきて平均 34 年の週期が存在する樣であると述べられておる。著者はここに用ひたる地震の表から、大地震に就き頻度の時間的分布を調べて見た。time-interval の單位を20年、23年、25年等と採り、又1570年以後は材料がそれ以前よりも增加しているので、間隔の單位を 10 年に採つたのも調べて見た。地震回數が少ない故に內側、中部、外側の地震帶に分けずに全國につき地震回數を算へた。Fig. 3 は 60 年間毎の地震回數を表はしたのである。

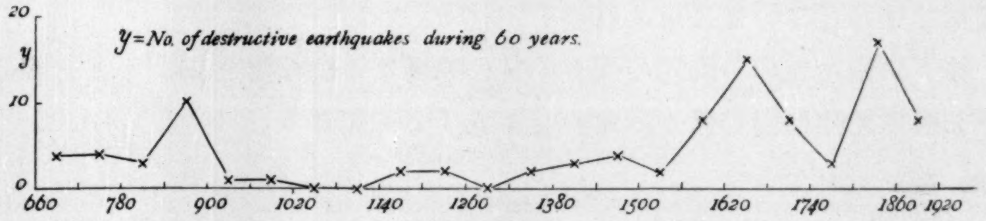

Fig. 3.

現在に近づくに從ひ地震回數が徐々に增加しておるのは、地震記錄が段々と豊富になつて來たと考へることが出來る。この樣な圖から cycle 又は見掛けの週期とも云ふべきもの卽ち頻度の極大から次の極大まで、及び極小から次の極小までの時間を測りそれの平均を以つて cycle としたのである。Table V に於て第三行及び第五行は cycle を表はし、第四行及び第六行に考へた time-interval とその cycle との比を記した。

---

4) 大森房吉　震災豫防調査會報告　第二十六號、第五十七號、第六十八號（乙）

Table V.

time interval taken	No. of Cycles	Cycle (max.-max.)	Cycle/time interval	Cycle (min.-min.)	Cycle/time interval
20 years	14	81 years	4·0	81 years	4·0
23	12	97	4·2	97	4·2
25	11, 12	103	4·1	97	3·9
40	7	154	3·8	149	3·7
46	5	184	4·0	202	4·4
50	5	200	4·0	190	3·8
60	4	240	4·0	240	4·0
10	9	34	3·4	33	3·3

寺田博士[5]によれば、各 interval に起る事柄が全く他に獨立の場合は、見掛けの週期として採つた間隔の約3倍餘のものが表はれ、連續的に起る事柄では4倍位のものが表はれると云ふことであるが、Table V から見れば殆どその通りになつている。週期又は cycle に就いてのこの判定法を以つてすれば、地震の頻度には週期又は cycle は上にとつた週期の範圍では殆どない様に思はれる。[6]

終りに臨み此等の問題の調査中常に懇篤なる御指導と御教示とを賜はりし藤原先生に對し深く感謝の意を表する次第なり。

(附　記)

週期又は cycle として得らたものが、全く偶然的のものであるか或いは意味あるものであるかを見る一方法として寺田博士は次の様なことを御注意せられた。cycle として得られた各の値を n とし、それの平均を ν とし、これが見掛けの週期に近い時に、若し cycle の各の値 n が ν の近くに normal distribution をなすならば、$\overline{|n-\nu/\nu|^2}=1/\nu$ なる關係式が成立する故に、$\overline{|n-\nu/\nu|^2}$ (obs.) と $1/\nu$ (cal.) とが大體一致する場合は、全く偶然的のものであり、然らざれば、或る物理的の意味あるものと考へ得られるであらうと云ふことである。これの計算の結果は次の Table VI の通りである。

5)　寺田寅彦　東京數學物理學會記事　8 (1916), 492.

6)　附記參照

Table VI.

Cycle (max.-max.)	$\overline{\|n-\nu\|/\nu^2}$ (bos.)	$1/\nu$ (cal.)	Cycle (min.-min.)	$\overline{\|n-\nu\|/\nu^2}$ (obs.)	$1/\nu$ (cal.)
76	0·35	0·01	76	0·15	0·01
97	0·3	0·01	97	0·11	0·01
94	0·2	0·01	90	0·1	0·01
154	0·22	0·006	149	0·28	0·007
184	0·17	0·005	202	0·14	0·005
200	0·15	0·005	190	0·12	0·005
240	0·07	0·004	240	0·008	0·004
34	0·13	0·03	33	0·29	0·03

Table VI より知れる通り $\overline{|n-\nu|/\nu^2}$ は $1/\nu$ より著しく大である。即ち各の n は ν の近くに normal distribution をして居ない。現在の所 data の數が僅少で充分にこの判定法を實行出來ないのは遺憾である。

---

15. *On the Relation between the Sunspot Number and the Destructive Earthquakes in Japan.*

By Takeo TAKAYAMA,
Earthquake Research Institute,

and

Takeo SUZUKI,
Seismological Institute.

The present investigation is a statistical study on the relation between the sunspot activity and the destructive earthquakes in Japan (Formosa excluded) for 318 years from 1608 to 1925 (Fig. 1). The method of this investigation is that, the number of destructive earthquakes which occurred for three years containing the year of sunspot maximum or minimum and the same in the other years, have been counted and reduced to the frequency in an equal duration, which at last were represented by the percentage frequency. Similarly, we calculated the earthquake percentage for five years of sunspot maximum or minimum

The values of percentage in Table I–IV in the text are the mean value of these two cases. We took statistics, dividing the whole time interval into two or four and also the space into three zones i.e., Omori's inner (Japan Sea side) and external (Pacific side) seismic zones and the inland zone of earthquakes which is aggregate of several local seismic zones between above two. The result obtained is summarized as follows;

1. We can not find any remarkable relation when we take statistics over the whole Japanese area. (Table 1)

2. When, however, the three seismic zones are considered separately, there exist remarkable relations, that is, (i) in the inner seismic zone the earthquake occurs more frequently in the vicinity of the sunspot maximum (Fig. 2a), (ii) in the external seismic zone, on the contrary the earthquake occurs more frequently in the vicinity of the sunspot minimum (Fig. 2c), (iii) in the inland or middle seismic zone the relation is not remarkable (Fig. 2b). These facts suggest us some possible relation in connection with the shift of the zone of the atmospheric high pressure.

3. On the cyclicity of the destructive earthquakes in Japan for from 660 to 1925, the curves of fluctuation of the seismic frequency have been constructed by taking various time intervals as unit of time in which the frequency is counted.

Each curve showed the apparent cyclic nature with its own period, which is found to be 3 or 4 times as long as the assumed unit interval as shown in Table V. This clearly shows us that the apparent periodicity is not the real one but is subjected to the accidental phenomena completely investigated by Professor T. Terada.

In conclusion, the authors wish to express their most sincere thanks to Professor S. Fujiwhara for his kind guidance.

16.　伊豆東海岸に於ける水準測量成果報告

今春伊豆東海岸地方に多數の地震發生せしを以て陸地測量部に依頼して附圖に示す範圍に於て該地方の水準測量を行へり。其成果を大正十三年同部により計測されしものと比較せしに同圖に示すが如き結果を得たり。此計測の精度に就ては彙報第三號百六十七頁を參照せられたし。

此測量は地震が引續き發生せる際に行はれたるものなるが故に地震鎮靜後を俟つて今一回計測を行ふ豫定なり。

此機會を以て陸地測量部員が本所の爲め此困難なる事業に從事せられしことを感謝す。(昭和五年六月廿日所長)

---

16. Precise Levellings in the Province of Idu.

In the spring of this year, abundant numbers of earthquakes, though not severe, took place in the eastern part of the Province of Idu. The work of precise levellings which was entrusted to the Military Land Survey Department, was carried out along a route crossing the shaken district, while the earthquakes were still incessantly occurring.

The result of the comparison of the data with those carried out in 1924 is embodied in the synoptical map reproduced in the accompanying figure. The accuracy of the levelling is the same as that carried out in the Tango district (see *Bull. Earthq. Res. Inst.*, **3** (1927), p. 167). Another surveying after the subsidence of the disturbance is now being contemplated. (June 20, 1930. The Director.)

線 路 圖
(數字ハ水準點番號ヲ示ス)

Map of route.
(Figures show the numbers of bench marks.)

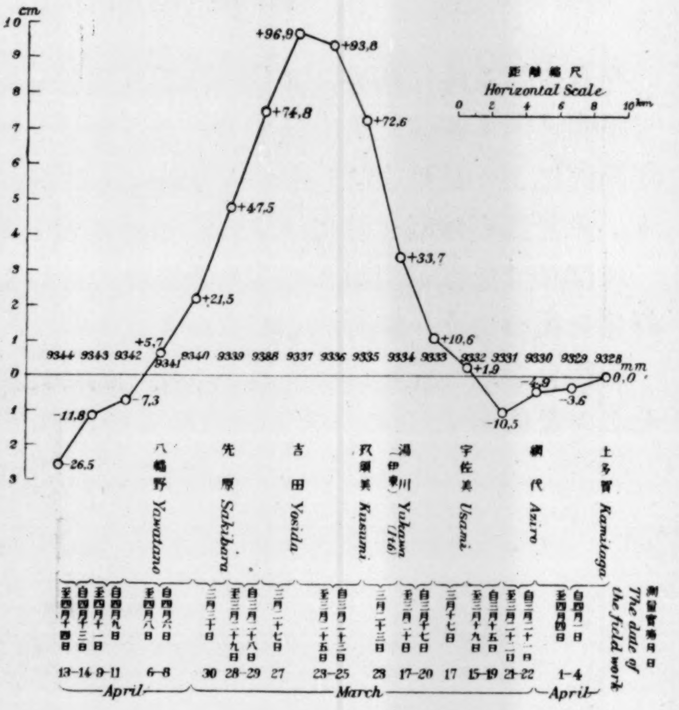

水 準 檢 測 斷 面 圖
(上多賀ヲ不動點ト假定ス)

Profile showing relative vertical displacement
(assuming No. 9328 to be stationary.)

伊豆東岸地方一等水準檢測圖

The Result of Precise Levellings on the East Coast of the Province of Idu.

――所　　報――

○　談話會記事

第五十回談話會　(昭和五年六月十七日)

1. 切り込みを有する板の撓曲に於ける內力の分布に就いて	藤原咲平 小穴純一 服部信一
1. 地震發生に關する氣壓の配置に就いて　(第一報)	石本巳四雄
1. 伊豆伊東附近の地質構造に就いて	津屋弘逵
1. 彈性波の分散性分散に就いて　(其一部)	妹澤克惟 西村源六郎
1. 筑波山に於ける傾斜變化觀側報告　(其二)	井上宇胤
1. 關東地震の再調査（イソスタシーの關係、地表の隆起と陷落の對比其他）	長岡半太郎 白井俊明
1. 丹後震災地三等三角測量の成果に就いて	鈴木三角科長
1. 土地の垂直運動と地形との關係	寺田寅彥 宮部直巳

第五十一回談話會　(昭和五年七月八日)

1. 內部の層源によるレーレー波の生成	妹澤克惟
1. 球面上に於けるラブ波の傳播とこれに關聯する一二の問題	妹澤克惟
1. 木造家屋の地震による破壞に關する力學的模型試驗	末廣恭二 佐藤小太郎
1. 關東震災地方の三等三角點の水平移動に就いて　(第一報)	坪井忠二 川嶋正治
1. 垂直振子地震計　(第一報)	高橋龍太郎
1. 地震傳播のホドグラフ的觀察	長岡半太郎 白井俊明

○　出張

昭和五年六月十四日地震事項調查の爲め靜岡縣下へ出張	高橋龍太郎
昭和五年七月十日地表傾斜觀測の爲め靜岡縣下へ出張	鹿熊金太郎
昭和五年七月十五日地震事項取調の爲め北海道へ出張	岸上冬彥
昭和五年七月十七日重力測定の爲め宮城、岩手の二縣下へ出張	坪井忠二
昭和五年七月三十一日地質調查の爲め靜岡縣下へ出張	津屋弘逵

昭和五年九月六日印刷
昭和五年九月九日發行

編纂兼發行者　東京帝國大學地震研究所

東京市深川區東大工町四十八番地
印刷者　星野　錫

東京市深川區東大工町四十八番地
印刷所　東京印刷株式會社

東京市神田區南神保町十六番地
賣捌所　岩波書店

Sold by

Iwanami Shoten,

Minamizinbôtyô, Kanda, Tôkyô.

Price of this copy: 0·63 Yen. (Postage exclusive.)

BULLETIN OF
THE EARTHQUAKE RESEARCH INSTITUTE
TOKYO IMPERIAL UNIVERSITY
Vol. VIII, Part 3. September, 1930.

Contents.

Papers and Reports.

Page

12. K. Sezawa and G. Nishimura, Dispersion of a Shock in Echoing- and Dispersive-Elastic Bodies. (in English) 321

13. C. Tsuboi, Investigation on the Deformation of the Earth's Crust in the Tango District connected with the Tango Earthquake of 1927. (Part 2.) (in English) 338

14. W. Inouye and T. Sugiyama, On Earth-tiltings observed at Mt. Tukuba. (in Japanese) 346

15. T. Takayama and T. Suzuki, On the Relation between the Sunspot Number and the Destructive Earthquakes in Japan. (in Japanese) 364

16. Precise Levellings in the Province of Idu. (in Japanese) 375

Institute Notes.

(For the papers written in Japanese or in occidental languages, the abstracts are given in occidental languages or in Japanese respectively.)

BULLETIN OF THE EARTHQUAKE RESEARCH INSTITUTE,
TOKYO IMPERIAL UNIVERSITY. Vol. VIII, Part 4. December, 1930.

東京帝國大學
地震研究所彙報

第八號　第四册

昭和五年十二月

目　次

論文及報告　　頁

17. 地殼の變形に因る熱の發生(英文)……寺田寅彦 377

18. 地殼の水平變動に就いて(英文)……坪井忠二 384

19. 地震と潮汐との關係(英文)……山口生知 393

20. 伊豆、伊東地方の地質構造に就いて(英文)……津屋弘逵 409

21. 伊東地震と地表傾斜變化の觀測(邦文)……石本巳四雄・高橋龍太郎 427

所　報

(The titles in occidental languages are given on the back cover.)

本彙報ハ年四回發行ス．　但シ第七號ニ限リ三冊トス．（第一號ヨリ第六號マデハ不定期ニ發行セリ.）

本彙報揭載ノ論文及ビ報告ノ內容ニ關シテハ著者ノミニ其責任アルモノトス．

本彙報ニ關スル照會通信ハ東京帝國大學地震研究所長へ宛テラレタシ．

The bulletin is published quarterly, excepting Vol. VII which consists of three parts. (Vols. I–VI were published at irregular intervals.)

The authors of the papers alone are responsible for the statements and opinions contained in their respective papers.

All communications relating to this bulletin should be addressed to the Director of the Earthquake Research Institute, Tokyo Imperial University.

17. *On the Heat Generated by the Deformation of the Earth Crust.*

By Torahiko TERADA,

Earthquake Research Institute.

(Read Jan. 21, 1930.—Received Sept. 20, 1930.)

Introduction.

Any inelastic deformation of the earth crust is accompanied with the generation of heat, which must be taken into account in any problem concerned with the thermal conditions of those parts of the crust subjected to sensible deformations. For example, it may be inquired whether the heat of some hot springs may not be supplied, at least partly, from such a source. Another example may be cited which is related with the hypothesis of continental drift; namely, the heat generated by the supposed slow displacement of the continental crust relative to the substratum may or may not affect the facility of such a motion.

Heat of Hot Spring.

The origins of the heat of hot springs have been repeatedly enumerated and discussed by generations of geologists. Besides the volcanic sources, the radioactive and chemical origins have been frequently dwelt upon. In the meanwhile, the possibility of a mechanical origin of heat seems to have be unduly neglected, though the present author was yet unable to make an exhaustive survey of the literatures.

In Saghalien, Honsyû, Formosa, Corea and also in China[1] we may point out numerous examples of a system of hot springs which are arranged along some conspicuous fault line, but could not be associated with any apparent volcanic activity of the region in question. In such cases, it is usual to attribute the heat of springs to the juvenile origin of the water. Even if such be the case, it will make an important difference whether the fault zone through which the juvenile water emerges is additionally heated by the mechanical cause or not.

1) Some of the papers consulted by the author are referred to at the end of this note.

For a rough estimation, we will assume that the deformation is limited to a region bounded by two parallel planes at a distance h from each other. One of the boundary plane, and the mass beyond it, moves parallel to the plane with a uniform velocity v relative to the other boundary plane. The region between the two planes is sheared uniformly on account of this relative motion of the boundary planes, behaving meanwhile as if it consisted of a viscous fluid with its coefficient of internal friction η. Let the motion continue for an interval of time τ. Then the total work done, which is mainly converted to heat, is

$$Q = \eta\left(\frac{v}{h}\right)^2 \tau \text{ erg/cm.}^3 = \eta\left(\frac{v}{h}\right)^2 \tau/4{\cdot}18\times 10^7 \text{ cal./cm.}^3$$

Assuming $\eta = 10^{13}$, for instance, with Wegener, we have

$$Q = \left(\frac{v}{h}\right)^2 \tau \times 2{\cdot}4\times 10^5 \text{ cal./cm.}^3$$

Suppose a fault takes place of which the total displacement $s=10$ m. is completed in $\tau=1$ minute. If the deformation is uniformly distributed within a zone of thickness $h=100$ m. and if it went on with the uniform velocity $v=s/\tau$, we obtain $Q=40$ cal. The temperature rise is $\theta=Q/\sigma$, where σ is the specific heat. If we assume $\sigma=1/4$, we have

$$\theta = 160°\text{C}.$$

which cannot be neglected in any case. If we assume $\eta=10^{12}$ instead, then $\theta=16°$C., which may still be of importance in the problem of hot springs at least.

The temporary excess of temperature in the zone of deformation will fail down due to the conduction into the external regions on both sides of the disturbed zone. For the present estimation, we will neglect the effect of the earth's surface, an effect which will decrease with the increasing depth, and consider the simplest one-dimensional case. Let the initial distribution of the temperature v be given by

$$v = f(x) \qquad \text{for } t = 0.$$

From the usual equation

$$\frac{dv}{dt} = k\frac{d^2v}{dx^2},$$

we have

$$v = \frac{1}{2\sqrt{\pi kt}} \int_{-\infty}^{\infty} f(x')\, e^{-\frac{(x-x')^2}{4kt}}\, dx'.$$

Assume

$$f(x) = T_0\, e^{-px^2},$$

as this may roughly represent the state immediately after the process of deformation as discussed above. Then, the subsequent course of matter goes on according to

$$v = \frac{T_0}{\sqrt{4kpt+1}}\, e^{-\frac{x^2}{4kpt+1}}.$$

If we put $p=1/b^2$, b will represent the effective *breadth* of the disturbed region and may roughly correspond to the thickness h above quoted. Take, for instance. $b=100$ m., i.e. $p=10^{-8}$ and $k=10^{-2}$ which is an approximate value for granite. Then the time, t_0, at which the temperature excess v at $x=0$, falls down to $1/\sqrt{2}$ will be given by

$$t_0 = \frac{1}{4kp} = 0{\cdot}25 \times 10^{10} \text{ sec.} \doteqdot 79 \text{ years,}$$

which is of an order of 100 years. If b be increased to 1000 m. t_0 will be accordingly increased to

$$t_0 = 7900 \text{ years.}$$

On the other hand, the heat must be estimated which is carried away by the spring water from the subterranean source to the earth's surface. Let V be the volume output of the spring in cm³. per sec., then the heat carried away is $cV\theta'$ cal./sec. where θ' is the temperature rise due to the heat source and c is the specific heat of the water, $\doteqdot 1$. The water, either juvenile or meteorological, will have acquired the temperature proper to the undisturbed region before entering the zone of disturbance and then be heated up to the excessive temperature of the hot zone on leaving that zone.

. Assuming, for example, $V=10^4$ or 10 litre/sec. and $\theta=80$°C., the heat loss is 8×10^5 cal./sec. For 1000 years, this will amount to a total loss of $2{\cdot}52\times 11^{16}$ cal.

The excess heat content of a rock with the specific heat of 1/4, heated 80° above the normal temperature, for a cube with its side of L km., is $2L^3\times10^5$ cal. Thence, if L be a little more than 2, the amount of the heat content will suffice to answer for the above calculated amount of the heat loss for 1000 years.

If the zone of deformation, as the heat source, has a thickness of $h=100$ m., while its areal extent is 10×10 km^2., its volume$=10$ km^2. is just of the same order of magnitude as above assumed. Thus, in short, a single spring of the assumed output will be able to exhaust the heat source of the above described extent and temperature during the lapse of time of an order of 1000 years. This is obiously a kind of lower limit of the time, as the rate of the heat loss decreases with the falling temperature.

An alternating way of estimating the heat produced by faulting is to regard the phenomenon as a simple slide along an ideal plane of contact with a definite coefficient of friction. If F be the force of friction per unit area, we may assume for the present purpose that F is of the same order of magnitude as the maximum breaking stress of rock materials. Put $F=s\times1000$ kg/cm. If the total slip is l m., the work done per unit area in thermal unit will amount to $sl\times2{\cdot}4\times10^3$ cal/cm. Taking $l=10$ m., for example, this is $2{\cdot}4\,s\times10^4$. If this heat be distributed uniformly within a prism of 100 m. height, with the unit area as its base, the heat content per unit volume will be $2{\cdot}4\ s$ cal., which will be equal to 40, i.e. the value estimated in the previous paragraph, if s be taken as 17. Ordinary compression tests in laboratory give s for usual hard rocks the values between 1 and 3. It is conceivable however, that the *effective* F in the present problem is much larger than the "strength," as the process of faulting is by no means that of a simple slipping, but involves the fracture of the adjoining zones.

The above estimations will show at least that the mechanical source of heat cannot be always put out of account in some problems concerning hot springs. It cannot be exactly said that any spring of importance might have derived its supply of heat through ages, solely out of the "mechanical fuel" as above discussed. It seems, however, quite probable that some springs might have undergone modifications in their thermal conditions by some processes as above considered.

There are many records of the cases in which the temperatures of springs were changed, temporarily or permanently, after destructive earthquakes. Rise as well as fall of the temperature are reported. It is, indeed, well known that the temperature of a hot spring is greatly

influenced by the change in its output, so that any change in the system of subterranean water circulation caused by the seismic crustal disturbances may affect the temperature of hot springs to a coniderable amount and thus completely eclipse the effect of the mechnical heat as above considered, even if the latter may be sensible. It seems, therefore, at first sight hopeless to discriminate the latter from the former. The situation will be, however, not so bad, if we could be furnished with an ample supply of data comprising the results of systematic observations regarding the temperature, output as well as the chemical constituents of water, for all the springs situated in the region where a conspicuous tectonic disturbance has been experienced. For the present, however, it will be scarcely worth while to develop here the feasible methods of analysis. What is urgently needed is an well-organised systematic observation, instead of a mass of fragmentary and temporary gleaning.

In passing it may also be suggested that the mechanical heat of the kind here considered could have played some rôle in the genetical process of petroleum.

Heat due to Continental Drift.

Consider a *sima* layer with the depth h, and suppose that its top-layer is moved with a uniform velocity v relative to the bottom layer which is assumed as fixed. The work done per unit time per unit volume is $\eta\,(v/h)^2$, where η is the coefficient of viscosity, as before. If $h=H\times 100$ km. and $v=V$ m/year and $\eta=10^{13}$, the heat produced is

$$Q \doteqdot \left(\frac{V}{H}\right)^2 \times 0{\cdot}24 \times 10^{-9} \text{ cal./cm}^3\text{. sec.}$$

On the other hand, the rate of heat production due to the radioactivity of plutonic rocks is, according to Holms,

$$Q' = 6{\cdot}4 \times 10^{-13} \text{ cal/cm}^3\text{. sec.}$$

Since H and V above defined are probably of the order of unity, the mechanical heat Q is safely negligible in comparison with the radioactive heat Q'. This holds even if $V=100$ and $H=1$.

In the case when a very thin layer is sheared with a sensible velocity, it may occur that the temperature is abnormally raised and

result in a considerable reduction of viscosity, in which case the drifting motion may be accelerated. As for an illustration take $V=10$ and $H=10^{-3}$, i.e. only 1 m. Then, $(V/H)^2=10^8$ and $Q\fallingdotseq 2{\cdot}4\times10^{-12}$, which decidedly exceeds Q'. As it is known that the plastic deformation of some material is frequently localized in a quite narrow zone of disturbance, for example "slip-plane", such an extreme case as above assumed may not be entirely excluded beyond the margin of possibility.

On the other hand, the mutual displacements of minor geotectonic units, i.e. "blocks", may involve the thermal process as above supposed. Slow gliding of two blocks along a common boundary zone may sometimes result in an accumulation of the mechanical heat and consequently to the acceleration of the motion, leading thus to a catastrophal acute disturbance. This idea, though crude enough, seems to harmonize with many observed facts concerning the relation between the chronic crustal motion and the occurrence of severe earthquakes.

參考文獻 (Literatures):

小川琢治, 地學雜誌, **15** (1903), 709; 韓山生, 同, **18** (1906), 257; 岩崎重三, 同, **19** (1907), 31; 比企忠, 同上, **23** (1911), 265; 小林儀一郎, 同, **26** (1914), 759; 河野密, 同, **27** (1915), 842; 大築洋之助, 同, **29** (1917), 8; 佐藤傳藏, 同, 同, 167; 山根新次, 同, **32** (1920), 301; 大江二郎, 同, **40** (1928), 555; 千谷好之助, 同, **40** (1928), 626, 698, **41** (1929), 46; 小川琢治, 地球, **2** (1924), 1; 石橋五郎, 同, 同, 91; 中村新太郎, 同, 同, 132; 藤田元春, 同, 同, 142; 石川成章, 同, 同, 152; 松原厚, 同, 同, 178; 三澤勝衞, 同, 同, 190; H. T. Chang, Proc. 3rd. Pan-Pacif. Sci. Congr., Vol. I, 812; etc.

---

17. 地殼の變形に因る熱の發生

地震研究所 寺 田 寅 彦

地殼の非彈性的變形が局部的に集中して起る時は其爲に發生する熱の爲に局部的の高溫を生じ得る。斷層の生ずる時の溫度上昇を概算して見ると、場合によつては、此れが溫泉の溫度等に影

響し得る程度のものとなる。故に温泉の熱源を論ずる際には、此點も考慮に加へる必要がある。

大陸移動説に於て考へらるゝやうな大陸と下層との間の相對運動の爲に、中間層に發生する熱は放射能性岩石の發する熱に比して小さいであらうと考へられる。併し陸塊相互の滑動の際に其境界層に發生する熱は必しもさうでない。此れは場合によつては其滑動を助長し急變を促がす効果があるかも知れない。

以上の如き熱源が從來余り注意されなかつたやうであるから、玆には唯極めて概略的な見積りをして、此方面の研究に注意を喚起したいと思つた迄である。

---

18. *A Note on the Analytical Treatments of the Horizontal Deformation of the Earth's Crust.*

By Chûji TSUBOI,

Earthquake Research Institute.

(Read Sept. 16, 1930.—Received Sept. 20, 1930.)

The horizontal deformation of the earth's crust which is going on in present days, whether chronic or acute, often has sufficiently large amount to be detected by means of precise triangulations. We have a number of such examples in this country, most of which were produced connected with earthquakes.[1] These unique data have been much discussed in this country from several points of view. It has been attempted by T. Terada, S. Fujiwhara, N. Miyabe and the writer to treat these data by means of analytical method.[2] From the observed horizontal displacements of the triangulation points in the district in question, they calculated the following quantities, viz. divergence, rotation and shear of the horizontal displacements and the directions and magnitudes of the axes of strain ellipses. They discussed the distributions of these quantities, compared them with those of other geophysical quantities, or interpreted them from geological point of view, and so on. The most fundamental assumption, implicitly taken as granted, underlying these investigations was that these calculated quantities are really exsisting ones but are not produced as a result of mere geometrical effect due to the accidental displacements to which the triangulation points were subjected. For the purpose of making these circumstances clear, we will reconsider for an example the process of calculation of the divergence

1) A. Imamura, *Pub. Earthq. Inv. Comm.*, 25 (1930).

2) S. Fujiwhara and T. Takayama, *Bull. Earthq. Res. Inst.*, 6 (1928), 149.
T. Terada and N. Miyabe, *ibid.*, 7 (1929), 223.
T. Terada and N. Miyabe, *Proc. Imp. Acad.*, 5 (1929), 322.
N. Miyabe, *Bull. Earthq. Res. Inst.*, 8 (1930), 45.
T. Terada and N. Miyabe, *Proc. Imp. Acad.*, 6 (1930), 49.
C. Tsuboi, *Bull. Earthq. Res. Inst.*, 8 (1930), 153.

of the horizontal displacement within a triangle with triangulation points at its vertices. The method of calculation initiated by T. Terada[3] was as follows. Let $o\ o$, x_2y_2, and x_3y_3 be the rectangular co-ordinates of the three triangulation points and u_1v_1, u_2v_2, and u_3v_3 be the respective components of the displacements σ_1, σ_2, σ_3 of the triangulation points in x and y directions. It is assumed that u and v of any point within the triangle is a linear function of x and y such that

$$u = u_1 + a_1x + b_1y,$$

$$v = v_1 + a_2x + b_2y.$$

Thus we have

$$\frac{\partial u}{\partial x} = a_1, \qquad \frac{\partial v}{\partial y} = b_2;$$

$$\text{div}\ \sigma = \frac{\partial u}{\partial x} + \frac{\partial v}{\partial y} = a_1 + b_2,$$

where

$$a_1 = \frac{u_2y_3 - u_3y_2 - u_1(y_3 - y_2)}{x_2y_3 - x_3y_2},$$

$$b_2 = -\frac{v_2x_3 - v_3x_2 - v_1(x_3 - x_2)}{x_2y_3 - x_3y_2}.$$

In this calculation, div σ naturally comes out to be constant throughout the triangle.

The method adopted by the writer[4] consists of, first, drawing contour lines of equal u and v over the region in question, and secondly calculating $\frac{\partial u}{\partial x}$ and $\frac{\partial v}{\partial y}$ for every point in the region and lastly taking the sum of $\frac{\partial u}{\partial x}$ and $\frac{\partial v}{\partial y}$ which is the divergence of horizontal displacement of that point.

It is clear that both methods involve the assumption that u and v within the triangle and whence the divergence are produced as a result of general deformation of the earth's crust, but are not produced by a merely accidental disturbances of the triangulation points. If the earth's crust underwent other kinds of deformation than is assumed in the

3) T. Terada and N. Miyabe, *Bull. Earthq. Res. Inst.*, **7** (1927), 223.

4) C. Tsuboi, *Bull. Earthq. Res. Inst.*, **8** (1930), 153.

above calculation, there will be no physical significances in them. Some of the remarkable examples of such cases will be shown in the following figure. In the first example, the real divergence of the horizontal displacement in the triangle is a large positive value

(1) (2) (3)

Fig. 1.

though the calculated divergence will be zero. In the second example the real divergence in the traiangle is practically zero though the calculated divergence will be of a large positive value. Still in the third example, the real divergence is a large negative value though the calculated divergence will be of a large positive value. In such cases, the calculated quantity has no physical significance being merely produced as a geometrical effect.

Though the assumptions made in the methods of the above mentioned authors seem to be plausible, yet it is of importance to make some check on the validity of these assumptions for developing any further discussion in this line.

Now we have an excellent case in which this crucial test is to be made. After the great Kwanto earthquake of 1923, the Military Land Survey Department[5] made revisions of triangulations of the first, second and third orders over the southern part of the Kwanto district where the damages caused by the earthquake were large. Still we have a standard rhombus base lines remeasured in the compound of the Tokyo Astronomical Observatory at Mitaka. They are a special set of base lines forming a rhombus which consists of two equilateral triangles. The successive changes of the lengths of the sides of the rhombus have been repeatedly measured. Then, if we can compare the divergence of Mitake region by four different sets of data, i.e. the results of the rhombus measurements and those of the triangulation of the first, second and third orders, we will get some informations regarding the validity of the assumptions made in the calculation of the divergence.

5) *Bull. Earthq. Inv. Comm.*, 11 (1930), 1.

The first order triangle, which contains in it Mitaka rhombus is composed of three points, Renkôzi, Kaminumabe and Tokumaru. The co-ordinates and the displacements of these points are given in table 1.

Table I.

	x	y	u	v
	m	m	m	m
Renkozi	0	0	−0·187	−1·438
Kaminumabe	18400	−4000	−0·053	−1·332
Tokumaru	17600	15600	−0·206	−0·793

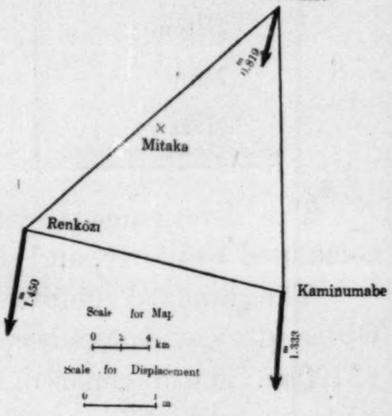

Fig. 2.

The divergence of horizontal displacements in this triangle was calculated after Terada's method. The value obtained was $3{\cdot}4\times10^{-5}$.

The second order triangle which contains in it Mitaka rhombus is composed of three points, Hitomi, Mure and Hosoyama. The co-ordinates and the displacements of these points are given in table 2.

Table II.

	x	y	u	v
	m	m	m	m
Hitomi	0	0	+0·088	−0·851
Mure	7300	950	−0·128	−0·841
Hosoyama	1500	−6750	+0·035	−1·322

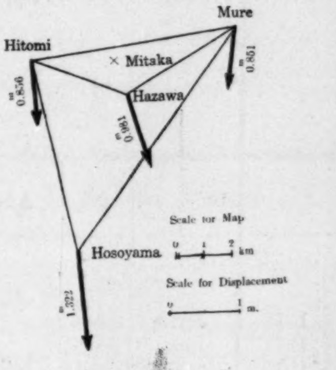

Fig. 3.

The divergence of horizontal displacements in this triangle was calculated similarly as in the case of the first order triangle. The value obtained was $3{\cdot}8\times10^{-5}$.

The smallest triangle which contains in it Mitaka rhombus is composed of Hitomi, Mure which are secondary points and Hazawa which is a tertiary triangulation point. The co-ordinates and the displacements of these points are given in table 3.

Table III.

	x	y	u	v
	m	m	m	m
Hitomi	0	0	+0·088	−0·851
Mure	7300	950	−0·128	−0·841
Hazawa	3400	−1300	+0·328	−0·925

The divergence of horizontal displacements in this triangle was calculated similarly, and the value obtained was $4{\cdot}5 \times 10^{-5}$.

The standard rhombus in the compound of the Tokyo Astronomical Observatory at Mitaka is composed of four base lines, each with the length of 100 m. The diagonals of this rhombus have the direction of EW and NS. The lengths of these sides have been measured fifteen times by the experts of the Military Land Survey Department under the supervision of the Imperial Japanese Geodetic Commission. The results obtained are shown in the following table.

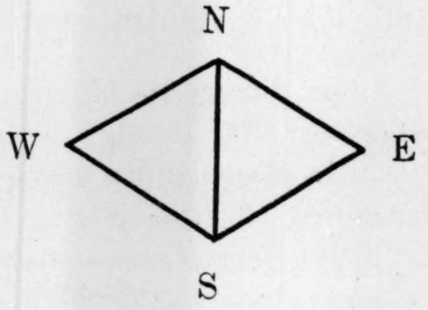

Fig. 4.

Table IV.

Date		NE	ΔNE	ES	ΔES	SW	ΔSW	WN	ΔWN	NS	ΔNS
		100 m +		100 m		100 m +		100 m +		100 m +	
		mm	mm	mm	mm	mm	mm	mm	mm	mm	mm
1916	June	+0·92		+0·26		+0·72		+0·78		+0.59	
1917	Feb.	+0·92	0	+0·25	−0·01	+0·69	−0·03	+0·78	0	+0·54	−0·05
1917	Oct.	+0·15	+0·23	+0·55	+0·30	+0·91	+0·22	+0·01	+0·23	+0·84	+0·30
1918	Feb.	+0·97	−0·18	+0·26	−0·29	+0·66	−0·25	+0·09	−0·82	+0·47	−0·37
1918	Oct.	+0·31	−0·66	+0·27	+0·01	+0·69	+0·03	+0·76	+0·67	+0·51	+0·04
1919	Nov.	+1·03	+0·72	+0·52	+0·25	+0·94	+0·25	+0·86	+0·10	+0·63	+0·12
1920	Nov.	+1·26	+0·23	+0·55	+0·03	+1·07	+0·07	+1·02	+0·16	+0·85	+0·22
1921	Nov.	+1·25	−0·01	+0·56	+0·01	+1·11	+0·04	+1·11	+0·09	+0·93	+0·08
1922	Nov.	+1·11	−0·14	+0·42	−0·14	+1·02	−0·09	+1·06	−0·05	+0·82	−0·11
1923	Sept.	+1·73	+0·62	+0·53	+0·11	+1·34	+0·32	+1·12	+0·06	+4·40	+3·54
1923	Oct.	+1·64	−0·09	+0·33	−0·20	+1·47	+0·13	+0·95	−0·17	+4·00	−0·40
1924	Jan.	+1·91	+0·27	+0·07	−0·26	+1·39	−0·08	+0·72	−0·23	+3·76	−0·24
1924	Aug.	+1·58	−0·33	−0·05	−0·12	+1·50	+0·11	+0·71	−0·01	+3·42	−0·34
1925	Dec.	+1·84	+0·26	+0·25	+0·30	+1·44	−0·06	+0·82	+0·11	+3·69	+0·27
1927	Dec.	+2·38	+0·54	+0·80	+0·55	+2·16	+0·72	+1·38	+0·56	+3·91	+0·29

By these data, we can calculate the increase of areas of triangles NWS and NSE both of which are equilateral. If we denote by S the area of a triangle whose sides are a, b and c, and if $s = \frac{1}{2}(a+b+c)$, we have

$$S = \sqrt{s(s-a)(s-b)(s-c)},$$

hence
$$\frac{dS}{S} = \frac{1}{2}\left\{\frac{ds}{s} + \frac{ds-da}{s-a} + \frac{ds-db}{s-b} + \frac{ds-dc}{s-c}\right\}.$$

If $a = b = c$ as in the present case,

$$da + db + dc = 2ds,$$

so that
$$\frac{dS}{S} = \frac{1}{2}\left\{\frac{2s-a}{s(s-a)}\right\}ds.$$

In the present case, $s = 150$ m and $a = 100$ m,

therefore
$$\frac{dS}{S} = \frac{ds}{75000},$$ ds being measured in mm.

In this way, we can calculate easily the increase of areas of the triangles NWS and NSE. The results are shown in the following table and figure.

Table V.

Date	Δ(NE+ES+NS)	div. (NES)		Δ(SW+WN+NS)	div. (SWN)	
			Integrated			Integrated
	mm			mm		
1916 June	−0·06	$-0·04\times10^{-5}$	$-0·04\times10^{-5}$	−0·08	$-0·05\times10^{-5}$	$-0·05\times10^{-5}$
1917 Feb.	+0·83	+0·55	+0·51	+0·75	+0·50	+0·45
1917 Oct.	−0·84	−0·56	−0·05	−1·54	−1·03	−0·58
1918 Feb.	−0·61	−0·41	−0·46	+0·73	+0·49	−0·09
1918 Oct.	+1·09	+0·73	+0·27	+0·47	+0·31	+0·22
1919 Nov.	+0·48	+0·32	+0·59	+0·51	+0·34	+0·56
1920 Nov.	+0·08	+0·05	+0·64	+0·21	+0·14	+0·70
1921 Nov.	−0·39	−0·26	+0·38	−0·25	−0·17	+0·53
1922 Nov.	+4·31	+2·87	+3·25	+3·96	+2·64	+3·17
1923 Sept.	−0·69	−0·46	+2·79	−0·44	−0·29	+2·88
1923 Oct.	−0·23	−0·15	+2·65	−0·55	−0·37	+2·51
1924 Jan.	−0·79	−0·53	+2·12	−0·24	−0·16	+2·35
1924 Aug.	+0·83	+0·55	+2·67	+0·32	+0·21	+2·56
1925 Dec.	+1·31	+0·87	+3·55	+1·50	+1·00	+3·56
1927 Dec.						

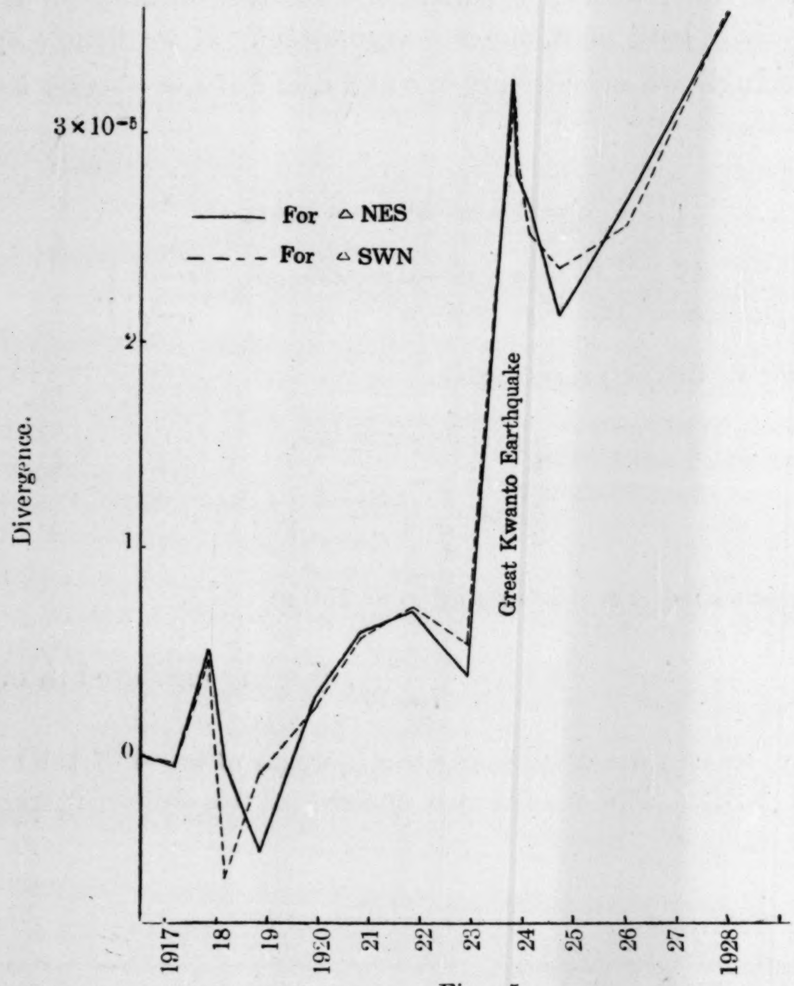

Fig. 5.

Two curves in Fig. 5 which represent the divergence of triangles NES and SWN respectively are alomost exactly similar in their forms. This seems to be a sufficient proof that the measurements of the variations in the lengths of the rhombus sides were precise enough and the deformation of the triangles were produced as the effect of the general deformation of the neighbouring earth's crust but not as the effect of the accidental displacements of one or some of the base stones. At the time of the great Kwanto earthquake of 1923, both triangles expanded in area and the divergences of the horizontal displacement in both triangles were,

$$2{\cdot}9\times10^{-5} \text{ for NES.}$$
$$2{\cdot}6\times10^{-5} \text{ for SWN.}$$

Now we have calculated the divergence of horizontal displacements of the neighbouring region of Mitake in four difference ways. The results are :—

(1) $3{\cdot}4\times10^{-5}$ ···for 1st order triangle.
(2) $3{\cdot}8\times$ „ ···for 2nd order triangle.
(3) $4{\cdot}5\times$ „ ···for 3rd order triangle.
(4) $2{\cdot}9\times$ „ ···for NES.
$2{\cdot}6\times$ „ ···for SWN.

As Prof. T. Terada kindly remarked the writer, the results (1), (2) and (3) must not be regarded as entirely independent, the displacements of the second order triangulation points having been calculated using the data of the displacements of the first order triangulation points. The results for rhombus are on the other hand entriely independent from those obtained from the results of triangulations. The values of divergence as calculated from these different date are seen to be of the same sign and their magnitudes are approximatey equal. This is a proof that the assumptions made in analytical treatments on the horizontal deformation of the earth's crust are to be justified.

One important point to be remarked in the above is that the divergence calculated from the data of the triangulations is that in the interval between the former and the later triangulations, which is some thirty years long. On the other hand, the divergence calculated from the data of the rhombus is that in the interval of about one year. As we can see from Fig. 5, the earth's crust in the neighbourhood of Mitaka has been generally expanding even when there was no remarkable earthquake. Thus we have no reason to expect that the divergence as calculated in different periods must come out to be exactly equal. It is rather plausible that the divergence calculated from the data of the triangulations comes out larger than that calculated from the data of the rhombus at the time of the earthquake of 1923.

In Fig. 5, the areas of the triangles of the rhombus are seen to have been subjected to gradual expansion. This expansion of the areas seems to have been disturbed in 1922 and suddenly came the earthquake of 1923 and after the earthquake the triangles decreased in their areas for one year and after that they again took their general course of expansion. In this respect the great earthquake of 1923 seems to have been an accidental event in the course of the expansion of the general area. It is

of special interest to note that a similar curve is obtained with other quantities such as the relative height of the mean sea level at Aburatubo which is the nearest mareographic station to the epicentre of the great Kwanto earthquake. This curve is shown in Fig. 6. The similarity in the forms of the curves in Fig. 5 and 6 suggests that there was some connections in the mechanisms of producing the divergence in Mitaka on the one hand and the vertical displacements at Aburatubo on the other hand.

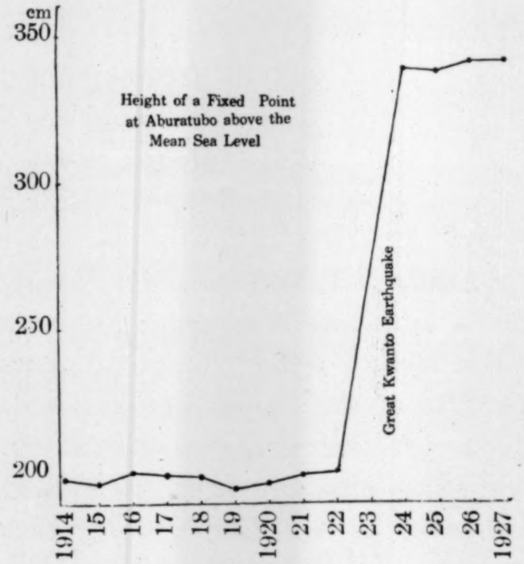

Fig. 6.

In conclusion, the writer wishes to express his deep thanks to Professor T. Terada for his interests and advices in this work.

---

18. 地殼の水平變動に就いて

地震研究所　坪　井　忠　二

地震の際の測量によつて明かにされた三角點の移動から該地域の地殼の變形を論ずる際には、此の三角點の移動が偶發的のものでなく近傍の一般の移動を代表して居ると看做されて居る。之は當然の假定であるが念の爲め事實果してさうであるかを調べた。1923 年の關東地震後一、二、三等三角測量が改測せられたのみならず三鷹村東京天文臺構内に於ける菱形基線の改測も行はれてゐるので、之等四つの材料から三鷹村近傍の divergence を求めた。その結果

$3{\cdot}4 \times 10^{-5}$	一等三角から
$3{\cdot}8 \times 10^{-5}$	二等三角から
$4{\cdot}5 \times 10^{-5}$	三等三角から
$2{\cdot}9 \times 10^{-5}$ $2{\cdot}6 \times 10^{-5}$	菱形から

なる値を得た。先づ大體に於いて一致してゐると見られるから、三角點の移動から地殼の一般の變動を求めても正鵠に近いものが得られるであらう。

菱形から求めた値が小さいのは、前後の測量の間の時間が三角測量では數十年、菱形では約一年であるからで、三鷹地方が緩慢に展張しつてあつた事實ともよく符合する。

菱形の約十年間に於ける面積の增減の有樣が油壺に於ける平均水面の上下と形が似てゐるのは注意すべき事である。

---

19. *Relation between Tidal Phases and the Earthquakes.*

By Seiti YAMAGUTI.

(Read April 15, 1930.—Received Sept. 20, 1930.)

Introduction.

The investigations on the relation between tidal phases and the occurrence of earthquakes, have already been made by Late Prof. Ômori[1], Prof. K. Honda[2] and others. In most of these investigations, however, the positions of the epicentres of the earthquakes referred to were not known and the earthquakes felt at a certain locality were taken together for the statistical investigation with regard to their lunar-hourly distribution.

The present investigation was made with the intention of studying the relation between the actual tidal phases and earthquakes, with reference to the numerous groups of the after-shocks which followed the recent destructive earthquakes, i. e. the Great Kwantô Earthquake[3] on Sept. 1, 1923, the Tango Earthquake[4] on March 7, 1927, the Tazima Earthquake[5] on May 23, 1925, and the Ômati Earthquake[6] on Nov. 11, 1918. In most of these cases, the positions of epicentres are approximately known and distributed within definite localities respectively, so that the comparison of the tidal phase in the neighbouring sea with the frequency of occurrence of these earthquakes may have a more definite significance than in the case of earlier investigations.

The materials for earthquakes were taken from the reports above cited, while for the tidal data, the Tide Table published by Naval Hydrographic Department was used.

---

1) F. Ômori, *Report E. I. C.*, **32** (1900), **54** (1906), etc.
2) K. Honda, *Pub. E. I. C.*, **18** (1904).
3) A. Imamura, *Bull. I. E. I. C.*, **101** (1928).
4) N. Nasu, *Report I. E. I. C.*, **101** (1927).
5) A. Imamura, *Journ. Fac. Sci. T. I. U.*, 111 (1929), Part 2.
6) F. Ômori, *Report I. E. I. C.*, **94** (1921).

Method of Investigation.

To determine the tidal phase at the time of an earthquake, the following procedure was taken. The time of the semidiurnal maximum occurring within 6 hours of the shock was taken as the time-origin, and the time of occurrence of the shock was marked along the time axis. The number of the points thus plotted within the successive time interval of an hour each before and after the maximum was counted. In a few cases, about 3 percent in number, the point fell outside the range of 6 hours, on account of the irregularity of the interval between the high waters. In these exceptional cases, the time of the earthquakes were counted from the neighbouring low water and plotted referring to $+6$ or -6 hours respectively. The number, n_x, at the time interval, x, was smoothed by taking $\frac{1}{4}(n_{x-1}+2n_x+n_{x+1})$ instead of n_x. Next, the value of n divided by the mean value, i. e. $12n/\Sigma n$, which is denoted by f, and called the *reduced frequency*, was calculated and plotted as ordinate against the time axis.

For the comparison, the number of shocks, falling within the successive solar time intervals of two hours each, was also counted and similarly treated as before.

Results and Discussions.

a) The After-shocks of the Great Kwantô Earthquake, and the Tide at Yokosuka.

For convenience's sake, we have taken the tide at Yokosuka for the comparison with the after-shocks of the Kwantô Earthquake.

According to Prof. Imamura's Report, the area of the region including the origins of the after-shocks was divided into the following four different localities :—

A. The area including Sagami Bay and the Province of Sagami as the main part.

B. Bôsô peninsula and the vicinity of its S. E. coast.

C. The drainage district of the River Tone.

D. Tôkyô and its environs.

In our present cases, the shocks originated in these respective areas are named A-, B-, C-, and D-type respectively, and investigated separately.

As to A-type, as the number of after-shocks on the first and second of september was extremely large, the after-shocks were divided into 5

epochs according to the following dates :—Sept. 1, Sept. 2, Sept. 3–6, Sept. 7—11, and Sept. 12–Oct. 1.

As to B- and D-types, they were divided into 3 epochs, Sept. 1–6, Sept. 7–11, and Sept. 12–Oct. 1.

As to C-type, the number of after-shocks were scanty, especially after Sept. 7, so that we were abliged to take only the interval, Sept. 1–6.

The values of the *reduced frequeney, f,* for these different epochs of each type are shown in Fig. 1. The curve (p) in Fig. 1 *f* is the curve corresponding to the "principal after-shocks" during the long period of Sept. 1, 1923—Feb. 12, 1928, for which 6 after-shocks immediately after the Great Earthquake on Sept. 1, are counted as 1.

The curves for the solar time distribution are shown in Fig. 2.

The curves showing the number of after-shocks for 4 types during the successive epochs of 4 hours from Sept. 1 to Sept 5, are shown in Fig. 3, from which the transference of the centre of the seismic activity first from the Sagami Bay to Bôsô peninsula and next to Tôkyô District, are clearly recognized.

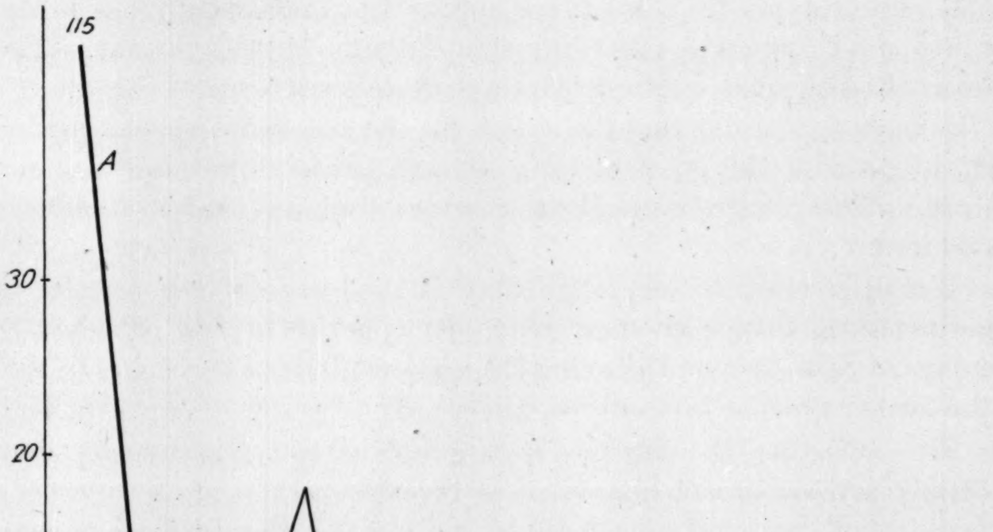

Fig. 3.

For the principal after-shocks during 4 years and 6 months above mentioned, there seems to exist a maximum frequency of occurrence of the shocks before 2 hours of the semidiurnal low water, a secondary maximum before 2 or 3 hours of the high water, and a minimum frequency near the high water.

Looking at Fig. 1, we may be able to remark the following :—

I) For A-type, the frequency of occurrence of the after-shocks, f, generally shows a maximum, a little before the low water and also a secondary maximum, is suggested between high water and the next low.

II) For B-type and D-type, which resemble to each other, f is maximum about at the low water, in common with all the other types, and besides, shows another maximum about 2 hours before the high water, as may be seen from the curves for (B+D) and (A+B+D) alike.

This characteristic feature of f may also be seen from the similar curve[7] for the shocks felt within the region of 160 km. from Tôkyô during the period of Jan.—Sept., 1926, so that we may consider this feature as real and proper to the region.

III) For C-type, (Fig. 1*d*) there appear two maxima of f, one before the low water, and the other immediately after the high water. The data are, however, too scanty to give a definite conclusion.

In general, it seems that the curves for the successive epochs change their forms with the lapse of time, though preserving some common feature. After a certain epoch, the curves seem to tend to a certain stable form.

It is interesting to see (Fig. 1*d*) that the curve of B-type, also in some measure, D-type shows a trend just opposite to that of A-type in the days of Sept. 1–6, and also that (Fig. 1*a*) the latter approaches to that of the former type, or inland type, afterwards.

The fact that the curves for different independent epochs show generally some common character as revealed in the mean curve of a long duration, may be considered as a proof for the existence of some real physical relation between the frequency of occurrence of shocks and the tidal phase.

The curves for solar time variation are shown in Fig. 2.

First, referring to the lowest curves of Fig. 2*a*, 2*b*, 2*c*, ..., which represent the mean variation for longer duration, we may observe a common semidiurnal wave of sensible amplitude, for all the types taken.

---

7) The data for the curve was taken from Prof. Imamura's paper, *Bull. E. R. I.*, (1927). The curve is here omitted.

The curves strongly suggest the relation with the semidiurnal waves of the atmospheric pressure, the maxima of pressure corresponding to the minima of f. On the other hand, the fact that the curves for the successive epochs, separated by 6 or 12 days from each other, shows quite different, often inverted, course may be taken as an evidence for the presence of some conspicuous lunar period interfering with the solar one. It is only by taking an average of a longer period that the lunar term is cancelled and the solar semidiurnal wave is revealed.

b) After-shocks of the Tango Earthquake and the Tides at Kôbe and Wazima.

As the tidal amplitude in the Japan Sea is generally very small, it seemed at first probable that it will not much affect the variation of the load on the earth crust near Tango, so that we have tried to take the tide at Kôbe for the comparison. Afterwards, however, the tide at Wazima was also taken for comparison[8)]

The after-shocks were firstly divided according to the dates into 15 parts, which are March 7–11, 12–20, 21–31; April 1, April 2–10, 11–20, 21–30, May 1–10, 11–20, 21–31, June 1–30, July 1–31, Aug. 1–31, Sept. 1–Dec. 31, in 1927 and Jan. 1–July 16 in 1928. These are similarly treated as in the case of the Great Kwantô Earthquake and are shown in Fig. 4 for the case of the tides at Wazima and in Fig. 5 for the case of the tides at Kôbe.

Next, the after-shocks, of which the positions of the epicentres are identified, are divided into 3 parts, namely, (1) those situated beneath the sea bed, (2) those on the northern side and, (3) those on the southern side of Yamada Fault.

The latter two parts were moreover divided into 4 or 5 parts according to the dates respectively, and compared with the tidal phase at Wazima, as shown in Fig. 6.

The frequency of the after-shocks plotted against the solar time, are shown in Fig. 7.

Individual curves shown in Fig. 4 and Fig. 5 are rather irregular and do not give any definite conclusion, except the invariable maximum

8) Mr. C. Tsuboi, who made a similar study of the Tango Earthquake referred to the tidal phase at Wazima, found the good correlation and informed me of his result. The comparison with Wazima tides was then made in the similar manner as for Kôbe tides. I am obliged to him for his kind information.

of f near the low water. The irregularity is, however, less in Fig. 4 than in Fig. 5. In Fig. 4, the individual curves show features more or less common to each other and to the lowest sum-curve. This will show that the earthquakes in this district is in some degree affected by the tides on the Japan Sea side. Fig. 5 is quite irregular if we compare the successive curves.

The sum-curve at the bottom of the figure, however, harmonizes very well with that of Fig. 4, if we take into account the difference of the tidal phase between Wazima and Kôbe amounting to about 5 hours on an average. In the latter station, the tidal waves are observed in irregular forms and this fact may also contribute to the irregularity of the curves in Fig. 5. At present stage, therefore, it is difficult to decide whether the Tango earthquakes are chiefly governed by the tides on the Japan Sea side.

On the other hand, it is very interesting to remark that the sum-curve of Fig. 4 shows some infallible resemblance to that of Fig. *1a*, *1b*··· etc. especially as regard to the maximum at the low tide and the minimum just preceding it.

From Fig. 6*b*, we may be able to say the followings :—

i) The after-shocks occurred in the sea bed has its maximum frequency at about one hour and a half respectively before and after the high water.

ii) The shocks on the northern side of Yamada Fault has its great maximum of f at about low water and the secondary at about high water.

iii) It is interesting to see that f of the shocks in sea bed shows entirely opposite course compared with that of the northern side of Yamada Fault.

These result may suggest some essential difference in the mechanism of earthquakes for the two sides of Yamada Fault.

Examining the curves of Fig. 4, we may remark that the curves for March 7–11, 21–31, and April 1 show markedly different form compared with the others. Severe earthquakes occured on March 7 and April 1. We may suggest that some change of curve form might take place immediately after and before the great shock, and then the form gradually settle down to the normal form as is represented by the curve of total sum above mentioned.

From the lowest sum-curve of Fig. 7, which shows the average solar time distribution of f, we can see clearly that the frequency of shocks is maximum at about 8 o'clock and 23 o'clock of the solar time and it is

minimum at about 3 and 18 o'clock. Comparing this with the corresponding curves in Fig. 2, we may notice that the curves for Kwantô and Tango are nearly reversed upside down. This suggests that the effect of the atmospheric semidiurnal waves is opposite on the two regions, one on the Pacific side and the other on the Japan Sea side.

c) The After-shocks of the Tazima Earthquake and the Tides at Wazima and Kôbe.

The after-shocks of the Tazima Earthquake of May 23, 1925, were treated similarly as in the case of the Tango Eorthquake and the results are shown in Fig. 8, for the tidal phase and in Fig. 9 for the solar time distribution.

From the curve (lowest in Fig. 8*a*) of the total sum for the tide at Wazima, we may be able to say that the frequency of occurence of shocks has its great maximum value at about the low water and also its small maximum value at about high water, while in the case of comparison with the tide at Kôbe (Fig. 8b), we see one more maximum of *f*.

From the curve (lowest Fig. 9) of the total sum for the solar time distribution, we can notice the maxima of *f* at about 8 and 23 o'clock, and minima of *f* at about 3 and 19 o'clock. This character of the curve is almost similar as in the case (Fig. 7 lowest curve) of Tango earthquakes. Another maximum of *f* may be seen at about 15 o'clock.

d) The After-shocks of the Ômati Earthquake and the Tides at Wazima and Yokosuka.

The after-shocks of Ômati Earthquake on Nov. 11, 1918, are similarly treated as in the preceding cases, and are shown in Fig. 10 and Fig. 11.

From the resultant curve (Fig. 10*a*, lowest) for the tide at Wazima, we can see the greatest maximum value of *f* at about low water as usual and the smaller secondary maximum of *f* at about 2 hours after the high water. As for the curve (Fig. 10*b*, lowest) for the tide of Yokosuka, we see maximum values of *f* at about the low water and at about 1.5 hours before and after the high water.

The amplitude of the sum-frequency curve for the tide at Yokosuka is only one thirds of that for the tide at Wazima, which may clearly show that the tide at Wazima affects the occurrence of shocks more than

the tide at Yokosuka. This result seems quite reasonable if we consider that Ômati is situated much nearer to Japan Sea than to the Pacific and the mechanical linkage with the Japan Sea Coast is more direct than with the Pacific Coast.

Looking at Fig. 11 for the solar time distribution, we must admit that the solar effect on the occurence of shocks is exceptionally large in the case of Ômati, being of the same order as in the case of the tide at Wazima. We see here the maximum values of f at about 9 and 18 o'clock and the minimum values at about 3 and 13 o'clock.

As shown in the above different cases the frequency curves of the after-shocks for the successive epochs separated from each other by several days or a little more than 10 days, do not show sufficient parallelisms. The sum-curve for a long duration of time show some feasures which seems to be real and physically significant.

One characteristic feature which is common to all the cases above mentioned is that the frequency of occurrence of the after-shocks is maximum at, or a little before the low water as shown in Fig. 12.

The secondary maximum appears before the high water in the case of Kwantô curve, whereas it is found a little after the high water for the cases of Tango, Tazima and Ômati curves, each referred to Wazima tides. Another feature worthy of notice is that a third maximum appear in the cases of Tango, Tazima and Ômati, when referred to the tides on the Pacific side.

Again, as to the f-curves referred to the solar time we may remark the following points, referring to Fig. 13: (i) Semidiurnal waves are suggested in all cases which are probably related with the daily variation of the atmospheric pressure. (ii) Kwantô curve is generally opposite to Tango and Tazima curves. (iii) Tango and Tazima curves are nearly parallel to each other. (iv) Omati curve in A. M. is parallel to, but in P. M. opposite to Tango-Tazima curves.

Theoretical discussions of these results will be reserved for a future.

In conclusion, I wish to express my best thanks to Prof. T. Terada under whose supervision the entire work has been carried out and who has given me many useful suggestions throughout the course of my investigation.

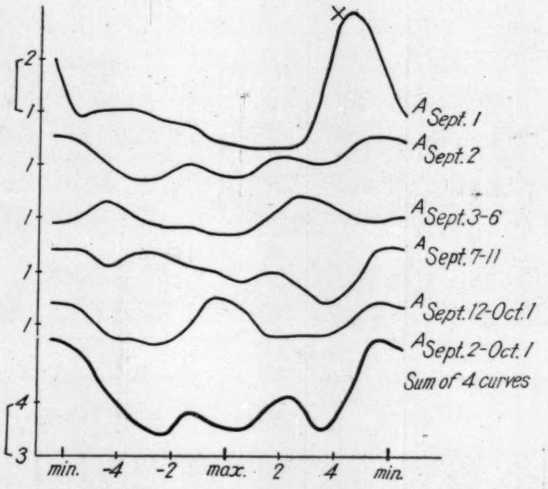

Fig. 1*a*. Frequency Curves of After-shocks of the Great Kwantô Earthquake, referred to the Tides at Yokosuka. A-Type.

× Marks the time, at which phase the Great Earthquake occurred.

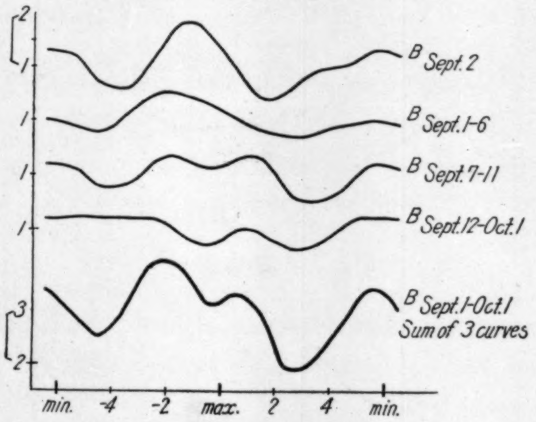

Fig. 1*b*. Do. B-Type.

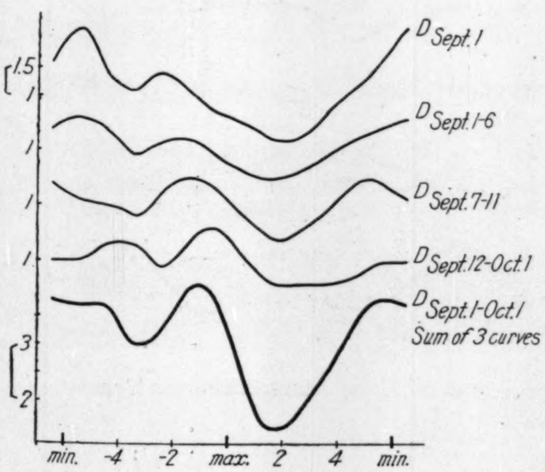

Fig. 1*c*. Do. D-Type.

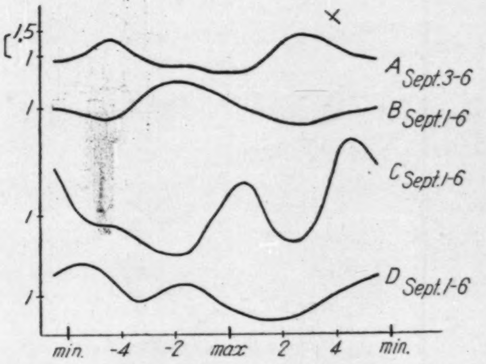

Fig. 1*d*. Comparison of 4-Types.

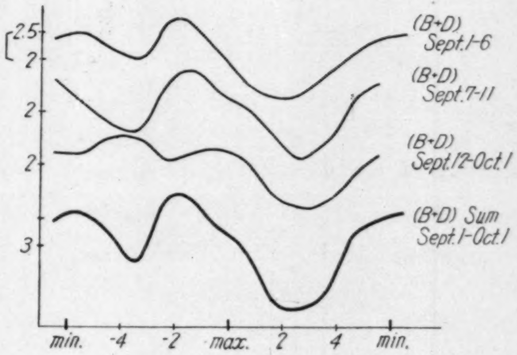

Fig. *e* 1. Sum B + D.

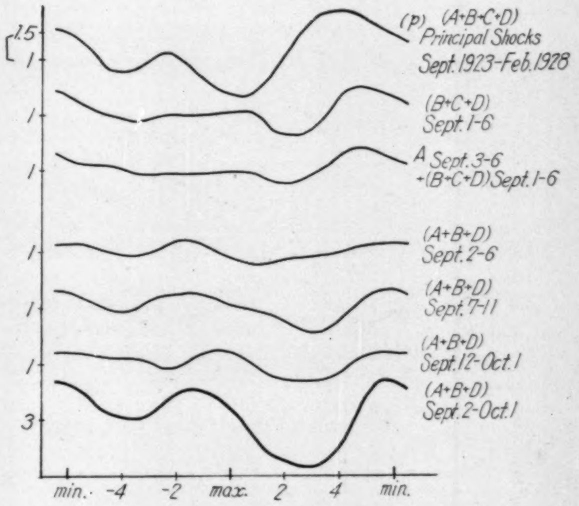

Fig. 1*f*. Sum of different Types.

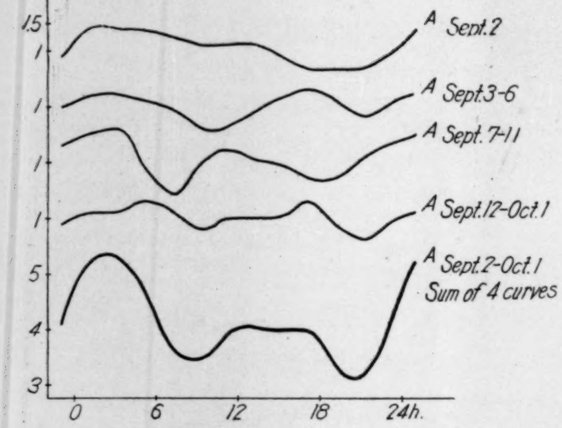

Fig. 2*a*. After-shocks of the Great Kwantô Earthquake referred to Solar Time.
A-Type.

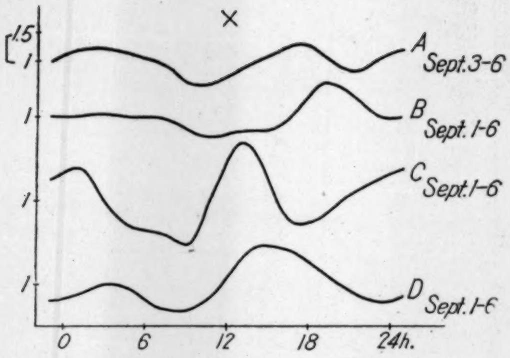

Fig. 2*d*. Do. Comparison of 4 Types.

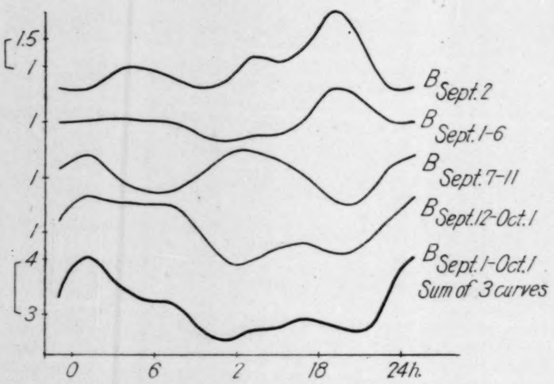

Fig. 2*b*. Do. B-Type.

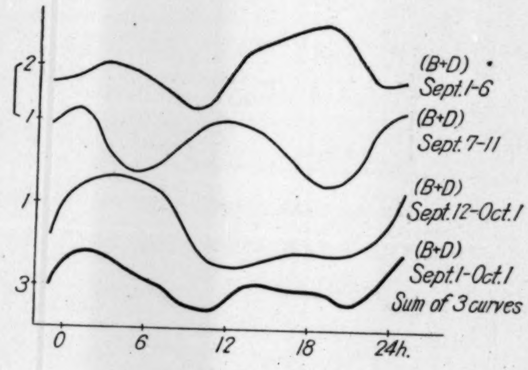

Fig. 2*e*. Sum B + D.

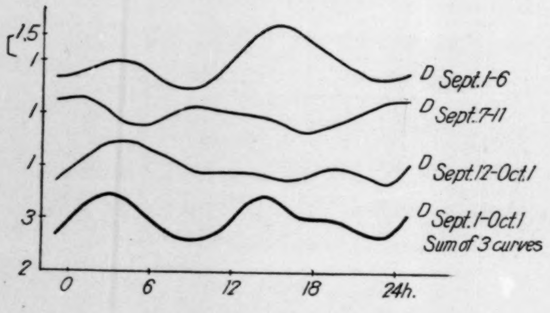

Fig. 2*c*. Do. D-Type.

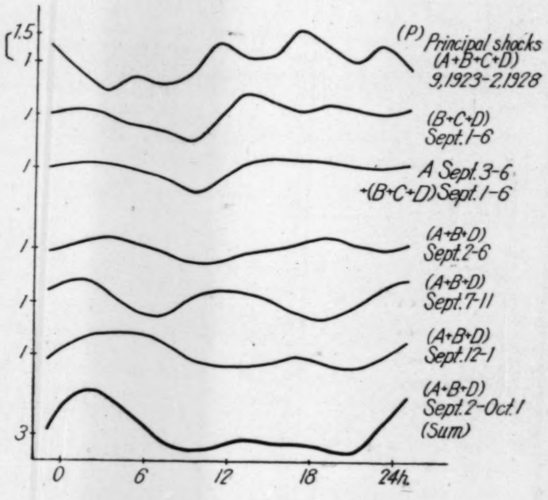

Fig. 2*f*. Do. Sum of different Types.

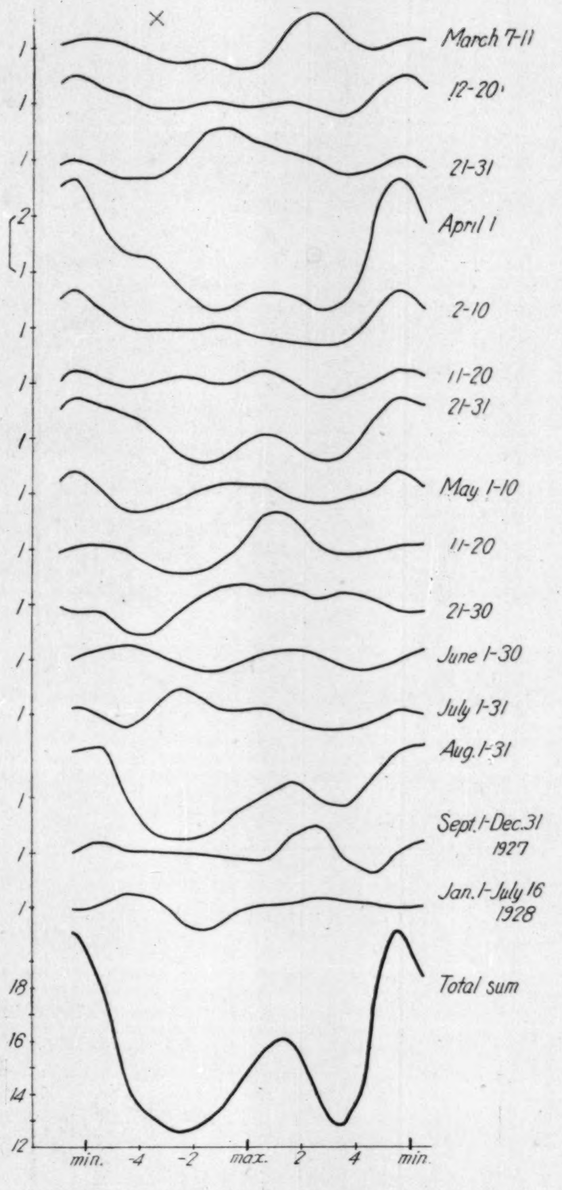

Fig. 4. After-shocks of the Tango Earthquake, referred to Tides at Wazima, 1927 & 1928.

× Marks the time, at which phase the Great Earthquake occurred.

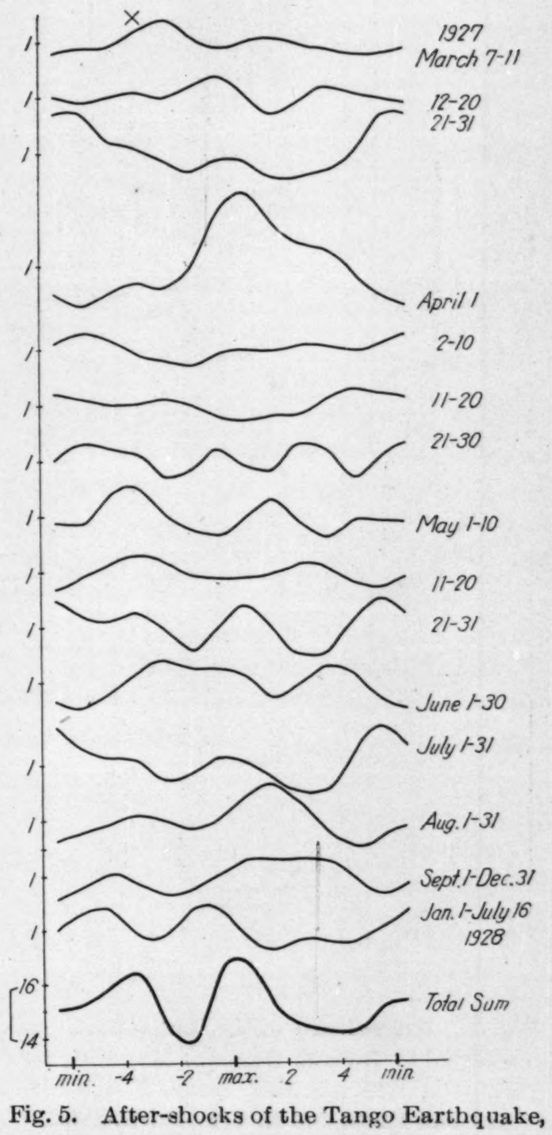

Fig. 5. After-shocks of the Tango Earthquake, referred to Tides at Kôbe, 1927 & 1928.

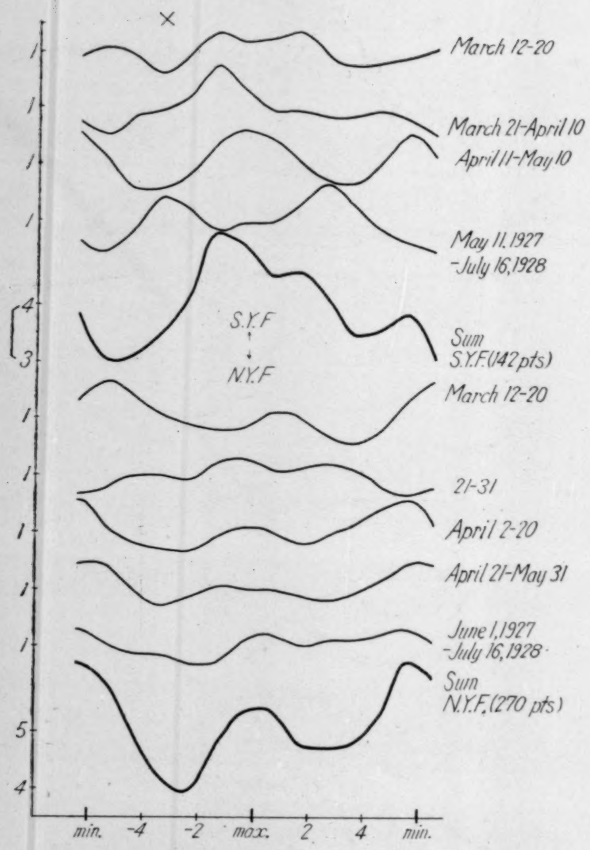

Fig. 6*a*. After-shocks of the Tango Earthquake, referred to Tides at Wazima, March 11, 1927—July 16, 1928. S. Y. F. means South Side of Yamada Fault, and N. Y. F., North Side.
× Marks the time, at which phase the Great Earthquake occurred.

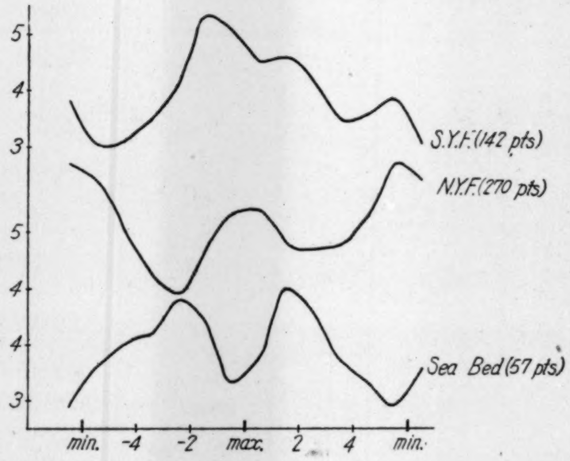

Fig. 6*b*. Compar son of 3 Types.

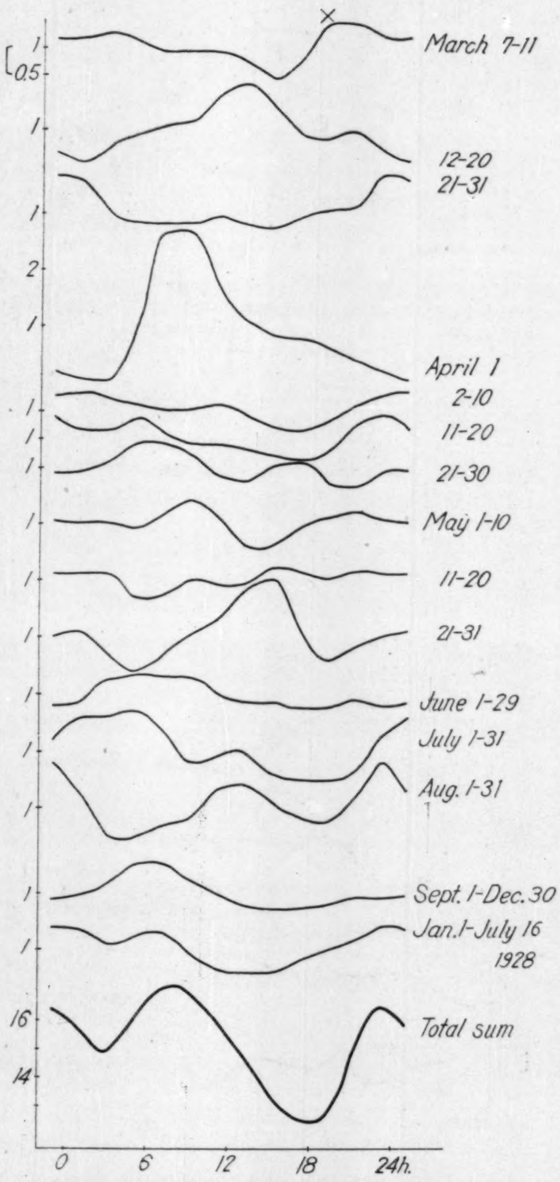

Fig. 7. After-shocks of the Tango Earthquake referred to Solar Time.

× Marks the time, at which phase the Great Earthquake occurred.

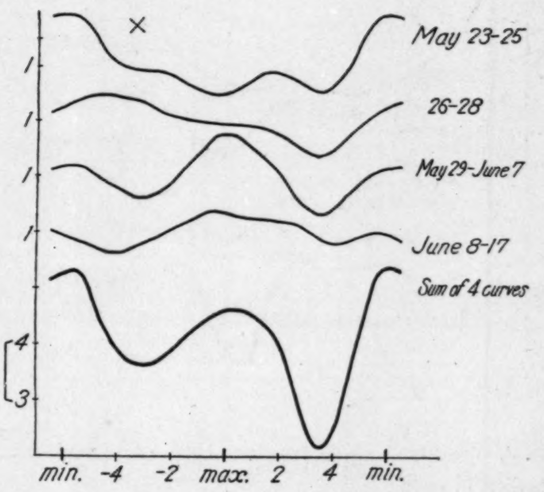

Fig. 8*a*. After-shocks of the Tazima Earthquake, 1925, referred to Tides at Wazima.

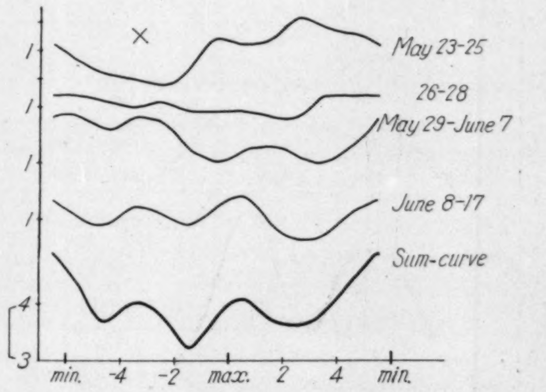

Fig. 8*b*. Tazima Earthquake, 1926, referred to Tides at Kôbe.

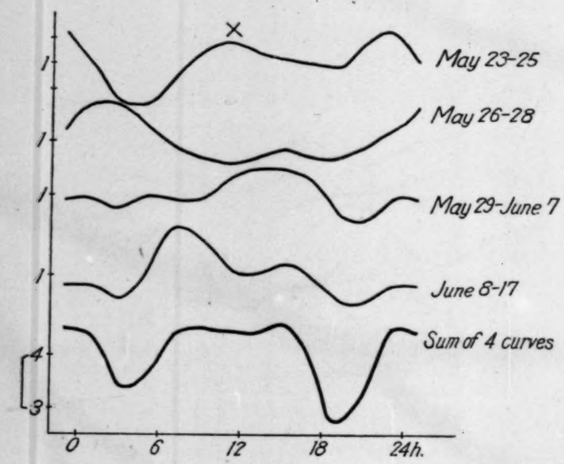

Fig. 9. Tazima Earthquake, 1925, referred to Solar Time.

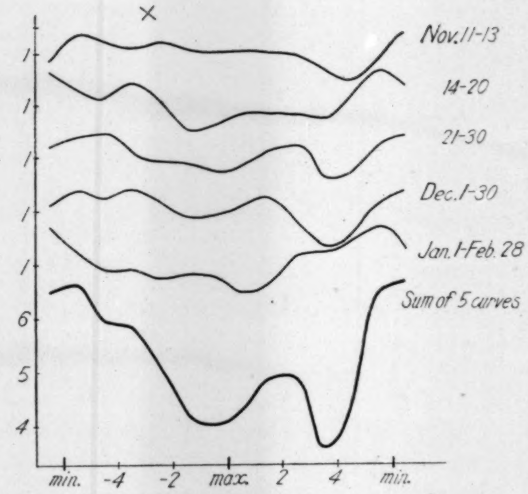

Fig. 10a. After-shocks of the Ômati Earthquake 1918 & 1919, referred to Tides at Wazima.

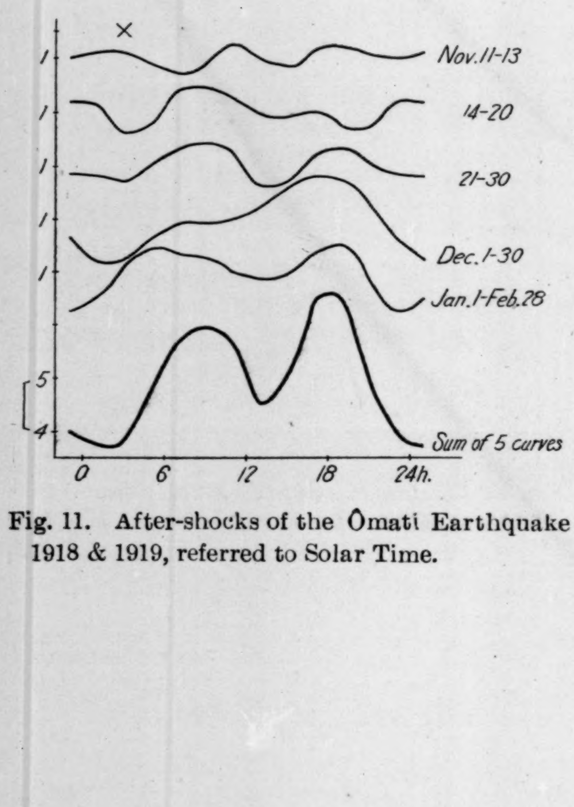

Fig. 11. After-shocks of the Ômati Earthquake 1918 & 1919, referred to Solar Time.

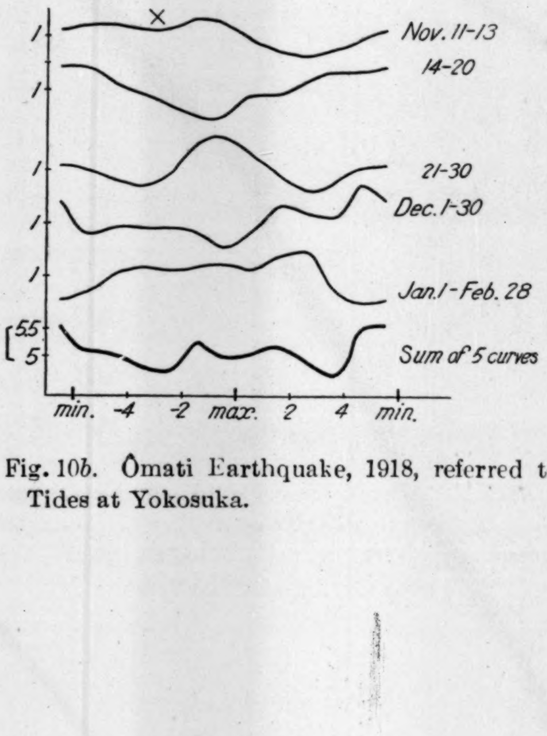

Fig. 10b. Ômati Earthquake, 1918, referred to Tides at Yokosuka.

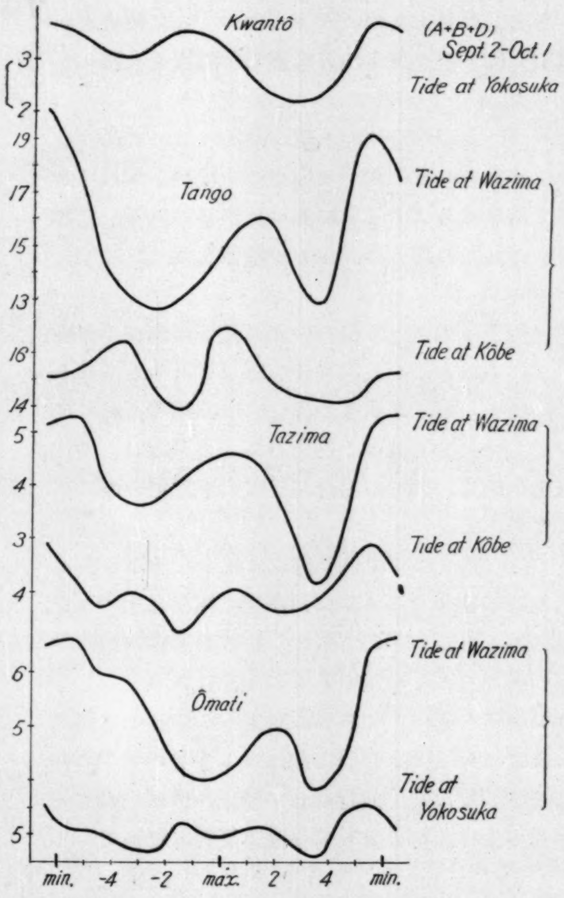

Fig. 12. Comparison of 4 Districts: Tidal Phase.

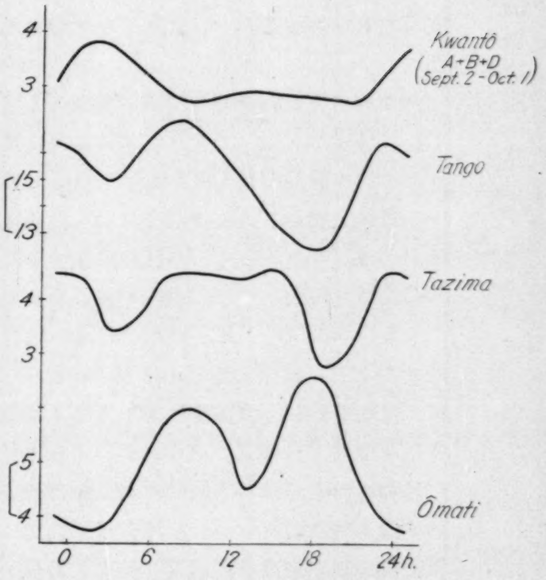

Fig. 13. Comparison of 4 Districts: Solar Time Distribution.

19. 地震と潮汐との關係

山口生知

地震と潮汐との關係に就ては故大森博士や、本多光太郎博士其他の人々に依つて既に研究されてゐる。併し之等の多くの場合は震源の位置が判明しないので或る地方に感じた地震を一纏めとして研究された。

それ故に我々は震源の位置の知れて居る最近に起つた左の四つの大地震の餘震に就いて其の附近の海の潮汐と比較研究した。卽ち第一は大正十二年九月一日に起つた關東の大地震、第二は昭和二年三月七日に起つた丹後の地震、第三は大正十四年五月二十三日に起つた但馬の地震、第四は大正七年十一月十一日に起つた大町の地震とそれぞれ其の附近の潮汐との關係を調べたのである。

其の調べ方は高潮時を時間の起點として其の前後潮汐の如何なる位相の處に餘震の時刻が分布されて居るかを調べて見た。其の結果四箇所共いづれの地方にも共通に低潮時（寧ろ少しく其の前）に於て餘震が最も多く起つて居ると云ふ著しい性質があり又關東の場合には高潮時の前に於て、丹後、但馬、大町の場合に於ては高潮時の少しく後に於て餘震の回數の第二の最大があると云ふこと、それからも一つ注意に價することは丹後、但馬、大町の場合に於て太平洋岸の潮汐に對し餘震の回數の第三の最大が存在すると云ふことである。

又も一つ面白いと思ふ結果は丹後の地震に就いて第六圖 b に示す通り海底に起つた餘震と山田斷層の北部に起つた餘震とは潮汐の位相に對して反對の關係にあるが山田斷層の南部に起つた餘震と海底の餘震とは潮汐に對して寧ろ類似の關係にあると云ふことである。此の結果は山田斷層の南北兩地方の地震の機巧に就いて根本的の差異のあることを暗示するものと思はれる。

又別に參考の爲め太陽時に對する餘震の分布をも調べて見たところ其の結果として第十三圖に示す通り四箇所共いづれの地方にも共通に地震に及ぼす大氣壓の影響と思はるゝ半日の週期の餘震回數の波が表はれて居る。併して丹後、但馬の波はお互に殆ど並行にして關東の波は一般に丹後但馬と反對であり大町の波は午前中は丹後、但馬の波と並行であるが午後は反對になつてゐると云ふ結論に到達したのである。

以上地震に及ぼす潮汐の影響並に大氣壓の影響に關する理論的の論議は將來の研究に委ねたいと思ふ。

20. *On the Geologic Structure of Itô District, Idu.*

By **Hiromichi TSUYA,**

Earthquake Research Institute.

(Read June 17, 1930.—Received Sept. 20, 1930.)

Introduction.

From February to May, 1930, there occurred numerous earthquakes which shook violently the northeastern coast-belt, including the hot-spring resort of Itô, of the Idu peninsula. These earthquakes were but local ones, starting for the most part from the sources distributed in the sea off the shore of the town of Itô[1].

This paper embodies the results of the study of the geologic structure of the Itô district, the coast-belt between Aziro on the north and Yawatano on the south. Of the distribution and petrographic characters of the rocks that occur in the district, only brief notes are given here, the detailed accounts of them being left for another occasion.

Topography.

The Idu peninsula projects into the Pacific at the southern coast of central Japan, separating the two bays, viz. Suruga on the west side and Sagami on the east. This peninsula consists geologically of later Tertiary and Quaternary volcanics of various kinds, together with contemporaneous sedimentaries composed essentially of volcanic materials; and exhibits as a whole a complicated topographical feature of maturely dissected volcanic tract. In the northern part of the peninsula there are three gigant volcanoes, viz. Daruma, Atami[2], and Amagi. The

1) A. Imamura, N. Nasu, F. Kishinouye and C. Yasuda, "On the Recent Itô Earthquakes", *Proc. Imp. Acad.*, 6 (1930), 190–193.

2) The term "Atami Volcano" was proposed originally by T. Hirabayashi to a volcano which he considered to exist in the vicinity of the hot-spring resort of Atami. In this paper the writer uses this term for a wider district including Hirabayashi's "Atami Volcano". Cf. p. 414.

Daruma volcano is situated at the side of Suruga Bay and is separated from the other two volcanoes on the side of Sagami Bay by the longitudinal valley of the river Kano which, running north through the central part of the northern half of the peninsula, flows into Suruga Bay at Numadu.

The Itô district is located where the southern skirt of the Atami volcano comes in contact with the northeastern skirt of the Amagi volcano. It is divided topographically into two parts. The one is the mountainous land included in the Atami and Amagi volcanoes; while the other the hill-land extending to the south of Itô. The former is dissected in the mature stage, and the crest of the divide, which ranges from the northern side of the Amagi volcano northward to the summit of the Atami volcano, separates the Suruga Bay drainage from the Sagami Bay drainage. The latter, being ramparted by the maturely dissected mountains of the former on the N. W., W., and S. W. sides, is a less dissected district within which lie many volcanoes, Oomuroyama, Komuroyama, etc. There are small intermontane basins, one of which holds water forming the Ooiké lake, drained through valleys between these volcanic masses.

In the Itô district there are three small but notable valleys. The southernmost valley runs N.W.—S.E. through the northeastern skirt of the Amagi volcano, transverse to its slope, and opens to the sea at Yawatano. The central valley assumes a winding course in the upper, but runs S.S.W.—N.N.E. in the lower, opening to the sea at the town of Itô. These two valleys mark at their lower courses the boundary between the two distinct physiographic units already mentioned of. The northernmost one runs W.N.W.—E.S.E. through the southern slope of the Atami volcano, transverse to its slope, and opens to the sea at Usami. The course of this valley was determined *a priori* by a tectonic line to be explained of later.

The general trend of the coast around the Idu peninsula appears for the most part to have been determined originally by faults, downthrow sides of which have been depressed under the sea; while the present shoreline is much indented with embayments and cliffed headlands, locally combined with long sand-beaches. On the coast no physiographic

feature indicating the land-upheaval in the recent geologic age—such as for example coastal terrace—is recognized. Moreover, the absence of any Diluvial sedimentaries from the peninsula shows that the land has been subsiding in the peninsula, since the Diluvial time without upheaval, at least in geologically recognizable amount. The present indented shorelines around the peninsula may be due largely to this subsidence; though minor irregularities in the shoreline may be attributed to marine erosion to which the coast has been constantly subjected.

The nearly straight coast-line from Aziro to Usami represents a fault. There is a clean-cut fault-facet, elevated abruptly from the sea, and with a narrow gravel-beach at its base. From Usami to Itô runs a reentrant fault-shoreline, as suggested by the steep mountain-slope along the coast; while from Itô to Yawatano a crenulate volcano-shoreline, along which the eastern skirts of the volcanoes on the hill-land terminate in sea-cliffs varying in height from a few meters (generally the skirt of younger volcano) to over one hundred meters (generally the skirt of older volcano). At several spots, there are sea-caves on the sea-cliffs. The most conspicuous of these is seen on the shore near Yawatano.

The coast along the Itô district does not show throughout its whole length any physiographic feature that indicates to the recent uplift of the land. It is, therefore, inferred that in the geologically recent date this coast-belt as a whole has not been uplifted at least in such a magnitude as to be recognized on the recent shore. Small changes of level, however, have actually taken place in recent years, as has been revealed from the precise levellings repeated thrice in 1903, 1923/24, and 1930 in this district by the Land Survey Department. The results of these levellings show a general tendency of negative movement between 1903 and 1923/24; while a general tendency of positive movement between 1923/24 and 1930. Whether these minor changes of land level are causally related with the earthquakes now under question or not, can not be determined.

Outline of the Geology of the Idu Peninsula.

Before treating the geologic structure of the Itô district, the general geology of the Idu peninsula will be briefly described.

The order of succession of the rocks in the peninsula has been variously determined by different writers[3]. The following scheme of the succession of the rocks in the peninsula is based on the present writer's own observations in the southern part of the peninsula.

Basal Tertiary complex:

Older group ·········Propylite with interbedded tuffs, tufaceous sandstone, agglomerate, and conglomerate.

Younger group ······Stratified series consisting of tuffs, tufaceous sandstone, tuff-breccia, and conglomerate, associated with liparite, dacite, and andesite.

Quaternary volcanics:

Andesite and basalt.

The Tertiary rocks of the Idu peninsula form the basal complex on which rest the Quaternary volcanoes—Daruma, Atami, and Amagi; and may be divided into two groups, older and younger[4]. Older is represented by the so-called propylite[5] mainly distributed in the central part of the peninsula. This rock is interstratified with a fossil-bearing series consisting of tuff, tufaceous sandstone, agglomerate, and conglomerate[6].

---

3) S. NISHIYAMA, *Explanatory Text of the Geologic Map, Sheet Yokohama*, 1:200,000, (1886).

T. HIRABAYASHI, "Geology of the Hakone and Atami Volcanoes", *Report Earthq. Invest. Com.*, **16** (1898), 58–73, (in Japanese).

H. ISHIWARA, "Geology of the Volcanoes of Idu Peninsula," *Report Earthq. Invest. Com.*, **17** (1898), 3–49, (in Japanese).

S. KOZU, "Geology of the Southern Part of Idu Peninsula," *Report Geological Survey*, **38** (1913), 1–19, (in Japanese).

J. SUZUKI, "Geology of the Amagi Volcanic Group, Prov. Idu," *Jour. Geol. Soc.*, Tokyo, **28** (1921), 431–448, (in Japanese).

H. TSUYA, "Volcanoes of Kozu-shima", *Bull. Earthq. Res. Inst.*, **7** (1929), 327–334.

4) A great deal of further detailed work is neccessary before the stratigraphic relation of all the rocks in these groups can be conclusively determined. R. Tayama and H. Niino in the Tôhoku Imperial University are now carrying out the stratigraphic study of these groups.

5) In the strict sense, "propylite" is hardly suitable to be applied to the rocks in the peninsula that have been called by this name. In this paper the writer restricts the term propylite to the altered andesite in the older group of the basal Tertiary complex.

6) It is doubtful whether the so-called propylite, together with the associating stratified series, are the products of a hypothetical Tertiary volcano, "Nekko Volcano", of H. Ishiwara. Probably, there may be some volcanic vents from which the whole piles of the so-called propylite have poured fourth, although none of such vents has come actually under the writer's notice.

Younger is represented by volcanic rocks—liparite, dacite, and andesite. They are associated with a fossil-bearing stratified series built up of their respective tuff, tufaceous sandstone, tuff-breccia, and agglomerate; and are distributed extensively in the southern part of the peninsula. The stratified series of the younger group shows local variations of its building materials, and there is no such definite order or succession in their lithic characters as can be applied throughout the whole area occupied by this series. The volcanic rocks occur either as lava-flows interbedded with the stratified series or as dikes penetrating the latter. The sequence of their eruption is not very simple, the andesitic and liparitic rocks having erupted alternately during the period represented by the younger group of the basal complex.

The Diluvial geology of the peninsula represented by the Diluvial volcanoes will be described later in connection with the local geology of the Itô district.

Geology of the Itô District.

The basal Tertiary complex exposed widely in the southern half of the peninsula extends considerably northward, forming the foundations of the Atami and Amagi volcanoes. Thus, the Itô district consists geologically of rocks of the basal Tertiary complex, exposed only in some limited areas, and of extensive Diluvial volcanics. See the annexed geologic map (Pl. XII.).

The chief rocks of the basal Tertiary complex in the Itô district is dark green-colored altered andesite, or the so-called propylite already referred to. It is exposed (1) on the upper course of the main river (the river which, running S.S.W.—N.N.E., flows into the sea at Itô), (2) near the mountain-pass, about 400 m. in height above sea level, on the highway from Itô to Numadu at about 4·5 km. southwest of Itô, in association with a conglomeratic agglomerate which exhibits indistinct stratification with northerly dip at high angle, and (3) in the vicinity of Usami. At these localities the altered andesite of the basal complex is overlain by the Diluvial volcanics, either of the Amagi volcano or of the Atami volcano. No member of the younger group of the basal complex is exposed in the Itô district; but it is well exposed in the area, immediate west of the Itô district, i.e. the northwestern foot of the Amagi volcano or the southwestern foot of the Atami volcano, where it is covered by the products of these volcanoes.

The Diluvial volcanoes are as follows, in the order from older to younger: Atami volcano, Amagi volcano, and Oomuroyama volcano group. The geologic structures of these volcanoes will be described below. Of the first two volcanoes, whose greater parts are out of the area now concerned, the description will be restricted only as to their certain peculiar features.

Atami Volcano. The term "Atami Volcano" is used here somewhat in different sense from that originally proposed by T. Hirabayashi, who meant by this "a volcano with its crater near the hot-spring resort of Atami".

The present writer means by "Atami Volcano" that volcanic tract which extends southward from Atami through Aziro and Usami far to Itô, and thus including Hirabayashi's "Atami Volcano".

Morphologically, the Atami volcano shows as a whole the aspect of demolished volcanic cone truncated at its top with a broad ring-wall. There is a long range of high ridges forming a wide ring-mountain, within which the village of Aziro and the town of Atami are located. The highest peak, Kurodaké, in the ring-mountain rises in an elevation of 799 m. above sea level. The flanks of the volcano are represented by the smooth ridges radiating outward from the crest of the ring-mountain. The inner side of the ring-mountain terminates in many branching spurs abruptly cut at the sea-shore on which Aziro and Atami are located. From their morphological features the ring-mountain is inferred to represent the dissected ring-wall of a gigant volcanic cone, the present writer's "Atami volcano". The dacite hills near Atami are the relics of a central cone within the caldera surrounded by the above-mentioned ring-wall.

The volcano was cut into two halves by a fault running in N.-S. direction through its central part. The eastern half of it depressed to be subjected to subsequent marine erosion and was lost beneath the sea. A striking shoreline feature on the coast between Aziro and Usami, where the eastern end of the southern ring-wall of the volcano is cut abruptly, is interpreted as representing the N.-S. fault just mentioned. At a distance of 6 km. to the east of this coast there is an isolated island called Hasima which is geologically composed of an andesite lava-flow overlain by an agglomerate-tuff. This island is probably a remnant of the depressed block of the Atami volcano.

The volcano is a stratified one built up of numerous, alternately accumulated layers of lava-flows and pyroclastics of andesitic nature.

The coast between Aziro and Usami runs nearly at right angle to the strike of the layers, and on the coast the inner structure of the volcano is exposed. There, is seen a section of very regular stratification of volcanic materials. On the northern four-fifths of the section lava-flows and pyroclastics are bedded with a general dip of about 30° southward (Fig. 1). The lavas are exclusively two-pyroxene-andesite. The finer and coarser pyroclastics including volcanic ashes, lapilli, and bombs of two-pyroxene-andesite, accumulate in distinct stratification. They are intruded by numerous dikes of olivine-two-pyroxene-andesite. On the southern one-fifth of the above-mentioned section a thick lava-flow of olivine-two-pyroxene-andesite is exposed, which rests conformably on the lower stratified part. The above facts show that in the volcano two-pyroxene-andesite erupted first, and then olivine-two-pyroxene-andesite. The uppermost lava of the volcano, olivine-two-pyroxene-andesite, caps the ring-mountain, and covers extensively its outer slope.

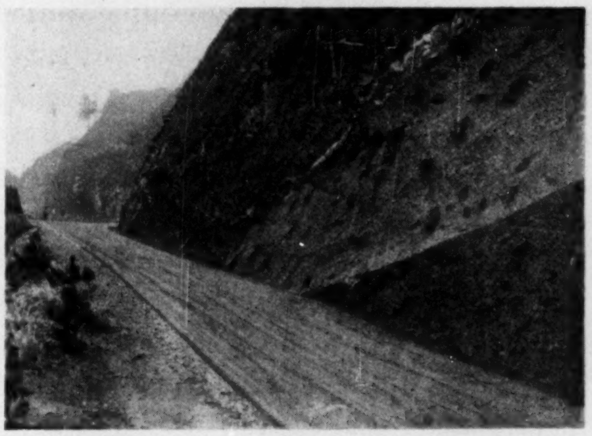

Fig. 1.—Highway along the coast between Aziro and Usami, viewed southwards. Alternated layers of pyroclastic accumulations are exposed.

On the outer slope of the southern part of the ring-mountain the lava of olivine-two-pyroxene-andesite is delimited by the valley which, running W.N.W.—E.S.E., opens to the sea at Usami (Fig. 2); and the greater part of the area south of this valley is occupied by lava-flows of two-pyroxene-andesite, intercalated with pyroclastics accumulating in layers with a general southward dip. This structure is interpreted as follows, under the supposition that the extrusion of

Fig. 2.—Valley at Usami, viewed northwestwards. The southern side of the Atami volcano is divided into two segments by this valley.

two-pyroxene-andesite preceded that of olivine-two-pyroxene-andesite: The southern slope of the volcano was cut into two segments by a strike fault or faults represented by the valley trending W.N.W.—E.S.E. through Usami, and the northern segment depressed relative to the southern one. The fault separating the two segments is either of a normal type or of a reverse one (an upthrust from the south). However, its exact location as well as its throw and dip are difficult to determine. Moreover, whether it is a normal or reverse fault can not be surely decided. But it is probably of a reverse fault, as is inferred from the exposure on the cliff-section between Aziro and Usami, where the layers of volcanic materials in the northern segment are traversed by a number of minor reverse faults.

The mass which forms the hills bordering the sea between Itô and Kawana is built up of alternating layers with a general southwestward dip of lava-flows and pyroclastics of two-pyroxene-andesite. This may be regarded as a land segment disjuncted by the N.-S. fault from the main mass of the Atami volcano.

At about 1 km. west-southwest of Itô a dike of pyroxene-dacite intrudes the body of two-pyroxene-andesite of the Atami volcano. This dike may be a feeder of the dacite-obsidian lava that covers the two-pyroxene-andesite body at the mountain-pass, about 2 km. southwest of the dike locality.

Sukumoyama volcano is a dome-shaped cinder-cone standing on a ridge, south of the fault that cuts the southern slope of the Atami volcano into two segments. It is 580·6 m. high above sea level, or about 150 m. high above the flank of the Atami volcano, and is underlain by a lava-flow of basalt containing abundant phenocrysts of olivine.

Amagi Volcano. This occupies the extensive area, south of the Itô district, and consists of a central main body and a number of parasitic volcanoes. The main body is a maturely dissected volcanic cone truncated at its top with a ring-wall surrounding an explosion-caldera, 6 km. in diameter. The highest peak in the ring-wall rises to an elevation of 1405·3 m. above sea level. The main body is built up of alternating layers of pyroclastics and lava-flows of two-pyroxene-andesite consisting of phenocrysts of labradorite, hypersthene, and augite, scattered through an aphanitic groundmass. The pyroclastics ejected at the beginning of eruption of the volcano often carry the fragments of the rocks of the basal Tertiary complex.

The parasitic volcanoes on the flanks of the main body are not much dissected. According to J. Suzuki[7], they may be divided into following three groups, each one of which represents a distinct stage of eruption :

(1) The parasitic volcanoes of the first stage are the nearest from the centre of the main body, except the one situated in the centre of the caldera, lying near the upper margin of the ring-wall around the caldera. The rocks of these volcanoes are petrographically similar to those of the main body. The one situated in the centre of the caldera may be regarded as the central crater-cone, being built up of hornblende-bearing two-pyroxene-andesite.

(2) The parasitic volcanoes of the second stage are arranged parallel with the circular outline of the caldera on the flank half-way down of the main body. The rocks of them are generally olivine-two-pyroxene-andesite.

(3) The parasitic volcanoes of the third stage are the farthest from the centre of the main body. These are the basaltic volcanoes, Oomuroyama, Komuroyama, etc. in the Itô district, which will be described later.

The Amagi volcano is contemporaneous with the Atami volcano in the age of formation ; while the former continued its activity on its flank after the latter had become extinct.

The northeastern flank of the Amagi volcano terminates in a fault trending S.E.—N.W. through Yawatano. The northwesterly extension of this fault is indicated by a deep valley with a straight course toward northwest. This fault, with another which represents probably the southerly extension of that fault traversing the Atami volcano bound respectively the southwest and west sides of a depressed area, the hill-land in the Itô district. All of J. Suzuki's "parasitic volcanoes of the third stage of the Amagi volcano" are located within this depressed area, and represent the last stage of the volcanic activity in the Idu peninsula. Thus, they may be treated of as a distinct and separate volcano group, Oomuroyama volcano group, from the parasitic volcanoes of the Amagi volcano ; though the rocks of all of these volcanoes may be comagmatic.

Oomuroyama Volcano Group. The volcanoes assigned to this are :

1. Umenokidaira volcano
2. Jôbosi volcano

---

7) J. Suzuki, *loc. cit.*

3. Komuroyama volcano
4. Oomuroyama volcano

A structural characteristic, common to all of these volcanoes, is that they are generally built up of lava-flows effused in earlier stage and pyroclastics ejected in later stage of their respective volcanic activity. Besides these volcanoes, there is a scoria-bed, Itô scoria-bed, in the vicinity of Itô, which is without prominent point of eruption. The chief characteristics, morphological as well as structural, of each of these volcanoes are given below in the order from older to younger.

1. Umenokidaira volcano. This volcano, the oldest of the Oomuroyama volcano group, situated at about 2 km. south of Itô, is a composite one, consisting of double homates—a somma and a central cone—and is built up of lava-flows overlain by a thick accumulation of pyroclastics.

The top of the somma is truncated with a ring-wall surrounding an oval caldera, the major and minor axes of which are 1·5 km. from N.N.W. to S.S.E. and 0·8 km. from E.N.E. to W.S.W. respectively. The crest line around the ring-wall is the highest in the southeast part where it rises about 90 m. above the bottom of the caldera, and becomes lower northwestward. In its northwestern part there is a great gap which is concealed under the northwestern flank of the central cone.

The eastern flank of the somma shows a smooth conical outline, terminating in sea-cliffs varying in height from 10 m. to 50 m. above sea level. When viewed from a distance east of this volcano, the flank of the somma exhibits a gentle upward slope and a smooth upper margin of the ring-wall at the top, 270 m. high above sea level (Fig. 3). The northern and southwestern flanks of the somma are covered with the lavas of the later volcanoes, Komuroyama and Oomuroyama, respectively. The northwestern flank of the somma is represented by a range of hills extending northwestward for a distance of 1·5 km., forming as a whole a broad fan-shaped stretch of lava-plateau. The undurated flowing outline of the range is broken by a

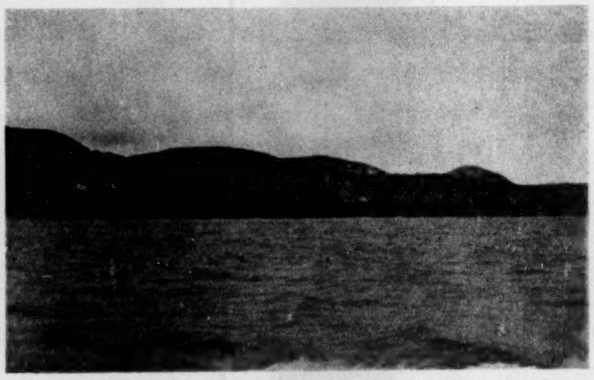

Fig. 3.—Umenokidaira volcano viewed northwestwards from the sea off the shore of Huto. Conical prominence in the right is the Komuroyama volcano.

prominence near the Ooiké lake. This prominence is a remnant of the northwestern wall of the nearby conical depression, 100 m. across and 30 m. deep, which is an explosion-crater buried under the later ejecta.

The central cone is about 70 m. in height above the bottom of the caldera and has a ruined crater at its top.

The whole area of the volcano—somma and central cone—is covered thickly with stratified beds of pyroclastics of all grades, viz. ashes, sands, lapilli, and bombs. These beds are underlain by lava-flows, as can be seen on the sea-cliffs at the eastern foot of the volcano and also in the valleys on its northwestern flank.

The rocks of the volcano are olivine-two-pyroxene-andesite and olivine-basalt. They often contain sporadic crystals of quartz and hornblende, probably xenocrysts derived from a hornblende-dacite, the presence of which at the base of the volcano is inferred from numerous hornblende-dacite blocks locally commingled in the pyroclastics of the volcano.

Resting on the southwest flank of the volcano, there is a parasitic volcano called Takamuroyama, 100 m. in height above the slope of the former. It consists of twin volcanic cones, the summits of which are so closely united that they make but one cone, and is built up of pyroclastics of basaltic nature. The northwestern half of this parasitic cone was blown away and the disrupted cone-materials spread down northwestward.

At a distance of about 1·5 km. southwest of Takamuroyama, there is another parasitic knob built up of the same materials as those of Takamuroyama.

These parasitic cones are surrounded by the lava-flow of the later volcano, Oomuroyama, and are more or less covered with the latter so that practically nothing is known of their relationship to the somma.

2. Jôbosi volcano. This volcano, about 1·5 km. south of Itô, lies on the back slope of the old mass composed of the two-pyroxene-andesite of the Atami volcano. It does not form an outstanding volcanic cone, but rather a plateau built up of a lava-flow overlain by repeated layers of volcanic ashes, sands, lapilli, etc. (Fig. 4). Its crater, located at the place called Jôbosi, is a circular dish-like one, 400 m. in diameter and about 50 m. in depth below the highest point of the wall surrounding it. Sections of the crater-wall show that it is composed of brown-colored scoriae.

The lava flowed out of a vent, probably represented by the crater at Jôbosi, and spread westward to form a lava-plateau with a gentle

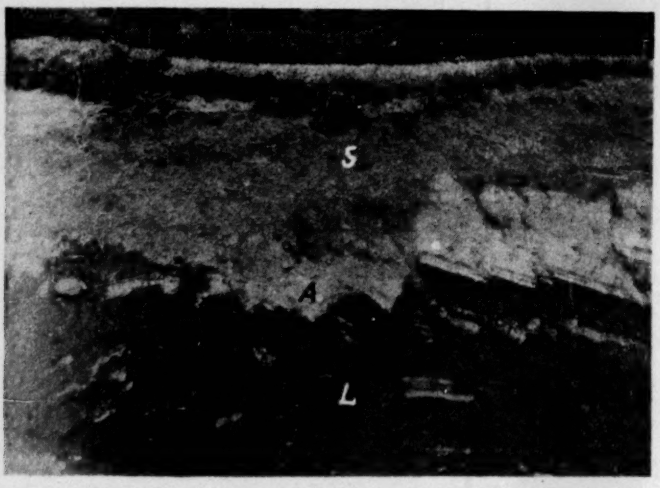

Fig. 4.—Pyroclastic accumulations of the Jôbosi volcano, traversed by minor faults. S-Subsoil; A-Ashes; L-lapilli.

westward dip. An off-shoot of the lava-flow run northward through a gap between the old masses and reached the valley in which the town of Itô is located. To the east and south, the lava-flow was stopped its advance by the old mass gradually elevated to these directions.

The rock of the volcano is a fine-grained basalt with abundant phenocrysts of olivine.

3. Komuroyama Volcano. This volcano, about 1 km. northeast of the Umenokidaira volcano, is a cinder-cone underlain by an extensive lava-sheet, morphologically representing an aspi-conide (Fig. 5).

The cinder-cone, about 150 m. in height above the surface of the lava-sheet or 321·2 m. in height above sea level, is built up of scoriaceous lapilli often associated with bombs exhibiting a spiral twist of plastic lava. At its summit there is a ruined crater, 20 m. across and 5 m. deep.

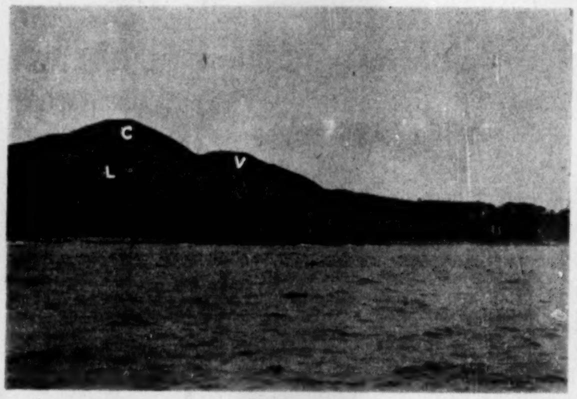

Fig. 5.—Komuroyama volcano viewed northwestwards. V-lava-mound showing the centre of eruption of the lava-flow; L-lava-flow; C-cinder cone.

The lava-sheet occupies a wide area around the

cinder-cone. It shows an uneven surface, "malapais" in Mexican term, the lava being broken into blocks that piled together in confused heaps. However, it is noted that the lava-sheet consists of several well-defined lava-streams which, flowing out in succession, were piled one on another, and that on each one of these lava-streams the lava-blocks piled in wave-like ridges, whose crests are 20–30 m. high above their troughs, probably resulting from pulsatory flowing of the lava.

The lava-sheet has an upward slope toward the cinder-cone and disappears beneath the covering of the latter. Near the northeastern foot of the cinder-cone there is a rugged lava-prominence, 270 m. in height above sea level, representing the place where outwelling of the lava took place, although there is no visible vent from which the lava proceeded. From this place outward the lava extended over the adjacent old land-surface. To the south and west it spread over the northeastern flank of the Umenokidaira volcano, and to the north over the mass composed of the products of the Atami volcano. To the east it reached to the sea, terminating in sea-cliffs.

The rock of the Komuroyama volcano is petrographically olivine-basalt. It is black, compact or scoriaceous, containing conspicuous phenocrysts of plagioclase and less conspicuous ones of olivine scattered through an aphanitic groundmass. It is to be noted that the lava contains sporadic crystals of quartz and that the plagioclase-phenocrysts (andesine) are more sodic than the plagioclase microcrysts (bytownite) in the groundmass. The plagioclase-phenocrysts, together with the quartz-crystals found in the lava, may be xenocrysts probably carried from a dacitic rock whose existence at the base of the Umenokidaira volcano was already inferred.

4. Oomuroyama Volcano. This volcano, about 1·5 km. southwest of the Umenokidaira volcano, is a composite one consisting of a lava-sheet and a cinder-cone properly called Oomuroyama which stands near the centre of the lava-sheet. It is similar in structure to the Komuroyama volcano, morphologically corresponding to an aspi-conide (Fig. 6).

Near the north eastern foot of the cinder-cone, there is a lava-mound, 50 m. high above the surface of the surrounding lava-sheet, representing the centre of extrusion of the lava. Its top is an uneven lava-field with circular outline, about 200 m. in diameter, where small eminences of lava-blocks surround a central depression (Fig. 7).

The lava-sheet is formed by several successive lava-flows, showing a downward slope in all directions from the lava-mound. The lava-flows extended outward, seeking the lowest part in the old land-surface. To

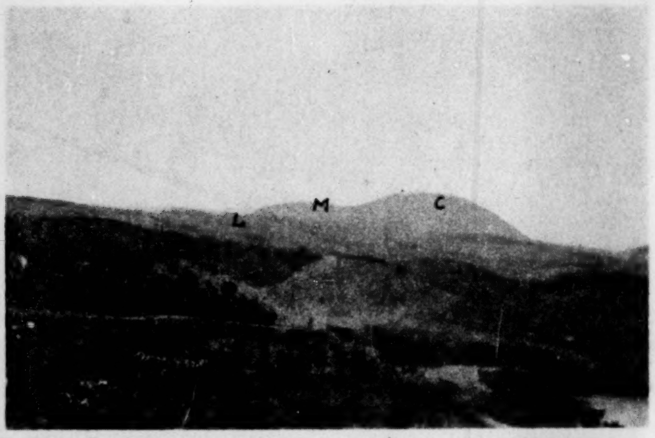

Fig. 6.—Oomuroyama volcano viewed southwards from Ooiké. M-lava-mound; L-lava-flow; C-cinder cone.

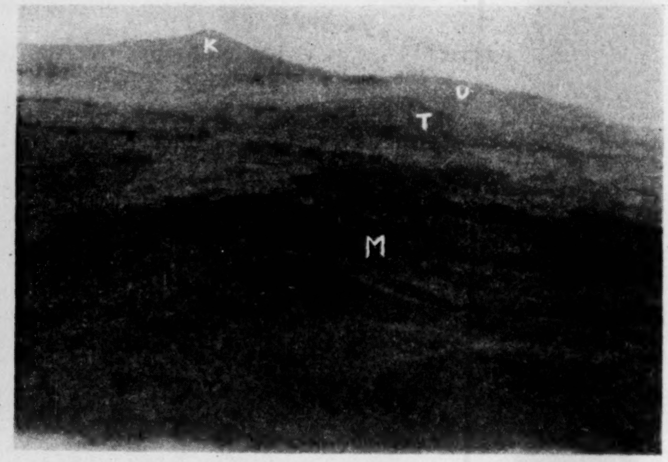

Fig. 7.—Top (M) of the lava-mound, (V in Fig. 6) looking down from the summit of the cinder-cone (C in Fig. 6) K-Komuroyama; U-Umenokidaira volcano; T-Takamuroyama.

the south and west the lava was prevented its advance by the scarps in which the northeastern foot of the Amagi volcano terminates, so that it spread eastward as well as northward, forming a lava-field nearly as wide as long. The lava run northward into the valley between the Umenokidaira volcano and the propylite mass overlain by the southern mass of the Atami volcano, and flowed as a narrow stream terminating in a thin edge. In one place the lava formed a dam which held the water in check and gave origin to the Ooiké lake. The lava extended eastward

over the southern slope of the Umenokidaira volcano, terminating in the southeast direction in a sea-cliff, 10–15 m. in height, along the coast from near Huto to Yawatano; while it may have extended more widely southeastward in the sea.

The surface of the lava-sheet is fresh in appearance and shows no trace of water-ways, indicating its original topographic feature. It is an uneven field of lava-blocks piled together in confused heaps with intervening depressions. There is no regular arrangement of them. Many of the minor irregularities of the surface of the lava-sheet may be attributed to the unevenness of the old land-surface over which the lava spread.

The cinder-cone, 200 m. in height above the surface of the underlying lava-sheet, or 581 m. in height above sea level, is a truncated cone, regular in form, with smooth flank whose slope is about 30°. At its summit there is a funnel-shaped crater, 300 m. across and 100 m. deep, floored with lapilli. The rim of the crater, in common with the entire surface of the cone, is covered with black scoriae, the larger fragments being about 10 cm. in diameter. A flank opening is seen on the southeastern slope of the cinder-cone.

The rock of the Oomuroyama volcano is olivine-basalt containing a few megascopic phenocrysts of plagioclase and olivine. It is to be noted that, as in the rock of the Komuroyama volcano, sporadic crystals of quartz are seen in the rock of this volcano.

Itô Scoria-bed. Extending over the ridges in the territory of the Atami volcano, which bound the Itô plain on the west, and also over the hills south of the Itô plain, there is a wide area covered with scoria-bed which is without prominent point of eruption. On the smooth ridges, west of the Itô plain the scoria-bed is separated from the underlying rocks of the Atami volcano by a soil-bed containing stumps of trees which once covered the latter; and on the hills, south of the Itô plain it rests on the lava-flow of the Jôbosi volcano and on the masses older than the latter. Accordingly, it is certain that the ejection of the scoriae is later than that of the lava of the Jôbosi volcano.

The scoria-bed shows indistinct layers and varies in thickness from a few meters at certain places on the border of the area covered with it, to over twenty meters on both sides of the Itô plain without, however, revealing its maximum vertical extent. It is cut by numerous minor faults, downthrow sides of which lie on the side of the Itô plain, a downthrow block of the scoria-bed, bounded on its southeast and

northwest sides by faults running in N.N.E.—S.S.W. direction. The downthrow block is covered with the alluvial deposit and may be genetically related with the hot-springs distributed in the plain. At Oka, the southern suberb of the town of Itô, the fragments in the scoria-bed vary in diameter from a few centimeters to over thirty centimeters and are piled without regular order of succession. It is inferred that, while there is no prominent point of eruption, the centre of eruption of the scoriae may not be very far from this place.

The scoriae are black or brown in color and are basaltic, containing sporadic phenocrysts of bytownite and olivine.

Summary and Conclusions.

As far as the visible parts are concerned, the geologic history of the Idu peninsula dates from the latter half of the Tertiary period. Its earliest time is represented by the volcanic activity which caused the eruption of a large quantity of the so-called propylite lavas associated with the interstratified pyroclastic materials. At the close of the Tertiary period there occurred again a great volcanic activity by which various rocks of two lineages—andesitic lineage and rhyolitic lineage—erupted alternately. At the same time the pyroclastic materials accumulated in the sea forming tuffite, tuff-breccia, etc.

After the cessation of this volcanic activity, the volcanic tract in the present Idu peninsula was subjected to crustal movements, generally in the sense of uplift.

The Diluvial volcanic activity took place on the eroded land-surface of the Tertiary volcanic tract, and constructed the gigant central volcanoes—Daruma, Atami, and Amagi—in which the andesitic rocks have been erupted in the order : two-pyroxene-andesite, olivine-bearing two-pyroxene-andesite, and olivine-two-pyroxene-andesite.

At the closing stage of this volcanic activity, the crustal movement culminated in dislocating the Diluvial volcanoes and in forming the general outline of the peninsula. The Atami volcano was cut into two by a north-south fault, the greater part of its eastern downthrow side being submerged. The southern side of this volcano was again segmented into two halves, north and south. The great tectonic trough including Tanna basin traversing from north to south the western flank of this volcano may date back in its appearance to this stage. The Amagi volcano was also cut at its northeastern skirt by a N.W.—S.E. fault.

The fourth and the last volcanic activity in the Idu peninsula occurred in the depression formed by the crustal movement at the northeastern foot of the Amagi volcano, and formed the basaltic volcanoes of the Oomuroyama volcano group. The Itô earthquakes occurred in the sea, immediate northeast of the land occupied by this volcano group.

All the volcanoes in the Oomuroyama volcano group are arranged in lines with some regularity, probably indicating the structural pattern of the ground on which they rest. There are two systems of the arrangement of these volcanoes, as can be seen on the annexed geologic map. One of them is represented by a distinct linear arrangement of the four volcanoes—Oomuroyama, Takamuroyama, Umenokidaira, and Komuroyama. These volcanoes mark a bow-shaped line extending in S.W.—N.E. direction from Oomuroyama to Komuroyama. The oldest volcano, Umenokidaira, is in its central part, and the youngest, Oomuroyama and Komuroyama, in the extremes. This is a remarkable example of the well-known fact that volcanoes are frequently located on fissures and that when one conduit becomes closed others are opened along the same line of fracture. The other one of the two systems of structural lines is represented by the two volcanoes—Komuroyama and Jôbosi—together with the assumed centre of eruption of the scoriae distributed in the vicinity of Itô, which mark a straight line in the S.E.—N.W. direction.

Although there are a great number of faults in the Itô district, no one was ascertained to have caused the earthquakes in Feb.-May, 1930. According to N. Nasu, the seismic foci of the Itô earthquakes, with a few exceptions "were confined to a narrow, conical region with its base, a circle of about 2 km. radius, on the sea-bottom in the inlet of Itô and the apex of this inverted cone some 6 km. below it". This conical region lies on the north-northeasterly extension of the volcano-structural line represented by the linear arrangement of the four volcanoes—Oomuroyama, Takamuroyama, Umenokidaira, and Komuroyama. These facts led the present writer to consider that the Itô earthquakes are probably the surface manifestation of a crypt-volcanic activity which took place at a depth, less than 6 km. below the sea bottom, of the earthcrust along the same line of fracture as that on which the activities of the youngest volcanoes, Oomuroyama and Komuroyama, occurred.

---

8) *loc. cit.*

20. 伊豆伊東地方の地質構造に就いて

地震研究所 津屋弘逵

先づ伊豆半島全般の地質を略述し、次に伊東地方の地質構造を論じた。

伊東地方の地質構造を研究せる結果、伊東地域には昭和五年二月より同年五月に亘つて起つた伊東地震と隨伴關係があると考へられる活斷層は見出されなかつた。天城火山の北東側第三次側火山と考へられてゐる大室山、小室等の火山群は熱海火山、天城火山等が斷層運動を受けて後に形成され伊豆半島に於ける最後の火山活動を代表するものであつて、その中大室山及び小室山火山の如きは最近地質時代に形成されたものである。この火山群に屬する火山は北東一南西、北西南東の二方向に配列し、地下にこの二方向の火山構造線の存在を示してゐる。大室山、高室山、梅ノ木平、小室山の四火山を結ぶ北東一南西の一線は殊に著しい。伊東地震の震原地域はこの線の北東延長上にある。この事實及び那須學士の研究された伊東地震々原の立體的分布より、伊東地震は伊豆半島に於ける最近の火山活動の行はれた大室山一小室山火山構造線の北東延長線に沿うて行はれた潜在火山活動を示すものと考へられる。

GEOLOGIC MAP OF ITÔ, IDU.

By Hiromichi Tsuya, 1930.

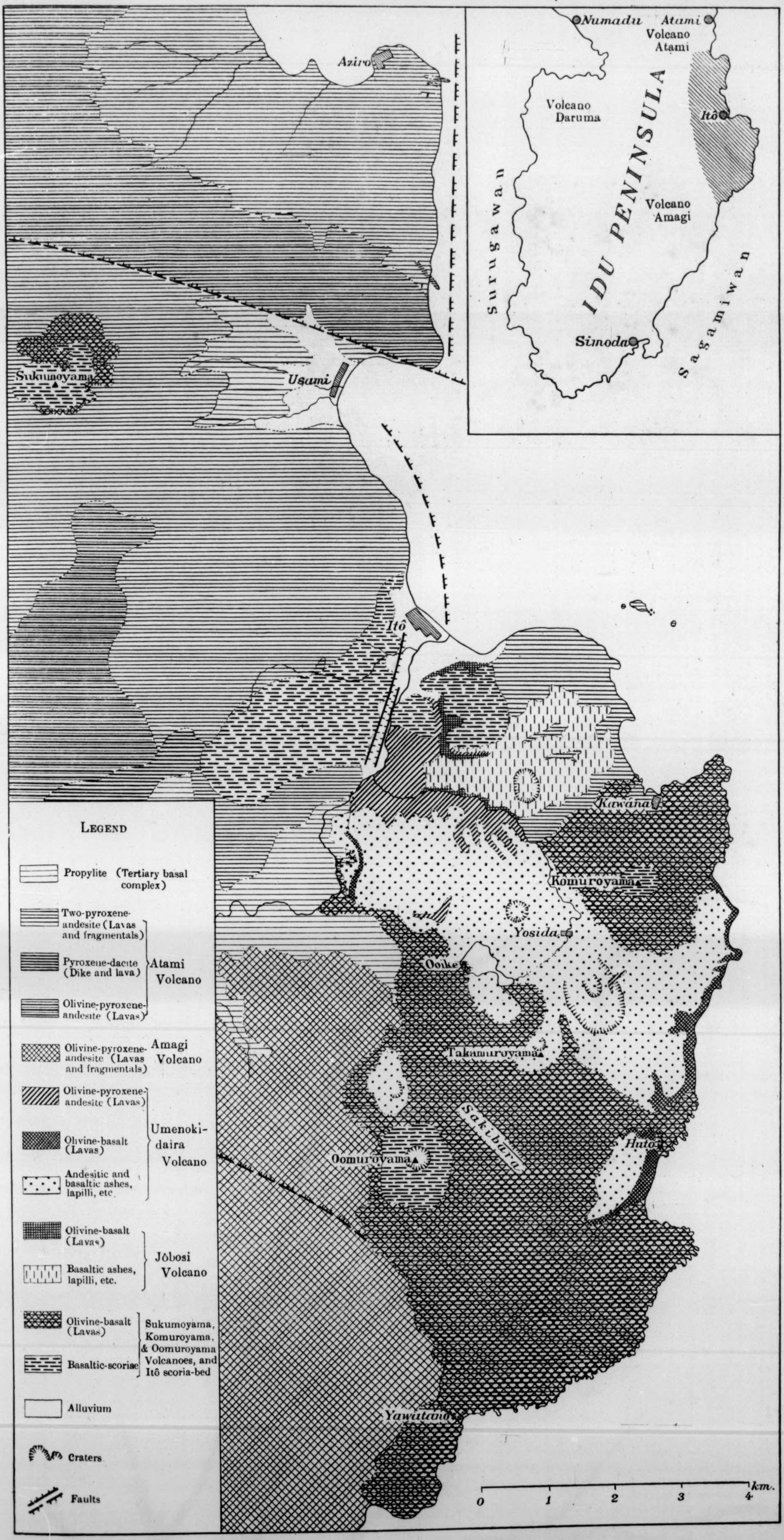

(震研彙報、第八號、圖版、津屋)

21. 伊東地震と地表傾斜變化の觀測

地震研究所 石本巳四雄
高橋龍太郎

(昭和五年九月二十日受理)

第一部 伊東及川奈に於ける觀測

I. 緒言

日本に於ける著名なる温泉地の一つである靜岡縣田方郡伊東町を中心とする地方は、昭和五年(1930年)二月十三日以後、約三ヶ月に亙つて數千回の地震に見舞はれたのである。

此の頻發性地震の經過は第一圖によつて、其の大體を窺ひ知る事が出來る。此圖は岸上冬彥氏の調査[1]に據るものであつて、地震回數は三崎に於ける百二十倍の地震計の記錄に據つて實動一ミクロン以上の振幅を有するものを數へたものである。此の數は大體、伊東町に於ける有感地震の回數と見做して差支ない。[2]

第一圖に於いて見らるゝ如く地震は明瞭に二つの活動期に分れて發生してゐる。第一の活動期は二月十四日に初まり四月十日頃に終るものであつて、三月九日に於て日々の地震回數は最大に達したのである。第二の活動期は五月八日頃より同月廿二日頃に到るものであつて、日々の地震回數は十日に最大に達してゐる。此等の地震の活動は間歇的であつて、平穩なる時には一時間中に一の地震をも發せざるに反し、活動時中にあつては、一分置き或は卅秒置きに相當の有感地震を發生したのである。此の活動の時刻は或時期に於いては潮汐の干潮時と可成りの程度に一致してゐた事は今村敎授の既に指摘せられたる所である。[3]

伊東に於いて感ぜられる地震は、性質急激なれども總震動時間短く、

---

1) 東京帝國大學地震研究所、同理學部地震學教室「伊東地震に就て(第二報)」地震 2 (1930), 293—300; 岸上冬彥「三崎に於ける伊東地震の觀測 (續き)」地震 2 (1930), 502.

2) 東京帝國大學地震研究所、同理學部地震學教室「伊東地震に就て」地震 2 (1930), 290.

3) 東京帝國大學地震研究所、同理學部地震學教室「伊東地震に就て(第二報)」地震 2 (1930), 292.

數回の主要動にて地震が終結する爲め、加速度の割合には建造物の受けた被害は僅少であつたのである。

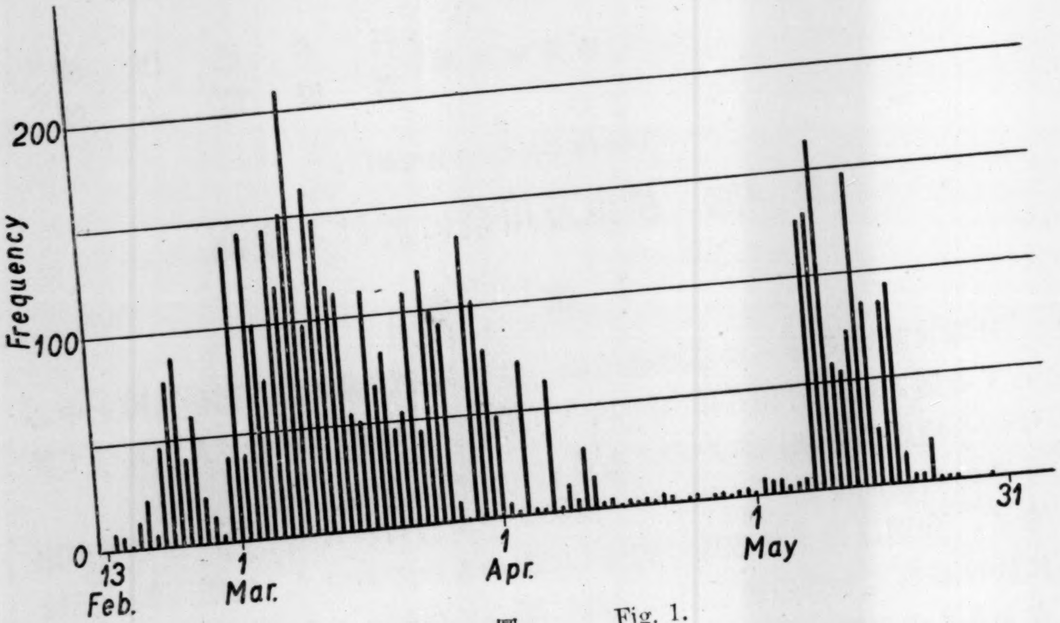

第 一 圖　　Fig. 1.

此等の地震に伴つて何等著しき地變の發生が氣づかれなかつた爲め、假令其の間の强震程度の地震は、數十粁を隔てたる東京に於ても尙數ミリメートルの振幅を與へたとは云へ、若し頻發性と言ふ事がなかつたならば或は特に吾〻の注意を惹かなかつたかも知れない。

此の種の頻發性地震は古來無かつたのでは無いが、伊東地震の場合は特に其の大きさに於て、又數に於て著しきものであり、地震現象の研究上、種〻の新しき事柄を明にすべく興味あるものであつたのである。地震研究所に於ては、此の地震の發生と共に伊東地方に二箇所に地塊の傾斜運動の觀測所を設置し、地震學教室との協力により震央を取卷く五ヶ所に地震計を設備して震原の分布を仔細に觀測し、[4] 又陸地測量部、[5] 海軍水路部に委托して海底及陸上の地形變動の詳細なる測量を爲したのである。

4)　東京帝國大學地震研究所、同理學部地震學教室「伊東地震に就て(第一報)」地震 2 (1920), 215—220;「伊東地震に就て（第二報）」地震 2 (1930), 281—300.

5)　「伊豆東海岸に於ける水準測量成果報告」地震研究所彙報 8 (1930), 375−376.

以下は此等研究事項の一つである、伊東地方に於ける地盤の傾斜變化の觀測に就いて述べるものである。

II. 器械及び其の設置

今回の地盤の傾斜變化の觀測に用ひたる器械は、熔融水晶製傾斜計[6]である。此は枠組も可動の水平棒も、又其をツエルナー型に吊す所の二本の細糸も悉く熔融水晶を以て製作されたる水平振子である。水晶糸と枠組及び水晶糸と可動水平棒との接合部は悉く熔接して製作されてあつて、水平振子を成す部分には熔融水晶以外の何等の物質も使用されてゐないのである。熔融水晶は熱に對する膨脹率極めて僅少であり、且又彈性後效果現象の殆ど無き物質なるを以て、此の如くして製作されたる水平振子傾斜計は、温度の變化に對して充分不感であり、且又地盤の傾斜位置が元に還りたる時には、傾斜計の偏位も亦舊に復して實際上ヒステリシスの現象を示さないのを特長とする。

此の熔融水晶製の水平振子は不銹鋼より成る精密なる螺子を有する三脚臺の上に載せられ地面の上に設置せられる。水平振子の傾斜に對する感度は自己振動周期の自乘に比例するものであるから、三脚臺の螺子を廻して振子の自己振動周期を適當に調整する事に依つて任意の感度を得る事が出來る。此の比例常數を定むる爲に傾斜計は一臺毎に檢定(Calibration) を爲してある事は勿論である。

可動水平棒の中央には焦點距離 50 cm. 直徑 5 mm. の小凹面鏡が取付けてある。記錄部分の下部にある小電球よりの光束を此の凹面鏡より反射せしめ、途中一枚の圓筒レンズを通じて光束を集注せしめ、ブロマイド寫眞紙上に光點を結ばしめる。地盤が傾斜する時は水平振子の可動水平棒は回轉する故にブロマイド紙上の光點も動いて傾斜變化を記錄するのである。ブロマイド紙は回轉圓筒上に卷付けてあつて一週間に一廻轉する。記錄速度は一日四糎になつてゐる。此の如き傾斜計二個を以て一組となし、傾斜變化を東西及南北の成分に分解して記錄せしめる。

從來の傾斜計に於ては小電燈は蓄電池に依つて不斷に點燈されてあつたのであるが、今回使用の傾斜計に於ては此點に改良を施して從來時間標の記入に用ひたる時計裝置によつて一時間毎に一回、電路を閉ぢて二

---

6) M. Ishimoto, "Construction d'un pendule horizontal de quartz et observations sur les variations de l'inclinaison de la surface terrestre," *Jap. Journ. Astron. Geophys.*, **6** (1928), 84.

M. Ishimoto, "Observations sur les variations de l'inclinaison de la surface terrestre," *Bull. Earthq. Res. Inst.*, **2** (1927), 1.

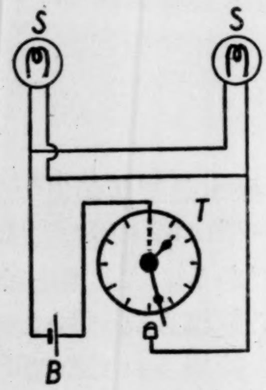

S……光源小電球
T……水銀斷續裝置付時計
B……乾電池

第二圖 Fig. 2.

分間宛點燈する事とした。東西及南北の成分に對する器械各個の小電球は第二圖の如き配線によつて並列に結がれ、同時に點滅する様になつてゐる。

此の改良によつて時間標を細かく記入する事を得、且又電源として一箇の乾電池を使用して約二ヶ月間觀測を繼續し得る事になつた。

此の如き裝置の傾斜計によつて得られたる記錄の一例として第三圖(圖版)に、四月廿六日より五月二日に到る期間の川奈の東西及南北兩成分の記錄を示してある。光源の間歇的點燈によつて、傾斜變化を示す曲線も據準を爲す直線も點々として記錄せられて居るのである。

伊東觀測所

伊東に於ける傾斜計は三月十一日に据付けられ、翌十二日より使用せられた。器械設置の場所は伊東町字廣野にある、小丘陵の麓、天然の火山礫岩層中に穿たれた横穴である。穴の大きさは間口約二米突、奧行約二米突、高さ約二米突半にして、東側に高さ二米突弱、幅八十糎の入口を有する。平常は物置として使用せられてゐたものである。穴の内面は何等の壁塗も爲さず掘鑿のまゝのものであつて乾燥し、床には天然の岩層を露出してゐる。器械は此の床上に直接に据付けられ、其の方向は正しく東西及南北に向けられた。器械の感度は一秒の傾斜變化が記錄紙上に一粍の偏れとして現れる様に調整した。此の感度は觀測の期間中變化なかつた。

此の横穴は入口に扉の設備を缺いてゐたので蓆を吊して扉の代用とした。横穴内に於ける器械の設置の方向は第四圖に於て見られる。

伊東に於ける傾斜計は三月廿二日の强震によつて南北成分の水平振子の水晶吊糸が切れて破損し、東西成分の水平振子は方向を狂はされた。此等は廿三日正午に到つて据付直し破損したものは新しき器械と換へられた。但し感度は前と變化なく調整された。

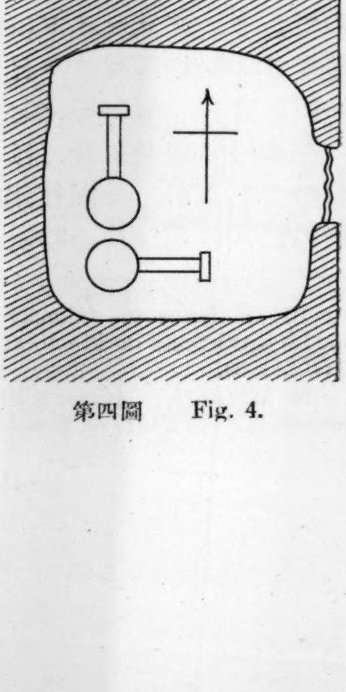

第四圖 Fig. 4.

川奈觀測所

伊東に於ける傾斜計の据付後一週間程の間に、伊東附近に發生する地震の震央區域が、地震計による五點觀測の結果漸次に明瞭となり、其等の地震の最多數は直徑約二粁に過ぎざる小區域內に震央を有し、其の震原の深さも餘り深からぬ事、其等の震央區域は伊東と、伊東の南に連る漁村川奈との間にある日蓮岬沖合なる事も判明するに到つた。從つて川奈に於ける地塊の傾斜運動も、伊東に於けると同樣地震發生と關係する所多きを知るに到つて川奈にも傾斜計を設置する事になつた。川奈に於ける傾斜計は三月十九日に据附けられ、翌十四日午前零時より使用せられた。

川奈に於ける觀測所の位置は川奈部落の西南を圍む急斜面の麓に現れてゐる天然の火山礫岩層中に穿たれたる橫穴であつて、穴の廣さは幅三米突、奥行二米突半、高さ約二米突半を算する。入口は略東南の方向を向き八十糎に五十糎程の扉を有してゐる。此穴は夏期捕獲せる魚類の貯藏に用ふるものである。穴の中は濕氣稍多く、雨天の時等天井より水滴の落ちる場合もあつた。穴は海面上の高さ約二十米突、海岸よりの距離約八十米突であつて、傾斜計は床上に直接に東西及南北の方向に据付けた。

傾斜計据付の當初は、川奈は伊東に比し震央區域により近く、地盤の傾斜運動も從つてより大ならんとの豫想の下に、傾斜計の感度を伊東のそれの二分の一、即ち一秒の傾斜が五粍の偏れとして記錄せらるゝ樣に調整したが、後に至つて、溫度の影響による日週變化全然なく、地盤の運動も豫想外に少にして且又海水の干滿によつて地盤の傾斜運動を惹起す現象が見らるゝ事に氣附き、四月廿一日に感度を從來の四倍、即ち一秒の傾斜が二糎の偏れとして記錄せらるゝ樣に調整し直した。而して觀測の期間中感度の變動は實際上無かつたと考へられる。

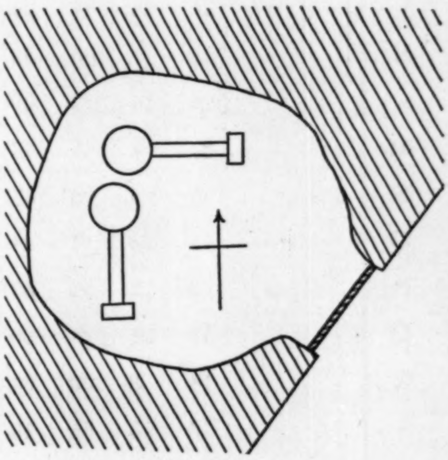

第五圖 Fig. 5.

川奈觀測所の穴の內の模樣は第五圖によつて大體を知る事が出來る。

川奈の觀測所の場所の撰定と、傾斜計の設置は岸上冬彥氏によつて爲

されたのである。又伊東町及川奈の傾斜計の取扱と管理に關しては牧野熈世氏、福本熊次氏及菊間勇氏の勞を煩はした。玆に岸上、牧野、福本、菊間の諸氏に厚く感謝の意を表する次第である。

伊東川奈兩觀測所の位置地形、地質等に關しては後出第十一圖及津屋所員の論文の挿繪を參照せられ度い。

III　觀測の結果

第六圖は、伊東及び川奈の第三圖に示せる如き記錄から各時に於ける傾斜曲線の偏位を讀み取つて、それを圖示したものである。同圖に於て、

第一表　東京に於ける有感伊東地震（保田氏による）

	Date					max. amplitude (2a)	Period
A	March	4	3^h	50^m	05^s	0·109 mm	0·7 sec.
B		4	5	11	17	0·500	1·1
C		9	4	39	53	0·224	0·7
D		9	19	54	49	0·538	0·9
E		13	4	29	45	0·128	1·1
F		14	14	18	41	0·093	1·1
G		14	21	5	30	0·040	0·56
H		15	18	34	04	0·218	0·7
I		19	10	16	57	0·207	1·3
J		21	23	04	24	0·170	1·1
K		22	17	50	52	1·280	1·0
L		26	14	22	59	0·422	1·5
M		27	1	41	47	0·433	1·2
N		30	0	06	37	0·072	1·3
O	April	1	23	4	44	0·248	1·1
P	May	9	12	52	50	0·159	1·1
Q		12	21	24	00	0·535	1·3
R		14	8	59	03	0·225	0·9
S		15	15	58	19	0·129	1·0
T		17	5	14	24	0·871	1·1

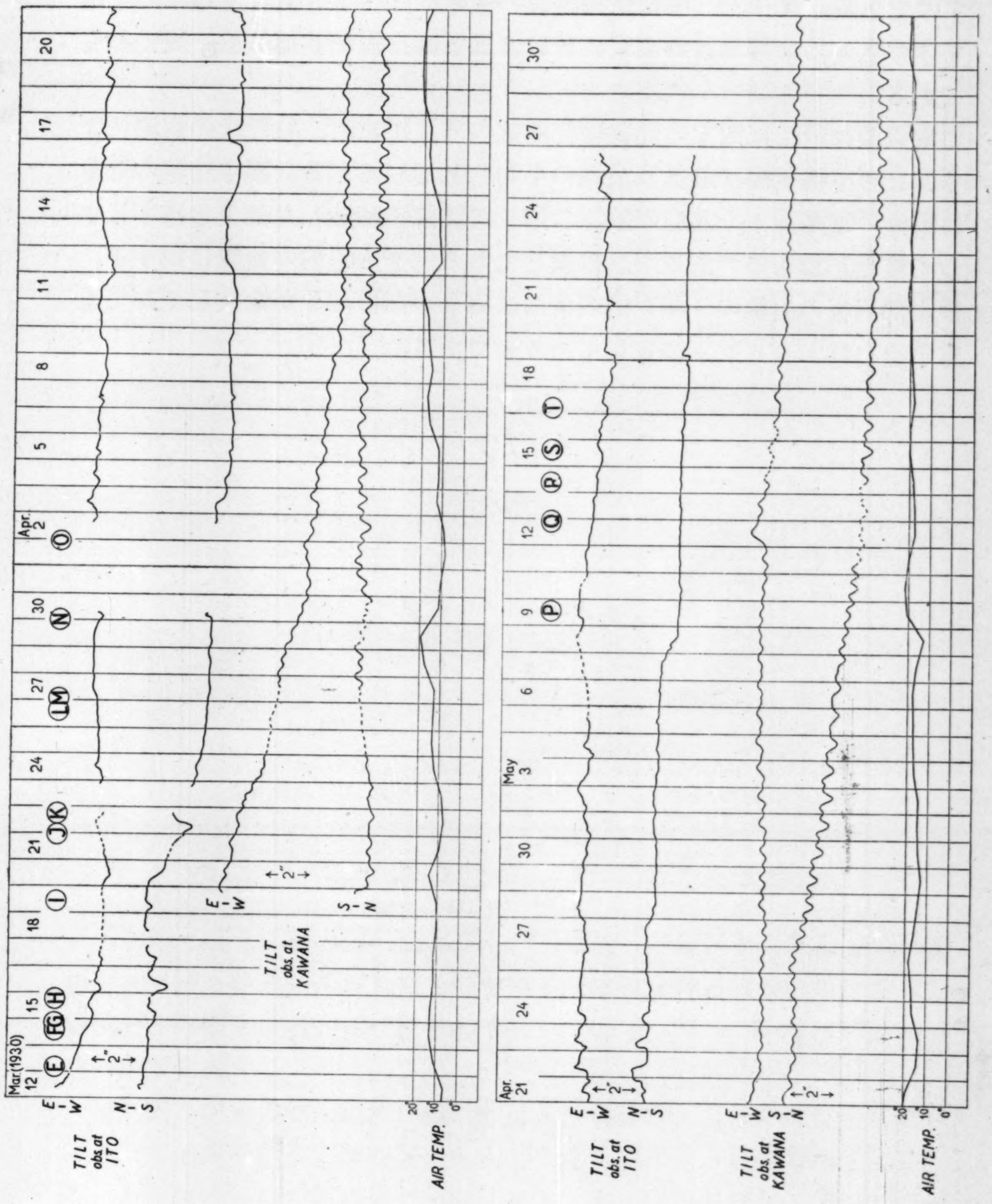
TILT obs. at ITO
TILT obs. at KAWANA
AIR TEMP.
E-W
N-S
S-N
Mar.(1930)
Apr.
May

第六圖 Fig. 6.

曲線が例へば W の方に片寄る事は、地盤が西下りの向きに傾く事を示すのである。又 E, F 等は伊東地震の中東京にても有感なりしものを示すのである。此等地震の東京に於ける發震時、震幅其他は第一表の如くである。

第六圖に於ては四本の傾斜變化曲線の外に伊東町、牧野氏の觀測による毎日の平均氣温（最低及最高の平均）を示してある。圖中點線の部分は電池の電壓降下、其他の故障に因つて記錄の缺除した部分を推定によつて連結したものであるが、缺損してゐる部より以前の曲線に對する、缺損部以後の曲線の、相互的の位置は假令中間の部分が缺損してゐても據準線の動かざる限り確定してゐるのである。

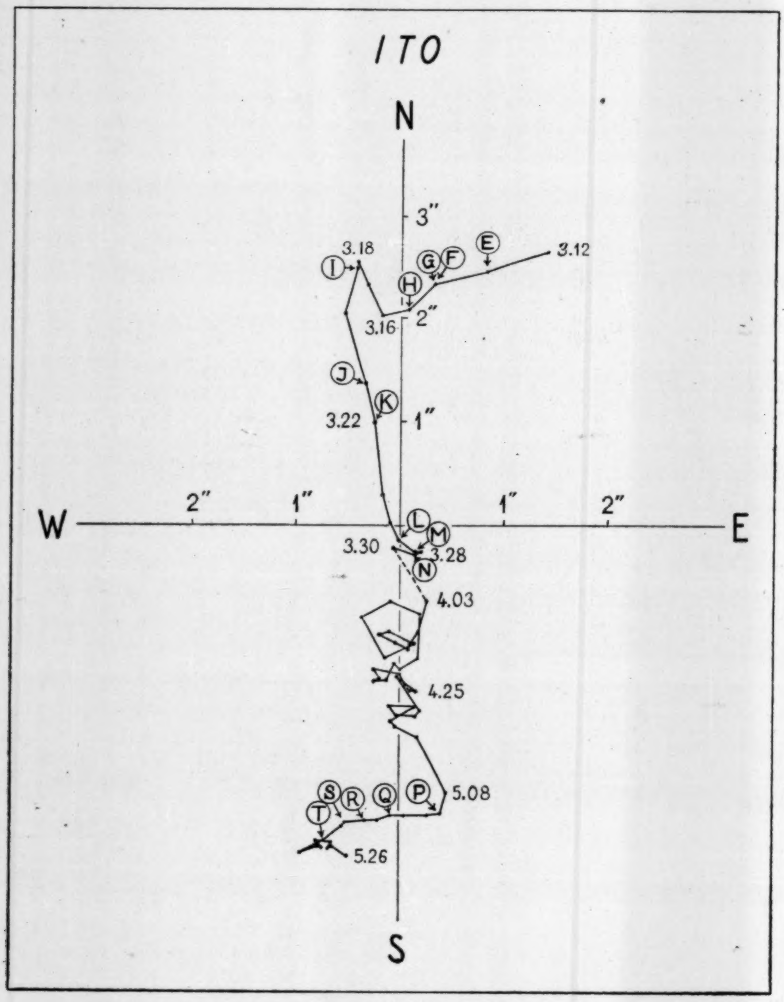

第七圖a　Fig. 7 a.

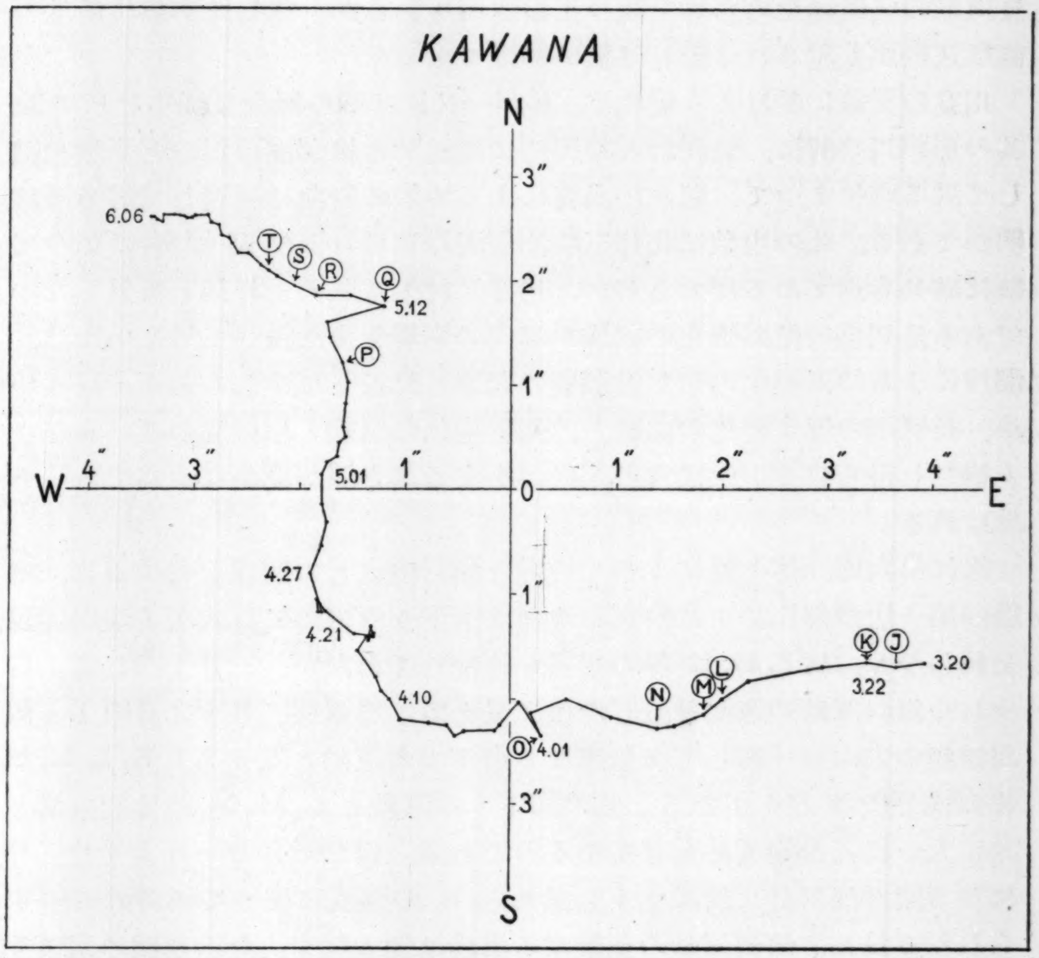

第七圖b　　Fig. 7 b.

第七圖a及bは第六圖の南北及東西の兩成分の偏位を合成して傾斜變化をヱクトル圖として表したものである。此圖を作るに當つては各日の偏位の平均値を其日の偏位値として用ひてゐる。又 **E, F** 等は前掲第一表の地震を表す。

第六圖の伊東の傾斜變化曲線に於ける小偏位は、氣溫の變化と日照熱によつて地面の極く表面の部分に歪を生ずる爲に起る日週傾斜變化である。此は穴の入口の簾の扉が不完全なりし爲太陽の光線が午前中穴の中に差込む爲に床面の溫度に不平均を生ずる爲であると考へられた爲め、三月の下旬より扉を完全にする事に依つて此の日週變化を大いに減少し得た。伊東の傾斜變化曲線は此の日週變化の外にも尙二三日間に亙る

長週期の氣溫變化の影響を被つてゐる所もあるが、然し此が爲に地塊の傾斜運動が蔽隱される恐れは無い程度である。

川奈の記錄に於ける小變化は、其が一日に二回の極大及極小を示す事、其の形が川奈灣に、傾斜計と略同時に設置せる檢潮儀の記錄と全然相似して居る事によつて、潮汐の負荷による地殼の彎曲に原因して居る事は明かである。此の現象は相模三崎油壺灣岸に於ける傾斜觀測に[7]依つて既に確められてゐる所であるが、川奈に於ても其の一好例を發見したのである。川奈の傾斜變化の記錄が溫度の影響を全然被つて居ない事は、潮汐による傾斜變化の形が檢潮儀の記錄と比較して少しも歪んで居ない事、長週期の溫度變化の曲線と、傾斜變化の曲線と相似點のない事等より推知し得られる。此は穴の入口の小なる事と扉が完全なる爲であると思はれる。

次に第六圖、第七圖によつて地震と傾斜變化との關係を考ふるに、地震の第一活動期に於ては伊東の地塊は西下りの方向に急速なる傾斜運動を爲しつゝ、E, F, G, H 等の强震を連發してゐたが、三月十四日頃から少しく傾斜運動の速度を減じた樣に見える。然る所三月十九日頃より傾斜運動の方向を一轉して又急速なる南下りの運動となり I, J, K, L, M, N 等の强震を連發してゐる。此の南下りの運動も L, M, N の地震發生と共に大いに其の速度を減じてゐるのである。但し三月廿一日より廿三日に至る間は傾斜計に故障ありし爲めと K の强震に因つて傾斜計破損せられたる爲め、傾斜運動の正確なる模樣は知り難く、此の期間の南下り運動は或は今少しく小であつたかも知れない。

伊東の地塊の傾斜運動の方向が E, F, G, H の諸地震の時には西下りであり、I, J, K, L, M, N の地震の場合には南下りである事を、那須信治氏の計測による其等地震の震原の位置と比較する時は興味深い事柄が判明するのである。

第八圖及第九圖は D, E, L, G, H の地震及 I, J, K, L, M, N の地震の震原の位置の東西垂直面への投影圖である。是に依つて見るに D, E, F, G, H の地震は一つの群を爲してゐて深き所より段々淺くなると共に次

7) R. Takahasi, "Tilting Motion of the Earth Crust caused by Tidal Loading," *Bull. Earthq. Res. Inst.*, 6 (1929), 85.

R. Takahasi, "Tilting Motion of the Earth Crust caused by the Secondary Undulations of Tides in a Bay," *Bull. Earthq. Res. Inst.*, 7 (1929), 95.

第に東方へ寄つて來てゐる。又 I, J, K, L, M, N の地震は他の一つの群を爲してゐて I, J の地震は深く K, L, M と次第に淺くなり北方へ片寄つて來てゐる。

卽ち D 以下の地震群と共に西下りの傾斜を爲しつゝあつた地塊は、新しき地震群 I, J, K, L, M, N の發生と共に南下りの傾斜運動に變化したと見得るのである。E, F, G, H の地震と I, J, K, L, M, N の地震と相異る群に屬する事、卽ち第一活動期が實際は二つに區別出來るのであつて、此の事は、第一圖の頻度圖に於ても、第一活動期の山を二つに分解し得る事からもいくらか想像し得るのである。

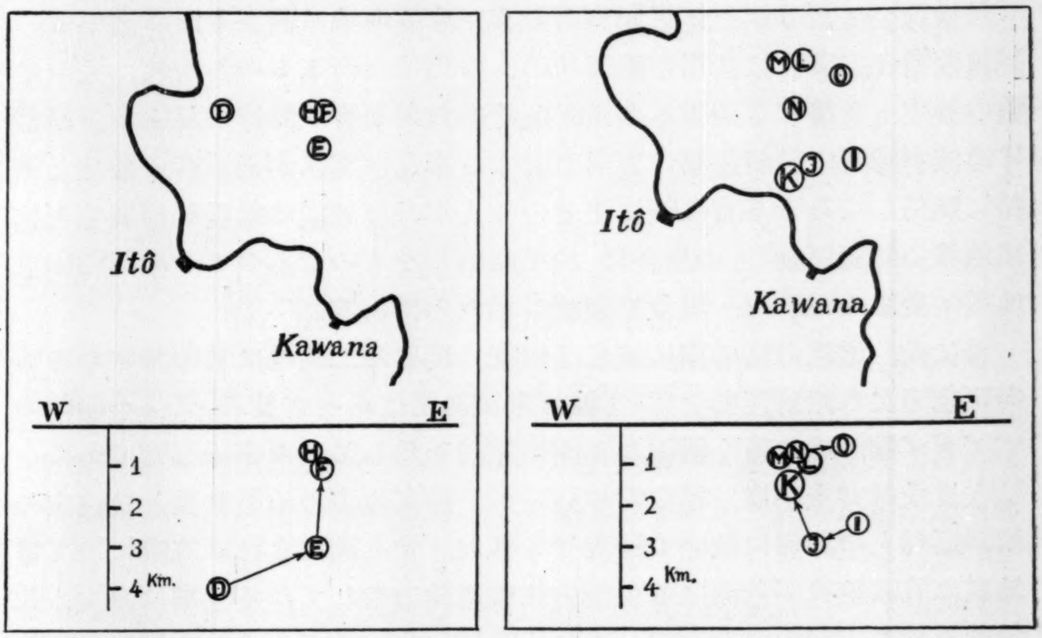

第八圖　Fig. 8.

伊東の地塊の傾斜運動は其後四月三日に到つて南下りの速度を減じ氣溫變化の影響と思はるゝ、逡々たるヂクザク狀或はループ狀の傾斜運動に入り、第一活動期の終塞する氣配を示した樣であつた。此のループ狀の運動は緩慢なる南下りの運動と重なつて第二活動期に入る直前迄續いてゐたのである。然る所五月七日に到り急に南下りの傾斜運動が急速となつて、再び活動の模樣を示し、八日第二活動期に入り、同時に傾斜運動は單純なる西下りと變つて、P, Q, R, S, T 等の强震を發生した。

而して第二活動期の終了と共に傾斜運動は再び緩慢なるヂクザク狀態に入つた。此等の有樣は第七圖 a に於て明瞭に認められる。

川奈の地塊も亦伊東の場合と類似の運動を示してゐる。卽ち、第一活動期の間は急激なる西下りの傾斜運動を續け、其間に J, K, L, M, N, O 等の强震を起してるが、四月十日に到り地震の鎭靜と共に傾斜運動は北下りの方向に變化して速度も緩慢となり、時に極く小さな振幅のヂクザク運動さへ爲す樣になつた。五月に入つて再び傾斜運動が速になつて間もなく第二の活動期に入り傾斜運動が西下りと變ると共に P, Q, R, S, T 等の强震を連發してゐるのである。此の傾斜運動も亦地震の鎭靜と共に遲々たるものとなつてゐる。此等の有樣は第七圖 b に明瞭に表れてゐて殆ど說明を要しない。

是に依つて觀るに、伊東觀測所の存在する地塊は西下り及び南下りの互に直角な二方向に、川奈觀測所のある地塊は西下りの方向に、夫々地震の發生と密接なる關係ある傾斜運動の方向を有する樣に見える。斯樣に地塊が特定の傾斜運動の方向を有する事及び其れが地震群の發生と密接に關係してゐる事實は旣に著者の一人が丹後地震の餘震群の發生と宮津地塊の傾斜運動[8]との場合に於て見出したものであつて、今回の伊東地震に於ても再び同一現象を觀測し得たのである。

兎に角、地震の活動期に於ては伊東、川奈の二地塊は其の特定なる方向に急速なる傾斜運動を爲し、鎭靜期に於てはループ狀の、又は小振幅のヂグザグ狀、或は極く緩慢なる傾斜運動を爲してゐた事は事實である。

なほ最近井上宇胤、杉山友紀兩氏が、[9] 關東地方の地震發生と筑波山の傾斜運動との關係に就いて發表せられた。井上氏によれば筑波に於ては地震は筑波地塊が急速なる東西の往復運動をなしてゐる時期に多く、比較的單純なる傾斜運動を爲してゐる時期に少いのである。今筑波、伊東、兩者の場合を考察するに、筑波と伊東とは地質に於て全く異なり、且つ筑波の傾斜運動は可成り震央の遠い地震及び震原の深い地震にまでも關係してゐるのであつて、數多くの地塊の聯絡狀態を初め、其他吾人の未

---

8) M. Ishimoto, "Constrnction d'un perndule horizontal de quartz et observations sur les variations de l'inclinaison de la surfsace terrestre," *Jap. Journ. Astron. Geophys.*, 6 (1928), 84.

M. Ishimoto, "Obervations sur les variations de l'inclinaison de la surface terrestre," *Bull. Earthq. Res. Inst.*, 2 (1927), 1.

9) 井上宇胤、杉山友紀「筑波山に於ける傾斜變化觀測報告」地震硏究所彙報 8 (1930), 346.

W. Inouye & T. Sugiyama, "On Preseismic Earth-tiltings observed at Mt. Tukuba," *Proc. Imp. Acad.*, 5 (1930), 457.

だ知り得ざる非常に複雜なるものが其間に介在してゐると考へらるゝのである。斯樣な場合を、伊東、川奈に於ける場合の如く非常に單純なる地塊運動と直ちに比較して、其の相違を云々する事は出來ない。吾々は寧ろ後に述べるが如き說明によつて其等が本質的には同じ事柄であると考ふるべきであらう。

尙、興味ある事柄は第六圖川奈の傾斜變化に於て、地震群中最强であつた K 地震を境界として、其の前後に於て傾斜運動の方向を少しく變ぜる事である。更に又 K 地震の後數日間は潮汐の負荷に依つて起る傾斜運動の振幅が著しく減少して居た事は注意すべき事柄である。

尙地震の發生と潮汐との關係、又地震、氣壓及地塊の傾斜運動間の相互關係、川奈における潮汐の記錄と此れによつて惹起せられたる地表傾斜變化の關係等に就いては後日稿を改めて發表する事とする。

（高橋）

第二部　伊東地震に關する考察

I. 緒　　論

伊東地震の經過に就いては已に二三の研究者[10]によつて發表されたものがあるから、此所に改めて詳述する必要はないが、此の地震の最も特長とする所は一般破壞的地震とは全く其の趣きを異にし、小地震續生を以て終始した事である。實際地震の出現する震央附近に於いて地殼變動を直接研究する事は最近開始された關係上、未だ實證の不足である事の非難は免れ得ない。幸に今回の地震に對して此等の方法が遺憾なく施行せられた結果地殼構造は元より、地震本質に對して一層進んだ議論をなし得る樣になつた事は事實である。

伊東地震發生の時間的關係は頻度曲線[11]の示す所によつて明かであるが、其の間多くの消長を示して居る。最も明瞭な事實として注意される事は二つの地震群に分けられる事である。第一群は二月中旬より四月初

10) 地震硏究所 今村硏究室、理學部地震學敎室　地震 2 (1930), 215, 281; 那須信治　地震 2 (1930), 301; 岸上冬彥　地震 2 (1930), 502; A. Imamura, N. Nasu, F. Kishinouye & C. Yasuda, *Proc. Imp. Acad.*, 6 (1730), 190.

11) 第一圖參照

旬に至るもの、第二群は五月中に發生したものである。此の外六月中にも多少群をなして發生したものが見受けられたが、其の數において以上の二群と全く比較し得る程度でない。地震群が如何なる原因により斯様な形式を以つて出現したかと云ふ根本的の疑問に對しては其の解答は恐らく不可能であらう。只小地震頻發原因が已に地下に具つて居り、且つ之れを出現せしむべき誘因は地表にも存在して居て、結局斯様な形式を生ぜしめたと考へる外に途はない様である。而して此の場合誘因として潮位と氣壓配置とを考へる事が出來る。

小地震の頻發に交つて勢力の大である地震の發生が行はれ、其の震動は東京においても弱震程度の地震であつた。此等東京における有感地震の表は已に掲げたものである。

此の表中三月廿二日に發生した地震は最大のものであり、伊東に於いて 12 mm. の振幅を有して居たと云ふ。東京伊東間は 100 km. の距離あるもにも拘らず東京に於いて 1.3 mm. の振幅を記録した事は一般の火山現象に關係する地震程度としては極めて激烈のものと云はなければならない。大正三年櫻島噴火に際しては此の程度以上の地震の發生を見た。地下狀況の變移がすべて地震發生となつて表面に達するとは誰も考へぬ事であらうが、相當急激な物質變位が地下に行はれる場合には必ず波動の成生が行はれて地震の發生を見るであらう。而して其の如何なる程度のものに限られて震動が發するかと云ふ問題に就いては研究すべき餘地が充分存在する樣である。此の點に關しては今回の小地震頻發と地表に於いて觀測される地形變動との間に明瞭な關係が存在するならば、前者は地下狀況が比較的急激なる狀態に置かれて發生したるものなるに反し、後者は比較的緩慢であると云ふ點において吾々は地震發生に關し重要なる論據を見出しうる事となる。

伊東地震群の發生が潮位の高低に支配されて居つた事實は、先づ伊東在住の人々によつて氣付かれ、其後油壺驗潮儀の記錄と比較[12]する事により其の事實が正確に認められる事となつた。但し全部の地震が潮汐に關係したのでは無く、或る時期を限つて潮位の低下した場合に多くの小地震の發生を見たのである。從來潮汐の高低が地震の發生と如何に關係

12) 前掲

するか統計的に研究したものが二三は存在[13]するが多くは其の間に密接の關係を否定する結論が得られて居る。然るに今回の地震中潮位が全く地震發生を支配した場合のあつた事は充分注目に價するものであり、以下述べんとする地震發生機巧に對しても密接の關係を有するものとなる。

2. 伊東地震に類似する諸地震

伊東地震は結局小地震の發生を以て一貫したものであるが、斯様な地震群の發生が大地震の前驅となるものなりや、或ひはかゝる地震群の發生は通常の事であつて日本全國に亘つて存在するものなりやと云ふ問に對しては相當の攻究を必要とする。

今村教授[14]は大地震に先立つて地震群の發生した例を擧げて居られるが、多くの場合は小地震群の發生のみで終るらしく、從來かゝる形式の下に發生した地震群の例に乏しくない。即ち此れ迄の報告中から次のものを撰出する事が出來る。

1. **有馬鳴動**[15] 明治三十二年(1899)より三十三年に亘つて兵庫縣有馬溫泉附近に發生したものであるが、其の始めは三十二年七月五日であつた。同月下旬から八月上旬に及んで鳴動の回數は非常に多く最も盛の時は一日二百回にも及んで居る。其後回數は次第に減少したとは云へ翌年迄も多少の鳴動は存在して居た。鳴動の原點は有馬町から約2 km. の六甲山中と推定され、多くは遠方で太砲を發射した如きか或ひは重い石を地上に落下した如き音あり、音響を聞いて後半秒乃至一秒を經て地響きが感知せられた。
2. **箱根山鳴動**[16] 大正六年(1917)一月十七日から微震が出現し始めたが三十日午後六時に至つて回數が急に增加し、同九時から三十一日午前二時頃迄は最も頻繁となり、同六時迄の十二時間に合計242回を算した。然し之等の震動は格別の震害を與へる事無く、其後增減を示し乍ら次第に平穩に赴き鎮靜した。天明六年二月にも同様の現象があつ

---

13) 大森房吉 震災豫防調査會報告 32 (1900), 35; 今村明恒 震災豫防調査會歐文報告 18 (1904), 41.

14) 今村明恒 震災豫防調査會報告 92 (1920).

15) 大森房吉 震災豫防調査會報告 88 b (1917), 73; 震災豫防調査會歐文紀要 2 (1908), 106.

16) 大森房吉 前掲

たと云ふ。

3. **大島地震**[17]　此の地震は最後に比較的大勢力を有する地震の出現で終つたものである。明治三十八年（1905）五月二十日頃より發生し、その中には相當の震度を有するものもあつたが、結局六月七日の强震で終局を告げた。地震總數は1000程であつた。

4. **上總地震群**[18]　大正四年（1915）十一月十二日より十七日迄出現したもので東京觀測によれば65回の地震が記錄された。

なほ以上の外、大正三年櫻島噴火に際して地震群の發生した事、或ひは諏訪地方に地震群の發生した事、[19]或ひは和歌山地方に數年に亘つて地震群の發生[20]を見た事等を數へるならば、其の間大小の差こそあれ形式上は何れも伊東地震に比較し得るものとなる。なほ人々の注意は殆ど惹かないが、多くの無感地震が群をなして出現する例は氣象要覽中に報告されて居るものが多數ある。今其の最近におけるものを摘出するならば

1. **長崎地方**　長崎地方に於いては大正十五年（1926）十月頃から小地震の發生あり、其間多少の消長はあつたが翌年三月迄續發して居る。一日の頻度は平均6回多い時は20回を越えて居る。而して大部分は無感地震であつた。

2. **花蓮港沖**　此の附近は大小の地震が頻々として發生する事を以て有名であるが、昭和四年（1929）九月十二日より十月二十六日に至るまで數多くの地震の出現を見た。總數214回でその中有感地震108回を數へた。一日別において最も多い日は有感地震14回無感地震16回であり、一日平均は4回と云ふ事になる。此の場合震央が海中にあつて、實際の地震の中小數のものの外は記錄されなかつたらしい。

3. **溫泉岳**　溫泉岳附近は小地震の常に發生する所であるが昭和四年（1927）十月二十五日より頻發的に小地震が出現した。二十五日には3回の有感地震と22回の無感地震、二十六日には2回の有感地震と20回の無感地震とがあり、それより次第に衰へた形勢であつたが十二月三十日には無感地震24回の出現があり、續いて翌年一月中相當

17）大森房吉　震災豫防調査會歐文紀要 **2** (1908), 96;　今村明恒　前揭
18）今村明恒　前揭
19）中村左衛門太郎　氣象集誌 **41** (1922), 233, 629.
20）中村左衛門太郎　同上　**34** (1915), 71; **41** (1922), 420.

の地震回數を算し、二月半迄も繼續して居た。これは火山地方ではあるが、火山噴火とは全く別箇のもので直接關係は認められて居ない。

4. **名瀨附近** 昭和四年 (1929) 二月、此の地方に小地震群が發生したが、何れも無感地震、最大頻度は一日 32 回であつた。

5. **石垣島附近** 昭和二年 (1927) 十月一日から石垣島附近に起つた小地震群は二週間で終熄したが、最も活動した時は一日四回の有感地震を數へた。

6. **水戸涸沼附近** 水戸涸沼附近においては大正十五年 (1926) 十一月地震群の發生を見たが、此の附近に昭和五年六月一日强震の發生を見た。

以上は比較的短時日の間に頻發した小地震群の例に過ぎないが、第九圖は此等地震の頻度を圖に表はしたものである。

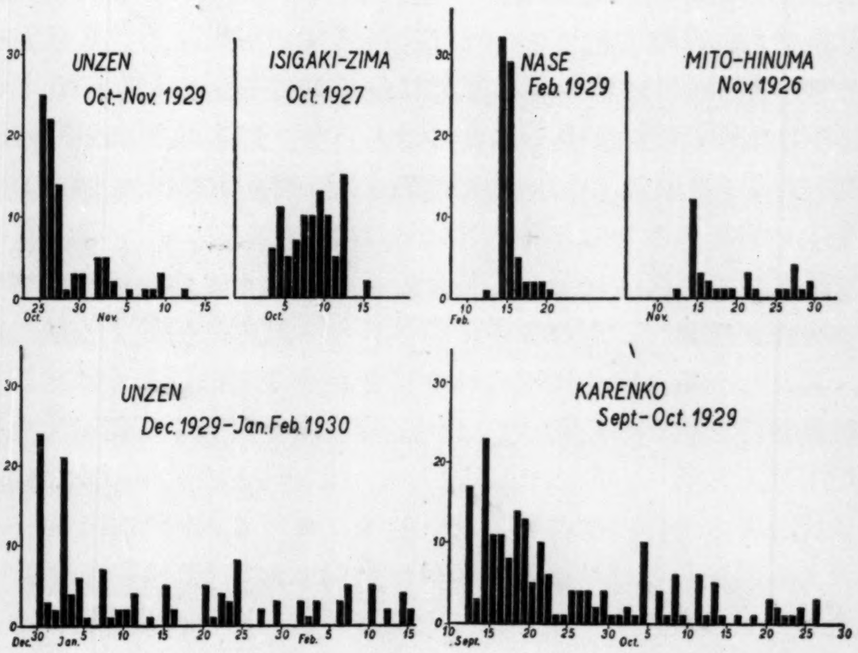

第九圖 Fig. 9.

なほ以上の外一層小規模と思はれる地震群を擧げるならば

震央	年月日	有感	無感
臺灣下淡水溪	昭和三年一月	14	34
岐阜附近	昭和三年四月廿四日	—	9
下甑五島附近	〃 六月	7	54
銚子附近	〃 十二月廿一日	6	33
布良附近	〃 九月廿三日	—	13

等である。また初めに强震程度の地震があり、其れに引續いて小地震群の發生する事、即ち餘震と稱せられる小地震群の發生であるが、此等の中最近のものを擧げれば

震央		有感	無感
九十九里濱北部	昭和五年五月一日	9	63
千々石灣	昭和二年十二月四日	6	46
日向ケ灘	昭和四年五月廿二日	6	25

等が得られるが、何れも數日を限度として起るもので一群をなす上において上記の地震群と聊も異る所がない。即ち此等の現象を見るに當つて餘震と云ふものを廣義に解釋して地震群として其の說明が爲さるべきではあるまいか。餘震の名稱は元來比較的大なる地震を冒頭として初まる小地震群を目標として使用されたものではあるが、實際餘震の發生狀況は伊東地震其他と性質上異るものとは考へられない。卽ち大地震により變動を與へられた地殼內においては小地震群の現出に適當な狀態に置かれると考へ得べく、一方かゝる狀態は地震地帶各所に存在するものらしく隨時小地震群の發生が見られるのであらう。卽ち地殼は相當複雜な構造を有して居るのであつて、特に地表に近い部分において以上の如き小地震發生を認容するものと考へなければならない。

從來學者の地震發生に關して論ずる場合に多くは地殼構造の構めて簡單なる場合を想像し、それより誘導されたる結果に信賴する傾向がある爲め、甚だしき先入觀念に捕はれる場合が少くない。吾々は地殼について一層複雜性を與へるに非ざれば到底地震發生に對する說明を充分に爲す事が不可能と考へられる樣になつた。卽ち目下地質學の立場において攻究されて居る地體の構造特に廣い意味における火山作用を考へに入れた議論から出發しなければならぬ事は勿論である。

小地震の數多發生する故を以て大地震が爲し崩しに勢力を出したものと考へる事の是非は不明である。但し小地震の頻發によつて地殼の進轉が實現される場合と大地震の發生が必然的に避くべからざる場合のある事を考ふるならば、其の間に地體構造上區別さるべきものがあると推定しなければならず、實際上も左樣であるであらう。之等は孰れも造山造陸運動に與る一分子の出現に寄與するものに相違ないが、表面的には比較的急激なる地塊運動を伴ふ土地隆起であり、かゝる地形變動を生ずる本源が地殼中に存在する事も當然の事と云はなければならない。

3. 水準測量結果より見たる此の地方の地塊運動

伊東地震の頻發に從つて種々の觀測が行はれた中に地塊運動を推定し得べきものとしては精密水準測量の實施と吾々の行つた傾斜變觀測とがある。なほ地形變動として肉眼に映ずる程度のものとして川奈海岸の漁夫によつて認められた海水の退減は此の地方の土地上昇を意味するものとなる。一方海底變化の有無を驗するために重錘による再測が試みられたが假令變化があつたにしても殆どすべて誤差の範圍内にあると考へて差支へ無いであらう。

水準測量の結果[21]は已に發表されて居り、川奈附近において最も隆起した事が示されて居るが、此等の結果を基として此の地方における地塊の存在と其の變動狀況とを論ずる事が出來る。然し乍ら吾々が斯樣な結果を取扱ふ場合水準線路の直線で無い事のために屢々間違つた結果に到達する事あるを恐れて、豫め水準線路の曲りに對する吟味をして置く事も強ち徒勞ではあるまい。即ち水準線路の曲りは何の程度まで許し得るものであるかと云ふ事を決定して置き度い。勿論水準測量自體の中にも誤差ある事、或ひは標高點相互の間に高さの差ある事等から問題は多少複雜となるが、今の場合は之等分子を全く顧みる事なく何れの標高點も一平面上にあり、且つ測量により得られた數字は全く正しいものとして議論を爲さんとするものであるから問題は自ら全く幾何學上のものとなる。

水準線路が全く直線を示す場合においては標高點の距離を其のまゝ圖上の横軸にとり二回の測量によつて求められた高さの差を縦軸にとる事により、その時間内における垂直變動の有樣、傾斜程度或ひは若しありとすれば傾斜の不連續等も見出す事が出來るのである。然し乍ら若し水準線路に彎曲のある場合においては假

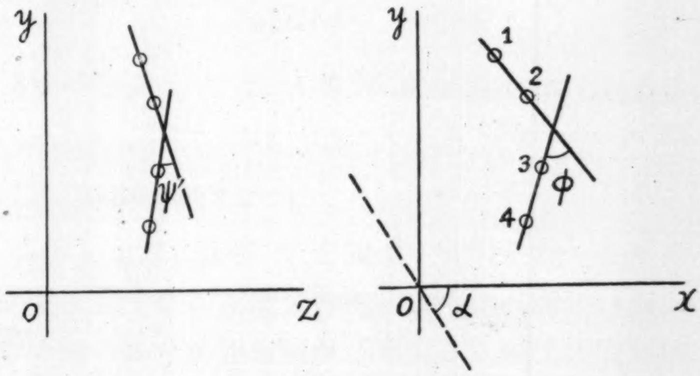

第十圖　Fig. 10.

21) 地震研究所彙報 8 (1930), 375.

令吾々が投影方法を使用するとも、その方法によつて傾斜の變化を見出す事は一般に不可能となる。今水準路の彎曲程度が如何程關係するものであるかを吟味するに當つて最も簡單なる場合として四個の標高點（1, 2, 3 及び 4）を二個づゝ（1, 2 及び 3, 4）結んだ二つの直線がある角をなす場合を考へやう（第十圖）。地面を水平と考へ、此れが x y 面にありとすれば二つの直線は次の式で表はす事が出來る。

$$y = a_1 x + b_1,$$

$$y = a_2 x + b_2.$$

今原點 O において x 軸と α 角をなす方向を軸として地面が此の二直線を乘せたまゝ小角 θ だけ傾斜するものとする。此の時各點の地面に直角の方向即ち z 軸の方向における變位は

$$z = x\theta\sin\alpha + y\theta\cos\alpha$$

となる。今此の二直線を yz 面に投影する場合二直線のなす角 ϕ が如何なる量として得られるかを見るのである。第十圖はおいて

$$\phi = \tan^{-1} a_1 - \tan^{-1} a_2.$$

若し $\tan^{-1}a_1$ 及び $\tan^{-1}a_2$ が 90° に近い場合、即ち二直線が殆ど一直線に近い場合においては

$$\phi \fallingdotseq \frac{1}{a_2} - \frac{1}{a_1}.$$

又 yz 面上における二直線のなす角 ψ は

$$\psi = \tan^{-1}\frac{a_1}{\theta\sin\alpha}\frac{1}{1+a_1\cot\alpha} - \tan^{-1}\frac{a_2}{\theta\sin\alpha}\frac{1}{1+a_2\cot\alpha}$$

となり、此の中 a_1, a_2 は甚だ大、θ は甚だ小であるから若し $a_1\cot\alpha$ 及び $a_2\cot\alpha$ が非常に大で無ければ

$$\psi \fallingdotseq \phi\cdot\theta\cdot\sin\alpha$$

となる。然るに吾々が圖上 θ を書き表はす場合 z の單位は xy の單位に比して極めて小なるものを用ふる事を常とする。例へば土地の垂直變動は實大を用ふるに反し地圖は五萬分の一或ひは二十萬分の一を使用するのである。今その單位の比を S とすれば

$$\psi' = \phi\cdot S\cdot\theta\cdot\sin\alpha$$

となり、若し $S\cdot\theta\cdot\sin\alpha$ が1に近い場合においては實際の水準線路の曲りが同程度に曲つて投影される事となる。今垂直方向の變位は實大となし、二十萬分の一の地圖を使用し、傾斜角は1秒、$\alpha=90°$ と置けば

$$S\cdot\theta\cdot\sin\alpha=0{\cdot}96$$

となり實際地圖上に見られる水準線路の屈曲がそのまゝ投影圖において見られる事となる。此の結果からすれば水準線路の屈曲に注意する事なく投影した圖中、假令其の中に傾斜不連續の存在を見出すとも、其等は實際の地面に不連續傾斜の存在する事を一般に意味するものとはならないのである。吾々は今回の測量中に此種の好例を見出す事が出來る。

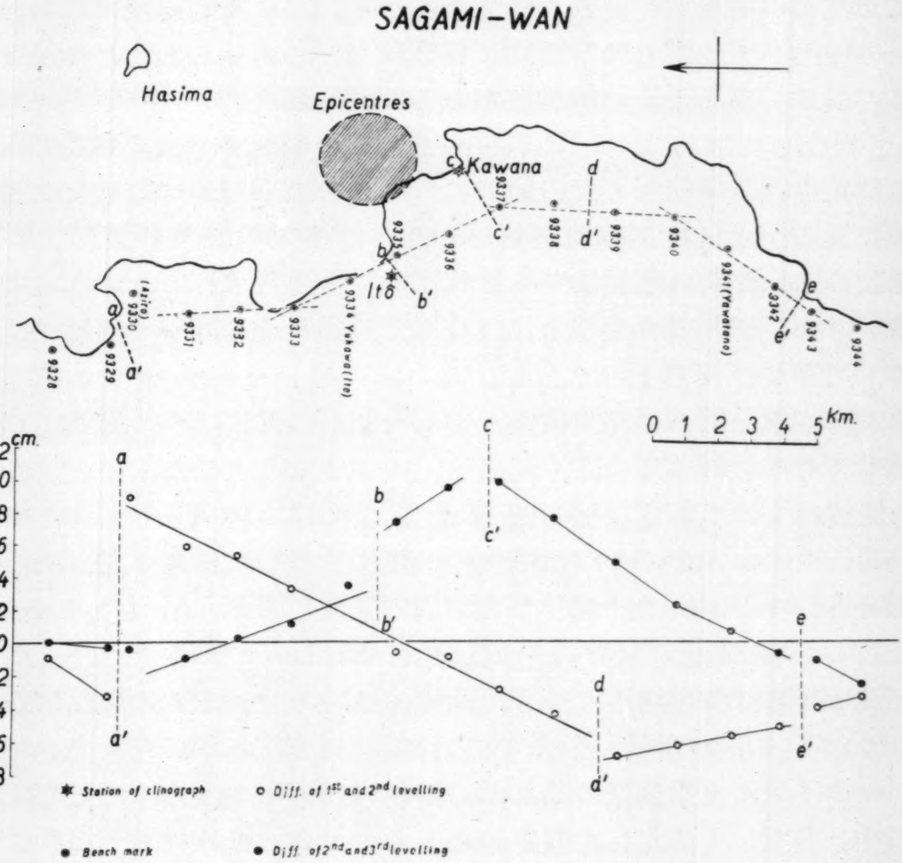

第 十 一 圖　　Fig. 11.

第十一圖上は伊東附近の略圖であり、水準線路は多少の屈曲を示して居る。但し一部分を取る場合には直線と見做して差支へない部分が多

い。此等の標高點が今回の地震によつて變動した量は知れて居るから、其れを用ひて實際の地塊存在と傾斜狀況とを見出さんとするものである。下圖は續いて行はれた二回の測量値の差を縱軸、横軸は南北線であつて此れに標高點位置を投影した。○印は第一回(明治卅六年)と第二回(大正十二年十三年)との測量値差、●印は第二回測量と第三回測量(本年)との差である。○印の期間中には關東大地震が發生して居ると云ふものゝ此の全部の變動が此の地震によつて惹起されたと考へる事は正當であるか否かは知り得べき限りでない。即ち此の變化は約 20 年間の積算値を意味するものに止るのであつて、此の量全部が大地震に關係して生じたものとは直ちに判定出來ない。但し大地震の際には此の地方に接して大隆起の出現が行はれたのであるから、恐らく此の地方においても以上の變動が大地震と殆ど同時に行はれたと判斷しても大した違いは無い樣である。而して此の變動においては網代附近における不連續境界(aa')の生じた事及び dd' に不連續の生じたる事は明瞭な事實である。即ち關東地震に附隨して此の地方に行はれた地形變動は網代を北端とし吉田に及ぶ一大地塊(南北徑約 14 km)の簡單なる傾斜運動に過ぎず、大地震の齎した全地形變動から見れば全く重要視されるものとは考へられない。而して此の大地塊上には今回の地震發生に關して問題とされた伊東、川奈が存在するのである。

第二回、第三回との測量値差、即ち今回の地震によつて惹起された地形變動と考へられるものは、關東地震により惹起されたものとは全く異つた性質のものである。即ち關東地震當時は大地塊として一方向きの傾斜を行つたものが、今回は數個の地塊に分裂して極めて局部的の地塊運動を行つたのである。而して大地震の際生じた網代附近の不連續線 aa' 或ひは吉田附近の dd' も今回は殆ど癒着したるが如く、たゞ川奈附近が最も隆起する地域となつて、此處に地塊の分裂と其の運動が行はれたのである。吾々は bb' 及び cc' の位置に便宜上不連續線を考へて居るが、此等は單に水準測量の結果から歸納したものではなく、地形上の觀察其他を顧慮して決定した假定的のものである。斯樣に考へる時は此の bb' と cc' とによつて劃されて居る小地塊(川奈地塊)が最も烈しい運動に與つた事は此等の圖からも推定し得るものであると同時に、幸ひ此の小地塊上に設置された傾斜計の記錄からも地震に直接關係した運動を取り出す事が出來るのである。此の小地塊が今回の伊東地震に關係して最

も重大なる役を演じたのは、此の地塊の直下或は此れに接して大部分の地震が發生した事、又一部分の地震は cc' に相當する地塊境界面にも發生して居る事から察すれば、此の地域全體としては隆起運動であると同時に川奈地塊及び此の兩端に接する二地塊（伊東地塊、富戶地塊）の傾斜運動が地震發生に密接の關係を有するものと推定される。

大地震の場合には地形變動量が大である關係上、其の狀況が明かにされる場合が多いが、伊東地震の如き小地震群生に對しても局部的に測定し得べき地形變動の存在して居た事は甚だ興味深いものであり、地震發生と地形變動との間に密接の關係ある事が逐次證明されて居るのである。斯樣に小區域の地塊運動が局部的地震に伴つて出現する事實は昭和二年十月の關原地震[22]により初めて見出された事であるが、此の際にも極めて僅かではあるが土地隆起が認められて居る。

關東地震においては一塊となつて傾斜運動を行つた地塊が今回の地震により數個に分裂して運動をなした事實に對し、吾々は地塊の分裂と云ふ現象に注意しなくてはならない。水準測量の結果から求められた地形變動の中、地震發生に關係なきものにおいては地塊の徑が比較大であつて、或るものは 50 km のもの[23]さへ存在する。然るに關東地震、丹後地震後行はれた水準測量の結果[24]からは其の地塊の徑が比較的小であつて平均 7 km であると云ふ事も云はれて居る。之れを以て之れを見れば地震發生に伴ふ直接の地形變動は寧ろ大地塊の存在を許す事なく小地塊に分裂せしめて運動せしめる事であつて、局部的に變動多い事を意味するのである。

地塊が分裂し或ひは密着して運動する事實は已に丹後地震の水準測量の結果中[25]に確められたのであるが、此回も且ては一地塊として傾斜運動をなしたものが、其の中央部に地震群發生を見ると同時に分裂して各自の運動が行はれたのである。斯樣な事實及び傾斜變化觀測結果等を顧慮する時は、恐らく地震終熄と同時に此等地塊は密着して各自運動を行はざる狀態に達するものと想像される。

22）石本巳四雄　地震研究所彙報 8 (1930), 222.

23）N. Yamasaki, *Proc. Imp. Acad.*, 4 (1928), 60.

24）武藤勝彥、熱海景良　地震研究所彙報 7 (1929), 495;　坪井忠二　地震研究所彙報 6 (1929), 71.

25）坪井忠二　前掲

以上の事實を說明するに當つては地塊相互間の密着狀況の變化する作用を先づ想像しなければならない。吾々が日常經驗する現象に比喩を求めるならば、二つの固體が水平力により壓迫される場合、其の境界における摩擦は大となつて相互運動の困難となる事を知つて居るから地塊運動も同樣なものであるかも知れない。但し實際の地塊が如何なる狀況に置かれてあるかと云ふ事に關しては別に新しい現象を見出さざる限り未決の問題として止る。なほ地塊が種々運動する條件としては、少くとも地殼の表面においては固體の集團であり各自の運動が可能である事實から、此の下に橫はる物質は比較的流動性に富むものであると想像せざるを得ない。

因に投影圖において 9340 號の標高點を境として傾斜の不連續が認められるが、此れは此の附近に不連續線の存在するものではなく、地圖上水準線路の屈曲して居る結果として說明出來るのである。此の事は已に幾何學上の問題として說明した事に相當するのである。

4. 傾斜變化に就いて

以上の如く水準測量の結果から吾々が地殼構造に就いて云々する樣になつたのは全く關東地震、丹後地震以來の事であり、今回も地殼變動と地震發生との間に密接の關係が認められるのである。然も最も變動の烈しいと考へられる川奈地塊及び此れに接する伊東地塊に傾斜計の設置が行はれた事から、此の二つの地塊の運動が論ぜられる事となつた。勿論傾斜計の示す變化はその設置された局部的のものには相當ないが、地塊の存在と其の運動の形式とが次第に明かにされた今日においては、溫度の影響が烈しくない限り、傾斜計の示す變化は其の地塊の傾斜變化と考へて差支へないものである。今回の如く觀測室が全く自然岩中に在り溫度の影響が絕無であるとさへ考へられる狀態においては傾斜計の示す變化は充分信用して差支へないものと信ずる。

傾斜計により求めれらたる變動は已に第一部において詳述されたものであるが、地塊の傾斜方向に特定のものが存在し、此の方向に地塊が傾斜しつゝ地震の發生が行はれるのである。此の事實は著者の一人が丹後地震直後宮津において[26]觀測した結果の中にも認められるものであつて、

26) 石本巳四雄 地震研究所彙報 4 (1928), 203.

宮津地塊は餘震群の發生と共にある特定方向に傾斜運動を行ひ、其の最後に發する比較的大なる餘震を以て傾斜變化は一段落を告げ靜止狀態に達するが、再び次の階段に進轉するのであつた。此れと同じく伊東、川奈の兩地塊とも特に傾斜し易き方向（伊東は西及び南下り、川奈は西下り）があつて、此の方向に傾斜する時に地震の發生が行はれて居るのである。宮津觀測と比較して殆ど同樣に明かであるが、比較的大餘震の發生に伴ふ靜止狀態は稍々明瞭を缺くのである。卽ち今回の地震に附隨して地塊の存在とその運動事實は水準測量の結果及び傾斜計觀測から得たる結果よりも證明し得るが何れも隆起運動を意味して居る。卽ち川奈、伊東兩地塊が何れも西下りである事[27]は海岸の比較的隆起する事實を示すものであり、地震發生に伴ひ地形變動がかゝる形式の下に進行する狀況が明かにされ、然も此の東上の傾向は全く震央附近の土地が地震發生に伴ひ上昇する事を意味するのである。

地塊運動が地震發生に關係する事は各地に於ける傾斜變化の觀測により次第に明かにされて居るが、地震發生は比較的急激な傾斜變化を先だてゝ居るのである。伊東地震においても群生する小地震の間において明かな傾斜變化をなして居る事實から、吾々は宮津における時と同じく此の現象は岩漿運動の結果行はれたものと推論するのである。幸今回の地震に對しては數臺の地震計による震原位置の決定が充分に行はれた爲め、此の方面からも岩漿運動を認めて地震發生を說明する事の適當[28]である事も唱へられて居る。

なほ地震が二群に分れて發生した事實は傾斜觀測上においても確められる事である。卽ち四月中地震發生の衰へた時期においては伊東地塊の傾斜運動は殆ど一個所に停頓して居たかの如く、川奈地塊は地震發生時に行はれる西下りの傾斜とは直角をなす北下りの傾斜を續けて居たのである。然も五月中旬に到つて再び地震の群發するに當つては、孰れの地塊も西下りの運動に移つたのである。此の西下りの運動は三月中兩地塊に行はれて居たものであり、海岸の隆起を起す方向である事は已に述べたものである。

地殼の傾斜運動が潮位の影響を受けて同期變化をなす事は川奈觀測に

27）第七圖參照
28）那須信治　前揭

おいて明かに認められ、地震發生に關係して此の振幅が多少變ぜられる事が見受けられて居るが、此等の現象は將來の研究に俟つべきものであると同時に、氣壓配置に關係した此等地塊の傾斜運動も將來の議論として殘されて居る。

要するに傾斜觀測の結果からは地塊の運動が地震發生と密接の關係を保ち短時間に生ずる地形變動を指示するものである事の實證が此回の觀測からも明かにされたと云へるのである。

5. 地震發生機巧について

伊東附近における地質構造は津屋所員の報告[29]に精しいから、此れを其のまゝ借用する事とする。伊豆半島は全部噴出岩を以て蔽はれて居る事から、幾回かの火山活動のあつた事を示すものであり、然も其の間に斷層、火山列の存在する事實は地塊の存在と地塊相互の間に運動の行はれた事を察するに難くない。水準測量の結果も地塊の存在を認めるのであるから、岩石の相違と地塊の存在と云ふ事とは別けて考ふべき性質のものであるらしい。

今回の地震發生に際して那須理學士は五臺の地震計を使用し、五つの觀測點における地震記象から其の震原の決定を行つた。震源位置の座標と大森公式の k とを未知數とする場合四點の觀測があれば充分である事は申迄もない。然も殆どすべての地震が五點を以て造られたる觀測網の中に存在した事は震原位置を充分精確に決定するに便宜であつた。而して以上の四量を計算する上に其の基礎となるものは、各記象の初期微動繼續時間であるから、其の精確さは第一に地震計ドラムの回轉の均一と云ふ問題である。而して次に起る問題は地震動の周期如何と云ふ事である。地震動の半周期以下においては相の變化を見出す事が殆ど不可能であると云ふ理由を以て、此の時間以下の精確さは望めない事となる。地震動の周期を 0.2 秒とすれば 0.1 秒以下の時間は信用度が少い事となる。那須氏は以上の事を顧慮した結果震原位置を圖上に表はしたのである。

同氏の結果[30]によれば地震發生上極めて興味ある事實が明かにされたのである。即ち大部分の震原は吾々が最も注目した小地塊に接して存在

29) 津屋弘逵　地震研究所彙報 8, (1930), 309.
30) 那須信治　前揭

する漏斗形をなす限界中に發生して居る事、又一部分の地震は川奈地塊と富戸地塊との境界面（cc'）において發生して居ると云ふ事である。此れらは全く川奈地塊の運動に密接の關係を有して出現した地震である事は直ちに氣の付くものである。從來の考へ方に從へば地震に關係する斷層の存在を明かにする事が試みられて居るが、若し今回の地震について斷層を云々せんと欲するならば、それは今述べた cc' に相當するものを擧ぐるが最も適當の樣である。但し此の斷層は地質學上に云ふものとは稍〻その赴きを異にして居る事は當然の事である。地質學上の斷層は且て此の場所に相互運動の行はれた痕跡あるものを總稱するものであるに反し、今云ふ斷層は地震學上、或ひは水準測量の結果得られた境界面であつて、現在其の活動が認められるものを限つて指摘するからである。

第十一圖の水準測量結果に見る如く關東地震に關係して運動の行はれた場所と今回の地震群によつて變動の行はれた所とにおいても已に全く異つたものゝある事は、地質學上から決定された斷層が必ずしも地震學上意味ある斷層とならない事を示すものである。然も關東地震の場合一地塊として存在したものが分裂して生じたる地形變動の外示さない極めて小規模の地震に向つて直ちに地質學上決定された大斷層に密接の關係を附會するが如きは當を得たるものでは無い樣である。

地震計の初動方面から斷層を推定する方法は屢〻試みられるものであるが、今回も各測候所に設置されたる地震計の記象から求められた初動方向分布の研究[3]が發表されて居る。其の論ずる所に從へば川奈を通過して殆ど南北に走る斷層が想像され、地質學上の斷層と關係ある事が主張されて居る。然し乍ら此の場所に假令如何なる大斷層が存在するとも、今回の伊東地震を説明する上には重要性は殆ど認められないのである。吾々は關東地震の際、網代附近に相當の不連續運動を認めたにも拘らず、今回の地震には何等關係ないものであつた事を思ひ合せるならば事は明瞭になると思ふ。なほ一層議論を進めるならば、關東地震において此の地方の有數斷層が地震發生に對し如何なる役を演じたかを考へて見る可きではあるまいか。相模灣沿岸、房總半島に亘つて二米突にも近い土地隆起運動の起つたにも拘らず、斷層として認むべき大規模のものが顯出しなかつたのは如何なる理由によるのであろうか。此等の問題に對

3）國富信一 岩波物理學及び化學講座特別題目，223.

して著者は再三論[32]を進めて居るから重複を避ける意味で此所には述べない。

地震計記象から求め得た初動方向を地圖上に劃き、それを解釋するに當つて注意すべき事柄のある事を忘れてはならない。例へば天龍川流域に震央を有した地震の初動方向の圖[33]において、其の押し引きを分類して直角に交る直線を引く事は容易である。然し乍ら此れが如何なる斷層機巧によつて發せられた波動に相當するかを決定する事は容易の技ではない。吾々は地震波を剪斷形式によつて起つたものとするか、或ひは斷層面に直角の方向に開閉する斷層形式を擇ぶかによつて、各 45° 度の間隔を保つ任意なる方向に斷層面を選擇する事が出來るのである。上記の地震においては天龍川と云ふ地形の存在がある爲めに、此れを斷層方向と假定する事により此の平面に沿ふて急に左右に開く樣な裂罅が出來たと想像し得たのである。然るに伊東地震の場合においては容易に斷層方向（若しありとするも）を決定する事は困難である。吾々が强いて斷層を考へるならば上述の cc' に相當するものを擧げるに止まるが、此の斷層は國富技師の決定したものに比較して正しく直角の位置にあるのである。因に斷層の存在は地形上重大の問題ではあらうが、假令此所に相當の運動が行はれても地震波發生機巧に對して吾々が議論を進める事の甚だしく困難である事を一言附加して置く。

伊東地震において最も注目すべきものゝ一つは震原位置の決定された事である。大部分の地震が漏斗形限界內に見出されたる事、然も地震は先づ深所に發し次第に表面近く來り、最も表面近い所において群生する如き發生は從來考へ來つた方法を以てしては全く說明に窮するのみである。

此の地方が全く火山噴出物によつて蔽はれて居る事實は何物か地下に存在する物質の地上に顯出せんとする傾向を意味する事に外ならないが、今回の地震も地下物質の地殼深所より上昇運動をなす結果發生した現象と察せられる。大正三年櫻島噴火に際して發生した數多くの地震は同じく小地震群であつた事を思ひ合せるならば、伊東地震は寧ろ廣い意味の潛伏的火山を意味するものであり、地下物質の地表に現はるゝ事なく、

32) 石本巳四雄 地震研究所彙報 6 (1929), 127 etc.
33) 松山基範 輓近地震學, 216; HASEGAWA, *Gerl. Beit. Geophys.*, 27 (1930), 203.

所謂深成岩の成生が行はれるものと信ぜられる。然も小地震が小局部に群生した事實から此れは深成岩の中にも大規模のもので無く、地殼の極めて表面に近い部分に發生する岩床或は岩脈の群生を意味するものゝ如くである。已にかゝる小地震發生の現象が日本各地に存在する事、又時間的にも多く存在する事實は地殼それ自體がかゝる現象を認容せしめる狀態に置かれてある事、即ち吾々が今日地表において見る種々の深成岩型の中何れかゞ今日地震を發生しつゝ地殼中に成生されて居る事を推定する事が出來るのである。

吾々が伊東地震を機として行つた傾斜觀測の結果は地震群の發生に從つて特定方向の傾斜變化をなす事がその主なるものであり、丹後地震直後行はれた觀測と極めてよく一致する事は已に述べた。今これを筑波觀測[34]と比較するならば、筑波においては地震發生に關して比較的急激な東西に動搖する傾斜變化のある事、然も比較的遠方の地震發生前にも此の現象のある事は伊東地震と多少趣きを異にして居る。元來筑波觀測所は深成岩である花崗岩に傾斜計の設置してある事が意味ある事の如く察せられる。即ち岩漿の運動に對して筑波は極めて敏感であるに反し、伊東地方の如く噴出岩よりなる地方は假令附近の極めて淺き部分に存在する岩漿運動に對しては動搖するとも筑波の如く、比較的深所に、然も廣い面積に亘る岩漿運動に關係する事が僅であると察せられる。

かゝる變動を基として吾々が地下狀況を想像するに當つて岩漿の存在とその運動とを認容する事となつたが、次の問題としては岩漿の性質を充分明かにして地震發生の機巧を充分說明すべきである。岩漿が地殼の深所から漫性的に地表近く上昇し來り次第に冷却する事實は充分信ぜられる事であるが此の冷却に際して岩漿內に存在する揮發性瓦斯の壓力は增加せられ外壓に抵抗する。外壓が此の壓力以下となる場合においては岩漿は猛烈の勢を以て流動を開始し、裂罅充塡が行はれると同時に地震波發生が行はれるのである。かゝる地震發生を假定する事により吾々は地震前に地塊運動の存在する事を充分說明する事が出來ると同時に潮位の高低に關して地震發生の左右される事も首肯し得られるであらう。

今回の地震が全く地殼內淺所に發生した事から地表における潮汐はそのまゝ外力の一部分となつて內氣壓と抵抗するものとなつたのであら

34) 井上宇胤、杉山友紀　地震研究所彙報 8 (1930), 346.

う。即ち干潮時に際しては外力の低減によつて內壓は岩漿流動を促し此所に地震發生を見る事となつたと想像される。一般地震においては震原位置が深い事及び半日の周期以て增減する壓力の作用は結局地殼が彈性を有すると云ふ事で傳達し得ず、かへつて其の量は小であつても長周期に亘る二點の氣壓差の變化は外壓の消長と見られ、結局從來地震發生の副因として働くものと考へられて居る。

以上は伊東地震に關し水準測量及び傾斜計觀測結果を根據として地震發生を論じたものであるが、結局此の地震も特別のものではなく地形變動を伴ひ、地塊傾斜を起さしめるものであり、一般地震、特に大地震後の餘震と比較して何等性質上異るもので無い事を附記して結尾とする。

（石本）

21. *Séismes d'Itô et l'observation sur les variations de l'inclinaison de la surface terrestre*

par M. ISHIMOTO et R. TAKAHASI,

Institut de Recherches sur les Tremblements de terre.

1ère partie: **Observations faites a Itô et à Kawana.**

Du 14 Février 1930 au 22 Avril de la même année, un grand nombre de séismes ont eu lieu dans la région d'Itô, ville d'eaux située au bord oriental de la presqu'île d'Idu. Dans le but d'étudier le mouvement de la croûte terrestre à l'occasion de ces séismes, on a installé un paire de pendules horizontaux (clinographes de silice fondu, inventées par le Prof. M. Ishimoto) à Itô afin d'observer les variations de l'inclinaison de la surface terrestre; les observations ont été effectuées à partir du 12 Mars. De plus, le 19 Mars une installation identique a été faite à Kawana et les deux observations ont été poursuivies jusqu'au 30 Juin. La sensibilité du clinographe à Itô était réglée de façon à donner 1 cm. de déviation pour 1 seconde d'inclinaison, tandis que la sensibilité du clinographe à Kawana était deux fois plus grande que celle du clinographe d' Itô. Les clinographes étaient installées dans des caves creusées dans la masse de scorie volcanique.

La figure 6 représente les courbes des variations de l'inclinaison obtenues par les observations faites à Itô et à Kawana, pendant la période du 12 Mars au 31 Mai, et la courve de la température moyenne de l'air observée à Itô. Dans cette figure, E, F etc. montrent les forts tremblements de terre, dont les données sont représentées par le Tableau 1. La figure 7a représente le diagramme-vecteur des variations de l'inclinaison à Itô composée avec des courbes de la figure 6. La figure 7b représente le diagramme-vecteur des variations de l'inclinaison à Kawana.

Comme on le voit dans la figure 7a, les forts séismes se groupent dans la période où les variations de l'inclinaison se trouvent rapides et simples, se faisant dans deux directions caractéristiques, c'est-a-dire l'Ouest et le Sud. Ce sont certainement les deux directions caractéristiques du bloc d'Itô. Quand il n'y a qu'un petit séisme, les variations de l'inclinaison restent comparativement relâchées et compliquée. Dans cette période la courbe se présente, parfois sous forme de zigzag et parfois sous forme de rouleau, et on y voit là influence des variations de la température de l'atmosphère. De plus, il est certain que les séismes E, F, G etc. correspondent à une inclinaison vers l'Ouest tandis que les séismes I, J, K etc. correspondent à une inclinaison vers le Sud formant deux séries différentes qui ont un rapport étroit avec leurs positions hypocentrales, comme on le voit dans la figure 8.

Le fait que la période active des séismes coïncide entièrement avec la période des variations remarquables de l'inclinaison s'accorde aussi très bien avec les résultats obtenus par les observations faites à Kawana comme on l'a représenté dans la figure 7b. Quant à la direction caractéristique du bloc de Kawana, on constate, qu'elle se dirige vers l'Ouest.

En outre, dans les résultats obtenus à Kawana (figure 6) on constate clairement les variations de l'inclinaison du terrain dues à la marée océanique. (Ryûtarô Takahasi)

2ème partie: Discussions sur le phénomène sismique d'Itô

1. Un grand nombre de séismes ont eu lieu aux environs de la ville d'Itô, et on les divise en deux groupes. Nous distingons parmi eux un certain nombre d'assez forts séismes qui ont été ressentis même à Tôkyô. Il a été aussi remarqué qu'une partie des séimes se sont produit successivement dans l'intervalle de la marée basse.

2. Nous distingons, partout au Japon, beaucoup d'exemples de sémismes qui resemblent aux séismes d'Itô quoique leur importance reste toujours inférieure. De ces faits il nous semble résulter qu'il n'y a aucune différence essentielle entre un groupe de petits séismes et les répliques.

3. D'après les résultats obtenus par le nivellement de précision exécuté dans la région d'Itô, nous pouvons constater l'existence de deux blocs au moment du grand tremblement de terre de 1923; tandis que un de deux s'est divisé en plusieurs cette fois-ci (Fig. 10). Il y a d'autre part, l'exhaussement maximum de terrain qui se place près de Kawana tout près de la région épicentrale. De ces faits nous constatons que les

séismes ont été accompagnées d'une inclinaison du bloc et d'un exhaussement de terrain.

4. Dans deux figures de vecteur-diagramme, nous pouvons remarquer, d'ailleurs, des sens prédominants qui ont un rapport avec l'apparition des séismes. Ce phénomène est comparable rigoureusement à celui qui a été observé à Miyadu juste après le grand tremblement de terre de Tango. Le fait que les deux blocs d'Itô et de Kawana s'inclinent vers l'Ouest, montre l'exhaussementn de la région littorale qui coïncide bien avec le témoignage oculaire.

5. L'exhaussement local de la surface terrestre est expliqué comme le résultat de l'injection magmatique dans la croûte rayonnant des ondes sismiques. D'après la détermination successive des positions hypocentrales, nous constatons qu'il existe quelque chose qui se soulève de la profondeur de la croûte vers sa surface. C'est certainement du magma, puisque ce quelque chose peut se mouvoir et cela nous porte à croire qu'il est l'origine du séisme. De la distribution des mouvements initiaux des ondes sismiques, on pose généralement qu'il s'est formé une faille dans la région épicentrale; mais cela n'ajoutera presque rien à l'explication de l'origine du séisme. (Mishio Ishimoto)

(震研彙報、第八號、圖版、石本、高橋)

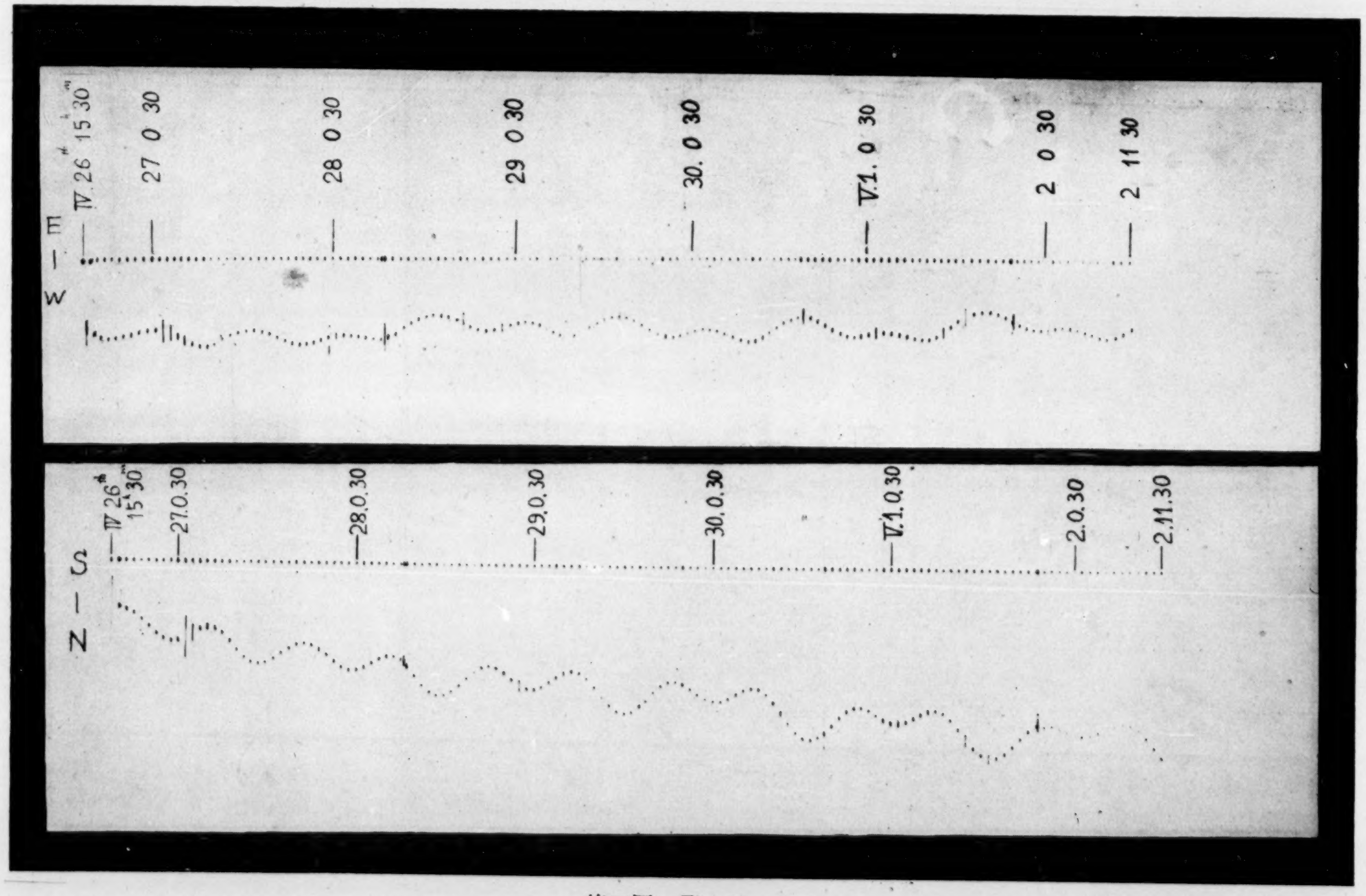

第三圖 Fig. 3.

——所　報——

○ 談話會記事

第五十二回談話會 （昭和五年九月十六日）

1. 加速度計による地震觀測　石本巳四雄
1. 地殼變動の解析的取扱に就いて　坪井忠二
1. 震源深き地震と日本嶋弧との關係　長岡半太郎
1. 山崩の調査 （第三報）　寺田寅彦・宮部直巳

第五十三回談話會 （昭和五年十月廿一日）

1. 駒ケ岳の地形變化に就いて　熱海景良・岸上冬彦
1. 伊東、川奈に於ける傾斜變化觀測 （續報）　高橋龍太郎
1. 丹後地方水準測量成果報告　末廣恭二
1. 土地の振動の習癖　末廣恭二
1. 地質時代の緯度變化に伴ふ地面の起伏と其他の現象　長岡半太郎・白井俊明

第五十四回談話會 （昭和五年十一月十八日）

1. 携帶用地震計及び記錄用同期電動機の製作　岸上冬彦
1. 昭和五年十月十七日大聖寺川附近の地震に就いて　岸上冬彦
1. 割れ目の出來方特に雁行性割れ目の出來方に就いて　藤原咲平・高山威雄
1. 地質時代（特に第三紀より現代まで）極の變位により生ずる地球表面の起伏　長岡半太郎・白井俊明

○ 出張

昭和五年九月十一日時報受信器修理の爲め神奈川縣下へ出張　波江野清藏
昭和五年九月十一日地震事項調査の爲め神奈川縣下へ出張　寺田寅彦
昭和五年九月十一日地震事項調査の爲め神奈川縣下へ出張　津屋弘逵
昭和五年九月十一日地震事項調査の爲め神奈川縣下へ出張　宮部直巳
昭和五年十月一日時報受信器修理の爲め千葉縣下へ出張　波江野清藏
昭和五年十月七日器械取片付の爲め新潟縣下へ出張　鹿熊金太郎
昭和五年十月七日地震事項調査の爲め神奈川縣下へ出張　宮部直巳
昭和五年十月十一日地震事項調査の爲め靜岡縣下へ出張　囑託　那須信治
昭和五年十月二十日地震事項調査の爲め福井、石川、兩縣下へ出張　岸上冬彦
昭和五年十一月五日傾斜計撤去の爲め靜岡縣下へ出張　高橋龍太郎

	那須信治	昭和五年十一月廿二日地震調査の爲め靜岡縣下へ出張
	岸上冬彦	昭和五年十一月廿二日地震調査の爲め靜岡縣下へ出張
囑託	齊田時太郎	昭和五年十一月廿七日地震調査の爲め靜岡縣下へ出張
	坪井誠太郎	昭和五年十一月廿七日地震調査の爲め靜岡縣下へ出張
	津屋弘逵	昭和五年十一月廿七月地震調査の爲め靜岡縣下へ出張
	大塚彌之助	昭和五年十一月廿七日地震調査の爲め靜岡縣下へ出張
	坪井忠二	昭和五年十一月廿八日地震調査の爲め靜岡縣下へ出張
	石本巳四雄	昭和五年十一月廿九日地震調査の爲め靜岡縣下へ出張
	宮部直巳	昭和五年十二月一日地震調査の爲め靜岡縣下へ出張
	高山威雄	昭和五年十二月一日地震調査の爲め靜岡縣下へ出張
	末廣恭二	昭和五年十二月五日地震調査の爲め靜岡縣下へ出張
	鹿熊金太郎	昭和五年十二月五日地震調査補助の爲め靜岡縣下へ出張

東京帝國大學

地震研究所彙報

第八號

昭和五年

BULLETIN

OF THE

EARTHQUAKE RESEARCH INSTITUTE

TOKYO IMPERIAL UNIVERSITY

Vol. VIII.

1930.

目　次

第八號

第一冊（昭和五年三月）

			頁
1.	地震波によつて土地の固有振動が誘起される可能度に就いて(英文)……………………	妹澤克惟	1
2.	地殼の群塊運動の可能度に就いて(英文)……	妹澤克惟 西村源六郎	13
3.	カリフオルニアに於ける地殼の變形(英文)‥	宮部直巳	45
4.	破壞的地震に就て(英文)……………………	寺田寅彦	61
5.	海水面に及ぼす海流の影響竝びに波浪の影響に就て(英文)…………………………	山口生知	75
6.	大阪近傍水準測量の結果に就て(邦文)……	梅本豐吉	85

第二冊（昭和五年六月）

7.	溫度分布が半無限彈性體の變形に及ぼす影響(英文)………………………………	西村源六郎	91
8.	十八米突の鐵管による地表傾斜變化の觀測(豫報)(英文)…………………………	高橋龍太郎	143
9.	昭和二年丹後地震に關聯せる丹後地方の地殼の變形に關する研究(第一報)(英文)……	坪井忠二	153
10.	地表の傾斜の變化に就て（第二報）關原における地震後の觀測(佛文)………	石本巳四雄	222

11. 昭和四年六月北海道駒ヶ嶽の噴火(英文)…… 津屋弘逵 坪井誠太郎 岸上冬彥 高橋龍太郎 坪井忠二 中田金市 宮部直巳 237

第三冊(昭和五年九月)

12. 彈性波の反響性及び分散性分散に就て(英文) 妹澤克惟 西村源六郎 321
13. 昭和二年丹後地震に關聯せる丹後地方の地殼の變形に關する研究(第二報)(英文)…… 坪井忠二 338
14. 筑波山に於ける傾斜變化觀測報告(邦文)…… 井上宇胤 杉山友紀 346
15. 大地震と太陽黑點との關係に就て(邦文)…… 高山威雄 鈴木武夫 364
16. 伊豆東海岸に於ける水準測量成果報告(邦文)…… 375

第四冊(昭和五年十二月)

17. 地殼の變形に因る熱の發生(英文)…… 寺田寅彥 377
18. 地殼の水平變動に就いて(英文)…… 坪井忠二 384
19. 地震と潮汐との關係(英文)…… 山口生知 393
20. 伊豆、伊東地方の地質構造に就いて(英文)…… 津屋弘逵 409
21. 伊東地震と地表傾斜變化の觀測(邦文)…… 石本巳四雄 高橋龍太郎 427

Contents.

Vol. VIII.

Part 1.—March, 1930.

Page

1. K. SEZAWA, Possibility of the Free-oscillations of the Surface-layer excited by the Seismic-waves. (in English) 1
2. K. SEZAWA and G. NISHIMURA, On the Possibility of the Block Movements of the Earth Crust. (in English) 13
3. N. MIYABE, Deformation of Earthcrust in California. (in English) 45
4. T. TERADA, On the Nature of Destructive Earthquakes. (in English) 61
5. S. YAMAGUTI, On the Effect of Ocean Current, "Kurosiwo", upon Sea Level. Effect of Waves. (in English) 75
6. T. UMEMOTO, Results of the Repeated Levellings in the Vicinity of Oosaka. (in Japanese) 85

Part 2.—June, 1930.

7. G. NISHIMURA, The Effect of Temperature Distribution on the Deformation of a Semi-infinite Elastic Body. (in English) 91
8. R. TAKAHASI, Preliminary Report on the Observation of the Tilting of the Earth's Crust with a Pair of Water Pipes. (in English) 143

9. C. Tsuboi, Investigation on the Deformation of the Earth's Crust in the Tango District connected with the Tango Earthquake of 1927. (Part 1.) (in English) 153

10. M. Ishimoto, Observations sur les variations de l'inclinaison de la surface terrestre (deuxième rapport). Résultats obtenus dans la région épicentrale du tremblement de terre de Sekibara. (en Français) 222

11. H. Tsuya, S. Tsuboi, F. Kishinouye, R. Takahasi, C. Tsuboi, K. Nakata and N. Miyabe, The Eruption of Komagatake, Hokkaidô, in 1929. (in English) 237

Part 3.—September, 1930.

12. K. Sezawa and G. Nishimura, Dispersion of a Shock in Echoing- and Dispersive-Elastic Bodies. (in English) 321

13. C. Tsuboi, Investigation on the Deformation of the Earth's Crust in the Tango District connected with the Tango Earthquake of 1927. (Part 2.) (in English) 338

14. W. Inouye and T. Sugiyama, On Earth-tiltings observed at Mt. Tukuba. (in Japanese) 346

15. T. Takayama and T. Suzuki, On the Relation between the Sunspot Number and the Destructive Earthquakes in Japan. (in Japanese) 364

16. Precise Levellings in the Province of Idu. (in Japanese) 375

Part 4.—December, 1930.

17. T. Terada, On the Heat generated by the Deformation of the Earth Crust. (in English) 377

18. C. Tsuboi, A Note on the Analytical Treatments of the Horizontal Deformation of the Earth's Crust. (in English) 384

19. S. Yamaguti, Relation between Tidal Phases and the Earthquakes. (in English) 393

20. H. Tsuya, On the Geological S ructure of Itô District, Idu. (in English) 409

21. M. Ishimoto et R. Takahasi, Séismes d'Itô et l'observation sur les variationsde l'inclinaison de la surface terrestre. (en japonais) 427

第八號索引

頁

井上宇胤、杉山友紀　(14) 筑波山に於ける傾斜變化觀測報告 (邦文)……346

石本巳四雄　(10) 地表の傾斜の變化に就て (第二報) 關原における地震後の觀測 (佛文)……222

石本巳四雄、高橋龍太郎　(21) 伊東地震と地表傾斜變化の觀測 (邦文)……421

岸上冬彥、津屋弘逵、坪井誠太郎、高橋龍太郎、坪井忠二、中田金市、宮部直巳；津屋弘逵、坪井誠太郎、岸上冬彥、高橋龍太郎、坪井忠二、中田金市、宮部直巳參照

宮部直巳　(3) カルフオルニアに於ける地殼の變形 (英文)……45

宮部直巳、津屋弘逵、坪井誠太郎、岸上冬彥、高橋龍太郎、坪井忠二、中田金市；津屋弘逵、坪井誠太郎、岸上冬彥、高橋龍太郎、坪井忠二、中田金市、宮部直巳參照

中田金市、津屋弘逵、坪井誠太郎、岸上冬彥、高橋龍太郎、坪井忠二、宮部直巳；津屋弘逵、坪井誠太郎、岸上冬彥、高橋龍太郎、坪井忠二、中田金市、宮部直巳參照

西村源六郎　(7) 溫度分布が半無限彈性體の變形に及ぼす影響 (英文)……91

西村源六郎、妹澤克惟；妹澤克惟、西村源六郎參照

妹澤克惟　(1) 地震波によつて土地の固有振動が誘起される可能度に就いて (英文)……1

妹澤克惟、西村源六郎　(2) 地殼の群塊運動の可能度に就いて (英文)……13

妹澤克惟、西村源六郎　(12) 彈性波の反響性及び分散性分散に就て (英文)……321

杉山友紀、井上宇胤；井上宇胤、杉山友紀參照

鈴木武夫、高山威雄；高山威雄、鈴木武夫參照

高橋龍太郎　(8) 十八米突の鐵管による地表傾斜變化の觀測(豫報)(英文)……143

高橋龍太郎、石本巳四雄；石本巳四雄、高橋龍太郎參照

高橋龍太郎、津屋弘逵、坪井誠太郎、岸上冬彥、坪井忠二、中田金市、宮部直巳；津屋弘逵、坪井誠太郎、岸上冬彥、高橋龍太郎、坪井忠二、中田金市、宮部直巳參照

高山威雄、鈴木武夫　(15) 大地震と太陽黑點との關係に就て(邦文)……364

寺田寅彥　(4) 破壞的地震に就いて(英文)……61

寺田寅彥　(17) 地殼の變形に因る熱の發生(英文)……377

坪井忠二　(9) 昭和二年丹後地震に關聯せる丹後地方の地殼の變形に關する研究(第一報)(英文)……153

坪井忠二　(13) 昭和二年丹後地震に關聯せる丹後地方の地殼の變形に關する研究(第二報)(英文)……338

坪井忠二　(18) 地殼の水平變動に就いて……377

坪井忠二、津屋弘逵、坪井誠太郎、岸上冬彥、高橋龍太郎、中田金市、宮部直巳；津屋弘逵、坪井誠太郎、岸上冬彥、高橋龍太郎、坪井忠二、中田金市、宮部直巳參照

坪井誠太郎、津屋弘逵、岸上冬彥、高橋龍太郎、坪井忠二、中田金市、宮部直巳；津屋弘逵、坪井誠太郎、岸上冬彥、高橋龍太郎、坪井忠二、中田金市、宮部直巳參照

津屋弘逵、坪井誠太郎、岸上冬彥、高橋龍太郎、坪井忠二、中田金市、宮部直巳　(11) 昭和四年六月北海道駒ヶ嶽の噴火(英文) 237

津屋弘逵　(20) 伊豆、伊東地方の地質構造に就いて(英文)……409

梅本豐吉　(6) 大阪近傍水準測量の結果に就いて(邦文)……85

山口生知　(5) 海水面に及ぼす海流の影響竝びに波浪の影響に就て(英文)……75

山口生知　(19) 地震と潮汐との關係(英文)……393

陸地測量部　(16) 伊豆東海岸に於ける水準測量成果報告(邦文)……375

Index to Vol. VIII.

Page

INOUYE, W. and SUGIYAMA, T. (14) On Earth-tiltings observed at Mt. Tsukuba. (in Japanese) 346

ISHIMOTO, M. (10) Observations sur les variations de l'inclinaison de la surface terrestre (deuxième rapport). Résultats obtenus dans la région épicentrale du tremblement de terre de Sekihara. (en français) 222

ISHIMOTO, M. et TAKAHASI, R. (21) Séismes d'Itô et l'observation sur les variations de l'inclinaison de la surface terrestre. (en japonais) 427

KISHINOUYE, F., TSUYA, H., TSUBOI, S., TAKAHASI, R., TSUBOI, C., NAKATA, K. and MIYABE, N., *See* TSUYA, H., TSUBOI, S., KISHINOUYE, F., TAKAHASI, R., TSUBOI, C., NAKATA, K. and MIYABE, N.

LAND SURVEY DEPARTMENT. (16) Precise Levellings in the Province of Idu. (in Japanese) 375

MIYABE, N. (3) Deformation of Earthcrust in California. (in English) 45

MIYABE, N., TSUYA, H., TSUBOI, S., KISHINOUYE, F., TAKAHASI, R., TSUBOI, C. and NAKATA, K., *See* TSUYA, H., TSUBOI, S., KISHINOUYE, F., TAKAHASI R., TSUBOI, C., NAKATA, K. and MIYABE, N.

NAKATA, K., TSUYA, H., TSUBOI, S., KISHINOUYE, F., TAKAHASI, R., TSUBOI, C. and MIYABE, N., *See* TSUYA, H., TSUBOI, S., KISHINOUYE, F., TAKAHASI, R., TSUBOI, C., NAKATA, K. and MIYABE, N.

NISHIMURA, G. (7) The Effect of Temperature Distribution on the Deformation of a Semi-infinite Elastic Body. (in English) .. 91

NISHIMURA, G. and SEZAWA, K., *See* SEZAWA, K. and NISHIMURA, G.

SEZAWA, K. (1) Possibility of the Free-oscillations of the Surface-layer excited by the Seismic-Waves. (in English) 1

SEZAWA, K. and NISHIMURA, G. (2) On the Possibility of the Block Movements of the Earth Crust. (in English) 13

SEZAWA, K. and NISHIMURA, G. (12) Dispersion of a Shock in Echoing- and Dispersive-Elastic Bodies. (in English) 321

SUGIYAMA, T. and INOUYE, W., *See* INOUYE, W. and SUGIYAMA, T.

SUZUKI, T and TAKAYAMA, T., *See* TAKAYAMA, T. and SUZUKI, T.

TAKAHASI, R. (8) Preliminary Report on the Observation of the Tilting of the Earth's Crust with a Pair of Water Pipes. (in English) 143

TAKAHASI, R. et ISHIMOTO, M., *See* ISHIMOTO, M. et TAKAHASI, R.

TAKAHASI, R., TSUYA, H., TSUBOI, S., KISHINOUYE, F., TSUBOI, C., NAKATA, K. and MIYABE, N., *See* TSUYA, H., TSUBOI, S., KISHINOUYE, F., TAKAHASI, R., TSUBOI, C., NAKATA, K. and MIYABE, N.

TAKAYAMA, T. and SUZUKI, T. (15) On the Relation between the Sunspot Number and the Destructive Earthquakes in Japan. (in Japanese) 364

TERADA, T. (4) On the Nature of Destructive Earthquakes. (in English) 61

TERADA, T. (17) On the Heat generated by the Deformation of the Earth Crust. (in English) 377

TSUBOI, C. (9) Investigation on the Deformation of the Earth's Crust in the Tango District connected with the Tango Earthquake of 1927. (Part 1.) (in English) 153

TSUBOI, C. (13) Investigation on the Deformation of the Earth's Crust in the Tango District connected with the Tango Earthquake of 1927. (Part 2) (in English) 338

TSUBOI, C. (18) A Note on the Analytical Treatments of the Horizontal Deformation of the Earth's Crust. (in English) ·· 384

TSUBOI, C., TSUYA, H., TSUBOI, S., KISHINOUYE, F., TAKAHASI, R., NAKATA, K. and MIYABE, N., *See* TSUYA, H., TSUBOI, S., KISHINOUYE, F., TAKAHASI, R., TSUBOI, C., NAKATA, K. and MIYABE, N.

TSUBOI, S., TSUYA, S., KISHINOUYE, F., TAKAHASI, R., TSUBOI, C., NAKATA, K. and MIYABE, N., *See* TSUYA, H., TSUBOI, S., KISHINOUYE, F., TAKAHASI, R., TSUBOI, C., NAKATA, K. and MIYABE, N.

TSUYA, H., TSUBOI, S., KISHINOUYE, F., TAKAHASI, R., TSUBOI, C., NAKATA, K. and MIYABE, N. (11) The Eruption of Komagatake Hokkaidô, in 1929. (in English) ········ 237

TSUYA, H. (20) On the Geological Structure of Itô District, Idu. (in English) ········ 409

UMEMOTO, T. (6) Results of the Repeated Levellings in the Vicinity of Oosaka. (in Japanese) ········ 85

YAMAGUTI, S. (5) On the Effect of Ocean Current, "Kurosiwo", upon Sea Level. Effect of Waves. (in English) ········ 75

YAMAGUTI, S. (19) Relation between Tidal Phases and the Earthquakes. (in English) ········ 393

昭和五年十二月廿三日印刷
昭和五年十二月廿六日發行

編纂兼發行者　東京帝國大學地震研究所

東京市深川區東大工町四十八番地
印刷者　星野　錫

東京市深川區東大工町四十八番地
印刷所　東京印刷株式會社

東京市神田區南神保町十六番地
賣捌所　岩波書店

Sold by

Iwanami Shoten,

Minamizinbôtyô, Kanda, Tôkyô.

Price of this copy: 0·95 Yen. (Postage exclusive.)

BULLETIN OF
THE EARTHQUAKE RESEARCH INSTITUTE
TOKYO IMPERIAL UNIVERSITY
Vol. VIII, Part 4. December, 1930.

Contents.

Papers and Reports.

Page

17. T. TERADA, On the Heat generated by the Deformation of the Earth Crust. (in English) 377

18. C. TSUBOI, A Note on the Analytical Treatments of the Horizontal Deformation of the Earth's Crust. (in English) 384

19. S. YAMAGUTI, Relation between Tidal Phases and the Earthquakes. (in English) ... 393

20. H. TSUYA, On the Geologic Structure of Itô District, Idu. (in English) 409

21. M. ISHIMOTO et R. TAKAHASI, Séismes d'Itô et l'observation sur les variations de l'inclinaison de la surface terrestre. (en japonais) 427

Institute Notes.

(For the papers written in Japanese or in occidental languages, the abstracts are given in occidental languages or in Japanese respectively.)